



**HAL**  
open science

# Extraction de composés phénoliques à partir d'une bio-huile de lignine

Laëtitia Cesari

► **To cite this version:**

Laëtitia Cesari. Extraction de composés phénoliques à partir d'une bio-huile de lignine. Génie des procédés. Université de Lorraine, 2017. Français. NNT : 2017LORR0148 . tel-01773073

**HAL Id: tel-01773073**

**<https://theses.hal.science/tel-01773073>**

Submitted on 20 Apr 2018

**HAL** is a multi-disciplinary open access archive for the deposit and dissemination of scientific research documents, whether they are published or not. The documents may come from teaching and research institutions in France or abroad, or from public or private research centers.

L'archive ouverte pluridisciplinaire **HAL**, est destinée au dépôt et à la diffusion de documents scientifiques de niveau recherche, publiés ou non, émanant des établissements d'enseignement et de recherche français ou étrangers, des laboratoires publics ou privés.



## AVERTISSEMENT

Ce document est le fruit d'un long travail approuvé par le jury de soutenance et mis à disposition de l'ensemble de la communauté universitaire élargie.

Il est soumis à la propriété intellectuelle de l'auteur. Ceci implique une obligation de citation et de référencement lors de l'utilisation de ce document.

D'autre part, toute contrefaçon, plagiat, reproduction illicite encourt une poursuite pénale.

Contact : [ddoc-theses-contact@univ-lorraine.fr](mailto:ddoc-theses-contact@univ-lorraine.fr)

## LIENS

Code de la Propriété Intellectuelle. articles L 122. 4

Code de la Propriété Intellectuelle. articles L 335.2- L 335.10

[http://www.cfcopies.com/V2/leg/leg\\_droi.php](http://www.cfcopies.com/V2/leg/leg_droi.php)

<http://www.culture.gouv.fr/culture/infos-pratiques/droits/protection.htm>

## Thèse

Présentée pour l'obtention du grade de

Docteur de l'Université de Lorraine

Spécialité Génie des Procédés et des Produits

par

Laëtitia Cesari

---

### **Extraction de composés phénoliques à partir d'une bio-huile de lignine**

---

Soutenue publiquement le 09 Octobre 2017 devant la commission d'examen :

Membres du jury :

Pr Christophe Coquelet (Mines de Paris CTP, rapporteur)

Dr Ilham Mokbel (Université de Lyon LMI, rapporteur)

Pr Nicolas Brosse (Université de Lorraine LERMAB, examinateur)

Pr Olivier Dangles (Université d'Avignon et des pays du Vaucluse INRA, examinateur)

Dr Fabrice Mutelet (Université de Lorraine LRGP, directeur de thèse)

Dr Laetitia L.S. Canabady-Rochelle (CNRS LRGP, co-directrice de thèse)

Membres invités :

Dr Mohammed Bouroukba (Université de Lorraine LRGP)

Dr Anthony Dufour (CNRS LRGP)

---

Laboratoire Réactions et Génie des Procédés (LRGP)

1 rue Grandville, 54000 Nancy, France



## Remerciements

Ce travail a été réalisé au Laboratoire Réactions et Génie des Procédés (LRGP-UMR 7274 CNRS) à Nancy et je tiens à remercier Monsieur Laurent Falk pour m'avoir accueilli dans ce laboratoire.

Ma gratitude va en tout premier lieu à mon directeur de thèse monsieur Fabrice Mutelet. Je n'oublierai jamais la confiance sans faille qu'il m'a accordée pendant ces trois années, ainsi que sa gentillesse, sa disponibilité, son écoute et ses conseils tant sur le plan scientifique et intellectuel que sur le plan humain.

Je tiens à remercier chaleureusement ma co-directrice de thèse madame Laetitia Canabady-Rochelle pour son soutien, ses conseils et sa contribution au bon déroulement de cette thèse.

Que monsieur Christophe Coquelet et madame Ilham Mokbel trouvent ici l'expression de ma sincère reconnaissance pour avoir accepté de juger ce travail en tant que rapporteur. Leur présence dans le jury m'honore. De plus, je tiens également à remercier messieurs Nicolas Brosse et Olivier Dangles qui ont accepté de faire partie du jury en tant qu'examineurs.

J'adresse mes vifs remerciements à messieurs Mohammed Bouroukba et Anthony Dufour pour leur aide et leurs conseils ainsi que nos nombreuses discussions scientifiques. Je les remercie également d'avoir accepté l'invitation à participer à ma soutenance.

J'adresse également ma gratitude à messieurs Yann Lebrech et Dominique Petitjean pour leur écoute et leurs conseils avisés. Que messieurs Steve Pontvianne et Emilien Girot trouvent également l'expression de ma sincère reconnaissance pour leur aide et leur grande disponibilité.

Je remercie aussi l'ensemble de l'équipe ThermE pour m'avoir accueillie et intégrée : Jean-Noël Jaubert, Romain Privat, Roland Solimando, Michel Dirand, Dominique Alonso, Viviane Renaudin, Jean-Charles Moise, Patrick Carré et Nathalie Hubert. Je pense également à mes collègues plus ou moins étudiants maintenant : Xiaochun « Peter » Xu, Vincent Plee, El Shaimaa Abumandour, Amal Ayad, Silvia Lasala, Mathieu Furet, Aurélien Allys, Airy Tilland, Lubin de Beauchene, Etienne Berger, Quentin Ribeyre et Kevin Villeneuve.

Un grand merci à l'ensemble des thésards restants : Sylvain Namysl, Nicolas Vin, Mathieu « Papy » Château, Jean-Patrick Barbé, Charlotte Godoy, Audrey Santandréa et aux membres du bureau des jeunes chercheurs : Lucie Barbier, Zeinab Chour, Daniela Florez, Mathilde Guilpain, Edouard Moine, Simon Picaud-Vannereux et Assia Saker. Je vous souhaite à tous bon courage !

J'adresse également mes vifs remerciements à l'ensemble des personnes de l'IUT Nancy-Brabois pour leur confiance et leur gentillesse. Grâce à vous, j'ai découvert les joies de l'enseignement et je vous en remercie. Je remercie également l'ensemble du LRGP que j'ai côtoyé pendant ces trois années et qui, d'une manière ou d'une autre, a eu une influence sur ce projet de thèse.

Je ne saurais terminer ces remerciements sans penser également à mes amis et à ma famille qui, de près ou de loin, ont contribué à celle que je suis devenue.

Tout d'abord à mes parents, qui m'ont toujours dit que je réussirai ce que j'entreprends, quelque en soit le projet. Votre amour et votre confiance ont toujours été sans faille.

Ensuite à mes frères qui, quoi que je fasse, me verront toujours comme leur petite sœur et me permettent de garder cette âme d'enfant.

A ma « happy family », qui demeure malgré la distance et le temps qui passe !

A mes futurs beaux-parents, qui m'ont acceptée telle que je suis et me confère le même soutien qu'à leur fils.

A Maxwell, qui a jugé qu'être réveillée dès potron-minet était le meilleur moyen de commencer la journée.

Enfin, et le plus important, je souhaite remercier de tout mon cœur mon collègue, ami et conjoint Yohann Le Guennec qui a toujours su trouver les mots et faire en sorte que je me dépasse chaque jour un peu plus. Pour cela et pour tout le reste, je souhaite te dédier cette thèse.

## Table des matières

Liste des figures .....	vi
Liste des tableaux .....	viii
Introduction .....	1
Chapitre I : Etude bibliographique .....	5
I-1. Contexte et enjeux environnementaux .....	5
I-2. La biomasse lignocellulosique .....	7
I-2.1. Composition de la biomasse .....	7
I-2.2. Prétraitement de la lignine .....	11
I-2.3. Valorisation de la lignine .....	13
I-2.4. Production de bio-huile issue de la lignine .....	14
I-2.5. Mécanismes réactionnels rencontrés lors de la pyrolyse .....	15
I-2.6. Composition des bio-huiles .....	17
I-3. Extraction de composés à forte valeur ajoutée présents dans une bio-huile .....	21
I-3.1. Procédés d'extraction .....	21
I-3.2. Vers de nouveaux milieux extractifs : les liquides ioniques .....	26
I-3.3. Etude microscopique et macroscopique des systèmes clés rencontrés dans le procédé d'extraction .....	28
I-4. Valorisation des composés phénoliques .....	33
I-5. Description des prochains chapitres .....	36
Références bibliographiques .....	38
Chapter II: Computational study on the molecular conformations of phenolic compounds....	49
Résumé .....	49
Abstract .....	50
II-1. Introduction .....	51
II-2. Computational methods .....	53
II-3. Results and discussion .....	54
II-3.1. Phenolic structures .....	54
II-3.2. Minimum structures .....	63
II-3.3. Potential functions .....	66
II-3.4. Calculation of intramolecular hydrogen bond enthalpy .....	70
II-4. Conclusion .....	72
References .....	73
Chapter III: Computational study of phenolic compounds-water clusters .....	77
Résumé .....	77

Abstract.....	78
III-1. Introduction .....	79
III-2. Computational methods.....	81
III-3. Result and discussion .....	82
III-3.1 Energies .....	82
III-3.2. Vibrational frequencies.....	89
III-3.3. Natural Bond Orbitals (NBO) analysis.....	96
III-3.4 HOMO-LUMO analysis .....	98
III-4. Study of the phenol-choline bis(trifluoromethylsulfonide)imide cluster .....	100
III-5. Conclusion.....	106
References: .....	107
Chapter IV: Phase equilibria of phenolic compounds in water or ethanol.....	113
Résumé .....	113
Abstract.....	114
IV-1. Introduction .....	115
IV-2. Material and Methods .....	117
IV-2.1. Chemicals .....	117
IV-2.2. Solubility of the phenolic compounds in water.....	119
IV-2.3. Solubility of water in the phenolic solution .....	119
IV-2.4. Vapor-Liquid equilibria of phenolic compound and ethanol .....	120
IV-2.5. Excess enthalpy between phenolic compounds and ethanol .....	121
IV-3. Theory/calculation .....	121
IV-3.1. Thermodynamic correlation .....	121
IV-3.2. Solid-Liquid Equilibria.....	122
IV-3.3. Vapor-Liquid equilibria.....	122
IV-4. Results and Discussion.....	123
IV-4.1. Solubility of the phenolic compounds in water.....	123
IV-4.2. Solubility of water in the phenolic solution .....	126
IV-4.3. Vapor-Liquid equilibria of phenolic compound and ethanol .....	127
IV-4.4 Excess enthalpy of the phenolic compound – ethanol systems.....	130
IV-5. Conclusion .....	132
References .....	134
Chapter V: Extraction of phenolic compounds from aqueous solution using choline bis(trifluoromethylsulfonyl)imide .....	139
Résumé .....	139

Abstract.....	140
V-1. Introduction .....	141
V-2. Materials and Methods .....	142
V-2.1. Chemicals and materials .....	142
V-2.2. Phase diagrams measurements of ternary mixtures {phenolic compounds + water + IL}.....	144
V-2.3. Extraction of phenolic compounds from aqueous solution .....	145
V-3. Thermodynamic correlation .....	145
V-4. Results and discussion.....	146
V-4.1. Ternary mixtures {phenolic compounds + water + IL} .....	146
V-4.2. Extraction of phenolic compounds from aqueous solution .....	154
V-4.3. Process sizing.....	156
V-5. Conclusion.....	159
References .....	162
Chapter VI: Separation of phenols from lignin pyrolysis oil using ionic liquid and comparison with ethyl acetate.....	165
Résumé .....	165
Abstract.....	166
VI-1. Introduction.....	167
VI-2. Materials and method.....	169
VI-2.1. Chemical reagents and solvents.....	169
VI-2.2. Bio-oil production .....	169
VI-2.3. Liquid-liquid extraction.....	170
VI-2.4. Sample analysis .....	172
VI-3. Results and discussion .....	173
VI-3.1. Influence of the experimental conditions used in the produced crude bio-oil before liquid liquid extraction.....	173
VI-3.2. Liquid-liquid extraction of phenolic compounds from bio oil using basic aqueous solutions. ....	173
VI-3.3. Extraction of phenolic compounds from the previous aqueous solution using various solvents.....	176
VI-3.4. Extraction of phenolic compounds from the aqueous solution using ethyl acetate. ....	177
VI-3.5. Extraction of phenolic compounds from aqueous solution using Choline bis(trifluoromethylsulfonyl)imide.....	179
VI-4. Conclusion .....	181
References .....	182

Chapter VII: Antioxidant Properties of Phenolic Compounds.....	187
Résumé .....	187
Abstract.....	188
VII-1. Introduction.....	189
VII-2. Materials and Method .....	191
VII-2.1. Chemicals.....	191
VII-2.2. Dosage of phenols by the Folin-Ciocalteu method.....	192
VII-2.3. Transition metal chelating capacity .....	193
VII-2.4. Radical scavenging activity .....	194
VII-2.5. Reducing power .....	195
VII-3. Results and discussion .....	197
VII-3.1. Total phenols quantification by the Folin-Ciocalteu method.....	199
VII-3.2. Iron(II) and Copper (II) chelating activity .....	200
VII-3.3. Radical scavenging activity .....	202
VII-3.4. Reducing capacity .....	204
VII-4. Conclusion .....	206
References .....	207
Conclusion et perspectives .....	211
APPENDIX .....	215
Appendix I: Computational study on the molecular conformations of phenolic compounds. .....	217
Appendix II: Computational study of phenolic compounds-water clusters .....	261
Appendix III: Phase equilibria of phenolic compounds in water or ethanol .....	287
Appendix IV: Extraction of phenolic compounds from aqueous solution using choline bis(trifluoromethylsulfonyl)imide .....	295
Appendix V: Antioxidant Properties of Phenolic Compounds .....	303



## Liste des figures

Figure I-1: Ressources mondiales pour la production d'énergie primaire en 1973 a) et 2014 b) d'après l'Agence Internationale de l'Energie[1] .....	5
Figure I-2 : Schéma de l'organisation structurale au sein d'une cellule végétale [8,9] .....	7
Figure I-3: Structure du motif cellobiose constitutif de la cellulose [14] .....	8
Figure I-4: Structure des monosaccharides issus des hémicelluloses [14].....	8
Figure I-5 : Structure des trois monolignols.....	9
Figure I-6 : Représentation schématique de la structure de la lignine issue d'une espèce feuillue [19] .....	10
Figure I-7 : Principales liaisons au sein de la structure de la lignine : (A) $\beta$ -O-4, (B) 5-5, (C) $\alpha$ -O-4, (D) $\beta$ -5, (E) $\beta$ - $\beta$ , (F) 4-O-5, (G) $\beta$ -1 [20].....	10
Figure I-8: Lignine Kraft[4,19,22] .....	11
Figure I-9 : Lignine lignosulfonate [4,19,22].....	12
Figure I-10 : Lignine organosolv [24].....	12
Figure I-11 : Lignine pyrolytique.....	13
Figure I-12: Procédés de valorisation de la lignine, produits obtenus et utilisations potentielles [20] .....	14
Figure I-13 : Schéma de dégradation de la lignine par élimination et déshydratation [9] .....	15
Figure I-14 : Schéma de rupture des liaisons éthers dans un réseau ligneux [9] .....	16
Figure I-15 : Schéma de l'évolution de la décomposition thermique de la structure de la lignine en fonction de la température [9] .....	17
Figure I-16 : Extraction liquide-liquide de phénols d'une bio-huile [34] .....	25
Figure I-17 : Classification des tests antioxydants d'après Huang et al [162] .....	34
Figure I-18 : Structures des molécules étudiées dans cette thèse : a) phénol, b) guaiacol, c) syringol, d) pyrocatechol, e) o-crésol, f) m-crésol, g) p-crésol, h) vanilline.....	36
Figure II-1: Global minimum energy structure of the studied phenolic compounds: a) phenol, b) o-cresol, c) trans-m-cresol, d) cis-m-cresol, e) p-cresol, f) pyrocatechol, g) guaiacol, h) vanillin, i) syringol. ....	55
Figure II-2: Potential Energy Surface of vanillin as a function of the torsion of C2-C3-O3-H3 (hydroxy) and C3-C4-O4-C7 (methoxyl) angles with C5-C6-C8-O8 (aldehyde) frozen at a) 180°, b) frozen at 0°, c) Potential Energy Surface of vanillin as a function of the torsion of C3-C4-O4-C7 (methoxyl) and C5-C6-C8-O8 (aldehyde) with C2-C3-O10-H11 (hydroxy) frozen at 180°, at B3LYP/cc-pVTZ.....	60
Figure II-3: a) Potential Energy Surface of syringol as a function of the torsion of C1-C2-O2-C7 (methoxyl) and C3-C4-O4-C8 (methoxyl) angles with C2-C3-O3-H3 (hydroxy) frozen at 180° at B3LYP/cc-pVTZ, b) Potential Energy Surface of syringol as a function of the torsion of C1-C2-O2-C7 (methoxyl) and C2-C3-O3-H3 (hydroxyl) angles with C3-C4-O4-C8 (methoxyl) frozen at 180° at B3LYP/cc-pVTZ.....	62
Figure III-1 Optimized structures of: a) the [Choline] cation, b) the [NTf <sub>2</sub> ] bis(trifluoromethylsulfonide)imide anion, c) the ILa ionic liquid conformation, d) the ILb conformation .....	101
Figure III-2 : Optimized cluster structures of a) [Choline]-phenol Ch-PhA, b) , [Choline]-phenol Ch-PhB, c) [NTf <sub>2</sub> ] -phenol N-PhA, d) [NTf <sub>2</sub> ] -phenol N-PhB .....	104
Figure III-3 : Optimized cluster structures of a) [Choline][NTf <sub>2</sub> ] - phenol ILa-PhA, b) [Choline][NTf <sub>2</sub> ] - phenol ILa-PhB, c) [Choline][NTf <sub>2</sub> ] - phenol ILa-PhC .....	105

Figure IV-1: Scheme of the VLE device[46]: 1. Temperature transmitter; 2. Pressure transducer (Druck-PMP4010); 3. Condenser; 4. Refrigerator; 5. Temperature sensor (T900 series); 6. Equilibrium vessel; 7. Constant temperature bath; 8. Magnetic stirrer; 9. Pressure buffer; 10. Vacuum control valve; 11. Vacuum pump.....	120
Figure IV-2: Solubility of phenolic compounds in water. Experimental measurements: ● Phenol, ● Guaiacol, ○ Syringol, ■ Pyrocatechol, ■ o-Cresol, □ m-Cresol, ▲ p-Cresol, Δ Vanillin. The solid lines have been calculated using NRTL model.....	123
Figure IV-3: Water solubility in phenolic phases. Experimental measurements: ● Guaiacol, ○ Syringol, ■ o-Cresol, □ m-Cresol, ▲ p-Cresol. The solid lines have been calculated using NRTL model. ....	126
Figure IV-4: Vapor-Liquid equilibria of the guaiacol-ethanol system in function of the molar fraction of guaiacol at different pressures. Experimental measurements at pressures: ● 0.09 bar, ■ 0.165 bar, ▲ 0.335 bar, ◆ 0.5 bar, ○ 0.7 bar, □ 0.83 bar, Δ 0.99 bar. The solid lines have been calculated using NRTL model.....	129
Figure IV-5: Mixing enthalpy of the phenolic compound - ethanol systems. ● Guaiacol, ■ o-Cresol, □ m-Cresol. ....	131
Figure V-1: Plot of the experimental data for the molar composition tie lines of the ternary system: a) {[choline][NTf <sub>2</sub> ] (1) – phenol (2) - water (3)}, b) {[choline][NTf <sub>2</sub> ] (1) – guaiacol (2) - water (3)}, c) {[choline][NTf <sub>2</sub> ] (1) –syringol (2) - water (3)}, d) {[choline][NTf <sub>2</sub> ] (1) – pyrocatechol (2) - water (3)} at 298 K and 0.1 MPa.....	151
Figure V-2: Influence of the mass ratio of ionic liquid/water on the efficiency of the extraction process.....	155
Figure V-3: Process design for the extraction of phenolic compound from aqueous solution .....	156
Figure VI-1: Scheme of the device for the lignin pyrolysis from [60] .....	170
Figure VI-2: Steps of the extraction of phenolic compounds from bio-oil.....	171
Figure VI-3: Scheme of the GC-GC MS-FID-FID device from [60] .....	172
Figure VI-4: Colour of the phase after liquid-liquid extraction: a) from left to right: ethyl acetate phase (4 stages mixing) and aqueous phase; b) from left to right: [choline][NTf <sub>2</sub> ] stages from 1 to 4 and aqueous phase.....	181
Figure VII-1: Dosage of phenols by the Folin-Ciocalteu method: ● Reference (Gallic acid), ● Phenol, ○ Guaiacol, ■ Syringol, ■ Pyrocatechol, □ Vanillin, ▲ O-cresol, ▲ M-cresol, Δ P-cresol. ....	199
Figure VII-2: Metal ion chelating activity. a) Iron(II) chelating activity: ● Phenol, ○ Guaiacol, ■ Syringol, ■ Pyrocatechol, □ Vanillin, ▲ O-cresol, ▲ M-cresol, Δ P-cresol. b) Copper(II) chelating activity: ● Reference (EDTA), ○ Guaiacol, ■ Pyrocatechol, □ Vanillin, ▲ O-cresol, ▲ M-cresol.....	201
Figure VII-3: Radical scavenging activity: ● Reference (Trolox), ● Phenol, ○ Guaiacol, ■ Syringol, ■ Pyrocatechol, □ Vanillin, ▲ O-cresol, ▲ M-cresol, Δ P-cresol.....	203
Figure VII-4: Reducing capacity. Panel a) ● Reference (ascorbic acid), ○ Guaiacol, ■ Syringol, ■ Pyrocatechol. Panel b) ● Phenol, □ Vanillin, ▲ O-cresol, ▲ M-cresol, Δ P-cresol.....	205

## Liste des tableaux

Tableau I-1 : Composition de diverses bio-huiles en pourcentage massique.....	18
Tableau I-2 : Extraction des composés à forte valeur ajoutée présent dans une bio-huile produite par conversion thermochimique de la biomasse .....	22
Tableau I-3 : Cations et anions présents dans la structure des liquides ioniques.....	27
Tableau I-4: Rang de températures et méthodes de mesure pour les systèmes {eau-composés phénoliques} issus de la littérature.....	31
Tableau I-5: Domaines d'utilisation des composés phénoliques présents dans les bio-huiles	33
Table II-1: Bond lengths for the ground state global minimum of phenolic compounds. ....	64
Table II-2: Bond angles for the ground state global minimum of phenolic compounds. ....	65
Table II-3: Potential constants for internal rotation (in $\text{kJ}\cdot\text{mol}^{-1}$ ).....	67
Table II-4: Intramolecular Hydrogen bond Enthalpy $\Delta H_{\text{HB}}$ calculated using different theories and basis sets. ....	71
Table III-1: Optimized conformations. ....	83
Table III-2: Lengths and frequencies of O-H bonds. ....	91
Table III-3: Calculated bond lengths ( $\text{\AA}$ ) of the global minimum conformations in the {phenolic compound – water} cluster.....	94
Table III-4: Calculated bond angles (in degrees) of the global minimum conformations in the {phenolic compound – water} cluster. ....	95
Table III-5: NBO population analysis.....	97
Table III-6: HOMO-LUMO parameters. ....	99
Table III-7: Energy of structures and binding energy for the Choline, $\text{NTf}_2$ , phenol and their clusters.....	102
Table IV-1: Temperature range and method of measurements for the {phenolic compounds-water} systems found in the literature.....	116
Table IV-2: Name, CAS number, abbreviation, molar mass, formula, source and purity of the used compounds .....	118
Table IV-3: Experimental LLE data of the {phenolic compound (PC) - water} systems at atmospheric pressure. ....	124
Table IV-4: Experimental SLE data of the {phenolic compound (PC)-water} systems at atmospheric pressure. ....	125
Table IV-5: NRTL parameters for the phenolic compound –water (SLE and LLE) systems	127
Table IV-6: Vapor-liquid equilibrium data of binary mixtures containing phenolic compounds and ethanol. ....	128
Table IV-7: NRTL parameters for the phenolic compound – ethanol (VLE) systems. ....	130
Table IV-8: Molar excess enthalpy of the {phenolic compound – ethanol} systems at $T=298.15\text{K}$ and $P=1\text{ atm}$ . ....	131
Table V-1: Names, CAS numbers, abbreviation, molar mass, chemical structures and source of compounds .....	143
Table V-2: Experimental LLE data of the tie-lines in mole fractions, solute distribution ratio $\beta$ and selectivity $S$ for the ternary system {[choline][ $\text{NTf}_2$ ] (1) –phenolic compound (2) – water (3)} at $298.15\text{K}$ and $0.1\text{ MPa}$ . <sup>a</sup> .....	148
Table V-3: Experimental SLE data of the tie-lines in mole fractions in the {[choline][ $\text{NTf}_2$ ] (1) –phenol (2) - water (3)}, {[choline][ $\text{NTf}_2$ ] (1) –syringol (2) - water (3)} and {[choline][ $\text{NTf}_2$ ] (1) –pyrocatechol (2) - water (3)} systems at $298\text{ K}$ and $0.1\text{ MPa}$ . <sup>a</sup> .....	150

Table V-4: Extraction parameters. ....	158
Table V-5: Composition in extract steam and energy required for single step evaporation. .	158
Table VI-1: Experimental conditions for the production of crude bio-oils.....	170
Table VI-2: Composition of the bio-oils before ( $w_b$ ) and after ( $w_a$ ) extraction with aqueous basic solutions and the respective extraction rates (%E).....	174
Table VI-3: Composition of the ethyl acetate final phase ( $w_f$ ) and the respective extraction rates (%E).....	178
Table VI-4: Composition of the [Choline][NTf <sub>2</sub> ] final phase ( $w_f$ ) and the respective extraction rates (%E).....	180
Table VII-1 : Mini-review on the literature concerning the antioxidant properties of bio-oils. ....	191
Table VII-2: Antioxidant properties of the studied phenolic compounds. a) GAER and EECC. b) TEAC and AERC.....	197



## Introduction

Depuis quarante ans, les ressources en pétrole ne cessent de diminuer. Dans le même temps, la production de dioxyde de carbone a plus que doublé, entraînant une accélération du réchauffement climatique. Malgré l'émergence de ressources renouvelables, l'utilisation du pétrole comme ressource primaire ne permettrait de tenir qu'une quarantaine d'années. Il est donc urgent de développer de nouvelles ressources renouvelables afin de compenser l'exploitation des énergies fossiles. Ce travail de recherche s'inscrit dans ce contexte sociétal, l'objectif de cette thèse étant de valoriser la biomasse, notamment la lignine, comme ressource énergétique complémentaire au pétrole, pour la production et l'extraction de composés phénoliques présentant une bioactivité.

En effet, la biomasse est une ressource particulièrement complexe, riche en cellulose et en hémicellulose. Ses constituants ont permis l'élaboration de bio-carburant de deuxième génération, pour la production de papier et/ou la valorisation de co-produits tels que des protéines, des acides aminés, des carbohydrates ou des acides organiques. Cependant, l'intérêt pour la lignine ne s'est développé que très récemment.

Jusqu'à aujourd'hui, la lignine a été principalement utilisée (combustion) pour fournir de l'énergie aux bioraffineries. Or la lignine est également valorisable par d'autres techniques pour produire, par exemple, des composés phénoliques. En effet, la pyrolyse de la lignine produit un liquide noir et visqueux appelé « bio-huile » qui contient de nombreux composés à forte valeur ajoutée, dont des composés phénoliques.

Compte-tenu de la composition complexe des bio-huiles et de leur instabilité thermique, il est très difficile de séparer et de purifier ces composés phénoliques. Différentes techniques d'extraction existent (distillation, chromatographie, CO<sub>2</sub> supercritique) mais la plus utilisée est l'extraction liquide-liquide avec utilisation de solvants (solution aqueuse, acétate d'éthyle, THF, etc.). Cependant, il faut faire face à de nombreuses contraintes, comme la redistribution des composés cibles dans les différentes phases, la forte quantité de solvant nécessaire ou encore un apport énergétique élevé afin de récupérer, par distillation, les composés cibles présents dans ces solvants.

Afin d'améliorer les procédés d'extraction, la connaissance microscopique des molécules étudiées est nécessaire. Ainsi, par calcul quantique, la structure des molécules dans leur état isolé ou dans un système multi-constituants peut être déterminée. Il est alors possible d'observer les modifications structurelles (allongement des liaisons, variation d'angles, présence de

liaisons hydrogènes, etc.) lors de l'ajout d'une molécule (par exemple une molécule d'eau) sur les composés phénoliques. De ce fait, la force des interactions régissant ces systèmes ainsi que les caractéristiques des liaisons hydrogènes permettent d'évaluer l'affinité d'un composé pour un solvant. Les composés phénoliques ont déjà été étudiés par calcul quantique, mais à différents niveaux de théorie et en utilisant différentes bases. De plus, plusieurs auteurs sont en désaccord sur la structure de certains composés, ce qui complique la comparaison entre molécules phénoliques.

Par ailleurs, l'amélioration des procédés d'extraction et de purification nécessite également la connaissance des propriétés macroscopiques des systèmes clés {composés phénoliques + solvant}. Or, il demeure un grand manque de données dans la littérature. De ce fait, la mise en place d'un modèle thermodynamique suffisamment robuste pour prédire les diagrammes de phases de systèmes contenant des composés phénoliques n'est pas envisageable.

De plus, les contraintes environnementales imposées par la Communauté Européenne poussent les industriels à réduire leur consommation de solvants organiques toxiques ainsi que les déchets rejetés dans la nature. La recherche de nouveaux solvants performants et plus respectueux de l'environnement semble donc une priorité. L'utilisation de liquides ioniques à la place de solvant organique constitue une alternative prometteuse afin d'extraire les composés phénoliques des phases aqueuses. En effet, la faible volatilité des liquides ioniques permet la récupération des composés phénoliques par distillation et limite la consommation énergétique. Les composés ainsi récupérés ne présentent pas de trace résiduelle de solvant. De plus, de par leur grande stabilité chimique et thermique, ces « nouveaux solvants verts » sont recyclables.

Enfin, il est possible que ces composés possèdent des propriétés antioxydantes, comme la plupart des composés phénoliques, ce qui leur confère une certaine « valeur ajoutée » et permet leur application industrielle dans des domaines pharmaceutique, alimentaire, et cosmétique.

A travers cette démarche, l'objectif de cette thèse est d'améliorer les procédés d'extractions de composés phénoliques. L'étude microscopique des composés seuls et en présence de solvant sera effectuée par calcul quantique. A l'échelle macroscopique, les données de la littérature seront complétées pour les systèmes {eau + composés phénoliques}. La possibilité d'utiliser un liquide ionique (Choline bistrifluorométhylsulfonyle), sera étudiée tout d'abord sur des systèmes ternaires {eau + composé phénolique + liquide ionique}. L'influence de différents paramètres physico-chimiques (cinétique, température, ratio massiques) sera examinée avant

de réaliser l'extraction sur des bio-huiles réelles. Enfin, les propriétés antioxydantes des composés seront étudiées par des différents tests biochimiques.

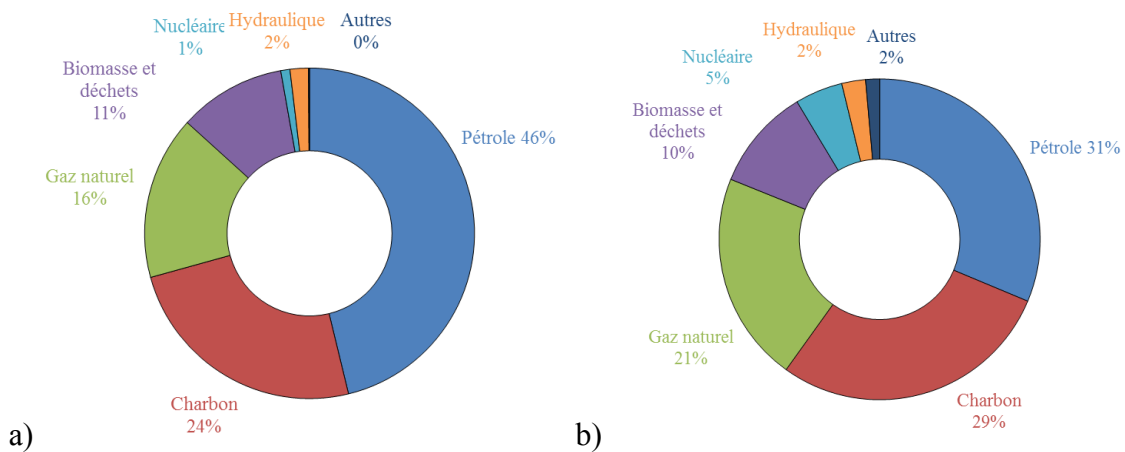


## Chapitre I : Etude bibliographique

### I-1. Contexte et enjeux environnementaux

Depuis quarante ans, l'industrialisation et l'urbanisation de plus en plus massive ont causé une augmentation considérable de la demande en énergie. En effet, depuis 1970, la production d'énergie a doublé (de 6,1 Gtep à 13,7 Gtep en 2014[1]) et son augmentation devrait continuer jusqu'à 18,5 Gtep en 2035. L'approvisionnement en énergie primaire est principalement issu des ressources géologiques (pétrole, charbon, gaz naturel et nucléaire) qui s'amenuisent au fil du temps. Si la dépendance au pétrole a diminué sur cette même période (de 46% à 31%), les ressources renouvelables (*i.e.* biomasse, nucléaire et hydraulique) peinent à émerger comme alternatives énergétiques (Figure I-1). En suivant ce rythme d'exploitation, les réserves existantes de pétrole ne permettraient de tenir qu'une quarantaine d'années [2].

**Figure I-1:** Ressources mondiales pour la production d'énergie primaire en 1973 a) et 2014 b) d'après l'Agence Internationale de l'Energie[1]



De plus, la consommation massive d'énergies fossiles a entraîné une augmentation de la production de gaz à effet de serre, passant de 15,5 Gt à 32,4 Gt de CO<sub>2</sub>, impactant directement le climat.

Enfin, l'ensemble du paysage mondial a fortement évolué. La difficulté d'accès à l'énergie pour les populations défavorisées et lors de perturbations politiques, militaires et économiques obligent à une réévaluation des impacts causés par l'industrie et à une transition énergétique, plus équitable et plus respectueuse de l'environnement.

Face à ces problématiques environnementales et humaines, les énergies bio-sourcées présentent un fort intérêt sociétal et économique. En effet, la biomasse ligno-cellulosique est une ressource répartie sur l'ensemble de notre planète ; elle émet peu de carbone en comparaison aux énergies fossiles sans être pour autant en compétition avec l'industrie agroalimentaire. Au sein des bioraffineries, la biomasse est utilisée comme une source de carbone permettant la production de biocarburant, d'énergie ou de divers composés chimiques.

Les différents constituants de la biomasse sont séparés selon leur finalité. Les sucres (cellulose, hémicellulose) et les huiles servent à la production de biocarburant ou de coproduits tels que des protéines, des acides aminés, des carbohydrates ou des acides organiques [3] alors que la lignine est considérée comme un composé à faible intérêt et est généralement brûlée afin de fournir l'énergie nécessaire au fonctionnement de la bioraffinerie. Cependant, la lignine constitue 30% du poids de la biomasse lignocellulosique et, chaque année, les bioraffineries produisent d'énormes quantités de lignine (près de 20 millions de tonnes par an). De ce fait, la lignine est la principale matière première renouvelable composée de motifs aromatiques (phénol, guaiacol, syringol, etc.). Tout comme la biomasse, la lignine peut être utilisée pour la production d'énergie, comme alternative à la production de carburant, ou de composés chimiques (fibres de carbones, polymères, BTX, phénols, quinones, polyaromatiques, etc. ) [4]. Ainsi, l'exploitation de la lignine doit être reconsidérée d'un point de vue sociétal et économique. En effet, elle pourrait devenir une source de matière première alternative au pétrole pour la production de certains composés possédant une forte valeur ajoutée (phénol, acides aromatiques, polyols aromatiques, quinones, etc.). Holladay et al [4] ont proposé six voies de valorisation potentielles permettant d'exploiter 225 millions de tonnes de lignine autrement que par la voie énergétique, et ainsi de réaliser une plus-value économique estimée entre 12 et 35 milliards de dollars. Certains procédés ont même dépassé l'échelle du laboratoire. En 2014, l'Union Européenne a finalisé un projet ayant pour objectif la production de molécules plateformes biosourcées à partir de glycérol et d'hydrolysats issus de biomasse. A ce jour, l'usine pilote mise au point dans le cadre de ce projet européen permet de traiter 50 kg de matière ligno-cellulosique sèche par heure [5].

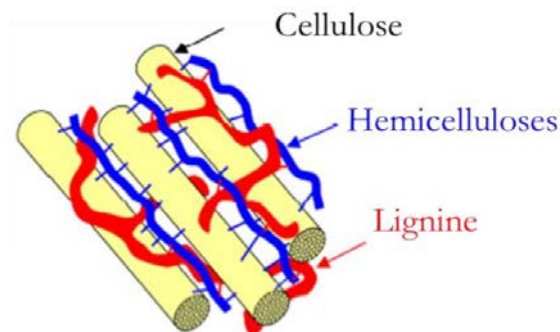
## I-2. La biomasse lignocellulosique

### I-2.1. Composition de la biomasse

La biomasse se définit d'après le code de l'énergie comme « la fraction biodégradable des produits, déchets et résidus provenant de l'agriculture, y compris les substances végétales et animales issues de la terre et de la mer, de la sylviculture et des industries connexes, ainsi que la fraction biodégradable des déchets industriels et ménagers ». [6] Dans le règne végétal, la biomasse correspond à la matière ligno-cellulosique présente dans les parois des cellules. Principalement composée de polysaccharides (40-60% cellulose (p/p) ; 10-30% d'hémicellulose (p/p)) et de lignine (20-25% p/p), sa structure et sa composition peuvent varier selon l'espèce végétale étudiée et ses conditions de croissance [7].

La cellulose constitue « le squelette » de la paroi cellulaire. Localisées à l'extérieur des fibres de cellulose, les hémicelluloses permettent la réticulation de la structure végétale, ce qui lui apporte une meilleure cohésion et lui confère sa structure. Enfin, la lignine rigidifie l'ensemble du système. (Figure I-2)

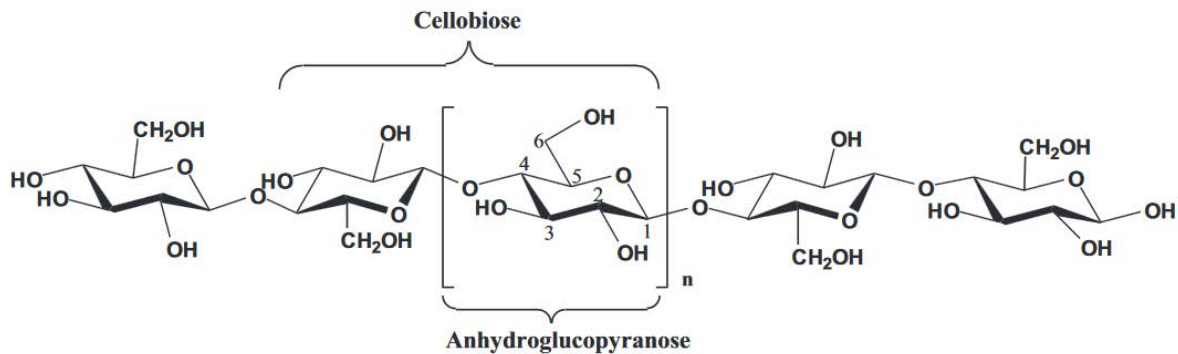
**Figure I-2 :** Schéma de l'organisation structurale au sein d'une cellule végétale [8,9]



*La cellulose* est le polysaccharide le plus abondant sur terre [10] avec une ressource totale estimée à 100 milliards de tonnes et une production annuelle de plus de 50 milliards de tonnes [11]. Principalement issue du bois (80% en masse), sa production sert à la fabrication du papier, à la synthèse d'additifs dans le domaine pharmaceutique [12], et plus récemment à la production de biocarburant [13]. Sa structure correspond à un homopolymère linéaire issu de la répétition du motif cellobiose, composé de deux unités de glucopyranose reliées par une liaison  $\beta$  1-4 (Figure I-3). La présence de groupements hydroxyles permet la formation de liaisons hydrogènes intra et intermoléculaires. Ainsi, les chaînes cellulosiques peuvent s'appareiller

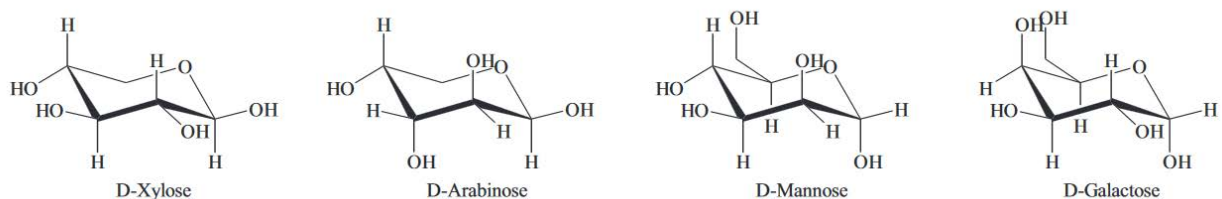
entre-elles afin de créer une structure fibreuse. Ces assemblages peuvent former, selon leur niveau d'organisation, des zones cristallines (organisation très structurée par de nombreuses liaisons hydrogènes) et des zones amorphes (forme peu structurée).

**Figure I-3:** Structure du motif cellobiose constitutif de la cellulose [14]



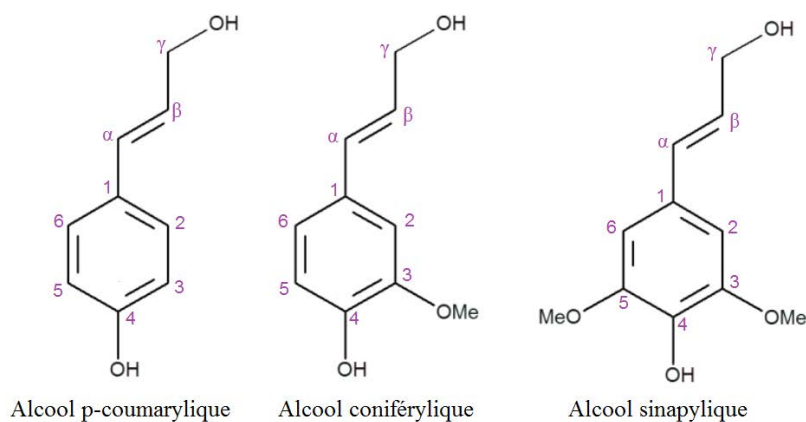
Les hémicelluloses constituent le second type de polysaccharides issus de la matière végétale. Contrairement à la cellulose, la structure des hémicelluloses comprend différents monosaccharides (Figure I-4) : des pentoses (arabinose, xylose, rhamnose) et des hexoses (mannose, galactose, acide manuronique, acide galacturonique). Les hémicelluloses formées peuvent être classées en quatre familles selon leur structure biochimique : les glucanes, les xylanes, les mannanes et les galactanes.

**Figure I-4:** Structure des monosaccharides issus des hémicelluloses [14]



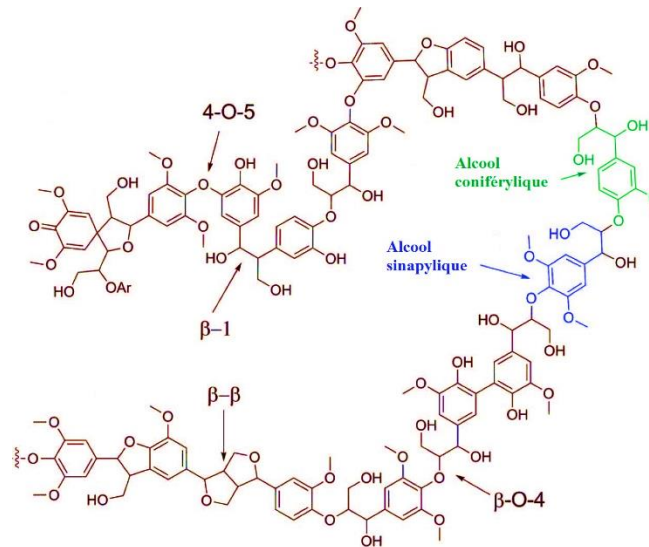
*La lignine* est un polymère amorphe issu de l'assemblage de groupements phénoliques.[15] Sa présence au sein d'une plante permet d'assurer la rigidité de sa structure tout en la protégeant contre les attaques biologiques extérieures.[16] Même si la structure exacte de la lignine ne peut être déterminée précisément, il est possible d'en faire une représentation schématique. En effet, la lignine est issue de la polymérisation de trois monolignols : l'alcool para-coumarylique (unité hydroxyphényl H), l'alcool coniférylique (unité guaiacyl G) et l'alcool sinapylique (unité syringyle S). Ces trois monolignols sont présentés Figure I-5 [17,18].

**Figure I-5 :** Structure des trois monolignols



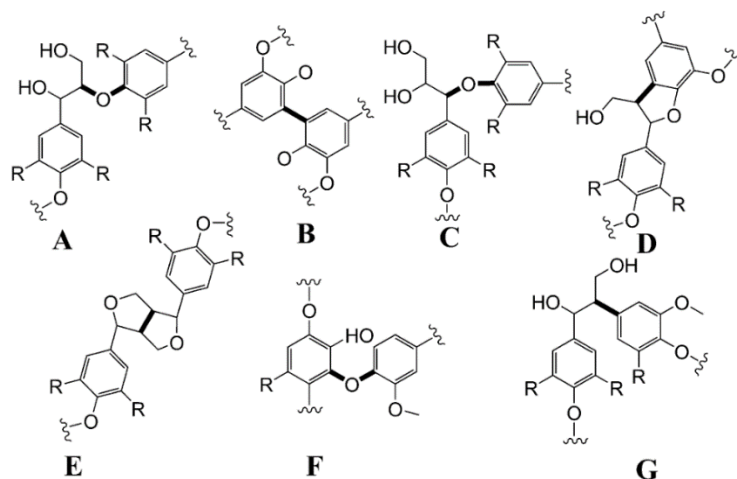
La quantité de lignine, sa composition et sa structure moléculaire dépendent de l'espèce végétale considérée. Ainsi, l'abondance de la lignine décroît selon l'ordre suivant : espèces résineuses (27-33%), feuillues (18-25%) puis graminées (17-24%) [4,19]. La lignine présente dans les espèces résineuses dérive principalement de l'alcool coniférylique et sera donc plus riche en unités G (90%). Inversement, les unités S seront plus abondantes dans les espèces feuillues (Figure I-6) et les unités H dans les espèces graminées.

**Figure I-6 :** Représentation schématique de la structure de la lignine issue d'une espèce feuillue [19]



Les unités H, G et S sont reliées entre-elles par différents types de liaisons :  $\beta$ -O-4,  $\alpha$ -O-4,  $\beta$ - $\beta$ ,  $\beta$ -5, 5-5, 4-O-5, and  $\beta$ -1. Parmi celles-ci, la liaison  $\beta$ -O-4 est la plus fréquente et correspond à plus de la moitié des liaisons au sein de la lignine [15]. (Figure I-7)

**Figure I-7 :** Principales liaisons au sein de la structure de la lignine : (A)  $\beta$ -O-4, (B) 5-5, (C)  $\alpha$ -O-4, (D)  $\beta$ -5, (E)  $\beta$ - $\beta$ , (F) 4-O-5, (G)  $\beta$ -1 [20]

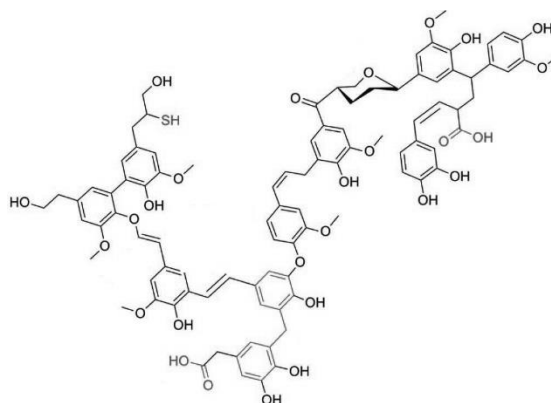


### I-2.2. Prétraitement de la lignine

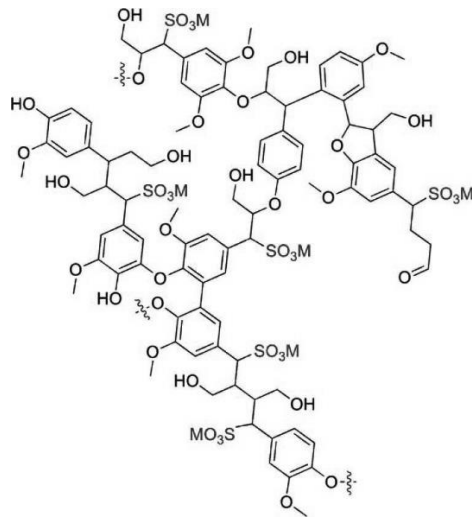
Afin de valoriser la lignine, un prétraitement est nécessaire pour séparer la lignine des autres composants de la biomasse ligno-cellulosique. Pour ce faire, différentes méthodes existent impliquant un traitement chimique, mécanique, biologique ou à l'aide de solvants.[21] Cependant, à l'instar de l'espèce végétale et de ses conditions de croissance, le prétraitement effectué a lui aussi une influence directe sur la structure de la lignine extraite. De ce fait, il existe différentes sortes de lignine, de qualité et de pureté variables.

*Le procédé Kraft* est la méthode la plus employée industriellement dans le monde, notamment dans l'industrie papetière. En effet, la majorité de la lignine produite est issue de ce procédé. La lignine obtenue (Figure I-8) est un liquide noir (également appelé « black liquor ») de poids moléculaire moyen compris entre 1000 et 3000 g.mol<sup>-1</sup> et contenant 1 à 1,5% de soufre en masse. Cependant, la mise en place du procédé kraft dépend de la fraction en lignine contenue dans le bois, sachant qu'une partie de celle-ci est brûlée comme carburant afin de produire l'énergie nécessaire au fonctionnement du procédé. Ainsi, la lignine « kraft » issue de ce même procédé ne peut pas être réellement considérée comme matière première pour la bioraffinerie.

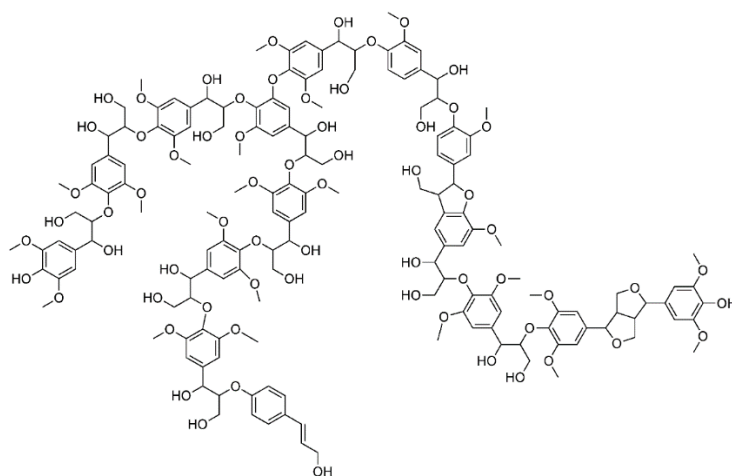
**Figure I-8:** Lignine Kraft[4,19,22]



*Le procédé lignosulfonate* est un autre procédé couramment utilisé en industrie papetière. La lignine ainsi obtenue (Figure I-9) a un poids moléculaire moyen supérieur à celui de la lignine Kraft (5000-20000 g.mol<sup>-1</sup>), et peut être utilisée pour la production de composés chimiques. Cependant, ce type de lignine est plus riche en soufre (entre 3 et 8% en masse), présent sous forme de groupes sulfonates.

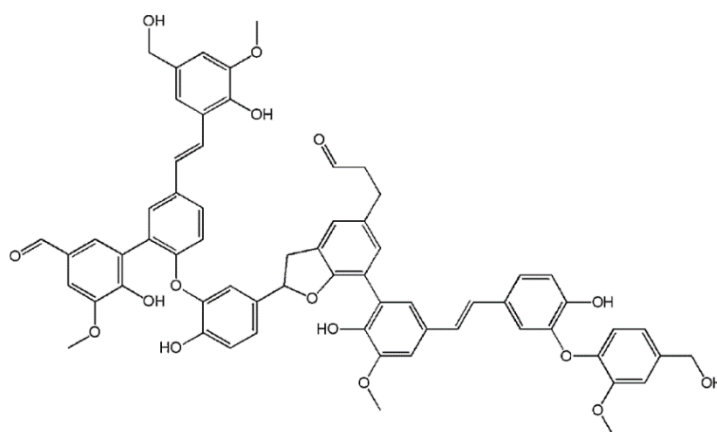
**Figure I-9 :** Lignine lignosulfonate [4,19,22]

*Le procédé organosolv* utilise des solvants organiques afin de produire une lignine de haute qualité et potentiellement valorisable.[4,19,23] Ce type de procédé permet de traiter la biomasse et d'en récupérer facilement ses composés (cellulose, hemicellulose et lignine) en trois flux différents. Cependant, son coût est élevé compte-tenu de utilisation des solvants organiques. La lignine « organosolv » est solide et libre de toute trace de soufre, avec un poids moléculaire inférieur à 5000 g.mol<sup>-1</sup> (Figure I-10). De plus, ce type de lignine est moins soluble dans l'eau que la lignine kraft ou la lignine lignosulfonate [4].

**Figure I-10 :** Lignine organosolv [24]

*Les procédés pyrolytiques* permettent la décomposition thermique de la biomasse en absence d'oxygène et sont utilisés pour produire une lignine sous forme de poudre sèche. Son poids moléculaire moyen est très faible par rapport aux autres lignines (650-1300 g.mol<sup>-1</sup>) du fait de sa dépolymérisation *via* le traitement thermique (723K [4]). Par ailleurs, cette lignine « pyrolytique » présente des différences structurales par la présence d'oligomères sous forme de C8 et non de C9, contrairement aux lignines obtenues par d'autres procédés de prétraitement de la biomasse (Figure I-11). Ainsi, l'utilisation de la lignine pyrolytique pourrait être la seule source de lignine envisageable pour l'obtention de molécules aromatiques.

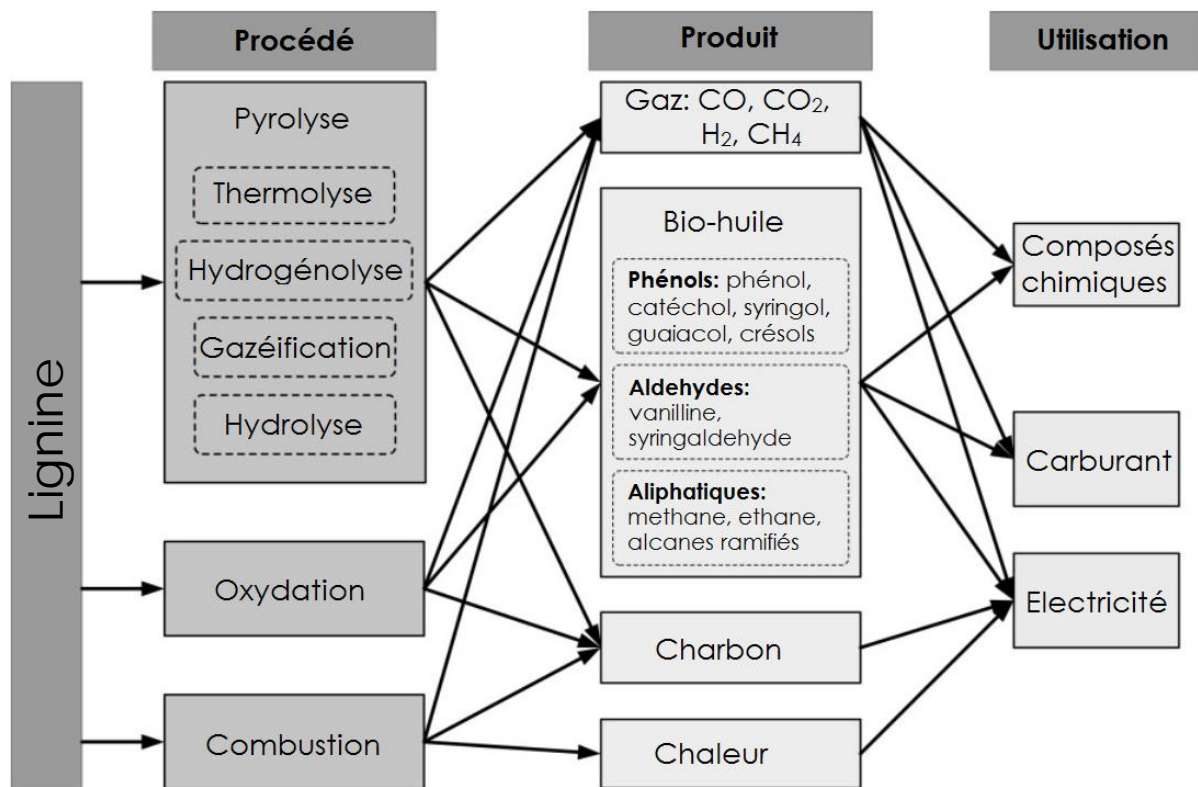
**Figure I-11** : Lignine pyrolytique



### I-2.3. Valorisation de la lignine

Les différents procédés de valorisation de la lignine, les produits formés et leurs utilisations potentielles sont représentés ci-après (Figure I-12). L'utilisation de la lignine peut être classée en trois catégories [4]. A court terme, la lignine pourrait être considérée comme une source de carbone pour fournir de l'énergie, comme gaz ou comme carburant. Dans ces conditions, la structure polymérique doit être dégradée dans des conditions drastiques. A moyen terme, la lignine pourrait être utilisée pour sa structure macromoléculaire (fibres de carbone, résines, polymères, etc.) [4] compte-tenu de son poids moléculaire élevé. Enfin, à long terme, la lignine pourrait produire certains composés aromatiques spécifiques (BTX, phénol, acides aromatiques, quinones, polyols aromatiques, etc.) [4] par sa déstructuration macromoléculaire tout en conservant ses blocs aromatiques.

**Figure I-12:** Procédés de valorisation de la lignine, produits obtenus et utilisations potentielles [20]



#### I-2.4. Production de bio-huile issue de la lignine

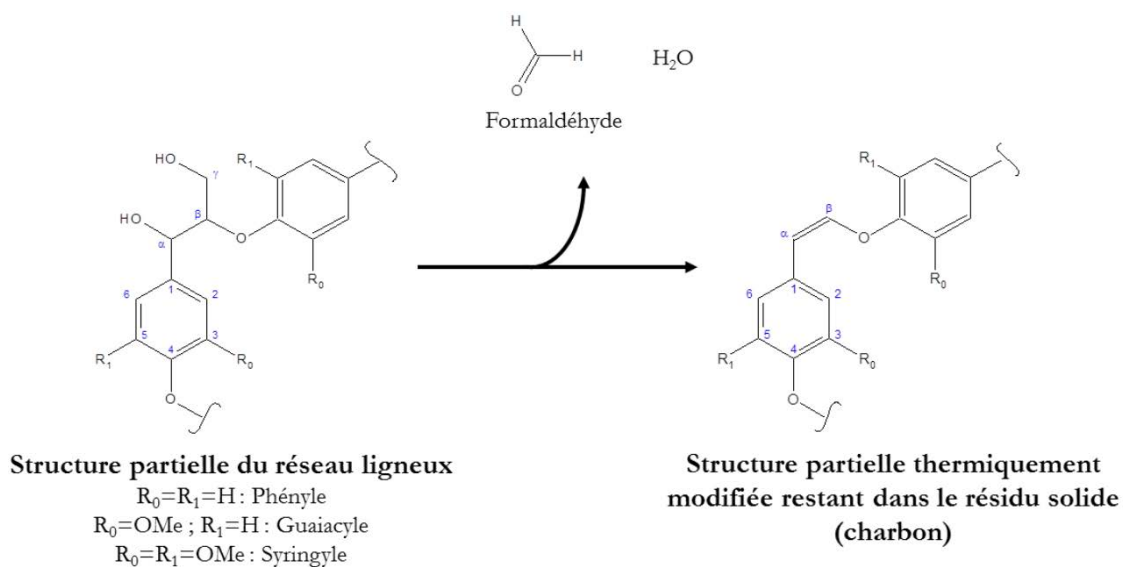
Le procédé de dépolymérisation de la lignine peut être effectué selon différentes conditions catalytiques référencées par Zakzeski et al [19] pour permettre son oxydation ou sa réduction. La production de composés phénoliques par hydrogénation ou hydrodeoxygénation catalytique a été résumée par Amen-Chen et al [25].

La *pyrolyse* de la lignine est un procédé de conversion thermique de la biomasse sous atmosphère inerte (absence de O<sub>2</sub>) conduisant à trois produits : du charbon sous forme solide (biochar), des gaz (CO<sub>2</sub>, CO, H<sub>2</sub>O, hydrocarbures) et une phase liquide appelée « bio-huile » ou « goudron » contenant de l'eau et de nombreux composés organiques. La composition et les rendements des différentes phases dépendent des conditions opératoires (*i.e.* température de réaction, rampe de température, matière première, additifs, etc.). On distingue deux types de pyrolyse : la pyrolyse lente qui favorise la production de charbon[26] et la pyrolyse rapide ou « flash pyrolysis » qui favorise la formation de bio-huile [27].

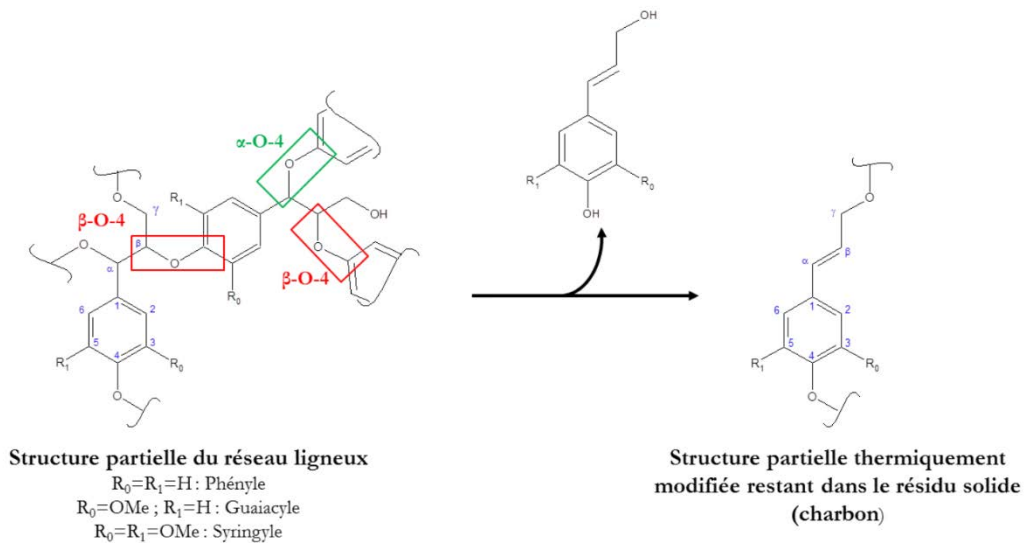
### I-2.5. Mécanismes réactionnels rencontrés lors de la pyrolyse

La dégradation de la lignine commence par la rupture des liaisons les plus faibles (liaisons C-O, liaisons carbonées) à basse température (120-300°C) qui conduit à la production d'acide formique, de formaldéhyde, de CO, de CO<sub>2</sub> et d'eau. La libération de molécules d'eau provient de la rupture des groupes fonctionnels OH liés aux carbones des chaînes aliphatiques. La production de formaldéhyde est due quant à elle à la rupture de la liaison carbonée β-γ (Figure I-13) [20,28]. Enfin, la dégradation des groupements carboxyliques et acétyles conduit à la formation d'acide formique et de CO<sub>2</sub> [28].

**Figure I-13** : Schéma de dégradation de la lignine par élimination et déshydratation [9]

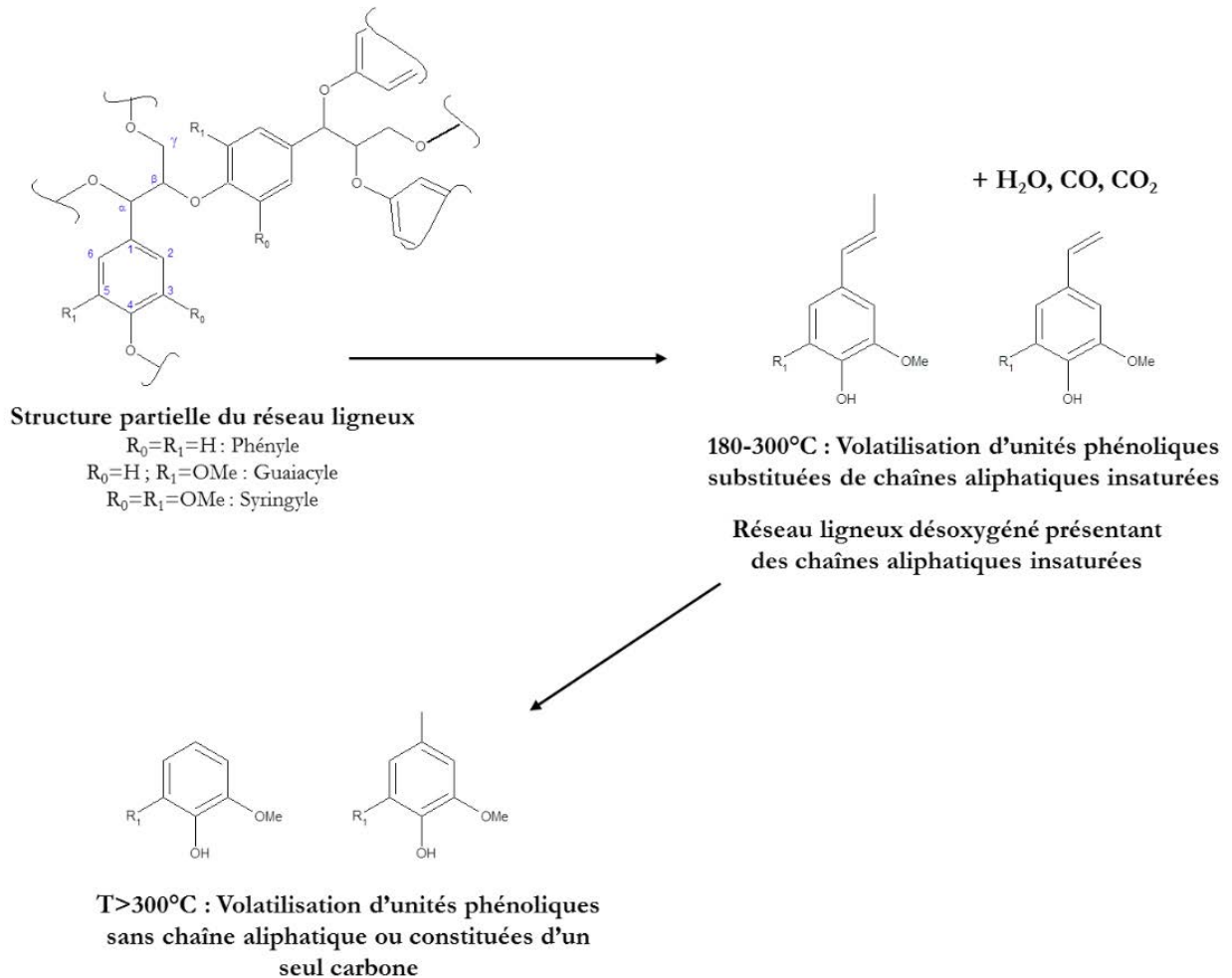


A cette température (120-300°C), le réseau polyphénolique est également détruit par la rupture des liaisons éthers ( $\alpha$ -O-4 et  $\beta$ -O-4), alors que les liaisons  $\gamma$ -O-4 sont plus résistantes thermiquement [20] (Figure I-14). Cependant, les températures spécifiques à la rupture de certaines liaisons et le rendement en un composé chimique donné dépendent du type de lignine. [29] Sa dépolymérisation provoque la libération d'unités phénoliques (phényle, guaiacyle ou syringyle), ainsi que de libération de plus petites molécules (CO, CO<sub>2</sub>, H<sub>2</sub>O) induite par un réarrangement du réseau ligneux [30,31].

**Figure I-14** : Schéma de rupture des liaisons éthers dans un réseau ligneux [9]

Les liaisons plus fortes se rompent à plus haute température. Ainsi, au-dessus de 300°C, la conversion des chaînes aliphatiques est totale [26] et provoque la volatilisation de monophénols (guaiacol, syringol) et de méthylphénols [32] (Figure I-15). Les groupements méthoxyles substitués sur les noyaux aromatiques deviennent réactifs vers 370°C [28] et engendrent la production de méthanol et de méthane respectivement par déméthoxylation et déméthylation. Enfin, au-delà de 500°C, les noyaux aromatiques craquent, libérant de l'hydrogène.

**Figure I-15** : Schéma de l'évolution de la décomposition thermique de la structure de la lignine en fonction de la température [9]



### I-2.6. Composition des bio-huiles

Les composés présents dans les bio-huiles sont majoritairement des monophénols, dérivés des trois monolignols à l'origine de la structure de la lignine, avec notamment une abondance de phénol, guaiacol et syringol ainsi que certains dérivés méthylés (crésols, 4-méthylguaiacol). Des composés oxydés (pyrocatechol, vanilline) sont également présents en forte concentration dans les bio-huiles, comme l'indique le Tableau I-1. Enfin, il est également possible de produire des composés aromatiques désoxygénés lors de pyrolyses catalytiques.

**Tableau I-1** : Composition de diverses bio-huiles en pourcentage massique

<b>Composition</b>	<b>Goudrons d'eucalyptus [33,34]</b>	<b>Huile de pyrolyse rapide d'épis de maïs[35]</b>	<b>Huile de lignine pyrolysée par micro-onde[36]</b>	<b>Huile de pyrolyse rapide de lignin EMAL (enzymatic mild acidolysis lignin) [37]</b>
Ethylbenzène	n.d.	n.d.	n.d.	8.64
p-xylène	n.d.	n.d.	n.d.	28.52
o-xylène	n.d.	n.d.	n.d.	9.35
Acide acétique	n.d.	n.d.	n.d.	2.17
4-methoxy-3-methylphénol	n.d.	n.d.	n.d.	0.23
Hydroxytoluène butylé	n.d.	n.d.	n.d.	0.17
Phénol	0.3	0.79	0.947	3.15
o-Crésol	0.1	0.17	0.883	n.d.
m-Crésol	0.2	0.17	n.d.	0.46
p-Crésol	0.1	0.19	1.115	3.14
2-éthylphenol	n.d.	n.d.	n.d.	0.18
4-éthylphenol	n.d.	n.d.	n.d.	3.24
2-ally-phénol	n.d.	n.d.	n.d.	0.36
2-allyl-4-methylphénol	n.d.	n.d.	n.d.	0.22
3-méthoxy-phénol	n.d.	n.d.	n.d.	0.23
Guaiacol	1	0.61	4.188	1.74
4-méthylguaiacol,	1.0	0.31	5.351	1.75
6-méthylguaiacol	n.d.	n.d.	0.530	n.d.
4-éthylguaiacol	n.d.	n.d.	2.637	0.95
3-allyguaiacol	n.d.	n.d.	0.408	n.d.

<b>Composition</b>	<b>Goudrons d'eucalyptus [33,34]</b>	<b>Huile de pyrolyse rapide d'épis de maïs[35]</b>	<b>Huile de lignine pyrolysée par micro-onde[36]</b>	<b>Huile de pyrolyse rapide de lignin EMAL (enzymatic mild acidolysis lignin) [37]</b>
4-vinyl-guaiacol	n.d.	n.d.	n.d.	1.87
4-propylguaiacol	n.d.	n.d.	0.301	n.d.
4-propenylguaiacol	n.d.	n.d.	0.833	n.d.
4-acétylguaiacol	n.d.	n.d.	0.559	n.d.
Syringol	2.5	0.63	n.d.	5.20
Pyrocatéchol	1.3	n.d.	n.d.	n.d.
3-méthylcatéchol	n.d.	n.d.	0.985	n.d.
4-méthylcatéchol	n.d.	n.d.	2.236	n.d.
4-éthylcatéchol	n.d.	n.d.	0.423	n.d.
2,6-diméthylphénol	n.d.	n.d.	n.d.	0.32
2,5-diméthylphénol	<0.05	n.d.	n.d.	n.d.
2,4-diméthylphénol	n.d.	0.05	0.456	1.0
2,3-diméthylphénol	n.d.	n.d.	1.243	n.d.
3,5diméthylphénol	n.d.	0.02	n.d.	n.d.
4-éthylphénol	n.d.	0.54	0.225	n.d.
3-éthylphénol	n.d.	0.02	n.d.	n.d.
2-éthylphénol	n.d.	0.01	n.d.	n.d.
2,5-diéthylphénol	n.d.	n.d.	n.d.	0.22
3-méthyl-4-éthylphénol	n.d.	n.d.	2.132	n.d.
Isoeugénol	n.d.	0.28	n.d.	n.d.
Vanilline	n.d.	n.d.	n.d.	1.85
2,3,5-triméthyl-1,4-benzènediol	n.d.	n.d.	n.d.	0.26
2,4,6-triméthyl-phénol	n.d.	n.d.	n.d.	0.27

<b>Composition</b>	<b>Goudrons d'eucalyptus [33,34]</b>	<b>Huile de pyrolyse rapide d'épis de maïs[35]</b>	<b>Huile de lignine pyrolysée par micro-onde[36]</b>	<b>Huile de pyrolyse rapide de lignin EMAL (enzymatic mild acidolysis lignin) [37]</b>
3-méthyl-5-(1-méthyléthyl)-phénol	n.d.	n.d.	n.d.	0.12
2éthyl-5-méthyl-phénol	n.d.	n.d.	n.d.	0.19
1-éthyl-4-méthoxy-benzène	n.d.	n.d.	n.d.	0.96
2-(1-méthyléthyl)phénol	n.d.	n.d.	n.d.	0.25
(E)-2-méthoxy-4-(1-propenyl)-phénol	n.d.	n.d.	n.d.	0.18
Acide 3-Hydroxy-4-méthoxybenzoïque	n.d.	n.d.	n.d.	4.82
2,3-Dihydro-benzofurane	n.d.	n.d.	n.d.	6.47
5-Tert-butylpyrogallol	n.d.	n.d.	n.d.	1.43
Acide 4-Hydroxy-3,5-diméthoxy-benzoïque	n.d.	n.d.	n.d.	1.26
3,4-Dihydro-2H-1-benzopyrane	n.d.	n.d.	n.d.	0.41
4-(2-Propényl)-phénol	n.d.	n.d.	n.d.	1.27
Acide 4-Hydroxy-3-méthoxy-benzoïque	n.d.	n.d.	n.d.	0.81
1-(4-Hydroxy-3-méthoxyphényl)-éthanone	n.d.	n.d.	n.d.	0.66
1-(4-Hydroxy-3-méthoxyphényl)-2-propanone	n.d.	n.d.	n.d.	0.71
2,6-Diméthoxy-4-(2-propenyl)-phénol	n.d.	n.d.	n.d.	3.36

n.d. : non déterminé

### **I-3. Extraction de composés à forte valeur ajoutée présents dans une bio-huile**

#### **I-3.1. Procédés d'extraction**

Les composés d'intérêt contenus dans une bio-huile sont séparés à l'aide de procédés utilisant la distillation[38–46] et/ou l'extraction par solvant [34,47–55]. D'autres méthodes telles que l'adsorption[53,55–59], la filtration sur membrane[60] ou encore l'extraction par le CO<sub>2</sub> supercritique [89-90] existent mais sont beaucoup moins utilisées. Le Tableau I-2 présente une synthèse non-exhaustive des procédés utilisés.

La distillation a été particulièrement étudiée comme technique de purification de bio-huiles[38–46]. Cependant, cette technique est difficile à appliquer compte-tenu des propriétés physico-chimiques intrinsèques des bio-huiles telles que leur instabilité thermique et leur composition complexe.[61] En effet, lors de la distillation des bio-huiles, des réactions entre les divers composés du mélange ont pu être observées [45,54] ainsi que de faibles sélectivités et efficacités [34,42,44,55].

Le dioxyde de carbone supercritique permet le fractionnement des bio-huiles mais les conditions expérimentales employées sont particulièrement drastiques. Feng et Meier[62] ont démontré que la pression avait un impact important sur la qualité de l'extraction par CO<sub>2</sub> supercritique. En effet, une augmentation de pression (de 15 à 25 MPa) augmente le rendement, mais diminue la sélectivité. De plus, l'extraction par CO<sub>2</sub> supercritique favorise l'enrichissement des molécules de faible poids moléculaire. Les composés aromatiques sont donc extractibles, à l'exception de certains tels que la vanilline, l'acétosyringone ou encore la propiosyringone qui demeurent dans le résidu. L'utilisation de la chromatographie liquide pourrait être une alternative, mais la consommation importante de solvant et la nécessité de régénérer la colonne rend cette technique peu compétitive économiquement [63].

**Tableau I-2 :** Extraction des composés à forte valeur ajoutée présent dans une bio-huile produite par conversion thermochimique de la biomasse

<b>Bio-huiles</b>	<b>Méthode d'extraction</b>	<b>Molécules cibles</b>	<b>Réf</b>
Huile issue de lignine hydrogénolytique	Distillation	Phénols monomériques	[38]
Goudrons de bois	Distillation flash	Phénols	[39]
Huile issue de pyrolyse sous vide	Distillation à pression réduite (0.7 kPa)	Syringol	[40]
Huile pyrolytique à partir de maïs	Distillation fractionnée (atmosphère, pression réduite et sous vide)	Composés aromatiques et oxygénés, phénols	[41]
Huile de pyrolyse rapide	Distillation moléculaire	3 fractions : composés légers, moyens et lourds	[42]
Huile de sciure	Distillation moléculaire	3 fractions : composés légers, moyens et lourds	[42]
Bio-huile brute	Distillation moléculaire	Cétones et acides carboxyliques	[43]
Huile de pin	Distillation moléculaire	Acides carboxyliques	[44]
Huile de pyrolyse rapide	Distillation atmosphérique	/	[45]
Hydrolyse acide de biomasse lignocellulosique dans un milieu biphasique (THF/H <sub>2</sub> O + NaCl)	Distillation en présence de solvant THF/H <sub>2</sub> O	Acide lévulinique, furfural, acide formique	[46]

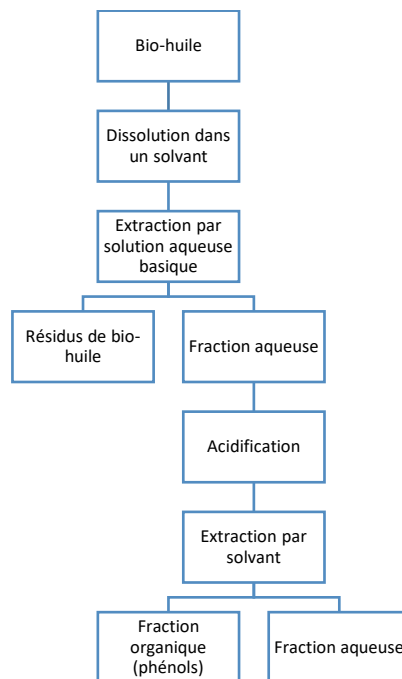
**Tableau I-2 : suite**

Huile de pyrolyse de bois	Extraction liquide-liquide par solution aqueuse alcaline	Phénols	[47–49]
Bio-huiles	Extraction liquide-liquide	Familles de molécules (aromatiques, phénols, acides, alcools, furfural)	[50]
Huile de pyrolyse du bois	Extraction alcaline aqueuse suivie par une acidification de la phase aqueuse et extraction par solvant organique	Phénols	[51]
Goudron de carbonisation	Distillation flash sous vide, puis extraction alcaline aqueuse suivie par une acidification de la phase aqueuse et extraction par solvant organique	Phénol, cresols, guaiacol, 4-methylguaiacol, syringol, pyrocatechol	[34]
Bio-pétrole directement deoxyliquéfié	Distillation sous vide puis extraction aqueuse basique, extraction acide et récupération avec dichlorométhane	Phénol, crésols, guaiacol, 4-méthylguaiacol, syringol	[52]
Huile d'hydrolyse rapide	Extraction par solvant		[53]
Huile d'hydrolyse rapide	Extraction aqueuse Solvant hydrophobe polaire/antisolvant	Composés phénoliques	[54]
Huile d'hydrolyse rapide	Séries d'extractions liquide-liquide	Fraction phénolique	[64]

**Tableau I-2 : suite**

Liquéfaction d'huile de lignine	Extraction liquide-liquide distillation sous vide  chromatographie liquide  cristallisation	Monomères de lignine	[55]
Huile d'hydrolyse rapide	Extraction en phase solide C18	/	[53]
Huile d'hydrolyse rapide	Extraction en phase solide HLB	/	[53]
Fraction d'huile de pyrolyse lente	Chromatographie sur colonne de silice	Fraction	[56]
Huile de pyrolyse sous vide	Chromatographie sur colonne de silice	Fraction	[57]
Huile de pyrolyse	Chromatographie sur colonne de silice	Fraction	[58]
Bio-huiles	Chromatographie sur colonne de silice avec fractionnement par solvant	Fraction	[59]
Bio-huile d'hydrolyse rapide	Nanofiltration et osmose inverse	Acides organiques	[60]

L'extraction liquide-liquide reste le procédé le plus utilisé pour l'extraction de composés présents au sein d'une bio-huile [34,50,52,54,55]. Généralement, le procédé est constitué de plusieurs étapes d'extraction liquide-liquide utilisant un milieu aqueux puis un milieu organique [40]. A titre d'exemple, un schéma du procédé d'extraction est présenté Figure I-16. La première étape du procédé consiste à extraire les composés phénoliques de la bio-huile à l'aide d'une solution aqueuse basique. Dans cette opération, le pH de la solution aqueuse est un paramètre influent sur l'efficacité du procédé (nombre de lavages requis, rendement, etc.) [65].

**Figure I-16** : Extraction liquide-liquide de phénols d'une bio-huile [34]

Ensuite, les composés sont extraits de la phase aqueuse en utilisant des solvants organiques tels que l'acétate d'éthyle [34], le méthylisobutylcétone MIBK [34,65], le dichlorométhane [66,67], le toluène [68], le diéthyl éther [51,69] ou encore le diisopropyl éther [65]. Les composés phénoliques sont ensuite récupérés par distillation.

Cependant, l'extraction liquide-liquide requiert une grande quantité de solvant ainsi que du matériel spécifique. En effet, certains auteurs ont remarqué une corrosion de métaux (aluminium, cuivre, acier) par les bio-huiles [70]. De plus, la miscibilité des solvants avec l'eau (solubilité de l'éthyl acétate dans l'eau : 90g/L à 20°C) fait que l'étape de distillation pour la récupération des composés est fortement énergivore.

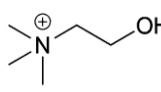
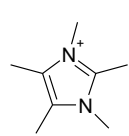
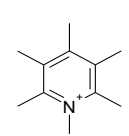
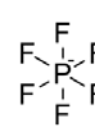
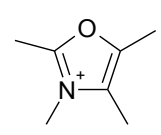
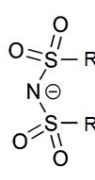
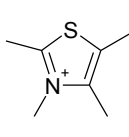
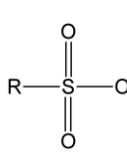
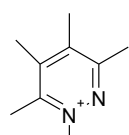
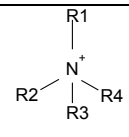
Aussi, la recherche de solvants innovants moins toxiques, plus stables et plus performants pourrait ouvrir de nouvelles perspectives pour l'extraction et la purification de ces composés cibles. Hou et al [71] ont démontré que les liquides ioniques constitués d'un cation de type dialkylimidasolium sont particulièrement efficaces pour l'extraction de phénol d'une bio-huile avec un taux d'extraction de 90%. Garron et al ont également montré que certains liquides ioniques hydrophobes (anion bis(trifluorométhylsulfonylimide) sont efficaces pour l'extraction du guaiacol d'une solution aqueuse [72].

### I-3.2. Vers de nouveaux milieux extractifs : les liquides ioniques

Les liquides ioniques sont des sels liquides dont la température de fusion est inférieure à 100°C. Ils sont liquides sur une large gamme de température (de la température ambiante jusqu'à 250°C), et très stables thermiquement [73] et chimiquement. Ils sont également non-inflammables et possèdent une forte capacité de solubilisation des composés. Leurs propriétés physico-chimiques peuvent être modifiées à souhait en jouant sur le choix de l'anion et du cation. Les liquides ioniques apparaissent depuis quelques années comme une alternative très prometteuse aux solvants organiques traditionnels. En effet, l'une de leurs propriétés les plus intéressantes est leur tension de vapeur négligeable permettant une récupération aisée des produits finaux par distillation, sans dégradation ni perte du solvant par évaporation et, par voie de conséquence, un taux de recyclage élevé du solvant. De ce fait, l'emploi des liquides ioniques contribue à la diminution des pollutions atmosphériques et des quantités d'effluents à traiter. Les ions les plus utilisés dans la synthèse de liquides ioniques sont présentés dans le Tableau I-4.

L'intérêt des liquides ioniques dans le domaine de la biomasse devient de plus en plus prononcé. En 2002, Rogers et al [74] furent les premiers à utiliser des liquides ioniques pour la dissolution de la cellulose. Depuis, de nombreux auteurs se sont penchés sur cette problématique [19]. La dissolution de la cellulose dans les liquides ioniques dépend de sa nature (degré de polymérisation, cristallinité et teneur en eau), des conditions opératoires (température, temps de séjour, fraction massique et activation par micro-ondes [75]) ainsi que de la structure du liquide ionique (choix du cation et de l'anion). Les liquides ioniques constitués d'anions tétrafluoroborate  $\text{BF}_4^-$ , hexafluorophosphate  $\text{PF}_6^-$ , bis(trifluorométhylsulfonyl)imide  $\text{NTf}_2^-$  et de dicyanamide  $\text{N}(\text{CN})_2^-$  ne permettent pas de dissoudre la cellulose [76]. Le liquide ionique le plus étudié pour la dissolution des sucres et de la cellulose est le 1-butyl-3-méthylimidazolium chlorure  $\text{BMIMCl}$  [74,77]. Cependant, sa viscosité et son point de fusion élevés réduisent considérablement ses applications. Les liquides ioniques performants dans le domaine de l'extraction de la cellulose sont des solvants ayant un caractère basique et constitués d'anions acétate, formate, phosphate ou phosphonate [78]. Concernant le cation, la présence de protons acides sur les noyaux hétérocycliques augmente fortement les interactions avec les groupements hydroxyles et éthers de la cellulose, et favorise donc sa solubilité [79].

**Tableau I-3** : Cations et anions présents dans la structure des liquides ioniques

Cations	Formule	Anions	Formule
Choline		Chloride Cl <sup>-</sup>	Cl <sup>-</sup>
Imidazolium		Tetrafluoroborate BF <sub>4</sub> <sup>-</sup>	
Pyridinium		Hexafluorophosphate PF <sub>6</sub> <sup>-</sup>	
Oxazolium		Imide : N- (SO <sub>2</sub> R) <sub>2</sub>	
Thiazolium		Sulfonate : O-(SO <sub>2</sub> R)	
Pyridazinium			
Tetraalkylammonium			

La dissolution de la lignine dans les liquides ioniques a été également étudiée [10,80–82]. Entre autres, Ragauskas et al ont montré que la solubilité de la lignine augmente avec la nature de l'anion selon : PF<sub>6</sub><sup>-</sup> << Br<sup>-</sup> < Cl<sup>-</sup> < MeSO<sub>4</sub><sup>-</sup> [10]. Par ailleurs, les liquides ioniques 1-hexyl-3-methylimidazolium trifluoromethanesulfonate [himm][CF<sub>3</sub>SO<sub>3</sub>], 1,3-dimethylimidazolium methylsulfate [mmim] [MeSO<sub>4</sub>] et 1-butyl-3-methylimidazolium methylsulfate [bmim][MeSO<sub>4</sub>] sont également efficaces pour la dissolution de la lignine [80]. De plus, Tan et al ont réussi à extraire de la lignine à partir de bagasse en utilisant un mélange de liquides

ioniques composés de 1-éthyl-3-méthylimidazolium comme cation et d'alkylbenzène sulfonates (principalement des xylènesulfonates) comme anions [81]. Xin et al ont également montré l'efficacité du THF pour l'extraction de la lignine dissoute dans un mélange de 1-éthyl-3-méthylimidazolium acétate et d'eau [82].

### **I-3.3. Etude microscopique et macroscopique des systèmes clés rencontrés dans le procédé d'extraction**

Une bonne connaissance des systèmes clés au niveau microscopique et macroscopique est essentielle afin de pouvoir apporter des modifications à un procédé. En effet, l'étude microscopique, effectuée par calcul quantique, permet de mieux comprendre les interactions entre soluté et solvant et donc d'orienter le choix sur les solvants extractifs. D'un point de vue macroscopique, les données expérimentales d'équilibre entre phases des systèmes sont d'une grande utilité pour la mise en place de modèles thermodynamiques robustes.

#### **I-3.3.1. Le calcul quantique**

Le calcul quantique est une méthode de calcul numérique basée sur les principes de chimie quantique qui permet la détermination de nombreuses propriétés de molécules, telles que la longueur des liaisons, l'énergie d'une structure, les structures les plus stables et les états de transition d'une molécule dans son état fondamental ou encore les spectres infra-rouge. Le calcul quantique s'inscrit également dans une étape de modélisation multi-échelle, par exemple afin de comprendre et de développer au mieux les techniques de conversion de la biomasse [83].

Le calcul de la structure électronique d'un système étudié dépend du niveau de théorie (méthode d'approximation des fonctions d'ondes) ainsi que de la base choisie (représentation des fonctions d'ondes). Appliqué à un système binaire, il permet la détermination des interactions entre les molécules (*i.e.* soluté et solvant) et permet d'évaluer leur affinité. En effet, la présence de liaisons hydrogènes intra ou intermoléculaires peut influencer la solubilité d'un composé dans un solvant. Il est donc important de connaître les interactions qui régissent ce système afin de prédire si le solvant pourra être utilisé comme milieu extractif et donc choisir au mieux le solvant adapté.

De nombreux auteurs se sont intéressés aux structures des molécules issues de la biomasse telle que la structure cristalline de la cellulose [84] et/ou son interaction avec l'eau [85]. De même, Hassan et al [86] ont étudié les interactions entre carbohydrates (glucose et cellobiose) et les liquides ioniques (1,3-diméthylimidazolium méthyl phosphonate DMIMMPh, 1-butyl-3-méthylimidazolium chloride BMIMCl, 1-éthanol-3-méthylimidazolium chloride EtOHMIMCl et 1-éthyl-3-méthylimidazolium thiocyanate EMIMSCN). Ils ont montré que les liquides ioniques basiques tels que le DMIMMPh sont efficaces pour la dissolution de la cellulose. Les interactions entre la lignocellulose et les liquides ioniques ont été modélisées par Janesko [87] en utilisant le (1,4)-diméthoxy- $\beta$ -D-glucopyranose et le 1-(4-méthoxyphényl)-2-méthoxyéthanol comme molécules modèles pour la cellulose et la lignine. Parmi les liquides ioniques étudiés, la cellulose interagit le plus fortement avec les anions Cl<sup>-</sup>, mais la lignine présente également de fortes liaisons hydrogène avec les cations imidazolium, démontrant ainsi l'influence du cation sur la solubilité de la biomasse lignocellulosique.

Les composés phénoliques ont été principalement étudiés dans leur état isolé [88–112]. Les études structurales (énergies, longueurs des liaisons et des angles, etc.) effectuées à différents niveaux de théorie et en utilisant différentes bases conduisent à des désaccords concernant la conformation la plus stable de composés [97–99]. Certains de ces composés ont également été étudiés en présence d'une ou de plusieurs molécules d'eau [88,90,103,105,113–119,119–127], mais aucune étude n'a été effectuée sur le m-crésol, le p-crésol, le syringol ou encore la vanilline dans ces conditions.

### **I-3.3.2. Etude bibliographique des systèmes clés du procédé d'extraction**

La mise en place d'un modèle thermodynamique robuste nécessite une base de données expérimentales riche et fiable. L'intérêt de ces données est double : d'une part, elles servent à optimiser les paramètres du modèle et d'autre part à tester sa capacité prédictive.

Les systèmes clés du procédé d'extraction (*cf.* Figure I-16) sont les systèmes rencontrés lors des deux extractions liquide-liquide c'est à dire les systèmes binaires {eau + composés phénoliques} et les systèmes ternaires {eau + composés phénoliques + liquide ionique}.

Une étude bibliographique des systèmes {eau + composés phénoliques} a permis de collecter les données des équilibres liquide-liquide (ELL) et liquide-solide (ELS) des systèmes binaires (Tableau I-4). La base de données recueillie, représente un ensemble de huit systèmes binaires {Eau + Phénol}, {Eau + Pyrocatecol}, {Eau + Vanilline}, {Eau + o-Crésol}, {Eau + m-Crésol},

{Eau + p-Crésol}, {Eau + Guaiacol}. Concernant les systèmes ternaires, les travaux se focalisent surtout sur les conditions d'extractions.[128–130] Seuls, Schuur et al [131] ont étudié le diagramme ternaire du système {tétradécyltrihexylphosphonium dicyanamide  $P_{66,14}[N(CN)_2]$  + eau + guaiacol}.

En examinant le Tableau I-4, nous constatons que le nombre de points expérimentaux est relativement faible dans les domaines de températures et de pressions modérées. Certains composés comme le phénol [132–135] ont été extrêmement étudiés, mais d'autres, tels que le guaiacol ou le syringol pourtant majoritairement présents dans les bio-huiles, ne présentent que peu ou pas de travaux les concernant [136,137]. De ce fait, ces données ne permettent pas la régression de paramètres thermodynamiques suffisamment robustes, pourtant nécessaire pour le dimensionnement et la simulation de procédés. Il est donc essentiel de poursuivre les études expérimentales pour améliorer la qualité des modèles thermodynamiques.

**Tableau I-4:** Rang de températures et méthodes de mesure pour les systèmes {eau-composés phénoliques} issus de la littérature.

<b>Système binaire</b>	<b>Température</b>	<b>Nombre de points</b>	<b>Méthode</b>	<b>Référence</b>
Eau + Phénol	[280-345K]	3 ; 15	Conductivité	[132,133]
	[274-338K]	40	Réfractométrie	[134]
	[293-339K]	16	Volumétrie	[135]
Eau + Pyrocatechol	[314-377K]	5	Méthode visuelle	[138]
	[295-326K]	20	/	[139]
Eau + Vanilline	[273-323K]	11	Méthode visuelle	[140]
	[273-303K]	3	Méthode visuelle	[141]
	[293-318K]	6	“Shake flask” méthode	[142]
Eau + o-Crésol	[298-435K]	18	Méthode visuelle	[143]
	298K	1	“Shake flask” méthode	[144]
	293K	1	Turbidité	[145]
	288;298K	2	/	[146]
	[298-363K]	6	Turbidité	[147]
Eau + m-Crésol	[273-420K]	20	Méthode visuelle	[143]
	298K	1	“Shake flask” méthode	[144]
	293K	1	Turbidité	[145]

	[288;298K]	2	/	[146]
	[293-371K]	5	Chromatographie	[148]
	[298-333K]	6	Turbidité	[147]
Eau + p-Crésol	[290-416K]	19	Méthode visuelle	[143]
	298K	1	“Shake flask” méthode	[144]
	293K	1	Turbidité	[145]
	[298-323K]	5	Turbidité	[147]
Eau + Guaiacol	298K	1	“Shake flask” méthode	[136]
	298K	1	Densitométrie	[137]

#### I-4. Valorisation des composés phénoliques

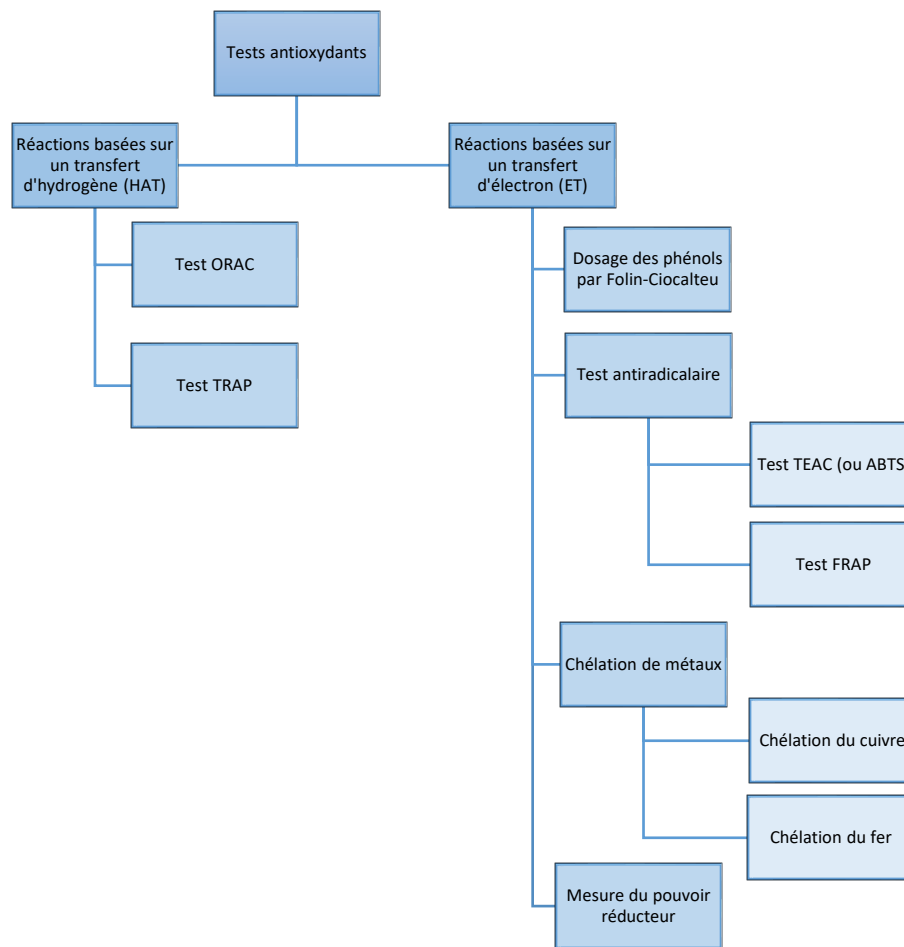
Les composés phénoliques présentent généralement des propriétés antioxydantes [149–153]. Ces molécules ont donc une forte valeur ajoutée et peuvent être utilisées industriellement dans différents domaines (Tableau I-5).

**Tableau I-5:** Domaines d'utilisation des composés phénoliques présents dans les bio-huiles

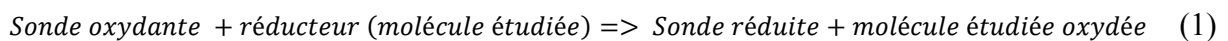
Composés	Utilisation	Ref
Phénol	Synthèse de résines, teintures, pigments, antioxydants	[4]
Guaiacol	Arôme, fragrance, goût synthétique, composé pharmaceutique	[154,155]
Syringol	Arôme alimentaire, composé pharmaceutique	[155,156]
Pyrocatechol	Antiseptique, révélateur photographique, teinture, encre, antioxydant, électroplaquage	[154]
Crésols	Synthèse d'herbicides, résines,	[157,158]
Vanilline	Arôme, synthèse de composé pharmaceutique	[159,160]

Les composés « antioxydants » sont définis comme des molécules capables de retarder, d'inhiber ou encore de prévenir l'oxydation de composés par des radicaux libres et de diminuer le stress oxydant. Ce dernier correspond à une quantité excessive d'oxygène et/ou d'azote provoquant l'oxydation de biomolécules (enzymes, protéines, ADN ou lipides) et entraînant des maladies dégénératives telles que le cancer, les maladies cardio-vasculaires ou encore le vieillissement [161].

La propriété « antioxydante » est un terme générique qui regroupe plusieurs mécanismes chimiques basés soit sur un transfert d'électrons (ET-based reactions), soit sur un transfert d'atome d'hydrogène (HAT-based reactions) [162]. Les tests antioxydants les plus souvent utilisés dans la littérature sont répertoriés dans la Figure I-17.

**Figure I-17** : Classification des tests antioxydants d'après Huang et al [162]

La plupart des tests HAT implique des réactions cinétiques en compétition et les propriétés antioxydantes sont quantifiées par rapport aux courbes de cinétique. Les tests ET sont basées sur une seule réaction chimique (Equation 1), où la sonde est une molécule oxydante qui, en présence d'une molécule antioxydante, change de couleur au cours de la réaction de réduction.



Ainsi, une étude spectroscopique permet de quantifier la propriété antioxydante étudiée. L'utilisation d'une molécule de référence permet une comparaison entre molécules étudiées. Cependant, il est nécessaire de toujours préciser les conditions opératoires dans lesquelles les tests ont été effectués. En effet, la plupart des tests publiés dans la littérature ont souvent été adaptés à un certain milieu réactionnel qui peut altérer les propriétés des molécules et engendrer des différences au niveau des résultats.

Du fait de la présence d'un groupement hydroxyle, les composés phénoliques sont capables de donner un atome d'hydrogène ou un électron à un radical libre. De plus, la délocalisation des charges sur leur noyau aromatique induit plusieurs formes de résonances qui stabilisent la forme radicalaire et ralentit les réactions en chaîne [163].

Certains composés phénoliques possédants deux groupements hydroxyles sont également capables de conjuguer des ions métalliques tels que le cuivre ou le fer. Cette capacité est particulièrement intéressante pour la prévention de la réaction de Fenton qui provoque la formation de radicaux libres  $\text{OH}\cdot$  à partir de peroxyde d'hydrogène ( $\text{H}_2\text{O}_2$ ) *via* une réaction d'oxydoréduction du fer ou du cuivre :



La présence de groupements catécholates ou gallates peut former des complexes avec ces métaux de transition par coordination ou *via* des interactions plus faibles [164,165].

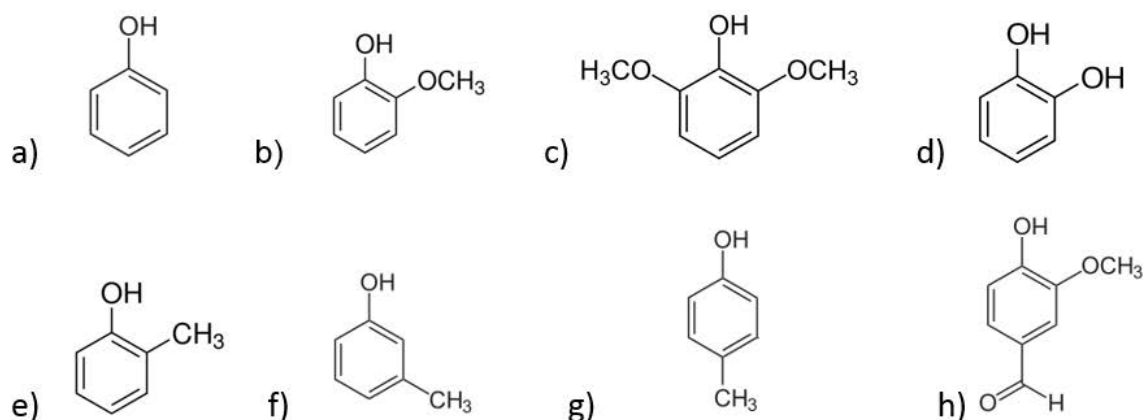
Les bio-huiles issues de la pyrolyse de la biomasse contiennent de nombreux composés phénoliques aux propriétés antioxydantes potentielles. Cependant, la composition complexe et la diversité des composés présents dans les bio-huiles font que la détermination des propriétés de chaque composé est très difficile. Ainsi, certains tests ont été créés afin de permettre la quantification d'une « efficacité antioxydante » pour des mélanges de composés. C'est le cas des tests TEAC (Trolox Equivalent Antioxidant Capacity), ORAC (Oxygen Radical Absorbance Capacity), TRAP (Total Radical-trapping Antioxidant Parameter) et FRAP (Ferric ion Reducing Antioxidant Power) qui permettent une quantification de la capacité antioxydante d'un échantillon complexe par rapport à une molécule de référence.

Enfin, le test de Folin-Ciocalteu permet également la détermination du pouvoir réducteur de certains composés car son mécanisme implique une réaction d'oxydo-réduction, même s'il est principalement utilisé pour le dosage des composés phénoliques totaux présents dans un échantillon.

### I-5. Description des prochains chapitres

L'étude porte principalement sur huit composés phénoliques (phénol, guaiacol, syringol, pyrocatechol, o-crésol, m-crésol, p-crésol et vanilline) considérés comme molécules modèles potentiellement valorisables dans les bio-huiles (Figure I-18).

**Figure I-18 :** Structures des molécules étudiées dans cette thèse : a) phénol, b) guaiacol, c) syringol, d) pyrocatechol, e) o-crésol, f) m-crésol, g) p-crésol, h) vanilline



Ce travail de recherche a été divisé en quatre objectifs principaux.

Une première étude concerne les structures des composés phénoliques par calcul quantique.

Dans le chapitre 2, les conformations des structures stables et des états de transitions de chaque molécule ont été déterminées dans leur état isolé en utilisant un haut niveau de théorie et une forte base (DFT/cc-pVTZ). L'influence des liaisons hydrogènes intramoléculaires sur la stabilité et la structure de la molécule a également été étudiée. Enfin, l'étude des potentiels de rotation a permis de mettre en évidence un certain schéma propre aux substituants du groupement benzénique ainsi qu'à l'environnement voisin.

Le chapitre 3 présente l'étude des composés phénoliques en présence d'une molécule d'eau par calcul quantique. Différentes conformations ont été étudiées pour l'ensemble des composés où la molécule d'eau est positionnée en tant qu'accepteur ou/et de donneur de liaison hydrogène. La simulation permet également d'identifier les modifications engendrées au niveau de la structure d'un composé phénolique. Enfin, une analyse NBO permet de déterminer l'électronégativité et la dureté des molécules dans le système. De plus, la détermination des

énergies d'interaction entre le phénol et le liquide ionique [Choline][NTf<sub>2</sub>] indique que ce dernier est efficace d'un point de vue microscopique, pour l'extraction de composés phénoliques présents dans une solution aqueuse.

La seconde étape consiste à étudier expérimentalement le comportement de ces huit composés phénoliques en contact avec divers solvants (eau, éthanol, liquide ionique). L'objectif principal de ce chapitre 4 est de pallier au manque de données expérimentales dans la littérature. L'étude des équilibres entre phases a tout d'abord été réalisée sur des systèmes binaires (composé phénolique + eau ou composé phénolique + éthanol). Ces mesures expérimentales permettent ensuite de régresser les paramètres du modèle thermodynamique NRTL.

Le chapitre 5 propose d'évaluer les performances d'un liquide ionique pour l'extraction des composés phénoliques d'un milieu aqueux. Ce travail présente les résultats des équilibres entre phases dans le cas de systèmes ternaires (composé phénolique + eau + liquide ionique choline bis(trifluorométhylsulfonide)imide). Ces mesures expérimentales ont également permis de régresser les paramètres des modèles thermodynamiques NRTL et UNIQUAC. Ces données ont ensuite permis de dimensionner un procédé d'extraction des composés phénoliques en solution aqueuse comprenant une colonne d'extraction multi-étagée et un ballon de séparation liquide-vapeur.

Le chapitre 6 présente les résultats obtenus lors d'extractions liquide-liquide de composés phénoliques de bio-huiles de lignine en utilisant un liquide ionique (choline bis(trifluorométhylsulfonide)imide) ou l'acétate d'éthyle. La quantification des phases par GC-MS (gas chromatography - mass spectroscopy) et GC-FID (gas chromatography - flamme ionization detector) a permis de comparer l'efficacité d'extraction de chaque solvant.

Enfin, les composés phénoliques sont connus d'après la littérature pour leurs propriétés antioxydantes. Cinq tests de mesure de pouvoir antioxydant ont été réalisés en microplaque afin de déterminer et de classer les molécules selon leurs propriétés : pouvoir anti-radicalaire, pouvoir réducteur, pouvoir de chélation du fer et du cuivre, et réponse au réactif de Folin-Ciocalteu (Chapitre 7).

## Références bibliographiques

- [1] IAE, Key World Energy Statistics 2016, (2016).
- [2] Les réserves de pétrole, (n.d.). <http://www.ifpenergiesnouvelles.fr/Espace-Decouverte/Tous-les-Zooms/Les-reserves-de-petrole> (accessed May 22, 2017).
- [3] H. Das, S.K. Singh, Useful Byproducts from Cellulosic Wastes of Agriculture and Food Industry—A Critical Appraisal, *Crit. Rev. Food Sci. Nutr.* 44 (2004) 77–89. doi:10.1080/10408690490424630.
- [4] J.J. Bozell, J.E. Holladay, D. Johnson, J.F. White, Top value added chemicals from biomass, Vol. II Results Screen. Potential Candidates Biorefinery Lignin Rep. PNNL-16983. (2007).
- [5] Les bioraffineries ont-elles un avenir?, *Tech. Ing.* (n.d.). <http://www.techniques-ingenieur.fr/actualite/articles/les-bioraffineries-ont-elles-un-avenir-25746/> (accessed May 10, 2017).
- [6] Code de l'énergie - Article L211-2, n.d.
- [7] M.B. Sticklen, Plant genetic engineering for biofuel production: towards affordable cellulosic ethanol, *Nat. Rev. Genet.* 9 (2008) 433–443. doi:10.1038/nrg2336.
- [8] R.N. Olcese, Valorisation des vapeurs de pyrolyse de lignine par hydrodéoxygénation directe catalysées par le fer, Université de Lorraine, 2012. <http://www.theses.fr/2012LORR0107> (accessed May 18, 2017).
- [9] Y. Le Brech, Analyse des mécanismes primaires de pyrolyse de la biomasse, Université de Lorraine, 2015. <http://www.theses.fr/2015LORR0106> (accessed May 9, 2017).
- [10] A.J. Ragauskas, G.T. Beckham, M.J. Bidddy, R. Chandra, F. Chen, M.F. Davis, B.H. Davison, R.A. Dixon, P. Gilna, M. Keller, P. Langan, A.K. Naskar, J.N. Saddler, T.J. Tschaplinski, G.A. Tuskan, C.E. Wyman, Lignin Valorization: Improving Lignin Processing in the Biorefinery, *Science*. 344 (2014) 1246843–1246843. doi:10.1126/science.1246843.
- [11] T. Stevanovic, D. Perrin, *Chimie du bois*, Presses polytechniques et universitaires romandes, 2009.
- [12] Y. Onda, Syntheses and Properties of Cellulose Derivatives for Pharmaceutical Use as Additive, *J. Synth. Org. Chem. Jpn.* 42 (1984) 602–606. doi:10.5059/yukigoseikyokaishi.42.602.
- [13] J.R. Hess, C.T. Wright, K.L. Kenney, Cellulosic biomass feedstocks and logistics for ethanol production, *Biofuels Bioprod. Biorefining*. 1 (2007) 181–190. doi:10.1002/bbb.26.
- [14] R. El Hage, Prétraitement du miscanthus x giganteus : vers une valorisation optimale de la biomasse lignocellulosique, Nancy 1, 2010. <http://www.theses.fr/2010NAN10063> (accessed May 5, 2017).
- [15] F.S. Chakar, A.J. Ragauskas, Review of current and future softwood kraft lignin process chemistry, *Ind. Crops Prod.* 20 (2004) 131–141. doi:10.1016/j.indcrop.2004.04.016.
- [16] S.K. Ritter, Lignocellulose: A Complex Biomaterial, 86 (2008) 15.
- [17] D. Fengel, G. Wegener, *Wood: chemistry, ultrastructure, reactions*, Walter de Gruyter, 1983.
- [18] N.G. Lewis, L.B. Davin, S. Sarkanen, Lignin and Lignan Biosynthesis: Distinctions and Reconciliations, in: N.G. Lewis, S. Sarkanen (Eds.), *Lignin Lignan Biosynth.*, American Chemical Society, Washington, DC, 1998: pp. 1–27. doi:10.1021/bk-1998-0697.ch001.
- [19] J. Zakzeski, P.C.A. Bruijninx, A.L. Jongerijs, B.M. Weckhuysen, The Catalytic Valorization of Lignin for the Production of Renewable Chemicals, *Chem. Rev.* 110 (2010) 3552–3599. doi:10.1021/cr900354u.

- [20] M.P. Pandey, C.S. Kim, Lignin Depolymerization and Conversion: A Review of Thermochemical Methods, *Chem. Eng. Technol.* 34 (2011) 29–41. doi:10.1002/ceat.201000270.
- [21] L. da Costa Sousa, S.P. Chundawat, V. Balan, B.E. Dale, “Cradle-to-grave” assessment of existing lignocellulose pretreatment technologies, *Curr. Opin. Biotechnol.* 20 (2009) 339–347. doi:10.1016/j.copbio.2009.05.003.
- [22] J.D. Gargulak, S.E. Lebo, Commercial Use of Lignin-Based Materials, in: W.G. Glasser, R.A. Northey, T.P. Schultz (Eds.), *Lignin Hist. Biol. Mater. Perspect.*, American Chemical Society, Washington, DC, 1999: pp. 304–320. doi:10.1021/bk-2000-0742.ch015.
- [23] P. Hughes, Cellulosic Ethanol-The Sustainable Fuel, *Lignol Energy Burnaby BC Can.* (2009).
- [24] K. Barta, T.D. Matson, M.L. Fettig, S.L. Scott, A.V. Iretskii, P.C. Ford, Catalytic disassembly of an organosolv lignin via hydrogen transfer from supercritical methanol, *Green Chem.* 12 (2010) 1640. doi:10.1039/c0gc00181c.
- [25] C. Amen-Chen, H. Pakdel, C. Roy, Production of monomeric phenols by thermochemical conversion of biomass: a review, *Bioresour. Technol.* 79 (2001) 277–299. doi:10.1016/S0960-8524(00)00180-2.
- [26] R.K. Sharma, J.B. Wooten, V.L. Baliga, X. Lin, W. Geoffrey Chan, M.R. Hajaligol, Characterization of chars from pyrolysis of lignin, *Fuel.* 83 (2004) 1469–1482. doi:10.1016/j.fuel.2003.11.015.
- [27] A. Bridgwater, Renewable fuels and chemicals by thermal processing of biomass, *Chem. Eng. J.* 91 (2003) 87–102. doi:10.1016/S1385-8947(02)00142-0.
- [28] E. Jakab, O. Faix, F. Till, T. Székely, Thermogravimetry/mass spectrometry study of six lignins within the scope of an international round robin test, *J. Anal. Appl. Pyrolysis.* 35 (1995) 167–179. doi:10.1016/0165-2370(95)00907-7.
- [29] D. Ferdous, A.K. Dalai, S.K. Bej, R.W. Thring, Pyrolysis of Lignins: Experimental and Kinetics Studies, *Energy Fuels.* 16 (2002) 1405–1412. doi:10.1021/ef0200323.
- [30] S. Wang, K. Wang, Q. Liu, Y. Gu, Z. Luo, K. Cen, T. Fransson, Comparison of the pyrolysis behavior of lignins from different tree species, *Biotechnol. Adv.* 27 (2009) 562–567. doi:10.1016/j.biotechadv.2009.04.010.
- [31] N. Brosse, R. El Hage, M. Chaouch, M. Pétrissans, S. Dumarçay, P. Gérardin, Investigation of the chemical modifications of beech wood lignin during heat treatment, *Polym. Degrad. Stab.* 95 (2010) 1721–1726. doi:10.1016/j.polymdegradstab.2010.05.018.
- [32] R.J. Evans, T.A. Milne, Molecular characterization of the pyrolysis of biomass, *Energy Fuels.* 1 (1987) 123–137. doi:10.1021/ef00002a001.
- [33] C.A. Luengo, M.O. Cencig, Biomass Pyrolysis in Brazil: Status Report, in: A.V. Bridgwater, G. Grassi (Eds.), *Biomass Pyrolysis Liq. Upgrad. Util.*, Springer Netherlands, Dordrecht, 1991: pp. 299–309. doi:10.1007/978-94-011-3844-4\_13.
- [34] C. Amen-Chen, H. Pakdel, C. Roy, Separation of phenols from Eucalyptus wood tar, *Biomass Bioenergy.* 13 (1997) 25–37. doi:10.1016/S0961-9534(97)00021-4.
- [35] C.A. Mullen, A.A. Boateng, N.M. Goldberg, I.M. Lima, D.A. Laird, K.B. Hicks, Bio-oil and bio-char production from corn cobs and stover by fast pyrolysis, *Biomass Bioenergy.* 34 (2010) 67–74. doi:10.1016/j.biombioe.2009.09.012.
- [36] D. Fu, S. Farag, J. Chaouki, P.G. Jessop, Extraction of phenols from lignin microwave-pyrolysis oil using a switchable hydrophilicity solvent, *Bioresour. Technol.* 154 (2014) 101–108. doi:10.1016/j.biortech.2013.11.091.
- [37] R. Lou, S. Wu, G. Lyu, Quantified monophenols in the bio-oil derived from lignin fast pyrolysis, *J. Anal. Appl. Pyrolysis.* 111 (2015) 27–32. doi:10.1016/j.jaap.2014.12.022.

- [38] U. Schuchardt, J.A.R. Rodrigues, A. Cotrim, J.L.M. Costa, Liquefaction of hydrolytic eucalyptus lignin with formate in water, using batch and continuous-flow reactors, *Bioresour. Technol.* 44 (1993) 123–129. doi:10.1016/0960-8524(93)90185-E.
- [39] A.N. Bagaev, Fractionation of wood tars and their products, *Gidroliz Lesokhim Promysh.* 18 (1965) 13–15.
- [40] J.N. Murwanashyaka, H. Pakdel, C. Roy, Separation of syringol from birch wood-derived vacuum pyrolysis oil, *Sep. Purif. Technol.* 24 (2001) 155–165. doi:10.1016/S1383-5866(00)00225-2.
- [41] J.A. Capunitan, S.C. Capareda, Characterization and separation of corn stover bio-oil by fractional distillation, *Fuel.* 112 (2013) 60–73. doi:10.1016/j.fuel.2013.04.079.
- [42] S. Wang, Y. Gu, Q. Liu, Y. Yao, Z. Guo, Z. Luo, K. Cen, Separation of bio-oil by molecular distillation, *Fuel Process. Technol.* 90 (2009) 738–745. doi:10.1016/j.fuproc.2009.02.005.
- [43] S. Ramaswamy, H.-J. Huang, B.V. Ramarao, *Separation and Purification Technologies in Biorefineries*, John Wiley & Sons, 2013.
- [44] Z. Guo, S. Wang, Y. Gu, G. Xu, X. Li, Z. Luo, Separation characteristics of biomass pyrolysis oil in molecular distillation, *Sep. Purif. Technol.* 76 (2010) 52–57. doi:10.1016/j.seppur.2010.09.019.
- [45] X.-S. Zhang, G.-X. Yang, H. Jiang, W.-J. Liu, H.-S. Ding, Mass production of chemicals from biomass-derived oil by directly atmospheric distillation coupled with co-pyrolysis, *Sci. Rep.* 3 (2013). doi:10.1038/srep01120.
- [46] J. Li, D. Ding, L. Xu, Q. Guo, Y. Fu, The breakdown of reticent biomass to soluble components and their conversion to levulinic acid as a fuel precursor, *RSC Adv.* 4 (2014) 14985. doi:10.1039/c3ra47923d.
- [47] D. Meier, D.R. Larimer, O. Faix, Direct liquefaction of different lignocellulosics and their constituents, *Fuel.* 65 (1986) 910–915. doi:10.1016/0016-2361(86)90197-3.
- [48] R. Maggi, B. Delmon, Comparison between “slow” and “flash” pyrolysis oils from biomass, *Fuel.* 73 (1994) 671–677. doi:10.1016/0016-2361(94)90007-8.
- [49] M.T. Galceran, L. Eek, Analisis de alquitran de extraccion de maderas duras, 2: Fraccion pesada., *Quimica Anal.* (1977). [http://agris.fao.org/agris-search/search.do;jsessionid=F583D9497F7B2141AF13ADC070ACD2C3?request\\_local\\_e=es&recordID=ES19780302092&sourceQuery=&query=&sortField=&sortOrder=&agrovocString=&advQuery=&centerString=&enableField=](http://agris.fao.org/agris-search/search.do;jsessionid=F583D9497F7B2141AF13ADC070ACD2C3?request_local_e=es&recordID=ES19780302092&sourceQuery=&query=&sortField=&sortOrder=&agrovocString=&advQuery=&centerString=&enableField=) (accessed May 10, 2017).
- [50] Y. Wei, H. Lei, L. Wang, L. Zhu, X. Zhang, Y. Liu, S. Chen, B. Ahring, Liquid–Liquid Extraction of Biomass Pyrolysis Bio-oil, *Energy Fuels.* 28 (2014) 1207–1212. doi:10.1021/ef402490s.
- [51] R.M. Gallivan, P.K. Matschei, Fractionation of oil obtained by pyrolysis of lignocellulosic materials to recover a phenolic fraction for use in making phenol-formaldehyde resins, n.d. <http://www.google.com/patents/US4209647> (accessed January 23, 2017).
- [52] J. Li, C. Wang, Z. Yang, Production and separation of phenols from biomass-derived biopetroleum, *J. Anal. Appl. Pyrolysis.* 89 (2010) 218–224. doi:10.1016/j.jaap.2010.08.004.
- [53] R. Lu, G.-P. Sheng, Y.-Y. Hu, P. Zheng, H. Jiang, Y. Tang, H.-Q. Yu, Fractional characterization of a bio-oil derived from rice husk, *Biomass Bioenergy.* 35 (2011) 671–678. doi:10.1016/j.biombioe.2010.10.017.
- [54] L. Fele Žilnik, A. Jazbinšek, Recovery of renewable phenolic fraction from pyrolysis oil, *Sep. Purif. Technol.* 86 (2012) 157–170. doi:10.1016/j.seppur.2011.10.040.
- [55] A. Vigneault, D.K. Johnson, E. Chornet, Base-Catalyzed Depolymerization of Lignin: Separation of Monomers, *Can. J. Chem. Eng.* 85 (2008) 906–916. doi:10.1002/cjce.5450850612.

- [56] Z. Wang, W. Lin, W. Song, L. Du, Z. Li, J. Yao, Component fractionation of wood-tar by column chromatography with the packing material of silica gel, *Chin. Sci. Bull.* 56 (2011) 1434–1441. doi:10.1007/s11434-010-4144-x.
- [57] T. Ba, A. Chaala, M. Garcia-Perez, C. Roy, Colloidal Properties of Bio-Oils Obtained by Vacuum Pyrolysis of Softwood Bark. Storage Stability, *Energy Fuels*. 18 (2004) 188–201. doi:10.1021/ef0301250.
- [58] P. Das, T. Sreelatha, A. Ganesh, Bio oil from pyrolysis of cashew nut shell-characterisation and related properties, *Biomass Bioenergy*. 27 (2004) 265–275. doi:10.1016/j.biombioe.2003.12.001.
- [59] S. XU, J. Liu, S. Li, Shu-qin Liu, Q. Lu, Solvent extraction-column chromatographic separation of bio-oil from fast pyrolysis of apricot stone and manufacture technology, *J. Dalian Univ. Technol.* 4 (2005).
- [60] A. Teella, G.W. Huber, D.M. Ford, Separation of acetic acid from the aqueous fraction of fast pyrolysis bio-oils using nanofiltration and reverse osmosis membranes, *J. Membr. Sci.* 378 (2011) 495–502. doi:10.1016/j.memsci.2011.05.036.
- [61] D. Radlein, Chemicals and materials from biomass, *PyNe Pyrolysis Netw.* 4 (1997).
- [62] Y. Feng, D. Meier, Extraction of value-added chemicals from pyrolysis liquids with supercritical carbon dioxide, *J. Anal. Appl. Pyrolysis*. 113 (2015) 174–185. doi:10.1016/j.jaap.2014.12.009.
- [63] H.-G. Zhang, Preparative Separation of Chemicals from Wood Vacuum Pyrolysis Oils by Liquid Chromatography, Université Laval, 1990.
- [64] H.L. Chum, S.K. Black, Process for fractionating fast-pyrolysis oils, and products derived therefrom, n.d. <http://www.google.com/patents/US4942269> (accessed May 10, 2017).
- [65] D.C. Greminger, G.P. Burns, S. Lynn, D.N. Hanson, C.J. King, Solvent extraction of phenols from water, *Ind. Eng. Chem. Process Des. Dev.* 21 (1982) 51–54. doi:10.1021/i200016a010.
- [66] R.W. Thring, J. Breau, Hydrocracking of solvolysis lignin in a batch reactor, *Fuel*. 75 (1996) 795–800. doi:10.1016/0016-2361(96)00036-1.
- [67] S. Wang, Y. Wang, Q. Cai, X. Wang, H. Jin, Z. Luo, Multi-step separation of monophenols and pyrolytic lignins from the water-insoluble phase of bio-oil, *Sep. Purif. Technol.* 122 (2014) 248–255. doi:10.1016/j.seppur.2013.11.017.
- [68] T. Radoykova, S. Nenkova, K. Stanulov, Production of phenol compounds by alkaline treatment of poplar wood bark, *Chem. Nat. Compd.* 46 (2010) 807–808. doi:10.1007/s10600-010-9751-x.
- [69] J.-M. Lavoie, W. Baré, M. Bilodeau, Depolymerization of steam-treated lignin for the production of green chemicals, *Bioresour. Technol.* 102 (2011) 4917–4920. doi:10.1016/j.biortech.2011.01.010.
- [70] H. Darmstadt, M. Garcia-Perez, A. Adnot, A. Chaala, D. Kretschmer, C. Roy, Corrosion of Metals by Bio-Oil Obtained by Vacuum Pyrolysis of Softwood Bark Residues. An X-ray Photoelectron Spectroscopy and Auger Electron Spectroscopy Study, *Energy Fuels*. 18 (2004) 1291–1301. doi:10.1021/ef0340920.
- [71] Y. Hou, Y. Ren, W. Peng, S. Ren, W. Wu, Separation of Phenols from Oil Using Imidazolium-Based Ionic Liquids, *Ind. Eng. Chem. Res.* 52 (2013) 18071–18075. doi:10.1021/ie403849g.
- [72] A. Garron, P.P. Arquilliere, W.A. Maksoud, C. Larabi, J.-J. Walter, C.C. Santini, From industrial black liquor to pure phenolic compounds: A combination of catalytic conversion with ionic liquids extraction, *Appl. Catal. Gen.* 502 (2015) 230–238. doi:10.1016/j.apcata.2015.06.012.
- [73] D.A. Fort, R.C. Remsing, R.P. Swatloski, P. Moyna, G. Moyna, R.D. Rogers, Can ionic liquids dissolve wood? Processing and analysis of lignocellulosic materials with 1-n-

- butyl-3-methylimidazolium chloride, *Green Chem.* 9 (2007) 63–69. doi:10.1039/B607614A.
- [74] R.P. Swatloski, S.K. Spear, J.D. Holbrey, R.D. Rogers, Dissolution of cellulose [correction of cellose] with ionic liquids, *J. Am. Chem. Soc.* 124 (2002) 4974–4975.
- [75] E.S.R.E.S. Hassan, *Use of Ionic Liquids for the Treatment of Biomass Materials and Biofuel Production*, Université de Lorraine, 2014. <http://www.theses.fr/2014LORR0043> (accessed June 2, 2017).
- [76] K.E. Gutowski, G.A. Broker, H.D. Willauer, J.G. Huddleston, R.P. Swatloski, J.D. Holbrey, R.D. Rogers, Controlling the Aqueous Miscibility of Ionic Liquids: Aqueous Biphasic Systems of Water-Miscible Ionic Liquids and Water-Structuring Salts for Recycle, Metathesis, and Separations, *J. Am. Chem. Soc.* 125 (2003) 6632–6633. doi:10.1021/ja0351802.
- [77] S. Zhu, Y. Wu, Q. Chen, Z. Yu, C. Wang, S. Jin, Y. Ding, G. Wu, Dissolution of cellulose with ionic liquids and its application: a mini-review, *Green Chem.* 8 (2006) 325. doi:10.1039/b601395c.
- [78] M. Gericke, P. Fardim, T. Heinze, Ionic Liquids — Promising but Challenging Solvents for Homogeneous Derivatization of Cellulose, *Molecules.* 17 (2012) 7458–7502. doi:10.3390/molecules17067458.
- [79] B. Lu, A. Xu, J. Wang, Cation does matter: how cationic structure affects the dissolution of cellulose in ionic liquids, *Green Chem.* 16 (2014) 1326–1335. doi:10.1039/C3GC41733F.
- [80] Y. Pu, N. Jiang, A.J. Ragauskas, Ionic Liquid as a Green Solvent for Lignin, *J. Wood Chem. Technol.* 27 (2007) 23–33. doi:10.1080/02773810701282330.
- [81] S.S.Y. Tan, D.R. MacFarlane, J. Upfal, L.A. Edey, W.O.S. Doherty, A.F. Patti, J.M. Pringle, J.L. Scott, Extraction of lignin from lignocellulose at atmospheric pressure using alkylbenzenesulfonate ionic liquid, *Green Chem.* 11 (2009) 339. doi:10.1039/b815310h.
- [82] Q. Xin, K. Pfeiffer, J.M. Prausnitz, D.S. Clark, H.W. Blanch, Extraction of lignins from aqueous-ionic liquid mixtures by organic solvents, *Biotechnol. Bioeng.* 109 (2012) 346–352. doi:10.1002/bit.24337.
- [83] S.H. Mushrif, V. Vasudevan, C.B. Krishnamurthy, B. Venkatesh, Multiscale molecular modeling can be an effective tool to aid the development of biomass conversion technology: A perspective, *Chem. Eng. Sci.* 121 (2015) 217–235. doi:10.1016/j.ces.2014.08.019.
- [84] T. Ishikawa, D. Hayakawa, H. Miyamoto, M. Ozawa, T. Ozawa, K. Ueda, Ab initio studies on the structure of and atomic interactions in cellulose III crystals, *Carbohydr. Res.* 417 (2015) 72–77. doi:10.1016/j.carres.2015.09.006.
- [85] Y. Li, M. Lin, J.W. Davenport, Ab Initio Studies of Cellulose I: Crystal Structure, Intermolecular Forces, and Interactions with Water, *J. Phys. Chem. C.* 115 (2011) 11533–11539. doi:10.1021/jp2006759.
- [86] E.-S.R.E. Hassan, F. Mutelet, M. Bouroukba, Experimental and theoretical study of carbohydrate–ionic liquid interactions, *Carbohydr. Polym.* 127 (2015) 316–324. doi:10.1016/j.carbpol.2015.03.042.
- [87] B.G. Janesko, Modeling interactions between lignocellulose and ionic liquids using DFT-D, *Phys. Chem. Chem. Phys.* 13 (2011) 11393. doi:10.1039/c1cp20072k.
- [88] W.-H. Fang, Theoretical characterization of the excited-state structures and properties of phenol and its one-water complex, *J. Chem. Phys.* 112 (2000) 1204–1211. doi:10.1063/1.480673.
- [89] S. Schumm, M. Gerhards, W. Roth, H. Gier, K. Kleinermanns, A CASSCF study of the S<sub>0</sub> and S<sub>1</sub> states of phenol, *Chem. Phys. Lett.* 263 (1996) 126–132. doi:10.1016/S0009-2614(96)01172-4.

- [90] D. Feller, M.W. Feyereisen, Ab initio study of hydrogen bonding in the phenol-water system, *J. Comput. Chem.* 14 (1993) 1027–1035. doi:10.1002/jcc.540140904.
- [91] M. Schütz, T. Bürgi, S. Leutwyler, Structures and vibrations of phenol · H<sub>2</sub>O and d-phenol · D<sub>2</sub>O based on ab initio calculations, *J. Mol. Struct. THEOCHEM.* 276 (1992) 117–132. doi:10.1016/0166-1280(92)80026-I.
- [92] H. Watanabe, S. Iwata, Theoretical studies of geometric structures of phenol-water clusters and their infrared absorption spectra in the O–H stretching region, *J. Chem. Phys.* 105 (1996) 420–431. doi:10.1063/1.471918.
- [93] T. Kojima, Potential Barrier of Phenol from its Microwave Spectrum, *J. Phys. Soc. Jpn.* 15 (1960) 284–287. doi:10.1143/JPSJ.15.284.
- [94] M. Pohl, K. Kleinermanns, Ab initio SCF calculations on hydrogen bonded cresol isomers, *Z. Für Phys. At. Mol. Clust.* 8 (n.d.) 385–392. doi:10.1007/BF01437106.
- [95] S.W. Dietrich, E.C. Jorgensen, P.A. Kollman, S. Rothenberg, A theoretical study of intramolecular hydrogen bonding in ortho-substituted phenols and thiophenols, *J. Am. Chem. Soc.* 98 (1976) 8310–8324. doi:10.1021/ja00442a002.
- [96] A. Welzel, A. Hellweg, I. Merke, W. Stahl, Structural and Torsional Properties of o-Cresol and o-Cresol-OD as Obtained from Microwave Spectroscopy and ab Initio Calculations, *J. Mol. Spectrosc.* 215 (2002) 58–65. doi:10.1006/jmsp.2002.8600.
- [97] V. Balachandran, M. Murugan, A. Nataraj, M. Karnan, G. Ilango, Comparative vibrational spectroscopic studies, HOMO–LUMO, NBO analyses and thermodynamic functions of p-cresol and 2-methyl-p-cresol based on DFT calculations, *Spectrochim. Acta. A. Mol. Biomol. Spectrosc.* 132 (2014) 538–549. doi:10.1016/j.saa.2014.04.194.
- [98] P.R. Richardson, M.A. Chapman, D.C. Wilson, S.P. Bates, A.C. Jones, The nature of conformational preference in a number of p-alkyl phenols and p-alkyl benzenes, *Phys. Chem. Chem. Phys.* 4 (2002) 4910–4915. doi:10.1039/b203954k.
- [99] A. Hellweg, C. Hättig, On the internal rotations in p-cresol in its ground and first electronically excited states, *J. Chem. Phys.* 127 (2007) 024307. doi:10.1063/1.2752163.
- [100] A. Hellweg, C. Hättig, I. Merke, W. Stahl, Microwave and theoretical investigation of the internal rotation in m-cresol, *J. Chem. Phys.* 124 (2006) 204305. doi:10.1063/1.2198842.
- [101] C. Puebla, T.-K. Ha, A theoretical study of conformations and rotational barriers in dihydroxybenzenes, *J. Mol. Struct. THEOCHEM.* 204 (1990) 337–351. doi:10.1016/0166-1280(90)85085-2.
- [102] T. Bürgi, S. Leutwyler, O–H torsional vibrations in the *S*<sub>0</sub> and *S*<sub>1</sub> states of catechol, *J. Chem. Phys.* 101 (1994) 8418–8429. doi:10.1063/1.468104.
- [103] M. Gerhards, W. Perl, S. Schumm, U. Henrichs, C. Jacoby, K. Kleinermanns, Structure and vibrations of catechol and catechol·H<sub>2</sub>O(D<sub>2</sub>O) in the *S*<sub>0</sub> and *S*<sub>1</sub> state, *J. Chem. Phys.* 104 (1996) 9362. doi:10.1063/1.471682.
- [104] R. Rudyk, M.A.A. Molina, M.I. Gómez, S.E. Blanco, F.H. Ferretti, Solvent effects on the structure and dipole moment of resorcinol, *J. Mol. Struct. THEOCHEM.* 674 (2004) 7–14. doi:10.1016/j.theochem.2003.12.019.
- [105] B. Gómez-Zaleta, R. Gómez-Balderas, J. Hernández-Trujillo, Theoretical analysis of hydrogen bonding in catechol–n(H<sub>2</sub>O) clusters (n = 0...3), *Phys. Chem. Chem. Phys.* 12 (2010) 4783. doi:10.1039/b922203k.
- [106] M. Mandado, A.M. Graña, R.A. Mosquera, Do 1,2-ethanediol and 1,2-dihydroxybenzene present intramolecular hydrogen bond?, *Phys Chem Chem Phys.* 6 (2004) 4391–4396. doi:10.1039/B406266C.
- [107] C. Agache, V.I. Popa, Ab Initio Studies on the Molecular Conformation of Lignin Model Compounds I. Conformational Preferences of the Phenolic Hydroxyl and Methoxy Groups

- in Guaiacol, *Monatshefte Für Chem. - Chem. Mon.* 137 (2006) 55–68. doi:10.1007/s00706-005-0404-x.
- [108] O.V. Dorofeeva, I.F. Shishkov, N.M. Karasev, L.V. Vilkov, H. Oberhammer, Molecular structures of 2-methoxyphenol and 1,2-dimethoxybenzene as studied by gas-phase electron diffraction and quantum chemical calculations, *J. Mol. Struct.* 933 (2009) 132–141. doi:10.1016/j.molstruc.2009.06.009.
- [109] M.A. Varfolomeev, D.I. Abaidullina, B.N. Solomonov, S.P. Verevkin, V.N. Emel'yanenko, Pairwise Substitution Effects, Inter- and Intramolecular Hydrogen Bonds in Methoxyphenols and Dimethoxybenzenes. Thermochemistry, Calorimetry, and First-Principles Calculations, *J. Phys. Chem. B.* 114 (2010) 16503–16516. doi:10.1021/jp108459r.
- [110] E.J. Cocinero, A. Lesarri, P. Écija, J.-U. Grabow, J.A. Fernández, F. Castaño, Conformational equilibria in vanillin and ethylvanillin, *Phys. Chem. Chem. Phys.* 12 (2010) 12486. doi:10.1039/c0cp00585a.
- [111] C.YOHANNAN PANICKER, HEMA TRESA VARGHESE, K. SAJINA, A.V. VAIDYAN, MEENU ANNA JOHN, B. HARIKUMAR, IR, Raman and ab-initio calculations of 2,6-dimethoxyphenol, *Orient. J. Chem.* 24 (2008) 973.
- [112] L. Zhang, G.H. Peslherbe, H.M. Muchall, Ultraviolet Absorption Spectra of Substituted Phenols: A Computational Study†, *Photochem. Photobiol.* 82 (2006) 324–331. doi:10.1562/2005-07-08-RA-605.
- [113] A. Plugatyr, I. Nahtigal, I.M. Svishchev, Spatial hydration structures and dynamics of phenol in sub- and supercritical water, *J. Chem. Phys.* 124 (2006) 024507. doi:10.1063/1.2145751.
- [114] W. Roth, M. Schmitt, C. Jacoby, D. Spangenberg, C. Janzen, K. Kleinermanns, Double resonance spectroscopy of phenol(H<sub>2</sub>O)<sub>1–12</sub>: evidence for ice-like structures in aromate–water clusters?, *Chem. Phys.* 239 (1998) 1–9. doi:10.1016/S0301-0104(98)00252-3.
- [115] C. Jacoby, W. Roth, M. Schmitt, C. Janzen, D. Spangenberg, K. Kleinermanns, Intermolecular Vibrations of Phenol(H<sub>2</sub>O)<sub>2-5</sub> and Phenol(D<sub>2</sub>O)<sub>2-5</sub> - *d*<sub>1</sub> Studied by UV Double-Resonance Spectroscopy and ab Initio Theory, *J. Phys. Chem. A.* 102 (1998) 4471–4480. doi:10.1021/jp9806157.
- [116] A. Lüchow, D. Spangenberg, C. Janzen, A. Jansen, M. Gerhards, K. Kleinermanns, Structure and energetics of phenol(H<sub>2</sub>O)<sub>n</sub>, n □ 7: Quantum Monte Carlo calculations and double resonance experiments, *Phys. Chem. Chem. Phys.* 3 (2001) 2771–2780. doi:10.1039/b101779i.
- [117] D.M. Benoit, D.C. Clary, Quantum Simulation of Phenol–Water Clusters, *J. Phys. Chem. A.* 104 (2000) 5590–5599. doi:10.1021/jp994420q.
- [118] I. Bandyopadhyay, H.M. Lee, K.S. Kim, Phenol vs Water Molecule Interacting with Various Molecules:  $\sigma$ -type,  $\pi$ -type, and  $\chi$ -type Hydrogen Bonds, Interaction Energies, and Their Energy Components, *J. Phys. Chem. A.* 109 (2005) 1720–1728. doi:10.1021/jp0449657.
- [119] M. Gerhards, M. Schmitt, K. Kleinermanns, W. Stahl, The structure of phenol(H<sub>2</sub>O) obtained by microwave spectroscopy, *J. Chem. Phys.* 104 (1996) 967–971. doi:10.1063/1.470820.
- [120] Y. Dimitrova, Ab initio and DFT studies of the vibrational spectra of hydrogen-bonded PhOH...(H<sub>2</sub>O)<sub>4</sub> complexes, *Spectrochim. Acta. A. Mol. Biomol. Spectrosc.* 60 (2004) 3049–3057. doi:10.1016/j.saa.2004.01.026.
- [121] R. Parthasarathi, V. Subramanian, N. Sathyamurthy, Hydrogen Bonding in Phenol, Water, and Phenol–Water Clusters, *J. Phys. Chem. A.* 109 (2005) 843–850. doi:10.1021/jp046499r.

- [122] F. Ramondo, L. Bencivenni, G. Portalone, A. Domenicano, Effect of intermolecular O-H ... O hydrogen bonding on the molecular structure of phenol: An ab initio molecular orbital study, *Struct. Chem.* 6 (n.d.) 37–45. doi:10.1007/BF02263526.
- [123] R. Wu, B. Brutschy, Study on the structure and intra- and intermolecular hydrogen bonding of 2-methoxyphenol · (H<sub>2</sub>O)<sub>n</sub> (n=1,2), *Chem. Phys. Lett.* 390 (2004) 272–278. doi:10.1016/j.cplett.2004.04.023.
- [124] S. Jalili, M. Akhavan, Study of hydrogen-bonded clusters of 2-methoxyphenol–water, *Theor. Chem. Acc.* 118 (2007) 947–957. doi:10.1007/s00214-007-0378-3.
- [125] M. Pohl, M. Schmitt, K. Kleinermanns, Microscopic shifts of size-assigned p-cresol/H<sub>2</sub>O-cluster spectra, *J. Chem. Phys.* 94 (1991) 1717. doi:10.1063/1.459944.
- [126] G. Myszkiewicz, W.L. Meerts, C. Ratzer, M. Schmitt, The structure of 4-methylphenol and its water cluster revealed by rotationally resolved UV spectroscopy using a genetic algorithm approach, *J. Chem. Phys.* 123 (2005) 044304. doi:10.1063/1.1961615.
- [127] H.S. Biswal, P.R. Shirhatti, S. Wategaonkar, O–H···O versus O–H···S Hydrogen Bonding I: Experimental and Computational Studies on the *p*-Cresol·H<sub>2</sub>O and *p*-Cresol·H<sub>2</sub>S Complexes, *J. Phys. Chem. A.* 113 (2009) 5633–5643. doi:10.1021/jp9009355.
- [128] V.M. Egorov, S.V. Smirnova, I.V. Pletnev, Highly efficient extraction of phenols and aromatic amines into novel ionic liquids incorporating quaternary ammonium cation, *Sep. Purif. Technol.* 63 (2008) 710–715. doi:10.1016/j.seppur.2008.06.024.
- [129] K.S. Khachatryan, S.V. Smirnova, I.I. Torocheshnikova, N.V. Shvedene, A.A. Formanovsky, I.V. Pletnev, Solvent extraction and extraction? voltammetric determination of phenols using room temperature ionic liquid, *Anal. Bioanal. Chem.* 381 (2005) 464–470. doi:10.1007/s00216-004-2872-y.
- [130] N. Deng, M. Li, L. Zhao, C. Lu, S.L. de Rooy, I.M. Warner, Highly efficient extraction of phenolic compounds by use of magnetic room temperature ionic liquids for environmental remediation, *J. Hazard. Mater.* 192 (2011) 1350–1357. doi:10.1016/j.jhazmat.2011.06.053.
- [131] X. Li, S.R.A. Kersten, B. Schuur, Extraction of Guaiacol from Model Pyrolytic Sugar Stream with Ionic Liquids, *Ind. Eng. Chem. Res.* 55 (2016) 4703–4710. doi:10.1021/acs.iecr.6b00100.
- [132] C. Achard, M. Jaoui, M. Schwing, M. Rogalski, Aqueous Solubilities of Phenol Derivatives by Conductivity Measurements, *J. Chem. Eng. Data.* 41 (1996) 504–507. doi:10.1021/je950202o.
- [133] M. Jaoui, C. Achard, M. Rogalski, Solubility as a Function of Temperature of Selected Chlorophenols and Nitrophenols in Aqueous Solutions Containing Electrolytes or Surfactants, *J. Chem. Eng. Data.* 47 (2002) 297–303. doi:10.1021/je0102309.
- [134] A.N. Campbell, A.J.R. Campbell, Concentrations, Total and Partial Vapor Pressures, Surface Tensions and Viscosities, in the Systems Phenol—Water and Phenol—Water—4% Succinic Acid, *J. Am. Chem. Soc.* 59 (1937) 2481–2488. doi:10.1021/ja01291a001.
- [135] A.E. Hill, W.M. Malisoff, The mutual solubility of liquids. III. The mutual solubility of phenol and water. IV. The mutual solubility of normal butylalcohol and water, *J. Am. Chem. Soc.* 48 (1926) 918–927. doi:10.1021/ja01415a011.
- [136] D. Tam, D. Varhanickova, W.Y. Shiu, D. Mackay, Aqueous solubility of chloroguaiacols, *J. Chem. Eng. Data.* 39 (1994) 83–86. doi:10.1021/je00013a022.
- [137] T. Shedlovsky, On guaiacol solutions: the electrical conductivity of sodium and potassium guaiaculates in guaiacol, *J. Gen. Physiol.* 17 (1934) 549–561. doi:10.1085/jgp.17.4.549.
- [138] W.H. Walker, A.R. Collett, C.L. Lazzell, The Solubility Relations of the Isomeric Dihydroxybenzenes, *J. Phys. Chem.* 35 (1930) 3259–3271. doi:10.1021/j150329a011.

- [139] X. Xia, D. Jiang, Determination and correlation of solubilities of catechol, *J. Chem. Ind. Eng.-CHINA-*. 58 (2007) 1082.
- [140] L.C. Cartwright, Vanilla-like Synthetics, Solubility and Volatility of Propenyl Guaethyl, Bourbonal, Vanillin, and Coumarin, *J. Agric. Food Chem.* 1 (1953) 312–314. doi:10.1021/jf60004a006.
- [141] C.E. Mange, O. Ehler, Solubilities of Vanillin., *Ind. Eng. Chem.* 16 (1924) 1258–1260. doi:10.1021/ie50180a017.
- [142] A. Noubigh, M. Abderrabba, E. Provost, Temperature and salt addition effects on the solubility behaviour of some phenolic compounds in water, *J. Chem. Thermodyn.* 39 (2007) 297–303. doi:10.1016/j.jct.2006.06.014.
- [143] N.V. Sidgwick, W.J. Spurrell, T.E. Davies, CXXXII.—The solubility of the nitrophenols and other isomeric disubstitution products of benzene, *J Chem Soc Trans.* 107 (1915) 1202–1213. doi:10.1039/CT9150701202.
- [144] D. Varhanickova, W.-Y. Shiu, D. Mackay, Aqueous Solubilities of Alkylphenols and Methoxyphenols at 25 .degree.C, *J. Chem. Eng. Data.* 40 (1995) 448–451. doi:10.1021/je00018a020.
- [145] C.R. Bailey, CCXCVIII.—The increased solubility of phenolic substances in water on addition of a third substance, *J Chem Soc Trans.* 123 (1923) 2579–2590. doi:10.1039/CT9232302579.
- [146] H. Brusset, H. Gillier-Pandraud, A. Neuman, Strukturbestimmung bei-150 grad c von 2, 5-und 2, 3-dimethylphenol, *Chem. Informationsdienst.* 3 (1972).
- [147] M. Klauck, A. Grenner, K. Taubert, A. Martin, R. Meinhardt, J. Schmelzer, Vapor–Liquid Equilibria in Binary Systems of Phenol or Cresols + Water, + Toluene, and + Octane and Liquid–Liquid Equilibria in Binary Systems of Cresols + Water, *Ind. Eng. Chem. Res.* 47 (2008) 5119–5126. doi:10.1021/ie071214t.
- [148] W.A. Leet, H.-M. Lin, K.-C. Chao, Mutual solubilities in six binary mixtures of water + a heavy hydrocarbon or a derivative, *J. Chem. Eng. Data.* 32 (1987) 37–40. doi:10.1021/je00047a010.
- [149] M.R. Rover, R.C. Brown, Quantification of total phenols in bio-oil using the Folin–Ciocalteu method, *J. Anal. Appl. Pyrolysis.* 104 (2013) 366–371. doi:10.1016/j.jaap.2013.06.011.
- [150] M. Andjelkovic, J. Vancamp, B. Demeulenaer, G. Depaemelaere, C. Socaciu, M. Verloo, R. Verhe, Iron-chelation properties of phenolic acids bearing catechol and galloyl groups, *Food Chem.* 98 (2006) 23–31. doi:10.1016/j.foodchem.2005.05.044.
- [151] S.Y. Yeung, W.H. Lan, C.S. Huang, C.P. Lin, C.P. Chan, M.C. Chang, J.H. Jeng, Scavenging property of three cresol isomers against H<sub>2</sub>O<sub>2</sub>, hypochlorite, superoxide and hydroxyl radicals, *Food Chem. Toxicol.* 40 (2002) 1403–1413.
- [152] G. Dobeles, T. Dizhbite, I. Urbanovich, A. Andersone, J. Ponomarenko, G. Telysheva, Pyrolytic oil on the basis of wood and the antioxidant properties of its water-soluble and -insoluble fraction, *J. Anal. Appl. Pyrolysis.* 85 (2009) 81–86. doi:10.1016/j.jaap.2008.12.006.
- [153] K. Zhou, J. Yin, L. Yu, ESR determination of the reactions between selected phenolic acids and free radicals or transition metals, *Food Chem.* 95 (2006) 446–457. doi:10.1016/j.foodchem.2005.01.026.
- [154] F. Helmut, V. Heinz-Werner, H. Toshikazu, P. Wilfrried, Phenol derivatives, *Ullmann's Encycl. Ind. Chem. VCH Ger.* 19 (1985) 299–357.
- [155] F. Ikegami, T. Sekine, Y. Fujii, [Anti-dermatophyte activity of phenolic compounds in “mokusaku-eki”], *Yakugaku Zasshi.* 118 (1998) 27–30.
- [156] J.A. Maga, I. Katz, Simple phenol and phenolic compounds in food flavor, *C R C Crit. Rev. Food Sci. Nutr.* 10 (1978) 323–372. doi:10.1080/10408397809527255.

- [157] R.N. Singru, A.B. Zade, W.B. Gurnule, Synthesis, characterization, and thermal degradation studies of copolymer resin derived from p-cresol, melamine, and formaldehyde, *J. Appl. Polym. Sci.* 109 (2008) 859–868. doi:10.1002/app.28197.
- [158] Filbert, Manufacture of dinitro-orthocresol, n.d. <http://www.google.com/patents/US2256195> (accessed May 10, 2017).
- [159] G.A. Burdock, *Fenaroli's Handbook of Flavor Ingredients*, Sixth Edition, CRC Press, 2016.
- [160] Vanillin Pharmaceutical, *Chem. Eng. News.* 34 (1956) 4778. doi:10.1021/cen-v034n040.p4778.
- [161] B.N. Ames, M.K. Shigenaga, T.M. Hagen, Oxidants, antioxidants, and the degenerative diseases of aging., *Proc. Natl. Acad. Sci. U. S. A.* 90 (1993) 7915–7922.
- [162] D. Huang, B. Ou, R.L. Prior, The Chemistry behind Antioxidant Capacity Assays, *J. Agric. Food Chem.* 53 (2005) 1841–1856. doi:10.1021/jf030723c.
- [163] J. Dai, R.J. Mumper, Plant Phenolics: Extraction, Analysis and Their Antioxidant and Anticancer Properties, *Molecules.* 15 (2010) 7313–7352. doi:10.3390/molecules15107313.
- [164] M. Yoshino, K. Murakami, Interaction of Iron with Polyphenolic Compounds: Application to Antioxidant Characterization, *Anal. Biochem.* 257 (1998) 40–44. doi:10.1006/abio.1997.2522.
- [165] N.R. Perron, J.L. Brumaghim, A Review of the Antioxidant Mechanisms of Polyphenol Compounds Related to Iron Binding, *Cell Biochem. Biophys.* 53 (2009) 75–100. doi:10.1007/s12013-009-9043-x.



## Chapter II: Computational study on the molecular conformations of phenolic compounds.

Laëtitia Cesari<sup>1</sup>, Laetitia Canabady-Rochelle<sup>1</sup>, Fabrice Mutelet<sup>1\*</sup>

1 : Université de Lorraine, Laboratoire Réactions et Génie des Procédés (LRGP, UMR CNRS-UL 7274), 1 rue Grandville, 54000 Nancy, France

Article paru dans Structural Chemistry :

L. Cesari, L. Canabady-Rochelle, F. Mutelet, Computational study on the molecular conformations of phenolic compounds, Struct. Chem. (2017). doi:10.1007/s11224-017-1017-9.

### Résumé

Ce chapitre est consacré à l'étude des conformations de huit composés phénoliques dans leur état isolé. Les conformations sont déterminées par calcul quantique en utilisant un haut niveau de théorie (B3LYP) et une base élevée (cc-pVTZ). Les surfaces d'énergie potentielle sont tracées en fonction de la rotation des substituants des composés phénoliques afin de pouvoir déterminer leurs minima et leurs états de transition. Il est montré que les conformations les plus stables sont obtenues lorsque les substituants se trouvent dans le plan du noyau benzénique entraînant alors la formation d'une liaison hydrogène intramoléculaire (cas du guaiacol, du pyrocatechol, du syringol et de la vanilline). Enfin, les barrières énergétiques et les fonctions potentielles présentent certaines similitudes suivant la rotation des substituants et leurs proches voisins.

**Abstract**

The study of the conformation of eight phenolic compounds (*i.e.* phenol, guaiacol, syringol, pyrocatechol, o-, m-, p-cresol and vanillin) was carried out using B3LYP method and cc-pVTZ basis set. Potential energy surfaces were plotted in order to identify the minimum energy structures and the transition states. For the first time, structures of vanillin and syringol were completely determined. Moreover, our work also confirms that the most stable conformations of m-cresol and p-cresol are obtained when the methyl group presents a hydrogen atom at the perpendicular of the benzene ring. The possibility of intramolecular hydrogen bonding and their parameters were investigated. Guaiacol, pyrocatechol, syringol and vanillin present a structure stabilized by the presence of a moderate hydrogen bond. Finally, potential energy barriers and rotational potential functions were also calculated. The comparisons of the rotational potential parameters for each molecule highlight the presence of similarities specific to each substituent and their neighbours.

## II-1. Introduction

Lignocellulosic residues produced by the forest industry have been considered as wastes until recently [1]. Yet, biomass can be used in many ways to provide either energy [2] or chemicals of high interest. With the increasing concerns about global warming and the depletion of fossil fuels resources, biochemicals arouse more interest as potential substitutes [3].

Studies have shown that pyrolysis of lignin could produce different kinds of bio-oils including several phenolic compounds such as phenol, guaiacol, syringol, o-, m-, p-cresol, pyrocatechol or vanillin [4–11]. After separation and purification, these compounds could be used as high value chemical feedstock in pharmaceuticals, agri-business, or chemicals industries [12–15]. Yet, pyrolytic oils derived from biomass are difficult to manipulate [16] and purification techniques such as distillation are not well adapted for the extraction of these compounds. Solvent extractions are preferably used, despite practical problems such as the redistribution of phenols in both phases [17] due to complex intermolecular phenomena.

The interactions between the compounds and the solvent play a major part into the extraction processes. For example, the presence of inter or intramolecular hydrogen bonds can either favour or reduce the solubility of a given molecule into the solvent. Thus, the knowledge of the preferential conformations of these phenolic compounds is required as a starting point for the further studies about interactions with solvent.

The parameters of intramolecular hydrogen bonding can be determined by different methods. Korth et al [18] studied the intramolecular hydrogen bonding in 2-substitued phenols by the cis-trans method which is the simplest and quickest one. Yet, Estácio et al [19] considered that the enthalpy of hydrogen bonding using this approach is overestimated, and preferred the ortho-para approach over the cis-trans and isodesmic ones.

Finally, quantum chemistry studies on the rotation of bonds in molecules allow the determination of conformers (*i.e.* global and local minima energy structures) and transition states. From these data, the energetic barriers can be calculated and the potential parameters regressed. The knowledge of such parameters facilitates the understanding of the behaviour of the molecules in a solvent.

Some studies were found in the literature on these phenolic compounds, but focusing only on one or few conformations and they related to different levels of theory and basis sets.

The conformation of phenol, already well investigated, showed that the energetically favoured position corresponds to a planar conformation [20–24].

Concerning cresols; Pohl and Kleinermanns [25] determined their structures by using *ab initio* calculations at low level of theory. The CNDO/2 molecular orbital method used by Dietrich et al [26] represented with good accuracy the experimental intramolecular hydrogen bond energy of o-cresol. Nevertheless, the most stable conformation cannot be determined using this method. Welzel et al [27] studied the internal rotation of the methyl group of o-cresol and evidenced 4 planar conformations corresponding to two different minima and two transition states.

P-cresol was subjected to many propositions of minimum energy structure. Balachandran et al [28] studied the p-cresol bonds variations with B3LYP and B3PW91 methods with the cc-pVDZ basis set. Their minimum structure did not present any negative frequency value and neither specified whether the global minimum was reached or not. Richardson et al [29] proposed a different minimum structure using the MP2 6-31G(d,p) level of theory. Hellweg et al [30] studied the internal rotation of the methyl group of p-cresol and evidenced 3 different structures: eclipsed, perpendicular and staggered at high level of theory and high basis set. They concluded that the global minimum structure is dependent on the level of theory and the basis set.

Helleweg et al [31] also investigated the internal rotation of the methyl group of m-cresol. In the same way, they discovered that the perpendicular position is stabilized by hyperconjugation and hence that this minimum cannot be observed with Hartree-Fock method.

The structure of pyrocatechol was well studied over the past decades. Puebla et al [32] studied the rotation barriers at the SCF/4-31G and 4-31G\* level of theory, and predicted two stable conformations. Bürgi and Leutwyler [33] found 6 structures at a high basis set. Yet, they only focused on one-dimensional calculation of one torsional vibration and thus neglected the effect of the coupling of two torsional modes. Conformations were also studied by other authors (Gerhards et al [34], Rudyk et al [35], Gómez-Zaleta et al [36], Mandado et al [37]). From experimental and theoretical studies, pyrocatechol is found in a planar conformation in which a hydrogen bond was observed between the OH groups [34]. Although Mandado et al [37] agreed with the conformations found, they rejected the hypothesis of a presence of intramolecular hydrogen bonding in the stable conformations.

The molecular conformations of guaiacol were completely studied by Agache and Popa [38] using MP2 and MP4SDQ methods with several basis sets. Conformation of minimum structures and transition states, including barrier heights and hydrogen bonds, were discussed. They demonstrated that the most stable structure is the cisoid conformation, confirmed by Dorofeeva et al [39] by gas-phase electron (GED) diffraction and *ab initio* calculations. Intramolecular hydrogen bond was observed between the hydroxyl group and the methoxy oxygen. Such interactions were studied computationally and experimentally by Varfolomeev et al [40].

Despite these numerous studies, there is still a lack of knowledge on the conformational structures of phenolic compounds of high interest such as vanillin [41] or syringol [42,43]. Indeed, the study of di-substituted phenol is quite complicated due to the various possible interactions between the different functional groups.

In the present work, we present a complete computational study of the conformational structures of eight phenols: phenol, guaiacol, syringol o-, m- p-cresol, pyrocatechol and vanillin. Potential energy surfaces were plotted to locate the minima and transition states. Energy barriers, potential parameters and intramolecular hydrogen bonds are also discussed.

## II-2. Computational methods

The quantum chemical calculations were performed with Gaussian[44] with Density Functional Theory (DFT) using Becke's three term hybrid exchange functional and the Lee, Yang and Parr correlation functional noted B3LYP [45–47]. Indeed, it is now well established that DFT can be used to determine the optimized geometry of molecules with high accuracy [48] and taking into account the electron correlation effects [49]. Because the global minimum energy structure can be basis set dependant, it is necessary to use a high basis set and a sufficient level of theory with a dynamic electron correlation to investigate and homogenize all different structures of the studied phenolic compounds.

The potential energy surfaces (PES) of the phenolic compounds were determined using the B3LYP method and cc-pVTZ basis set for the simultaneous rotations of specific dihedral angles from  $-180^\circ$  to  $+180^\circ$  with a step of  $30^\circ$ , then for each dihedral angle with a step of  $10^\circ$  while the others were set at specific values. Minima and transition states located on the PES were fully optimized (B3LYP/cc-pVTZ) using Berny algorithm with tight convergence criteria. No geometrical constraints were imposed on the molecule under study. Frequencies of the

optimized structures were calculated at the same level of theory in order to confirm if they correspond to a minimum or a transition state.

Quantitative potential energy profiles for rotation of substituents were calculated using least-squares fitted Fourier-type functions of a dihedral angle  $\tau$  [50].

$$V = \sum_{n=1}^n V_n [1 - \cos(n\tau)] + \sum_{m=1}^m V'_m \sin(m\tau) \quad (1)$$

The parameters  $V_n$  and  $V'_m$  correspond to potential energy relative to a reference value. When the molecule presents a symmetry around  $180^\circ$ , the sin terms are not considered.

Evaluation of the intramolecular hydrogen bond enthalpy was determined by the cis-trans method [19] calculated for the optimized structures.

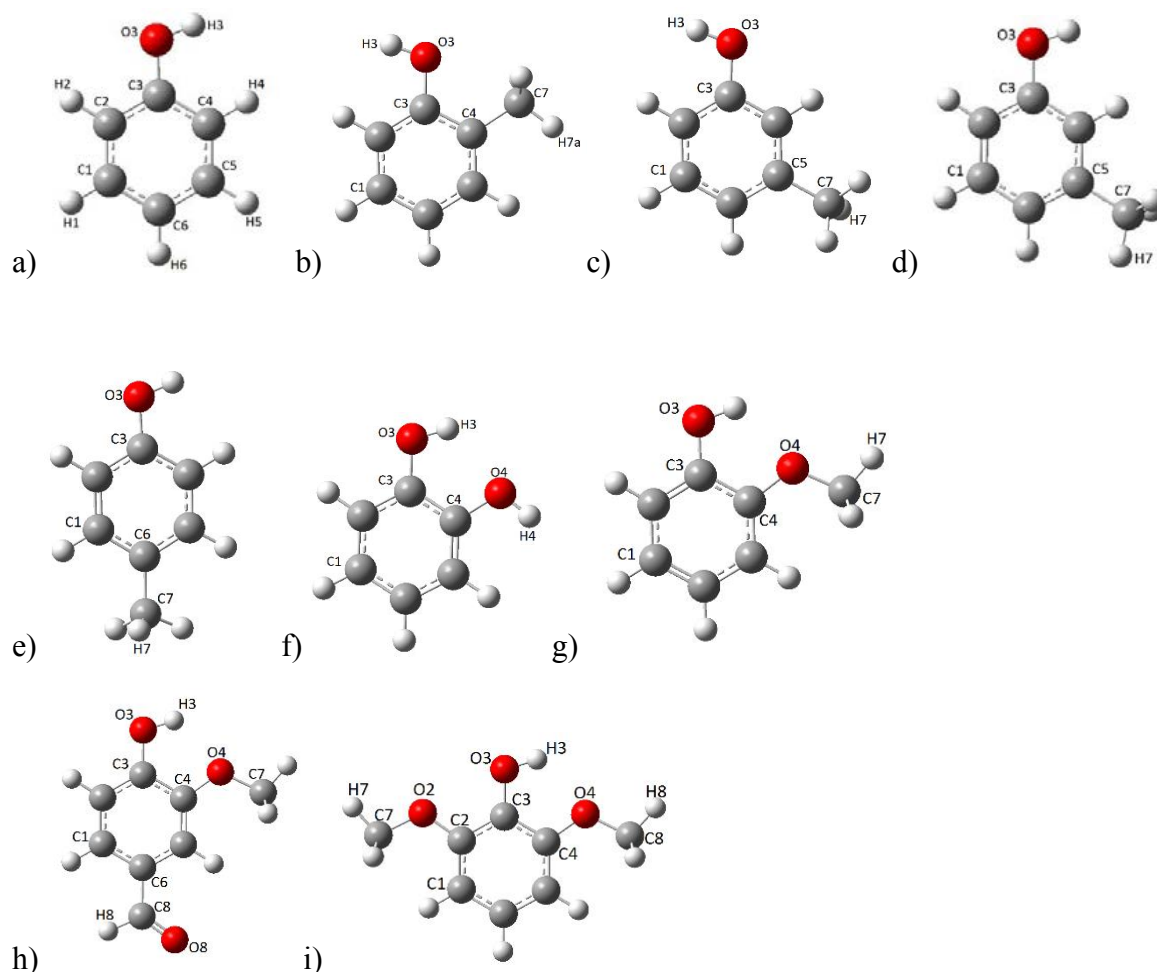
## II-3. Results and discussion

### II-3.1. Phenolic structures

Potential energy surfaces and structures of all of the conformations of the phenolic compounds are provided in supporting information. Global minima are depicted in Figure II-1.

**Phenol.** The potential energy curve for the rotation of the dihedral angle C2-C3-O3-H3 corresponding to the hydroxyl group of phenol is plotted in Figure S1 (Appendix I). Two global minima ( $C_{1a}$ ,  $C_{1b}$ ) are indistinguishable and correspond to the hydroxyl group in the aromatic plane at  $0^\circ$  or  $180^\circ$  [22][43]. The internal rotation of the hydroxyl group is made through two indistinguishable transition states  $TS_{1a}$  and  $TS_{1b}$  corresponding to a configuration with the hydroxyl group at the perpendicular of the benzene plane. This rotation presents an energy barrier of  $15.97 \text{ kJ}\cdot\text{mol}^{-1}$ . Structures are presented in Table S1.

**Figure II-1:** Global minimum energy structure of the studied phenolic compounds: a) phenol, b) o-cresol, c) *trans*-m-cresol, d) *cis*-m-cresol, e) p-cresol, f) pyrocatechol, g) guaiacol, h) vanillin, i) syringol.



***O*-cresol.** The potential energy surface for the rotation of the C2-C3-O3-H3 and C3-C4-C7-H7 dihedral angles of *o*-cresol, for the hydroxyl and methyl groups respectively, is presented in Figure S2. Specific potential energy curves with frozen coordinates of the *o*-cresol groups are displayed in Figure S3 and the corresponding structures are detailed in Tables S2a and S2b. All structures (minimum C and transition states TS) are obtained when one hydrogen atom of the methyl group is in the aromatic plane. Minimum structures are found when one hydrogen atom of the methyl group C3-C4-C7-H7 is at 180° and the hydroxyl group C2-C3-O3-H3 is respectively at 0° (*trans*-*o*-cresol C<sub>1</sub>) [25]·[27]·[43] or at 180° (*cis*-*o*-cresol C<sub>2</sub>). *Trans*-*o*-cresol conformer corresponds to the global minimum because of its higher stability than *cis*-*o*-cresol ( $\Delta E = 1.63\text{kJ}\cdot\text{mol}^{-1}$ ).

The structure of *trans*-o-cresol can be observed through three similar conformations ( $C_{1a}$ ,  $C_{1b}$ ,  $C_{1c}$ ) corresponding to the same structure with respect to the internal rotation of the hydrogen atoms. The transition between two structures  $C_1$  goes by three similar conformations ( $TS_{1a}$ ,  $TS_{1b}$ ,  $TS_{1c}$ ) with an energy barrier of  $3.99 \text{ kJ}\cdot\text{mol}^{-1}$  corresponding to the methyl group rotation. The same phenomenon is observed for *cis*-o-cresol with an energy barrier of  $6.43 \text{ kJ}\cdot\text{mol}^{-1}$ . A good agreement is observed with calculated values obtained by Aota et al [51]. Indeed, the former authors found that the energy value of *trans*-o-cresol is  $4.01 \text{ kJ}\cdot\text{mol}^{-1}$  lower than those obtained for *cis* o-cresol. Welzel and al [27] found the energy barrier in the same range of value for the MP2/6-311G\*\* level of theory. The interconversion of the  $C_1$  and  $C_2$  conformations goes by two symmetrical transition states  $TS_3$  and  $TS_4$  and requires an energy of  $16 \text{ kJ}\cdot\text{mol}^{-1}$  from *trans* to *cis* conformations and  $14.37 \text{ kJ}\cdot\text{mol}^{-1}$  for the reverse one.

***M-cresol.*** The potential energy surface corresponding to the torsion of the C2-C3-O3-H3 (hydroxyl) and C4-C5-C7-H7 (methyl) angles of m-cresol is plotted in Figure S4. One can observe that the conformations are more stable when the hydroxyl group is in the plane of the benzene ring, while the rotation of the methyl group does not seem to need a huge amount of energy. The rotation of each group in specific conditions are plotted in Figures S5 and S6. Figure S5 shows that the potential energy curves plotted in function of the variation of the methyl angle (C2-C3-O3-H3 fixed at  $0^\circ$  or  $180^\circ$ ) are in the same range of values (inferior to  $0.4 \text{ kJ}\cdot\text{mol}^{-1}$ ). Figure S6 presents the energy variation in function of the hydroxyl angle in *trans* m-cresol. The maximum energy is found with an angle of  $90^\circ$  and it corresponds to a barrier of rotation of  $16.04 \text{ kJ}\cdot\text{mol}^{-1}$  (equivalent to  $1340 \text{ cm}^{-1}$ ). This result is in good agreement with experimental data from microwave spectroscopy that shows a rotation barrier of about  $1300 \text{ cm}^{-1}$  [25]. The global energy minima of m-cresol correspond to the conformations when one methyl hydrogen is almost at the perpendicular of the benzene ring ( $C_1$  and  $C_2$ ) and the hydroxyl group in *trans*-position. Two rotation barriers for the *trans* m-cresol exist and are equal to  $0.06$  and  $0.07 \text{ kJ}\cdot\text{mol}^{-1}$  ( $4.8$  and  $5.9 \text{ cm}^{-1}$ ). This result is in good agreement with laser induced fluorescence that found a doublet spacing at about  $4 \text{ cm}^{-1}$  due to the hindered rotation of the methyl group [52]. Two other minima similar at  $C_1$  and  $C_2$  are found, but with a *cis*-configuration of the hydroxyl group ( $C_3$  and  $C_4$ ). The difference of energy between *trans* and *cis* conformations is so low ( $0.094 \text{ kJ}\cdot\text{mol}^{-1}$ ) that both *trans* and *cis* conformations can be considered as global energy minima. Same conclusion was also observed by Pohl and Kleinermanns [25] and by Hellweg and al [31]. Finally, another conformation is found with a

*cis*-position for the hydroxyl group and a *trans*-position for the methyl one, in the plane of the benzene ring (C<sub>5</sub>).

The inversion between C<sub>1</sub> and C<sub>2</sub> can be made through the rotation of the methyl group. Two transition states (TS<sub>1</sub> and TS<sub>2</sub>) were found in which one of the methyl hydrogen is in the plane of the benzene ring (respectively in *cis* and *trans*-positions). Each configuration can be represented by three different values of the C4-C5-C7-H7 angle, due to the position of the hydrogen atoms. In the *cis*-conformation of the hydroxyl group, the rotation of the methyl hydrogens shows that the two conformations C<sub>3</sub> and C<sub>4</sub> can be achieved at very low energy barrier (about 3.7 J.mol<sup>-1</sup>). This rotation goes through the other conformation C<sub>5</sub> and two transition states TS<sub>4</sub> and TS<sub>5</sub>. Such conformations can only be observed if the step on the rotation of the methyl group is small enough (Figure S5b). The hydrogen atoms in the C<sub>3</sub> or C<sub>4</sub> configurations can also rotate *via* a transition state TS<sub>3</sub> when the two groups (hydroxyl and methyl) are in the *cis*-position. In this case, an energy barrier of about 0.26 kJ.mol<sup>-1</sup> is required. Figure S6 shows the rotation of the hydroxyl group C2-C3-O3-H3 while the methyl angle C4-C5-C7-H7 is fixed at 180°. Transition states (TS<sub>6</sub> and TS<sub>7</sub>) are found when the angle reaches the value of -90° and 90°. Between this two states, the C2-C3-O3-H3 angle goes by 0°, corresponding to the TS<sub>2</sub> conformation. All the conformations were optimized at the B3LYP/cc-pVTZ level of theory. Details are presented in Table S3.

***P-cresol***. The potential energy surface corresponding to the rotation of the C2-C3-O3-H3 (hydroxy) and C5-C6-C7-H7 (methyl) groups is plotted in Figure S7. As for *m-cresol*, one can observe that the conformations presenting the minimum energy are when the hydroxyl group is in the plane of the benzene ring [25][28][30][53]. *P-cresol* has three different minimum energy conformations: two of them when one methyl hydrogen is almost at the perpendicular of the benzene ring (C<sub>1</sub> and C<sub>2</sub>), and another one when the hydrogen atom is in the plane in *cis*-position with respect to the hydroxyl hydrogen (C<sub>3</sub>) (Table S4a). Figure S8a shows that the three conformations are very close in terms of energy to each other. Many papers present only one configuration as the most stable conformation: Hameka et al [53] and Richardson et al [29] found that the planar conformation (C<sub>3</sub>) is the most stable conformation, whereas Pohl et al [25] and Balachandran [28] figured out the most stable conformation does not have a hydrogen in the plane of the benzene ring. Only Hellweg et al [30] came up with the influence of the basis set and the level of theory on the conformation optimization. Without a dynamic electron

correlation and a sufficient basis set, the perpendicular conformations ( $C_1$  and  $C_2$ ) cannot be evidenced.

The inversion between  $C_1$  and  $C_2$  can be made with the rotation of the hydroxyl group through two transition states  $TS_1$  and  $TS_2$  when the C2-C3-O3-H3 angle reaches respectively  $-90^\circ$  and  $90^\circ$  (Figure S9). As expected, the required energy ( $13.77\text{kJ}\cdot\text{mol}^{-1}$ , equivalent to  $1151\text{ cm}^{-1}$ ) is weaker than those for the o- or m-cresol. The rotation of the methyl group allows the molecule to switch between the 3 conformations through different transition states. The  $TS_3$  structure corresponds to an anti-planar position of the methyl group with respect to the hydroxyl group and presents a very high energy barrier ( $0.22\text{kJ}\cdot\text{mol}^{-1}$ ) compared to transition states  $TS_4$  and  $TS_5$  ( $0.007\text{kJ}\cdot\text{mol}^{-1}$ ) as seen in Figure S8b.

**Pyrocatechol.** The potential energy surface and potential energy curves for the rotation of the hydroxyl groups (C3-C4-O4-H4 and C2-C3-O3-H3 dihedral angles) of pyrocatechol are plotted in Figures S10 and S11. Two global minima ( $C_{1a}$ ,  $C_{1b}$ ) are observed, symmetric to one another and correspond to the *cisoid* conformations [32][34][35]. The hydroxyl groups present the same angle value ( $180^\circ$  or  $0^\circ$ ) and therefore allow the formation of a moderate intramolecular hydrogen bond [35][54] whose characteristics are detailed as follows: distance between the donor-acceptor atoms dH3-O4:  $2.146\text{ \AA}$ , distance between the two electronegative atoms dO3-O4 :  $2.682\text{ \AA}$ , bond angle O3-H3--O4:  $113.6^\circ$  and bonding energy  $\Delta H_{\text{intra-HB}}$ :  $16.02\text{ kJ}\cdot\text{mol}^{-1}$ . Similar values were found by Rudyk et al [35] and Korth et al [18] at the B3LYP/6-31G(d,p) level of theory: dH-O:  $2.123\text{ \AA}$ , dO-O:  $2.675\text{ \AA}$ , O-H--O:  $114.6^\circ$ . The passage of one *cisoid* conformation to another one can be made by a transition structure ( $TS_3$ ) of  $27.43\text{ kJ}\cdot\text{mol}^{-1}$  with the hydrogen atoms of the hydroxyl groups next to each other in the aromatic plane. A local minimum ( $C_2$ ) is also noticed presenting a *transoid* conformation ( $\Delta E=16.02\text{ kJ}\cdot\text{mol}^{-1}$ ). In the literature, the energy difference between  $C_1$  and  $C_2$  is 19.1, 18.94, 7.52 and  $14.59\text{ kJ}\cdot\text{mol}^{-1}$  with HF using 6-31G(d,p), 6-311++G(d,p), PM3 and AM1 basis sets, respectively [33][55].

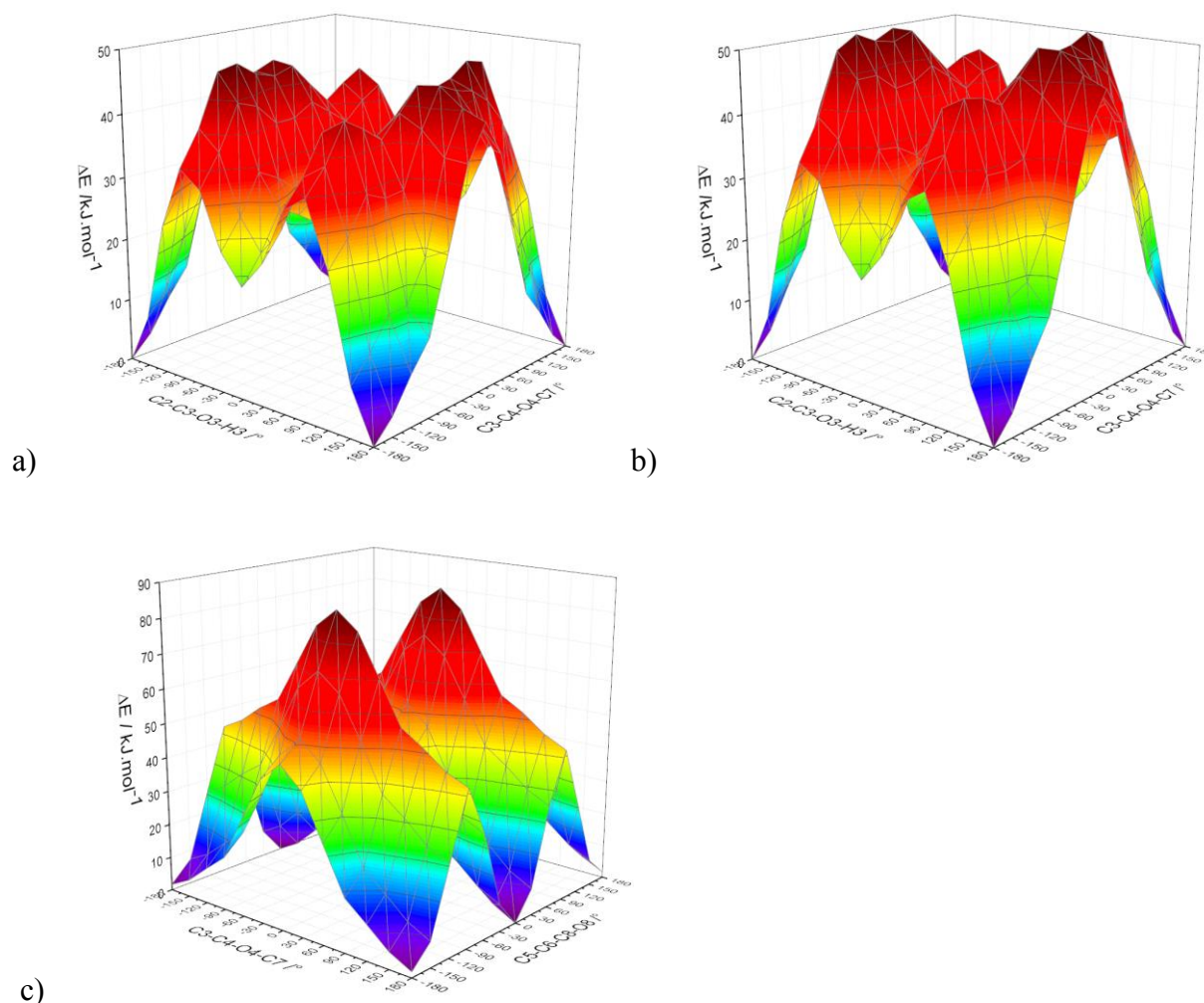
The interconversion between the *cisoid* and the *transoid* conformations goes through symmetrical transitions states ( $TS_{1a}$ ,  $TS_{1b}$ ,  $TS_{2a}$ ,  $TS_{2b}$ ) with one hydroxyl group in the perpendicular of the aromatic plane and an energy barrier of  $26.94\text{ kJ}\cdot\text{mol}^{-1}$  for the pathway  $C_1$  to  $C_2$  and  $10.92\text{ kJ}\cdot\text{mol}^{-1}$  for the reverse one.

**Guaiacol.** The potential energy surface and potential energy curves for the rotation of the guaiacol groups are presented in Figures S12 and S13. The C3-C4-O4-C7 and C2-C3-O3-H3 dihedral angles correspond respectively to the methoxy and hydroxyl groups. A global minimum is observed when the two dihedral angles are almost at a value of  $180^\circ$ , which corresponds to a *cisoid* conformation [38][39]. As for pyrocatechol, it is stabilized by the formation of a moderate intramolecular hydrogen bond between the phenolic hydrogen and the methoxy oxygen, whose details are as follows: distance between the donor-acceptor atoms dH3-O4: 2.099 Å, distance between the two electronegative atoms dO3-O4 : 2.649 Å, bond angle O3-H3--O4:  $114.5^\circ$ , bonding energy  $\Delta H_{\text{intra-HB}}$ : 17.56 kJ.mol<sup>-1</sup>. Similar values were found by Korth and al [18] at the B3LYP/6-31G(d,p) level of theory: dH-O: 2.077 Å, bond angle O-H--O:  $115.5^\circ$ . The bonding energy value is coherent with those found in the literature: Agache and al (2006) [38]: 18.09kJ.mol<sup>-1</sup> for MP2/6-311G(d,p), Varfolomeev and al [40]: 18.8 kJ.mol<sup>-1</sup> for B3LYP/6-31++G(d,p), 18.9 kJ.mol<sup>-1</sup> for B3LYP/6-311++G(d,p), 17.1 kJ.mol<sup>-1</sup> for B3LYP/6-311++G(2df,2p) and 16.9 kJ.mol<sup>-1</sup> for B3LYP/6-311++G(3dfd,2pd).

Another minimum conformation can be noticed with a *transoid* conformation where the methoxy angle is maintained at  $180^\circ$  and the hydroxyl group moves to an angle of  $0^\circ$ . This rotation is made through two symmetrical transition states TS<sub>1</sub> and TS<sub>2</sub> where the hydroxyl group is almost perpendicular at the aromatic plane. One can remark two other minima symmetrical to each other (C<sub>3</sub> and C<sub>4</sub>) with the methoxy group not in the aromatic plane (dihedral angle C3-C4-O4-C7 of  $\pm 67^\circ$ ). These two conformations can be achieved from the *transoid* molecule *via* two transition states TS<sub>3</sub> and TS<sub>4</sub> also symmetrical to each other. The last transition state TS<sub>5</sub> allows the interconversion between C<sub>3</sub> and C<sub>4</sub> with an energy barrier at 5.9 kJ.mol<sup>-1</sup>. The structures are detailed in Table S6.

**Vanillin.** The potential energy surfaces and potential energy curves for the rotation of the vanillin's groups are presented in Figure II-2 and in appendix I (Figure S14). The C2-C3-O3-H3, C3-C4-O4-C7 and C5-C6-C8-O8 dihedral angles correspond respectively to the hydroxyl, methoxy and aldehyde groups.

**Figure II-2:** Potential Energy Surface of vanillin as a function of the torsion of C2-C3-O3-H3 (hydroxy) and C3-C4-O4-C7 (methoxy) angles with C5-C6-C8-O8 (aldehyde) frozen at a) 180°, b) frozen at 0°, c) Potential Energy Surface of vanillin as a function of the torsion of C3-C4-O4-C7 (methoxy) and C5-C6-C8-O8 (aldehyde) with C2-C3-O10-H11 (hydroxy) frozen at 180°, at B3LYP/cc-pVTZ.



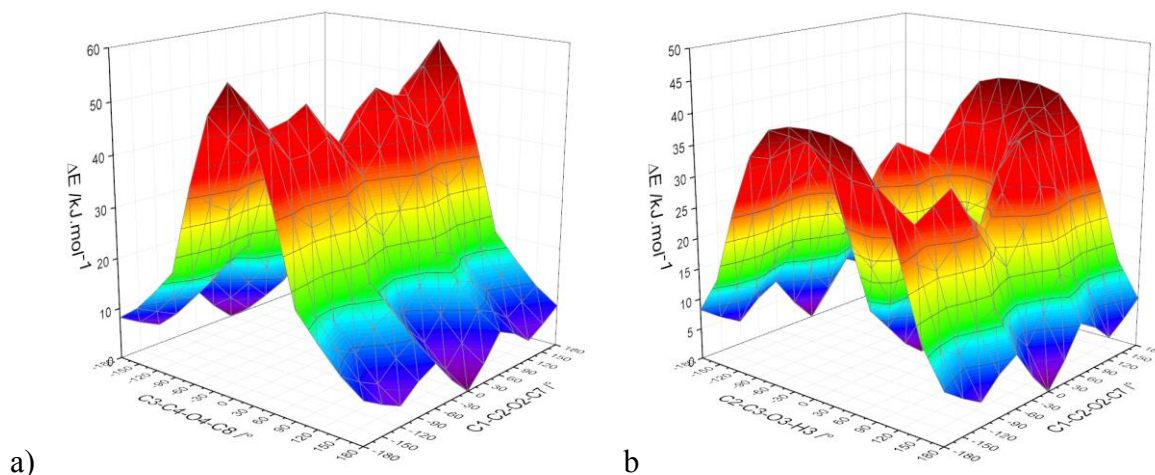
One can observe that the potential energy surfaces of vanillin looks like the guaiacol's one. Indeed, the chemical structure of vanillin is similar to the guaiacol one, only with the addition of an aldehyde group on the benzene ring. The configurations present minimum energy structures when the aldehyde is located in the plane of the benzene ring. The same configurations as for guaiacol are observed, with respect to the orientation of the aldehyde: two *cisoid* conformations with the hydroxyl and methoxy dihedral angles at 180° (C<sub>1</sub> and C<sub>2</sub>), two *transoid* conformations with the hydroxyl dihedral angle moving to 0° (C<sub>3</sub> and C<sub>4</sub>), and two groups of symmetrical conformations when the methoxy group is not in the plane of the benzene ring (C<sub>5</sub>-C<sub>7</sub> and C<sub>6</sub>-C<sub>8</sub>).

The *cisoid* configurations are more stable because of the presence of a moderate intramolecular hydrogen bonding between the phenolic hydrogen and the methoxy oxygen. Characteristics of the bond are described as follows: distance between the donor-acceptor atoms dH3-O4: 2.083 Å, bond angle O3-H3--O4: 114.6°, distance between the two electronegative atoms O3-O4: 2.635 Å, bonding energy  $\Delta H_{\text{intra-HB}}$ : 18.92 kJ.mol<sup>-1</sup> for C<sub>1</sub> conformation, and distance between the donor-acceptor atoms dH3-O4: 2.092 Å, bond angle O3-H3--O4: 114.3°, distance between the two electronegative atoms O3-O4: 2.641 Å, bonding energy  $\Delta H_{\text{intra-HB}}$ : 17.74 kJ.mol<sup>-1</sup> for C<sub>2</sub> conformation. Intermolecular hydrogen bonding data of C<sub>2</sub> are similar with those obtained for guaiacol (see above). The global minimum is found in the *cisoid* conformation, when the oxygen atom from the aldehyde is facing the methoxy group (C<sub>1</sub>), corresponding to a dihedral angle of 0°. This structure seems to interact with the methoxy group and reduces the length of the hydrogen bond. This explains the small differences obtained for this configuration with guaiacol. Our results confirm the hypothesis made by Cocinero and al [41] that the two most stable conformations of vanillin are the ones with the intermolecular hydrogen bonds.

Transition from a structure to another one can be obtained through the rotation of the hydroxyl (Figure S15), methoxy (Figure S16) or aldehyde group (Figure S17) around the benzene ring. The rotation for the *transoid* conformation to the *cisoid* ones can easily be made with the rotation of the hydroxyl group through an energy barrier of 16.19 kJ.mol<sup>-1</sup> and 16.16 kJ.mol<sup>-1</sup> respectively to the C<sub>3</sub>-C<sub>1</sub> through TS<sub>9</sub> or TS<sub>10</sub> and C<sub>4</sub>-C<sub>2</sub> rotations through TS<sub>11</sub> or TS<sub>12</sub>. The symmetrical configurations C<sub>6</sub> and C<sub>8</sub> (respectively C<sub>5</sub> and C<sub>7</sub>) can be switched from one to another with the rotation of the methoxy group through a transition state TS<sub>15</sub> (respectively TS<sub>18</sub>) with a barrier of 6.0 kJ.mol<sup>-1</sup> (respectively 6.38 kJ.mol<sup>-1</sup>) or to the *transoid* conformation C<sub>3</sub> (respectively C<sub>4</sub>) through two transition states TS<sub>13</sub> and TS<sub>14</sub> (respectively TS<sub>16</sub> and TS<sub>17</sub>). The inversion between the configurations through the rotation of the aldehyde can be observed but it requires much more energy (43.77 kJ.mol<sup>-1</sup> for the *cisoid* conformations C<sub>2</sub> toward C<sub>1</sub>).

**Syringol.** The conformations of syringol are investigated with the rotation of the three groups located around the benzene ring. The dihedral angles C2-C3-O3-H3, C1-C2-O2-C7 and C3-C4-O4-C8 describe respectively the angle between the hydroxyl, methoxyl and methoxyl group with the plane of the benzene ring. The potential energy surfaces of syringol are displayed in Figures II-3 a) and b).

**Figure II-3:** a) Potential Energy Surface of syringol as a function of the torsion of C1-C2-O2-C7 (methoxyl) and C3-C4-O4-C8 (methoxyl) angles with C2-C3-O3-H3 (hydroxy) frozen at 180° at B3LYP/cc-pVTZ, b) Potential Energy Surface of syringol as a function of the torsion of C1-C2-O2-C7 (methoxyl) and C2-C3-O3-H3 (hydroxyl) angles with C3-C4-O4-C8 (methoxyl) frozen at 180° at B3LYP/cc-pVTZ.



One can see that the minimum energy structures are obtained when the hydroxyl group is in the plane of the benzene ring. Figure S19 and S20 show the rotation of some dihedral angles in specific conditions. The minimum energy structures of syringol are found when the hydroxyl group is in the plane of the benzene ring (C2-C3-O3-H3 at 180°) creating a moderate intramolecular hydrogen bond with one of the methoxy group (C3-C4-O4-C8 at 180°). Figure S19 shows the variation of the energy of the structure with the rotation of the C1-C2-O2-C7 angle while the C2-C3-O3-H3 and C3-C4-O4-C8 dihedral angles are maintained at 180°. Three minima structures can be observed: one in the plane of the benzene ring with C1-C2-O2-C7 at 0° (C<sub>1</sub>) [43], and two others symmetrical with C1-C2-O2-C7 at -120° (C<sub>2</sub>) and +120° (C<sub>3</sub>).

The characteristics about the intramolecular hydrogen bonding for C<sub>1</sub> is detailed as follows: distance between the donor-acceptor atoms dH3-O4: 2.088 Å, bond angle O3-H3--O4: 114.8°, distance between the two electronegative atoms O3-O4: 2.643 Å. Due to the symmetry of the molecule, the bonding energy  $\Delta H_{\text{intra-HB}}$  could not be calculated by the cis-trans method.

The torsion of the methoxy group C1-C2-O2-C7 allows the switch from C<sub>2</sub> or C<sub>3</sub> conformations towards C<sub>1</sub> through two symmetrical transition states TS<sub>1</sub> and TS<sub>2</sub> where C1-C2-O2-C7 reaches the value of -64° and 64° respectively. The interconversion between C<sub>2</sub> and C<sub>3</sub> can also happen

directly through the transition state TS<sub>3</sub> when the C1-C2-O2-C7 is at 180° with an energy barrier of 4.4 kJ.mol<sup>-1</sup>.

The torsion of the hydroxyl group C2-C3-O3-H3 can also serve the conversion from one conformation to another but it requires more energy. The C<sub>1</sub> conformation can achieve its symmetrical form (C2-C3-O3-H3 at 180° to 0°) through the transition state TS<sub>4</sub> when the hydroxyl group is at the perpendicular of the plane of the benzene ring, with an energy barrier of 22.98 kJ.mol<sup>-1</sup>. Two transition states TS<sub>5</sub> and TS<sub>6</sub> also exist corresponding to the dihedral angles C2-C3-O3-H3 at 90° and C1-C2-O2-C7 at -120° (respectively -90° and 120°). These two transition states are also connected to another transition state TS<sub>7</sub> as seen in Figure S20. TS<sub>5</sub> and TS<sub>6</sub> can also achieve the TS<sub>4</sub> conformation by rotation of their methoxyl group C1-C2-O2-C7 from their value to 0° (not shown in graphs).

### II-3.2. Minimum structures

The bond lengths and angles of the ground state are listed in Tables II-1 and II-2 for each phenolic compound. Three dimensional single crystal X-ray diffraction data taken from literature[56–61] are also listed as reference points for comparison.

One can observe that the results for phenol is in good agreement with the experimental geometry parameters obtained by Larsen et al[61]. The maximum deviation is noticed for C5-C6, C3-O3 and O3-H3 (0.42%, 0.60% and 0.55% respectively), which are very small. The average deviation of 0.3° is obtained for the bond angle, with a maximum in the C2-C3-C4 angle of 0.9°.

Bois observed experimentally two structures for the o-cresol [58] and m-cresol [60] molecules. These structures correspond to the *cis* and *trans* configurations with respect to the hydroxyl group. However, only one structure was observed for p-cresol [59]. One conformation was found experimentally for vanillin and pyrocatechol by Velavan et al [57] and Brown [56] respectively, which are in agreement with those obtained by quantum calculations in this work. No experimental data are available in the literature for guaiacol or syringol.

Lei Zhang et al [43] have demonstrated that the C-C bond length increases at the substituent position for guaiacol, o-,m-,p-cresol and syringol. Same behaviour is observed in this work, even for pyrocatechol and vanillin (bold numbers in Table II-1). Moreover, these bonds are antiperiplanar to the C-O (for methoxyl) or C-H (for methyl) bond of the substituent.

**Table II-1:** Bond lengths for the ground state global minimum of phenolic compounds.

Phenol			Guaiacol			O-cresol			M-cresol				P-cresol			Pyrocatechol			Syringol		Vanillin		
bond	calc	exp	bond	calc	bond	calc	exp	cis		exp	bond	calc	exp	bond	calc	exp	bond	calc	bond	calc	bond	calc	exp
								calc	calc														
C1-C2	1.387	1.392	C1-C2	1.393	C1-C2	1.390	1.39	C1-C2	1.385	1.390	1.38	C1-C2	1.386	1.395	C1-C2	1.392	1.391	C1-C2	1.396	C1-C2	1.389	1.378	1.378
C2-C3	1.393	1.391	C2-C3	1.385	C2-C3	1.391	1.38	C2-C3	1.393	1.392	1.40	C2-C3	1.393	1.387	C2-C3	1.387	1.381	C2-C3	<b>1.399</b>	C2-C3	1.386	1.381	1.381
C3-C4	1.393	1.391	C3-C4	<b>1.405</b>	C3-C4	<b>1.401</b>	1.40	C3-C4	1.391	1.392	1.40	C3-C4	1.390	1.388	C3-C4	<b>1.400</b>	1.389	C3-C4	<b>1.397</b>	C3-C4	<b>1.413</b>	1.403	1.403
C4-C5	1.390	1.394	C4-C5	1.387	C4-C5	1.392	1.40	C4-C5	<b>1.396</b>	1.392	1.39	C4-C5	1.391	1.401	C4-C5	1.385	1.372	C4-C5	1.391	C4-C5	1.377	1.370	1.370
C5-C6	1.389	1.395	C5-C6	1.396	C5-C6	1.392	1.40	C5-C6	1.393	<b>1.397</b>	1.41	C5-C6	1.392	1.396	C5-C6	1.393	1.399	C5-C6	1.389	C5-C6	<b>1.404</b>	1.400	1.400
C6-C1	1.392	1.395	C6-C1	1.386	C6-C1	1.387	1.40	C6-C1	1.392	1.388	1.40	C6-C1	<b>1.398</b>	1.399	C6-C1	1.388	1.378	C6-C1	1.389	C6-C1	1.392	1.379	1.379
C1-H1	1.082	1.084	C1-H1	1.081	C1-H1	1.082	-	C1-H1	1.082	1.082	-	C1-H1	1.083	1.0	C1-H1	1.081	-	C1-H1	1.079	C1-H1	1.083	-	-
C2-H2	1.081	1.081	C2-H2	1.081	C2-H2	1.084	-	C2-H2	1.081	1.084	-	C2-H2	1.081	1.1	C2-H2	1.081	-	C5-H5	1.079	C2-H2	1.081	-	-
C4-H4	1.084	1.086	C5-H5	1.080	C5-H5	1.083	-	C4-H4	1.085	1.082	-	C4-H4	1.084	1.0	C5-H5	1.084	-	C6-H6	1.081	C5-H5	1.080	-	-
C5-H5	1.082	1.084	C6-H6	1.081	C6-H6	1.081	-	C6-H6	1.082	1.082	-	C5-H5	1.083	1.0	C6-H6	1.081	-	-	-	-	-	-	-
C6-H6	1.081	1.080	-	-	-	-	-	-	-	-	-	-	-	-	-	-	-	-	-	-	-	-	
C3-O3	1.367	1.375	C3-O3	1.362	C3-O3	1.370	1.38	C3-O3	1.367	1.368	1.39	C3-O3	1.368	1.391	C3-O3	1.363	1.364	C3-O3	1.361	C3-O3	1.352	1.348	1.348
O3-H3	0.962	0.957	O3-H3	<u>0.966</u>	O3-H3	0.962	-	O3-H3	0.962	0.962	-	O3-H3	0.962	1.0	O3-H3	0.965	-	O3-H3	<u>0.966</u>	O3-H3	<u>0.967</u>	-	-
-	-	-	C4-O4	1.372	C4-C7	1.503	1.52	C5-C7	1.507	1.507	1.54	C6-C7	1.507	1.517	C4-O4	1.377	1.380	C4-O4	1.373	C4-O4	1.367	1.360	1.360
-	-	-	O4-C7	1.418	C7-H7a	1.089	-	C7-H7a	1.093	1.090	-	C7-H7a	1.093	-	O4-H4	<u>0.961</u>	-	O4-C8	1.418	O4-C7	1.423	1.430	1.430
-	-	-	C7-H7a	1.087	C7-H7b	1.092	-	C7-H7b	1.091	1.090	-	C7-H7b	1.091	1.0	-	-	-	C8-H8a	1.093	C7-H7a	1.092	-	-
-	-	-	C7-H7b	1.093	C7-H7c	1.092	-	C7-H7c	1.089	1.093	-	C7-H7c	1.090	-	-	-	-	C8-H8b	1.087	C7-H7b	1.092	-	-
-	-	-	C7-H7c	1.093	-	-	-	-	-	-	-	-	-	-	-	-	-	C8-H8c	1.093	C7-H7c	1.086	-	-
-	-	-	-	-	-	-	-	-	-	-	-	-	-	-	-	-	-	C2-O2	1.360	C6-C8	1.468	1.459	1.459
-	-	-	-	-	-	-	-	-	-	-	-	-	-	-	-	-	-	O2-C7	1.416	C8-H8	1.109	-	-
-	-	-	-	-	-	-	-	-	-	-	-	-	-	-	-	-	-	C7-H7a	1.087	C8=O8	1.212	1.205	1.205
-	-	-	-	-	-	-	-	-	-	-	-	-	-	-	-	-	-	C7-H7b	1.094	-	-	-	-
-	-	-	-	-	-	-	-	-	-	-	-	-	-	-	-	-	-	C7-H7c	1.094	-	-	-	-

Table II-2: Bond angles for the ground state global minimum of phenolic compounds.

Phenol			Guaiacol			O-Cresol			M-Cresol				P-Cresol			Pyrocatechol			Syringol			Vanillin				
									cis		trans															
angle	calc	exp litt	angle	calc	angle	calc	exp litt	angle	calc	calc	exp litt	angle	calc	exp litt	angle	calc	exp litt	angle	calc	angle	calc	angle	calc	exp litt		
C1-C2-C3	119.6	119.2	C1-C2-C3	120.1	C1-C2-C3	120.1	120	C1-C2-C3	119.0	119.2	118	C1-C2-C3	119.8	119.7	C1-C2-C3	120.2	119.5	C1-C2-C3	119.5	C1-C2-C3	119.6	120.0				
C2-C3-C4	120.0	120.9	C2-C3-C4	119.7	C2-C3-C4	121.1	122	C2-C3-C4	120.2	120.2	122	C2-C3-C4	119.5	120.5	C2-C3-C4	119.4	120.4	C2-C3-C4	119.6	C2-C3-C4	120.1	119.9				
C3-C4-C5	119.8	119.4	C3-C4-C5	120.1	C3-C4-C5	117.6	117	C3-C4-C5	120.9	120.7	120	C3-C4-C5	119.9	118.7	C3-C4-C5	120.4	120.4	C3-C4-C5	121.0	C3-C4-C5	120.1	119.8				
C4-C5-C6	120.5	120.5	C4-C5-C6	119.7	C4-C5-C6	122.0	122	C4-C5-C6	118.6	118.9	119	C4-C5-C6	121.5	121.6	C4-C5-C6	119.9	119.2	C4-C5-C6	118.8	C4-C5-C6	119.7	120.2				
C5-C6-C1	119.3	119.2	C5-C6-C1	120.1	C5-C6-C1	119.4	120	C5-C6-C1	120.3	120.3	121	C5-C6-C1	117.5	117.8	C5-C6-C1	119.8	120.6	C5-C6-C1	121.0	C5-C6-C1	120.0	119.6				
C6-C1-C2	120.8	120.8	C6-C1-C2	120.2	C6-C1-C2	119.9	119	C6-C1-C2	120.9	120.7	121	C6-C1-C2	121.7	121.2	C6-C1-C2	120.3	119.9	C6-C1-C2	120.1	C6-C1-C2	120.5	120.6				
C1-C2-H2	121.4	121.6	C1-C2-H2	121.4	C1-C2-H2	120.3	-	C1-C2-H2	121.7	120.6	-	C1-C2-H2	121.2	-	C1-C2-H2	121.4	-	C4-C5-H5	120.9	C1-C2-H8	121.7	-				
C3-C4-H4	119.9	120.0	C4-C5-H5	120.5	C4-C5-H5	118.5	-	C3-C4-H4	119.5	118.5	-	C3-C4-H4	120.0	-	C4-C5-H5	119.6	-	C5-C6-H6	119.5	C4-C5-H9	122.2	-				
C4-C5-H5	119.3	119.5	C5-C6-H6	119.4	C5-C6-H6	120.1	-	C5-C6-H6	119.7	119.8	-	C4-C5-H5	118.9	-	C5-C6-H6	119.7	-	C6-C1-H1	119.7	C6-C1-H7	119.6	-				
C5-C6-H3	120.3	120.3	C6-C1-H1	120.3	C6-C1-H1	120.5	-	C6-C1-H1	119.7	119.9	-	C6-C1-H1	119.4	-	C6-C1-H1	120.2	-	-	-	-	-	-	-	-	-	-
C6-C1-H1	120.0	119.8	-	-	-	-	-	-	-	-	-	-	-	-	-	-	-	-	-	-	-	-	-	-	-	
C2-C3-O3	117.5	117.0	C2-C3-O3	120.1	C2-C3-O3	122.0	120	C2-C3-O3	117.4	122.5	cis 118/trans120.75	C2-C3-O3	117.6	117.4	C2-C3-O3	120.0	118.6	C2-C3-O3	119.6	C2-C3-O3	120.0	118.3				
C4-C3-O3	122.5	-	C4-C3-O3	120.2	C4-C3-O3	116.9	-	C4-C3-O3	122.4	117.3	cis 121/trans117	C4-C3-O3	122.8	121.3	C4-C3-O3	120.6	120.4	C4-C3-O3	120.8	C4-C3-O3	119.9	121.8				
C3-O3-H3	109.4	108.8	C3-O3-H3	107.6	C3-O3-H3	109.3	-	C3-O3-H3	109.4	109.3	-	C3-O3-H3	109.3	117.5	C3-O3-H3	108.1	-	C3-O3-H3	107.0	C3-O3-H3	107.8	-				
-	-	-	C3-C4-O4	114.0	C3-C4-C7	120.2	122	C4-C5-C7	120.1	120.4	120	C5-C6-C7	121.5	121.7	C3-C4-O4	115.3	117.1	C3-C4-O4	113.5	C3-C4-O4	113.6	114.2				
-	-	-	C5-C4-O4	125.9	C5-C4-C7	122.2	-	C6-C5-C7	121.2	120.7	121	C1-C6-C7	121.0	120.2	C5-C4-O4	124.3	122.5	C5-C4-O4	125.5	C5-C4-O4	126.3	126.1				
-	-	-	C4-O4-C7	118.4	C4-C7-H7a	110.8	-	C5-C7-H7a	111.1	111.5	-	C6-C7-H7a	111.4	-	C4-O4-H4	110.0	-	C4-O4-C8	118.4	C4-O4-C7	118.2	117.3				
-	-	-	O4-C7-H7a	106.2	C4-C7-H7b	111.3	-	C5-C7-H7b	111.4	111.3	-	C6-C7-H7b	111.5	-	-	-	-	O4-C8-H8a	111.3	O4-C7-H7a	111.0	-				
-	-	-	O4-C7-H7b	111.3	C4-C7-H7c	111.3	-	C5-C7-H7c	111.3	110.9	-	C6-C7-H7c	111.3	-	-	-	-	O4-C8-H8b	106.2	O4-C7-H7b	111.0	-				
-	-	-	O4-C7-H7c	111.3	H7a-C7-H7b	108.4	-	H7a-C7-H7b	107.2	108.2	-	H7a-C7-H7b	107.1	-	-	-	-	O4-C8-H8c	111.3	O4-C7-H7c	106.1	-				
-	-	-	H7a-C7-H7b	109.4	H7a-C7-H7c	108.4	-	H7a-C7-H7c	107.7	107.4	-	H7a-C7-H7c	107.5	-	-	-	-	H8a-O8-H8b	109.3	H7a-C7-H7b	109.5	-				
-	-	-	H7a-C7-H7c	109.4	H7b-C7-H7c	106.5	-	H7b-C7-H7c	108.0	107.3	-	H7b-C7-H7c	107.8	-	-	-	-	H8a-O8-H8c	109.3	H7a-C7-H7c	109.6	-				
-	-	-	H7b-C7-H7c	109.3	-	-	-	-	-	-	-	-	-	-	-	-	-	H8b-O8-H8c	109.3	H7b-C7-H7c	109.6	-				
-	-	-	-	-	-	-	-	-	-	-	-	-	-	-	-	-	-	C1-C2-O2	125.1	C1-C6-C8	120.0	119.5				
-	-	-	-	-	-	-	-	-	-	-	-	-	-	-	-	-	-	C3-C2-O2	115.4	C5-C6-C8	120.0	121.0				
-	-	-	-	-	-	-	-	-	-	-	-	-	-	-	-	-	-	C2-O2-C7	118.3	C6-C8-H8	114.3	-				
-	-	-	-	-	-	-	-	-	-	-	-	-	-	-	-	-	-	O2-C7-H7a	105.9	C6-C8=O8	125.2	126.1				
-	-	-	-	-	-	-	-	-	-	-	-	-	-	-	-	-	-	O2-C7-H7b	111.6	H8-C8=O8	120.5	-				
-	-	-	-	-	-	-	-	-	-	-	-	-	-	-	-	-	-	O2-C7-H7c	111.6	-	-	-				
-	-	-	-	-	-	-	-	-	-	-	-	-	-	-	-	-	-	H7a-C7-H7b	109.2	-	-	-				
-	-	-	-	-	-	-	-	-	-	-	-	-	-	-	-	-	-	H7a-C7-H7c	109.2	-	-	-				
-	-	-	-	-	-	-	-	-	-	-	-	-	-	-	-	-	-	H7b-C7-H7c	109.2	-	-	-				

The C-O and O-H bonds (underlined values) in phenol have a length of 1.367 Å and 0.962 Å respectively, and the same is observed for the cresols. Yet, in guaiacol, pyrocatechol, syringol and vanillin, the length of the C-O bond decreases as same as the O-H increases. This result agrees with the possibility of a moderate intramolecular hydrogen bond. It must be clarified that the bond angle O-H--O of these compounds is too low (smaller than 120°) to be properly considered as an intramolecular hydrogen bond.

In Table II-2, one can observe that the C-C-O angle of the hydroxyl group is larger when the hydroxyl hydrogen is pointing through the same side (bold values). Similar results were experimentally observed for these molecules [56–61] and others such as 2,5-dimethylphenol [62] or 2,3-dimethylphenol [62]. The value of the C-C-O angles are a little smaller (120°) in the case of hydrogen bond compared to free hydroxyl group (122°). For guaiacol and vanillin, the two angles have almost the same value. The C-C-O angle is also more important for the methoxy group when it is pointing on the same side (underlined values).

Deformations in the benzene ring were noticed at the angle whose summit corresponds to the carbon with the methyl group. Values are always inferior to 120° (italic values). Such deformation was also observed experimentally by Bois [58–60] who suggests that this would be due to the donor character of the methyl group.

### II-3.3. Potential functions

Because phenolic compounds were not completely studied, only few information are found in the literature concerning the parameters of the potential functions. The values obtained in this work are listed in Table II-3. Comparisons were made with the results found in the literature for the methyl rotation of cresols [27,30,31], and for the hydroxyl rotation of phenol [63] and catechol [34]. Signs of the results depend on the definition of the angle, and comparisons must be done with absolute values. The methyl rotation in o-cresol was investigated by Welzel et al [27]. They determined a value for  $V_3$  of 4.187 kJ.mol<sup>-1</sup> and 7.228 kJ.mol<sup>-1</sup> for *trans* o-cresol and *cis* o-cresol respectively from calculation, and 4.4256 and 7.912 kJ.mol<sup>-1</sup> from experiment. These results are similar with those obtained in this work:  $V_3=4.005$  kJ.mol<sup>-1</sup> for *trans*-o-cresol and  $V_3=6.413$  kJ.mol<sup>-1</sup> for *cis*-o-cresol.

**Table II-3:** Potential constants for internal rotation (in kJ.mol<sup>-1</sup>)

Compounds	Fixed dihedral angle	Value(°)	Rotation	V <sub>1</sub>	V <sub>2</sub>	V <sub>3</sub>	V <sub>4</sub>	V <sub>5</sub>	V <sub>6</sub>	V' <sub>1</sub>	V' <sub>2</sub>	V' <sub>3</sub>	V' <sub>4</sub>
Phenol	/	/	C2-C3-O3-H3	0.479	15.938	-0.452	-	-	-	-	-	-	-
O-cresol	C2-C3-O3-H3	180	C3-C4-C7-H7	-0.111	-0.090	-6.413	-	-	-0.259	-	-	-	-
	C2-C3-O3-H3	0	C3-C4-C7-H7	0.054	0.021	-4.005	-	-	0.026	-	-	-	-
	C3-C4-C7-H7	180	C2-C3-O3-H3	1.425	15.214	0.111	-	-	-	-	-	-	-
M-cresol	C2-C3-O3-H3	180	C4-C5-C7-H7	-	-	-0.260	-	-	-0.060	-	-	-	-
	C2-C3-O3-H3	0	C4-C5-C7-H7	-	-	-0.008	-	-	-0.061	-	-	-	-
	C4-C5-C7-H7	180	C2-C3-O3-H3	0.000	15.881	-0.765	-	-	-	-	-	-	-
	C4-C5-C7-H7	11	C2-C3-O3-H3	0.612	16.027	-0.568	-	-	-	0.008	0.007	-	-
	C4-C5-C7-H7	-11	C2-C3-O3-H3	0.612	16.027	-0.568	-	-	-	-0.008	-0.007	-	-
P-cresol	C2-C3-O3-H3	180	C5-C6-C7-H7	-	-	0.212	-	-	-0.074	-	-	-	-
	C5-C6-C7-H7	90	C2-C3-O3-H3	-0.448	14.805	0.437	-	-	-	-	-	-	-
Pyrocatechol	C2-C3-O3-H3	0	C3-C4-O4-H4	16.392	17.883	-0.311	-	-	-	-	-	-	-
	C2-C3-O3-H3	180	C3-C4-O4-H4	-25.013	-2.817	-2.212	-0.424	-0.177	-0.034	-	-	-	-
	C3-C4-O4-H4	0	C2-C3-O3-H3	24.623	-3.309	2.471	-0.720	0.298	-0.092	-	-	-	-
	C3-C4-O4-H4	180	C2-C3-O3-H3	-15.358	18.348	-0.754	-	-	-	-	-	-	-
Guaiacol	C3-C4-O4-C7	180	C2-C3-O3-H3	-17.787	19.272	0.136	-	-	-	-	-	-	-
	C2-C3-O3-H3	180	C3-C4-O4-C7	-37.421	-8.733	-3.294	2.274	0.468	-0.373	-	-	-	-
	C2-C3-O3-H3	0	C3-C4-O4-C7	-4.461	2.130	-6.560	0.363	0.038	-0.152	-	-	-	-
Vanillin	C2-C3-O3-H3	180	C5-C6-C8=O8	5.329	45.675	0.144	-4.208	-0.392	0.656	-	-	-	-
	C3-C4-O4-C7	180											
	C2-C3-O3-H3	0	C5-C6-C8=O8	0.063	42.768	-0.015	-3.723	-0.300	0.467	0.421	-0.123	-	-
	C3-C4-O4-C7	-65											
	C2-C3-O3-H3	0	C5-C6-C8=O8	0.062	42.767	-0.015	-3.723	-0.300	0.466	-0.421	0.123	-	-
	C3-C4-O4-C7	65											
	C2-C3-O3-H3	0	C5-C6-C8=O8	3.970	44.829	0.376	-4.056	-0.446	0.612	-	-	-	-

	C3-C4-O4-C7	180											
	C5-C6-C8=O8	0	C2-C3-O3-H3	-17.834	25.150	-1.120	-	-	-	-	-	-	-
	C3-C4-O4-C7	180											
	C5-C6-C8=O8	180	C2-C3-O3-H3	-16.591	24.621	-1.186	-	-	-	-	-	-	-
	C3-C4-O4-C7	180											
	C5-C6-C8=O8	0	C3-C4-O4-C7	-9.821	3.783	-6.772	0.419	0.142	-0.198	-	-	-	-
	C2-C3-O3-H3	0											
	C5-C6-C8=O8	180	C3-C4-O4-C7	-5.403	2.422	-6.582	0.417	0.104	-0.190	-	-	-	-
	C2-C3-O3-H3	0											
	C5-C6-C8=O8	0	C3-C4-O4-C7	-43.533	-6.920	-3.267	2.238	0.351	-0.521	-	-	-	-
	C2-C3-O3-H3	180											
	C5-C6-C8=O8	180	C3-C4-O4-C7	-38.742	-8.039	-3.109	2.236	0.311	-0.492	-	-	-	-
	C2-C3-O3-H3	180											
Syringol	C3-C4-O4-C8	180	C2-C3-O3-H3	-17.581	18.092	-1.039	0.386	0.051	0.061	-4.476	-3.032	-1.065	-0.405
	C1-C2-O2-C7	-120											
	C3-C4-O4-C8	180	C2-C3-O3-H3	-17.505	18.016	-0.964	0.372	0.204	0.085	4.476	3.032	1.065	0.285
	C1-C2-O2-C7	120											
	C3-C4-O4-C8	180	C2-C3-O3-H3	0.504	23.030	-0.580	0.468	0.069	-0.015	-	-	-	-
	C1-C2-O2-C7	0											
	C2-C3-O3-H3	180	C1-C2-O2-C7	2.366	2.647	5.799	0.271	-0.062	-0.092	-	-	-	-
	C3-C4-O4-C8	180											
	C2-C3-O3-H3	180	C3-C4-O4-C8	-39.088	-8.752	-1.869	2.688	-0.084	-0.769	-	-	-	-
	C1-C2-O2-C7	0											

Using Watson's A reduction, Hellweg et al obtained  $V_3=0.268 \text{ kJ.mol}^{-1}$  and  $V_6=0.134 \text{ kJ.mol}^{-1}$  for *cis*-m-cresol and  $V_3=0.038 \text{ kJ.mol}^{-1}$  and  $V_6=0.166 \text{ kJ.mol}^{-1}$  for *trans*-m-cresol[31]. Using the same base with DFT theory, we obtain similar value for  $V_3$  ( $0.260 \text{ kJ.mol}^{-1}$ ) for *cis*-m-cresol. Yet, our value of  $V_3$  for *trans* m cresol ( $0.008 \text{ kJ.mol}^{-1}$ ) and for  $V_6$  are much lower ( $0.06$  and  $0.061 \text{ kJ.mol}^{-1}$ ).

The methyl rotation parameters in p-cresol were determined by Hellweg and Hättig [30] using MP2 and CC2 levels with different basis sets. For cc-pVTZ basis set, they obtained  $V_3= 0.2037$  and  $V_6 = 0.1775 \text{ kJ.mol}^{-1}$  (converted values), that are close to our results (values of  $V_3=0.212$  and  $V_6 = 0.074 \text{ kJ.mol}^{-1}$ ).

The microwave investigations on phenol shows that the potential barrier can be represented by only a  $V_2$  parameter at the value of  $13.16 \text{ kJ.mol}^{-1}$  (converted value) [63]. This corresponds to our value of  $15.938 \text{ kJ.mol}^{-1}$  for  $V_2$ . Finally, the local torsions of the hydroxyl groups in pyrocatechol were evaluated by Gerhards et al. [34]. They discovered that the hydroxyl group can be described by a  $V_2/V_1$  ( $V_2 = 21.641 \text{ kJ.mol}^{-1}$  and  $V_1 = 19.18 \text{ kJ.mol}^{-1}$ ) potential when bound and by a  $V_1$  potential (value of  $32.30 \text{ kJ.mol}^{-1}$ ) when the hydroxyl group is free. In the same way, we obtain values of  $V_2 = 17.883$  and  $V_1=16.392 \text{ kJ.mol}^{-1}$  when the hydroxyl is bound, and value of  $V_1=25.013 \text{ kJ.mol}^{-1}$  when it is free.

When comparing the rotation of groups in the structure of the phenolic compounds studied in this work, similarities in behaviors can be observed.

The rotation of the hydroxyl group in phenol can be described as a value of  $V_2$  approximately  $15 \text{ kJ.mol}^{-1}$ . The same phenomenon can be seen in the rotation of the free hydroxyl group in cresols and in syringol. Yet, the presence of substituents increases the energy barrier ( $23.03 \text{ kJ.mol}^{-1}$ ), therefore, increases the value of the potential group.

On the other way, the hydroxyl rotation involved in a hydrogen bond as a donor is characterized by two major parameters  $V_1$  and  $V_2$  between  $15$  and  $20 \text{ kJ.mol}^{-1}$  as observed in pyrocatechol, guaiacol or syringol. In the case of vanillin, the value of  $V_2$  is a little higher (approximately  $25 \text{ kJ.mol}^{-1}$ ) caused by the presence of the aldehyde group.

When the hydroxyl (or methoxy) group is involved in a hydrogen bond as an acceptor, the potential rotation is mainly characterized by a  $V_1$  parameter. The value depends on the substituent: the bigger it is, the higher the value will be ( $25 \text{ kJ.mol}^{-1}$  for pyrocatechol,  $37.4 \text{ kJ.mol}^{-1}$  for guaiacol,  $39.088 \text{ kJ.mol}^{-1}$  for syringol). The position of the aldehyde group in the

case of vanillin also has an influence. When the group is in *cis* position (dihedral angle C5-C6-C8=O8 at 0°), the methoxy group is stabilized and the value of  $V_2$  is higher (43.533 kJ.mol<sup>-1</sup>) compared to the *trans* position ( $V_2 = 38.742$  kJ.mol<sup>-1</sup>).

The potential function of free methoxy groups is defined by the influence of three parameters  $V_1$ ,  $V_2$  and  $V_3$  almost fairly.  $V_3$  is always around 6 kJ.mol<sup>-1</sup>, but  $V_1$  and  $V_2$  can be affected by the presence of others substituents. For example, in vanillin, a position of the aldehyde oxygen pointing to the methoxy group increases the value of  $V_1$  (9.821 kJ.mol<sup>-1</sup> compared to 5.403 kJ.mol<sup>-1</sup>).

The rotation of the aldehyde group is only observed in the structure of vanillin. The potential function is mostly qualified by the  $V_2$  terms with high value (around 42-45 kJ.mol<sup>-1</sup>). The fact that the methoxy group is in the plane of the benzene ring slightly decreases the value of  $V_2$  and increases the influence of  $V_1$ .

Finally, the rotation of a methyl group can be investigated through the study of the cresols' structures. Potential functions need the  $V_3$  and  $V_6$  parameters to be correctly defined. Values for *cis*-o-cresol are a little higher ( $V_3 = 6.413$  and  $V_6 = 0.259$  kJ.mol<sup>-1</sup>) than those obtained for *trans*-o-cresol ( $V_3 = 4.005$  and  $V_6 = 0.026$  kJ.mol<sup>-1</sup>), probably caused by the presence of a hydrogen bond in the *cis*-conformation and the steric hindrance of the methyl group. When the methyl group is placed further from the hydroxyl group, as in m-cresol or p-cresol, the values of  $V_3$  and  $V_6$  decrease.

### II-3.4. Calculation of intramolecular hydrogen bond enthalpy

Table II-4 presents the results of calculation of intramolecular hydrogen bond enthalpy,  $\Delta H_{HB}$  of o-cresol, pyrocatechol, guaiacol and vanillin using different level of theory (HF, DFT and MP2) and different basis sets.

The choice of basis set is important and the use of polarization functions reduced considerably the  $\Delta H_{HB}$  value. Results obtained with DTF are in good agreement with those obtained with MP2 when the cc-pVTZ basis set is used. This confirms our choice to optimize phenolic compounds with DFT/cc-pVTZ.

**Table II-4:** Intramolecular Hydrogen bond Enthalpy  $\Delta H_{\text{HB}}$  calculated using different theories and basis sets.

Theory level	$\Delta H_{\text{HB}}$ (kJ.mol <sup>-1</sup> )			
	O-cresol	Pyrocatechol	Guaiacol	Vanillin
HF/3-21G	5.36	-29.96	-32.09	-33.80
HF/6-31G	4.04	-29.88	-31.78	-33.62
HF/6-311G	4.10	-28.79	-30.83	-32.62
HF/cc-pVTZ	2.87	-16.70	-18.19	-19.45
DFT/3-21G	4.70	-27.25	-29.28	-31.10
DFT/6-31G	3.16	-25.41	-26.62	-28.38
DFT/6-311G	2.70	-25.66	-27.35	-29.10
DFT/cc-pVTZ	1.63	-16.02	-17.56	-18.92
MP2/3-21G	5.89	-26.78	-28.43	-29.44
MP2/6-31G	4.15	-26.08	-27.12	-28.28
MP2/6-31G(d)	3.30	-19.10	-20.93	-22.03
MP2/6-311G	3.63	-25.52	-27.28	-28.43
MP2/6-311G(d,p)	2.30	-17.31	-19.92	-20.81
MP2/6-311+G(d,p)	2.58	-17.38	-19.69	-20.55
MP2/6-311++G(d,p)	2.51	-17.70	-19.67	-20.52
MP2/cc-pVTZ	1.29	-16.25	-18.23	-19.22

Calculated values of  $\Delta H_{\text{HB}}$  for pyrocatechol, guaiacol and vanillin are negative because the *cis* conformations are more stable than the *trans* ones, unlike for o-cresol. Results are in good agreements with those obtained by Rozas et al [64]: 0.5 kcal.mol<sup>-1</sup> (2.09 kJ.mol<sup>-1</sup>) for o-cresol and -4.19 kcal.mol<sup>-1</sup> (-17.51 kJ.mol<sup>-1</sup>) for pyrocatechol.

Experimentally, the intramolecular hydrogen-bond energy can be measured by gas chromatography using polar columns [65][66], by calorimetry [40] or infra-red (IR) [67]. Nevertheless, there is still a lack of data concerning the phenolic compounds. The  $\Delta H_{\text{HB}}$  value calculated for guaiacol is in good agreement with GC measurements (15.9 kJ.mol<sup>-1</sup>) and IR (17.1 kJ.mol<sup>-1</sup>). Larger deviation is observed with calorimetry solution data (14.3 kJ.mol<sup>-1</sup>). Evaluation of hydrogen bonding energy based on calorimetry required IR data and calculations of specific data such as cavity formation enthalpy that required assumptions. Moreover, it is well established that spectroscopy data is an useful tool to highlight the intramolecular hydrogen bonding but it cannot provide a quantitative value.

#### II-4. Conclusion

The conformational analysis of these eight phenolic compounds was performed at the B3LYP/cc- pVTZ level of theory. For all the phenolic compounds, it was observed that each optimal conformation presents the hydroxyl group in the plane of the benzene ring. Vanillin, guaiacol, syringol (and pyrocatechol) are also more stable with the methoxy (hydroxyl) group in the plane. Moreover, these molecules have the specificity to create intramolecular hydrogen bond between the phenolic hydrogen and the methoxy (hydroxyl) oxygen, which stabilizes the conformations. O-cresol conformation is also the most stable when its groups are in the plane of the benzene ring, but in *trans*-position. The m-cresol and p-cresol conformations have the particularity to be more stable with one hydrogen on their methyl almost at the perpendicular of the plane of the benzene ring.

This conformational analysis could lead to future studies for a better knowledge of the behavior of these compounds in particular situations. In fact, the interaction energy between phenolic compounds and solvent molecules could help to highlight and understand the differences in their behaviors in the same environment. Such a work could help to improve the separation of the phenolic compounds through solvent extraction.

## References

- [1] H. Pakdel, C. Amen-Chen, J. Zhang, C. Roy, Phenolic compounds from vacuum pyrolysis of biomass, *Bio-Oil Prod. Util.* CPL Press UK. (1996) 124–136.
- [2] A.V. Bridgwater, D. Meier, D. Radlein, An overview of fast pyrolysis of biomass, *Org. Geochem.* 30 (1999) 1479–1493. doi:10.1016/S0146-6380(99)00120-5.
- [3] A.V. Bridgwater, S.A. Bridge, A Review of Biomass Pyrolysis and Pyrolysis Technologies, in: A.V. Bridgwater, G. Grassi (Eds.), *Biomass Pyrolysis Liq. Upgrad. Util.*, Springer Netherlands, Dordrecht, 1991: pp. 11–92. [http://www.springerlink.com/index/10.1007/978-94-011-3844-4\\_2](http://www.springerlink.com/index/10.1007/978-94-011-3844-4_2) (accessed January 20, 2017).
- [4] H. Pakdel, C. Roy, C. Amen-Chen, Phenolic compounds from vacuum pyrolysis of wood wastes, *Can. J. Chem. Eng.* 75 (1997) 121–126. doi:10.1002/cjce.5450750119.
- [5] C. Amen-Chen, H. Pakdel, C. Roy, Production of monomeric phenols by thermochemical conversion of biomass: a review, *Bioresour. Technol.* 79 (2001) 277–299. doi:10.1016/S0960-8524(00)00180-2.
- [6] J. Zakzeski, P.C.A. Bruijninx, A.L. Jongerius, B.M. Weckhuysen, The Catalytic Valorization of Lignin for the Production of Renewable Chemicals, *Chem. Rev.* 110 (2010) 3552–3599. doi:10.1021/cr900354u.
- [7] J.N. Murwanashyaka, H. Pakdel, C. Roy, Separation of syringol from birch wood-derived vacuum pyrolysis oil, *Sep. Purif. Technol.* 24 (2001) 155–165. doi:10.1016/S1383-5866(00)00225-2.
- [8] M. Kleinert, T. Barth, Phenols from Lignin, *Chem. Eng. Technol.* 31 (2008) 736–745. doi:10.1002/ceat.200800073.
- [9] C. Amen-Chen, H. Pakdel, C. Roy, Separation of phenols from Eucalyptus wood tar, *Biomass Bioenergy.* 13 (1997) 25–37. doi:10.1016/S0961-9534(97)00021-4.
- [10] S. Wang, Y. Wang, Q. Cai, X. Wang, H. Jin, Z. Luo, Multi-step separation of monophenols and pyrolytic lignins from the water-insoluble phase of bio-oil, *Sep. Purif. Technol.* 122 (2014) 248–255. doi:10.1016/j.seppur.2013.11.017.
- [11] J.-M. Lavoie, W. Baré, M. Bilodeau, Depolymerization of steam-treated lignin for the production of green chemicals, *Bioresour. Technol.* 102 (2011) 4917–4920. doi:10.1016/j.biortech.2011.01.010.
- [12] F. Helmut, V. Heinz-Werner, H. Toshikazu, P. Wilfried, Phenol derivatives, *Ullmann's Encycl. Ind. Chem. VCH Ger.* 19 (1985) 299–357.
- [13] F. Ikegami, T. Sekine, Y. Fujii, [Anti-dermatophyte activity of phenolic compounds in “mokusaku-eki”], *Yakugaku Zasshi.* 118 (1998) 27–30.
- [14] J.A. Maga, I. Katz, Simple phenol and phenolic compounds in food flavor, *C R C Crit. Rev. Food Sci. Nutr.* 10 (1978) 323–372. doi:10.1080/10408397809527255.
- [15] H. Fiege, H.-W. Voges, T. Hamamoto, S. Umemura, T. Iwata, H. Miki, Y. Fujita, H.-J. Buysch, D. Garbe, W. Paulus, Phenol Derivatives, in: *Wiley-VCH Verlag GmbH & Co. KGaA (Ed.), Ullmanns Encycl. Ind. Chem., Wiley-VCH Verlag GmbH & Co. KGaA, Weinheim, Germany, 2000.* [http://doi.wiley.com/10.1002/14356007.a19\\_313](http://doi.wiley.com/10.1002/14356007.a19_313) (accessed August 23, 2016).
- [16] D. Radlein, Chemicals and materials from biomass, *PyNe Pyrolysis Netw.* 4 (1997).
- [17] D. Meier, D.R. Larimer, O. Faix, Direct liquefaction of different lignocellulosics and their constituents, *Fuel.* 65 (1986) 910–915. doi:10.1016/0016-2361(86)90197-3.
- [18] H.-G. Korth, M.I. de Heer, P. Mulder, A DFT Study on Intramolecular Hydrogen Bonding in 2-Substituted Phenols: Conformations, Enthalpies, and Correlation with Solute Parameters, *J. Phys. Chem. A.* 106 (2002) 8779–8789. doi:10.1021/jp025713d.
- [19] S.G. Estácio, P. Cabral do Couto, B.J. Costa Cabral, M.E. Minas da Piedade, J.A. Martinho Simões, Energetics of Intramolecular Hydrogen Bonding in Di-substituted

- Benzenes by the ortho–para Method, *J. Phys. Chem. A.* 108 (2004) 10834–10843. doi:10.1021/jp0473422.
- [20] W.-H. Fang, Theoretical characterization of the excited-state structures and properties of phenol and its one-water complex, *J. Chem. Phys.* 112 (2000) 1204–1211. doi:10.1063/1.480673.
- [21] S. Schumm, M. Gerhards, W. Roth, H. Gier, K. Kleinermanns, A CASSCF study of the  $S_0$  and  $S_1$  states of phenol, *Chem. Phys. Lett.* 263 (1996) 126–132. doi:10.1016/S0009-2614(96)01172-4.
- [22] D. Feller, M.W. Feyereisen, Ab initio study of hydrogen bonding in the phenol-water system, *J. Comput. Chem.* 14 (1993) 1027–1035. doi:10.1002/jcc.540140904.
- [23] M. Schütz, T. Bürgi, S. Leutwyler, Structures and vibrations of phenol · H<sub>2</sub>O and d-phenol · D<sub>2</sub>O based on ab initio calculations, *J. Mol. Struct. THEOCHEM.* 276 (1992) 117–132. doi:10.1016/0166-1280(92)80026-I.
- [24] H. Watanabe, S. Iwata, Theoretical studies of geometric structures of phenol-water clusters and their infrared absorption spectra in the O–H stretching region, *J. Chem. Phys.* 105 (1996) 420–431. doi:10.1063/1.471918.
- [25] M. Pohl, K. Kleinermanns, Ab initio SCF calculations on hydrogen bonded cresol isomers, *Z. Für Phys. At. Mol. Clust.* 8 (1988) 385–392. doi:10.1007/BF01437106.
- [26] S.W. Dietrich, E.C. Jorgensen, P.A. Kollman, S. Rothenberg, A theoretical study of intramolecular hydrogen bonding in ortho-substituted phenols and thiophenols, *J. Am. Chem. Soc.* 98 (1976) 8310–8324. doi:10.1021/ja00442a002.
- [27] A. Welzel, A. Hellweg, I. Merke, W. Stahl, Structural and Torsional Properties of o-Cresol and o-Cresol-OD as Obtained from Microwave Spectroscopy and ab Initio Calculations, *J. Mol. Spectrosc.* 215 (2002) 58–65. doi:10.1006/jmsp.2002.8600.
- [28] V. Balachandran, M. Murugan, A. Nataraj, M. Karnan, G. Ilango, Comparative vibrational spectroscopic studies, HOMO–LUMO, NBO analyses and thermodynamic functions of p-cresol and 2-methyl-p-cresol based on DFT calculations, *Spectrochim. Acta. A. Mol. Biomol. Spectrosc.* 132 (2014) 538–549. doi:10.1016/j.saa.2014.04.194.
- [29] P.R. Richardson, M.A. Chapman, D.C. Wilson, S.P. Bates, A.C. Jones, The nature of conformational preference in a number of p-alkyl phenols and p-alkyl benzenes, *Phys. Chem. Chem. Phys.* 4 (2002) 4910–4915. doi:10.1039/b203954k.
- [30] A. Hellweg, C. Hättig, On the internal rotations in p-cresol in its ground and first electronically excited states, *J. Chem. Phys.* 127 (2007) 024307. doi:10.1063/1.2752163.
- [31] A. Hellweg, C. Hättig, I. Merke, W. Stahl, Microwave and theoretical investigation of the internal rotation in m-cresol, *J. Chem. Phys.* 124 (2006) 204305. doi:10.1063/1.2198842.
- [32] C. Puebla, T.-K. Ha, A theoretical study of conformations and rotational barriers in dihydroxybenzenes, *J. Mol. Struct. THEOCHEM.* 204 (1990) 337–351. doi:10.1016/0166-1280(90)85085-2.
- [33] T. Bürgi, S. Leutwyler, O–H torsional vibrations in the  $S_0$  and  $S_1$  states of catechol, *J. Chem. Phys.* 101 (1994) 8418–8429. doi:10.1063/1.468104.
- [34] M. Gerhards, W. Perl, S. Schumm, U. Henrichs, C. Jacoby, K. Kleinermanns, Structure and vibrations of catechol and catechol·H<sub>2</sub>O(D<sub>2</sub>O) in the  $S_0$  and  $S_1$  state, *J. Chem. Phys.* 104 (1996) 9362. doi:10.1063/1.471682.
- [35] R. Rudyk, M.A.A. Molina, M.I. Gómez, S.E. Blanco, F.H. Ferretti, Solvent effects on the structure and dipole moment of resorcinol, *J. Mol. Struct. THEOCHEM.* 674 (2004) 7–14. doi:10.1016/j.theochem.2003.12.019.
- [36] B. Gómez-Zaleta, R. Gómez-Balderas, J. Hernández-Trujillo, Theoretical analysis of hydrogen bonding in catechol–n(H<sub>2</sub>O) clusters (n = 0...3), *Phys. Chem. Chem. Phys.* 12 (2010) 4783. doi:10.1039/b922203k.

- [37] M. Mandado, A.M. Graña, R.A. Mosquera, Do 1,2-ethanediol and 1,2-dihydroxybenzene present intramolecular hydrogen bond?, *Phys Chem Chem Phys*. 6 (2004) 4391–4396. doi:10.1039/B406266C.
- [38] C. Agache, V.I. Popa, Ab Initio Studies on the Molecular Conformation of Lignin Model Compounds I. Conformational Preferences of the Phenolic Hydroxyl and Methoxy Groups in Guaiacol, *Monatshefte Für Chem. - Chem. Mon.* 137 (2006) 55–68. doi:10.1007/s00706-005-0404-x.
- [39] O.V. Dorofeeva, I.F. Shishkov, N.M. Karasev, L.V. Vilkov, H. Oberhammer, Molecular structures of 2-methoxyphenol and 1,2-dimethoxybenzene as studied by gas-phase electron diffraction and quantum chemical calculations, *J. Mol. Struct.* 933 (2009) 132–141. doi:10.1016/j.molstruc.2009.06.009.
- [40] M.A. Varfolomeev, D.I. Abaidullina, B.N. Solomonov, S.P. Verevkin, V.N. Emel'yanenko, Pairwise Substitution Effects, Inter- and Intramolecular Hydrogen Bonds in Methoxyphenols and Dimethoxybenzenes. Thermochemistry, Calorimetry, and First-Principles Calculations, *J. Phys. Chem. B*. 114 (2010) 16503–16516. doi:10.1021/jp108459r.
- [41] E.J. Cocinero, A. Lesarri, P. Écija, J.-U. Grabow, J.A. Fernández, F. Castaño, Conformational equilibria in vanillin and ethylvanillin, *Phys. Chem. Chem. Phys.* 12 (2010) 12486. doi:10.1039/c0cp00585a.
- [42] C.Y. Panicker, H.T. Varghese, K. Sajina, A.V. Vaidyan, M.A. John, B. Harikumar, IR, Raman and ab-initio calculations of 2,6-dimethoxyphenol, *Orient. J. Chem.* 24 (2008) 973.
- [43] L. Zhang, G.H. Peslherbe, H.M. Muchall, Ultraviolet Absorption Spectra of Substituted Phenols: A Computational Study†, *Photochem. Photobiol.* 82 (2006) 324–331. doi:10.1562/2005-07-08-RA-605.
- [44] M.J. Frisch, G.W. Trucks, H.B. Schlegel, G.E. Scuseria, M.A. Robb, J.R. Cheeseman, G. Scalmani, V. Barone, B. Mennucci, G.A. Petersson, others, Gaussian 09, rev. A. 02, Gaussian Inc Wallingford CT. (2009).
- [45] A.D. Becke, Density-functional exchange-energy approximation with correct asymptotic behavior, *Phys. Rev. A*. 38 (1988) 3098–3100. doi:10.1103/PhysRevA.38.3098.
- [46] C. Lee, W. Yang, R.G. Parr, Development of the Colle-Salvetti correlation-energy formula into a functional of the electron density, *Phys. Rev. B Condens. Matter.* 37 (1988) 785–789.
- [47] P.J. Stephens, F.J. Devlin, C.F. Chabalowski, M.J. Frisch, Ab Initio Calculation of Vibrational Absorption and Circular Dichroism Spectra Using Density Functional Force Fields, *J. Phys. Chem.* 98 (1994) 11623–11627. doi:10.1021/j100096a001.
- [48] J.A. Montgomery, M.J. Frisch, J.W. Ochterski, G.A. Petersson, A complete basis set model chemistry. VI. Use of density functional geometries and frequencies, *J. Chem. Phys.* 110 (1999) 2822–2827. doi:10.1063/1.477924.
- [49] E. VanBesien, M.P.M. Marques, Ab initio conformational study of caffeic acid, *J. Mol. Struct. THEOCHEM.* 625 (2003) 265–275. doi:10.1016/S0166-1280(03)00026-5.
- [50] L. Radom, W.J. Hehre, J.A. Pople, Molecular orbital theory of the electronic structure of organic compounds. XIII. Fourier component analysis of internal rotation potential functions in saturated molecules, *J. Am. Chem. Soc.* 94 (1972) 2371–2381. doi:10.1021/ja00762a030.
- [51] T. Aota, T. Ebata, M. Ito, Rotational isomers and internal rotation of the methyl group in S<sub>0</sub>, S<sub>1</sub> and ion of o-cresol, *J. Phys. Chem.* 93 (1989) 3519–3522. doi:10.1021/j100346a031.

- [52] I. Appel, K. Kleinermanns, Fluorescence excitation spectra of hydrogen-bonded cresol-isomers in supersonic free jets, *Berichte Bunsenges. Für Phys. Chem.* 91 (1987) 140–152. doi:10.1002/bbpc.19870910213.
- [53] H.F. Hameka, J.O. Jensen, Calculations of the energies, geometries and vibrational frequencies of the ground and first excited singlet states of toluene and p-cresol, *J. Mol. Struct. THEOCHEM.* 331 (1995) 203–214. doi:10.1016/0166-1280(94)03888-R.
- [54] G.A. Jeffrey, *An Introduction to Hydrogen Bonding*, Oxford University Press, 1997.
- [55] F.J. Ramírez, J.T. López Navarrete, Normal coordinate and rotational barrier calculations on 1,2-dihydroxybenzene, *Vib. Spectrosc.* 4 (1993) 321–334. doi:10.1016/0924-2031(93)80006-2.
- [56] C.J. Brown, The crystal structure of catechol, *Acta Crystallogr.* 21 (1966) 170–174. doi:10.1107/S0365110X66002482.
- [57] R. Velavan, P. Sureshkumar, K. Sivakumar, S. Natarajan, Vanillin-I, *Acta Crystallogr. C.* 51 (1995) 1131–1133. doi:10.1107/S0108270194011923.
- [58] C. Bois, Structure de l'o-crésol, *Acta Crystallogr. B.* 28 (1972) 25–31. doi:10.1107/S0567740872001815.
- [59] C. Bois, Structure du p-crésol à basse température, *Acta Crystallogr. B.* 26 (1970) 2086–2092. doi:10.1107/S0567740870005411.
- [60] C. Bois, Structure du m-crésol, *Acta Crystallogr. B.* 29 (1973) 1011–1017. doi:10.1107/S0567740873003778.
- [61] N.W. Larsen, Microwave spectra of the six mono-<sup>13</sup>C-substituted phenols and of some monodeuterated species of phenol. Complete substitution structure and absolute dipole moment, *J. Mol. Struct.* 51 (1979) 175–190. doi:10.1016/0022-2860(79)80292-6.
- [62] H. Brusset, H. Gillier-Pandraud, A. Neuman, Strukturbestimmung bei-150 grad c von 2, 5-und 2, 3-dimethylphenol, *Chem. Informationsdienst.* 3 (1972).
- [63] T. Kojima, Potential Barrier of Phenol from its Microwave Spectrum, *J. Phys. Soc. Jpn.* 15 (1960) 284–287. doi:10.1143/JPSJ.15.284.
- [64] I. Rozas, I. Alkorta, J. Elguero, Intramolecular Hydrogen Bonds in *ortho*-Substituted Hydroxybenzenes and in 8-Substituted 1-Hydroxynaphthalenes: Can a Methyl Group Be an Acceptor of Hydrogen Bonds?, *J. Phys. Chem. A.* 105 (2001) 10462–10467. doi:10.1021/jp013125e.
- [65] E.E. Fedorov, O.E. Makarov, A.N. Pankratov, V.S. Grinev, Gas–liquid chromatography-obtained differences in the dissolution enthalpy between two positional isomers in a polar stationary phase: A measure of the inter- or intramolecular hydrogen bond energy?, *J. Chromatogr. A.* 1241 (2012) 76–83. doi:10.1016/j.chroma.2012.04.010.
- [66] I.M. Skvortsov, O.E. Makarov, E.E. Fedorov, Further consideration of the gas–liquid chromatographic method for determining the intramolecular hydrogen bond energies with the example of 2-substituted phenols, *J. Chromatogr. A.* 1132 (2006) 248–255. doi:10.1016/j.chroma.2006.07.057.
- [67] G.S. Denisov, M.I. Sheikh-Zade, M.V. Eskin, Determination of the energy of an intramolecular hydrogen bond with the help of competing equilibria, *Zh Prikl Spektrosk.* 27 (1977) 1049–1054.

## Chapter III: Computational study of phenolic compounds-water clusters

Laëtitia Cesari<sup>1</sup>, Laetitia Canabady-Rochelle<sup>1</sup>, Fabrice Mutelet<sup>1\*</sup>

1 : Université de Lorraine, Laboratoire Réactions et Génie des Procédés (LRGP, UMR CNRS-UL 7274), 1 rue Grandville, 54000 Nancy, France

Article en cours de soumission au journal Structural Chemistry (Octobre 2017).

### Résumé

Dans ce chapitre, nous étudions, par calcul quantique, huit composés phénoliques en présence d'une molécule d'eau. Les calculs sont effectués au niveau B3LYP/cc-pVTZ. La détermination des structures les plus stables se fait par l'évaluation de l'énergie d'interaction. Les termes correctifs BSSE et ZPE sont également calculés. Trois conformations sont observées avec les composés phénoliques : cyclique (guaiacol, syringol), translinéaire (phénol, crésol, pyrocatechol) ou perpendiculaire (vanilline). Des analyses NBO et HUMO-LUMO sont effectuées afin d'observer les changements apportés au niveau des charges et de la réactivité des composés phénoliques par une molécule d'eau. Enfin, les structures du liquide ionique choline bis(trifluorométhylsulfonyle)imide ([choline][NTf<sub>2</sub>]) sont déterminées. Le calcul de l'énergie d'interaction entre le liquide ionique et le phénol montre que ce liquide ionique est un excellent choix pour l'extraction du phénol en solution aqueuse.

**Abstract**

A study of eight molecules (phenol, o-cresol, m-cresol, p-cresol, pyrocatechol, guaiacol, syringol and vanillin) were investigated in their one water complex forms by quantum calculations using B3LYP/cc-pVTZ level of theory. For the first time, the structures of o-cresol, m-cresol, syringol and vanillin with water were determined. Phenol, cresols and pyrocatechol present a translinear structure while guaiacol and syringol are in cyclic configurations in contact with water. It was found that vanillin and water interact via the aldehyde function and the presence of H<sub>2</sub>O does not affect the intramolecular hydrogen bond in the structure of vanillin. The NBO analysis indicates that the electronegativity of water increases in the structures as follows: translinear < cyclic < vanillin. The HOMO-LUMO energy gap shows that the presence of water increases the hardness of guaiacol and syringol caused by their cyclic conformations. Vanillin is the least hard but the most electronegative molecule with or without water

### III-1. Introduction

Lignin is one of the main structural components of biomass. Produced in high amounts in the forest industry, it has been considered as a waste for many years and burned as cheap fuel to provide energy [1, 2]. Yet, lignin has presented a new interest since the last decades. Indeed, the structure of lignin results from the association of phenolic groups and it could become a new resource for their production [3]. Under thermochemical treatments such as liquefaction or pyrolysis, lignin can produce a significant quantity of chemical compounds such as monophenols [4–11]. These high added-value compounds could be used in various fields such as pharmaceuticals, agri-business or chemicals industries [12–15].

Researches already investigated the possibility to extract phenolic compounds from biomass. Various techniques such as supercritical CO<sub>2</sub> [16–21] to distillation [22] were investigated [23]. However, the most commonly used method seems to be the liquid-liquid extraction (LLE) [24] probably because of its user-friendliness. The process requires two step liquid-liquid extraction using water and organic solvent as extraction media [8–10, 25, 26]. Yet, the extracted fraction results in a complex mixture constituted of many phenolic compounds with similar structures and properties. Therefore, their separation becomes arduous. A better knowledge of the interactions between the compounds and the solvent could improve the selectivity in the extraction process. For example, the presence of hydrogen bond has a direct influence on the solubility of the compounds. In the same way, the solvent has a huge effect on the hydrogen abstraction and directly impacts their properties. Phenolic hydrogen in an intramolecular hydrogen bond are more abstractable than the one involved in a linear intermolecular hydrogen bond [27, 28].

The behaviour of phenolic compounds could be described through a computational study using quantum calculations. Lots of studies have already elucidated the conformational structures of phenolic compounds [29–53]. For the last decades, the authors have begun to investigate the interaction between phenolic compounds and water [27, 29, 31, 44, 46, 54–67]. Phenol complexes with water were strongly studied experimentally [55–57, 60, 68–70] and computationally [29, 31, 54–63]. Several structures were investigated, especially the ones presenting interaction between water and the hydroxyl group of phenol. From the analysis of the structure and vibrations in the phenol-water complexes, the modification of the C-O and O-H bonds was observed in the phenol structure. Moreover, the complexation with water induces several spectral shifts related to the frequency modes of the molecule [71]. Furthermore, in

addition to the hydrophilic conformations, water can also form interaction with the centre of the benzene ring [54–59].

Ahn et al [72] studied the hydrogen bonding between water and phenol complexes. They observed the influence of the substituting group (i.e. fluoro, chloro, hydroxyl and amino) on ortho and para position. For para-substituted phenols, the binding energy is directly affected by the electrostatic effect, depending on the position of the hydroxyl group (as donor or acceptor). In the case of ortho-substituted phenols, many parameters such as geometry changes or the nature of the substituting group have an influence on the strength of the hydrogen bonds. Therefore, the pattern of the binding energy of the complexes is difficult to highlight.

Wu and Brutschy [64] studied the structure of guaiacol in the presence of one or two water molecules and how it affects the intramolecular hydrogen bond. Experimental studies based on resonant two-photon ionization (R2PI) lead to the conclusion that the previous intramolecular hydrogen bond in guaiacol is destroyed. Same results were found by Jalili et al [27], who also studied the possibility of a bifurcated hydrogen bond.

The structures of catechol and catechol-(H<sub>2</sub>O)<sub>n</sub> complexes were also investigated experimentally and computationally by Gerhards et al [44, 73] and Gómez-Zaleta [46]. Translinear structure seems the most stable conformation compared to the cyclic one.

The p-cresol structures with water were already studied by Pohl and al [65], Myszkiewicz et al [66] and Biswal et al [67]. These works found that the hydroxyl group in translinear conformation constitutes the most stable form.

Finally, no information has been found on the structure of o-cresol, m-cresol, syringol nor vanillin in their one-water cluster configurations.

In this work, we investigated the interaction between water and phenolic compounds regularly found in bio-oils: phenol, guaiacol, syringol, pyrocatechol, o-, m-, p-cresol and vanillin. All calculations were carried out with the same level of theory and the same basis set to allow homogenisation of the results and to properly compare the clusters conformations. The lengths of bonds and frequencies are also discussed.

### III-2. Computational methods

Quantum calculations were carried out using the Gaussian 09 program. Several trial structures of the phenolic compound-water complexes were studied depending on the position on the water molecule around the phenolic compound. Geometrical structures were optimized at B3LYP [74–76] level of theory using the cc-pVTZ basis set. The frequency calculations were performed to verify the absence of imaginary frequency and to calculate the ZPE corrective term. The ZPE correction was scaled by a factor 0.9889 according to the literature [77] and the fundamental frequencies by a factor of 0.9665 [77]. Basis set superposition error BSSE were estimated using the counterpoise method.

The binding energy was calculated as follows:

$$E_{bind} = E_{cluster} - (E_{phenolic\ compound} + E_{water}) \quad (1)$$

Where  $E_{cluster}$ ,  $E_{phenolic\ compound}$  and  $E_{water}$  correspond to the energy of the optimized geometry of the dimer, and the separated optimized geometry of the phenolic compound and water, respectively.

In order to understand the interactions between donor and acceptor atoms in the hydrogen bonds, natural population analysis were performed using the Natural Bond Orbitals (NBO) calculations.

Finally, the HOMO-LUMO (Highest Occupied Molecular Orbital - Lowest Unoccupied Molecular Orbital) energy gap was used as a criterion to understand the reactivity of the molecules [78]. Because the DFT method provides huge differences with experimental values [79], calculations were made at HF/cc-pVTZ using the B3LYP/cc-pVTZ optimized conformation structure. The hardness  $\eta$  and electronegativity  $\chi$  of the phenolic compounds and of the clusters were determined by the following expressions defined by Mulliken [80]:

$$\text{Electronegativity } \chi = \frac{IP + EA}{2} \quad (2)$$

$$\text{Hardness } \eta = IP - EA \quad (3)$$

Where IP and EA are the ionization potential and the electron affinity, respectively. Using the Koopmanns' theoreme,  $IP \approx -E(\text{HOMO})$  and  $EA \approx -E(\text{LUMO})$ .

Where  $E(\text{LUMO})$  and  $E(\text{HOMO})$  correspond respectively to the energy of the lowest unoccupied molecular orbital LUMO and the highest occupied molecular orbital HOMO.

### III-3. Result and discussion

#### III-3.1 Energies

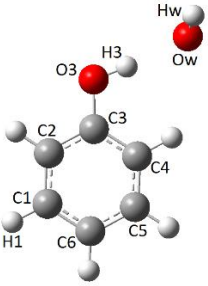
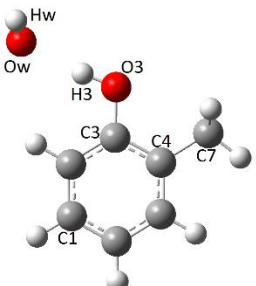
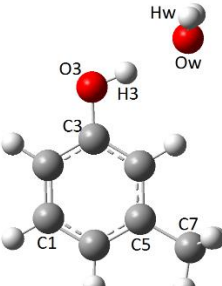
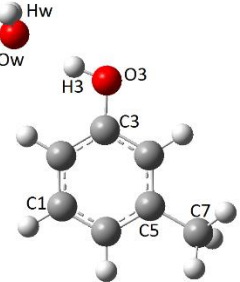
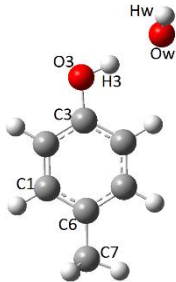
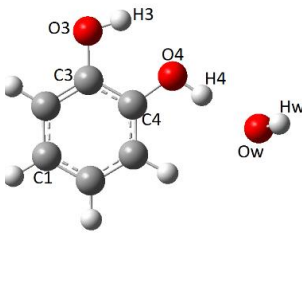
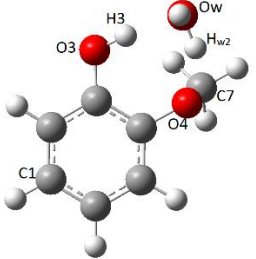
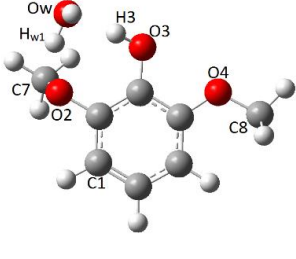
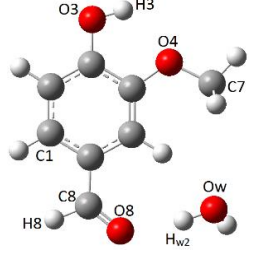
##### *Water*

Before studying its interactions with the phenolic compounds, the structure of water has to be determined in its isolated form. In its ground state, the global minimum energy structure of water at the B3LYP/cc-pVTZ level of theory corresponds to an energy of -76.45983971 Hartree and a zero point vibrational energy (ZPE) of 0.021279 Hartree. These results are in good agreement with the work of Xantheas[81] at the MP2/aug-cc-pVTZ level (Energy = -76.344148 Hartree). The Ow-Hw bond are 0.9614 Å long and oriented by an angle Hw1-Ow-Hw2 of 104.52°. The frequencies of the Ow-Hw bonds are 3800.36 and 3900.72 cm<sup>-1</sup> for the symmetric and anti-symmetric vibration, respectively.

##### *Phenolic compounds*

The structures of the phenolic compounds (C<sub>0</sub>) in their isolated forms were taken from the previous chapter and are reminded in Appendix II (Table S1). Table III-1 represents the structures of the most stable conformations of the phenolic·H<sub>2</sub>O complexes. The conformations of all the one water-cluster forms (C<sub>n</sub>) of the phenolic compounds are depicted in Tables S1 to S9 (Appendix II). The conformations are listed for each compound from the global energy conformation to the less stable one.

Table III-1: Optimized conformations.

	<b>Phenol</b>	<b>O-cresol</b>	<b>Cis m-cresol</b>
			
Energy (Hartree)	-384.0580447	-423.38956669	-423.3891244
$\Delta E$ (kJ.mol <sup>-1</sup> )	-32.85	-32.53	-32.32
$\Delta E + ZPE + BSSE$ (kJ.mol <sup>-1</sup> )	-17.94	-17.93	-17.56
	<b>Trans m-cresol</b>	<b>P-cresol</b>	<b>Pyrocatechol</b>
			
Energy (Hartree)	-423.3891357	-423.3881675	-459.3116508
$\Delta E$ (kJ.mol <sup>-1</sup> )	-32.26	-32.25	-35.91
$\Delta E + ZPE + BSSE$ (kJ.mol <sup>-1</sup> )	-17.63	-17.13	-20.54
	<b>Guaiacol</b>	<b>Syringol</b>	<b>Vanillin</b>
			
Energy (Hartree)	-498.6225336	-613.182495	-611.9960588
$\Delta E$ (kJ.mol <sup>-1</sup> )	-26.35	-26.34	-35.04
$\Delta E + ZPE + BSSE$ (kJ.mol <sup>-1</sup> )	-7.66	-8.02	-18.11

*Phenol*

Table S2 depicted the parameters of the different conformations of phenol in its ground state and in contact with water. In its ground state, the hydroxyl group of phenol is in the plane of the benzene ring. Its conformation is maintained in the phenol·H<sub>2</sub>O cluster. Three conformations were found (C<sub>1</sub>, C<sub>2</sub> and C<sub>3</sub>), and the most stable energetically conformation is C<sub>1</sub> [29, 31, 54–63].

In the C<sub>1</sub> and C<sub>2</sub> conformations, the water molecule is close to the hydroxyl group of phenol, creating a hydrogen bond. As an acceptor (C<sub>1</sub>), it places itself symmetrically at the perpendicular of the benzene ring. This so-called translinear conformation is the most stable one. The associated binding energy is -32.85 kJ.mol<sup>-1</sup> and goes up to -17.94 kJ.mol<sup>-1</sup> with the correction by ZPE and BSSE. Similar results are obtained by Ahn et al [72] with MP2/6-311G\*\* level of theory (-22.93 kJ.mol<sup>-1</sup> with ZPE and BSSE correction). As a donor (C<sub>2</sub>), one part of the water molecule is in the plan of the benzene ring. Another conformation is found with water as an acceptor (C<sub>3</sub>). In the C<sub>3</sub> conformation, the water molecule is at the perpendicular to the benzene ring and the interaction is towards the benzene hydrogens. The benzene ring of phenol acts as a donor because of its electronegativity.

*O-cresol*

The conformations of o-cresol are presented in Table S3. Six conformations of the one water cluster were investigated. The most stable conformation (C<sub>1</sub>) is found when the water molecule is at the perpendicular of the plan of the benzene ring, next to the hydroxyl group. In this case, water acts as a hydrogen acceptor. This C<sub>1</sub> conformation presents a  $\Delta E$  of -32.53 kJ.mol<sup>-1</sup> and -17.93 kJ.mol<sup>-1</sup> without any correction or with ZPE and BSSE corrective terms, respectively. Water behaves similarly in the C<sub>1</sub> and C<sub>2</sub> conformations. The main different between both conformations is the rotation of 180° of the hydroxyl group of o-cresol. In the C<sub>3</sub> and C<sub>4</sub> conformations, water is placed between the hydroxyl and the methyl groups of o-cresol. In C<sub>3</sub>, water is as a donor, but in C<sub>4</sub>, a triangular bridge is observed. Thus, water presents two roles: donor towards the hydroxyl group and acceptor towards the methyl one. In the C<sub>5</sub> and C<sub>6</sub> conformations, the water is not placed next to the hydroxyl group. In the C<sub>5</sub> conformation, water interacts in a bifurcated hydrogen bond with the hydrogen atoms of the methyl and of the benzene ring, whereas in the C<sub>6</sub>, it interacts only with the benzene one. No information for this system are provided in the literature for comparison.

*M-cresol*

The conformations of m-cresol in its isolated and one-water complex states are listed in **Table S4**. In its isolated form, m-cresol presents two ground states depending on the hydroxyl group in *cis* or *trans* position. Two m-cresol·H<sub>2</sub>O conformations were studied for *trans* m-cresol and three for *cis* m-cresol. In the most stable conformations of *trans* and *cis* m-cresol (C<sub>1</sub> *trans* and C<sub>1</sub> *cis*), water is in translinear position. It creates a hydrogen bond as an acceptor with the hydroxyl group of m-cresol. The corresponding  $\Delta E$  are -32.26 and -32.32 kJ.mol<sup>-1</sup> respectively for *trans* and *cis* m-cresol (-17.63 and -17.56 kJ.mol<sup>-1</sup> with ZPE and BSSE corrective terms). In the C<sub>2</sub> conformations, one part of the water molecule is in the plan of the benzene ring. Water acts in this way as a hydrogen donor towards the hydroxyl group. In the third conformation of *cis* m-cresol, water interacts with the hydrogens of the benzene ring and the methyl group in a bifurcated hydrogen bond. For these systems, no data are available in the literature.

*P-cresol*

Details about the conformations of p-cresol·H<sub>2</sub>O complexes are provided in **Table S5**. Four conformations were investigated for p-cresol. The most stable C<sub>1</sub> ( $\Delta E = -32.25$  kJ.mol<sup>-1</sup> without correction) corresponds to a translinear conformation. This results agrees well with Myszkiewicz et al [66] and Pohl et al [65] ( $\Delta E = -32.0$  kJ.mol<sup>-1</sup> at the HF/STO-3G level). Water interacts with the hydroxyl group of p-cresol as a hydrogen acceptor. In the C<sub>2</sub> conformation, water is partially in the plan of the benzene ring. It acts as a hydrogen donor towards the hydroxyl group. In the last two conformations, water forms a bifurcated hydrogen bond with the hydrogens of the methyl and the benzene ring. Yet, in C<sub>3</sub>, the methyl hydrogen interacting with water is pointing towards the same side than the hydrogen of the hydroxyl group. In the C<sub>4</sub> conformation, the methyl hydrogen is pointing towards the other side.

*Pyrocatechol*

The five conformations of the pyrocatechol·H<sub>2</sub>O complexes are depicted in **Table S6**. In the most stable conformation (C<sub>1</sub>), the intramolecular hydrogen bond between the two hydroxyl groups of pyrocatechol in its isolated state is retained. Water is placed next to the hydrogen available to create a hydrogen bond as an acceptor [44, 46, 73]. The C<sub>1</sub> conformation presents an energy  $\Delta E$  of -20.54 kJ.mol<sup>-1</sup> and -35.91 kJ.mol<sup>-1</sup> respectively with and without the ZPE and BSSE correction terms. These values are similar to the ones found by Gerhards et al [44] at the HF/6-31G(d,p) level (-24.92 kJ.mol<sup>-1</sup> and -33.32 kJ.mol<sup>-1</sup>) and by Gomez-Zaleta et al [46] (-17.15 kJ.mol<sup>-1</sup>). In the C<sub>2</sub> conformation, water is placed between the two hydroxyl groups. Therefore, the intramolecular hydrogen bond is destroyed to create a bridge where water is both an acceptor and a donor. In the C<sub>3</sub> conformation, one part of the water molecule is in the plane of the benzene ring, interacting as a donor towards the oxygen available. The rotation of one hydroxyl group allows the formation of the C<sub>4</sub> conformation in which the intramolecular hydrogen bond no longer exists. The water molecule is involved as an acceptor in the same way than in C<sub>1</sub>. Yet, the C<sub>4</sub> structure is less stable due to the lack of the intramolecular hydrogen bond. Finally, the C<sub>5</sub> structure corresponds to an interaction between the water and the hydrogen of the benzene ring.

*Guaiacol*

The seven conformations of the guaiacol·H<sub>2</sub>O complexes are presented in **Table S7**. In its ground state, guaiacol presents an intramolecular hydrogen bond between its hydroxyl and methoxy groups. In some of the complexes conformations, this hydrogen bond is destroyed (C<sub>1</sub>, C<sub>2</sub>, C<sub>6</sub>). In the C<sub>1</sub> and C<sub>2</sub> conformations, water inserts between the hydroxyl and methoxy groups of guaiacol, creating a double hydrogen bond, where water is at the same time a donor with the methoxy group, and as an acceptor towards the hydroxyl one. The difference between C<sub>1</sub> and C<sub>2</sub> conformations is the position of the methoxy group. In C<sub>2</sub> conformation, the methoxy group is in the plan of the benzene ring while it forms a dihedral angle C3-C4-O3-C7 of -86.97° in C<sub>1</sub>. When the binding energy is calculated only with the energy of the clusters, C<sub>1</sub> is the most stable conformation (-26.35 kJ.mol<sup>-1</sup> for C<sub>1</sub> and -26.29 kJ.mol<sup>-1</sup> for C<sub>2</sub>). Nevertheless, the ZPE and BSSE corrected relative energies show that C<sub>2</sub> conformation is a slightly more stable than C<sub>1</sub> (-7.66 kJ.mol<sup>-1</sup> for C<sub>1</sub> and -8.37 kJ.mol<sup>-1</sup> for C<sub>2</sub>). For Jalili et al [27] and Wu et al [64], the minimum structure corresponds to the methoxy group in the plan of the benzene ring (C<sub>2</sub>). Yet,

these authors did not investigate the potential improvement of the stability upon the rotation of the methoxy group corresponding to another minimum (structure  $C_1$ ). The conformation in the work of Wu et al [64] presents a binding energy of  $-35.94 \text{ kJ}\cdot\text{mol}^{-1}$  at the MP2/6-31+G(d,p) level of theory and a value of  $-13.81 \text{ kJ}\cdot\text{mol}^{-1}$  with the BSSE and the ZPE correction obtained at the B3LYP/6-31+G(d,p) level of theory. Lower energies in absolute were obtained by Jalili and al [27] at the B3LYP/6-31+G\*\* calculated on the 6-31G\*\* geometry ( $-21.09 \text{ kJ}\cdot\text{mol}^{-1}$  without any correction and  $-7.66 \text{ kJ}\cdot\text{mol}^{-1}$  with ZPE and BSSE terms). These results are in good agreement with the binding energy obtained for the same conformation ( $C_2$ ) in this work. In the  $C_3$  conformation, water acts as a hydrogen donor towards the hydroxyl group. The previous intramolecular hydrogen bond is maintained in guaiacol. Similar phenomenon is observed in the  $C_4$  conformation although water is now involved as an acceptor towards the hydrogen of the methoxy group. The  $C_5$  conformation is particularly complex. Indeed, water inserts between the hydroxyl and methoxy group of guaiacol but the intramolecular hydrogen bond of the molecule is not destroyed. Water is placed as a donor towards the hydroxyl group and an acceptor towards the methoxy one. The  $C_6$  conformation is similar that the one observed in the phenol·H<sub>2</sub>O complex. To be accessible, the hydroxyl group rotates to  $180^\circ$  and therefore it destroys the intramolecular bond. Then, water is put in a translinear position towards the hydroxyl group as an acceptor. Finally, the last conformation  $C_7$  presents the water molecule as an acceptor towards the hydrogen of benzene ring.

### *Syringol*

The conformations of syringol in its ground state and in its complex forms with water are presented in **Table S8**. In its ground state, syringol presents an intramolecular hydrogen bond between the hydroxyl and methoxy groups. Using the cc-pVTZ basis set, the minimum energy structure corresponds to all substituents placed in the plan of the benzene ring. In the syringol·H<sub>2</sub>O complexes, five different conformations were investigated. As for guaiacol, several conformations destroys the previous intramolecular hydrogen bond ( $C_1$ - $C_4$ ). In the  $C_1$  and  $C_2$  conformations, water inserts between the hydroxyl and methoxy groups of syringol. Thus, water is involved in a double hydrogen bond: as an acceptor towards the hydroxyl group and as a donor towards the methoxy one. The difference between  $C_1$  and  $C_2$  conformations corresponds to the position of the methoxy group. In  $C_1$ , the methoxy inclines to a dihedral angle  $C_1$ - $C_2$ - $O_2$ - $C_7$  of  $-94.61^\circ$  while in  $C_2$ , it is in the plan of the benzene ring. The  $C_1$

conformation is the most stable with a binding energy of  $-26.34 \text{ kJ.mol}^{-1}$  ( $-8.02 \text{ kJ.mol}^{-1}$  with ZPE and BSSE correction). The  $C_3$  and  $C_4$  conformations are similar to  $C_1$ . Water is still between the hydroxyl and the oriented methoxy groups but the second methoxy is no longer in the plan of the benzene ring. Oriented with a dihedral angle C3-C4-O4-C8 around  $65^\circ$ , it is either facing the first methoxy in the same side of the benzene ring ( $C_3$ ) or it is placed on the other side ( $C_4$ ). Finally, the last structure  $C_5$  does not destroy the previous intramolecular hydrogen bond. Water is placed as a hydrogen donor next to the free methoxy group. The water molecule is involved into a double hydrogen bond with a hydroxyl and an oriented methoxy group (similar to  $C_1$ ) for the lowest energy conformation. No data are available in the literature for comparison.

### *Vanillin*

The conformation of vanillin in its ground state and in its nine forms with water are depicted in **Table S9**. As for guaiacol and syringol, vanillin also presents an intramolecular hydrogen bond between the hydroxyl and methoxy groups. In the first two conformations  $C_1$  and  $C_2$ , water is placed as a hydrogen donor next to the oxygen atom of the aldehyde group. Therefore, the intramolecular hydrogen bond present in the vanillin's isolated form remained in these conformations with water. The position of the water molecule close to the aldehyde and the benzene ring ( $C_1$ ) stabilizes the hydrogen bonding with water compared to the  $C_2$  conformation. The binding energy corresponding to the  $C_1$  conformation has a value of  $-35.04 \text{ kJ.mol}^{-1}$  ( $-18.11 \text{ kJ.mol}^{-1}$  with ZPE and BSSE corrective terms). The  $C_3$  conformation corresponds to the cyclic one: water is involved in a double hydrogen bond between the hydroxyl and methoxy groups. In the  $C_4$  conformation, water placed as a hydrogen donor towards the hydroxyl group maintains the intramolecular hydrogen bond. The  $C_5$  conformation corresponds to the translinear conformation. The rotation of the hydroxyl group destroys the previous intramolecular hydrogen bond. Therefore, the water molecule can interact as an acceptor towards the hydroxyl group. Vanillin also presents a structure where water interacts with the hydrogen of the benzene ring. Yet, in the  $C_6$  conformation, water is involved in a bifurcated hydrogen bond with the aromatic moiety and the aldehyde hydrogens. For the last two structures, the hydroxyl group is rotated of an angle of  $180^\circ$ . Water is placed between the hydroxyl and methoxy groups. In the  $C_7$  conformation, each hydrogen of water interacts with one oxygen of vanillin while in the  $C_8$  conformation, only one hydrogen of water interacts with the two oxygens of vanillin. .

### *Comparison of the global minimum structures*

The phenol·H<sub>2</sub>O complex is the most stable when the water molecule is placed in a translinear position to the benzene ring next to the hydroxyl group. Same observations are drawn with o-cresol·H<sub>2</sub>O, *cis* m-cresol·H<sub>2</sub>O, *trans* m-cresol·H<sub>2</sub>O and p-cresol·H<sub>2</sub>O complexes. In the pyrocatechol·H<sub>2</sub>O conformation, the translinear conformation is also favoured. Indeed, the structure is stabilized by the intramolecular hydrogen bond between the two hydroxyl groups but also by the symmetrical interaction with water around the plan of the benzene ring.

When the phenolic compound presents initially an intramolecular hydrogen bond, water inserts between the two functional groups in a cyclic structure. Therefore, the previous hydrogen bond is destroyed and replaced by a double intermolecular hydrogen bond (guaiacol and syringol). Moreover, the complex structure is more stable when the involved methoxy group does not remain in the plan of the benzene ring. In the case of vanillin, the intramolecular hydrogen bond is preserved since water prefers to interact with the aldehyde group.

### **III-3.2. Vibrational frequencies**

The lengths and the scaled frequency of specific bonds are listed in Table III-2.

#### *Phenol*

In the phenol·H<sub>2</sub>O complex, the O<sub>3</sub>-H<sub>3</sub> bond is extended due to the presence of the water molecule as an acceptor. The O-H bond reaches 0.973 Å in the complex conformation while the length is only 0.962 Å in pure phenol. This phenomenon is also observed in the vibration frequencies where the O<sub>3</sub>-H<sub>3</sub> free vibration is of 3689.38 cm<sup>-1</sup> and drops to 3490.02 cm<sup>-1</sup> in the complex conformation. Similar observations were previously observed experimentally by Tanabe et al [83] (free OH group presents a stretching frequency of 3657 cm<sup>-1</sup> while in contact with water, the frequency has a value of 3524 cm<sup>-1</sup>) and computationally by Ahn [72] with BLYP/6-31G\*\* level (3667.49 cm<sup>-1</sup> and 3465.4 cm<sup>-1</sup> for isolated form and the complex with water, respectively). In this translinear conformation, water is involved symmetrically in the complex. The O<sub>w</sub>-H<sub>w</sub> bonds in water are also longer up to 0.962 Å, in agreement with the observed redshift in the frequencies (3669.54 cm<sup>-1</sup> and 3765.19 cm<sup>-1</sup> for the symmetrical and anti-symmetrical vibrations, respectively). These results are in accordance with the work of Tanabe et al [83]. They determined experimental frequencies for water of 3650 cm<sup>-1</sup> and 3748

$\text{cm}^{-1}$  for symmetrical and anti-symmetrical stretching modes, respectively. Similar behaviors were observed for the other translinear conformations, especially for o-cresol, m-cresol, p-cresol and pyrocatechol.

### *Pyrocatechol*

The previous intramolecular hydrogen bond observed between the two hydroxyl groups (noted O3-H3 for the donor and O4-H4 for the acceptor) of pyrocatechol in its isolated state is preserved in its one water conformation complex. The O3-H3 bond length is not affected (pure pyrocatechol: 0.965 Å, pyrocatechol·H<sub>2</sub>O: 0.966 Å). In the translinear position, water forms a hydrogen bond as an acceptor with the hydroxyl group available. The original O4-H4 bond increases from 0.961 Å (3706.37  $\text{cm}^{-1}$ ) to 0.974 Å (3468.68  $\text{cm}^{-1}$ ). Similar frequencies were obtained experimentally by Gerhards et al [73] (3673  $\text{cm}^{-1}$  for pure catechol and 3499  $\text{cm}^{-1}$  with one water molecule). The water bonds also increase to a value of 0.962 Å, like for the other translinear conformations. This elongation is concomitant with the drop of the frequencies to 3671.41  $\text{cm}^{-1}$  and 3767.30  $\text{cm}^{-1}$  (initially 3673.05  $\text{cm}^{-1}$  and 3770.05  $\text{cm}^{-1}$ ) for the symmetric and the anti-symmetric vibration, respectively. The range of value is the same as for the other translinear complexes.

**Table III-2:** Lengths and frequencies of O-H bonds.

System	Bond	Lengths (Å)	Scaled frequency (cm <sup>-1</sup> ) <sup>b</sup>
H <sub>2</sub> O	Symmetrical (Sym)	0.961	3673.05
	Antisymmetrical (Antisym)	0.961	3770.05
Phenol	Phenolic O3-H3	0.962 <sup>a</sup>	3689.38
	Phenolic O3-H3	0.973	3490.02
Phenol·H <sub>2</sub> O	H2O sym Ow-Hw	0.962	3669.54
	H2O antisym Ow-Hw	0.962	3765.19
O-cresol	Phenolic O3-H3	0.962 <sup>a</sup>	3690.24
	Phenolic O3-H3	0.973	3492.04
O-cresol·H <sub>2</sub> O	H2O sym Ow-Hw	0.962	3668.20
	H2O antisym Ow-Hw	0.962	3763.92
Cis m-cresol	Phenolic O3-H3	0.962 <sup>a</sup>	3688.41
	Phenolic O3-H3	0.973	3492.36
Cis m-cresol·H <sub>2</sub> O	H2O sym Ow-Hw	0.962	3668.39
	H2O antisym Ow-Hw	0.962	3764.00
Trans m-cresol	Phenolic O3-H3	0.962 <sup>a</sup>	3688.99
	Phenolic O3-H3	0.973	3492.94
Trans m-cresol·H <sub>2</sub> O	H2O sym Ow-Hw	0.962	3668.39
	H2O antisym Ow-Hw	0.962	3764.13
P-cresol	Phenolic O3-H3	0.962 <sup>a</sup>	3690.91
	Phenolic O3-H3	0.972	3495.39
P-cresol·H <sub>2</sub> O	H2O sym Ow-Hw	0.962	3669.00
	H2O antisym Ow-Hw	0.962	3764.65
Pyrocatechol	Phenolic O3-H3	0.965 <sup>a</sup>	3653.77
	Phenolic O4-H4	0.961	3706.37
	Phenolic O3-H3	0.966	3639.95
Pyrocatechol·H <sub>2</sub> O	Phenolic O4-H4	0.974	3468.68
	H2O sym Ow-Hw	0.962	3671.41
	H2O antisym Ow-Hw	0.962	3767.30
Guaiacol	Phenolic O3-H3	0.966 <sup>a</sup>	3641.27
	Phenolic O3-H3	0.979	3364.24
Guaiacol·H <sub>2</sub> O	H2O bound Ow-Hw2	0.972	3520.86
	H2O non bound Ow-Hw1	0.962	3733.77
Syringol	Phenolic O3-H3	0.966 <sup>a</sup>	3641.57
	Phenolic O3-H3	0.979	3369.01
Syringol·H <sub>2</sub> O	H2O bound Ow-Hw1	0.972	3517.97
	H2O non bound Ow-Hw2	0.962	3733.33
Vanillin	Phenolic O3-H3	0.967 <sup>a</sup>	3622.40
	ketone C8=O8	1.212 <sup>a</sup>	1701.16
Vanilline·H <sub>2</sub> O	phenolic O3-H3	0.968	3615.00
	ketone C8=O8	1.219	1675.87
	H2O bound Ow-Hw2	0.973	3510.99
	H2O non bound Ow-Hw1	0.961	3733.98

<sup>a</sup> : from previous chapter, <sup>b</sup>: scaled factor of 0.9665 [77]

*Guaiacol*

For guaiacol·H<sub>2</sub>O complex, the previous intramolecular hydrogen bond present in the isolated form does no longer exist. Water acts as a hydrogen acceptor towards the hydroxyl group and as a donor towards the methoxy one. Therefore, the O3-H3 bond of guaiacol increases from 0.966 Å to 0.979 Å. This is confirmed by the red shift in the frequencies from 3641.27 cm<sup>-1</sup> to 3364.24 cm<sup>-1</sup>. Similar results were obtained computationally by Jalili et al [27] with the B3LYP/6-31G\*\* basis set (3688.2 cm<sup>-1</sup> for the hydroxyl group involved in the intramolecular hydrogen bond in the isolated form and 3443.7 cm<sup>-1</sup> for intermolecular hydrogen bond in the water cluster conformation). Wu and Brutschy [64] observed by IR/R2PI measurements a red shift in the stretching vibration frequency of the hydroxyl group in guaiacol with the addition of one water molecule. The hydroxyl group presents a frequency of 3599 cm<sup>-1</sup> in the pure guaiacol conformation whereas its frequency drops down to 3477 cm<sup>-1</sup> in the presence of water. Unlike in the trans-linear conformations, the water molecule is not involved symmetrically in the intermolecular hydrogen bond. The water bonded Ow-Hw2 is longer (0.972 Å) than the free one Ow-Hw1 (0.962 Å). Therefore, the frequency of the bonded Ow-Hw2 is lower 3520.86 cm<sup>-1</sup> than the free one Ow-Hw1 3733.77 cm<sup>-1</sup>. Similar frequencies were determined experimentally by Wu and Brutschy [64] (free OwHw: 3731cm<sup>-1</sup>, bonded OwHw: 3605 cm<sup>-1</sup>), and computationally by Jalili et al [27] (free OwHw: 3784.3 cm<sup>-1</sup>, bonded OwHw: 3629.7 cm<sup>-1</sup>).

*Syringol*

In its one water complex, the previous intramolecular hydrogen bond between the hydroxyl and one methoxy group of syringol does not longer exist. The increase of the O3-H3 bond (from 0.966 Å to 0.979 Å) in syringol is highlighted by its frequency drops from 3641.57 cm<sup>-1</sup> down to 3369.01 cm<sup>-1</sup>. These frequencies are in the same range of values than those observed for the guaiacol conformations. Indeed, the water molecule has a similar behavior with syringol or guaiacol: acceptor towards the hydroxyl group and donor to the methoxyl one. Therefore, the bond lengths are similar: 0.972 Å for the bonded Ow-Hw1 and 0.962 Å for the free Ow-Hw2. Similarities are also observed in the frequencies (3517.97 cm<sup>-1</sup> for bonded Ow-Hw1 and 3733.33 cm<sup>-1</sup> for the free Ow-Hw2).

*Vanillin*

In the vanillin·H<sub>2</sub>O conformation, the previous intramolecular hydrogen bond between the hydroxyl and methoxy groups is maintained. The length of the O3-H3 bond is slightly increased (from 0.967 to 0.968 Å) by the presence of water. Because it interacts directly with water, the carboxyl bond C8=O8 increases from 1.212 Å in its isolated state to 1.219 Å in the water complex form. This observation is in agreement with the red shift in the frequency. The C=O vibration has a value of 1701.16 cm<sup>-1</sup> in the isolated state and achieves 1675.87 cm<sup>-1</sup> in the complex form. The frequency of the C=O vibration of the isolated vanillin is in accordance with the work of Balachandran et al [84], both computationally (1689 cm<sup>-1</sup> at B3LYP/6-311++G\*\*) and experimentally (1687 cm<sup>-1</sup> by infra-red spectroscopy). The water molecule is not involved symmetrically in the hydrogen bond. Therefore, the OH bonds are not the same. In the bonded Ow-Hw2, the length is of 0.973 Å with a frequency of 3510.99 cm<sup>-1</sup>, whereas the free Ow-Hw1 has a smaller length of 0.961 Å, characterized by a higher vibration frequency (3733.98 cm<sup>-1</sup>).

*Comparison*

Tables III-3 and III-4 list all the bonds lengths and angles of the global minimum conformations of the phenolic compounds in their one water complex forms.

It is worth to notice that these parameters fluctuates like pure phenolic molecules [53, 82]. Indeed, the C-C bond length in the benzene ring increases as a function of the substituent position for guaiacol, o-,m-,p-cresol, syringol, pyrocatechol and vanillin. Same behaviour is observed in the case of the one water complex forms (bold numbers in Table III-3). Moreover, these bonds are antiperiplanar to the C-O (for methoxyl) or C-C (for methyl) bond of the substituent.

In the translinear conformations, the O3-H3 bond increases to 0.973 Å (*italic values*) caused by the donor behavior of the phenolic molecule in the hydrogen bond. Water is placed symmetrically at the perpendicular of the benzene ring. Therefore, the lengths of the two Ow-Hw bonds are equal (0.962 Å). The role of water as the hydrogen acceptor slightly affects the lengths of the Ow-Hw bonds.

**Table III-3:** Calculated bond lengths (Å) of the global minimum conformations in the {phenolic compound – water} cluster.

Phenol		O-cresol		Cis M-cresol		Trans M-cresol		P-cresol		Pyrocatechol		Guaiacol		Syringol		Vanillin	
bond	Length	bond	Length	bond	Length	Bond	Length	Bond	Length	Bond	Length	Bond	Length	Bond	Length	Bond	Length
C1-C2	1.387	C1-C2	1.390	C1-C2	1.385	C1-C2	1.389	C1-C2	1.385	C1-C2	1.393	C1-C2	1.387	C1-C2	1.392	C1-C2	1.387
C2-C3	1.396	C2-C3	1.394	C2-C3	1.396	C2-C3	1.396	C2-C3	1.395	C2-C3	1.386	C2-C3	1.396	C2-C3	1.396	C2-C3	1.387
C3-C4	1.396	C3-C4	<b>1.403</b>	C3-C4	1.394	C3-C4	1.394	C3-C4	1.393	C3-C4	<b>1.402</b>	C3-C4	<b>1.403</b>	C3-C4	<b>1.412</b>	C3-C4	<b>1.414</b>
C4-C5	1.390	C4-C5	1.391	C4-C5	<b>1.396</b>	C4-C5	1.392	C4-C5	1.391	C4-C5	1.387	C4-C5	1.388	C4-C5	1.391	C4-C5	1.377
C5-C6	1.390	C5-C6	1.392	C5-C6	1.393	C5-C6	<b>1.397</b>	C5-C6	1.392	C5-C6	1.394	C5-C6	1.389	C5-C6	1.394	C5-C6	<b>1.407</b>
C1-C6	1.392	C1-C6	1.388	C1-C6	1.393	C1-C6	1.389	C1-C6	<b>1.398</b>	C1-C6	1.388	C1-C6	1.391	C1-C6	1.383	C1-C6	1.395
C1-H1	1.082	C1-H1	1.082	C1-H1	1.082	C1-H1	1.083	C1-H1	1.084	C1-H1	1.081	C1-H1	1.082	C1-H1	1.081	C1-H1	1.083
C2-H2	1.081	C2-H2	1.083	C2-H2	1.081	C2-H2	1.082	C2-H2	1.082	C2-H2	1.081	C2-H2	1.081	C2-H2	<u>1.393</u>	C1-H2	1.081
-	-	-	-	-	-	-	-	-	-	-	-	-	-	O2-C7	1.436	-	-
-	-	-	-	-	-	-	-	-	-	-	-	-	-	C7-H7a	1.091	-	-
-	-	-	-	-	-	-	-	-	-	-	-	-	-	C7-H7b	1.088	-	-
-	-	-	-	-	-	-	-	-	-	-	-	-	-	C7-H7c	1.091	-	-
C3-O3	1.359	C3-O3	1.362	C3-O3	1.359	C3-O3	1.359	C3-O3	1.360	C3-O3	1.364	C3-O3	1.355	C3-O3	1.354	C3-O3	1.350
O3-H3	<i>0.973</i>	O3-H3	<i>0.973</i>	O3-H3	<i>0.973</i>	O3-H3	<i>0.973</i>	O3-H3	<i>0.972</i>	O3-H3	0.966	O3-H3	<u>0.979</u>	O3-H3	<u>0.979</u>	O3-H3	0.968
C4-H4	1.083	C4-C7	1.503	C4-H4	1.084	C4-H4	1.083	C4-H4	1.083	C4-O4	1.369	C4-O4	<u>1.393</u>	C4-O4	1.359	C4-O4	1.364
C5-H5	1.083	C7-H7a	1.089	C5-C7	1.508	C5-C7	1.507	C5-H5	1.083	O4-H4	<i>0.974</i>	O4-C7	1.437	O4-C8	1.416	O4-C7	1.428
C6-H6	1.081	C7-H7b	1.092	C7-H7a	1.092	C7-H7a	1.090	C6-C7	1.507	C5-H5	1.083	C7-H7a	1.088	C8-H8a	1.087	C7-H7a	1.091
-	-	C7-H7c	1.091	C7-H7b	1.089	C7-H7b	1.093	C7-H7a	1.090	C6-H6	1.081	C7-H7b	1.091	C8-H8b	1.094	C7-H7b	1.091
-	-	C5-H5	1.083	C7-H7c	1.092	C7-H7c	1.090	C7-H7b	1.093	-	-	C7-H7c	1.091	C8-H8c	1.094	C7-H7c	1.086
-	-	C6-H6	1.081	C6-H6	1.082	C6-H6	1.082	C7-H7c	1.093	-	-	C5-H5	1.082	C5-H5	1.079	C5-H5	1.080
-	-	-	-	-	-	-	-	-	-	-	-	C6-H6	1.081	C6-H6	1.081	C6-C8	1.460
-	-	-	-	-	-	-	-	-	-	-	-	-	-	-	-	C8-H8	1.107
-	-	-	-	-	-	-	-	-	-	-	-	-	-	-	-	C8=O8	1.219
-	-	-	-	-	-	-	-	-	-	-	-	-	-	-	-	-	-
Ow-Hw1	0.962	Ow-Hw1	0.962	Ow-Hw1	0.962	Ow-Hw1	0.962	Ow-Hw1	0.962	Ow-Hw1	0.962	Ow-Hw1	0.962	Ow-Hw1	<u>0.972</u>	Ow-Hw1	0.961
Ow-Hw2	0.962	Ow-Hw2	0.962	Ow-Hw2	0.962	Ow-Hw2	0.962	Ow-Hw2	0.962	Ow-Hw2	0.962	Ow-Hw2	<u>0.972</u>	Ow-Hw2	0.962	Ow-Hw2	<u>0.973</u>
-	-	-	-	-	-	-	-	-	-	-	-	-	-	-	-	-	-
-	-	-	-	-	-	-	-	-	-	-	-	-	-	-	-	-	-
-	-	-	-	-	-	-	-	-	-	H3--O4	2.114	-	-	-	-	H3--O4	2.079
-	-	-	-	-	-	-	-	-	-	O3--O4	2.669	-	-	-	-	O3--O4	2.634
-	-	-	-	-	-	-	-	-	-	-	-	-	-	-	-	-	-
H3--Ow	1.867	H3--Ow	1.869	H3-Ow	1.873	H3-Ow	1.870	H3-Ow	1.871	H4--Ow	1.830	H3--Ow	1.823	H3--Ow	1.827	Hw2--O8	1.912
O3--Ow	2.837	O3--Ow	2.838	O3-Ow	2.842	O3-Ow	2.839	O3-Ow	2.840	O4--Ow	2.803	O3--Ow	2.796	O3--Ow	2.800	Ow--O8	2.869
-	-	-	-	-	-	-	-	-	-	-	-	-	-	-	-	-	-
-	-	-	-	-	-	-	-	-	-	-	-	Hw2--O4	1.904	Hw1--O2	1.899	H5--Ow	2.294
-	-	-	-	-	-	-	-	-	-	-	-	Ow--O4	2.748	Ow--O2	2.749	C5--Ow	3.3424

**Table III-4:** Calculated bond angles (in degrees) of the global minimum conformations in the {phenolic compound – water} cluster.

Phenol		O-cresol		Cis M-cresol		M-cresol trans		P-cresol		Pyrocatechol		Guaiacol		Syringol		Vanillin	
Angles	Values	Angles	Values	Angles	Values	Angles	Values	Angles	Values	Angles	Values	Angles	Values	Angles	Values	Angles	Values
C1-C2-C3	119.9	C1-C2-C3	120.1	C1-C2-C3	119.4	C1-C2-C3	119.3	C1-C2-C3	120.1	C1-C2-C3	120.1	C1-C2-C3	120.8	C1-C2-C3	121.7	C1-C2-C3	119.5
C2-C3-C4	119.6	C2-C3-C4	120.7	C2-C3-C4	119.8	C2-C3-C4	119.8	C2-C3-C4	119.1	C2-C3-C4	119.8	C2-C3-C4	118.3	C2-C3-C4	118.2	C2-C3-C4	120.2
C3-C4-C5	119.9	C3-C4-C5	118.0	C3-C4-C5	120.9	C3-C4-C5	121.0	C3-C4-C5	120.0	C3-C4-C5	120.0	C3-C4-C5	120.7	C3-C4-C5	120.1	C3-C4-C5	120.3
C4-C5-C6	120.7	C4-C5-C6	121.9	C4-C5-C6	118.9	C4-C5-C6	118.9	C4-C5-C6	121.7	C4-C5-C6	119.9	C4-C5-C6	120.5	C4-C5-C6	120.4	C4-C5-C6	119.5
C5-C6-C1	119.1	C5-C6-C1	119.3	C5-C6-C1	120.2	C5-C6-C1	120.1	C5-C6-C1	117.4	C5-C6-C1	120.0	C5-C6-C1	119.2	C5-C6-C1	120.2	C5-C6-C1	120.0
C6-C1-C2	120.7	C6-C1-C2	120.1	C6-C1-C2	120.9	C6-C1-C2	120.9	C6-C1-C2	121.7	C6-C1-C2	120.1	C6-C1-C2	120.5	C6-C1-C2	119.4	C6-C1-C2	120.6
C2-C1-H1	119.3	C2-C1-H1	119.5	C2-C1-H1	119.4	C2-C1-H1	119.3	C2-C1-H1	118.9	C2-C1-H1	119.6	C2-C1-H1	119.4	C2-C1-H1	118.8	C2-C1-H1	119.8
C6-C1-H1	120.0	C6-C1-H1	120.4	C6-C1-H1	119.7	C6-C1-H1	119.8	C6-C1-H1	119.4	C6-C1-H1	120.3	C6-C1-H1	120.1	C6-C1-H1	121.8	C6-C1-H1	119.6
C1-C2-H2	121.3	C1-C2-H2	120.6	C1-C2-H2	121.6	C1-C2-H2	120.9	C1-C2-H2	121.1	C1-C2-H2	121.4	C1-C2-H2	121.3	C1-C2-H2	119.1	C1-C2-H2	121.7
C3-C2-H2	118.8	C3-C2-H2	119.3	C3-C2-H2	119.0	C3-C2-H2	119.8	C3-C2-H2	118.8	C3-C2-H2	118.6	C3-C2-H2	117.9	C3-C2-H2	119.3	C3-C2-H2	118.7
-	-	-	-	-	-	-	-	-	-	-	-	-	-	C2-O2-C7	113.9	-	-
-	-	-	-	-	-	-	-	-	-	-	-	-	-	O2-C7-H7a	110.2	-	-
-	-	-	-	-	-	-	-	-	-	-	-	-	-	O2-C7-H7b	106.7	-	-
-	-	-	-	-	-	-	-	-	-	-	-	-	-	O2-C7-H7c	110.9	-	-
-	-	-	-	-	-	-	-	-	-	-	-	-	-	H7a-C7-H7b	109.7	-	-
-	-	-	-	-	-	-	-	-	-	-	-	-	-	H7a-C7-H7c	109.7	-	-
-	-	-	-	-	-	-	-	-	-	-	-	-	-	H7b-C7-H7c	109.7	-	-
C2-C3-O3	117.8	C2-C3-O3	122.2	C2-C3-O3	117.7	C2-C3-O3	122.6	C2-C3-O3	117.9	C2-C3-O3	120.3	C2-C3-O3	118.3	C2-C3-O3	123.8	C2-C3-O3	120.1
C4-C3-O3	122.6	C4-C3-O3	117.1	C4-C3-O3	122.5	C4-C3-O3	117.6	C4-C3-O3	123.0	C4-C3-O3	119.9	C4-C3-O3	123.4	C4-C3-O3	118.0	C4-C3-O3	119.8
C3-O3-H3	110.5	C3-O3-H3	110.5	C3-O3-H3	110.5	C3-O3-H3	110.4	C3-O3-H3	110.4	C3-O3-H3	107.2	C3-O3-H3	112.0	C3-O3-H3	111.4	C3-O3-H3	107.7
C3-C4-H4	119.6	C3-C4-C7	119.9	C3-C4-H4	119.1	C3-C4-H4	118.3	C3-C4-H4	119.7	C3-C4-O4	115.4	C3-C4-O4	120.1	C3-C4-O4	115.2	C3-C4-O4	113.8
C5-C4-H4	120.6	C5-C4-C7	122.1	C5-C4-H4	120.0	C5-C4-H4	120.7	C5-C4-H4	120.4	C5-C4-O4	124.7	C5-C4-O4	119.3	C5-C4-O4	124.8	C5-C4-O4	126.0
C4-C5-H5	119.3	C4-C7-H7a	110.9	C4-C5-C7	120.0	C4-C5-C7	120.3	C4-C5-H5	118.9	C4-O4-H4	111.1	C4-O4-C7	113.9	C4-O4-C8	118.3	C4-O4-C7	118.0
C6-C5-H5	120.0	C4-C7-H7b	111.3	C6-C5-C7	121.1	C6-C5-C7	120.7	C6-C5-H5	119.4	C4-C5-H5	119.3	O4-C7-H7a	106.7	O4-C8-H8a	105.9	O4-C7-H7a	111.2
C1-C6-H6	120.5	C4-C7-H7c	111.3	C5-C7-H7a	111.3	C5-C7-H7a	111.4	C1-C6-C7	121.0	C6-C5-H5	120.8	O4-C7-H7b	110.3	O4-C8-H8b	111.7	O4-C7-H7b	110.9
C5-C6-H6	120.4	H7a-C7-H7b	108.4	C5-C7-H7b	111.3	C5-C7-H7b	111.0	C5-C6-C7	121.6	C1-C6-H6	120.4	O4-C7-H7c	110.9	O4-C8-H8c	111.6	O4-C7-H7c	105.9
-	-	H7a-C7-H7c	108.4	C5-C7-H7c	111.2	C5-C7-H7c	111.5	C6-C7-H7a	111.2	C5-C6-H6	119.6	H7a-C7-H7b	109.7	H8a-C8-H8b	109.2	H7a-C7-H7b	109.0
-	-	H7b-C7-H7c	106.4	H7a-C7-H7b	107.9	H7a-C7-H7b	107.3	C6-C7-H7b	111.6	-	-	H7a-C7-H7c	109.7	H8a-C8-H8c	109.2	H7a-C7-H7c	110.0
-	-	C4-C5-H5	118.6	H7a-C7-H7c	107.1	H7a-C7-H7c	108.2	C6-C7-H7c	111.6	-	-	H7b-C7-H7c	109.6	H8b-C8-H8c	109.1	C4-C5-H5	121.2
-	-	C6-C5-H5	119.5	H7b-C7-H7c	107.8	H7b-C7-H7c	107.3	H7a-C7-H7b	107.6	-	-	C4-C5-H5	118.3	C4-C5-H5	120.1	C6-C5-H5	119.4
-	-	C1-C6-H6	120.5	C1-C6-H6	120.0	C1-C6-H6	120.0	H7a-C7-H7c	107.6	-	-	C6-C5-H5	121.2	C6-C5-H5	119.5	C1-C6-C8	118.9
-	-	C5-C6-H6	120.2	C5-C6-H6	119.8	C5-C6-H6	119.8	H7b-C7-H7c	107.0	-	-	C1-C6-H6	120.6	C1-C6-H6	120.2	C5-C6-C8	121.1
-	-	-	-	-	-	-	-	-	-	-	-	C5-C6-H6	120.1	C5-C6-H6	119.6	C6-C8-H8	114.3
-	-	-	-	-	-	-	-	-	-	-	-	-	-	-	-	C6-C8=O8	126.5
-	-	-	-	-	-	-	-	-	-	-	-	-	-	-	-	H8-C8=O8	119.3
-	-	-	-	-	-	-	-	-	-	-	-	-	-	-	-	-	-
-	-	-	-	-	-	-	-	-	-	O3-H3-O4	114.9	-	-	-	-	O3-H3-O4	114.7
-	-	-	-	-	-	-	-	-	-	-	-	-	-	-	-	-	-
O3-H3-Ow	174.5	O3-H3-Ow	174.1	O3-Hw-Ow	173.5	O3-Hw-Ow	174.0	O3-H3-Ow	173.9	O4-H4-Ow	176.8	O3-H3-Ow	171.9	O3-H3-Ow	172.4	Ow-Hw2-O8	167.3
H3-Ow-Hw1	113.5	H3-Ow-Hw1	113.6	H3-Ow-Hw1	112.5	H3-Ow-Hw1	113.2	H3-Ow-Hw1	112.6	H4-Ow-Hw1	116.4	H3-Ow-Hw1	113.8	H3-Ow-Hw1	84.2	Hw2-O8-C8	132.1
H3-Ow-Hw2	113.5	H3-Ow-Hw2	113.6	H3-Ow-Hw2	112.5	H3-Ow-Hw2	112.9	H3-Ow-Hw2	112.6	H4-Ow-Hw2	116.4	H3-Ow-Hw2	84.8	H3-Ow-Hw2	113.0	-	-
-	-	-	-	-	-	-	-	-	-	-	-	-	-	-	-	-	-
-	-	-	-	-	-	-	-	-	-	-	-	Ow-Hw2-O4	143.7	Ow-Hw1-O2	144.5	C5-H5-Ow	163.0
-	-	-	-	-	-	-	-	-	-	-	-	Hw2-O4-C4	116.6	Hw1-O2-C2	116.4	H5-Ow-Hw1	123.1
-	-	-	-	-	-	-	-	-	-	-	-	Hw2-O4-C7	109.3	Hw1-O2-C7	110.2	H5-Ow-Hw2	68.3
-	-	-	-	-	-	-	-	-	-	-	-	-	-	-	-	-	-
Hw1-Ow-Hw2	105.6	Hw1-Ow-Hw2	105.6	Hw1-Ow-Hw2	105.6	Hw1-Ow-Hw2	105.6	Hw1-Ow-Hw2	105.574	Hw1-Ow-Hw2	105.8	Hw1-Ow-Hw2	106.4	Hw1-Ow-Hw2	106.3	Hw1-Ow-Hw2	104.5

In the cyclic (guaiacol and syringol) and perpendicular (vanillin) conformations, water is the donor molecule in the hydrogen bond. Its asymmetrical interactions lead to different bond lengths. The interacting Ow-Hw bond presents longer lengths (0.972 Å, underlined values) than the free Ow-Hw one. The O3-H3 and C-O bonds interact in the cyclic bonds. Therefore, their lengths hugely increase compared to a simple intramolecular or intermolecular hydrogen bond (double underlined values).

The C-C-O angle of the hydroxyl group is larger when the hydroxyl, methoxy or aldehyde hydrogen is pointing through the same side (**bold values** in Table III-4). Similar results were previously observed for these molecules in their isolated configuration [53, 82]. In the cresols conformations, the deformation in the methyl-substituted aromatic carbon angle still remains in the water complex forms [82] (similar to [85–87]). The C-C-C angle values are always inferior to  $119^\circ$  (*italic values*). Finally, the angle in the water molecule is larger in the cyclic conformations (underlined values) than in the translinear ones.

### III-3.3. Natural Bond Orbitals (NBO) analysis

The charges obtained from the natural population analysis are listed in Table III-5. In the translinear conformations, the presence of the water molecule does not have a huge influence on the charges of the aromatic atoms. Only the aromatic hydrogen atom in the same side of the hydroxyl one is submitted to an increase of its charge (*italic values*). The main modification corresponds to the hydroxyl group with the increase of electronegativity for the oxygen and of electro positivity (**bold values**).

**Table III-5:** NBO population analysis.

Phenol			O-cresol		Cis M-cresol		Trans M-cresol		P-cresol		Pyrocatechol		Guaiacol		Syringol		Vanillin									
C0	C1		C0	C1	C0	C1	C0	C1	C0	C1	C0	C1	C0	C1	C0	C1	C0	C1								
C1	-0.177	-0.181	C1	-0.188	-0.191	C1	-0.167	-0.173	C1	-0.168	-0.172	C1	-0.183	-0.188	C1	-0.207	-0.191	C1	-0.309	-0.260	C1	-0.162	-0.155			
C2	-0.260	-0.265	C2	-0.281	-0.284	C2	-0.269	-0.272	C2	-0.300	-0.302	C2	-0.249	-0.252	C2	-0.245	-0.250	C2	-0.249	-0.244	C2	0.250	0.221	C2	-0.256	-0.260
C3	0.319	0.324	C3	0.312	0.316	C3	0.329	0.334	C3	0.329	0.333	C3	0.311	0.316	C3	0.269	0.267	C3	0.280	0.279	C3	0.235	0.240	C3	0.316	0.324
C4	-0.290	-0.293	C4	-0.054	-0.058	C4	-0.299	-0.302	C4	-0.271	-0.274	C4	-0.281	-0.284	C4	0.244	0.249	C4	0.237	0.208	C4	0.272	0.276	C4	0.242	0.244
C5	-0.178	-0.182	C5	-0.186	-0.190	C5	0.022	0.018	C5	0.023	0.018	C5	-0.186	-0.189	C5	-0.271	-0.275	C5	-0.281	-0.228	C5	-0.306	-0.295	C5	-0.241	-0.245
C6	-0.237	-0.245	C6	-0.227	-0.235	C6	-0.246	-0.253	C6	-0.246	-0.253	C6	-0.036	-0.044	C6	-0.215	-0.219	C6	-0.216	-0.227	C6	-0.194	-0.203	C6	-0.166	-0.176
H1	0.202	0.198	H1	0.202	0.198	H1	0.202	0.198	H1	0.201	0.197	H1	0.197	0.194	H1	0.203	0.200	H1	0.202	0.203	H1	0.208	0.211	H1	0.205	0.206
H2	0.214	0.208	H2	0.196	0.207	H2	0.213	0.209	H2	0.197	0.207	H2	0.213	0.208	H2	0.214	0.211	H2	0.214	0.214	H5	0.208	0.208	H2	0.219	0.220
H4	0.197	0.207	H5	0.197	0.193	H4	0.191	0.202	H4	0.209	0.204	H4	0.196	0.207	H5	0.198	0.208	H5	0.207	0.211	H6	0.201	0.202	H5	0.230	<u>0.249</u>
H5	0.202	0.198	H6	0.202	0.199	H6	0.198	0.194	H6	0.198	0.194	H5	0.197	0.193	H6	0.203	0.199	H6	0.202	0.203	-	-	-	-	-	-
H6	0.203	0.200	-	-	-	-	-	-	-	-	-	-	-	-	-	-	-	-	-	-	-	-	-	-	-	
O3	-0.660	<b>-0.686</b>	O3	-0.669	<b>-0.695</b>	O3	-0.661	<b>-0.687</b>	O3	-0.661	<b>-0.687</b>	O3	-0.662	<b>-0.688</b>	O3	<u>-0.658</u>	<u>-0.664</u>	O3	-0.659	<b>-0.692</b>	O3	-0.650	<b>-0.683</b>	O3	<u>-0.648</u>	<u>-0.645</u>
H3	0.466	<b>0.493</b>	H3	0.468	<b>0.495</b>	H3	0.466	<b>0.492</b>	H3	0.466	<b>0.493</b>	H3	0.465	<b>0.492</b>	H3	<u>0.482</u>	<u>0.482</u>	H3	0.482	<b>0.503</b>	H3	0.482	<b>0.502</b>	H3	<u>0.490</u>	<u>0.492</u>
-	-	-	C7	-0.595	-0.593	C7	-0.597	-0.595	C7	-0.597	-0.595	C7	-0.592	-0.591	O4	-0.694	<b>-0.721</b>	O4	-0.521	<b>-0.570</b>	O2	-0.522	<b>-0.570</b>	O4	-0.519	-0.520
-	-	-	H7a	0.200	0.197	H7a	0.205	0.204	H7a	0.205	0.202	H7a	0.205	0.199	H4	0.478	<b>0.505</b>	C7	-0.215	-0.212	C7	-0.214	-0.212	C7	-0.216	-0.218
-	-	-	H7b	0.212	0.209	H7b	0.204	0.201	H7b	0.210	0.207	H7b	0.204	0.202	-	-	-	H7a	0.187	0.182	H7a	0.167	0.168	H7a	0.174	0.185
-	-	-	H7c	0.212	0.209	H7c	0.208	0.205	H7c	0.205	0.203	H7c	0.201	0.202	-	-	-	H7b	0.168	0.168	H7b	0.187	0.182	H7b	0.174	0.176
-	-	-	-	-	-	-	-	-	-	-	-	-	-	-	-	-	-	H7c	0.168	0.174	H7c	0.167	0.175	H7c	0.190	0.187
-	-	-	-	-	-	-	-	-	-	-	-	-	-	-	-	-	-	-	-	-	O4	-0.476	-0.474	C8	0.410	0.424
-	-	-	-	-	-	-	-	-	-	-	-	-	-	-	-	-	-	-	-	-	C8	-0.218	-0.219	H8	0.098	0.106
-	-	-	-	-	-	-	-	-	-	-	-	-	-	-	-	-	-	-	-	-	H8a	0.187	0.188	O8	-0.538	<u>-0.583</u>
-	-	-	-	-	-	-	-	-	-	-	-	-	-	-	-	-	-	-	-	-	H8b	0.163	0.162	-	-	-
-	-	-	-	-	-	-	-	-	-	-	-	-	-	-	-	-	-	-	-	-	H8c	0.163	0.163	-	-	-
Ow	-	-0.923	Ow	-	-0.923	Ow	-	-0.922	Ow	-	-0.922	Ow	-	-0.925	Ow	-	-0.925	Ow	-	-0.938	Ow	-	-0.938	Ow	-	-0.948
Hw1	-	0.473	Hw1	-	0.473	Hw1	-	0.473	Hw1	-	0.473	Hw1	-	0.473	Hw1	-	0.476	Hw1	-	0.467	Hw1	-	0.489	Hw1	-	0.451
Hw2	-	0.473	Hw2	-	0.473	Hw2	-	0.473	Hw2	-	0.473	Hw2	-	0.473	Hw2	-	0.476	Hw2	-	0.489	Hw2	-	0.466	Hw2	-	0.487

In the cyclic forms, the meta carbons on the same side of the intermolecular cycle go through a huge modification in their charge (*italic values*), becoming less electronegative. The same phenomenon is observed for the other aromatic carbons. The atoms involved in the cyclic interactions present an increase of ~~in~~ their charge (**bold values**). As for the translinear conformations, there is an increase of the electronegativity and electropositivity of the oxygen and hydrogen atoms respectively. The differences in the charges upon complexation are more important in the cyclic forms than in the translinear ones.

The atoms in the intramolecular hydrogen bonds of pyrocatechol and vanillin are weakly affected by the complexation with water (underlined values). Finally, only the aromatic hydrogen interacting with water in the vanillin complex presents a major modification in its charge (double underlined value). The oxygen atom of the aldehyde group is not affected by the complexation.

The electronegativity of the water oxygen increases as follows: translinear < cyclic < vanillin. The hydrogen atoms involved non-symmetrically are more electropositive than the free ones.

### III-3.4 HOMO-LUMO analysis

The results for the HOMO-LUMO analysis are presented in Table III-6. In their isolated forms, the hardness of the molecules decreases as follows: phenol > o-cresol > pyrocatechol > guaiacol > trans m-cresol > cis m-cresol > syringol > p-cresol > vanillin. Upon the complexation with water, the hardness of the phenolic compounds decreases, except for guaiacol and syringol. Moreover, the interaction energy is weaker for the cyclic conformations of guaiacol and syringol than for the translinear ones. Therefore, the cyclic conformations are less stable than the translinear ones, and this behaviour leads to a higher reactivity of the guaiacol and syringol compounds.

**Table III-6:** HOMO-LUMO parameters.

Compounds	isolated				water cluster			
	HOMO (Hartree)	LUMO (Hartree)	$\chi$ (eV)	$\eta$ (eV)	HOMO (Hartree)	LUMO (Hartree)	$\chi$ (eV)	$\eta$ (eV)
Phenol	-0.31498	0.12423	2.59529	11.95152	-0.29750	0.11606	2.46862	11.25355
O-cresol	-0.30829	0.13043	2.41991	11.93819	-0.29167	0.11628	2.38630	11.10089
Cis m-cresol	-0.31062	0.12415	2.53705	11.83070	-0.29441	0.11662	2.41896	11.18470
Trans m-cresol	-0.31099	0.12735	2.49855	11.92785	-0.29419	0.11709	2.40957	11.19150
P-cresol	-0.30405	0.12332	2.45896	11.62934	-0.28764	0.11723	2.31855	11.01708
Pyrocatechol	-0.30615	0.13004	2.39610	11.86934	-0.28984	0.11041	2.44127	10.89136
Guaiacol	-0.30107	0.13483	2.26181	11.86145	-0.31133	0.12760	2.49978	11.94390
Syringol	-0.29471	0.13836	2.12725	11.78444	-0.29827	0.13508	2.22031	11.79206
Vanillin	-0.31881	0.07856	3.26877	10.81299	-0.32060	0.07018	3.40714	10.63367

The electronegativity of the phenolic compounds in their isolated forms decreases as follows: vanillin > phenol > cis m-cresol > trans m-cresol > p-cresol > o-cresol > pyrocatechol > guaiacol > syringol. With the presence of water, phenol and cresols are less electronegative than in their isolated forms whereas pyrocatechol, guaiacol, syringol and vanillin are more electronegative. Vanillin is the least hard but the most electronegative molecule of the studied compounds with or without water.

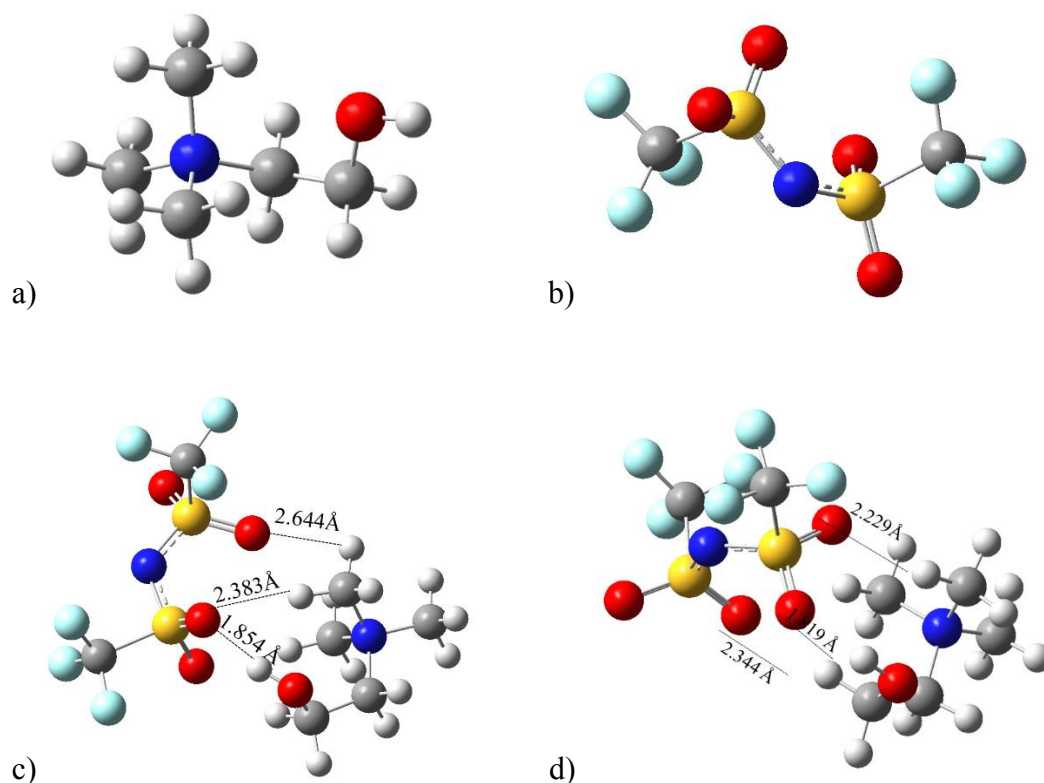
#### **III-4. Study of the phenol-choline bis(trifluoromethylsulfonide)imide cluster**

The most stable structures of the [choline] cation and the bis(trifluoromethylsulfonide)imide [NTf<sub>2</sub>] anion are presented in Figure III-1. In the NTf<sub>2</sub> anion's structure, the CF<sub>3</sub><sup>-</sup> groups lie on each side of the S-N-S plane. This result agrees well with conformations obtained by Fujii et al [87] and Paulechka [88]. In the choline's structure, the rotation of the N-C-C-O dihedral angles provides two structures: the most stable conformation with a dihedral value of -58.23°, and another less stable conformation with a dihedral value of -180°. The value of the N-C-C-O dihedral is in agreement with the value obtained in crystal structure of ionic liquid containing choline cation [89–91].

To obtain the stable configurations of [Choline][NTf<sub>2</sub>] ionic liquid, the anion was located at different positions around the cation. Two conformations IL1 and IL2 were investigated, where the anion was placed next to the hydroxyl group of the choline with the S-N-S plane parallel of the choline's structure ILa, and next to the hydroxyl group of the choline but with the S-N-S plane at the perpendicular of the choline's structure ILb.

**Figure III-1** Optimized structures of: a) the [Choline] cation, b) the [NTf<sub>2</sub>] bis(trifluoromethylsulfonide)imide anion, c) the ILa ionic liquid conformation, d) the ILb conformation

Yellow correspond to sulfur atoms, dark blue to nitrogen, light blue to chloride, red to oxygen, grey to carbon and white to hydrogen.



Choline-based ionic liquids are known to present hydrogen bonds between the cation and the anion [89–91]. In both structures ILa and ILb, the hydroxyl group of the choline cation interacts with one oxygen atom of the NTf<sub>2</sub> anion in a medium hydrogen bond [92]. The O-H bond and the O-H ---O angle present values of 1.854 Å and 164.27° respectively for the ILa conformation, and 1.819 Å and 165.48° for the ILb one. The interaction energy of the ionic liquids' structures is calculated as in equation 1. The conformation ILa presents the highest interaction energy (327.78 kJ.mol<sup>-1</sup> in absolute). Therefore, its conformation is chosen as the best optimized structure for the rest of the work (Table III-7). Nockemann et al [93] also observed experimentally a hydrogen bond between the hydroxyl proton of choline and the sulfonyl oxygen atom of NTf<sub>2</sub> in the crystal structure.

**Table III-7:** Energy of structures and binding energy for the Choline, NTf<sub>2</sub>, phenol and their clusters

	Energy (Hartree)	$\Delta E$ (kJ.mol <sup>-1</sup> )
Choline	-328.81583316	/
[NTf <sub>2</sub> ]	-1827.75494749	/
Phenol	-307.585694	/
[Choline][NTf <sub>2</sub> ] ILa	-2156.69562	-327.78
[Choline][NTf <sub>2</sub> ] ILb	-2156.69492	-325.94
[Choline] + Phenol Ch-PhA	-636.417353	-41.55
[Choline] + Phenol Ch-PhB	-636.412978	-30.07
[NTf <sub>2</sub> ] + Phenol N-PhA	-2135.36087	-53.11
[NTf <sub>2</sub> ] + Phenol N-PhB	-2135.35903	-48.27
[Choline][NTf <sub>2</sub> ] + Phenol ILa-PhA	-2464.29988	-48.73
[Choline][NTf <sub>2</sub> ] + Phenol ILa-PhB	-2464.29889	-46.13
[Choline][NTf <sub>2</sub> ] + Phenol ILa-PhC	-2464.29867	-45.57

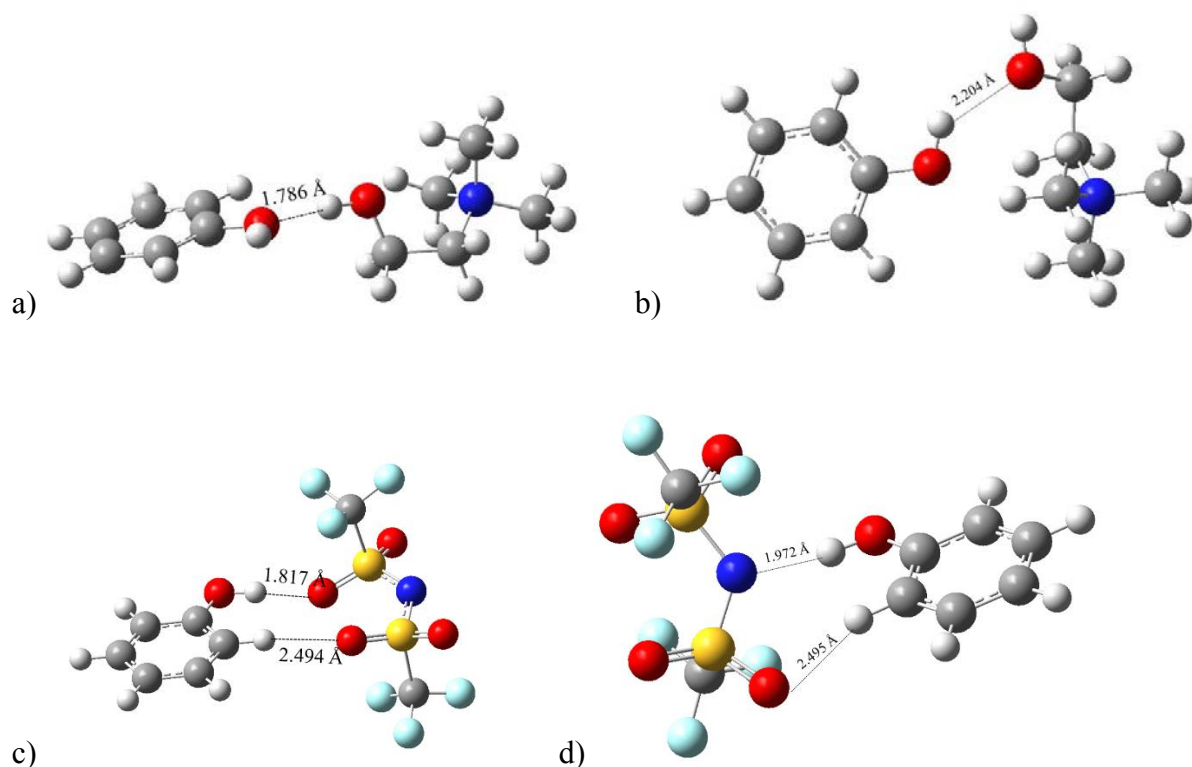
The interactions with phenol was investigated for each ion of the ionic liquid separately (Figure III-2). As previously, several conformations were investigated with the phenol located at different positions around the ion. The interaction energy between the phenol and the ion was calculated according to the same procedure described previously.

In contact with the choline cation, two conformations were investigated (Figure III-2). In the Ch-PhA structure, the hydroxyl group of choline is pointing towards the hydroxyl group of phenol. In this conformation, the molecules interact through a hydrogen bond where choline acts as a donor and phenol as an acceptor. The O--H bond presents a length of 1.786 Å and an O-H--O angle of 175.48°, corresponding to a medium hydrogen bond [92]. In the second conformation Ch-PhB, the two molecules also interact through a hydrogen bond but in this case, choline acts as the acceptor and phenol as the donor. The length of the O--H bond is high (2.204 Å) and the O-H--O angle low (134.63°) in comparison with the Ch-PhA conformation leading to a weaker hydrogen bond. Therefore, the Ch-PhB structure is less stable than the Ch-PhA one. The interaction energy also confirms this result. Indeed, the Ch-PhA conformation presents an interaction energy of 41.55 kJ.mol<sup>-1</sup>, namely 11 kJ.mol<sup>-1</sup> higher than the Ch-PhB conformation (Table III-7).

Two conformations were also investigated for the NTf<sub>2</sub>-phenol clusters (Figure III-2). The first one named N-PhA presents the NTf<sub>2</sub> anion and the phenol molecule interacting through hydrogen bonding. In this conformation, the hydroxyl group of phenol acts as a donor towards the oxygen atom of the NTf<sub>2</sub> anion with a length O--H of 1.817 Å and an angle O-H--O of 176.68°. The structure is also stabilized by another weaker hydrogen bond between one hydrogen of the benzene ring of phenol and another oxygen atom of the NTf<sub>2</sub> anion. The second conformation N-PhB also presents the two molecules interacting through hydrogen bonding with phenol as a donor and NTf<sub>2</sub> as acceptor. In this case, the hydroxyl group of phenol is pointing in direction of the nitrogen atom of NTf<sub>2</sub> with a bond length of H--N 1.972 Å and an angle O-H--N of 170.59°. This conformation is also stabilized by another weaker hydrogen bond between one hydrogen of the benzene ring of phenol and the other oxygen atom of the NTf<sub>2</sub> anion. As for the choline-phenol system, the high strength of the hydrogen bond of the N-PhA conformation stabilized the structure and leads to a higher interaction energy (53.11 kJ.mol<sup>-1</sup>) than this obtained with the N-PhB conformation (48.27 kJ.mol<sup>-1</sup>) (Table III-7).

The absolute interaction energies are higher in the NTf<sub>2</sub>-phenol systems in comparison to the [choline]-phenol ones. Therefore, the NTf<sub>2</sub> anion plays a dominant role into the interaction of the ionic liquid with phenol. The major influence of the anion was also observed by Hassan et al [94] for the interaction of ionic liquids with carbohydrates.

**Figure III-2 :** Optimized cluster structures of a) [Choline]-phenol Ch-PhA, b) , [Choline]-phenol Ch-PhB, c) [NTf<sub>2</sub>]-phenol N-PhA, d) [NTf<sub>2</sub>]-phenol N-PhB

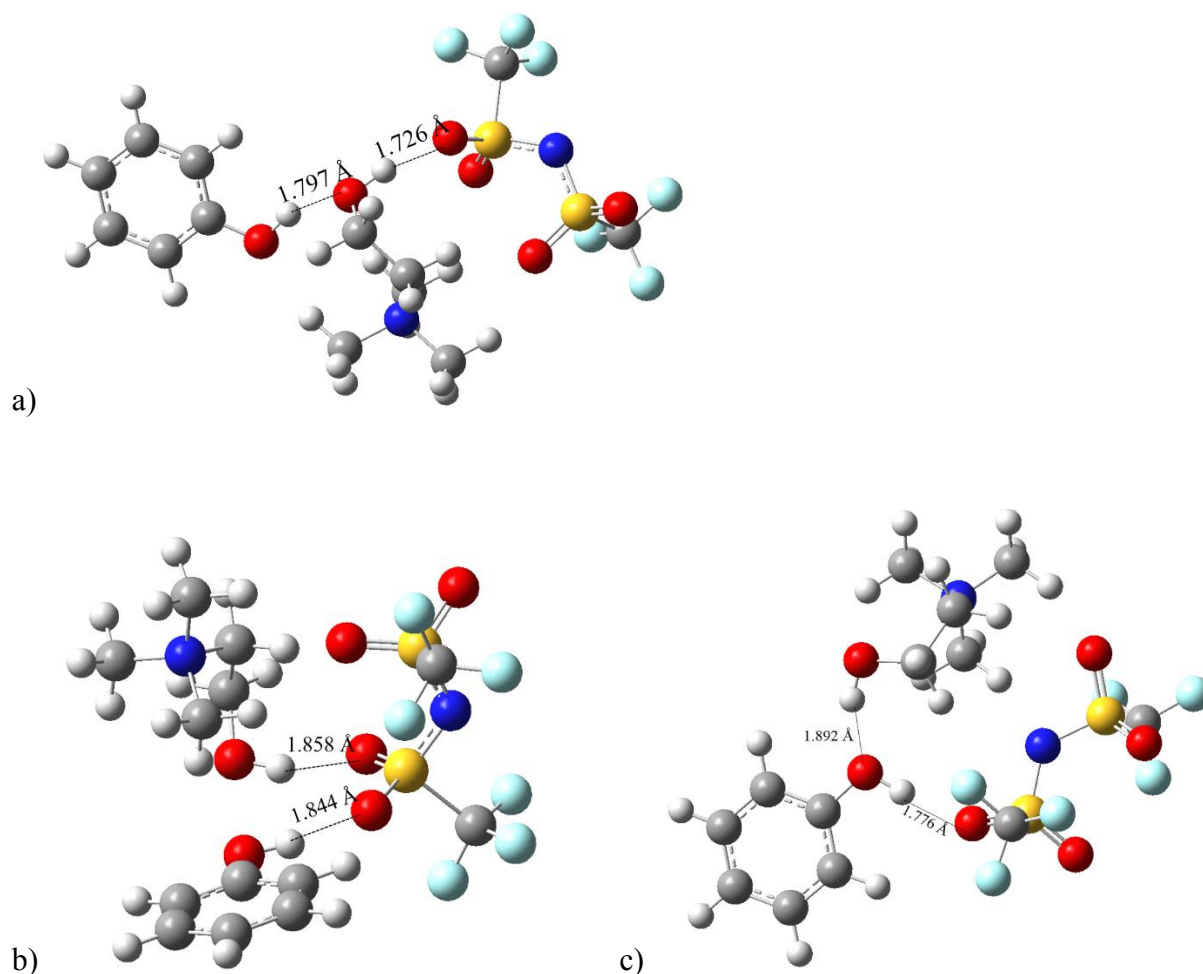


For the ionic liquid-phenol system, three conformations were investigated as previously between phenol and the optimized structure of ionic liquid ILa (Figure III-3).

In the first one named ILa-PhA, the hydroxyl group of phenol acts as a hydrogen donor towards the hydroxyl group of choline, itself acting as a donor towards one oxygen atom of the NTf<sub>2</sub> anion. The O--H bonds present length of 1.797 Å and 1.726 Å and the O-H--O angles values of 153.67° and 166.46° respectively. Moreover, some of the hydrogen atoms of the choline cation are very close to the oxygen atom of phenol (O--H bonds between 2.34 and 2.96 Å) and allow them to interact and stabilize the interaction between phenol and the ionic liquid. Therefore, this conformation is the most stable with an absolute interaction energy of 48.73 kJ.mol<sup>-1</sup>. In the second studied conformation ILa-PhB, both hydroxyl groups of phenol and of choline act as hydrogen donor towards two oxygen atoms linked to the same sulfur atom. In this conformation, the O--H bonds are longer than in the ILa-PhA conformation with length of 1.844 Å and 1.858 Å for phenol and choline molecules, respectively. The third conformation named ILa-PhC allows the phenol molecule to interact with the two ions of the ionic liquid. The choline acts as a hydrogen donor towards the hydroxyl group of phenol, itself acting as hydrogen donor

towards an oxygen atom of the ionic liquid. The length of the O--H bonds are as follows: 1.892 Å for the choline-phenol hydrogen bond and 1.776 Å for the phenol-NTf<sub>2</sub> one.

**Figure III-3** : Optimized cluster structures of a) [Choline][NTf<sub>2</sub>] – phenol ILa-PhA, b) [Choline][NTf<sub>2</sub>] – phenol ILa-PhB, c) [Choline][NTf<sub>2</sub>] – phenol ILa-PhC



In comparison with the phenol-water cluster (32.85kJ.mol<sup>-1</sup>), the interaction energy between phenol and the [Choline][NTf<sub>2</sub>] ionic liquid is much higher (48.73 kJ.mol<sup>-1</sup>) meaning that in contact with these two molecules, phenol is more likely to interact with the ionic liquid than with water. Therefore, this ionic liquid could be an excellent solvent for the extraction of phenol from aqueous solution.

### III-5. Conclusion

The structures of the eight phenolic compounds in their one water complex forms were fully determined. Phenol, o-cresol, m-cresol, p-cresol and pyrocatechol present a translinear conformation whereas guaiacol and syringol present a cyclic one. Vanillin interacts with water through its aldehyde function.

In all translinear conformations, the hydroxyl bond of the phenolic compounds increases, corresponding to a red shift in the frequency. Same phenomenon is observed in the cyclic conformations. The NBO analysis indicates that the electronegativity of water increases in the structures as follows: translinear < cyclic < vanillin. The cyclic conformations of guaiacol and syringol increase their hardness and therefore their reactivity. Vanillin is the least hard but the most electronegative molecule of the studied compounds with or without water.

**References:**

- [1] H. Pakdel, C. Amen-Chen, J. Zhang, C. Roy, Phenolic compounds from vacuum pyrolysis of biomass, *Bio-Oil Prod. Util.* CPL Press UK. (1996) 124–136.
- [2] A.V. Bridgwater, D. Meier, D. Radlein, An overview of fast pyrolysis of biomass, *Org. Geochem.* 30 (1999) 1479–1493. doi:10.1016/S0146-6380(99)00120-5.
- [3] A.V. Bridgwater, S.A. Bridge, A Review of Biomass Pyrolysis and Pyrolysis Technologies, in: A.V. Bridgwater, G. Grassi (Eds.), *Biomass Pyrolysis Liq. Upgrad. Util.*, Springer Netherlands, Dordrecht, 1991: pp. 11–92. [http://www.springerlink.com/index/10.1007/978-94-011-3844-4\\_2](http://www.springerlink.com/index/10.1007/978-94-011-3844-4_2) (accessed January 20, 2017).
- [4] H. Pakdel, C. Roy, C. Amen-Chen, Phenolic compounds from vacuum pyrolysis of wood wastes, *Can. J. Chem. Eng.* 75 (1997) 121–126. doi:10.1002/cjce.5450750119.
- [5] C. Amen-Chen, H. Pakdel, C. Roy, Production of monomeric phenols by thermochemical conversion of biomass: a review, *Bioresour. Technol.* 79 (2001) 277–299. doi:10.1016/S0960-8524(00)00180-2.
- [6] J. Zakzeski, P.C.A. Bruijninx, A.L. Jongerius, B.M. Weckhuysen, The Catalytic Valorization of Lignin for the Production of Renewable Chemicals, *Chem. Rev.* 110 (2010) 3552–3599. doi:10.1021/cr900354u.
- [7] M. Kleinert, T. Barth, Phenols from Lignin, *Chem. Eng. Technol.* 31 (2008) 736–745. doi:10.1002/ceat.200800073.
- [8] J.N. Murwanashyaka, H. Pakdel, C. Roy, Separation of syringol from birch wood-derived vacuum pyrolysis oil, *Sep. Purif. Technol.* 24 (2001) 155–165. doi:10.1016/S1383-5866(00)00225-2.
- [9] C. Amen-Chen, H. Pakdel, C. Roy, Separation of phenols from Eucalyptus wood tar, *Biomass Bioenergy.* 13 (1997) 25–37. doi:10.1016/S0961-9534(97)00021-4.
- [10] S. Wang, Y. Wang, Q. Cai, X. Wang, H. Jin, Z. Luo, Multi-step separation of monophenols and pyrolytic lignins from the water-insoluble phase of bio-oil, *Sep. Purif. Technol.* 122 (2014) 248–255. doi:10.1016/j.seppur.2013.11.017.
- [11] J.-M. Lavoie, W. Baré, M. Bilodeau, Depolymerization of steam-treated lignin for the production of green chemicals, *Bioresour. Technol.* 102 (2011) 4917–4920. doi:10.1016/j.biortech.2011.01.010.
- [12] F. Helmut, V. Heinz-Werner, H. Toshikazu, P. Wilfried, Phenol derivatives, *Ullmann's Encycl. Ind. Chem. VCH Ger.* 19 (1985) 299–357.
- [13] F. Ikegami, T. Sekine, Y. Fujii, [Anti-dermatophyte activity of phenolic compounds in “mokusaku-eki”], *Yakugaku Zasshi.* 118 (1998) 27–30.
- [14] J.A. Maga, I. Katz, Simple phenol and phenolic compounds in food flavor, *C R C Crit. Rev. Food Sci. Nutr.* 10 (1978) 323–372. doi:10.1080/10408397809527255.
- [15] H. Fiege, H.-W. Voges, T. Hamamoto, S. Umemura, T. Iwata, H. Miki, Y. Fujita, H.-J. Buysch, D. Garbe, W. Paulus, Phenol Derivatives, in: *Wiley-VCH Verlag GmbH & Co. KGaA (Ed.), Ullmanns Encycl. Ind. Chem., Wiley-VCH Verlag GmbH & Co. KGaA, Weinheim, Germany, 2000.* [http://doi.wiley.com/10.1002/14356007.a19\\_313](http://doi.wiley.com/10.1002/14356007.a19_313) (accessed August 23, 2016).
- [16] P. Garcia-Salas, A. Morales-Soto, A. Segura-Carretero, A. Fernández-Gutiérrez, Phenolic-Compound-Extraction Systems for Fruit and Vegetable Samples, *Molecules.* 15 (2010) 8813–8826. doi:10.3390/molecules15128813.
- [17] V. Louli, N. Ragoussis, K. Magoulas, Recovery of phenolic antioxidants from wine industry by-products, *Bioresour. Technol.* 92 (2004) 201–208. doi:10.1016/j.biortech.2003.06.002.

- [18] R.N. Patel, S. Bandyopadhyay, A. Ganesh, Extraction of cardanol and phenol from bio-oils obtained through vacuum pyrolysis of biomass using supercritical fluid extraction, *Energy*. 36 (2011) 1535–1542. doi:10.1016/j.energy.2011.01.009.
- [19] E. Reverchon, I. De Marco, Supercritical fluid extraction and fractionation of natural matter, *J. Supercrit. Fluids*. 38 (2006) 146–166. doi:10.1016/j.supflu.2006.03.020.
- [20] F. Le Floch, M. Tena, A. Ríos, M. Valcárcel, Supercritical fluid extraction of phenol compounds from olive leaves, *Talanta*. 46 (1998) 1123–1130. doi:10.1016/S0039-9140(97)00375-5.
- [21] H.I. Castro-Vargas, L.I. Rodríguez-Varela, S.R.S. Ferreira, F. Parada-Alfonso, Extraction of phenolic fraction from guava seeds (*Psidium guajava* L.) using supercritical carbon dioxide and co-solvents, *J. Supercrit. Fluids*. 51 (2010) 319–324. doi:10.1016/j.supflu.2009.10.012.
- [22] P.K. Rout, M.K. Naik, S.N. Naik, V.V. Goud, L.M. Das, A.K. Dalai, Supercritical CO<sub>2</sub> Fractionation of Bio-oil Produced from Mixed Biomass of Wheat and Wood Sawdust, *Energy Fuels*. 23 (2009) 6181–6188. doi:10.1021/ef900663a.
- [23] J.A. Capunitan, S.C. Capareda, Characterization and separation of corn stover bio-oil by fractional distillation, *Fuel*. 112 (2013) 60–73. doi:10.1016/j.fuel.2013.04.079.
- [24] D. Radlein, Chemicals and materials from biomass, *PyNe Pyrolysis Netw.* 4 (1997).
- [25] R.W. Thring, J. Breau, Hydrocracking of solvolysis lignin in a batch reactor, *Fuel*. 75 (1996) 795–800. doi:10.1016/0016-2361(96)00036-1.
- [26] D. Fu, S. Farag, J. Chaouki, P.G. Jessop, Extraction of phenols from lignin microwave-pyrolysis oil using a switchable hydrophilicity solvent, *Bioresour. Technol.* 154 (2014) 101–108. doi:10.1016/j.biortech.2013.11.091.
- [27] S. Jalili, M. Akhavan, Study of hydrogen-bonded clusters of 2-methoxyphenol–water, *Theor. Chem. Acc.* 118 (2007) 947–957. doi:10.1007/s00214-007-0378-3.
- [28] D.V. Avila, K.U. Ingold, J. Lusztyk, W.H. Green, D.R. Procopio, Dramatic Solvent Effects on the Absolute Rate Constants for Abstraction of the Hydroxylic Hydrogen Atom from tert-Butyl Hydroperoxide and Phenol by the Cumyloxyl Radical. The Role of Hydrogen Bonding, *J. Am. Chem. Soc.* 117 (1995) 2929–2930. doi:10.1021/ja00115a029.
- [29] W.-H. Fang, Theoretical characterization of the excited-state structures and properties of phenol and its one-water complex, *J. Chem. Phys.* 112 (2000) 1204–1211. doi:10.1063/1.480673.
- [30] S. Schumm, M. Gerhards, W. Roth, H. Gier, K. Kleinermanns, A CASSCF study of the S<sub>0</sub> and S<sub>1</sub> states of phenol, *Chem. Phys. Lett.* 263 (1996) 126–132. doi:10.1016/S0009-2614(96)01172-4.
- [31] D. Feller, M.W. Feyereisen, Ab initio study of hydrogen bonding in the phenol-water system, *J. Comput. Chem.* 14 (1993) 1027–1035. doi:10.1002/jcc.540140904.
- [32] M. Schütz, T. Bürgi, S. Leutwyler, Structures and vibrations of phenol · H<sub>2</sub>O and d-phenol · D<sub>2</sub>O based on ab initio calculations, *J. Mol. Struct. THEOCHEM.* 276 (1992) 117–132. doi:10.1016/0166-1280(92)80026-I.
- [33] H. Watanabe, S. Iwata, Theoretical studies of geometric structures of phenol-water clusters and their infrared absorption spectra in the O–H stretching region, *J. Chem. Phys.* 105 (1996) 420–431. doi:10.1063/1.471918.
- [34] T. Kojima, Potential Barrier of Phenol from its Microwave Spectrum, *J. Phys. Soc. Jpn.* 15 (1960) 284–287. doi:10.1143/JPSJ.15.284.
- [35] M. Pohl, K. Kleinermanns, Ab initio SCF calculations on hydrogen bonded cresol isomers, *Z. Für Phys. At. Mol. Clust.* 8 (n.d.) 385–392. doi:10.1007/BF01437106.
- [36] S.W. Dietrich, E.C. Jorgensen, P.A. Kollman, S. Rothenberg, A theoretical study of intramolecular hydrogen bonding in ortho-substituted phenols and thiophenols, *J. Am. Chem. Soc.* 98 (1976) 8310–8324. doi:10.1021/ja00442a002.

- [37] A. Welzel, A. Hellweg, I. Merke, W. Stahl, Structural and Torsional Properties of o-Cresol and o-Cresol-OD as Obtained from Microwave Spectroscopy and ab Initio Calculations, *J. Mol. Spectrosc.* 215 (2002) 58–65. doi:10.1006/jmsp.2002.8600.
- [38] V. Balachandran, M. Murugan, A. Nataraj, M. Karnan, G. Ilango, Comparative vibrational spectroscopic studies, HOMO–LUMO, NBO analyses and thermodynamic functions of p-cresol and 2-methyl-p-cresol based on DFT calculations, *Spectrochim. Acta. A. Mol. Biomol. Spectrosc.* 132 (2014) 538–549. doi:10.1016/j.saa.2014.04.194.
- [39] P.R. Richardson, M.A. Chapman, D.C. Wilson, S.P. Bates, A.C. Jones, The nature of conformational preference in a number of p-alkyl phenols and p-alkyl benzenes, *Phys. Chem. Chem. Phys.* 4 (2002) 4910–4915. doi:10.1039/b203954k.
- [40] A. Hellweg, C. Hättig, On the internal rotations in p-cresol in its ground and first electronically excited states, *J. Chem. Phys.* 127 (2007) 024307. doi:10.1063/1.2752163.
- [41] A. Hellweg, C. Hättig, I. Merke, W. Stahl, Microwave and theoretical investigation of the internal rotation in m-cresol, *J. Chem. Phys.* 124 (2006) 204305. doi:10.1063/1.2198842.
- [42] C. Puebla, T.-K. Ha, A theoretical study of conformations and rotational barriers in dihydroxybenzenes, *J. Mol. Struct. THEOCHEM.* 204 (1990) 337–351. doi:10.1016/0166-1280(90)85085-2.
- [43] T. Bürgi, S. Leutwyler, O–H torsional vibrations in the  $S_0$  and  $S_1$  states of catechol, *J. Chem. Phys.* 101 (1994) 8418–8429. doi:10.1063/1.468104.
- [44] M. Gerhards, W. Perl, S. Schumm, U. Henrichs, C. Jacoby, K. Kleinermanns, Structure and vibrations of catechol and catechol·H<sub>2</sub>O(D<sub>2</sub>O) in the  $S_0$  and  $S_1$  state, *J. Chem. Phys.* 104 (1996) 9362. doi:10.1063/1.471682.
- [45] R. Rudyk, M.A.A. Molina, M.I. Gómez, S.E. Blanco, F.H. Ferretti, Solvent effects on the structure and dipole moment of resorcinol, *J. Mol. Struct. THEOCHEM.* 674 (2004) 7–14. doi:10.1016/j.theochem.2003.12.019.
- [46] B. Gómez-Zaleta, R. Gómez-Balderas, J. Hernández-Trujillo, Theoretical analysis of hydrogen bonding in catechol–n(H<sub>2</sub>O) clusters (n = 0...3), *Phys. Chem. Chem. Phys.* 12 (2010) 4783. doi:10.1039/b922203k.
- [47] M. Mandado, A.M. Graña, R.A. Mosquera, Do 1,2-ethanediol and 1,2-dihydroxybenzene present intramolecular hydrogen bond?, *Phys Chem Chem Phys.* 6 (2004) 4391–4396. doi:10.1039/B406266C.
- [48] C. Agache, V.I. Popa, Ab Initio Studies on the Molecular Conformation of Lignin Model Compounds I. Conformational Preferences of the Phenolic Hydroxyl and Methoxy Groups in Guaiacol, *Monatshefte Für Chem. - Chem. Mon.* 137 (2006) 55–68. doi:10.1007/s00706-005-0404-x.
- [49] O.V. Dorofeeva, I.F. Shishkov, N.M. Karasev, L.V. Vilkov, H. Oberhammer, Molecular structures of 2-methoxyphenol and 1,2-dimethoxybenzene as studied by gas-phase electron diffraction and quantum chemical calculations, *J. Mol. Struct.* 933 (2009) 132–141. doi:10.1016/j.molstruc.2009.06.009.
- [50] M.A. Varfolomeev, D.I. Abaidullina, B.N. Solomonov, S.P. Verevkin, V.N. Emel'yanenko, Pairwise Substitution Effects, Inter- and Intramolecular Hydrogen Bonds in Methoxyphenols and Dimethoxybenzenes. Thermochemistry, Calorimetry, and First-Principles Calculations, *J. Phys. Chem. B.* 114 (2010) 16503–16516. doi:10.1021/jp108459r.
- [51] E.J. Cocinero, A. Lesarri, P. Écija, J.-U. Grabow, J.A. Fernández, F. Castaño, Conformational equilibria in vanillin and ethylvanillin, *Phys. Chem. Chem. Phys.* 12 (2010) 12486. doi:10.1039/c0cp00585a.
- [52] C.Y. Panicker, H. T. Varghese, K. Sajina, A.V. Vaidyan, A. J. Meenu, B. Harikumar, IR, Raman and ab-initio calculations of 2,6-dimethoxyphenol, *Orient. J. Chem.* 24 (2008) 973.

- [53] L. Zhang, G.H. Peslherbe, H.M. Muchall, Ultraviolet Absorption Spectra of Substituted Phenols: A Computational Study†, *Photochem. Photobiol.* 82 (2006) 324–331. doi:10.1562/2005-07-08-RA-605.
- [54] A. Plugatyr, I. Nahtigal, I.M. Svishchev, Spatial hydration structures and dynamics of phenol in sub- and supercritical water, *J. Chem. Phys.* 124 (2006) 024507. doi:10.1063/1.2145751.
- [55] W. Roth, M. Schmitt, C. Jacoby, D. Spangenberg, C. Janzen, K. Kleinermanns, Double resonance spectroscopy of phenol(H<sub>2</sub>O)<sub>1–12</sub>: evidence for ice-like structures in aromate–water clusters?, *Chem. Phys.* 239 (1998) 1–9. doi:10.1016/S0301-0104(98)00252-3.
- [56] C. Jacoby, W. Roth, M. Schmitt, C. Janzen, D. Spangenberg, K. Kleinermanns, Intermolecular Vibrations of Phenol(H<sub>2</sub>O)<sub>2-5</sub> and Phenol(D<sub>2</sub>O)<sub>2-5</sub> - *d*<sub>1</sub> Studied by UV Double-Resonance Spectroscopy and ab Initio Theory, *J. Phys. Chem. A.* 102 (1998) 4471–4480. doi:10.1021/jp9806157.
- [57] A. Lüchow, D. Spangenberg, C. Janzen, A. Jansen, M. Gerhards, K. Kleinermanns, Structure and energetics of phenol(H<sub>2</sub>O)<sub>n</sub>, *n* ≤ 7: Quantum Monte Carlo calculations and double resonance experiments, *Phys. Chem. Chem. Phys.* 3 (2001) 2771–2780. doi:10.1039/b101779i.
- [58] D.M. Benoit, D.C. Clary, Quantum Simulation of Phenol–Water Clusters, *J. Phys. Chem. A.* 104 (2000) 5590–5599. doi:10.1021/jp994420q.
- [59] I. Bandyopadhyay, H.M. Lee, K.S. Kim, Phenol vs Water Molecule Interacting with Various Molecules:  $\sigma$ -type,  $\pi$ -type, and  $\chi$ -type Hydrogen Bonds, Interaction Energies, and Their Energy Components, *J. Phys. Chem. A.* 109 (2005) 1720–1728. doi:10.1021/jp0449657.
- [60] M. Gerhards, M. Schmitt, K. Kleinermanns, W. Stahl, The structure of phenol(H<sub>2</sub>O) obtained by microwave spectroscopy, *J. Chem. Phys.* 104 (1996) 967–971. doi:10.1063/1.470820.
- [61] Y. Dimitrova, Ab initio and DFT studies of the vibrational spectra of hydrogen-bonded PhOH... (H<sub>2</sub>O)<sub>4</sub> complexes, *Spectrochim. Acta. A. Mol. Biomol. Spectrosc.* 60 (2004) 3049–3057. doi:10.1016/j.saa.2004.01.026.
- [62] R. Parthasarathi, V. Subramanian, N. Sathyamurthy, Hydrogen Bonding in Phenol, Water, and Phenol–Water Clusters, *J. Phys. Chem. A.* 109 (2005) 843–850. doi:10.1021/jp046499r.
- [63] F. Ramondo, L. Bencivenni, G. Portalone, A. Domenicano, Effect of intermolecular O-H ... O hydrogen bonding on the molecular structure of phenol: An ab initio molecular orbital study, *Struct. Chem.* 6 (n.d.) 37–45. doi:10.1007/BF02263526.
- [64] R. Wu, B. Brutschy, Study on the structure and intra- and intermolecular hydrogen bonding of 2-methoxyphenol · (H<sub>2</sub>O)<sub>n</sub> (*n*=1,2), *Chem. Phys. Lett.* 390 (2004) 272–278. doi:10.1016/j.cplett.2004.04.023.
- [65] M. Pohl, M. Schmitt, K. Kleinermanns, Microscopic shifts of size-assigned *p*-cresol/H<sub>2</sub>O-cluster spectra, *J. Chem. Phys.* 94 (1991) 1717. doi:10.1063/1.459944.
- [66] G. Myszkiewicz, W.L. Meerts, C. Ratzler, M. Schmitt, The structure of 4-methylphenol and its water cluster revealed by rotationally resolved UV spectroscopy using a genetic algorithm approach, *J. Chem. Phys.* 123 (2005) 044304. doi:10.1063/1.1961615.
- [67] H.S. Biswal, P.R. Shirhatti, S. Wategaonkar, O–H...O versus O–H...S Hydrogen Bonding I: Experimental and Computational Studies on the *p*-Cresol·H<sub>2</sub>O and *p*-Cresol·H<sub>2</sub>S Complexes, *J. Phys. Chem. A.* 113 (2009) 5633–5643. doi:10.1021/jp9009355.
- [68] T. Watanabe, T. Ebata, S. Tanabe, N. Mikami, Size-selected vibrational spectra of phenol-(H<sub>2</sub>O)<sub>n</sub> (*n*=1–4) clusters observed by IR–UV double resonance and stimulated Raman-

- UV double resonance spectroscopies, *J. Chem. Phys.* 105 (1996) 408–419. doi:10.1063/1.471917.
- [69] T. Ebata, A. Fujii, N. Mikami, Vibrational spectroscopy of small-sized hydrogen-bonded clusters and their ions, *Int. Rev. Phys. Chem.* 17 (1998) 331–361. doi:10.1080/014423598230081.
- [70] R.M. Helm, H.J. Neusser, Highly resolved UV spectroscopy of clusters: isotope substitution studies of hydrogen-bonded phenol·water, *Chem. Phys.* 239 (1998) 33–47. doi:10.1016/S0301-0104(98)00256-0.
- [71] M. Schütz, T. Bürgi, S. Leutwyler, T. Fischer, Intermolecular bonding and vibrations of phenol-H<sub>2</sub>O (D<sub>2</sub>O), *J. Chem. Phys.* 98 (1993) 3763. doi:10.1063/1.464055.
- [72] D.-S. Ahn, S.-W. Park, S. Lee, B. Kim, Effects of Substituting Group on the Hydrogen Bonding in Phenol–H<sub>2</sub>O Complexes: Ab Initio Study, *J. Phys. Chem. A* 107 (2003) 131–139. doi:10.1021/jp021519f.
- [73] M. Gerhards, C. Unterberg, K. Kleinermanns, Structures of catechol(H<sub>2</sub>O)<sub>1,3</sub> clusters in the S<sub>0</sub> and D<sub>0</sub> states, *Phys. Chem. Chem. Phys.* 2 (2000) 5538–5544. doi:10.1039/b006744j.
- [74] A.D. Becke, Density-functional exchange-energy approximation with correct asymptotic behavior, *Phys. Rev. A* 38 (1988) 3098–3100. doi:10.1103/PhysRevA.38.3098.
- [75] C. Lee, W. Yang, R.G. Parr, Development of the Colle-Salvetti correlation-energy formula into a functional of the electron density, *Phys. Rev. B Condens. Matter* 37 (1988) 785–789.
- [76] P.J. Stephens, F.J. Devlin, C.F. Chabalowski, M.J. Frisch, Ab Initio Calculation of Vibrational Absorption and Circular Dichroism Spectra Using Density Functional Force Fields, *J. Phys. Chem.* 98 (1994) 11623–11627. doi:10.1021/j100096a001.
- [77] M.K. Kesharwani, B. Brauer, J.M.L. Martin, Frequency and Zero-Point Vibrational Energy Scale Factors for Double-Hybrid Density Functionals (and Other Selected Methods): Can Anharmonic Force Fields Be Avoided?, *J. Phys. Chem. A* 119 (2015) 1701–1714. doi:10.1021/jp508422u.
- [78] The Principle of Maximum Hardness, in: *Chem. Hardness*, Wiley-VCH Verlag GmbH & Co. KGaA, Weinheim, FRG, 2005: pp. 99–124. doi:10.1002/3527606173.ch4.
- [79] U. Salzner, R. Baer, Koopmans' springs to life, *J. Chem. Phys.* 131 (2009) 231101. doi:10.1063/1.3269030.
- [80] R.S. Mulliken, A New Electroaffinity Scale; Together with Data on Valence States and on Valence Ionization Potentials and Electron Affinities, *J. Chem. Phys.* 2 (1934) 782–793. doi:10.1063/1.1749394.
- [81] S.S. Xantheas, *Ab initio* studies of cyclic water clusters (H<sub>2</sub>O)<sub>n</sub>, *n*=1–6. II. Analysis of many-body interactions, *J. Chem. Phys.* 100 (1994) 7523–7534. doi:10.1063/1.466846.
- [82] S. Tanabe, T. Ebata, M. Fujii, N. Mikami, OH stretching vibrations of phenol–(H<sub>2</sub>O)<sub>n</sub> (*n*=1–3) complexes observed by IR-UV double-resonance spectroscopy, *Chem. Phys. Lett.* 215 (1993) 347–352. doi:10.1016/0009-2614(93)85726-5.
- [83] V. Balachandran, K. Parimala, Vanillin and isovanillin: Comparative vibrational spectroscopic studies, conformational stability and NLO properties by density functional theory calculations, *Spectrochim. Acta. A. Mol. Biomol. Spectrosc.* 95 (2012) 354–368. doi:10.1016/j.saa.2012.03.087.
- [84] C. Bois, Structure de l'o-crésol, *Acta Crystallogr. B* 28 (1972) 25–31. doi:10.1107/S0567740872001815.
- [85] C. Bois, Structure du m-crésol, *Acta Crystallogr. B* 29 (1973) 1011–1017. doi:10.1107/S0567740873003778.
- [86] C. Bois, Structure du p-crésol à basse température, *Acta Crystallogr. B* 26 (1970) 2086–2092. doi:10.1107/S0567740870005411.

- [87] K. Fujii, T. Fujimori, T. Takamuku, R. Kanzaki, Y. Umebayashi, S. Ishiguro, Conformational Equilibrium of Bis(trifluoromethanesulfonyl) Imide Anion of a Room-Temperature Ionic Liquid: Raman Spectroscopic Study and DFT Calculations, *J. Phys. Chem. B.* 110 (2006) 8179–8183. doi:10.1021/jp0612477.
- [88] Y.U. Paulechka, G.J. Kabo, V.N. Emel'yanenko, Structure, Conformations, Vibrations, and Ideal-Gas Properties of 1-Alkyl-3-methylimidazolium bis(trifluoromethylsulfonyl)imide Ionic Pairs and Constituent Ions, *J. Phys. Chem. B.* 112 (2008) 15708–15717. doi:10.1021/jp804607n.
- [89] P. Nockemann, B. Thijs, K. Driesen, C.R. Janssen, K. Van Hecke, L. Van Meervelt, S. Kossmann, B. Kirchner, K. Binnemans, Choline Saccharinate and Choline Acesulfamate: Ionic Liquids with Low Toxicities, *J. Phys. Chem. B.* 111 (2007) 5254–5263. doi:10.1021/jp068446a.
- [90] K. Frydenvang, B. Jensen, K. Nielsen, Structure of choline picrate, *Acta Crystallogr. C.* 48 (1992) 1343–1345. doi:10.1107/S0108270191014610.
- [91] K. Frydenvang, G. Hjelvang, B. Jensen, S.M. Martinho Do Rosario, Structures of the choline ion in different crystal surroundings, *Acta Crystallogr. C.* 50 (1994) 617–623. doi:10.1107/S0108270193007589.
- [92] G.A. Jeffrey, *An introduction to hydrogen bonding*, 1997.
- [93] P. Nockemann, K. Binnemans, B. Thijs, T.N. Parac-Vogt, K. Merz, A.-V. Mudring, P.C. Menon, R.N. Rajesh, G. Cordoyiannis, J. Thoen, J. Leys, C. Glorieux, Temperature-Driven Mixing-Demixing Behavior of Binary Mixtures of the Ionic Liquid Choline Bis(trifluoromethylsulfonyl)imide and Water, *J. Phys. Chem. B.* 113 (2009) 1429–1437. doi:10.1021/jp808993t.
- [94] E.-S.R.E. Hassan, F. Mutelet, M. Bouroukba, Experimental and theoretical study of carbohydrate–ionic liquid interactions, *Carbohydr. Polym.* 127 (2015) 316–324. doi:10.1016/j.carbpol.2015.03.042.

## Chapter IV: Phase equilibria of phenolic compounds in water or ethanol

Laëtittia Cesari<sup>1</sup>, Sylvain Namysl<sup>1</sup>, Laetitia Canabady-Rochelle<sup>1</sup>, Fabrice Mutelet<sup>1</sup>

1 : Université de Lorraine, Ecole Nationale Supérieure des Industries Chimiques, Laboratoire Réactions et Génie des Procédés (UMR CNRS 7274), 1 rue Grandville, 54000 NANCY, France.

Article paru dans Fluid Phase Equilibria :

L. Cesari, S. Namysl, L. Canabady-Rochelle, F. Mutelet, Phase equilibria of phenolic compounds in water or ethanol, Fluid Phase Equilibria. 453 (2017) 58–66. doi:10.1016/j.fluid.2017.09.008.

### Résumé

L'objectif de ce chapitre est de compléter les données de la littérature sur des systèmes clés rencontrés dans les procédés d'extraction de composés phénoliques à partir d'une bio-huile. Ainsi, les systèmes {eau-composé phénolique} sont étudiés expérimentalement entre 293 et 323 K. Les systèmes {eau + pyrocatechol}, {eau + syringol} et {eau + vanilline} présentent des équilibres solide-liquide alors que les systèmes {eau + phénol}, {eau + guaiacol}, {eau + syringol} et {eau + crésol} présentent des équilibres liquide-liquide. La solubilité des composés phénoliques dans l'eau décroît selon l'ordre suivant : pyrocatechol > phénol > o-crésol > m-crésol > p-crésol > guaiacol > syringol > vanilline. Enfin, les équilibres liquide-vapeur et les enthalpies de mélange des systèmes {éthanol + composé phénolique} sont également mesurés. L'ensemble des données expérimentales est utilisé afin de déterminer les paramètres d'interaction du modèle NRTL.

**Abstract**

The mutual solubilities of water and eight phenolic compounds (*i.e.* phenol, guaiacol, syringol, pyrocatechol, o-, m-, p-cresol and vanillin) were investigated between 293.15 and 323.15K. The solubility of the phenolic compounds in water increases as follows: vanillin < syringol < guaiacol < p-cresol < m-cresol < o-cresol < phenol < pyrocatechol. For the molecules presenting liquid-liquid equilibria, the solubility of water into the phenolic phase increases as follows: guaiacol < o-cresol < m-cresol < p-cresol < syringol. The vapor-liquid equilibria of binary mixtures composed of ethanol and phenol or guaiacol or o-cresol were measured in a range of pressure from 0.09 bar to atmospheric pressure. Finally, the mixing enthalpies of the phenolic compounds with ethanol indicate that the reactions are exothermic. It was found that NRTL model is suitable for the representation of phase diagrams of systems containing phenolic compounds and water or ethanol.

### IV-1. Introduction

Most of the chemicals, such as phenolic compounds, are produced from the petrochemical industry. Yet, with the rise of global warming and the limited stocks of fossil fuels, there is an urgent need to find new ways of production for such compounds. For the last years, lignin has become as interesting tool for the production of monophenols [1]. Indeed, the thermochemical conversion processes of lignin can provide liquid fuels [2] as well as bio-oils rich in valuable chemicals. With specific bioactivities, such as antioxidant or antimicrobial properties, phenolic compounds are used as intermediate or raw material in the food, pharmaceutical and cosmetic industries [3–6].

Bio-oils can be produced by various thermochemical treatments, the famous ones being pyrolysis and liquefaction. Many studies have investigated the influence of solvent on the liquefaction process, including formic acid [7], water [8–10], methanol, 2-propanol [10], or ethanol [10–13]. In order to reduce the CO<sub>2</sub> emission and be more economically competitive, more and more processes are using solvents coming from biomass for liquefaction processes [14]. Besides, biomass pyrolysis also produces aromatic compounds-rich bio-oils. The condensed vapors obtained during a pyrolysis process are generally collected in solvents such as aqueous solution or ethanol. The extraction of high value compounds from this diluted bio-oil is difficult to perform due to its thermal instability and its complex composition. Most of the processes generally start with the recovery of the solvent by distillation. Then, liquid-liquid extraction using water [15], basic aqueous solutions [16–18] or polar organic solvent [19] are predominantly preferred. Although the distillation of ethanol and the liquid-liquid extraction of phenolic compounds with water are regularly used in the extraction process, only few data are available in the literature [20–39]. The method and the range of temperature of the {phenolic compounds-water} systems found in the literature are presented in Table IV-1.

**Table IV-1:** Temperature range and method of measurements for the {phenolic compounds-water} systems found in the literature

System	Temperature	Method	Reference
Phenol-water	[280-345K]	Conductivity	[31,34]
Phenol-water	[274-338K]	Refractometry	[32]
Phenol-water	[293-339K]	Volumetry	[33]
Pyrocatechol-water	[314-377K]	Synthetic method Visual observation	[29]
Pyrocatechol-water	[295-326K]	/	[30]
Vanillin-water	[273-323K]	Heating/cooling + increment of solvent Visual observation	[26]
Vanillin-water	[273-303K]	Rise of temperature Visual observation	[27]
Vanillin-water	[293-318K]	Shake flask method Chromatography	[28]
Cresol-water	[273-450K]	Decrease of temperature Visual observation	[21]
Cresol-water	298K	Shake flask method Chromatography	[22]
Cresol-water	293K	Turbidity	[23]
Cresol-water	288;298K	/	[24]
m-cresol-water	[293-350K]	Chromatography	[25]
Cresol-water	[298-360K]	Turbidity	[36]
Guaiacol-water	298K	Shake flask method Chromatography	[20]
Guaiacol-water	298K	Density measurements	[35]

No data has been found for the syringol-water system. The vapor-liquid equilibria (VLE) of the {phenol+ethanol} system were only investigated at atmospheric pressure [40,41], at 288.15K [42] and 293.15 K [43]. Only one isothermal VLE at 290.15 K can be found for the binary

{guaiacol + ethanol} [38] and two sets of VLE data for the binary system {o-cresol + ethanol} (0.9576 bar [37] and 291.15K [39]).

To date, there is still a huge lack of information about the behavior of phenolic compounds with such solvents, especially for guaiacol and syringol. It is therefore difficult to determine the most adapted solvent for such extraction and to estimate its feasibility and extraction capacity.

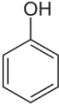
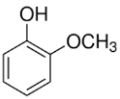
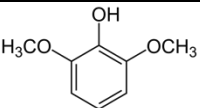
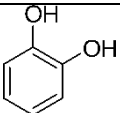
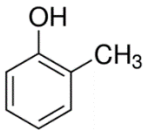
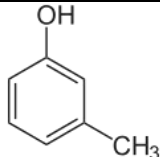
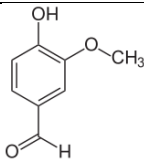
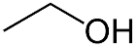
In this work, we studied the behavior of eight phenolic compounds (*i.e.* phenol, guaiacol, syringol, pyrocatechol, o-cresol, m-cresol, p-cresol and vanillin) with water or ethanol. The mutual solubilities of the compounds with water were investigated as a function of temperature. Bubble curves of phenolic compounds with ethanol as well as their mixing enthalpy were also studied. The phase equilibrium data of the systems were used to regress parameters on the Non-Random Two-Liquids (NRTL) [44] thermodynamic models.

## **IV-2. Material and Methods**

### **IV-2.1. Chemicals**

Phenol (CAS 108-95-2), guaiacol (CAS 90-05-1), syringol (CAS 91-10-1), pyrocatechol (CAS 120-80-9), o-cresol (CAS 95-48-7), m-cresol (CAS 108-39-4), p-cresol (CAS 106-44-5) and vanillin (CAS 121-33-5) were supplied by Sigma Aldrich. All chemicals were used as received without any further purification. Deionized water and absolute ethanol were used for all experiments. Table IV-2 summarizes the parameters of the compounds used in this work.

**Table IV-2:** Name, CAS number, abbreviation, molar mass, formula, source and purity of the used compounds

Name and CAS	Abbreviation	Molar mass g.mol <sup>-1</sup>	Formula	Source and purity (wt%)
Phenol 108-95-2		94.11		Sigma Aldrich >99.5%
2-methoxyphenol 90-05-1	Guaiacol	124.14		Sigma Aldrich >99%
2,6-dimethoxyphenol 91-10-1	Syringol	154.16		Sigma Aldrich 99%
1,2-benzenediol 120-80-9	Pyrocatechol	110.11		Sigma Aldrich >99%
2-Methylphenol 95-48-7	o-Cresol	108.14		Sigma Aldrich >99%
3-Methylphenol 108-39-4	m-Cresol	108.14		Sigma Aldrich >99%
4-Methylphenol 106-44-5	p-Cresol	108.14		Sigma Aldrich >99%
4-Hydroxy-3-methoxybenzaldehyde 121-33-5	Vanillin	152.15		Sigma Aldrich >99%
Ethanol 64-17-5		46.07		Carlo Erba absolute anhydrous

### IV-2.2. Solubility of the phenolic compounds in water

Aqueous solubility of the phenolic compounds was determined using the shake-flask method between 293 and 323K. Saturated solutions of each phenolic compound in water were prepared and put in a thermostatic water bath to maintain a constant temperature in the solutions. The temperature was measured with a RTD-126U thermometer ( $\pm 0.1$ K). The mixtures were stirred for 48 hours with a coated magnetic stirring bar. Then, the solutions were left for another 48 hours without stirring to allow the phases to settle down. Samples of the aqueous phase were taken with a syringe. In the case of solid-liquid equilibria, a 0.45- $\mu$ m filter was connected to the syringe. Samples were diluted by factor  $10^4$  with deionized water before analysis. Quantification of the fraction of the phenolic compound was made using a UV-visible spectrophotometer at the maximum of absorbance for each compound. Maximum wavelengths are provided in Table S1 (Appendix III). For each studied compounds, a calibration curve was carried out with six known concentrations solutions, comprised within 1 and 10 mg/L. Linear calibration curves (absorbance *A* versus the concentration *C*) provided  $R^2$  correlation coefficients of 0.998 or higher.

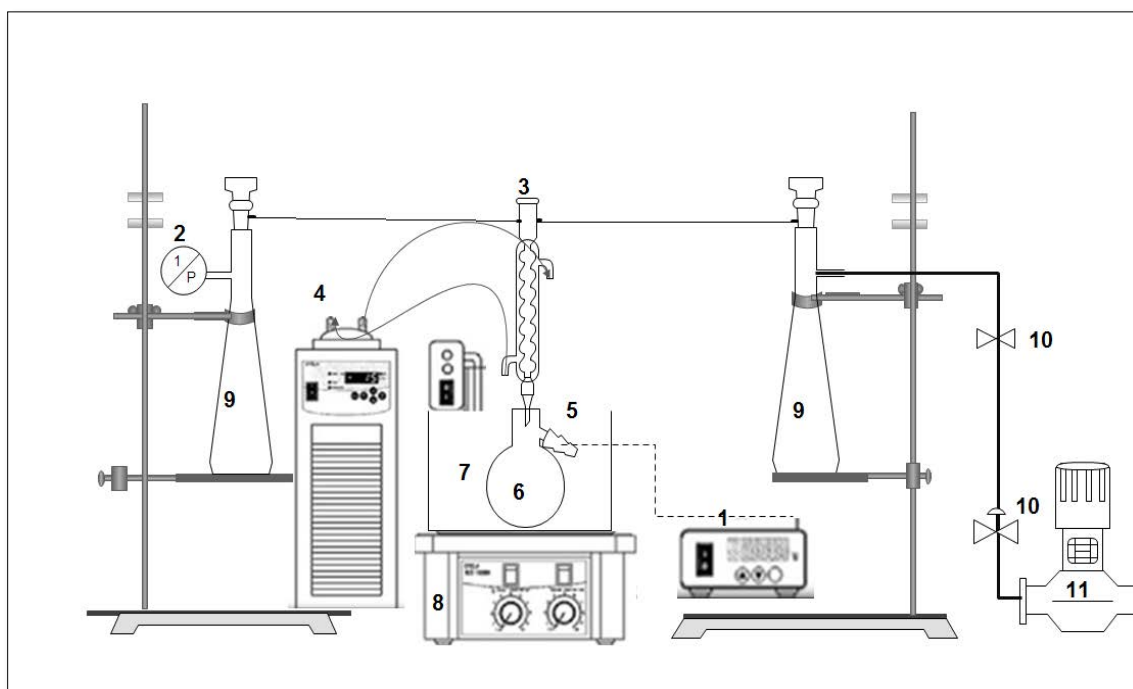
### IV-2.3. Solubility of water in the phenolic solution

In the case of liquid-liquid equilibria between water and phenolic compound (*i.e.* phenol, guaiacol, o-, m-, p-cresol), the determination of the fraction of water in the phenolic phase was determined by the trouble point method [45] between 293 and 323K. An amount of phenolic compound was put into a jacketed glass cell and connected to a thermostatic bath. The temperature was measured with a RTD-126U thermometer ( $\pm 0.1$ K) and maintained constant all over the experiment. Solutions were stirred with a coated magnetic bar and known amounts of water were added stepwise until a second phase appears.

#### IV-2.4. Vapor-Liquid equilibria of phenolic compound and ethanol

Apparatus used for the VLE measurements was described in our previous work [46]. Figure IV-1 presents the device used for the determination of the bubble point of isobaric VLE.

**Figure IV-1:** Scheme of the VLE device[46]: 1. Temperature transmitter; 2. Pressure transducer (Druck-PMP4010); 3. Condenser; 4. Refrigerator; 5. Temperature sensor (T900 series); 6. Equilibrium vessel; 7. Constant temperature bath; 8. Magnetic stirrer; 9. Pressure buffer; 10. Vacuum control valve; 11. Vacuum pump.



A volume of 50 mL of a known mixture of phenolic compound and ethanol was introduced into a round-bottom flask (6). The flask was put into a controlled oil bath (7) and connected to a condenser (3) cooled by a glycol aqueous solution. This condenser was kept at a sufficiently low temperature (267.15 K) to minimize the amount of vapor lost through the vacuum pump section, and hence, to avoid variation of the initial composition of the sample solution. To confirm the measuring accuracy, the seal fittings in the device had to be kept in good connection to avoid air leakage. Then, the pressure was set at the desired value with the pump (11). The temperature was measured by a temperature sensor (T900 series) thermocouple calibrated with high measuring accuracy ( $T900 \pm 0.06 \text{ }^\circ\text{C}$ ) and the pressure was determined by a pressure transducer (Druck-PMP4010) with an accuracy of ( $\pm 0.4 \text{ mbar}$ ). The mixture was stirred by a

coated magnetic bar. After 15 min the heating has been turned on, the temperature of the solution was generally stable and the vapor-liquid equilibrium was reached.

### IV-2.5. Excess enthalpy between phenolic compounds and ethanol

Excess molar enthalpies were measured using a Setaram C80 differential calorimeter (Setaram Instrumentation, France, 2010). The apparatus was calibrated using the Joule effect (electrical calibration) on a vessel containing a platinum resistance. Calibration was performed using several precise heat inputs to simulate experimental samples [47–49]. The phenolic compound and ethanol were initially in two compartments of the cell, separated by a mercury joint. The mixing was obtained by reversing the calorimeter. The calorimeter principle and the scheme of the cell have been described elsewhere [50].

## IV-3. Theory/calculation

### IV-3.1. Thermodynamic correlation

The phase equilibrium data of the binary systems were represented using the NRTL [44] model. This thermodynamic model allows to calculate the activity coefficient  $\gamma_i$ , for any component  $i$  of the binary system using the following expression:

$$\ln \gamma_i = \frac{\sum_{j=1}^m \tau_{ji} G_{ji} x_j}{\sum_{l=1}^m G_{li} x_l} + \sum_{j=1}^m \frac{x_j G_{ij}}{\sum_{l=1}^m G_{lj} x_l} \left( \tau_{ij} - \frac{\sum_{r=1}^m x_r \tau_{rj} G_{rj}}{\sum_{l=1}^m G_{lj} x_l} \right) \quad (2)$$

with  $G_{ji} = \exp(-\alpha_{ji} \tau_{ji})$ ,  $\tau_{ji} = \frac{g_{ji} - g_{ii}}{RT} = \frac{\Delta g_{ji}}{RT}$ ,  $\Delta g_{ij} = a_{ij} + b_{ij}T$  and  $\alpha_{ji} = \alpha_{ij} = \alpha$

where:  $g$  is an energy parameter characterizing the interaction of species  $i$  and  $j$ ,  $x_i$  is the mole fraction of component  $i$ ,  $T$  the temperature,  $R$  the ideal gas constant and  $m$  the number of components. The value of the non-randomness parameter  $\alpha$  was set to 0.3 according to the literature [51]. The use of NRTL model requires the knowledge of two sets of parameters  $a_{ij}$  and  $b_{ij}$ . The parameters were determined from experimental data, and by minimizing the following objective function:

$$F_{obj} = \sum_{k=1}^N \sum_{i=1}^2 \{ (x_{i,k}^{I,exp} - x_{i,k}^{I,calc})^2 + (x_{i,k}^{II,exp} - x_{i,k}^{II,calc})^2 \} \quad (3)$$

Where N is the number of tie lines in the data set,  $x_{i,k}^{I,exp}$ ,  $x_{i,k}^{I,calc}$  are the experimental and calculated mole fractions of the aqueous phase and  $x_{i,k}^{II,exp}$ ,  $x_{i,k}^{II,calc}$  are the experimental and calculated mole fractions of the phenolic phase.

The rmsd values, which provide a measure of the accuracy of the correlations, were calculated according to the following equation:

$$rmsd = \left\{ \frac{\sum_{k=1}^N \sum_{i=1}^2 \{ (x_{i,k}^{I,exp} - x_{i,k}^{I,calc})^2 + (x_{i,k}^{II,exp} - x_{i,k}^{II,calc})^2 \}}{4N} \right\}^{\frac{1}{2}} \quad (4)$$

### IV-3.2. Solid-Liquid Equilibria

The solubility of phenolic compounds in water *via* solid-liquid equilibria (*ie* pyrocatechol, syringol and vanillin) were determined using the simplified thermodynamic equation [52]:

$$\ln(x_{PC}\gamma_{PC}) = \frac{\Delta_{fus}H_{PC}}{RT_{fus PC}} \left( 1 - \frac{T_{fus PC}}{T} \right) \quad (5)$$

where  $\Delta_{fus}H_{PC}$  is the melting enthalpy calculated at the melting temperature  $T_{fus PC}$  of the phenolic compound. The objective function and the rmsd definition were similar to the equations 3 and 4. The solid phase was supposed to be pure phenolic component.

### IV-3.3. Vapor-Liquid equilibria

The vapor-liquid equilibria was determined through the following expression:

$$P \cdot y_i = P_i^{sat} \cdot x_i \cdot \gamma_i \cdot \mathcal{P} \quad (6)$$

where P and  $P_i^{sat}$  are respectively the pressure and saturated pressure of compound i, with y and x the molar fractions in the vapor and liquid phases, respectively. The Poynting coefficient  $\mathcal{P}$  was supposed equal to 1 since the fixed pressure was below the atmospheric one. The saturated pressures of the components were calculated using the Antoine equation [53–55] (Table S2 in Appendix III).

The objective function used to regress the  $a_{ij}$  and  $b_{ij}$  parameter is presented as follows:

$$F_{obj} = abs(1 - \frac{P_{calculated}}{P_{experimental}}) \quad (7)$$

The corresponding rmsd was calculated with the expression:

$$rmsd = \left\{ \frac{\sum_{i=1}^N (P_{i_{experimental}} - P_{i_{calculated}})^2}{N} \right\}^{\frac{1}{2}} \quad (8)$$

## IV-4. Results and Discussion

### IV-4.1. Solubility of the phenolic compounds in water

For a better display, the solubilities of the phenolic compounds in water were plotted in Figure IV-2 with a natural log scale. Experimental data are provided in Tables IV-3 and IV-4.

**Figure IV-2:** Solubility of phenolic compounds in water. Experimental measurements: ● Phenol, ● Guaiacol, ○ Syringol, ■ Pyrocatechol, ■ o-Cresol, □ m-Cresol, ▲ p-Cresol, △ Vanillin. The solid lines have been calculated using NRTL model.

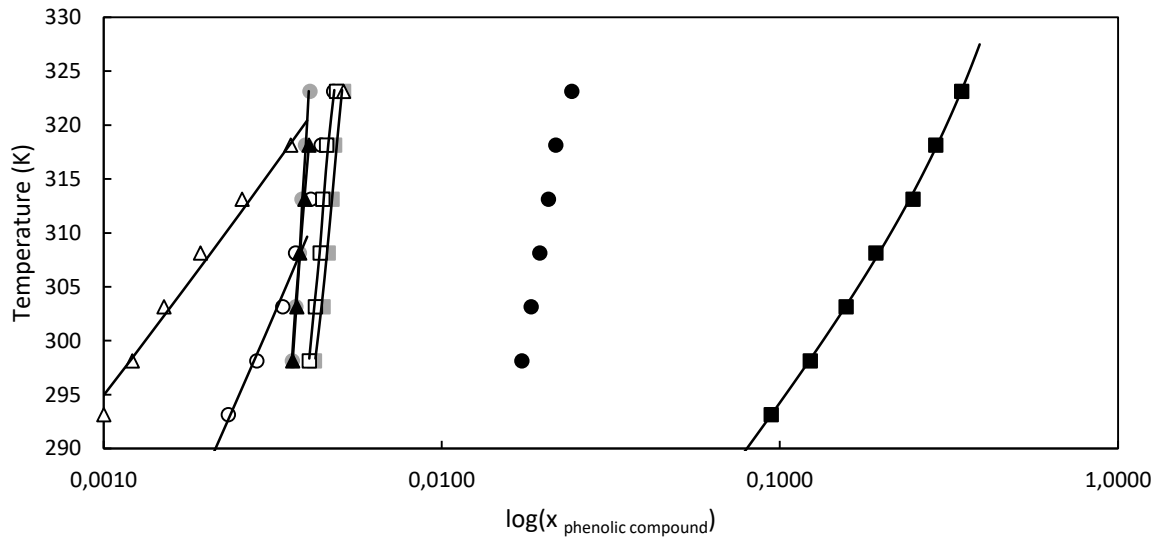


**Table IV-3:** Experimental LLE data of the {phenolic compound (PC) - water} systems at atmospheric pressure.

Temperature (K)	Aqueous phase		Phenolic phase	
	X <sub>PC</sub>	X <sub>water</sub>	X <sub>PC</sub>	X <sub>water</sub>
<i>Phenol-water</i>				
298.15	0.0172	0.9828		
303.15	0.0184	0.9816		
308.15	0.0195	0.9805		
313.15	0.0207	0.9793		
318.15	0.0217	0.9783		
323.15	0.0242	0.9758		
<i>Guaiacol-water</i>				
298.15	0.0036	0.9964	0.7522	0.2478
303.15	0.0037	0.9963	0.7346	0.2654
308.15	0.0038	0.9962	0.7226	0.2774
313.15	0.0039	0.9961	0.6952	0.3048
318.15	0.0039	0.9961	0.6739	0.3261
323.15	0.0041	0.9959	0.6443	0.3557
<i>Syringol-Water</i>				
313.15	0.0041	0.9959	0.3516	0.6484
318.15	0.0044	0.9956	0.3278	0.6722
323.15	0.0048	0.9952	0.3136	0.6864
<i>o-Cresol-water</i>				
298.15	0.0042	0.9958	0.5152	0.4848
303.15	0.0044	0.9956	0.5102	0.4898
308.15	0.0046	0.9954	0.5046	0.4954
313.15	0.0047	0.9953	0.4990	0.5010
318.15	0.0048	0.9952	0.4944	0.5056
323.15	0.0051	0.9949	0.4846	0.5154
<i>m-Cresol-water</i>				
298.15	0.0041	0.9959	0.5209	0.4791
303.15	0.0042	0.9958	0.5087	0.4913
308.15	0.0044	0.9956	0.4998	0.5002
313.15	0.0044	0.9956	0.4859	0.5141
318.15	0.0046	0.9954	0.4692	0.5308
323.15	0.0049	0.9951	0.4573	0.5427
<i>p-Cresol-water</i>				
298.15	0.0036	0.9964	0.4843	0.5157
303.15	0.0037	0.9963	0.4720	0.5280
308.15	0.0038	0.9962	0.4617	0.5383
313.15	0.0039	0.9961	0.4518	0.5482
318.15	0.0040	0.9960	0.4455	0.5545

$u(T) = 0.1K, u(x) < 0.005$

**Table IV-4:** Experimental SLE data of the {phenolic compound (PC)-water} systems at atmospheric pressure.

Temperature (K)	$x_{PC}$	$x_{water}$
<i>Syringol+water</i>		
293.15	0.0023	0.9977
298.15	0.0028	0.9972
303.15	0.0034	0.9966
308.15	0.0037	0.9963
<i>Pyrocatechol+water</i>		
293.15	0.0942	0.9058
298.15	0.1229	0.8771
303.15	0.1568	0.8432
308.15	0.1923	0.8077
313.15	0.2477	0.7523
318.15	0.2892	0.7108
323.15	0.3450	0.6550
<i>Vanillin+water</i>		
293.15	0.0010	0.9990
298.15	0.0012	0.9988
303.15	0.0015	0.9985
308.15	0.0019	0.9981
313.15	0.0026	0.9974
318.15	0.0036	0.9964
323.15	0.0051	0.9949

$$u(T) = 0.1K, u(x) < 0.005$$

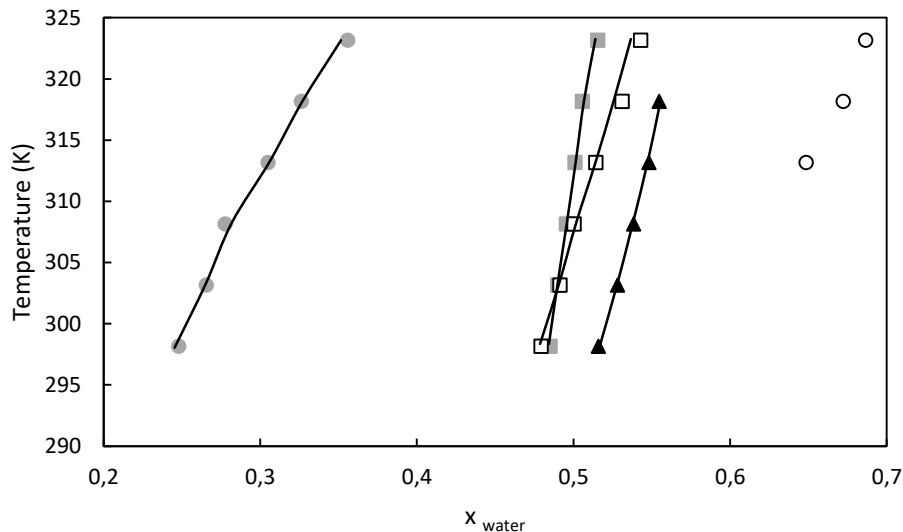
The solubility of each compounds in water increases with the increasing of temperature. Pyrocatechol, vanillin and syringol present a solid-liquid equilibria while the other compounds are in liquid-liquid equilibria with water. Note that syringol presents also a liquid-liquid equilibria but for a temperature beyond 308.15K. The solubility of pyrocatechol, phenol and vanillin is the most influenced by temperature. At 298.15 K, pyrocatechol presents the highest solubility in water ( $x_{pyrocatechol} = 0.123$ ), followed by phenol ( $x_{phenol} = 0.017$ ). The solubility of the others compounds are in the same range of values, according to the following rank: o-cresol > m-cresol > p-cresol > guaiacol > syringol > vanillin. The pyrocatechol and phenol molecules present respectively two and one hydroxyl groups, which are easily accessible to interact with water. In the case of cresols, the presence of a methyl group hinders the interactions of water with the hydroxyl group and therefore reduces the solubility of the compound. Finally, for guaiacol, syringol and vanillin, the presence of a methoxy group creates an intramolecular hydrogen bond with the hydroxyl group of the phenolic compounds. For these three former molecules, their hydroxyl groups are less available to interact with water. Generally,

measurements are in good agreement with those found in literature [20–34]. Nevertheless, our experimental data obtained for the vanillin-water system presents some deviation with those measured by Noubigh et al [28]. Indeed, this difference can be explained by the fact these authors waited only 3 hours of stirring and did not reach the equilibria [56–58]. Besides, for the vanillin-water system, the results presented in this work are in good agreement with those from Cartwright [26] and Mange et al [27]. Moreover, our experimental data for the guaiacol-water system is in disagreement with those found in the work of Jaspersen et al [59]. For the solubility of syringol in water, no data have been found in the literature. Plot of the different data are provided in supporting information for comparison (Figures S1 to S7 in Appendix III).

#### IV-4.2. Solubility of water in the phenolic solution

Tables VI-3 and VI-4 and Figure VI-3 gather the results of the solubility of water in the phenolic solutions.

**Figure IV-3:** Water solubility in phenolic phases. Experimental measurements: ● Guaiacol, ○ Syringol, ■ o-Cresol, □ m-Cresol, ▲ p-Cresol. The solid lines have been calculated using NRTL model.



Water is more soluble in the phenolic solutions with the rise of temperature. The guaiacol system is the most temperature-dependent. At 300 K, the solubility of water increases in the phenolic compounds as follows: guaiacol < o-cresol < m-cresol < p-cresol < syringol. The solubility of water in guaiacol is very low compared to those obtained in cresols or in syringol. This behavior is mainly due to the fact that guaiacol presents in its structure an intramolecular

hydrogen bond between its hydroxyl and methoxy group [60]. Therefore, the hydroxyl group is less accessible to interact with water. In the case of cresols, the solubility of water increases with the increasing distance of the methyl group. The hydroxyl group is less hindered in the para position compared to the ortho position and therefore can interact with water more easily. In the case of syringol, there is an intramolecular hydrogen bond between its hydroxyl and methoxy groups but its second methoxy group remains available to interact with water molecules. Experimental solubility measurements are in good agreement with those found in the literature [21,23–25,35] with a deviation between 0.15 and 1.4%. Comparisons are provided in Appendix III (Figures S4 to S7).

The regression of the parameter  $a_{ij}$  and  $b_{ij}$  of the NRTL model are listed in Table IV-5 for the phenolic compound-water systems. It can be noted that the number of experimental data of the two binary systems {phenol-water} and {syringol-water} does not allow to regress the NRTL parameters. The rmsd values are very low (inferior to 0.3%) for all systems which means that the correlated values fit well with the experimental data (Figures IV-2 and IV-3).

**Table IV-5:** NRTL parameters for the phenolic compound –water (SLE and LLE) systems

Compounds	$a_{12}$ (J.mol <sup>-1</sup> )	$a_{21}$ (J.mol <sup>-1</sup> )	$b_{12}$ (J.mol <sup>-1</sup> .K <sup>-1</sup> )	$b_{21}$ (J.mol <sup>-1</sup> .K <sup>-1</sup> )	rmsd (%)
Guaiacol	-2904.47	14631.14	50.56	-41.82	0.1363
o-Cresol	2238.76	4062.37	36.27	-14.81	0.0403
m-Cresol	-678.03	8057.33	46.23	-27.99	0.0298
p-Cresol	-839.66	6804.87	48.39	-25.14	0.0399
Syringol <sup>a</sup>	-4.48	-4.73	40.04	92.25	0.0041
Pyrocatechol <sup>a</sup>	2049.51	18565.35	182.94	-60.35	0.1488
Vanillin <sup>a</sup>	23464.72	5611.93	-30.50	2754755.83	0.0085

a: solid-liquid equilibrium

#### IV-4.3. Vapor-Liquid equilibria of phenolic compound and ethanol

The results of the vapor-liquid equilibria between the phenolic compounds (*i.e.* phenol, guaiacol, o-cresol) and ethanol are summarized hereafter (Table IV-6). The boiling temperature increases with the increase of pressure. Same phenomenon is observed with the increase of the molar fraction of the phenolic compounds. No azeotrope point is observed for the three systems, neither is a demixing of the liquid phase. Figure IV-4 presents the plot of the guaiacol-ethanol system as example.

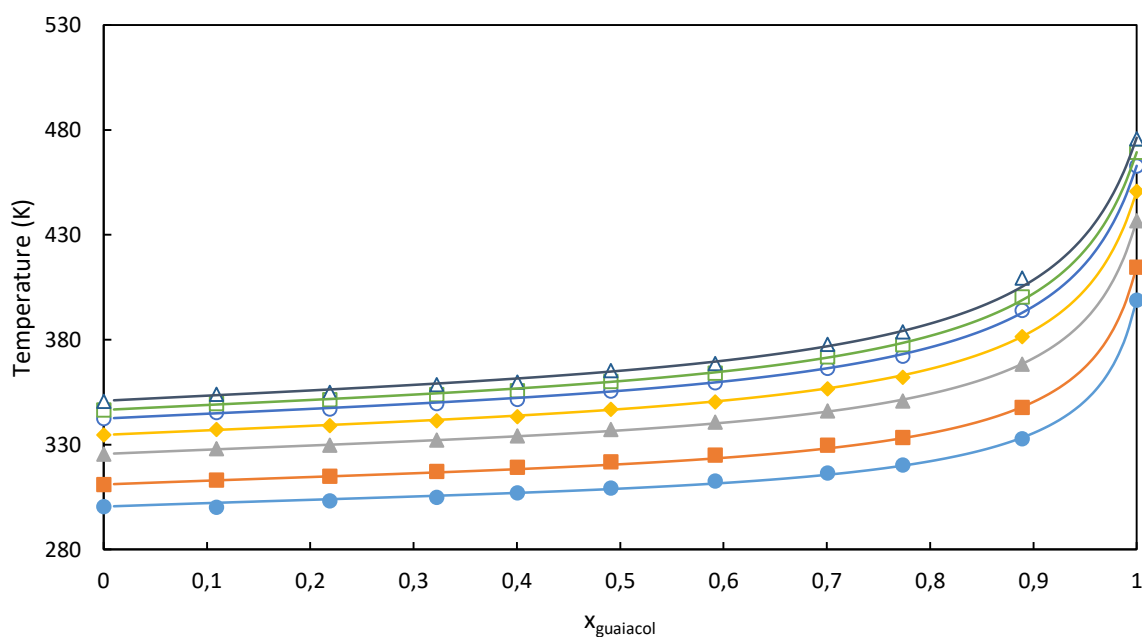
**Table IV-6:** Vapor-liquid equilibrium data of binary mixtures containing phenolic compounds and ethanol.

P (bar)	$X_{\text{phenol}}$	T (K)	P (bar)	$X_{\text{guaiacol}}$	T (K)	P (bar)	$X_{\text{o-cresol}}$	T (K)
0.090	0.100	303.09	0.090	0.109	300.25	0.090	0.097	302.23
	0.198	305.10		0.219	303.33		0.206	305.46
	0.300	310.04		0.322	304.88		0.304	308.67
	0.400	313.16		0.400	307.11		0.390	312.21
	0.495	319.73		0.491	309.40		0.507	319.01
	0.588	325.77		0.592	312.76		0.597	326.79
	0.692	333.65		0.701	316.55		0.699	333.07
	0.794	342.26		0.773	320.29		0.791	342.80
0.883	353.85	0.889	332.80	0.898	359.99			
0.150	0.100	312.58	0.164	0.109	313.11	0.150	0.097	311.87
	0.198	315.16		0.219	315.03		0.206	315.32
	0.300	319.57		0.322	317.28		0.304	319.29
	0.400	323.66		0.400	319.36		0.390	322.19
	0.495	330.26		0.491	321.93		0.507	329.86
	0.588	337.31		0.592	325.08		0.597	336.50
	0.692	345.08		0.701	329.79		0.699	344.12
	0.794	355.05		0.773	333.56		0.791	354.31
0.883	366.57	0.889	347.75	0.898	373.10			
0.330	0.100	328.70	0.333	0.109	328.13	0.351	0.097	329.36
	0.198	331.35		0.219	329.87		0.206	333.25
	0.300	336.15		0.322	332.29		0.304	337.22
	0.400	339.90		0.400	334.17		0.390	340.16
	0.495	347.78		0.491	337.32		0.507	348.90
	0.588	355.56		0.592	340.83		0.597	356.03
	0.692	364.32		0.701	346.20		0.699	363.84
	0.794	376.11		0.773	350.90		0.791	375.90
0.883	388.50	0.889	368.35	-	-	-		
0.550	0.100	340.09	0.500	0.109	337.36	0.551	0.097	339.54
	0.198	342.95		0.219	339.06		0.206	343.48
	0.300	348.05		0.322	341.49		0.304	347.87
	0.400	352.38		0.400	343.46		0.390	350.35
	0.495	360.94		0.491	346.85		0.507	360.29
	0.588	369.17		0.592	350.46		0.597	367.82
	0.692	378.58		0.701	356.72		0.699	376.33
	0.794	389.90		0.773	362.19		0.791	389.39
-	-	-	0.889	381.56	-	-	-	
0.750	0.100	347.53	0.700	0.109	345.35	0.750	0.097	346.85
	0.198	350.61		0.219	347.10		0.206	351.09
	0.300	355.78		0.322	349.65		0.304	355.53
	0.400	360.18		0.400	351.60		0.390	357.50
	0.495	369.28		0.491	355.68		0.507	368.40

	0.588	378.05		0.592	359.53		0.597	376.10
	0.692	387.67		0.701	366.51		0.699	385.84
-	-	-		0.773	372.24	-	-	-
-	-	-		0.889	394.05	-	-	-
	0.100	350.58		0.109	349.63		0.097	349.95
	0.198	353.70		0.219	351.45		0.206	354.17
0.851	0.300	359.06	0.832	0.322	354.00	0.851	0.304	358.80
	0.400	363.56		0.400	355.80		0.390	360.75
	0.495	373.06		0.491	360.20		0.507	371.88
	0.588	381.78		0.592	364.10		0.597	379.52
-	-	-		0.701	371.89	-	0.699	389.62
-	-	-		0.773	377.68	-	-	-
-	-	-		0.889	400.47	-	-	-
	0.100	354.51	0.996	0.109	354.12	0.991	0.097	353.75
	0.198	357.65	0.961	0.219	354.92	0.977	0.206	357.95
0.986	0.300	362.97	0.992	0.322	358.70	0.997	0.304	363.05
	0.400	367.75	0.977	0.400	359.87	0.999	0.390	364.60
	0.495	376.85	0.990	0.491	365.43	0.991	0.507	374.97
	0.588	386.30	0.971	0.592	368.80	0.985	0.597	384.56
-	-	-	0.997	0.701	377.89	0.994	0.699	394.11
-	-	-	0.990	0.773	383.82	-	-	-
-	-	-	0.965	0.889	409.48	-	-	-

$u(T) = 0.06$  K,  $u(P) = 0.4$  mbar,  $u(x) < 0.005$

**Figure IV-4:** Vapor-Liquid equilibria of the guaiacol-ethanol system in function of the molar fraction of guaiacol at different pressures. Experimental measurements at pressures: ● 0.09 bar, ■ 0.165 bar, ▲ 0.335 bar, ◆ 0.5 bar, ○ 0.7 bar, □ 0.83 bar, △ 0.99 bar. The solid lines have been calculated using NRTL model.



The temperature dependency is more important at high fraction of phenolic compounds ( $x_{\text{phenolic}} = 0.8-1$ ). The binary system {guaiacol-ethanol} is less temperature-dependent compared to the phenol or o-cresol systems (Figures S8 and S9 in Appendix III). Indeed, the slope in the guaiacol system is higher compared to the other systems. Moreover, for the {o-cresol-ethanol} and {phenol-ethanol} systems, the increase of the boiling temperature is more regularly distributed on the range of the studied molar fraction. The final boiling temperature is decreasing depending on the phenolic compounds as follows: guaiacol > o-cresol > phenol.

The regression of the parameter  $a_{ij}$  and  $b_{ij}$  of the NRTL model are listed in Table IV-7 for the phenolic compound-ethanol system. The rmsd values are very low (inferior to 0.02 bar) for all systems showing that the correlated values fit well with the experimental data.

**Table IV-7:** NRTL parameters for the phenolic compound – ethanol (VLE) systems.

Compounds	$a_{12}$ (J.mol <sup>-1</sup> )	$a_{21}$ (J.mol <sup>-1</sup> )	$b_{12}$ (J.mol <sup>-1</sup> .K <sup>-1</sup> )	$b_{21}$ (J.mol <sup>-1</sup> .K <sup>-1</sup> )	rmsd (bar)
Phenol	-0.04	0.01	-10.99	5.47	0.021
Guaiacol	3327.95	2215.75	-9.21	-1.38	0.022
o-Cresol	142951.43	-4284.01	-4.65	5.11	0.025

#### IV-4.4 Excess enthalpy of the phenolic compound – ethanol systems

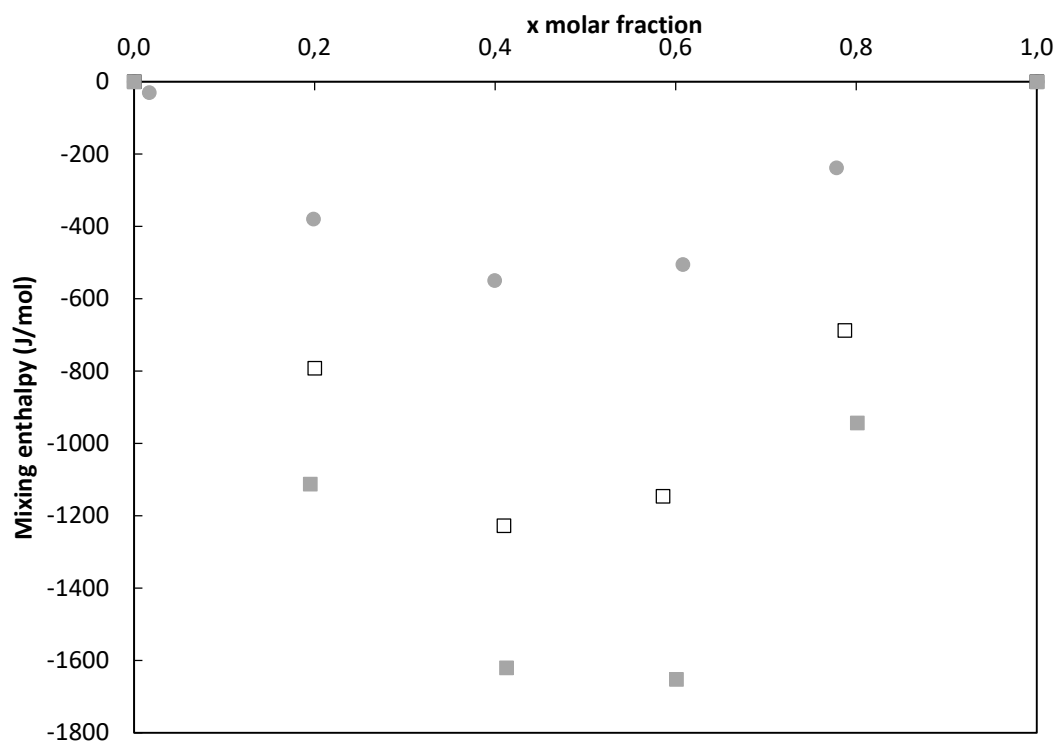
Excess properties give information for understanding the origin of the nonideality of mixtures. Molar excess enthalpy ( $h^E$ ) provides a measure of the intermolecular interactions in the mixture. During mixing, energy is required to break the interactions between the molecules of the pure solvent in order to form new interactions between unlike species releasing energy. The results of the molar excess enthalpy ( $h^E$ ) for guaiacol, o-cresol and m-cresol and ethanol systems are listed in Table IV-8 and plotted in Figure IV-5.

**Table IV-8:** Molar excess enthalpy of the {phenolic compound – ethanol} systems at T=298.15K and P= 1 atm.

$X_{\text{Guaiacol}}$	$h^E \text{ (J.mol}^{-1}\text{)}$	$X_{\text{o-cresol}}$	$h^E \text{ (J.mol}^{-1}\text{)}$	$X_{\text{m-cresol}}$	$h^E \text{ (J.mol}^{-1}\text{)}$
0.0168	-29.95	0.1954	-1112.03	0.2003	-791.99
0.1988	-379.49	0.4127	-1620.73	0.4097	-1227.70
0.3994	-549.10	0.6007	-1652.17	0.5861	-1146.24
0.6080	-505.33	0.8013	-943.58	0.7875	-687.42
0.7783	-237.77	-	-	-	-

$u(T)=0.02\text{K}$ ;  $u(h^E)=5 \text{ J.mol}^{-1}$ ;  $u(x) < 0.005$

**Figure IV-5:** Mixing enthalpy of the phenolic compound - ethanol systems. ● Guaiacol, ■ o-Cresol, □ m-Cresol.



The mixing of ethanol and phenolic compounds studied in this work is exothermic and the curves are practically symmetrical towards the molar fraction  $x=0.5$ . In first approximation, the exothermic effect may be related to stronger interactions between phenolic compounds and ethanol than ethanol-ethanol or phenolic-phenolic compounds interactions. Finally, the mixing

enthalpy values decrease as follows: guaiacol > m-cresol > o-cresol. It is worth noting that molar excess enthalpy of {ethanol + guaiacol} is quite small (0 to  $-550 \text{ J}\cdot\text{mol}^{-1}$ ). Replacing the methoxy group of the guaiacol by a methyl group in o-cresol leads to a strong increase of the  $h^E$  values.

#### **IV-5. Conclusion**

The mutual solubilities of water and eight phenolic compounds (*i.e.* phenol, guaiacol, syringol, pyrocatechol, o-, m-, p-cresol and vanillin) were investigated between 293.15 and 323.15K. Vapor-liquid equilibria and mixing enthalpy of binary mixtures {phenol or guaiacol or o-cresol + ethanol} were also investigated for different molar compositions. The information provided by this work help to understand the behavior of the phenolic compounds in green solvents. This knowledge is vital for the development of extraction and purification processes of phenolic compounds from bio-oils produced upon biomass thermochemical conversion. Moreover, parameters of the NRTL thermodynamic model were determined and correlate well with the experimental measurements.

*List of symbols*

$\alpha$	Non-randomness parameter
$\gamma_i$	Activity coefficient
$a_{ij}, b_{ij}$	NRTL parameters
$g$	Interaction energy parameter (NRTL)
$h^E$	Molar excess enthalpy
$\Delta_{fus}H$	Fusion enthalpy
K	Kelvin
LLE	Liquid-Liquid Equilibrium
N	Number of tie-lines
$\mathcal{P}$	Poynting coefficient
P	Pressure
$P^{sat}$	Saturated pressure
PC	Phenolic Compound
R	Ideal gas constant
rmsd	Root mean square deviation
SLE	Solid Liquid Equilibrium
T	Temperature
$T_{fus}$	Fusion temperature
VLE	Vapor-Liquid Equilibrium
x	Molar fractions (liquid phase)
y	Molar fraction (vapor phase)

## References

- [1] A.V. Bridgwater, D. Meier, D. Radlein, An overview of fast pyrolysis of biomass, *Org. Geochem.* 30 (1999) 1479–1493. doi:10.1016/S0146-6380(99)00120-5.
- [2] R.K. Sharma, N.N. Bakhshi, Catalytic upgrading of biomass-derived oils to transportation fuels and chemicals, *Can. J. Chem. Eng.* 69 (1991) 1071–1081. doi:10.1002/cjce.5450690505.
- [3] M.D. Guillén, M.L. Ibargoitia, New Components with Potential Antioxidant and Organoleptic Properties, Detected for the First Time in Liquid Smoke Flavoring Preparations, *J. Agric. Food Chem.* 46 (1998) 1276–1285. doi:10.1021/jf970952x.
- [4] F. Helmut, V. Heinz-Werner, H. Toshikazu, P. Wilfried, Phenol derivatives, *Ullmann's Encycl. Ind. Chem. VCH Ger.* 19 (1985) 299–357.
- [5] F. Ikegami, T. Sekine, Y. Fujii, [Anti-dermatophyte activity of phenolic compounds in “mokusaku-eki”], *Yakugaku Zasshi.* 118 (1998) 27–30.
- [6] J.A. Maga, I. Katz, Simple phenol and phenolic compounds in food flavor, *C R C Crit. Rev. Food Sci. Nutr.* 10 (1978) 323–372. doi:10.1080/10408397809527255.
- [7] X. Ouyang, X. Huang, Y. Zhu, X. Qiu, Ethanol-Enhanced Liquefaction of Lignin with Formic Acid as an *in Situ* Hydrogen Donor, *Energy Fuels.* 29 (2015) 5835–5840. doi:10.1021/acs.energyfuels.5b01127.
- [8] Wahyudiono, T. Kanetake, M. Sasaki, M. Goto, Decomposition of a Lignin Model Compound under Hydrothermal Conditions, *Chem. Eng. Technol.* 30 (2007) 1113–1122. doi:10.1002/ceat.200700066.
- [9] Wahyudiono, M. Sasaki, M. Goto, Conversion of biomass model compound under hydrothermal conditions using batch reactor, *Fuel.* 88 (2009) 1656–1664. doi:10.1016/j.fuel.2009.02.028.
- [10] X. Yuan, H. Li, G. Zeng, J. Tong, W. Xie, Sub- and supercritical liquefaction of rice straw in the presence of ethanol–water and 2-propanol–water mixture, *Energy.* 32 (2007) 2081–2088. doi:10.1016/j.energy.2007.04.011.
- [11] H.-M. Liu, Y.-L. Liu, Characterization of milled solid residue from cypress liquefaction in sub- and super ethanol, *Bioresour. Technol.* 151 (2014) 424–427. doi:10.1016/j.biortech.2013.10.050.
- [12] R. Singh, A. Prakash, S.K. Dhiman, B. Balagurumurthy, A.K. Arora, S.K. Puri, T. Bhaskar, Hydrothermal conversion of lignin to substituted phenols and aromatic ethers, *Bioresour. Technol.* 165 (2014) 319–322. doi:10.1016/j.biortech.2014.02.076.
- [13] C. Xu, T. Etcheverry, Hydro-liquefaction of woody biomass in sub- and super-critical ethanol with iron-based catalysts, *Fuel.* 87 (2008) 335–345. doi:10.1016/j.fuel.2007.05.013.
- [14] Z. Liu, F.-S. Zhang, Effects of various solvents on the liquefaction of biomass to produce fuels and chemical feedstocks, *Energy Convers. Manag.* 49 (2008) 3498–3504. doi:10.1016/j.enconman.2008.08.009.
- [15] J.N. Murwanashyaka, H. Pakdel, C. Roy, Separation of syringol from birch wood-derived vacuum pyrolysis oil, *Sep. Purif. Technol.* 24 (2001) 155–165. doi:10.1016/S1383-5866(00)00225-2.
- [16] C. Amen-Chen, H. Pakdel, C. Roy, Separation of phenols from Eucalyptus wood tar, *Biomass Bioenergy.* 13 (1997) 25–37. doi:10.1016/S0961-9534(97)00021-4.
- [17] R.W. Thring, J. Breau, Hydrocracking of solvolysis lignin in a batch reactor, *Fuel.* 75 (1996) 795–800. doi:10.1016/0016-2361(96)00036-1.
- [18] S. Wang, Y. Wang, Q. Cai, X. Wang, H. Jin, Z. Luo, Multi-step separation of monophenols and pyrolytic lignins from the water-insoluble phase of bio-oil, *Sep. Purif. Technol.* 122 (2014) 248–255. doi:10.1016/j.seppur.2013.11.017.

- [19] S. Czernik, R. Maggi, G.V.C. Peacocke, A review of physical and chemical methods of upgrading biomass-derived fast pyrolysis liquids, in: Biomass Proc. 4th Biomass Conf. Am., 1999: pp. 1235–1240.
- [20] D. Tam, D. Varhanickova, W.Y. Shiu, D. Mackay, Aqueous solubility of chloroguaiacols, *J. Chem. Eng. Data.* 39 (1994) 83–86. doi:10.1021/je00013a022.
- [21] N.V. Sidgwick, W.J. Spurrell, T.E. Davies, CXXXII.—The solubility of the nitrophenols and other isomeric disubstitution products of benzene, *J Chem Soc Trans.* 107 (1915) 1202–1213. doi:10.1039/CT9150701202.
- [22] D. Varhanickova, W.-Y. Shiu, D. Mackay, Aqueous Solubilities of Alkylphenols and Methoxyphenols at 25 .degree.C, *J. Chem. Eng. Data.* 40 (1995) 448–451. doi:10.1021/je00018a020.
- [23] C.R. Bailey, CCXCVIII.—The increased solubility of phenolic substances in water on addition of a third substance, *J Chem Soc Trans.* 123 (1923) 2579–2590. doi:10.1039/CT9232302579.
- [24] H. Brusset, H. Gillier-Pandraud, A. Neuman, Strukturbestimmung bei-150 grad c von 2, 5-und 2, 3-dimethylphenol, *Chem. Informationsdienst.* 3 (1972).
- [25] W.A. Leet, H.-M. Lin, K.-C. Chao, Mutual solubilities in six binary mixtures of water + a heavy hydrocarbon or a derivative, *J. Chem. Eng. Data.* 32 (1987) 37–40. doi:10.1021/je00047a010.
- [26] L.C. Cartwright, Vanilla-like Synthetics, Solubility and Volatility of Propenyl Guaethyl, Bourbonal, Vanillin, and Coumarin, *J. Agric. Food Chem.* 1 (1953) 312–314. doi:10.1021/jf60004a006.
- [27] C.E. Mange, O. Ehler, Solubilities of Vanillin., *Ind. Eng. Chem.* 16 (1924) 1258–1260. doi:10.1021/ie50180a017.
- [28] A. Noubigh, M. Abderrabba, E. Provost, Temperature and salt addition effects on the solubility behaviour of some phenolic compounds in water, *J. Chem. Thermodyn.* 39 (2007) 297–303. doi:10.1016/j.jct.2006.06.014.
- [29] W.H. Walker, A.R. Collett, C.L. Lazzell, The Solubility Relations of the Isomeric Dihydroxybenzenes, *J. Phys. Chem.* 35 (1930) 3259–3271. doi:10.1021/j150329a011.
- [30] X. Xia, D. Jiang, Determination and correlation of solubilities of catechol, *J. Chem. Ind. Eng.-CHINA-* 58 (2007) 1082.
- [31] C. Achard, M. Jaoui, M. Schwing, M. Rogalski, Aqueous Solubilities of Phenol Derivatives by Conductivity Measurements, *J. Chem. Eng. Data.* 41 (1996) 504–507. doi:10.1021/je950202o.
- [32] A.N. Campbell, A.J.R. Campbell, Concentrations, Total and Partial Vapor Pressures, Surface Tensions and Viscosities, in the Systems Phenol—Water and Phenol—Water—4% Succinic Acid, *J. Am. Chem. Soc.* 59 (1937) 2481–2488. doi:10.1021/ja01291a001.
- [33] A.E. Hill, W.M. Malisoff, The mutual solubility of liquids. III. The mutual solubility of phenol and water. IV. The mutual solubility of normal butylalcohol and water, *J. Am. Chem. Soc.* 48 (1926) 918–927. doi:10.1021/ja01415a011.
- [34] M. Jaoui, C. Achard, M. Rogalski, Solubility as a Function of Temperature of Selected Chlorophenols and Nitrophenols in Aqueous Solutions Containing Electrolytes or Surfactants, *J. Chem. Eng. Data.* 47 (2002) 297–303. doi:10.1021/je0102309.
- [35] T. Shedlovsky, On guaiacol solutions: the electrical conductivity of sodium and potassium guaiaculates in guaiacol, *J. Gen. Physiol.* 17 (1934) 549–561. doi:10.1085/jgp.17.4.549.
- [36] M. Klauck, A. Grenner, K. Taubert, A. Martin, R. Meinhardt, J. Schmelzer, Vapor–Liquid Equilibria in Binary Systems of Phenol or Cresols + Water, + Toluene, and + Octane and Liquid–Liquid Equilibria in Binary Systems of Cresols + Water, *Ind. Eng. Chem. Res.* 47 (2008) 5119–5126. doi:10.1021/ie071214t.

- [37] T.E.V. Prasad, A. Jaiswal, S. Prasad, G. Harish, N. Krupavaram, N.M. Sirisha, K. Ashok, Y.N. Kumar, N. Venkanna, D.H.L. Prasad, Activity coefficients of the binary mixtures of o-cresol or p-cresol with C1–C4 aliphatic alcohols near ambient pressure, *Fluid Phase Equilibria*. 244 (2006) 86–98. doi:10.1016/j.fluid.2006.03.018.
- [38] G. Weissenberger, R. Henke, L. Bregmann, Zur Kenntnis organischer Molekülverbindungen: XVI. Zweiwertige Phenole und ihre Äther, *Monatshefte Chem.* 46 (1925) 471–482. doi:10.1007/BF01525702.
- [39] G. Weissenberger, L. Piatti, The Molecular Compounds of the Phenols. I. The Behavior of Cresols against Alcohol, *Monatsh Chem.* 45 (n.d.) 187–206. doi:10.1007/BF01524660.
- [40] C.H. Chou, J.L. Perng, M.D. Lee, Y.P. Chen, Vapor-Liquid Equilibrium Measurements of the Ternary System of Ethanol, Water and Phenol at 760 mm Hg, *J Chin Inst Chem En.* 18 (1987) 393–399.
- [41] N.V. Novikova, V.N. Ponomarev, V.S. Timofeev, Investigation of the separation technology of the mixture ethanol - water - butyl acetate - phenol, *Osn. Org Sint Neft.* 25 (1989) 124–129.
- [42] G. Weissenberger, F. Schuster, K. Schuler, The molecular compounds of phenols. IV. The behavior of the binary systems with phenol and phenol ethers, *Monatsh Chem.* 45 (1924) 425–435.
- [43] G. Weissenberger, R. Henke, E. Sperling, Zur Kenntnis organischer Molekülverbindungen XVII. Das Verhalten des Dekahydronaphthalins, *Monatshefte Chem.* 46 (1925) 483–497. doi:10.1007/BF01526344.
- [44] H. Renon, J.M. Prausnitz, Local compositions in thermodynamic excess functions for liquid mixtures, *AIChE J.* 14 (1968) 135–144. doi:10.1002/aic.690140124.
- [45] M. Rogošić, M. Bakula, M. Župan, Liquid-liquid Equilibria in the Ternary Systems H<sub>2</sub>O–Phenol – 2-Butanone and H<sub>2</sub>O–Phenol – 2-Propanol, *Chem. Biochem. Eng. Q.* 26 (2012) 155–162.
- [46] E.-S. Abumandour, F. Mutelet, D. Alonso, Performance of an absorption heat transformer using new working binary systems composed of {ionic liquid and water}, *Appl. Therm. Eng.* 94 (2016) 579–589. doi:10.1016/j.applthermaleng.2015.10.107.
- [47] C80. The brochure, Setaram Instrumentation, Caluire, France, (2009).
- [48] C80. Commissioning, Setaram Instrumentation, Caluire, France, (2010).
- [49] I. Letyanina, N. Tsvetov, I. Zvereva, A. Samarov, A. Toikka, Excess molar enthalpies for binary mixtures of n-propanol, acetic acid, and n-propyl acetate at 313.15K and atmospheric pressure, *Fluid Phase Equilibria*. 381 (2014) 77–82. doi:10.1016/j.fluid.2014.08.022.
- [50] P.M. Ghogomu, M. Bouroukba, J. Dellacherie, D. Balesdent, M. Dirand, On the ideality of liquid mixtures of long-chain n-alkanes, *Thermochim. Acta.* 306 (1997) 69–71. doi:10.1016/S0040-6031(97)00301-8.
- [51] L.D. Simoni, A. Chapeaux, J.F. Brennecke, M.A. Stadtherr, Asymmetric Framework for Predicting Liquid–Liquid Equilibrium of Ionic Liquid–Mixed-Solvent Systems. 2. Prediction of Ternary Systems, *Ind. Eng. Chem. Res.* 48 (2009) 7257–7265. doi:10.1021/ie9004628.
- [52] J.M. Prausnitz, R.N. Lichtenthaler, E.G. de Azevedo, *Molecular thermodynamics of fluid-phase equilibria*, Prentice-Hall, 1986.
- [53] <http://www.engr.umd.edu/~nsw/ench250/antoine.dat> - Antoine\_coefficient\_table.PDF, (n.d.).  
[http://www.eng.auburn.edu/~drmill/mans486/Diffusion%20Tube/Antoine\\_coefficient\\_table.PDF](http://www.eng.auburn.edu/~drmill/mans486/Diffusion%20Tube/Antoine_coefficient_table.PDF) (accessed April 12, 2017).
- [54] E. Von Terres, F. Gebert, H. Hulsemann, P. Heinz, H. Toepsch, W. Ruppert, Zur Kenntnis der Physicalisch-Chemischen Grundlagen der Gewinnung und Zerlegung

- derPheolfractionen von Steibohlentee und Braunkohlenschwefel, Brennst. Chem. 36 (1955) 272.
- [55] S. Henke, P. Kadlec, Z. Bubník, Physico-chemical properties of ethanol – Compilation of existing data, J. Food Eng. 99 (2010) 497–504. doi:10.1016/j.jfoodeng.2009.06.050.
- [56] F.L. Mota, A.J. Queimada, S.P. Pinho, E.A. Macedo, Aqueous Solubility of Some Natural Phenolic Compounds, Ind. Eng. Chem. Res. 47 (2008) 5182–5189. doi:10.1021/ie071452o.
- [57] A.J. Queimada, F.L. Mota, S.P. Pinho, E.A. Macedo, Solubilities of Biologically Active Phenolic Compounds: Measurements and Modeling, J. Phys. Chem. B. 113 (2009) 3469–3476. doi:10.1021/jp808683y.
- [58] L.-L. Lu, X.-Y. Lu, Solubilities of Gallic Acid and Its Esters in Water, J. Chem. Eng. Data. 52 (2007) 37–39. doi:10.1021/je0601661.
- [59] L.V. Jaspersen, R.J. McDougal, V. Diky, E. Paulechka, R.D. Chirico, K. Kroenlein, K. Iisa, A. Dutta, Liquid–Liquid Equilibrium Measurements for Model Systems Related to Catalytic Fast Pyrolysis of Biomass, J. Chem. Eng. Data. 62 (2017) 243–252. doi:10.1021/acs.jced.6b00625.
- [60] C. Agache, V.I. Popa, Ab Initio Studies on the Molecular Conformation of Lignin Model Compounds I. Conformational Preferences of the Phenolic Hydroxyl and Methoxy Groups in Guaiacol, Monatshefte Für Chem. - Chem. Mon. 137 (2006) 55–68. doi:10.1007/s00706-005-0404-x.



## Chapter V: Extraction of phenolic compounds from aqueous solution using choline bis(trifluoromethylsulfonyl)imide

Laëtitia Cesari<sup>1</sup>, Laetitia Canabady-Rochelle<sup>1</sup>, Fabrice Mutelet<sup>1</sup>

<sup>1</sup> : Université de Lorraine, Laboratoire Réactions et Génie des Procédés (LRGP, UMR CNRS-UL 7274), 1 rue Grandville, 54000 Nancy, France

Article paru dans Fluid Phase Equilibria :

L. Cesari, L. Canabady-Rochelle, F. Mutelet, Extraction of phenolic compounds from aqueous solution using choline bis(trifluoromethylsulfonyl)imide, Fluid Phase Equilibria. 446 (2017) 28–35. doi:10.1016/j.fluid.2017.04.022.

### Résumé

Ce chapitre a pour objectif d'évaluer les performances d'un liquide ionique comme solvant pour l'extraction de composés phénoliques d'un milieu aqueux. Le liquide ionique choisi est la [choline][NTf<sub>2</sub>] (choline bis(trifluoromethylsulfonyl)imide) pour son caractère hydrophobe et sa faible toxicité. Les équilibres solide-liquide et liquide-liquide de quatre systèmes ternaires {eau + composé phénolique (phénol, guaiacol, syringol ou pyrocatechol) + liquide ionique} sont mesurés à 298 K et à pression atmosphérique. Le calcul de la sélectivité et du coefficient de distribution montrent que ce liquide ionique est un excellent choix pour l'extraction des composés phénoliques en phase aqueuse. De plus, les données expérimentales ont été utilisées afin de déterminer les paramètres d'interaction des modèles NRTL et UNIQUAC. L'influence de paramètres tels que la cinétique, la température ou le rapport massique solvant/solution est évaluée lors de l'extraction de composés phénoliques d'une solution aqueuse synthétique. Cette étude montre que l'extraction des composés phénoliques est quasiment instantanée, efficace à température ambiante et ne requiert qu'une faible quantité de solvant. Enfin, le procédé proposé montre que le guaiacol et le syringol sont facilement extraits. De plus, cette extraction nécessite une colonne avec un faible nombre d'étages théoriques et peu d'énergie comparé à des solvants organiques.

**Abstract**

The efficiency of choline bis(trifluoromethylsulfonyl)imide [choline][NTf<sub>2</sub>] was evaluated as extractant media for the extraction of phenolic compounds from aqueous solution. Solid-liquid and liquid-liquid equilibria of the ternary mixtures {water + phenolic compounds (phenol, guaiacol, syringol or pyrocatechol) + ionic liquid} were first measured at 295.15K at atmospheric pressure. The selectivity and the solute distribution ratio values calculated from experimental data indicate that [choline][NTf<sub>2</sub>] is suitable for the extraction of phenolic compounds. Thermodynamic data of ternary mixtures were used to regress the parameters of the NRTL and UNIQUAC thermodynamic models. The influence of experimental conditions on the extraction of phenolic compounds from aqueous solutions using [choline][NTf<sub>2</sub>] were evaluated. Process design shows that phenol, guaiacol and syringol are easily extractable with few amount of solvent, number of theoretical steps and energy.

## V-1. Introduction

Plants produce a large variety of natural compounds, among them, phenolic compounds. Known for their antioxidant or antimicrobial properties, phenolic compounds are often used as raw material or intermediate for the production of resins [1], food additives [2], food flavor, pharmaceutical or perfumery products [3–5]. To date, most of the phenolic compounds are produced from petroleum. Yet, due to the increasing of greenhouse effect and the reducing stocks of fossil fuels, researches lean towards new sources of fuel and chemicals, such as lignin [6]. These last decades, thermochemical conversion processes of biomass have demonstrated their potentials to produce gasoline-compatible liquid fuels [7]. The liquefaction of lignin produces mixtures rich in phenolic compounds but their extraction required several and complex steps [8]. For example, the separation of phenolic compounds from primary oils of Eucalyptus wood tar can be obtained after 5-stage alkaline extraction and 4-stage ethyl acetate extraction [9]. Separation processes require a good knowledge of phase diagrams of mixtures and of the interactions between the solutes and the extractant media. Liquid-liquid equilibria of systems containing water, phenolic compounds and a solvent allow evaluating the performance of the extraction processes through the calculation of selectivity and solute distribution ratio values. Many organic solvents such as esters [10],[11], ether [12], carbonates [13],[14], ketones [15–21], alcohols [16],[22], aromatic [23],[24] and aliphatic hydrocarbons [25] have been tested but mostly in systems containing phenol and water, even if researches are more concerned about other monophenols such as guaiacol [26] or pyrocatechol [27]. Ghanadzadeh Gilani et al [28] and Alvarez Gonzalez et al [29] have studied the extracting capability of several solvents and shown that organic esters are the most effective solvent for the extraction of phenol from water. Recently, new solvents such as ionic liquids or deep eutectic solvents have shown an important interest in various processes extraction due to their unique physico-chemical properties. These solvents could replace ethyl acetate or esters for the extraction of phenol from aqueous solution. The use of such solvents may lead to a simplification of the process. Indeed, their low volatility implies an easy way to recover the phenolic compounds. Moreover, such processes could improve the yield and purity of the products. Because ionic liquid (IL) are easily recovered and reusable, their use could also reduce the cost of the process. Pili et al. [30] demonstrated the performance of ILs to remove phenol from aqueous solution using supported ionic liquid membrane. However, studies on the extraction of phenolic compounds using of ionic liquid are still lacking [26]. It is now well established that bis(trifluoromethylsulfonyl)imide based ILs are hydrophobic. Therefore, this family can be used as an extractive media in aqueous liquid-liquid extraction.

Indeed, Nockemanns et al. studied the binary system {choline bis(trifluoromethylsulfonyl)imide + water}. They showed that these compounds are partially miscible and present an upper critical solution temperature at 72°C [31]. The choice of choline as cation was dictated for its low toxicity compared to imidazolium or pyridinium IL [32]. This family of ILs is more environmentally friendly than some traditional industrial solvents.

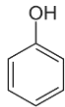
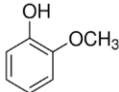
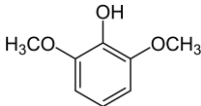
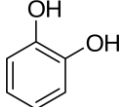
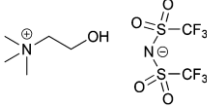
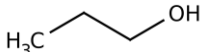
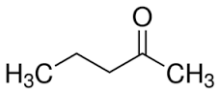
The aim of this study was to evaluate the feasibility of the use of choline bis(trifluoromethylsulfonyl)imide for the extraction of phenolic compounds from aqueous solution. For the first time, full phase diagrams of ternary systems containing {water + phenol or guaiacol or syringol or pyrocatechol + choline bis(trifluoromethylsulfonide)imide} required for the process design were first determined. Thermodynamic data were then used to fit interaction parameters of NRTL [33] and UNIQUAC [34] models and then to facilitate the process simulation. The last part of the paper is devoted to the process sizing of a column for the extraction of phenolic compounds using choline bis(trifluoromethylsulfonyl)imide.

## **V-2. Materials and Methods**

### **V-2.1. Chemicals and materials**

The names, abbreviation, CAS numbers, molar masses, structures, producers and purity of the substances are listed in Table V-1.

**Table V-1:** Names, CAS numbers, abbreviation, molar mass, chemical structures and source of compounds

Name	Abbreviation	CAS	Molar mass g.mol <sup>-1</sup>	Formula	Source and purity (wt%)
Phenol		108-95-2	94.1112		Sigma Aldrich >99.5%
2-methoxyphenol	Guaiacol	90-05-1	124.1372		Sigma Aldrich >99%
2,6-dimethoxyphenol	Syringol	91-10-1	154.1632		Sigma Aldrich 99%
1,2-benzenediol	Pyrocatechol	120-80-9	110.1106		Sigma Aldrich >99%
Choline bis(trifluoromethylsulfonide)imide	[Choline][NTf <sub>2</sub> ]	827027-25-8	384.31		Io-li-tec >99%
1-propanol		71-23-8	60.0950		Sigma Aldrich >99%
2-pentanone		107-87-9	86.1323		Sigma Aldrich >99%

Phenol (CAS 108-95-2), guaiacol (CAS 90-05-1), syringol (CAS 91-10-1), pyrocatechol (CAS 120-80-9), 1-propanol (CAS 71-23-8) and 2-pentanone (CAS 107-87-9) were supplied by Sigma Aldrich. All materials were used as received without any further purification. The ionic liquid choline bis(trifluoromethylsulfonide)imide [choline][NTf<sub>2</sub>] was supplied by Io-li-tec with a purity of 99%. The IL was dried at 323.15K during 5h under high vacuum before use. Water content was determined with a TIM550 Karl Fischer volumetric titration (Titralab) using the hydranal-Solvent E as analyte (from Sigma-Aldrich). The water content was less than 61 ppm for [choline][NTf<sub>2</sub>]. The error on the water content was  $\pm 2\%$ . Deionized water was used for all experiments.

### V-2.2. Phase diagrams measurements of ternary mixtures {phenolic compounds + water + IL}

The liquid-liquid equilibrium tie-lines were measured for the phenolic compound (phenol, guaiacol, syringol, pyrocatechol) + water + choline bis(trifluoromethylsulfonide)imide systems at 298.15K under atmospheric pressure. Mixtures with compositions comprised within the immiscible region of the systems were introduced into a jacketed glass cell of 30 cm<sup>3</sup> volume. The cell was closed and connected to a thermostatic bath to maintain a constant temperature of 298.15K ( $\pm 0.1$ K) measured with a RTD-126U thermometer. The mixtures were stirred for 48 hours with a coated magnetic stirring bar and then left for 48 hours without stirring to allow the phases to settle down. Composition of each phases were determined by gas chromatography coupled with FID (Perichrom PR2100 with ALS 104 autosampler) and TCD (Shimadzu GC-2010 with AOC-20i auto injector) detectors. Samples were taken from both phases with a syringe. 1-propanol was added to all studied samples in order to avoid phases splitting and to maintain a homogenous mixture. 2-pentanone was added as an internal standard. Details of the operating conditions are presented in Tables S1 and S2 (Appendix IV). The low-volatility of ILs requires the use of a pre-column in order to protect the GC column. In each phase, the IL fraction was obtained by subtracting the fraction of phenolic compound and water from one.

Solid-liquid equilibria of the ternary systems {water + (phenol or syringol or pyrocatechol) + choline bis(trifluoromethylsulfonide)imide} were determined *via* the trouble point method [16]. Mixtures containing phenolic compound and choline bis(trifluoromethylsulfonide)imide with different compositions were put into glass cell connected to a thermostatic bath. The temperature was set to 298.15 K and measured with a RTD-126U thermometer with an

uncertainty of 0.1K. Solutions were stirred and known amounts of water were added regularly until the solid totally disappears.

### V-2.3. Extraction of phenolic compounds from aqueous solution

Extraction of phenolic compounds from synthetic aqueous solutions were experimented with [choline][NTf<sub>2</sub>]. A stock solution of aqueous solution containing precise amounts of four phenolic compounds (phenol, guaiacol, syringol and pyrocatechol) was prepared. The concentrations were 5.05 g.L<sup>-1</sup>, 5.13 g.L<sup>-1</sup>, 5.08 g.L<sup>-1</sup> and 5.21g.L<sup>-1</sup> for phenol, guaiacol, syringol and pyrocatechol, respectively. A weight of this solution was put into a glass cell connected to a thermostatic bath. The [choline][NTf<sub>2</sub>] ionic liquid was then added to the mixture under stirring. A sample of the ionic liquid rich-phase was diluted in 1-propanol to avoid phase splitting. 2-pentanone was also added to the sample and as an intern standard. Sample were analyzed by gas chromatography with the same procedures as described previously.

Several parameters (time, temperature and weight ratio of ionic liquid/water) were studied in order to evaluate their influence on the extraction ratio of phenolic compounds in the IL phase and to determine the experimental conditions to obtain an optimal extraction.

### V-3. Thermodynamic correlation

The liquid-liquid equilibrium data of the investigated ternary systems {phenolic compounds + water + IL} were correlated using the NonRandom Two-Liquid equation (NRTL) [33] and the UNIVersal QUAsi-Chemical (UNIQUAC) theory [34]. For NRTL model, the value of the non-randomness parameter  $\alpha$  was set to 0.3 according to the literature [35]. For UNIQUAC model, the relative volume and surface area of the pure component I,  $r_i$  and  $q_i$ , were calculated using the same method as in [36].

Two parameters per binary  $\Delta g_{ji}$  or  $\Delta u_{ji}$  must be fitted for both thermodynamic model. These binary interaction parameters were obtained by minimizing the following objective function:

$$F_{obj.} = \sum_{k=1}^N \sum_{i=1}^3 \left\{ \left( x_{i,k}^{I,exp} - x_{i,k}^{I,calc} \right)^2 + \left( x_{i,k}^{II,exp} - x_{i,k}^{II,calc} \right)^2 \right\} \quad (1)$$

Where  $N$  is the number of tie lines in the data set,  $x_{i,k}^{I,exp}$ ,  $x_{i,k}^{I,calc}$  are the experimental and calculated mole fractions of the aqueous phase and  $x_{i,k}^{II,exp}$ ,  $x_{i,k}^{II,calc}$  are the experimental and calculated mole fractions of the IL phase.

The rmsd values, which provide a measure of the accuracy of the correlations, were calculated according to the following equation:

$$rmsd = \left( \frac{\sum_{k=1}^N \sum_{i=1}^3 \left\{ \left( x_{i,k}^{I,exp} - x_{i,k}^{I,calc} \right)^2 + \left( x_{i,k}^{II,exp} - x_{i,k}^{II,calc} \right)^2 \right\}}{6N} \right)^{\frac{1}{2}} \quad (2)$$

## V-4. Results and discussion

### V-4.1. Ternary mixtures {phenolic compounds + water + IL}

The liquid-liquid equilibrium (LLE) and solid-liquid equilibrium (SLE) compositions for the ternary systems {[choline][NTf<sub>2</sub>] (1) + phenol (2) + water (3)}, {[choline][NTf<sub>2</sub>] (1) + guaiacol (2) + water (3)}, {[choline][NTf<sub>2</sub>] (1) + syringol (2) + water (3)}, {[choline][NTf<sub>2</sub>] (1) + pyrocatechol (2) + water (3)} at 298.15K under atmospheric pressure are listed in Tables V-2 and V-3 and the corresponding triangular phase diagrams are presented in Figure V-1.

The consistency of the LLE experimental tie-line data was determined through the Othmer–Tobias equation given by:

$$\ln \left( \frac{1-x_3^I}{x_3^I} \right) = a_1 + b_1 \ln \left( \frac{1-x_1^{II}}{x_1^{II}} \right) \quad (3)$$

Where  $a_1$  and  $b_1$  are the Othmer–Tobias parameters and  $x_3^I$ ,  $x_1^{II}$  are the molar fraction of water in aqueous rich phase and the molar fraction of [choline][NTf<sub>2</sub>] in IL rich phase, respectively. Results presented in Table S3 (Appendix IV) indicate a good consistency for our LLE ( $R^2 > 0.98$ ).

Guaiacol and [choline][NTf<sub>2</sub>] are completely miscible at 298.15K unlike {guaiacol + water} or {water + [choline][NTf<sub>2</sub>]} binary mixtures. Binary mixture {water + [choline][NTf<sub>2</sub>]} is partially miscible at 298 K. Liquid-liquid equilibria data of {water + [choline][NTf<sub>2</sub>]} found in this work is in good agreement with those published by Nockemann et al. [31]. The

{[choline][NTf<sub>2</sub>] (1) + guaiacol (2) + water (3)} presents only one phase envelop with no plait point (Figure V-1b). This system exhibits a type-2 LLE behavior according to the Treybal classification [37].

**Table V-2:** Experimental LLE data of the tie-lines in mole fractions, solute distribution ratio  $\beta$  and selectivity  $S$  for the ternary system {[choline][NTf<sub>2</sub>] (1) – phenolic compound (2) – water (3)} at 298.15K and 0.1 MPa.<sup>a</sup>

Aqueous-rich layer			[Choline][NTf <sub>2</sub> ]-rich layer			$\beta$	$S$
$x_1^I$	$x_2^I$	$x_3^I$	$x_1^{II}$	$x_2^{II}$	$x_3^{II}$		
<i>{[choline][NTf<sub>2</sub>] (1) – phenol (2) - water (3)}</i>							
0.006	0	0.994	0.29	0	0.71		
0.008	0.004	0.988	0.281	0.094	0.625	23.50	32.7
0.005	0.008	0.987	0.17	0.209	0.621	26.13	41.3
0.002	0.012	0.986	0.095	0.292	0.612	24.33	38.7
0.001	0.0135	0.9855	0.072	0.299	0.629	22.15	35.7
0.001	0.0138	0.9852	0.06	0.309	0.631	22.39	35.1
0	0.016	0.984	0.026	0.316	0.658	19.75	30.8
0.0005	0.017	0.9825	0.011	0.316	0.673	18.59	27.8
0	0.017	0.983	0	0.328	0.672	19.29	28.2
<i>{[choline][NTf<sub>2</sub>] (1) – guaiacol (2) - water (3)}</i>							
0.006	0	0.994	0.29	0	0.71		
0.006	0.0005	0.9935	0.292	0.083	0.625	166.00	232.4
0.0045	0.0025	0.993	0.201	0.295	0.505	118.00	187.6
0.004	0.0034	0.9926	0.173	0.383	0.445	112.65	221.5
0.002	0.006	0.992	0.103	0.522	0.375	87.00	194.1
0.002	0.007	0.991	0.07	0.592	0.337	84.57	223.7
0.001	0.011	0.988	0.02	0.655	0.314	59.55	175.1
0	0.003	0.997	0	0.752	0.248		
<i>{[choline][NTf<sub>2</sub>] (1) – syringol (2) - water (3)}</i>							
0.006	0	0.994	0.29	0	0.71		
0.006	0.0005	0.993	0.278	0.109	0.613	218.00	304.9
0.005	0.001	0.9932	0.236	0.191	0.573	191.00	309.4
0.004	0.002	0.9937	0.151	0.294	0.555	147.00	254.8
0.004	0.003	0.9939	0.121	0.32	0.559	106.67	191.0
0.003	0.003	0.994	0.109	0.337	0.554	112.33	199.7
0.001	0.004	0.995	0.027	0.368	0.605	92.00	165.1
0	0.003	0.997	0	1	0		

<i>{[choline][NTf<sub>2</sub>] (1) - pyrocatechol (2) - water (3)}</i>							
0.006	0	0.994	0.29	0	0.71		
0.006	0.004	0.99	0.248	0.048	0.704	12.00	16.8
0.007	0.006	0.988	0.236	0.06	0.704	10.00	14.1
0.008	0.008	0.986	0.226	0.073	0.7	9.13	12.8
0.009	0.01	0.983	0.21	0.087	0.703	8.70	12.3
0.011	0.017	0.978	0.178	0.108	0.714	6.35	8.9
0.015	0.03	0.955	0.122	0.127	0.751	4.23	5.8
0.024	0.042	0.890	0.071	0.087	0.842	2.07	2.6

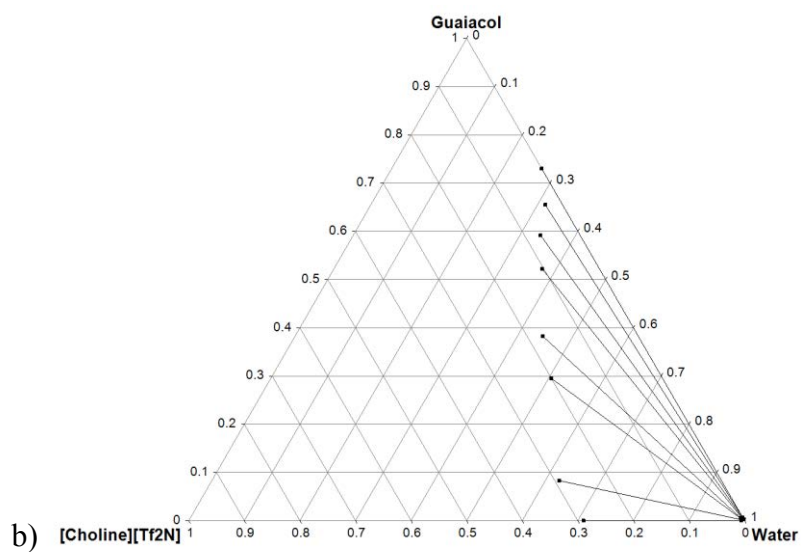
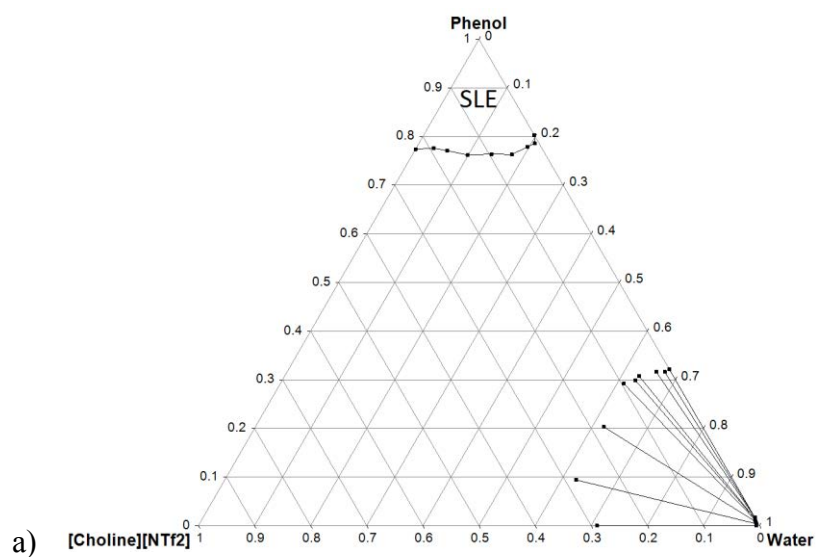
a:  $u(T) = 0.1K$ ,  $u(x) < 0.005$

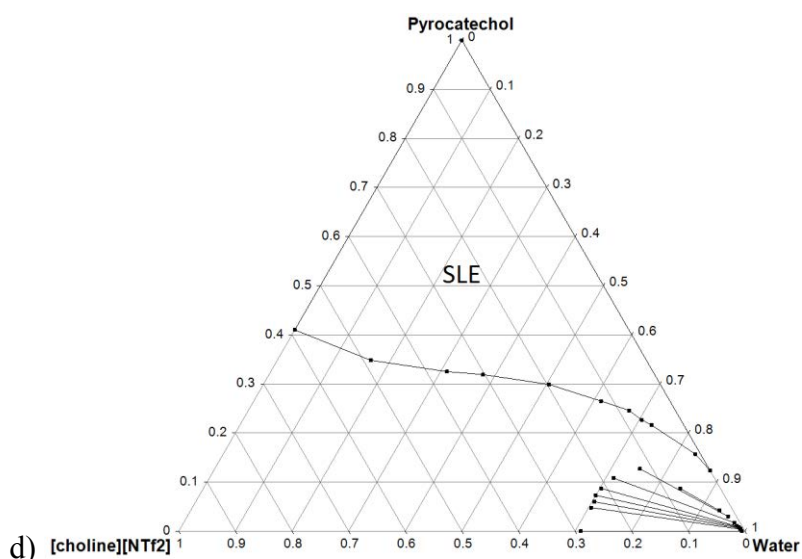
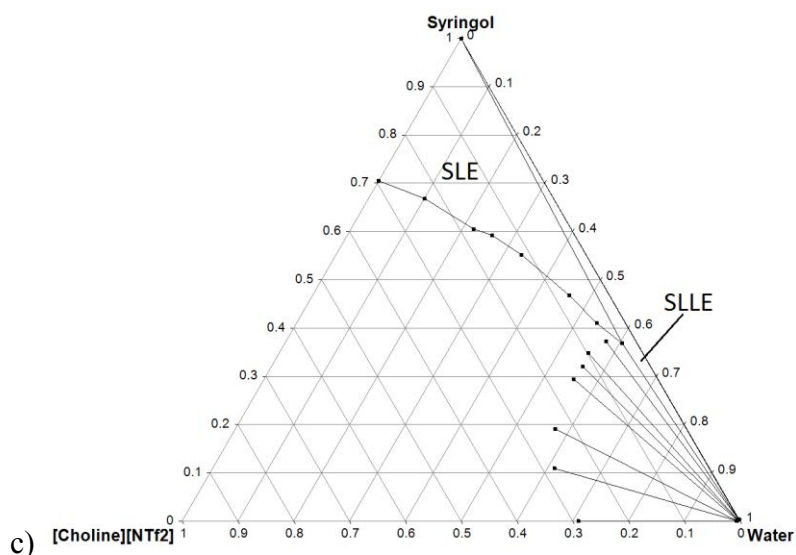
**Table V-3:** Experimental SLE data of the tie-lines in mole fractions in the {[choline][NTf<sub>2</sub>] (1) –phenol (2) - water (3)}, {[choline][NTf<sub>2</sub>] (1) –syringol (2) - water (3)} and {[choline][NTf<sub>2</sub>] (1) –pyrocatechol (2) - water (3)} systems at 298 K and 0.1 MPa.<sup>a</sup>

Liquid layer			Equilibrium solid phase
$x_1^I$	$x_2^I$	$x_3^I$	
<i>{[choline][NTf<sub>2</sub>] (1) – phenol (2) - water (3)}</i>			
0.226	0.774	0.000	Phenol
0.194	0.776	0.031	Phenol
0.170	0.771	0.058	Phenol
0.140	0.762	0.099	Phenol
0.096	0.764	0.140	Phenol
0.060	0.763	0.177	Phenol
0.024	0.779	0.197	Phenol
0.007	0.786	0.206	Phenol
0.000	0.803	0.197	Phenol
<i>{[choline][NTf<sub>2</sub>] (1) – syringol (2) - water (3)}</i>			
0.295	0.705	0.000	Syringol
0.231	0.668	0.101	Syringol
0.175	0.605	0.220	Syringol
0.149	0.592	0.260	Syringol
0.115	0.552	0.332	Syringol
0.071	0.467	0.461	Syringol
0.052	0.410	0.538	Syringol
<i>{[choline][NTf<sub>2</sub>] (1) – pyrocatechol (2) - water (3)}</i>			
0.590	0.410	0.000	Pyrocatechol
0.487	0.348	0.165	Pyrocatechol
0.364	0.325	0.311	Pyrocatechol
0.303	0.319	0.378	Pyrocatechol
0.197	0.299	0.504	Pyrocatechol
0.121	0.265	0.613	Pyrocatechol
0.082	0.246	0.672	Pyrocatechol
0.069	0.227	0.704	Pyrocatechol
0.057	0.216	0.727	Pyrocatechol
0.010	0.157	0.834	Pyrocatechol
0.000	0.123	0.877	Pyrocatechol

a:  $u(T) = 0.1\text{K}$ ,  $u(x) < 0.005$

**Figure V-1:** Plot of the experimental data for the molar composition tie lines of the ternary system: a) {[choline][NTf<sub>2</sub>] (1) – phenol (2) - water (3)}, b) {[choline][NTf<sub>2</sub>] (1) – guaiacol (2) - water (3)}, c) {[choline][NTf<sub>2</sub>] (1) – syringol (2) - water (3)}, d) {[choline][NTf<sub>2</sub>] (1) – pyrocatechol (2) - water (3)} at 298 K and 0.1 MPa.





Binary {phenol + [choline][NTf<sub>2</sub>]}, {syringol + [choline][NTf<sub>2</sub>]}, and {pyrocatechol + [choline][NTf<sub>2</sub>]}, are partially miscible since the corresponding ternary mixtures present a solid-liquid equilibrium (Figures V-1a, V-1c and V-1d respectively). The associated ternary systems exhibit type-4 behavior.

The {[choline][NTf<sub>2</sub>] (1) + phenol (2) + water (3)} system exhibits two different areas: one with liquid-liquid equilibria with no plait point at low fraction in phenol and another one with solid-liquid equilibria at high fraction in phenol (Figure V-1a). The {[choline][NTf<sub>2</sub>] (1) + pyrocatechol (2) + water (3)} system also presents two areas with liquid-liquid and liquid-solid equilibria, except that these phase envelopes present a plait point (Figure V-1d). The

{[choline][NTf<sub>2</sub>] (1) + syringol (2) + water (3)} system also presents an area with solid-liquid-liquid equilibria at high molar fraction of [choline][NTf<sub>2</sub>] and an area with liquid-liquid equilibria at low molar fraction (Figure V-1c). Yet, these areas are linked *via* a three-phase area presenting a solid-liquid-liquid equilibrium, with an aqueous-rich layer, a liquid-ionic rich layer and syringol in its solid form. At very low fraction of ionic liquid, a gel was observed but its composition was not determined.

Solute distribution ratios  $\beta$  and selectivities  $S$  were calculated for each system. These parameters were used to evaluate the possible use of the [choline][NTf<sub>2</sub>] as a solvent for the extraction of phenolic compounds from aqueous solutions. These parameters are defined by the following expressions:

$$\beta = \frac{x_2^{II}}{x_2^I} \quad (4)$$

$$S = \frac{x_2^{II} x_3^I}{x_2^I x_3^{II}} \quad (5)$$

where:  $x$  is the mole fraction. Superscripts I and II refer to the aqueous rich phase and the IL-rich phase respectively. Subscripts 2 and 3 refer to the phenolic compounds (phenol, guaiacol, syringol or pyrocatechol) and water respectively.

The distribution ratio ( $\beta$ ) and the selectivity ( $S$ ) values obtained for each ternary system are displayed in Table V-2. Both parameters are higher than 1 for each systems, showing the suitability of the [Choline][NTf<sub>2</sub>] to extract phenolic compounds from aqueous solution.

For the ternary mixtures containing guaiacol or syringol, the selectivity  $S$  and the solute distribution ratio values  $\beta$  are higher than 50. In the case of phenol, these values are about 40 and 20 for selectivity and solute distribution ratio, respectively. The values are even lower (inferior to 20) in the case of pyrocatechol. These differences is explained by the solubility of the phenolic compounds in water increasing in the following order: syringol and guaiacol < phenol < pyrocatechol. Therefore, the order of the extraction applicability in [choline][NTf<sub>2</sub>] is syringol > guaiacol > phenol > pyrocatechol.

The selectivity values for the phenol, guaiacol and pyrocatechol system were compared to those found in literature for organic solvents (1-octanol [28], cyclohexanone [28], isobutylacetate [28], 2-ethyl-1-hexanol [28], 2-butanone [16], 2-propanol [16], MTBK [19], MBK [17], 2-methoxy-2-methylpropane [12], toluene [24], m-xylene [24], 2-pentanone [20], MIPK [21]). No data were found for the syringol system. The selectivity ( $S$ ) and solute distribution ratio

were plotted as a function of the phenol molar fraction in aqueous solution ( $x_2^1$ ) from literature data (Figures S3 and S4 in Appendix IV). The selectivity values of the system with [choline][NTf<sub>2</sub>] are low compared to the classical solvents (*i.e.* 2-ethyl-1-hexanol 3-12x, isobutylacetate 5-20x) but this IL is as efficient as 2-propanol or toluene. Moreover, its selectivity and the solute distribution values are almost not affected by the concentration of phenol in the solution.

The selectivity and solute distribution ratio for the systems {water + guaiacol + trihexyltetradecylphosphonium dicyanamide [P666.14[N(CN)<sub>2</sub>]} and {water + guaiacol + ethyl acetate} are reported in the literature [26], as well as for the {water – pyrocatechol – n-butyl acetate} system [27]. Performances of [choline][NTf<sub>2</sub>] are compared to others solvents (Figures S5 and S6 in Appendix IV). For the systems containing guaiacol, the solute distribution ratio of the [choline][NTf<sub>2</sub>] system is in the same range of value than the ethyl acetate one [26], and also than the [P666.14[N(CN)<sub>2</sub>] [26] ionic liquid from  $x_2^1 = 0.003$ . At infinite dilution, selectivity value of the [choline][NTf<sub>2</sub>] is lower than the value obtained with ethyl acetate or [P666.14[N(CN)<sub>2</sub>]. For the systems containing pyrocatechol, the selectivity and solute distribution ratio of the [choline][NTf<sub>2</sub>] vary less with the molar composition of pyrocatechol in the aqueous phase, compared to the n-butyl acetate system [27]. [choline][NTf<sub>2</sub>] presents a lower selectivity and solute distribution ratio values than those obtained with n-butyl acetate at infinite dilution. Starting from  $x_2^1 = 0.02$ , both systems present the same efficiency.

#### V-4.2. Extraction of phenolic compounds from aqueous solution

The results of the extraction experiments are plotted in Figures S7, S8 (Appendix IV) and V-2.

The extraction rate is defined as below:

$$\% \text{Extraction: } \frac{\text{weight of phenolic compound in the ionic liquid phase}}{\text{weight of phenolic compound in the synthetic aqueous solution}} \quad (6)$$

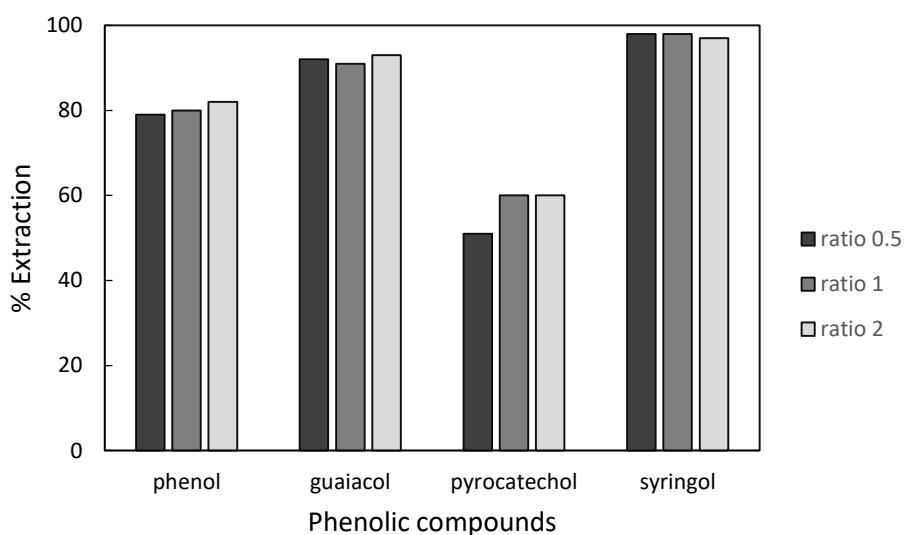
The influence of the extraction time on the extraction efficiency is represented in Figure S7 (Appendix IV). The extraction rate strongly increases during the five first minutes and within 10 minutes, a maximum extraction rate is observed for each phenolic compound. The extraction rate is increasing as follow: pyrocatechol < phenol < guaiacol < syringol, in accordance with the higher aqueous solubility of pyrocatechol and phenol than guaiacol or syringol. Therefore, phenol and pyrocatechol are more difficult to extract in IL. Moreover, these results are in

agreement with those obtained from the study of the values of coefficient distribution factor  $\beta$  and the selectivity  $S$  of the ternary diagrams.

The influence of the temperature was studied between 298.15 and 318.15K using an ionic liquid/water weight ratio of 1:1 during 180 minutes. The temperature was not studied over 318.15K due to the increasing miscibility between the two phases until an upper critical solution temperature at 345.15K [31]. In the range studied, the temperature effect is negligible on the extraction efficiency (Figure S8 in Appendix IV).

The influence of the weight ratio of ionic liquid/water on the extraction (%) was studied at three different ratios: 0.5, 1 and 2 (Figure V-2). An increase of the ratio from 0.5 to 1 has an influence on the extraction of pyrocatechol which goes from 50% to 60%. However, beyond a ratio of 1, there is no improvement on the extraction of any compounds. Others phenolic compounds are not affected by this decrease.

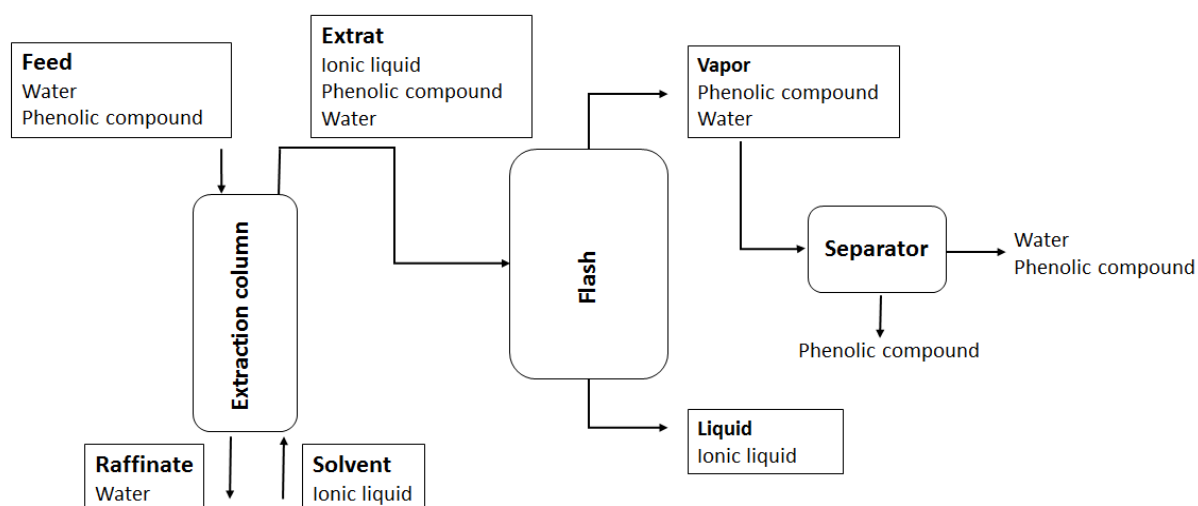
**Figure V-2:** Influence of the mass ratio of ionic liquid/water on the efficiency of the extraction process.



### V-4.3. Process sizing

NRTL model (Table S4 in Appendix IV) was used to evaluate the efficiency of [choline][NTf<sub>2</sub>] as an extractive media for the extraction of a phenolic compound from aqueous solutions and for further process sizing. A possible LLE process is depicted in Figure V-3. The feed and solvent flows are in contact in a liquid-liquid extraction column. The extract stream containing the phenolic compound and amounts of water in the ionic liquid phase is then sent to an evaporator. Because of the low volatility of IL, no further distillation is required. After evaporation of water and recovery of the phenolic compound, the ionic liquid could be reused as extraction solvent, which constitutes its main advantage as compared to other organic solvents commonly used in the literature.

**Figure V-3:** Process design for the extraction of phenolic compound from aqueous solution



To design the extraction column, the resulting extract and raffinate flows were assumed approximately equal to the solvent and feed flows respectively. The column was operated as counter-flow at 298.15K and the extraction was considered effective at a 99.995% rate. We also assumed that the composition in the ionic liquid phase is proportional to the composition in the aqueous phase at a factor  $D$  called equilibrium coefficient.

The feed was constituted of an aqueous solution containing the phenolic compound at a low mass fraction. This high dilution behavior is representative of the percent found in bio-oils.

The solvent used was considered to be a pure ionic liquid [choline][NTf<sub>2</sub>]. The minimum L/F ratio was determined using the following expression:

$$\frac{L}{F} \min = \frac{w_f - w_r}{w_{emax} - w_l} \quad (7)$$

Where  $w_{emax} = D * w_f$

L and F are the mass flows of solvent and feed respectively, w correspond to the mass fraction. The subscripts f, r, emax and l correspond to the feed, raffinate, maximum in extract and solvent phases. D is the mass equilibrium coefficient. For calculations, a good starting value for initialization is generally  $\frac{L}{F} = 2 \frac{L}{F} \min$ .

Under these conditions, the number of stages n required can be determined by:

$$\frac{w_r}{w_f} = \frac{E-1}{E^{n+1}-1} \quad (8)$$

Where E is the extraction factor, calculated by:

$$E = D \frac{L}{F} \quad (9)$$

The composition of the extract streams following these extraction conditions was determined using the NRTL parameters. The calculation of the energy needed for the evaporation required some NRTL parameters for liquid-vapor equilibrium. Nevertheless, no information is found in the literature concerning liquid-vapor equilibrium between water and [choline][NTf<sub>2</sub>] nor between phenol and [choline][Ntf<sub>2</sub>]. Therefore, it is supposed that the remaining liquid phase only contains pure ionic liquid. The energy needed for the evaporation was calculated taking into account the heating of the mixture to the boiling point of the phenolic compound, the evaporation of the phenolic compound and the co-extracted water.

The extraction parameters from this process are listed in Table V-4 for phenolic compounds at different mass ratios (0.5% and 1.5%). The increase of the mass fraction from 0.5 to 1.5% does not influence a lot the L/F<sub>min</sub> solvent ratio. Moreover, this ratio is very low for phenol, guaiacol and syringol showing that the extraction column required small amount of [choline][NTf<sub>2</sub>]. Pyrocatechol is the only studied compounds which presents difficulties with high S/F ratio. Whatever the compound, the number of theoretical stages calculated according to equation 8 was in the same range of value. Moreover, an increase in the mass fraction of the phenolic compound in the feed leads to an increase of the number of theoretical stages for the same L/F ratio (Table V-4). These results are in good agreements with those obtained experimentally.

**Table V-4:** Extraction parameters.

Compounds	D	$w_f$	$\frac{L}{F}$ min	$\frac{L}{F}$	n (decimals)	n (integer)
Phenol	7	0.005	0.14	0.3	5.34	6
		0.015	0.14	0.3	6.83	7
Guaiacol	14	0.005	0.07	0.3	3.02	4
		0.015	0.07	0.3	3.79	4
Syringol	22	0.005	0.05	0.1	5.08	6
		0.015	0.05	0.1	6.48	7
Pyrocatechol	1.6	0.005	0.62	1.3	5.41	6
		0.015	0.62	1.3	6.91	7

The composition of the extraction steams and the energy required for evaporation are listed in Table 5. Thermodynamic data of pure compounds required for the calculation are presented in Table S7 (Appendix IV). An increase of the mass fraction of phenolic compound (0.5% to 1.5%) in the feed increase the mass fraction of phenolic compound in the extract (1.3% to 4% respectively) and reduce the energy required for the evaporation (*i.e.* from 30.43 to 10.75 MJ/kg for phenol).

**Table V-5:** Composition in extract steam and energy required for single step evaporation.

Compounds	mass fraction in feed		mass fraction in extract		energy MJ/kg of PC
	$w_{PC}$	$w_{PC}$	$w_{water}$	$w_{IL}$	
Phenol	0.005	0.013	0.086	0.900	30.43
	0.015	0.040	0.088	0.871	10.75
Guaiacol	0.005	0.054	0.088	0.858	8.41
	0.015	0.143	0.079	0.778	3.41
Syringol	0.005	0.013	0.096	0.891	43.55
	0.015	0.085	0.086	0.830	6.57
Pyrocatechol	0.005	0.004	0.092	0.904	134.98
	0.015	0.011	0.095	0.894	45.64

Energy in MJ/kg of phenolic compound (PC)

As expected, pyrocatechol is the compound the least easily extractable with a very low mass fraction recovered in the extract whatever the feed composition. Therefore, the extraction process for pyrocatechol requires much more energy (46.64 MJ/kg) than for phenol, guaiacol and syringol (10.75, 3.41 and 6.57MJ/kg, respectively). Compared to an ethyl acetate based

process [26] and for the same feed, our design for the extraction of guaiacol from water using IL required less energy and less equipment.

The vapor steam coming from the distillation is composed of water and phenolic compound. In some cases, the fraction of phenolic compound is above its limit of aqueous solubility when this steam is cooled to 298 K. Two phases, one aqueous and one phenolic, should be observed. This process is particularly interesting for the recovery of syringol. Indeed, syringol presents a solid-liquid equilibrium with water. Therefore, a simple filtration could allow the recovery of syringol with high purity. For phenol and guaiacol presenting a liquid-liquid equilibria, the elimination of water in the phenolic phase could be made with a drying molecule such as magnesium sulfate.

### V-5. Conclusion

Ternary diagrams of mixture containing {water, phenolic compound (phenol, guaiacol, syringol or pyrocatechol), [choline][NTf<sub>2</sub>]} were studied at 298.15K at atmospheric pressure. [choline][NTf<sub>2</sub>] is a suitable solvent for the extraction of phenolic compounds from aqueous solution. Such process required less equipment (one extraction column and one flash) and less energy compared to other organic based ones. After distillation, the vapor stream can allow the recovery of phenolic compounds in few steps. Phenol, guaiacol and syringol are the easily extractable compounds.

Although the [choline][NTf<sub>2</sub>] ionic liquid presents a lower selectivity and solute distribution ratio than other organic solvent in the system {water + phenolic compound + solvent}, others properties must be taken in account for the extraction of phenolic compounds. For example, the very low vapor pressure of ionic liquids favours an easier recovery of the phenolic compounds. Besides, the low purity caused by solvent residue in the compounds is a real issue in the food, flavor, fragrance and pharmaceutical industries.[38] Thus, the recovery of phenol from the ionic liquid layer could be easily made *via* distillation and [choline][NTf<sub>2</sub>] could be reusable.

*List of symbols*

$a_1, b_1$	Othmer-Tobias constant parameter
$C_p$	Heat capacity at constant pressure
$D$	Mass equilibrium coefficient
$E$	Extraction factor
$g$	Interaction energy parameter (NRTL)
$F$	Mass flows of feed
$\Delta H_{\text{vap}}$	Latent heat of vaporization
$L$	Mass flows of solvent
$n$	Number of stages (decimal)
$N$	Number of tie-lines
$q_i$	Surface area factor
$R$	Ideal gas constant
$r_i$	Volume area factor
rmsd	root mean square deviation
$S$	Selectivity
$T$	Temperature
$T_b$	Boiling temperature
$u$	Interaction energy parameter (UNIQUAC)
$V_m$	Molar volume
$w_i$	Mass fraction
$x_i$	Mole fraction
$Z$	Coordination number

*Greek letters*

$\alpha$  non-randomness parameter

$\beta$  solute distribution ratio

$\gamma_i$  activity coefficient

## References

- [1] R.M. Gallivan, P.K. Matschei, Fractionation of oil obtained by pyrolysis of lignocellulosic materials to recover a phenolic fraction for use in making phenol-formaldehyde resins, n.d. <http://www.google.com/patents/US4209647>.
- [2] M.D. Guillén, M.L. Ibargoitia, New Components with Potential Antioxidant and Organoleptic Properties, Detected for the First Time in Liquid Smoke Flavoring Preparations, *J. Agric. Food Chem.* 46 (1998) 1276–1285. doi:10.1021/jf970952x.
- [3] F. Helmut, V. Heinz-Werner, H. Toshikazu, P. Wilfrried, Phenol derivatives, *Ullmann's Encycl. Ind. Chem. VCH Ger.* 19 (1985) 299–357.
- [4] F. Ikegami, T. Sekine, Y. Fujii, [Anti-dermatophyte activity of phenolic compounds in “mokusaku-eki”], *Yakugaku Zasshi.* 118 (1998) 27–30.
- [5] J.A. Maga, I. Katz, Simple phenol and phenolic compounds in food flavor, *C R C Crit. Rev. Food Sci. Nutr.* 10 (1978) 323–372. doi:10.1080/10408397809527255.
- [6] A.V. Bridgwater, D. Meier, D. Radlein, An overview of fast pyrolysis of biomass, *Org. Geochem.* 30 (1999) 1479–1493. doi:10.1016/S0146-6380(99)00120-5.
- [7] R.K. Sharma, N.N. Bakhshi, Catalytic upgrading of biomass-derived oils to transportation fuels and chemicals, *Can. J. Chem. Eng.* 69 (1991) 1071–1081. doi:10.1002/cjce.5450690505.
- [8] C. Amen-Chen, H. Pakdel, C. Roy, Production of monomeric phenols by thermochemical conversion of biomass: a review, *Bioresour. Technol.* 79 (2001) 277–299. doi:10.1016/S0960-8524(00)00180-2.
- [9] C. Amen-Chen, H. Pakdel, C. Roy, Separation of phenols from Eucalyptus wood tar, *Biomass Bioenergy.* 13 (1997) 25–37. doi:10.1016/S0961-9534(97)00021-4.
- [10] K.S. Narasimhan, C.C. Reddy, K.S. Chari, Solubility and Equilibrium Data of Phenol-Water-Isoamyl Acetate and Phenol-Water-Methyl Isobutyl Ketone Systems at 30° C., *J. Chem. Eng. Data.* 7 (1962) 457–460. doi:10.1021/je60015a003.
- [11] K.S. Narasimhan, C.C. Reddy, K.S. Chari, Solubility and Equilibrium Data of Phenol-Water-n-Butyl Acetate System at 30° C., *J. Chem. Eng. Data.* 7 (1962) 340–343. doi:10.1021/je60014a005.
- [12] Y. Lei, Y. Chen, X. Li, Y. Qian, S. Yang, C. Yang, Liquid–Liquid Equilibria for the Ternary System 2-Methoxy-2-methylpropane + Phenol + Water, *J. Chem. Eng. Data.* 58 (2013) 1874–1878. doi:10.1021/je400295z.
- [13] I.-C. Hwang, S.-J. Park, Liquid–liquid equilibria of ternary mixtures of dimethyl carbonate, diphenyl carbonate, phenol and water at 358.15K, *Fluid Phase Equilibria.* 301 (2011) 18–21. doi:10.1016/j.fluid.2010.11.012.
- [14] S.-J. Park, I.-C. Hwang, S.-H. Shin, Liquid–Liquid Equilibria for Ternary Mixtures of Methylphenyl Carbonate, Dimethyl Carbonate, Diphenyl Carbonate, Anisole, Methanol, Phenol, and Water at Several Temperatures, *J. Chem. Eng. Data.* 59 (2014) 323–328. doi:10.1021/je400776b.
- [15] C. Yang, Y. Qian, Y. Jiang, L. Zhang, Liquid–liquid equilibria for the quaternary system methyl isobutyl ketone–water–phenol–hydroquinone, *Fluid Phase Equilibria.* 258 (2007) 73–77. doi:10.1016/j.fluid.2007.05.026.

- [16] M. Rogošić, M. Bakula, M. Župan, Liquid-liquid Equilibria in the Ternary Systems H<sub>2</sub>O– Phenol – 2-Butanone and H<sub>2</sub>O– Phenol – 2-Propanol, *Chem. Biochem. Eng. Q.* 26 (2012) 155–162.
- [17] Y. Chen, Z. Wang, L. Li, Liquid–Liquid Equilibria for Ternary Systems: Methyl Butyl Ketone + Phenol + Water and Methyl Butyl Ketone + Hydroquinone + Water at 298.15 K and 323.15 K, *J. Chem. Eng. Data.* 59 (2014) 2750–2755. doi:10.1021/je500532v.
- [18] H. Wang, L. Li, R. Lv, Y. Chen, Measurement and Correlation of Liquid–Liquid Equilibria for the Ternary Methyl Isobutyl Ketone + Phenol + Water System at (333.15, 343.15 and 353.15) K under Atmospheric Pressure, *J. Solut. Chem.* 45 (2016) 875–884. doi:10.1007/s10953-016-0472-z.
- [19] D. Liu, L. Luo, L. Li, Y. Chen, Liquid–Liquid Equilibria for the Methyl Tert-Butyl Ketone + Phenol + Water Ternary System at 298.15, 313.15 and 323.15 K, *J. Solut. Chem.* 44 (2015) 1891–1899. doi:10.1007/s10953-015-0382-5.
- [20] R. Lv, L. Li, H. Wang, Y. Chen, Phase Equilibrium for Phenol Extraction from Aqueous Solution with 2-Pentanone at Different Temperatures, *J. Solut. Chem.* 45 (2016) 1414–1424. doi:10.1007/s10953-016-0517-3.
- [21] R. Lv, L. Li, H. Wang, Y. Chen, Experimental Determination and Correlation of Liquid–Liquid Equilibria for Methyl Isopropyl Ketone + Phenol + Water Mixtures at 298.15, 313.15, and 323.15 K, *J. Chem. Eng. Data.* 61 (2016) 2221–2225. doi:10.1021/acs.jced.5b00895.
- [22] L.H. de Oliveira, M. Aznar, (Liquid+liquid) equilibrium of {water+phenol+(1-butanol, or 2-butanol, or tert-butanol)} systems, *J. Chem. Thermodyn.* 42 (2010) 1379–1385. doi:10.1016/j.jct.2010.06.007.
- [23] A. Martin, M. Klauck, K. Taubert, A. Precht, R. Meinhardt, J. Schmelzer, Liquid–Liquid Equilibria in Ternary Systems of Aromatic Hydrocarbons (Toluene or Ethylbenzene) + Phenols + Water, *J. Chem. Eng. Data.* 56 (2011) 733–740. doi:10.1021/je100069q.
- [24] M. Mohsen-Nia, I. Paikar, Ternary and Quaternary Liquid + Liquid Equilibria for Systems of (Water + Toluene + m -Xylene + Phenol), *J. Chem. Eng. Data.* 52 (2007) 180–183. doi:10.1021/je060345i.
- [25] A. Martin, M. Klauck, A. Grenner, R. Meinhardt, D. Martin, J. Schmelzer, Liquid–Liquid(–Liquid) Equilibria in Ternary Systems of Aliphatic Hydrocarbons (Heptane or Octane) + Phenols + Water, *J. Chem. Eng. Data.* 56 (2011) 741–749. doi:10.1021/je1007923.
- [26] X. Li, S.R.A. Kersten, B. Schuur, Extraction of Guaiacol from Model Pyrolytic Sugar Stream with Ionic Liquids, *Ind. Eng. Chem. Res.* 55 (2016) 4703–4710. doi:10.1021/acs.iecr.6b00100.
- [27] B. Wang, M. Rong, P. Wang, S. Chen, Liquid–Liquid Equilibria for the Ternary System n -Butyl Acetate + Pyrocatechol + Water at Different Temperatures at 101.3 kPa, *J. Chem. Eng. Data.* 61 (2016) 3184–3189. doi:10.1021/acs.jced.6b00280.
- [28] H. Ghanadzadeh Gilani, A. Ghanadzadeh Gilani, M. Sangashekan, Tie-line data for the aqueous solutions of phenol with organic solvents at T=298.2K, *J. Chem. Thermodyn.* 58 (2013) 142–148. doi:10.1016/j.jct.2012.10.028.

- [29] J.R. Alvarez Gonzalez, E.A. Macedo, M.E. Soares, A.G. Medina, Liquid-liquid equilibria for ternary systems of water-phenol and solvents: data and representation with models, *Fluid Phase Equilibria*. 26 (1986) 289–302. doi:10.1016/0378-3812(86)80024-3.
- [30] S.R. Pilli, T. Banerjee, K. Mohanty, Performance of different ionic liquids to remove phenol from aqueous solutions using supported liquid membrane, *Desalination Water Treat.* 54 (2015) 3062–3072. doi:10.1080/19443994.2014.907750.
- [31] P. Nockemann, K. Binnemans, B. Thijs, T.N. Parac-Vogt, K. Merz, A.-V. Mudring, P.C. Menon, R.N. Rajesh, G. Cordoyiannis, J. Thoen, J. Leys, C. Glorieux, Temperature-Driven Mixing-Demixing Behavior of Binary Mixtures of the Ionic Liquid Choline Bis(trifluoromethylsulfonyl)imide and Water, *J. Phys. Chem. B*. 113 (2009) 1429–1437. doi:10.1021/jp808993t.
- [32] D.J. Couling, R.J. Bernot, K.M. Docherty, J.K. Dixon, E.J. Maginn, Assessing the factors responsible for ionic liquid toxicity to aquatic organisms via quantitative structure–property relationship modeling, *Green Chem.* 8 (2006) 82–90. doi:10.1039/B511333D.
- [33] H. Renon, J.M. Prausnitz, Local compositions in thermodynamic excess functions for liquid mixtures, *AIChE J.* 14 (1968) 135–144. doi:10.1002/aic.690140124.
- [34] D.S. Abrams, J.M. Prausnitz, Statistical thermodynamics of liquid mixtures: A new expression for the excess Gibbs energy of partly or completely miscible systems, *AIChE J.* 21 (1975) 116–128. doi:10.1002/aic.690210115.
- [35] L.D. Simoni, A. Chapeaux, J.F. Brennecke, M.A. Stadtherr, Asymmetric Framework for Predicting Liquid–Liquid Equilibrium of Ionic Liquid–Mixed-Solvent Systems. 2. Prediction of Ternary Systems, *Ind. Eng. Chem. Res.* 48 (2009) 7257–7265. doi:10.1021/ie9004628.
- [36] U. Domańska, M. Laskowska, A. Pobudkowska, Phase Equilibria Study of the Binary Systems (1-Butyl-3-methylimidazolium Thiocyanate Ionic Liquid + Organic Solvent or Water) ‡, *J. Phys. Chem. B*. 113 (2009) 6397–6404. doi:10.1021/jp900990s.
- [37] R.E. Treybal, *Liquid Extraction*, McGraw Hill Book Company Inc., 1951. <http://archive.org/details/liquidextraction030155mbp> (accessed October 6, 2016).
- [38] R.N. Patel, S. Bandyopadhyay, A. Ganesh, Extraction of cardanol and phenol from bio-oils obtained through vacuum pyrolysis of biomass using supercritical fluid extraction, *Energy*. 36 (2011) 1535–1542. doi:10.1016/j.energy.2011.01.009.
- [39] H. Wang, Z. Wang, L. Li, Y. Chen, Ternary and Quaternary Liquid–Liquid Equilibria for Systems of Methyl Butyl Ketone + Water + Hydroquinone + Phenol at 313.2 K and Atmospheric Pressure, *J. Chem. Eng. Data*. 61 (2016) 1540–1546. doi:10.1021/acs.jced.5b00918.

## Chapter VI: Separation of phenols from lignin pyrolysis oil using ionic liquid and comparison with ethyl acetate.

Laëtitia Cesari<sup>1</sup>, Fabrice Mutelet<sup>1</sup>, Laetitia Canabady-Rochelle<sup>1\*</sup>

1 : Université de Lorraine, Laboratoire Réactions et Génie des Procédés (LRGP, UMR CNRS-UL 7274), 1 rue Grandville, 54000 Nancy, France

Article à soumettre

### Résumé

Les résultats encourageants des chapitres précédents ont conduit à utiliser la [choline][NTf<sub>2</sub>] pour l'extraction des composés phénoliques sur des bio-huiles réelles. Les bio-huiles utilisées sont issues de la pyrolyse rapide de lignine. Les extractions des composés phénoliques sont effectuées en deux étapes. Une première extraction est effectuée à l'aide d'une solution aqueuse basique. Cinq lavages sont effectués sur la bio-huile avant de collecter les fractions. Une seconde extraction comprenant quatre lavages est ensuite effectuée avec de l'acétate d'éthyle (solvant organique classique) ou avec le liquide ionique (comme alternative verte). Des analyses effectuées par GC-FID et GC-MS permettent de quantifier l'efficacité de chacune des étapes d'extraction. Il est montré que le liquide ionique [choline][NTf<sub>2</sub>] est un excellent solvant pour la récupération des composés phénoliques en solution aqueuse. En effet, il permet d'extraire les composés phénoliques avec un taux d'extraction plus important et moins de lavages qu'avec l'acétate d'éthyle.

**Abstract**

Bio-oils rich in phenolic compounds were produced by lignin pyrolysis. The extraction of phenolic compounds from the crude bio-oils was performed in two steps. First, a 5-stages liquid-liquid extraction (LLE) was performed with a basic aqueous solution. Then, in a second step, a 4-stages LLE was carried out with either ethyl acetate – a commonly used organic solvent - or [Choline][NTf<sub>2</sub>] ionic liquid, as a green alternative. It was found that the extraction of the phenolic compounds with the basic aqueous solution in the first LLE needs improvement. The extraction rates show that [Choline][NTf<sub>2</sub>] is an excellent solvent for the recovery of phenolic compounds from aqueous solution as compared to the classical ethyl acetate organic solvent.

## VI-1. Introduction

Lignocellulosic biomass (*i.e.* wood, straw, etc.) is a natural widespread resource, which present a huge potential of valorisation for various industrial sectors, especially foods, cosmetic and pharmaceuticals without being in competition with agro-business. Many high added-value compounds can be extracted from lignocellulosic biomass and its derivatives, such as acids, alcohols, aldehydes, ketones esters, heterocyclic derivatives and phenolic compounds [1]. The acetyl groups of hemicelluloses provides acetic acid [2] while the lignin produces phenolic compounds of different size [3,4]. Most of these phenolic compounds present valuable properties such as antiallergenic, antimicrobial or antiviral effect [5], antioxidant properties [6–9], but also cardioprotective activities[10] or protective effects on hormone-dependent breast tumors [11]. Thus, phenolic compounds are valorized as raw materials or intermediates in the synthesis of pharmaceuticals [12–14], food flavours [15,16], food additives [16,17], fragrances [13,14,16], herbicides [18], and for the production of resins [19–21] or adhesives [20,22,23] as well.

Pyrolysis is a thermochemical conversion process, well investigated to date [24]. Biomass pyrolysis produces solid (char), liquid (the so-called bio-oil) and gas (*i.e.* CO<sub>2</sub>, CO, CH<sub>4</sub>, H<sub>2</sub>, etc). According to the pyrolysis conditions, two main pyrolysis processes can be defined. Flash pyrolysis is lead with moderate temperature (450-600°C), high heating rates (>1000°C) and low residence time of the biomass inside the pyrolysis furnace (<2 seconds). Inversely, the slow pyrolysis is carried out at low temperature and high residence time. According to the operating conditions used, the production of one or several phases will be optimized. While the slow pyrolysis favours the production of char [25], the flash pyrolysis provides high added-value compounds [26].

These last decades, the extraction of phenolic compounds from various natural resources rises more interest. Among various techniques described in the literature, phenolics were extracted using membrane [27], preparative chromatography [28–33]), distillation [34–42], the liquid-liquid extraction (LLE) using various solvent [20,32,33,43–49] being the most commonly used. Indeed, many issues were reported with distillation, such as the reactivity of bio-oil [41,49] or the poor selectivity and efficiency [32,38,40,47] caused by their complex composition and the non-stability of the bio-oil. To date, liquid-liquid extraction seems the easiest way of phenolic compounds extraction using small device and occurring under mild conditions (*i.e.* atmospheric pressure and room temperature). In LLE, the phenolic compounds extraction is based on the partial miscibility of aqueous and organic solvents.

For liquid-liquid extraction of phenolic compounds, several solvents are at disposal with some advantages and drawbacks. Alkaline solutions are often investigated for the extraction of compounds from the crude bio-oil [20,43–45,47,50,51]. Some authors succeeded to effectively extract families of compounds such as phenols.[50,51]. Yet, for Amen-Chen et al [47] and Greminger et al [52], an efficient extraction using aqueous solution requires pH higher than 11 and a multiple stages LLE. Nevertheless, according to Meier and coworkers, Maggi and Delmon, and Galceran and Eek [43–45], this method of extraction was not effective enough, causing the redistribution of the compounds in the phase and (sometimes) precipitation. Hence, another LLE is often performed consecutively.

Many organic solvents were investigated for the recovery of phenolic compounds from the previous aqueous phase resulting from this first alkaline extraction, among them ethyl acetate [47], methylisobutylketone MIBK [47,52], dichloromethane [53,54], toluene [55], ether [20,56], or diisopropyl ether [52]. Then, the recovery of the compounds from the organic phase is generally performed *via* distillation. Since many organic solvents are very or partially miscible with water, a distillation step following LLE is carried out for a partial recovery of the solvent [57] and require lots of energy. Yet, the huge volumes of solvent, constitutes the main LLE drawback related to organic solvent use, especially for health applications, which strongly restrict them. Hence, the improvement of process needs solvent with higher extraction capacity and lower toxicity than those reported for commonly used organic solvents.

These last few years, ionic liquids have been investigated for the extraction of phenolic compounds as a potential alternative of organic solvent. Indeed, ionic liquids are a new kind of solvent with specific properties such as a low vapor pressure and a high thermal and chemical stability. To date, only few studies investigated the possibility to use ionic liquids as a way to extract phenolic compounds. Garron et al [58] showed that some hydrophobic imidazolium ionic liquids containing bis(trifluoromethylsulfonylimide) [NTf<sub>2</sub>] anion are effective for the extraction of guaiacol from aqueous solutions. In our previous work [59], we also evidenced that [Choline][NTf<sub>2</sub>] was a good solvent for the extraction of phenol, guaiacol and syringol from aqueous solution.

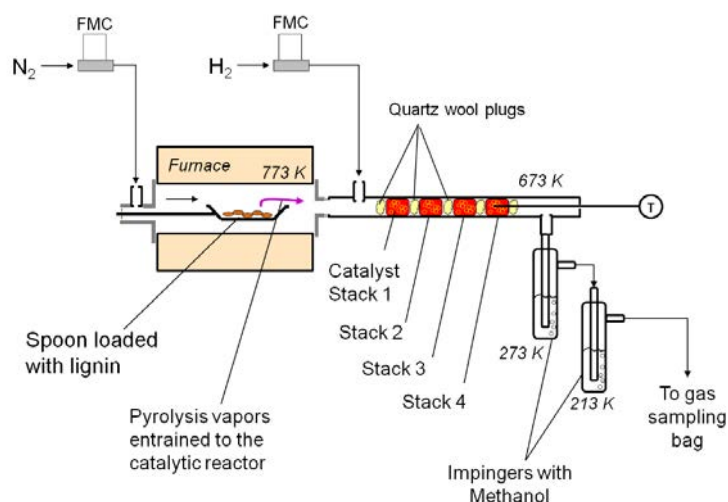
## VI-2. Materials and method

### VI-2.1. Chemical reagents and solvents

Standards of phenol (CAS 108-95-2), guaiacol (CAS 90-05-1), syringol (CAS 91-10-1), pyrocatechol (CAS 120-80-9), o-cresol (CAS 95-48-7), vanillin (CAS 121-33-5), toluene (CAS 108-88-3) and o-xylene (CAS 95-47-6) were purchased from Sigma-Aldrich. Ethyl acetate (CAS 141-78-6) was supplied from Sigma-Aldrich and ethanol (CAS 64-17-5) from Carlo Erba. 1-octene (CAS 111-66-0) was purchased from Sigma-Aldrich. Sodium hydroxide (CAS 1310-73-2) in pellets was purchased from Sigma-Aldrich. Protobind lignin 1000 was purchased from Green Value. Choline bis(trifluoromethylsulfonyl)imide [Choline][Ntf<sub>2</sub>] ionic liquid was purchased from Io-li-tec with a purity of 99% (w/w). Deionized water was used for all the experiments.

### VI-2.2. Bio-oil production

The device used for lignin pyrolysis is described elsewhere[60]. Briefly, lignin was introduced with a steel sample boat into a heated steel tubular reactor (Figure VI-1). The pyrolysis of lignin was conducted under hydrogen and with iron-based catalysts. It has been shown that iron is selective and cheap catalyst for hydrodeoxygenation reactions [61,62] The vapours were collected into methanol-containing impingers. The fractions were collected into a flask and sample was added with 0.2µL of 1-octene as internal standard for quantification. Then, the methanol of the diluted bio-oil was removed using rotary evaporation to obtain the crude bio-oil (vacuum, 40°C). Methanol was used as a solvent to improve pyrolysis vapour sampling in impingers. It is a light solvent easy to be evaporated at low temperature by rotary evaporation. Furthermore, bio-oils produced by hydrodeoxygenation of lignin are much more stable than bio-oils produced by (non-catalytic) pyrolysis of lignocellulosic biomass. It has been checked that after evaporation of methanol, no modification of composition was observed in the bio-oils. Six bio-oils were collected and notated from 1 to 6. These former ones were produced with different experimental catalyst compositions as detailed in Table VI-1. A, B, C and D correspond to catalyst precursors (confidential).

**Figure VI-1:** Scheme of the device for the lignin pyrolysis from [60]**Table VI-1:** Experimental conditions for the production of crude bio-oils

Bio-oils	Catalyst composition in iron	Catalyst precursor	Additive	Catalyst precursor
1	10%	A	None	None
2	None	None	None	None
3	10%	A	2%	B
4	10%	C	2%	D
5	10%	A	5%	B
6	10%	A	2%	B

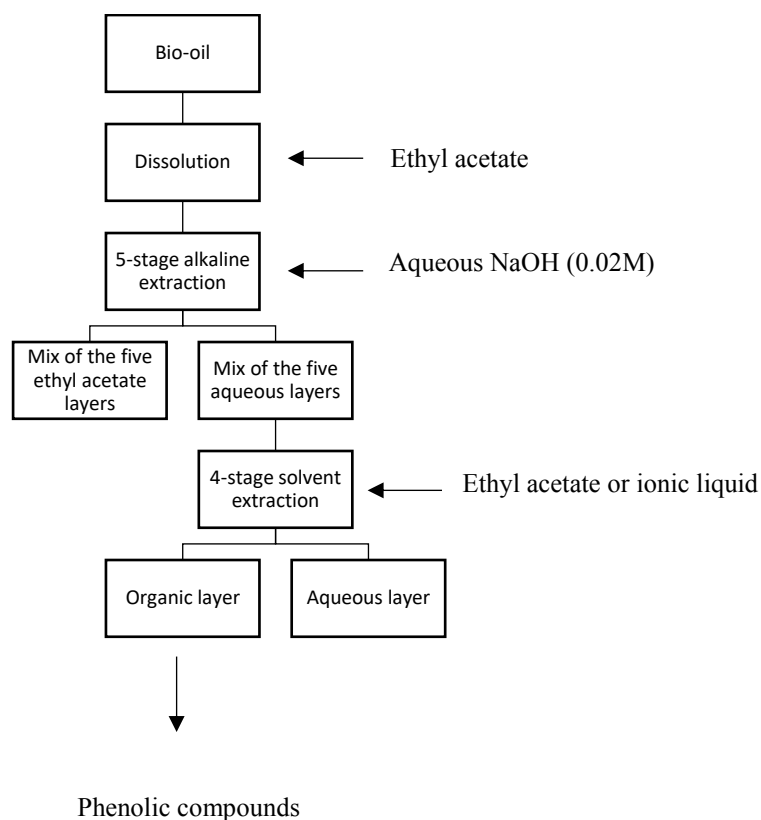
### VI-2.3. Liquid-liquid extraction

The main liquid-liquid extraction procedure was described in Amen-Chen et al [47] with some modifications. The procedure was divided into four steps (Figure VI-2): 1) dilution of the bio-oil in ethyl acetate, 2) liquid-liquid extraction with basic aqueous solutions, 3) acidification of the aqueous layer with chloride acid (2M) and 4) liquid-liquid extraction with a solvent.

Briefly, the crude bio-oil diluted in ethyl acetate (1:1 weight ratio) was washed with an aqueous hydroxide solution NaOH at 0.02M (1:1 weight ratio, pH value of 12.1). The phases were splitted in a separatory funnel, and the aqueous phase was collected in a flask. The bio-oil was washed five times with fresh aqueous sodium hydroxide solution. Then, the resulting bio-oil

was diluted in ethanol and a volume of 0.5 $\mu$ L of 1-octene was introduced for quantification of the remaining compounds.

**Figure VI-2:** Steps of the extraction of phenolic compounds from bio-oil

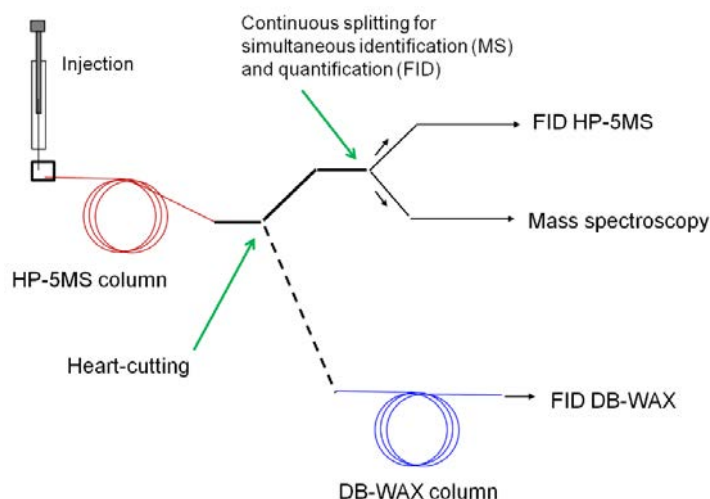


The five aqueous layers were combined and acidified with acid chloride (2M) until reaching a pH 6 value. The studied solvent (ethyl acetate or [choline][NTf<sub>2</sub>]) was then added to the mixture (0.5:1 solvent/aqueous phase, w/w) for the recovery of the phenol. The phases were separated with a separatory funnel and the organic layer containing phenolic compounds was collected. The aqueous phase was washed four times with fresh solvent (ethyl acetate or ionic liquid) solution. A volume of 0.5 $\mu$ L of 1-octene was introduced to each organic sample for quantification. Before analysis, the ionic liquid samples were diluted into ethanol to reduce their viscosity.

### VI-2.4. Sample analysis

The analysis of the oil fractions was performed with an Agilent 7890A Gas Chromatography coupled to an Agilent 5975C MS analyser. The samples (1 $\mu$ L) were injected by an Agilent 7683B autosampler with a split ratio of 20. First, the sample was sent to an Agilent HP-5MS (30m $\times$ 250 $\mu$ m $\times$ 0.25 $\mu$ m) column. The exit of the HP-5MS column was connected either to an Agilent DB-Wax123 (30m $\times$ 320 $\mu$ m $\times$ 0.25 $\mu$ m) column connected to a flame ionization detector (FID) or simultaneously to a (FID) and a mass spectroscopy (MS) (Figure VI-3). The temperature programming was as follows: the temperature oven was firstly maintained at 323 K during 5 minutes and then heated with a ramp rate of 5K/min up to 523 K. The temperature was then held at 523 K during 15 minutes. More details of the device are provided elsewhere [60,63].

**Figure VI-3:** Scheme of the GC-GC MS-FID-FID device from [60]



The quantification of the phenolic compounds was performed using FID results. Four mixtures containing eight phenolic compounds as standards were prepared with various concentrations to determine their relative response factor (GC/FID and response factor predicted by de Saint Laumer). For the other phenolic compounds, the relative response factors were determined by the Saint-Laumer method [64]. The database used for the identification was provided by the NIST.

### VI-3. Results and discussion

#### VI-3.1. Influence of the experimental conditions used in the produced crude bio-oil before liquid liquid extraction.

More than 50 compounds are present in the bio-oil [60] but this work is mainly focused on the 23 more abundant components listed in Table VI-2. The composition of the crude bio-oils before extraction ( $w_b$ ) are listed in Table VI-2. When the lignin is pyrolysed without catalyst (bio-oil 2), the production of methoxyl compounds is favoured, especially 2-methoxyphenol, 2-methoxy-p-cresol, 4-ethyl-2-methoxyphenol, 2,6-dimethoxyphenol and 1-(4-hydroxy-3-5-dimethoxyphenyl)-ethanone. Same results are observed with the presence of catalyst using 10% C and 2% D (bio-oil 4). The use of 10% A and 2% B as catalyst favours the production of phenol (bio-oils 3 and 6), 2-methoxyphenol, 2-methoxy-4-methylphenol, 4-methylphenol and 1-(4-hydroxy-3-5-dimethoxyphenyl)-ethanone. The presence of B does not highly influence the production of compounds in the bio-oils. Indeed, the bio-oils 1 (10% A) and 5 (10% A and 5% B) present similar ratio of phenolic compounds with phenol and 2-methoxyphenol as major compounds.

#### VI-3.2. Liquid-liquid extraction of phenolic compounds from bio oil using basic aqueous solutions.

This first step allowed the extraction of phenolic compounds from the former crude bio-oil “n” (n= 1 to 6, corresponding to the 6 various bio-oils produced) using an aqueous NaOH solution numbered “n” (n= 1 to 6). The composition of the bio-oil after extraction ( $w_a$ ) and the extraction rate of each compound are listed in Table VI-2. The extraction rate of phenolic compounds  $i$  from the bio-oil  $n$  using the basic aqueous solution  $n$  is calculated as follows:

$$\text{Extraction rate with water}(\%) = \frac{w_i^b - w_i^a}{w_i^b} \cdot 100 \quad (1)$$

Where  $w_i$  is the mass fraction of the compound  $i$ . The superscripts “b” and “a” correspond to the bio-oil phase before and after extraction, respectively.

**Table VI-2:** Composition of the bio-oils before ( $w_b$ ) and after ( $w_a$ ) extraction with aqueous basic solutions and the respective extraction rates (%E).

Compounds	% w/w of crude bio oil																	
	Bio oil 1			Bio oil 2			Bio oil 3			Bio oil 4			Bio oil 5			Bio oil 6		
	$w_b$	$w_a$	% E	$w_b$	$w_a$	% E	$w_b$	$w_a$	% E	$w_b$	$w_a$	% E	$w_b$	$w_a$	% E	$w_b$	$w_a$	% E
phenol	0.78	0.31	61	0.86	0.4904	43	1.80	1.45	19	1.48	1.20	19	1.17	0.86	27	0.36	0.18	49
o-cresol	0.17	0.08	53	0.23	0.1106	51	0.56	0.46	18	0.33	0.28	15	0.26	0.19	27	0.09	0.05	56
p-cresol	0.31	0.14	55	0.38	0.2358	38	1.02	0.87	15	0.80	0.70	13	0.53	0.38	29	0.17	0.09	52
guaiacol	0.72	0.24	66	2.62	1.4754	44	0.99	0.79	21	2.95	2.08	29	0.99	0.68	32	0.30	0.13	45
1-ethyl-4-methoxybenzene	0.08	0.01	82	0.08	0.0160	79	0.06	0.02	64	0.05	0.02	69	0.10	0.03	68	0.03	0.01	30
2,5-dimethylphenol	0.11	0.05	54	0.09	0.0380	56	0.29	0.25	14	0.18	0.16	13	0.15	0.09	42	0.05	0.03	54
1-ethenyl-4-methoxybenzene	0.09	0.01	84	0.04	0.0105	70	0.18	0.07	63	0.03	0.02	33	0.12	0.06	50	0.03	0.01	45
4-ethylphenol	0.36	0.20	45	0.65	0.4145	37	0.74	0.65	11	1.04	0.91	12	0.44	0.35	20	0.12	0.08	69
2-methoxy-3-methylphenol	0.05	0.02	56	0.14	0.0759	46	0.07	0.05	27	0.14	0.12	16	0.08	0.04	52	0.02	0.01	54
2-methoxy-p-cresol	0.33	0.14	58	1.40	0.8540	39	0.72	0.53	27	2.27	1.65	27	0.39	0.23	42	0.12	0.06	49
2,3-dihydrobenzofuran	0.23	0.11	55	0.24	0.1275	46	0.70	0.62	12	0.60	0.54	10	0.38	0.29	24	0.09	0.06	63
3-(1-methylethyl)phenol	0.03	0.01	62	0.04	0.0321	19	0.05	0.04	13	0.09	0.06	40	0.05	0.04	11	0.01	0.01	71
1-methoxy-2-(methoxymethyl)benzene	0.11	0.05	55	0.10	0.0681	31	0.18	0.14	21	0.17	0.15	16	0.11	0.08	22	0.03	0.02	67
4-ethyl-2-methoxyphenol	0.56	0.28	50	1.68	1.1922	29	0.60	0.53	12	2.18	1.91	12	0.64	0.52	19	0.13	0.09	66
2-methoxy-4-vinylphenol	0.46	0.22	52	0.54	0.2890	47	1.36	1.24	9	1.36	1.19	13	0.73	0.60	18	0.17	0.12	70
4-ethyl-1,2-dimethoxybenzene	0.03	0.02	54	0.06	0.0204	66	0.12	0.09	23	0.05	0.03	48	0.05	0.03	29	0.03	0.01	20
syringol	0.21	0.04	83	1.94	0.6985	64	0.45	0.30	34	2.44	1.59	35	0.26	0.12	54	0.07	0.02	32
4-methoxy-3-(methoxymethyl)-phenol	0.15	0.04	70	0.87	0.5089	41	0.27	0.20	27	1.27	0.92	27	0.18	0.10	44	0.05	0.02	36
2-methoxy-4-(1-propenyl)-phenol	0.07	0.05	24	0.08	0.0632	20	0.27	0.24	11	0.33	0.30	9	0.11	0.09	12	0.02	0.02	64
5-tert-butylpyrogallol	0.15	0.05	69	0.66	0.4087	38	0.21	0.17	21	0.90	0.73	19	0.16	0.09	46	0.04	0.02	45

1-(4-hydroxy-3-5-dimethoxyphenyl)-ethanone	0.25	0.05	82	1.03	0.3284	68	1.03	0.54	48	2.02	1.18	42	0.46	0.09	80	0.15	0.03	23
methyl ester	0.11	0.06	44	0.05	0.0375	25	0.07	0.05	29	0.05	0.03	42	0.17	0.16	11	0.03	0.03	78
hexadecanoic acid																		
9,10-anthracenedione	0.07	0.07	62	0.06	0.0413	27	0.13	0.10	24	0.11	0.09	11	0.10	0.08	16	0.03	0.02	58

$u(w) = 10\%$

The extraction rate tends to decrease when the mass fraction of a given phenolic compound increases in the bio-oil (see bio-oils 3 and 4). For instance, the percentage of phenol in the bio-oils 3 (1.795%) and 4 (1.484%) is higher than in the other bio-oils but the extraction rate for this compound is quite low (19% compared to 60% in bio-oil 1 with a percentage of phenol of 0.78%). The acidic character of phenolic compounds has also an impact on their extraction. Indeed, the most extracted compound, 1-(4-hydroxy-3-5-dimethoxyphenyl)-ethanone (68% in bio-oil 2 and 48.22% in bio-oil 3) has a pKa of 7.8 [65] compared to the other compounds (pKa of phenol 9.95). Nevertheless, acidity is not the only parameter influencing the extraction. Indeed, the polarity of the molecule has an impact on their solubility in the aqueous solution as well. For instance, 2-methoxy-4-(1-propenyl)-phenol presents the lowest extraction rate upon the basic aqueous solution extraction (extraction rate varying between 9 and 25% for most of the studied bio-oils), despite a pKa (9.88[66]) lower than the one of the other compounds.

Thus, the basic aqueous solution (pH 12.1) is a good solvent for the liquid-liquid extraction of phenolic compounds from bio-oil but that could be still improved. One solution could consist to perform a higher number of stages of extraction but it will consequently increase the quantity of solvents needed. Another possibility is the use of a 5M NaOH solution for the first extraction [47]. Yet, such solution led to monophasic solutions in our work.

### VI-3.3. Extraction of phenolic compounds from the previous aqueous solution using various solvents.

In this second step of the LLE process, the phenolic compounds were extracted from the aqueous layer  $n$  ( $n= 1$  to  $6$ ) using ethyl acetate or [Choline][NTf<sub>2</sub>] solutions  $n$  ( $n= 1$  to  $6$ ). The composition of the final phase  $w_f$  (ethyl acetate or ionic liquid) and their extraction rates are listed in Table VI-3. The extraction rate of the phenolic compounds  $i$  from the aqueous solution  $n$  is calculated as follows:

$$\text{Extraction rate (\%)} = \frac{w_i^f}{w_i^{aq}} \cdot 100 \quad (2)$$

$$\text{With } w_i^{aq} = w_i^b - w_i^a$$

Where  $w_i$  is the mass fraction of the compound  $i$ . The superscripts “f” and “aq” refers to the final phase (ethyl acetate or ionic liquid) and the aqueous initial phase respectively, while the superscript “b” and “a” correspond to the bio-oil phase before and after extraction,

respectively. Bio-oils 1 to 4 were extracted with ethyl acetate, whereas bio-oils 5 and 6 were extracted with [Choline][NTf<sub>2</sub>] ionic liquid.

#### **VI-3.4. Extraction of phenolic compounds from the aqueous solution using ethyl acetate.**

Before the extraction with ethyl acetate, the major phenolic components present in the aqueous phase 1 are phenol and 2-methoxy phenol. After a 4-stage process using ethyl acetate, these components are extracted with a rate of 40%. In the case of the aqueous solution 3, 1-(4-hydroxy-3-5-dimethoxyphenyl)-ethanone and phenol are the major components and are extracted in the final phase with a rate of 57% and 83%, respectively. In the case of aqueous solutions 2 and 4, the major components present are 2-methoxyphenol, 2,6-dimethoxyphenol and 1-(4-hydroxy-3-5-dimethoxyphenyl)-ethanone. These compounds are well extracted with ethyl acetate (extraction rates comprised within 45 and 75%). On the other hand, methyl ester hexadecanoic acid, 1-ethyl-4-methoxybenzene, 1-ethenyl-4-methoxybenzene, 4-ethyl-1-2dimethoxybenzene and 1-methoxy-2-methoxy-methylbenzene are the less extracted phenolic compounds with a rate inferior to 20% in most of the cases. Finally, after 4 process stages with ethyl acetate, ethyl acetate solutions 3 and 4 present higher extraction rates for most of the components than the solutions 1 and 2 (Table VI-3). Moreover, all the aqueous phases still remained yellow after the extraction, suggesting that not all the phenolic compounds were recovered (Figure VI-4a).

**Table VI-3:** Composition of the ethyl acetate final phase ( $w_f$ ) and the respective extractions rates (%E).

Compounds	% w/w of crude bio oil											
	Bio oil 1			Bio oil 2			Bio oil 3			Bio oil 4		
	$w_{aq}$	$w_f$	%E	$w_{aq}$	$w_f$	%E	$w_{aq}$	$w_f$	%E	$w_{aq}$	$w_f$	%E
Phenol	0.47	0.21	44	0.37	0.19	51	0.34	0.28	83	0.28	0.23	80
o-cresol	0.09	0.03	34	0.12	0.03	23	0.10	0.06	58	0.05	0.04	81
p-cresol	0.17	0.05	32	0.15	0.05	37	0.15	0.12	81	0.11	0.08	80
guaiacol	0.48	0.19	40	1.15	0.55	48	0.21	0.18	89	0.86	0.47	54
1-ethyl-4-methoxybenzene	0.06	0.00	4	0.06	n.d.	n.d.	0.04	0.00	5	0.04	0.00	3
2,5-dimethylphenol	0.06	0.01	14	0.05	0.01	24	0.04	0.03	62	0.02	0.02	64
1-ethenyl-4-methoxybenzene	0.07	n.d.	n.d.	0.03	n.d.	n.d.	0.12	0.01	11	0.01	n.d.	n.d.
4-ethylphenol	0.16	0.03	20	0.24	0.04	17	0.08	0.06	70	0.12	0.06	49
2-methoxy-3-methylphenol	0.03	0.005	15	0.06	0.01	16	0.02	0.01	28	0.02	0.01	45
2-methoxy-p-cresol	0.19	0.08	40	0.55	0.37	68	0.19	0.19	96	0.62	0.50	81
2,3-dihydrobenzofuran	0.13	0.02	15	0.11	0.02	14	0.08	0.05	61	0.06	0.03	56
3-(1-methylethyl)phenol	0.02	0.01	24	0.01	0.01	68	0.01	n.d.	n.d.	0.04	0.01	20
1-methoxy-2-(methoxymethyl)benzene	0.06	0.08	14	0.03	0.01	17	0.04	0.01	34	0.03	0.01	36
4-ethyl-2-methoxyphenol	0.28	0.05	17	0.48	0.12	25	0.07	0.06	78	0.26	0.14	54
2-methoxy-4-vinylphenol	0.24	0.04	16	0.25	0.04	16	0.12	0.12	96	0.18	0.10	54
4-ethyl-1,2-dimethoxybenzene	0.02	0.00	11	0.04	n.d.	n.d.	0.03	0.00	11	0.02	0.00	17
syringol	0.17	0.09	51	1.24	0.66	53	0.15	0.11	72	0.85	0.59	69
4-methoxy-3-(methoxymethyl)-phenol	0.10	0.03	32	0.36	0.20	57	0.07	0.04	56	0.35	0.19	54
2-methoxy-4-(1-propenyl)-phenol	0.02	0.01	49	0.02	0.01	60	0.03	0.02	81	0.03	0.03	80
5-tert-butylpyrogallol	0.10	0.02	19	0.25	0.08	32	0.04	0.02	50	0.17	0.09	51
1-(4-hydroxy-3-5-dimethoxyphenyl)-ethanone	0.21	0.12	60	0.70	0.52	75	0.50	0.29	58	0.85	0.64	76
methyl ester hexadecanoic acid	0.05	0.00	8	0.01	0.01	43	0.02	0.00	18	0.02	0.00	9
9,10-anthracenedione	0.04	0.01	11	0.02	0.01	55	0.03	0.01	27	0.01	0.01	73

$u(w) = 10\%$

### **VI-3.5. Extraction of phenolic compounds from aqueous solution using Choline bis(trifluoromethylsulfonyl)imide.**

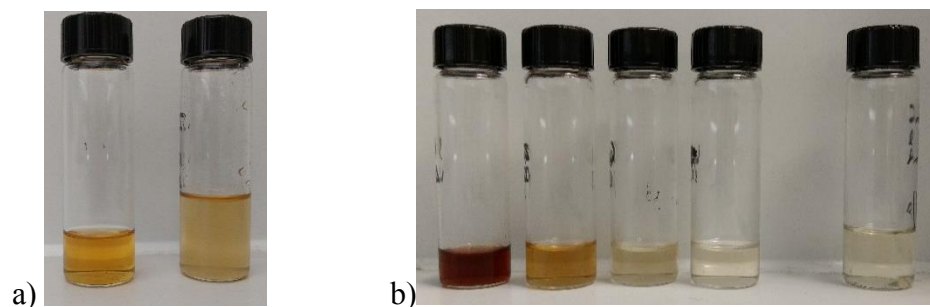
After the first stage of extraction with [Choline][NTf<sub>2</sub>], most of the phenolic compounds are extracted from the aqueous solutions with a rate higher than 40% (Table VI-4). The use of the [Choline][NTf<sub>2</sub>] ionic liquid allows the recovery of the major components (in aqueous phases 5 and 6) which are phenol, guaiacol and 1-(4-hydroxy-3-5-dimethoxyphenyl)-ethanone with similar extraction rate (70%, 67% and 79%, respectively). These rates are a little lower than those obtained after 4 stages of extraction with ethyl acetate (83%, 86% and 57% in bio-oil 3, 43%, 40% and 60% for bio-oil 1). 1-ethyl-4-methoxybenzene and 1-ethenyl-4-methoxybenzene are the less extracted compounds (rate inferior to 15%), as observed with ethyl acetate. This behaviour could be explained by the apolar alkyl chain grafted on the benzene moiety leading to repulsive interactions with the ionic liquid. The second stage of the extraction with the ionic liquid allows the recovery of the major compounds: phenol, cresols, guaiacol, 2-methoxy-p-cresol, 4-ethyl-2-methoxyphenol, 2-methoxy-4-vinylphenol, syringol and 1-(4-hydroxy-3-5-dimethoxyphenyl)-ethanone. No phenolic components are observed in the ionic liquid phase of the third and fourth extraction stages. Moreover, the aqueous phase is colourless after the second extraction (Figure VI-4b). Hence, the ionic liquid [Choline][NTf<sub>2</sub>] is an efficient solvent for the extraction of phenol, guaiacol and syringol with an excellent extraction rate (superior than 80%) in only two stages.

**Table VI-4:** Composition of the [Choline][NTf<sub>2</sub>] final phase ( $w_f$ ) and the respective extraction rates (%E).

Compounds	% w/w of crude bio oil									
	Bio-oil 5					Bio oil 6				
	$w_{aq}$	1 <sup>st</sup> stage		2 <sup>nd</sup> stage		$w_{aq}$	1 <sup>st</sup> stage		2 <sup>nd</sup> stage	
	$w_f$	%E	$w_f$	%E		$w_f$	%E	$w_f$	%E	
Phenol	0.31	0.22	71	0.05	16	0.18	0.13	69	0.04	21
o-cresol	0.07	0.04	50	0.01	8	0.04	0.02	55	0.01	13
p-cresol	0.15	0.09	56	0.01	9	0.08	0.05	63	0.01	13
guaiacol	0.32	0.21	67	0.05	14	0.17	0.11	682	0.03	19
1-ethyl-4-methoxybenzene	0.07	0.01	7	n.d.	n.d.	0.02	n.d.	n.d.	n.d.	n.d.
2,5-dimethylphenol	0.06	0.02	26	n.d.	n.d.	0.02	0.02	73	n.d.	n.d.
1-ethenyl-4-methoxybenzene	0.06	0.01	8	n.d.	n.d.	0.02	0.00	14	n.d.	n.d.
4-ethylphenol	0.09	0.06	64	n.d.	n.d.	0.04	0.03	92	n.d.	n.d.
2-methoxy-3-methylphenol	0.04	0.01	14	n.d.	n.d.	0.01	0.00	41	n.d.	n.d.
2-methoxy-p-cresol	0.17	0.08	45	0.01	7	0.06	0.03	57	0.01	14
2,3-dihydrobenzofuran	0.09	0.04	42	n.d.	n.d.	0.04	0.02	58	n.d.	n.d.
3-(1-methylethyl)phenol	0.01	0.01	89	n.d.	n.d.	0.00	0.00	75	n.d.	n.d.
1-methoxy-2-(methoxymethyl)benzene	0.02	0.01	55	n.d.	n.d.	0.01	0.01	84	n.d.	n.d.
4-ethyl-2-methoxyphenol	0.12	0.09	75	0.01	9	0.05	0.04	87	0.01	13
2-methoxy-4-vinylphenol	0.13	0.08	58	n.d.	n.d.	0.05	0.05	89	0.01	11
4-ethyl-1,2-dimethoxybenzene	0.01	0.00	31	n.d.	n.d.	0.02	0.01	21	n.d.	n.d.
syringol	0.14	0.10	70	0.03	20	0.05	0.04	83	0.01	23
4-methoxy-3-(methoxymethyl)-phenol	0.08	0.04	48	n.d.	n.d.	0.03	0.02	72	n.d.	n.d.
2-methoxy-4-(1-propenyl)-phenol	0.01	0.01	86	n.d.	n.d.	0.01	0.00	32	n.d.	n.d.
5-tert-butylpyrogallol	0.07	0.04	49	n.d.	n.d.	0.02	0.02	79	n.d.	n.d.
1-(4-hydroxy-3-5-dimethoxyphenyl)-ethanone	0.36	0.21	79	0.05	20	0.11	0.09	80	0.02	19
methyl ester hexadecanoic acid	0.02	0.01	14	n.d.	n.d.	0.01	0.00	25	n.d.	n.d.
9,10-anthracenedione	0.02	0.01	81	n.d.	n.d.	0.01	0.01	48	n.d.	n.d.

u(w) = 10%; n.d.: not determined

**Figure VI-4:** Colour of the phase after liquid-liquid extraction: a) from left to right: ethyl acetate phase (4 stages mixing) and aqueous phase; b) from left to right: [choline][NTf<sub>2</sub>] stages from 1 to 4 and aqueous phase.



#### VI-4. Conclusion

Alkaline solution with high pH allows the partial extraction of phenolic compounds from crude bio-oils. Improvement can be made by increasing the number of stages of extraction or by using alkaline solution with higher concentration. Yet, precaution must be made in order to prevent reactions with the bio oils. The use of ethyl acetate for the recovery of the phenolic compounds from the aqueous phase is partially effective. It appears that [Choline][NTf<sub>2</sub>] is a good solvent for the recovery of phenolic compounds since it requires only two stages to extract 80% of phenol, guaiacol, syringol or 1-(4-hydroxy-3-5-dimethoxyphenyl)-ethanone.

## References

- [1] D.L. Klass, *Biomass for Renewable Energy, Fuels, and Chemicals*, Academic Press, 1998.
- [2] D. Güllü, A. Demirbas, Biomass to methanol via pyrolysis process, *Energy Convers. Manag.* 42 (2001) 1349–1356. doi:10.1016/S0196-8904(00)00126-6.
- [3] J. Zakzeski, P.C.A. Bruijninx, A.L. Jongerius, B.M. Weckhuysen, The Catalytic Valorization of Lignin for the Production of Renewable Chemicals, *Chem. Rev.* 110 (2010) 3552–3599. doi:10.1021/cr900354u.
- [4] C. Amen-Chen, H. Pakdel, C. Roy, Production of monomeric phenols by thermochemical conversion of biomass: a review, *Bioresour. Technol.* 79 (2001) 277–299. doi:10.1016/S0960-8524(00)00180-2.
- [5] F.L. Mota, A.J. Queimada, S.P. Pinho, E.A. Macedo, Aqueous Solubility of Some Natural Phenolic Compounds, *Ind. Eng. Chem. Res.* 47 (2008) 5182–5189. doi:10.1021/ie071452o.
- [6] R.C. Hider, Z.D. Liu, H.H. Khodr, Metal chelation of polyphenols, *Methods Enzymol.* 335 (2001) 190–203.
- [7] V.L. Singleton, R. Orthofer, R.M. Lamuela-Raventós, [14] Analysis of total phenols and other oxidation substrates and antioxidants by means of folin-ciocalteu reagent, in: *Methods Enzymol.*, Elsevier, 1999: pp. 152–178. doi:10.1016/S0076-6879(99)99017-1.
- [8] A.C. Jennings, The determination of dihydroxy phenolic compounds in extracts of plant tissues, *Anal. Biochem.* 118 (1981) 396–398. doi:10.1016/0003-2697(81)90600-X.
- [9] S.Y. Yeung, W.H. Lan, C.S. Huang, C.P. Lin, C.P. Chan, M.C. Chang, J.H. Jeng, Scavenging property of three cresol isomers against H<sub>2</sub>O<sub>2</sub>, hypochlorite, superoxide and hydroxyl radicals, *Food Chem. Toxicol.* 40 (2002) 1403–1413.
- [10] H.K. Obied, M.S. Allen, D.R. Bedgood, P.D. Prenzler, K. Robards, R. Stockmann, Bioactivity and Analysis of Biophenols Recovered from Olive Mill Waste, *J. Agric. Food Chem.* 53 (2005) 823–837. doi:10.1021/jf048569x.
- [11] M. Kampa, V.-I. Alexaki, G. Notas, A.-P. Nifli, A. Nistikaki, A. Hatzoglou, E. Bakogeorgou, E. Kouimtoglou, G. Blekas, D. Boskou, A. Gravanis, E. Castanas, Antiproliferative and apoptotic effects of selective phenolic acids on T47D human breast cancer cells: potential mechanisms of action., *Breast Cancer Res.* 6 (2004) R63. doi:10.1186/bcr752.
- [12] Vanillin Pharmaceutical, *Chem. Eng. News.* 34 (1956) 4778. doi:10.1021/cen-v034n040.p4778.
- [13] F. Helmut, V. Heinz-Werner, H. Toshikazu, P. Wilfried, Phenol derivatives, *Ullmann's Encycl. Ind. Chem. VCH Ger.* 19 (1985) 299–357.
- [14] F. Ikegami, T. Sekine, Y. Fujii, [Anti-dermatophyte activity of phenolic compounds in “mokusaku-eki”], *Yakugaku Zasshi.* 118 (1998) 27–30.
- [15] G.A. Burdock, *Fenaroli's Handbook of Flavor Ingredients*, Sixth Edition, CRC Press, 2016.
- [16] J.A. Maga, I. Katz, Simple phenol and phenolic compounds in food flavor, *C R C Crit. Rev. Food Sci. Nutr.* 10 (1978) 323–372. doi:10.1080/10408397809527255.
- [17] M.D. Guillén, M.L. Ibargoitia, New Components with Potential Antioxidant and Organoleptic Properties, Detected for the First Time in Liquid Smoke Flavoring Preparations, *J. Agric. Food Chem.* 46 (1998) 1276–1285. doi:10.1021/jf970952x.
- [18] Filbert, Manufacture of dinitro-orthocresol, n.d. <http://www.google.com/patents/US2256195> (accessed May 10, 2017).
- [19] J.J. Bozell, J.E. Holladay, D. Johnson, J.F. White, Top value added chemicals from biomass, Vol. II Results Screen. Potential Candidates Biorefinery Lignin Rep. PNNL-16983. (2007).

- [20] R.M. Gallivan, P.K. Matschei, Fractionation of oil obtained by pyrolysis of lignocellulosic materials to recover a phenolic fraction for use in making phenol-formaldehyde resins, n.d. <http://www.google.com/patents/US4209647> (accessed January 23, 2017).
- [21] R.N. Singru, A.B. Zade, W.B. Gurnule, Synthesis, characterization, and thermal degradation studies of copolymer resin derived from p-cresol, melamine, and formaldehyde, *J. Appl. Polym. Sci.* 109 (2008) 859–868. doi:10.1002/app.28197.
- [22] H.L. Chum, S.K. Black, Process for fractionating fast-pyrolysis oils, and products derived therefrom, n.d. <http://www.google.com/patents/US4942269> (accessed May 10, 2017).
- [23] T. Suzuki, H. Nozaki, T. Yamada, T. Homma, Preparation of wood tar-based phenol-resin adhesives, *Japan Wood Res Soc* 1-1-17, Mukogaoka, Bunkyo-Ku, Tokyo, 113-0023, Japan, 1992.
- [24] S. Yaman, Pyrolysis of biomass to produce fuels and chemical feedstocks, *Energy Convers. Manag.* 45 (2004) 651–671. doi:10.1016/S0196-8904(03)00177-8.
- [25] R.K. Sharma, J.B. Wooten, V.L. Baliga, X. Lin, W. Geoffrey Chan, M.R. Hajaligol, Characterization of chars from pyrolysis of lignin, *Fuel.* 83 (2004) 1469–1482. doi:10.1016/j.fuel.2003.11.015.
- [26] A.V. Bridgwater, P. Carson, M. Coulson, A comparison of fast and slow pyrolysis liquids from mallee, *Int. J. Glob. Energy Issues.* 27 (2007) 204. doi:10.1504/IJGEI.2007.013655.
- [27] A. Teella, G.W. Huber, D.M. Ford, Separation of acetic acid from the aqueous fraction of fast pyrolysis bio-oils using nanofiltration and reverse osmosis membranes, *J. Membr. Sci.* 378 (2011) 495–502. doi:10.1016/j.memsci.2011.05.036.
- [28] Z. Wang, W. Lin, W. Song, L. Du, Z. Li, J. Yao, Component fractionation of wood-tar by column chromatography with the packing material of silica gel, *Chin. Sci. Bull.* 56 (2011) 1434–1441. doi:10.1007/s11434-010-4144-x.
- [29] T. Ba, A. Chaala, M. Garcia-Perez, C. Roy, Colloidal Properties of Bio-Oils Obtained by Vacuum Pyrolysis of Softwood Bark. Storage Stability, *Energy Fuels.* 18 (2004) 188–201. doi:10.1021/ef0301250.
- [30] P. Das, T. Sreelatha, A. Ganesh, Bio oil from pyrolysis of cashew nut shell-characterisation and related properties, *Biomass Bioenergy.* 27 (2004) 265–275. doi:10.1016/j.biombioe.2003.12.001.
- [31] S. XU, J. Liu, S. Li, Shu-qin Liu, Q. Lu, Solvent extraction-column chromatographic separation of bio-oil from fast pyrolysis of apricot stone and manufacture technology, *J. Dalian Univ. Technol.* 4 (2005).
- [32] A. Vigneault, D.K. Johnson, E. Chornet, Base-Catalyzed Depolymerization of Lignin: Separation of Monomers, *Can. J. Chem. Eng.* 85 (2008) 906–916. doi:10.1002/cjce.5450850612.
- [33] R. Lu, G.-P. Sheng, Y.-Y. Hu, P. Zheng, H. Jiang, Y. Tang, H.-Q. Yu, Fractional characterization of a bio-oil derived from rice husk, *Biomass Bioenergy.* 35 (2011) 671–678. doi:10.1016/j.biombioe.2010.10.017.
- [34] U. Schuchardt, J.A.R. Rodrigues, A. Cotrim, J.L.M. Costa, Liquefaction of hydrolytic eucalyptus lignin with formate in water, using batch and continuous-flow reactors, *Bioresour. Technol.* 44 (1993) 123–129. doi:10.1016/0960-8524(93)90185-E.
- [35] A.N. Bagaev, Fractionation of wood tars and their products, *Gidroliz Lesokhim Promysh.* 18 (1965) 13–15.
- [36] J.N. Murwanashyaka, H. Pakdel, C. Roy, Separation of syringol from birch wood-derived vacuum pyrolysis oil, *Sep. Purif. Technol.* 24 (2001) 155–165. doi:10.1016/S1383-5866(00)00225-2.
- [37] J.A. Capunitan, S.C. Capareda, Characterization and separation of corn stover bio-oil by fractional distillation, *Fuel.* 112 (2013) 60–73. doi:10.1016/j.fuel.2013.04.079.

- [38] S. Wang, Y. Gu, Q. Liu, Y. Yao, Z. Guo, Z. Luo, K. Cen, Separation of bio-oil by molecular distillation, *Fuel Process. Technol.* 90 (2009) 738–745. doi:10.1016/j.fuproc.2009.02.005.
- [39] S. Ramaswamy, H.-J. Huang, B.V. Ramarao, *Separation and Purification Technologies in Biorefineries*, John Wiley & Sons, 2013.
- [40] Z. Guo, S. Wang, Y. Gu, G. Xu, X. Li, Z. Luo, Separation characteristics of biomass pyrolysis oil in molecular distillation, *Sep. Purif. Technol.* 76 (2010) 52–57. doi:10.1016/j.seppur.2010.09.019.
- [41] X.-S. Zhang, G.-X. Yang, H. Jiang, W.-J. Liu, H.-S. Ding, Mass production of chemicals from biomass-derived oil by directly atmospheric distillation coupled with co-pyrolysis, *Sci. Rep.* 3 (2013). doi:10.1038/srep01120.
- [42] J. Li, D. Ding, L. Xu, Q. Guo, Y. Fu, The breakdown of reticent biomass to soluble components and their conversion to levulinic acid as a fuel precursor, *RSC Adv.* 4 (2014) 14985. doi:10.1039/c3ra47923d.
- [43] D. Meier, D.R. Larimer, O. Faix, Direct liquefaction of different lignocellulosics and their constituents, *Fuel.* 65 (1986) 910–915. doi:10.1016/0016-2361(86)90197-3.
- [44] R. Maggi, B. Delmon, Comparison between “slow” and “flash” pyrolysis oils from biomass, *Fuel.* 73 (1994) 671–677. doi:10.1016/0016-2361(94)90007-8.
- [45] M.T. Galceran, L. Eek, Analisis de alquitran de extraccion de maderas duras, 2: Fraccion pesada., *Quimica Anal.* (1977). [http://agris.fao.org/agris-search/search.do;jsessionid=F583D9497F7B2141AF13ADC070ACD2C3?request\\_local\\_e=es&recordID=ES19780302092&sourceQuery=&query=&sortField=&sortOrder=&agrovocString=&advQuery=&centerString=&enableField=](http://agris.fao.org/agris-search/search.do;jsessionid=F583D9497F7B2141AF13ADC070ACD2C3?request_local_e=es&recordID=ES19780302092&sourceQuery=&query=&sortField=&sortOrder=&agrovocString=&advQuery=&centerString=&enableField=) (accessed May 10, 2017).
- [46] Y. Wei, H. Lei, L. Wang, L. Zhu, X. Zhang, Y. Liu, S. Chen, B. Ahring, Liquid–Liquid Extraction of Biomass Pyrolysis Bio-oil, *Energy Fuels.* 28 (2014) 1207–1212. doi:10.1021/ef402490s.
- [47] C. Amen-Chen, H. Pakdel, C. Roy, Separation of phenols from Eucalyptus wood tar, *Biomass Bioenergy.* 13 (1997) 25–37. doi:10.1016/S0961-9534(97)00021-4.
- [48] J. Li, C. Wang, Z. Yang, Production and separation of phenols from biomass-derived biopetroleum, *J. Anal. Appl. Pyrolysis.* 89 (2010) 218–224. doi:10.1016/j.jaap.2010.08.004.
- [49] L. Fele Žilnik, A. Jazbinšek, Recovery of renewable phenolic fraction from pyrolysis oil, *Sep. Purif. Technol.* 86 (2012) 157–170. doi:10.1016/j.seppur.2011.10.040.
- [50] O. Beaumont, Flash Pyrolysis Products From Beech Wood, *Wood Fiber Sci.* 17 (2007) 228–239.
- [51] G.E. Achladas, Analysis of biomass pyrolysis liquids: separation and characterization of phenols, *J. Chromatogr. A.* 542 (1991) 263–275. doi:10.1016/S0021-9673(01)88766-5.
- [52] D.C. Greminger, G.P. Burns, S. Lynn, D.N. Hanson, C.J. King, Solvent extraction of phenols from water, *Ind. Eng. Chem. Process Des. Dev.* 21 (1982) 51–54. doi:10.1021/i200016a010.
- [53] R.W. Thring, J. Breaux, Hydrocracking of solvolysis lignin in a batch reactor, *Fuel.* 75 (1996) 795–800. doi:10.1016/0016-2361(96)00036-1.
- [54] S. Wang, Y. Wang, Q. Cai, X. Wang, H. Jin, Z. Luo, Multi-step separation of monophenols and pyrolytic lignins from the water-insoluble phase of bio-oil, *Sep. Purif. Technol.* 122 (2014) 248–255. doi:10.1016/j.seppur.2013.11.017.
- [55] T. Radoykova, S. Nenkova, K. Stanulov, Production of phenol compounds by alkaline treatment of poplar wood bark, *Chem. Nat. Compd.* 46 (2010) 807–808. doi:10.1007/s10600-010-9751-x.
- [56] J.-M. Lavoie, W. Baré, M. Bilodeau, Depolymerization of steam-treated lignin for the production of green chemicals, *Bioresour. Technol.* 102 (2011) 4917–4920. doi:10.1016/j.biortech.2011.01.010.

- [57] X. Li, S.R.A. Kersten, B. Schuur, Extraction of Guaiacol from Model Pyrolytic Sugar Stream with Ionic Liquids, *Ind. Eng. Chem. Res.* 55 (2016) 4703–4710. doi:10.1021/acs.iecr.6b00100.
- [58] A. Garron, P.P. Arquilliere, W.A. Maksoud, C. Larabi, J.-J. Walter, C.C. Santini, From industrial black liquor to pure phenolic compounds: A combination of catalytic conversion with ionic liquids extraction, *Appl. Catal. Gen.* 502 (2015) 230–238. doi:10.1016/j.apcata.2015.06.012.
- [59] L. Cesari, L. Canabady-Rochelle, F. Mutelet, Extraction of phenolic compounds from aqueous solution using choline bis(trifluoromethylsulfonyl)imide, *Fluid Phase Equilibria.* 446 (2017) 28–35. doi:10.1016/j.fluid.2017.04.022.
- [60] R.N. Olcese, Valorisation des vapeurs de pyrolyse de lignine par hydrodéoxygénation directe catalysées par le fer, Université de Lorraine, 2012. <http://www.theses.fr/2012LORR0107> (accessed May 18, 2017).
- [61] R.N. Olcese, M. Bettahar, D. Petitjean, B. Malaman, F. Giovanella, A. Dufour, Gas-phase hydrodeoxygenation of guaiacol over Fe/SiO<sub>2</sub> catalyst, *Appl. Catal. B Environ.* 115–116 (2012) 63–73. doi:10.1016/j.apcatb.2011.12.005.
- [62] R.N. Olcese, J. Francois, M.M. Bettahar, D. Petitjean, A. Dufour, Hydrodeoxygenation of Guaiacol, A Surrogate of Lignin Pyrolysis Vapors, Over Iron Based Catalysts: Kinetics and Modeling of the Lignin to Aromatics Integrated Process, *Energy Fuels.* 27 (2013) 975–984. doi:10.1021/ef301971a.
- [63] R. Olcese, V. Carré, F. Aubriet, A. Dufour, Selectivity of Bio-oils Catalytic Hydrotreatment Assessed by Petroleomic and GC\*GC/MS-FID Analysis, *Energy Fuels.* 27 (2013) 2135–2145. doi:10.1021/ef302145g.
- [64] J.-Y. de Saint Laumer, E. Cicchetti, P. Merle, J. Egger, A. Chaintreau, Quantification in Gas Chromatography: Prediction of Flame Ionization Detector Response Factors from Combustion Enthalpies and Molecular Structures, *Anal. Chem.* 82 (2010) 6457–6462. doi:10.1021/ac1006574.
- [65] F. Xu, Effects of redox potential and hydroxide inhibition on the pH activity profile of fungal laccases, *J. Biol. Chem.* 272 (1997) 924–928.
- [66] M. Ragnar, C.T. Lindgren, N.-O. Nilvebrant, pK<sub>a</sub>-Values of Guaiacyl and Syringyl Phenols Related to Lignin, *J. Wood Chem. Technol.* 20 (2000) 277–305. doi:10.1080/02773810009349637.



## Chapter VII: Antioxidant Properties of Phenolic Compounds

Laëtitia Cesari<sup>1</sup>, Fabrice Mutelet<sup>1</sup>, Laetitia Canabady-Rochelle<sup>1\*</sup>

1 : Université de Lorraine, Laboratoire Réactions et Génie des Procédés (LRGP, UMR CNRS-UL 7274), 1 rue Grandville, 54000 Nancy, France

Article à soumettre.

### Résumé

Les composés phénoliques régulièrement présents dans les bio-huiles sont susceptibles de présenter des propriétés anti-oxydantes. Dans ce dernier chapitre, cinq tests de propriétés anti-oxydantes (réactif de Folin-Ciocalteu, test antiradicalaire, chélation d'ions métalliques (fer et cuivre) et pouvoir réducteur) sont effectués sur huit composés phénoliques. Afin de pouvoir comparer les propriétés des composés phénoliques, les résultats sont normalisés via une molécule de référence spécifique à chacun des tests. L'étude des propriétés étudiées suivant un rang de concentration permet de déterminer un indice (GAER, TEAC, EECC ou AERC) qui quantifie la propriété antioxydante. Les composés étudiés présentent un fort pouvoir antiradicalaire et un pouvoir réducteur, mais une chélation aux métaux relativement faible.

**Abstract**

The thermochemical conversion of biomass such as pyrolysis or liquefaction provides bio-oils containing molecules, which present antioxidant properties and hence some potential industrial applications in foods, cosmetics or pharmaceuticals. Five different antioxidant tests were performed on eight phenolic compounds, which are common surrogates found in lignin bio-oils: phenol, guaiacol, syringol, pyrocatechol, o-, m-, p-cresol and vanillin. Results were compared to reference molecules in order to classify the phenolic compounds towards each antioxidant mechanism (*i.e.* iron or copper chelating capacity, radical scavenging capacity, reducing power and response to the Folin-Ciocalteu's reagent). The studied phenolic compounds do not present a high transition metal chelation ability but they exhibit good reducing power and radical scavenging activity. The adaptation of the Folin-Ciocalteu's assay allowed the determination of a Gallic Acid Equivalent Response (GAER), index defined by analogy to the TEAC (Trolox Equivalent Antioxidant Capacity) one, for which guaiacol is the most responsive molecule.

## VII-1. Introduction

Phenolic compounds can be used for various industrial applications in foods, cosmetics or pharmaceuticals among them, food additives, food flavors, drugs or perfumery [1–3]. These molecules, regularly found in all kind of vegetal sources (*i.e.* woods, straw, agricultural residues) can be produced from biomass materials upon thermochemical conversion such as pyrolysis or liquefaction. Indeed, the thermochemical conversion of lignin produces bio-oils, rich in a variety of chemicals, especially phenolic compounds [4–6]. Among them, some compounds contain one or more hydroxyl groups associated to the aromatic ring. Phenolic moieties are present in wide variety of compounds in lignin bio-oils, in monomers or in oligomers, depending on the biomass source, on the process conditions and catalysts used [4–7].

Phenolic compounds produced from lignin have risen more and more interests [8,9] considering their biological activities reported in the literature. Many of them present antiallergenic, antimicrobial, antiviral [10], cardio-protective activities [11] or beneficial effects against hormone-dependent breast tumors [12]. Among various bioactivities, the antioxidant properties are a topic of high interest [13–16] especially for phenolic acids [17–21] or phenolic derivatives [22–24].

The antioxidant capacity of a biomolecule gathers many and various chemical mechanisms, classified into two main types based either on a hydrogen atom transfer (HAT) or on an electron atom transfer (ET) [25]. Various antioxidant capacity tests are reported in the literature [13–26] involving either an HAT or ET-based chemical reaction that are media dependent (solvent, pH, etc.). The ET-based chemical reaction includes several common assays such as the TEAC (Trolox Equivalent Antioxidant Capacity), the response to the Folin-Ciocalteu's reagent (FCR) or even the transition metal ion chelating activity, which can be determined as an indirect antioxidant method. Indeed in living organisms, the presence of iron catalyzes the Haber-Weiss reaction ( $\bullet\text{O}_2^- + \text{H}_2\text{O}_2 \rightarrow \bullet\text{OH} + \text{OH}^- + \text{O}_2$ ) [27]. During the first step of this former reaction, the iron oxidation degree is reduced by a free radical molecule (radical dioxygen  $\bullet\text{O}_2^-$ ). The second step of the Haber-Weiss reaction, the so-called Fenton reaction, produces a hydroxide radical molecule ( $\bullet\text{OH}$ ) by oxidation of the iron. Therefore, the presence of an iron-chelating molecule would limit oxidation while inhibiting the production of reactive oxygen species.

Among the antioxidant properties, phenolic compounds are likely to act as scavengers. For example, the investigation of o-, m- and p-cresol by Yeung et al demonstrated that all three

cresols acted as H<sub>2</sub>O<sub>2</sub> scavengers [16]. Moreover, their 50% inhibitory concentration (IC<sub>50</sub>) decrease as follows: o-cresol > p-cresol > m-cresol.

Due to the presence of phenolic compounds in bio-oils, many studies directly evaluated the antioxidant properties of bio-oils for their further valorization. Bio-oils composition differs from one another in their phenolic compounds depending on the biomass source and the thermochemical process applied. Moreover, due to their complex mixture, it is very difficult to determine the compounds of interest towards one antioxidant property, and the presence of other chemical classes of molecules can interfere with the monophenols' response. Dobelet al (2011) studied the radical scavenging activity and the inhibition of lipid oxidation of the phenolic fractions of wood pyrolytic. More recently, Qazi et al (2017) [28] studied the antioxidant activity of the lignins derived from fluidized-bed fast pyrolysis. In their work, the 2,2-diphenyl-1-picrylhydrazyl radical scavenging activity (DPPH), the total phenolic content (TPC) and the trolox equivalent antioxidant capacity (TEAC) were investigated and significant correlations were observed between the various antioxidant indices. As reported in Hussin et al (2014) who studied ethanol organosolv lignin obtained from oil palm fronds, free phenolic hydroxyl groups are mainly reported responsible of antioxidant activity while aliphatic hydroxyl groups have an opposite effect on the radical scavenging activity [29]. The main studies on antioxidant properties of various bio-oils are reviewed in Table VII-1.

In this work, we investigated the antioxidant properties of phenolic compounds regularly found in lignin bio-oils [40–44]: *i.e.* phenol, guaiacol, syringol, pyrocatechol, o-, m-, p-cresol and vanillin. First the Folin-Ciocalteu assay was carried out on phenolic compounds. Although this former method is convenient, simple and reproducible to quantify total polyphenols, this assay presents some limitations. Among them, it is not specific enough to quantify bio-oils since various phenolic compounds have various responses [39]. Lastly, this reagent can be interfered by other non-phenolic reducing molecules [39]. Hence, we further investigated three other complementary antioxidant tests (*i.e.* metal ion chelating capacity, radical scavenging capacity, and reducing power) to assess the antioxidant behavior of these compounds in details.

**Table VII-1** : Mini-review on the literature concerning the antioxidant properties of bio-oils.

Lignin or lignin-derived bio-oils	Antioxidant tests performed	Reference
Ethanol organosolv lignin from oil palm fronds	Oxygen uptake measurement	[30]
Lignin derived from fluidised-bed fast pyrolysis	Radical scavenging activities (DPPH, TEAC) Total phenolic content	[28]
Wood pyrolytic oil obtained by fast pyrolysis	Radical scavenging activities (DPPH, TEAC, hypoxanthine/xanthine oxidase) Inhibition of lipid oxidation	[31]
Phenolics derived from pyrolysis oil	Antioxidative effect studied on diesters and Poly- $\alpha$ -olefins ATSM standards	[32]
Pyrolytic lignins	Radical scavenging activities (DPPH, TEAC)	[33]
Technical lignin (BiologninTM)	Radical scavenging activities (DPPH, TEAC)	[34]
Lignin	Radical scavenging activities (DPPH)	[35]
Slow pyrolysis bio-oil of birch wood	Mihaljevic, Rancimat and PDSC test methods	[36]
Pyrolysis bio-oils	Radical scavenging activities (TEAC)	[37]
Hydrothermal lignocellulosic bio-oil	Oxidation stability measurement (PetroOXY equipment)	[38]
Fast pyrolysis bio-oil	Total phenol quantification (Folin-Ciocalteu)	[39]

## VII-2. Materials and Method

### VII-2.1. Chemicals

The studied phenolic compounds (*i.e.* phenol (CAS 108-95-2), guaiacol (CAS 90-05-1), syringol (CAS 91-10-1), pyrocatechol (CAS 120-80-9), o-cresol (CAS 95-48-7), m-cresol (CAS 108-39-4), p-cresol (CAS 106-44-5) and vanillin (CAS 121-33-5)) were supplied by Sigma Aldrich (see Appendix V for structures and properties of these phenolic compounds, Table S1). Trolox (CAS 53188-07-1), gallic acid (CAS 149-91-7), and ascorbic acid (CAS 62624-30-0), the reference molecules used in antioxidant tests, were supplied by Sigma Aldrich. Ethylenediaminetetraacetic acid (EDTA; CAS 60-00-4) was provided by FlukaChemie. The reagents 2,2'-azino-bis(3-ethylbenzothiazoline-6-sulphonic acid) (ABTS; CAS 30931-67-0), Na<sub>2</sub>HPO<sub>4</sub> (CAS 10039-32-4), NaH<sub>2</sub>PO<sub>4</sub> (CAS 13472-35-0), K<sub>2</sub>S<sub>2</sub>O<sub>8</sub> (CAS

7727-21-1), Ferrozine (CAS 63451-29-6), FeCl<sub>2</sub> (7758-94-3), potassium ferricyanide (CAS 13746-66-2), FeCl<sub>3</sub> (CAS 7705-08-0), Na<sub>2</sub>CO<sub>3</sub> (CAS 497-19-8), Folin-Ciocalteu's phenol reagent, hexamine (CAS 100-97-0) and KCl (CAS 7447-40-7) were supplied by Sigma-Aldrich. Tri-Chloroacetic Acid (TCA) was provided from Fischer Scientific (CAS 76-03-9). All chemicals were used as received without any further purification. Deionized water (conductivity of 18.2 mΩ.cm<sup>-1</sup>) was used for all experiments. In the various experimental protocols, all the concentrations referred to the final concentration in solution, taking into account the volume of all the added reagents. All tests were carried out in microplate reader, which enable investigation of each molecule in a range of concentration.

### VII-2.2. Dosage of phenols by the Folin-Ciocalteu method

The response of each phenolic compound towards the Folin-Ciocalteu method was determined by the method of Singleton and Rossi [45] and adapted for a microplate by Mussatto et al [46]. A 5-μL volume of aqueous solutions of phenolic compounds and gallic acid used as reference were deposited in 96-well microplate. Then, 60 μL of sodium carbonate solution (7.5 % w/v), 15 μL of Folin-Ciocalteu reagent (1 N) and 200 μL of ultrapure water were added to each well. The plates were incubated at 60°C for 5 min. After cooling at room temperature (25°C), the absorbance was read at 760 nm. Phenolic compounds were studied in the range of 0 to 15 mM and gallic acid between 0 and 8 mM. The chemical reaction involved in this test is schematized in Figure S1 (Appendix V, panel a). An increase of the absorbance corresponds to a higher concentration of phenols in the system, according to the Beer-Lambert equation:

$$A = \varepsilon \cdot l \cdot C \quad (1)$$

Where A is the absorbance,  $\varepsilon$  the molar extinction coefficient (M<sup>-1</sup>.cm<sup>-1</sup>), l the path length of the light beam through the sample (cm<sup>-1</sup>) and C the concentration.

The response factor of the phenolic compounds was compared to the gallic acid and expressed as a Gallic Acid Equivalent Response (GAER) calculated as follows:

$$GAER = \frac{a_s}{a_{GA}} \quad (2)$$

With  $a_s$  and  $a_{GA}$ , the line slopes of absorbance plotted as a function of concentration (mM) for phenolic samples and gallic acid, respectively.

The value of the 50% effective concentration (EC<sub>50</sub>) was calculated as follows:

$$EC_{50} = \frac{A_{max}}{2 \cdot a_s} \quad (3)$$

Where  $A_{max}$  is the maximum of absorbance reached by the studied compound and  $a_s$  the line slopes of absorbance plotted as a function of concentration (mM).

### VII-2.3. Transition metal chelating capacity

#### VII-2.3.1. Iron(II) chelating activity

The ability of phenolic compounds to chelate  $Fe^{2+}$  was adapted from a method described by Dinis et al. [47]. This test gives the potential of a studied molecule to act as an indirect antioxidant while inhibiting or delaying the radical production due to the Haber-Weiss and Fenton reactions. A volume of 277.5  $\mu$ L of aqueous phenolic solutions (at various concentrations) was deposited in the 96-well microplate. 7.5  $\mu$ L of aqueous iron(II) chloride solution (2 mM) was added to the samples. After 3 min of incubation at room temperature (25°C), 15  $\mu$ L of aqueous ferrozine solution (5 mM) were added to each well. The absorbance was measured at 562 nm (corresponding to the iron(II)-ferrozine complex) after 10 min of incubation at room temperature (25°C). EDTA, a metal-chelating agent, was used as reference from 0 to 100  $\mu$ M. Phenol and pyrocatechol were tested from 0 to 600  $\mu$ M and until 150  $\mu$ M for the other phenolic compounds. The chemical reaction involved in the iron(II) chelation activity is described elsewhere [48]. The increase in the chelating capacity was visualized by a decrease of absorbance. The iron chelating capacity was quantified as follows:

$$Iron\ chelation\ capacity\ (\%) = \frac{(A_0 - A_s)}{A_0} \times 100 \quad (4)$$

Where  $A_0$  and  $A_s$  are the blank (distilled water) and the sample absorbance, respectively.

The EDTA Equivalent iron(II) Chelation Capacity (EECC) index was determined by comparison of the line slope for each phenolic compound towards the EDTA one, from the following expression:

$$EECC = \frac{a_s}{a_{EDTA}} \quad (5)$$

With  $a_s$  and  $a_{EDTA}$ : the line slopes of iron chelating activity (%) plotted as a function of concentration ( $\mu$ M) for phenolic samples and EDTA, respectively.

The value of the 50% effective concentration ( $EC_{50}$ ) was calculated as follows:

$$EC_{50} = \frac{50}{a_s} \quad (6)$$

With  $a_s$  the line slopes of iron chelating activity (%) plotted as a function of concentration ( $\mu\text{M}$ ).

### VII-2.3.2. Copper(II) chelating activity

The ability of phenolic compounds to chelate  $\text{Cu}^{2+}$  was determined by the method of Wu et al [49] with some modifications. This method is complementary to the iron-chelating assay since, the copper (II)-chelating test was carried out in another pH.

First, a hexamine buffer solution was prepared constituted of 10 mM hexamine and 10 mM KCl. A copper(II) solution was prepared with 3 mM  $\text{CuSO}_4$  dissolved in this former hexamine buffer. Both former solutions were adjusted at pH 5 with 1N HCl. Then, solutions of phenolic compounds and EDTA (the metal-chelating reference) were prepared in the hexamine buffer. A volume of 143  $\mu\text{L}$  of sample solutions were mixed with 143  $\mu\text{L}$  of copper(II) solution. Then, 14  $\mu\text{L}$  of murexide (1mM in ultrapure  $\text{H}_2\text{O}$ ) was added. After 3 min of incubation at room temperature ( $25^\circ\text{C}$ ), the absorbance was read at 485 nm and 520 nm, corresponding to the absorbance of copper(II)-murexide complex and to the free murexide, respectively. The ratio of absorbance measured at the two wavelengths ( $A_{485}/A_{520}$ ) was considered proportional to the copper(II) free in solution. Phenolic compounds were studied in a range of concentration comprised within 0 and 50 mM (and up to 90 mM for pyrocatechol) and between 0 and 2 mM for EDTA. The chemical reaction involved in this test is schematized in Figure S1 (Appendix V, panel b). The copper chelation capacity was quantified by the Equation 7:

$$\text{Copper chelation capacity (\%)} = \frac{\left(\frac{A_{485}}{A_{520}}\right)_0 - \left(\frac{A_{485}}{A_{520}}\right)_s}{\left(\frac{A_{485}}{A_{520}}\right)_0} \times 100 \quad (7)$$

Where  $A_0$  and  $A_s$  are respectively the blank (hexamine buffer) and the sample absorbance.

The EDTA Equivalent copper(II) Chelation Capacity (EECC) index and the value of the 50% effective concentration ( $EC_{50}$ ) were determined by the same equations than those described in the iron chelation capacity test (Equation 5 and Equation 6, respectively).

### VII-2.4. Radical scavenging activity

The radical scavenging activity of each phenolic compound solution was investigated by the TEAC method described by Sadat et al [50] with some modifications. A 7 mM solution of

ABTS was prepared in ultrapure water in the presence of potassium persulfate (2.45 mM) to generate the ABTS<sup>•+</sup> radical. The solution was stored in the dark for at least 4 hours. Then, the ABTS<sup>•+</sup> solution was diluted in phosphate buffer (pH 7.4) to reach an absorbance value of  $0.70 \pm 0.02$  at 734 nm. The diluted ABTS<sup>•+</sup> solution (150  $\mu$ L) was mixed with phenolic or Trolox buffer solutions (150  $\mu$ L) directly in a 96-well microplate. After 10 min of incubation at 30°C, the absorbance was measured at 734 nm. Phenolic compounds were studied from 0 to 180  $\mu$ M and Trolox from 0 to 32  $\mu$ M. The chemical reaction involved in this radical scavenging test is described elsewhere [48]. An absorbance decrease at 734 nm corresponds to an increase of the radical scavenging activity. This activity was calculated using the following equation:

$$\text{Radical scavenging activity (\%)} = \frac{(A_0 - A_s)}{A_0} \times 100 \quad (8)$$

Where  $A_0$  and  $A_s$  correspond respectively to the blank (buffer) and the sample absorbance.

The Trolox Equivalent Antioxidant Capacity (TEAC) index was determined by the comparison of the line slope for each compound towards the one obtained for Trolox.

$$\text{TEAC} = \frac{a_s}{a_{\text{Trolox}}} \quad (9)$$

With  $a_s$  and  $a_{\text{Trolox}}$ , the line slopes of radical scavenging activity (%) plotted as a function of concentration ( $\mu$ M) for phenolic samples and for Trolox, respectively.

The 50% effective concentration ( $EC_{50}$ ) value of each compound was calculated as in Equation 6.

### VII-2.5. Reducing power

The reducing capacity of each phenolic compound was determined by the method of Oyaizu [51] with some modifications. Phenolic compounds and ascorbic acid (used as reference) solutions were prepared in 200 mM phosphate buffer (pH 6.6). A 70- $\mu$ L volume of sample or reference solution at various concentrations was mixed with 35  $\mu$ L of 1% (m/v) potassium ferricyanide (in phosphate buffer) in a 96-well microplate. After 20 min of incubation at 50°C, 135  $\mu$ L of ultrapure water, 33  $\mu$ L of trichloroacetic acid (10% m/v in phosphate buffer) and 27  $\mu$ L of iron(III)chloride (0.1% m/v in H<sub>2</sub>O) were added to the former mixtures. After 10 min of incubation at room temperature (25°C), the absorbance was read at 700 nm. The ranges of concentration varied from 0 to 140  $\mu$ M for ascorbic acid, from 0 to 160  $\mu$ M for guaiacol, syringol and pyrocatechol, and until 100 mM for the other phenolic compounds. The chemical

reaction involved in the reducing power is described elsewhere [48]. In this test, an increase of the reducing power was visualized by an increase of the absorbance at 700 nm. The reducing capacity of the compounds was calculated as follows:

$$\text{Reducing capacity (\%)} = \left(1 - \frac{A_0 - A_s}{A_0}\right) \times 100 \quad (10)$$

Where  $A_s$  is the sample absorbance.  $A_0$  is the absorbance of a 66  $\mu\text{M}$  Prussian blue solution measured in the same reaction medium. Here,  $A_0$  was equal to 0.8.[48]

The comparison of the line slope for each phenolic compound towards the one for ascorbic acid allowed the determination of the Ascorbate Equivalent Reducing Capacity (AERC) index.

$$\text{AERC} = \frac{a_s}{a_{\text{Ascorbate}}} \quad (11)$$

With  $a_s$  and  $a_{\text{Ascorbate}}$ , line slopes of reducing capacity (%) plotted as a function of concentration ( $\mu\text{M}$ ) for phenolic samples and ascorbate, respectively.

The value of the 50% effective concentration ( $\text{EC}_{50}$ ) was calculated as in Equation 6.

## VII-3. Results and discussion

**Table VII-2:** Antioxidant properties of the studied phenolic compounds. a) GAER and EECC. b) TEAC and AERC.

a)

Compounds	Gallic acid equivalent response					Iron(II) chelation activity					Copper(II) chelation activity					
	a	GAER	SEM	EC50	SEM	a	EECC	SEM	EC50	SEM	a	EECC	SEM	EC50	SEM	
	mM <sup>-1</sup>			mM	mM	mM <sup>-1</sup>			mM	mM	mM <sup>-1</sup>			mM	mM	
Trolox	-	-	-	-	-	-	-	-	-	-	-	-	-	-	-	-
Ascorbate	-	-	-	-	-	-	-	-	-	-	-	-	-	-	-	-
EDTA	-	-	-	-	-	1939	1.00	0.00	0.03	0.00	19.07	1.000	0.00	2.62	0.06	
Gallic acid	4.74	1.00	0.00	0.35	0.00	-	-	-	-	-	-	-	-	-	-	-
Phenol	6.65	1.40	0.02	0.15	0.00	0.09	4.56E-05	1.66E-06	565	789.20	-	-	-	-	-	-
Guaiacol	7.55	1.59	0.02	0.17	0.00	0.06	3.11E-05	4.20E-06	830	106.88	0.24	1.26E-02	3.90E-04	207	10.60	
Syringol	5.05	1.07	0.01	0.27	0.00	0.09	4.68E-05	3.32E-06	550	52.19	-	-	-	-	-	-
Pyrocatechol	2.94	0.62	0.01	0.45	0.01	0.13	6.72E-05	2.61E-05	383	43.96	3.01	1.58E-01	6.21E-03	16.63	1.32	
O-cresol	5.98	1.26	0.01	0.21	0.00	0.04	1.96E-05	5.82E-06	1314	183.61	0.134	7.11E-03	2.97E-03	368	151	
M-cresol	5.80	1.22	0.01	0.19	0.00	0.08	4.13E-05	2.94E-06	623	60.45	0.04	2.20E-03	3.48E-04	1193	699	
P-cresol	5.31	1.12	0.01	0.23	0.00	0.03	1.28E-05	2.83E-06	2008	79.81	-	-	-	-	-	-
Vanillin	5.39	1.14	0.02	0.34	0.01	0.19	9.70E-05	3.26E-05	265	89.84	1.84	9.64E-02	2.66E-02	27.20	1.18	

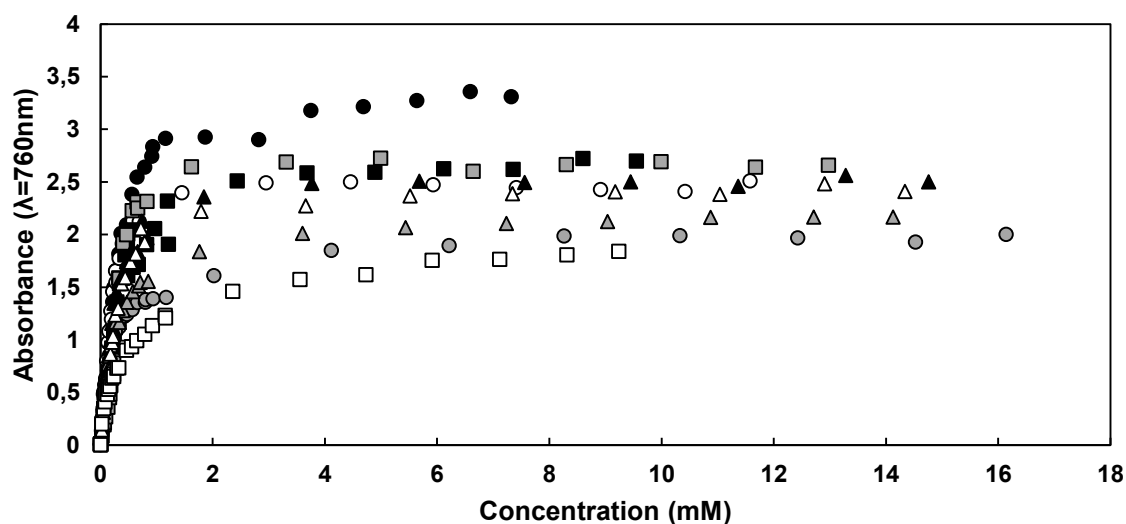
b)

Compounds	Radical scavenging activity					Reducing capacity				
	a $\mu\text{M}^{-1}$	TEAC	SEM	EC50 $\mu\text{M}$	SEM $\mu\text{M}$	a $\mu\text{M}^{-1}$	AERC	SEM	EC50 $\mu\text{M}$	SEM $\mu\text{M}$
Trolox	6.38	1.00	0.00	7.84	0.05	-	-	-	-	-
Ascorbate	-	-	-	-	-	1.21	1.00	0.00	41.24	0.89
EDTA	-	-	-	-	-	-	-	-	-	-
Gallic acid	-	-	-	-	-	-	-	-	-	-
Phenol	9.21	1.44	1.38E-03	5.43	0.03	1.40E-03	1.15E-03	1.77E-05	35714.29	672
Guaiacol	15.06	2.36	9.94E-03	3.32	0.04	1.42	1.17	0.02	35.19	0.30
Syringol	7.28	1.14	3.20E-03	6.87	0.03	2.11	1.74	0.03	23.66	0.08
Pyrocatechol	8.17	1.28	6.96E-03	6.12	0.07	5.83	4.81	0.11	8.58	0.03
O-cresol	15.60	2.45	1.45E-02	3.21	0.04	3.30E-02	2.72E-02	3.29E-04	1515	15.53
M-cresol	7.62	1.19	7.39E-03	6.57	0.08	3.80E-03	3.13E-03	2.00E-05	13157	297
P-cresol	18.42	2.89	1.01E-02	2.72	0.01	4.60E-02	3.79E-02	6.27E-04	1086	12.62
Vanillin	4.56	0.72	2.31E-03	10.96	0.09	1.44E-02	1.19E-02	1.84E-04	3472	44.26

### VII-3.1. Total phenols quantification by the Folin-Ciocalteu method

In this assay, the gallic acid molecule was used as the reference for comparison. The results are gathered in Table VII-2 and plotted in Figure VII-1. The linearization of the absorbance as a function of the concentration of the compounds is provided in supporting information (Figure S2). The GAER of the compounds decreases as follows: guaiacol > phenol > o-cresol > m-cresol > vanillin > p-cresol > syringol > gallic acid > pyrocatechol (Table VII-2 and Figure S3). All the phenolic compounds are in the same range of value (higher than 1) except for pyrocatechol, which has a GAER of 0.62. Indeed, it was evidenced that vicinal dihydroxyl phenols present a lower reactivity with the Folin-Ciocalteu's reactant if the alkali solution is put first in the mixture [15], that explains the lower value for the pyrocatechol assay. The  $EC_{50}$  response is inversely dependent of the slope of the molecules' response. Therefore, an increase of the response of the molecules towards the FCR corresponds to a lower  $EC_{50}$  (Figure S4).

**Figure VII-1:** Dosage of phenols by the Folin-Ciocalteu method: ● Reference (Gallic acid), ○ Phenol, ○ Guaiacol, ■ Syringol, □ Pyrocatechol, □ Vanillin, ▲ O-cresol, ▲ M-cresol, ▲ P-cresol.



In their phenolate forms, one electron can be easily removed from the phenolic structure. Indeed, the oxidation is favored by the decreasing acidity of the phenolic compounds. Hence according to their  $pK_a$  values (Table S1), the rank of acidity of phenolic compounds is the

following one, considering the lower the pKa, the stronger the acid: o-cresol < m- and p-cresol < gallicol and syringol < phenol < pyrocatechol < vanillin. Thus, guaiacol reacts more to the Folin-Ciocalteu's reagent than phenol. For the same reason, vanillin reacts less. Syringol is as acid as guaiacol, but the presence of the second methoxy group in syringol involves a steric effect that inhibits the oxidation reaction. Finally, cresols are the less acid studied molecules and their reactivity towards the Folin-Ciocalteu's reagent may be the highest. Yet, since the reactive media is at pH around 10, the cresols are probably still in their acid forms considering their respective pKa values.

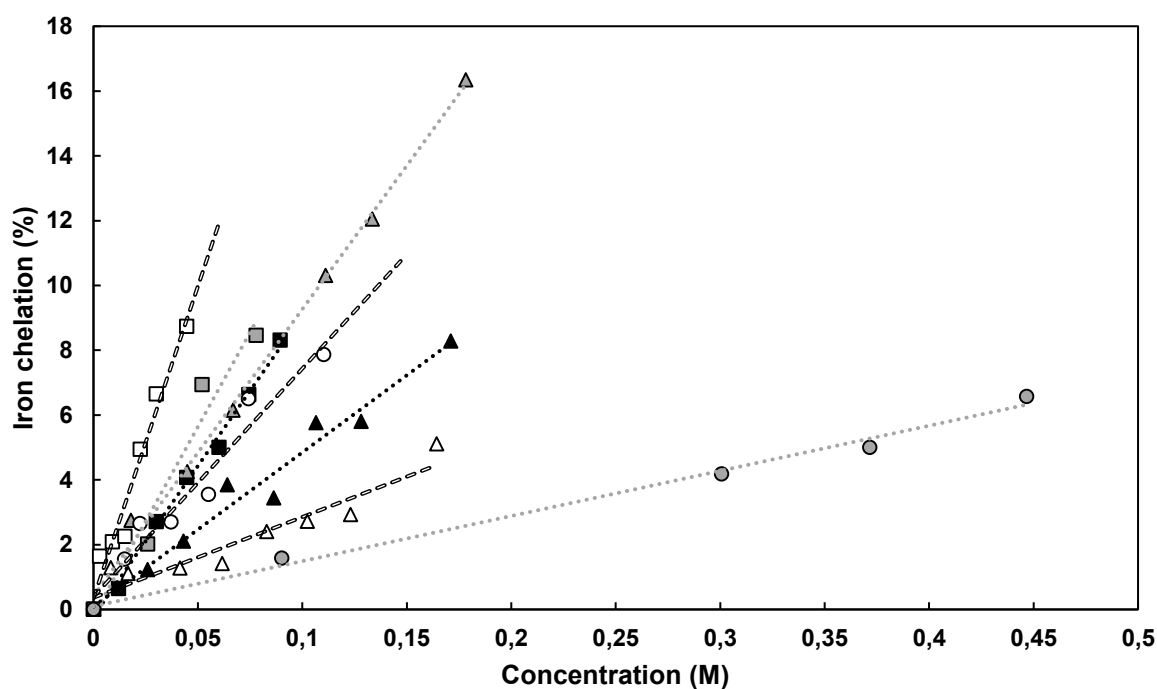
### VII-3.2. Iron(II) and Copper (II) chelating activity

The tests for the iron(II) and copper(II) chelation activity were adapted for microplate study. In both tests, the EDTA molecule was used as the reference for comparison. The results of metal transition chelating activity are displayed in Table VII-2.

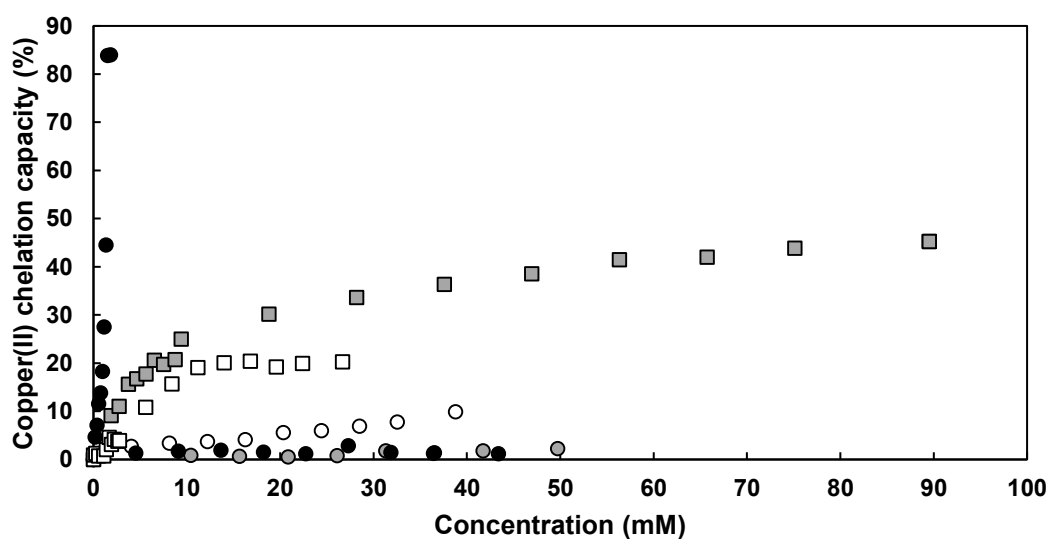
Figure VII-2 (panel a) shows the iron(II) chelation activity as a function of concentration. All of the phenolic compounds present a linear response towards the iron chelation capacity. The molecules were studied up to their limit of solubility in the solvent. In the range of concentration studied, their iron chelation capacity is very low. The comparison with EDTA gives values of EECC largely inferior to 1. Vanillin is the phenolic molecule with the higher EECC ( $9.5 \cdot 10^{-5}$ ) (see Table VII-2 and Figure S5), corresponding to the lower EC<sub>50</sub> value (Figure S6). These results are in good agreement with those reported by [17], who evidenced that the phenolic acids not bearing neither catechol nor galloyl moiety did not show any complex formation with iron.

**Figure VII-2:** Metal ion chelating activity. a) Iron(II) chelating activity: ● Phenol, ○ Guaiacol, ■ Syringol, □ Pyrocatechol, □ Vanillin, ▲ O-cresol, ▲ M-cresol, ▲ P-cresol. b) Copper(II) chelating activity: ● Reference (EDTA), ○ Guaiacol, □ Pyrocatechol, □ Vanillin, ▲ O-cresol, ▲ M-cresol.

a)



b)



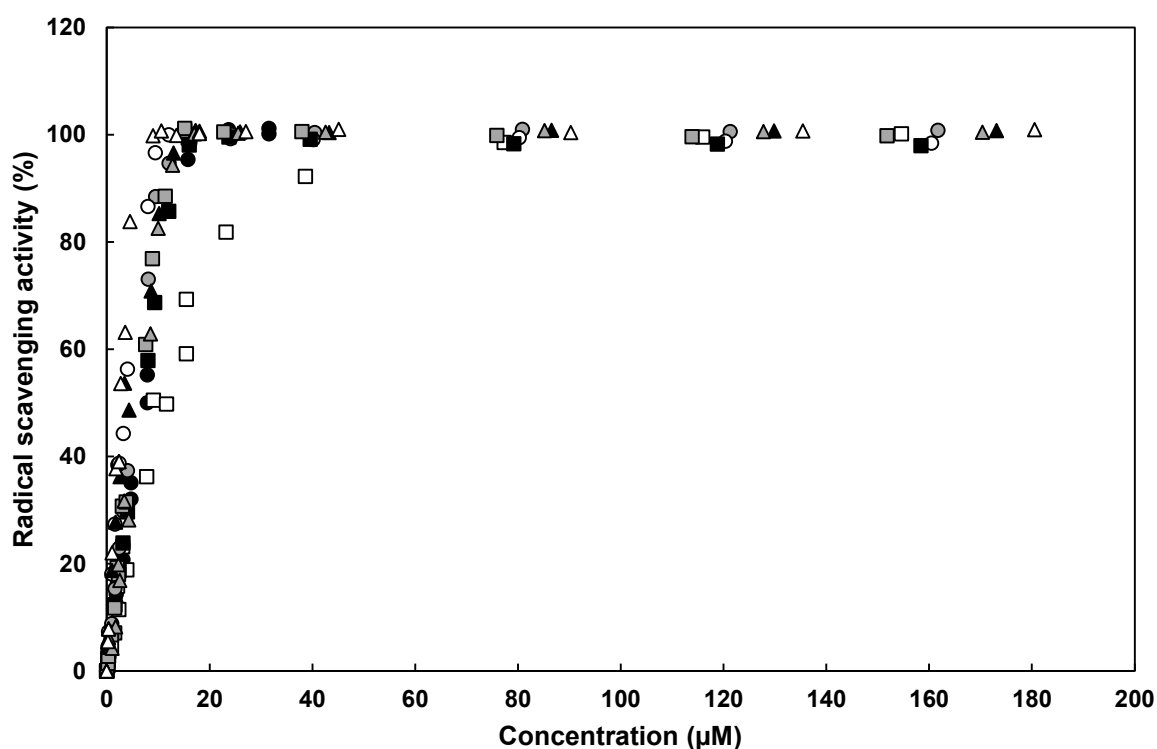
The copper(II) chelating activity test presents some interferences for syringol, pyrocatechol, and vanillin due to the natural absorption of these former molecules at the same wavelength than the murexide one. Indeed, the phenolic solutions turned orange upon the addition of the copper buffer even in the absence of murexide. Therefore, to overcome such interference phenomena between these former phenolic compounds and murexide, we carried out an additional control experiment, where murexide volume was replaced by water, in order to subtract the absorbance due to the phenolic compound in the absence of murexide. Thus, the optical path was not modified since the final volume in a well remained constant. The absorbance at a given wavelength was then calculated by the subtraction of the absorbance measured in the absence of murexide to the whole absorbance measured in the presence of murexide. This data treatment corrected the overestimation in the chelating capacity measurement, caused by the initial coloration. For instance, the syringol solution absorbed in the considered wavelength (*i.e.* orange coloration in the copper buffer), but syringol does not present any copper chelating activity. The copper(II) chelation activity is plotted in Figure VII-2 (panel b) as a function of concentration. The copper chelating capacity decreases as follows: EDTA > pyrocatechol > vanillin > guaiacol > o-cresol > m-cresol (Table VII-2 and Figure S7). Phenol, syringol and p-cresol do not present any copper chelating capacity. The presence of one substituent in ortho position towards the hydroxyl group seems to increase the copper chelation ability. Moreover, the more electronegative the substituent is (OH > OCH<sub>3</sub> > CH<sub>3</sub>), the higher the chelating power is (pyrocatechol > guaiacol > o-cresol). In the case of syringol, the presence of two methoxy groups (OCH<sub>3</sub>) provide a steric effect that probably reduce the chelating capacity. The corresponding EC<sub>50</sub> values are displayed in Figure S8 when calculation was possible. The EC<sub>50</sub> values for the copper chelating capacity are lower compared to the EC<sub>50</sub> of the iron chelating capacity (Figure S6). For example, pyrocatechol that presents both iron and copper chelating capacities has an EC<sub>50</sub> of 383 mM in the case of the iron chelation and 16.63 mM for the copper chelation. Hence, pyrocatechol presents a higher affinity for copper (II) as compared to iron (II).

### VII-3.3. Radical scavenging activity

The radical scavenging activity of the phenolic compounds was measured by the ABTS test where the unstable free cationic radical ABTS<sup>o+</sup> can potentially receive one electron by the

investigated molecule, involving a discoloration of the ABTS<sup>•+</sup> dark blue solution. Trolox<sup>®</sup> was used as a radical scavenger reference for the comparison of the radical scavenging activities of phenolic compounds. Molecules were studied in a range of concentrations up to observe saturation (Figure VII-3). Regressions were made on the linearization range of studied concentrations (Figure S9) and respective results (a, TEAC and EC<sub>50</sub>) are summarized in Table VII-2 (panel b).

**Figure VII-3:** Radical scavenging activity: ● Reference (Trolox), ○ Phenol, ○ Guaiacol, ■ Syringol, ■ Pyrocatechol, □ Vanillin, ▲ O-cresol, ▲ M-cresol, ▲ P-cresol.



According to the TEAC and the EC<sub>50</sub> values (Figures S10 and S11, respectively), the radical scavenging activity decreases for the phenolic compounds as follows: p-cresol > o-cresol > guaiacol > phenol > pyrocatechol > m-cresol > syringol > trolox > vanillin. All the investigated phenolic compounds present a higher radical scavenging activity than Trolox at the exception of vanillin (TEAC = 0.72; EC<sub>50</sub> = 10.96 µM). This result is surprising because at this pH (pH 7.4), vanillin is partially ionized in the reaction medium and therefore should present a higher antioxidant capacity than the other phenolic compounds.

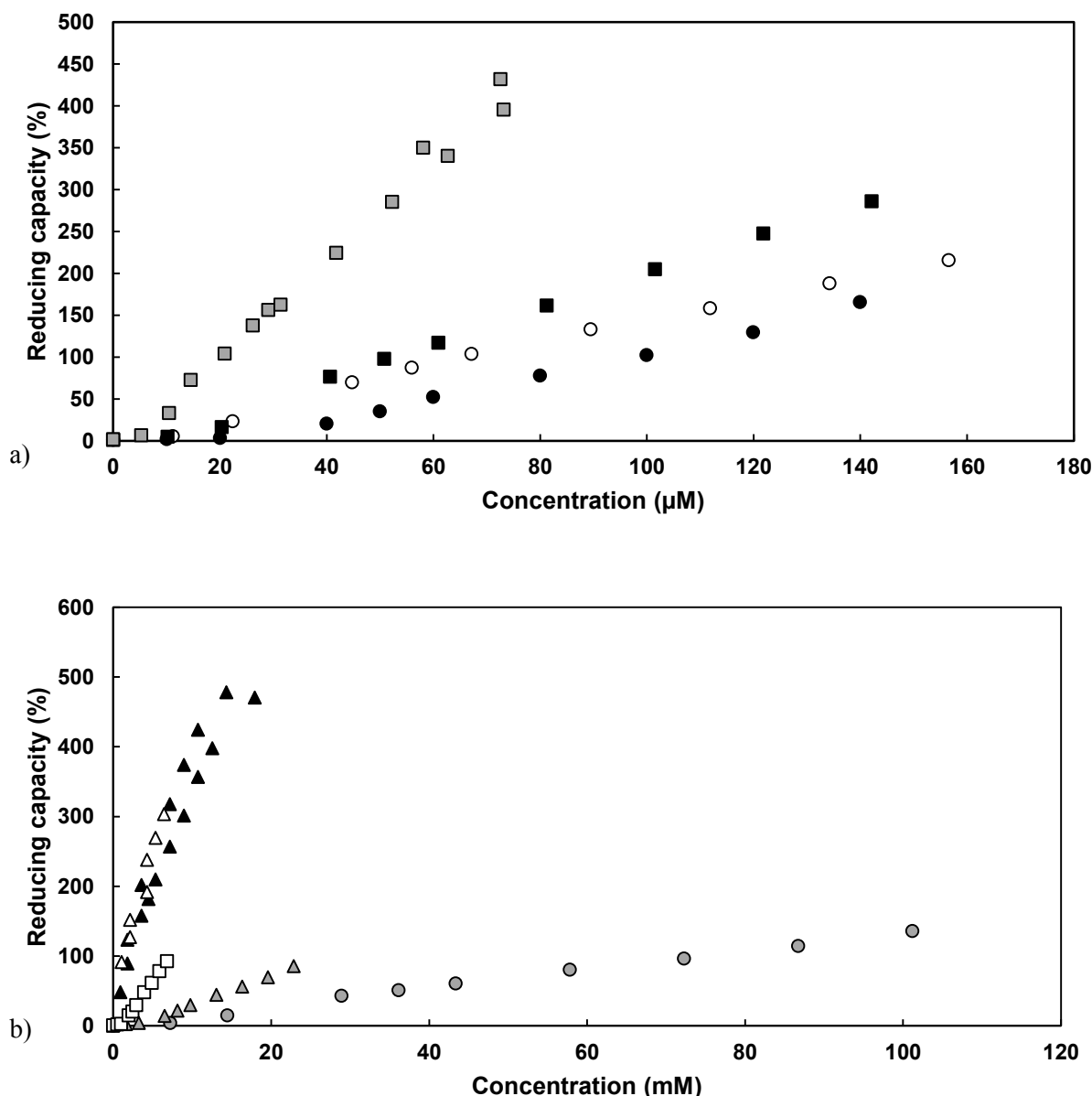
The presence of a single donor group (*i.e.* CH<sub>3</sub>, OCH<sub>3</sub> or OH) in para or ortho position increases the number of resonance forms and therefore increases the radical scavenging capacity of the molecule compared to phenol. Secondly, the more the substituent presents a donor behavior (OH > OCH<sub>3</sub> > CH<sub>3</sub>), the less the radical scavenging capacity will be. Considering this former donor scale, pyrocatechol presents therefore a radical scavenging capacity lower than guaiacol, itself lower than o-cresol. In the same way, the further the substituent is, then decreasing its donor effect, the higher the scavenging capacity will be (p-cresol > o-cresol). Nenadis et al [52] studied the influence of the position of the hydroxyl groups in phenolic compounds and their results are in good agreements with our observations. In their study, former authors reported a radical scavenging activity higher for resorcinol and phloroglucin than pyrocatechol or hydroquinone. The hydroxyl group in meta position presents only an inductive attractive effect that stabilizes the molecule whereas the ortho or para positions have a mesomeric repulsive effect. The results are surprising because the trend in phenolic compounds 'structure is known to increase the antioxidant property with the increase of the donor effect in the substituent group and the number of substituents [53,54,21]. Therefore, pyrocatechol is supposed to be the most reactive molecule, followed by syringol and guaiacol. Nevertheless, the presence of solvent must be considered since it can interfere in the system [55] and make difficult the possibility to define structure-activity relationships.

Finally, in accordance with the literature, the presence of a single methoxy group (*i.e.* guaiacol) increases the radical scavenging capacity compared to phenol [56]. Inversely, the presence of several methoxy groups, such as in syringol, provides a steric effect that can reduce the hydroxyl group availability and therefore decrease the radical scavenging capacity.

#### VII-3.4. Reducing capacity

The reducing capacity was evaluated in comparison to the ascorbate as a reducing reference. In this aim, the Oyaizu's test [57] was modified and miniaturized as in Canabady-Rochelle et al [48]. Linear relationships are found between the reducing capacity and the concentration of all the compounds (Figures VII-4). The studied phenolic compounds can be divided in two families: guaiacol, syringol and pyrocatechol constitutes the first one (panel a), phenol, cresols and vanillin the second one (panel b).

**Figure VII-4:** Reducing capacity. Panel a) ● Reference (ascorbic acid), ○ Guaiacol, ■ Syringol, □ Pyrocatechol. Panel b) ○ Phenol, □ Vanillin, ▲ O-cresol, △ M-cresol, △ P-cresol.



Indeed, the reducing capacity of guaiacol, syringol and pyrocatechol is observed at low concentration (from 0 to 160  $\mu\text{M}$ ). These molecules also present an AERC higher than 1 (Table VII-2, panel b and Figure S12, panel a). Therefore, the corresponding  $\text{EC}_{50}$  are low ( $< 40 \mu\text{M}$ ), meaning that former phenolic compounds have high reducing capacities. On the other side, the reducing capacity of phenol, cresols and vanillin had to be investigated at higher concentration, from 0 up to 100 mM. In that case, the resulting AERC is far below 1 (Table VII-2, panel b and

Figure S12, panel b). The corresponding  $EC_{50}$  are higher, going up to 35 mM for phenol (Figure S13) indicating a low reducing capacity of such molecules.

Therefore, the presence of an oxygenated substituent ( $OCH_3$  or  $OH$ ) may directly impact the reducing capacity of the molecules. Yet, the presence of the aldehyde group in the vanillin molecule stabilizes the negative charge in the phenolate structure and hinders its reducing capacity ( $AERC = 1.19 \times 10^{-2}$ ;  $EC_{50} = 3.472$  mM).

#### **VII-4. Conclusion**

In this work, various tests were performed to investigate the antioxidant properties of eight phenolic compounds potentially extractable from bio-oils. The comparison with reference molecules allows the determination of 4 indices to classify the response of the compounds to the reference one for each studied test. All phenolic compounds present a radical scavenging capacity, with the best TEAC values obtained for guaiacol, o-cresol and p-cresol. Moreover, all phenolic compounds present high reducing capacities, especially pyrocatechol, guaiacol and syringol. Guaiacol is also the most reactive molecule towards the Folin-Ciocalteu's reagent. Finally, all the studied compounds present difficulties to chelate transition metals. Only pyrocatechol and vanillin show a low chelation capacity.

Thus, some of these compounds could be used for their antioxidant properties, particularly guaiacol and pyrocatechol. These tests could be used for the determination of the antioxidant properties of bio-oils (compared to reference molecules). Yet, some precaution must be made. For example, the Folin-Ciocalteu's reagent is known to interact with other non-phenolic molecules. Besides, the copper chelation assay showed some interference phenomenon. Lastly, the choice of the antioxidant properties to study on a given bio-oil must be based on its composition. Indeed, this work demonstrated that monophenols are not very good iron chelators but have huge reducing capacity.

## References

- [1] F. Helmut, V. Heinz-Werner, H. Toshikazu, P. Wilfried, Phenol derivatives, Ullmann's Encycl. Ind. Chem. VCH Ger. 19 (1985) 299–357.
- [2] F. Ikegami, T. Sekine, Y. Fujii, [Anti-dermatophyte activity of phenolic compounds in “mokusaku-eki”], Yakugaku Zasshi. 118 (1998) 27–30.
- [3] J.A. Maga, I. Katz, Simple phenol and phenolic compounds in food flavor, C R C Crit. Rev. Food Sci. Nutr. 10 (1978) 323–372. doi:10.1080/10408397809527255.
- [4] D.J. Nowakowski, A.V. Bridgwater, D.C. Elliott, D. Meier, P. de Wild, Lignin fast pyrolysis: Results from an international collaboration, J. Anal. Appl. Pyrolysis. 88 (2010) 53–72. doi:10.1016/j.jaap.2010.02.009.
- [5] R. Olcese, V. Carré, F. Aubriet, A. Dufour, Selectivity of Bio-oils Catalytic Hydrotreatment Assessed by Petroleomic and GC\*GC/MS-FID Analysis, Energy Fuels. 27 (2013) 2135–2145. doi:10.1021/ef302145g.
- [6] R.N. Olcese, G. Lardier, M. Bettahar, J. Ghanbaja, S. Fontana, V. Carré, F. Aubriet, D. Petitjean, A. Dufour, Aromatic Chemicals by Iron-Catalyzed Hydrotreatment of Lignin Pyrolysis Vapor, ChemSusChem. 6 (2013) 1490–1499. doi:10.1002/cssc.201300191.
- [7] R. Bayerbach, D. Meier, Characterization of the water-insoluble fraction from fast pyrolysis liquids (pyrolytic lignin). Part IV: Structure elucidation of oligomeric molecules, J. Anal. Appl. Pyrolysis. 85 (2009) 98–107. doi:10.1016/j.jaap.2008.10.021.
- [8] C. Amen-Chen, H. Pakdel, C. Roy, Production of monomeric phenols by thermochemical conversion of biomass: a review, Bioresour. Technol. 79 (2001) 277–299. doi:10.1016/S0960-8524(00)00180-2.
- [9] J.N. Murwanashyaka, H. Pakdel, C. Roy, Separation of syringol from birch wood-derived vacuum pyrolysis oil, Sep. Purif. Technol. 24 (2001) 155–165. doi:10.1016/S1383-5866(00)00225-2.
- [10] F.L. Mota, A.J. Queimada, S.P. Pinho, E.A. Macedo, Aqueous Solubility of Some Natural Phenolic Compounds, Ind. Eng. Chem. Res. 47 (2008) 5182–5189. doi:10.1021/ie071452o.
- [11] H.K. Obied, M.S. Allen, D.R. Bedgood, P.D. Prenzler, K. Robards, R. Stockmann, Bioactivity and Analysis of Biophenols Recovered from Olive Mill Waste, J. Agric. Food Chem. 53 (2005) 823–837. doi:10.1021/jf048569x.
- [12] M. Kampa, V.-I. Alexaki, G. Notas, A.-P. Nifli, A. Nistikaki, A. Hatzoglou, E. Bakogeorgou, E. Kouimtzoglou, G. Blekas, D. Boskou, A. Gravanis, E. Castanas, Antiproliferative and apoptotic effects of selective phenolic acids on T47D human breast cancer cells: potential mechanisms of action., Breast Cancer Res. 6 (2004) R63. doi:10.1186/bcr752.
- [13] R.C. Hider, Z.D. Liu, H.H. Khodr, Metal chelation of polyphenols, Methods Enzymol. 335 (2001) 190–203.
- [14] V.L. Singleton, R. Orthofer, R.M. Lamuela-Raventós, [14] Analysis of total phenols and other oxidation substrates and antioxidants by means of folin-ciocalteu reagent, in: Methods Enzymol., Elsevier, 1999: pp. 152–178. doi:10.1016/S0076-6879(99)99017-1.
- [15] A.C. Jennings, The determination of dihydroxy phenolic compounds in extracts of plant tissues, Anal. Biochem. 118 (1981) 396–398. doi:10.1016/0003-2697(81)90600-X.
- [16] S.Y. Yeung, W.H. Lan, C.S. Huang, C.P. Lin, C.P. Chan, M.C. Chang, J.H. Jeng, Scavenging property of three cresol isomers against H<sub>2</sub>O<sub>2</sub>, hypochlorite, superoxide and hydroxyl radicals, Food Chem. Toxicol. 40 (2002) 1403–1413.
- [17] M. Andjelkovic, J. Vancamp, B. Demeulenaer, G. Depaemelaere, C. Socaciu, M. Verloo, R. Verhe, Iron-chelation properties of phenolic acids bearing catechol and galloyl groups, Food Chem. 98 (2006) 23–31. doi:10.1016/j.foodchem.2005.05.044.

- [18] H. Liu, J. Cao, W. Jiang, Evaluation and comparison of vitamin C, phenolic compounds, antioxidant properties and metal chelating activity of pulp and peel from selected peach cultivars, *LWT - Food Sci. Technol.* 63 (2015) 1042–1048. doi:10.1016/j.lwt.2015.04.052.
- [19] J.-M. Noh, Y.-S. Lee, Inhibitory activities of hydroxyphenolic acid–amino acid conjugates on tyrosinase, *Food Chem.* 125 (2011) 953–957. doi:10.1016/j.foodchem.2010.09.087.
- [20] M.A. Soobrattee, V.S. Neergheen, A. Luximon-Ramma, O.I. Aruoma, T. Bahorun, Phenolics as potential antioxidant therapeutic agents: Mechanism and actions, *Mutat. Res. Mol. Mech. Mutagen.* 579 (2005) 200–213. doi:10.1016/j.mrfmmm.2005.03.023.
- [21] K. Zhou, J. Yin, L. Yu, ESR determination of the reactions between selected phenolic acids and free radicals or transition metals, *Food Chem.* 95 (2006) 446–457. doi:10.1016/j.foodchem.2005.01.026.
- [22] S.B. Bukhari, S. Memon, M. Mahroof-Tahir, M.I. Bhangar, Synthesis, characterization and antioxidant activity copper–quercetin complex, *Spectrochim. Acta. A. Mol. Biomol. Spectrosc.* 71 (2009) 1901–1906. doi:10.1016/j.saa.2008.07.030.
- [23] Y. Iwasaki, T. Hirasawa, Y. Maruyama, Y. Ishii, R. Ito, K. Saito, T. Umemura, A. Nishikawa, H. Nakazawa, Effect of interaction between phenolic compounds and copper ion on antioxidant and pro-oxidant activities, *Toxicol. In Vitro.* 25 (2011) 1320–1327. doi:10.1016/j.tiv.2011.04.024.
- [24] S. Khokhar, R.K. Owusu Apenten, Iron binding characteristics of phenolic compounds: some tentative structure–activity relations, *Food Chem.* 81 (2003) 133–140. doi:10.1016/S0308-8146(02)00394-1.
- [25] D. Huang, B. Ou, R.L. Prior, The Chemistry behind Antioxidant Capacity Assays, *J. Agric. Food Chem.* 53 (2005) 1841–1856. doi:10.1021/jf030723c.
- [26] C.A. Rice-Evans, N.J. Miller, P.G. Bolwell, P.M. Bramley, J.B. Pridham, The relative antioxidant activities of plant-derived polyphenolic flavonoids, *Free Radic. Res.* 22 (1995) 375–383.
- [27] J.P. Kehrer, The Haber–Weiss reaction and mechanisms of toxicity, *Toxicology.* 149 (2000) 43–50. doi:10.1016/S0300-483X(00)00231-6.
- [28] S. Qazi, D. Li, C. Briens, F. Berruti, M. Abou-Zaid, Antioxidant Activity of the Lignins Derived from Fluidized-Bed Fast Pyrolysis, *Molecules.* 22 (2017) 372. doi:10.3390/molecules22030372.
- [29] V. Ugartondo, M. Mitjans, M. Vinardell, Comparative antioxidant and cytotoxic effects of lignins from different sources, *Bioresour. Technol.* 99 (2008) 6683–6687. doi:10.1016/j.biortech.2007.11.038.
- [30] M.H. Hussin, A.A. Rahim, M.N. Mohamad Ibrahim, M. Yemloul, D. Perrin, N. Brosse, Investigation on the structure and antioxidant properties of modified lignin obtained by different combinative processes of oil palm fronds (OPF) biomass, *Ind. Crops Prod.* 52 (2014) 544–551. doi:10.1016/j.indcrop.2013.11.026.
- [31] G. Dobeles, T. Dizhbite, J. Ponomarenko, I. Urbanovich, J. Kreicberga, V. Kampars, Isolation and characterization of the phenolic fractions of wood pyrolytic oil, *Holzforschung.* 65 (2011) 503–510. doi:10.1515/hf.2011.049.
- [32] A. Olejniczak, A. Kucinska, A.W. Cyganiuk, J.P. Lukaszewicz, Effect of Salix viminalis Pyrolysis Derived Antioxidants on Oxidative Stability of Diesters and Diester–Poly- $\alpha$ -olefin Mixtures, *Ind. Eng. Chem. Res.* 51 (2012) 5117–5123. doi:10.1021/ie2007054.
- [33] R.Y. Nsimba, N. West, A.A. Boateng, Structure and Radical Scavenging Activity Relationships of Pyrolytic Lignins, *J. Agric. Food Chem.* 60 (2012) 12525–12530. doi:10.1021/jf3037787.
- [34] A. Arshanitsa, J. Ponomarenko, T. Dizhbite, A. Andersone, R.J.A. Gosselink, J. van der Putten, M. Lauberts, G. Telysheva, Fractionation of technical lignins as a tool for

- improvement of their antioxidant properties, *J. Anal. Appl. Pyrolysis*. 103 (2013) 78–85. doi:10.1016/j.jaap.2012.12.023.
- [35] M. Azadfar, A.H. Gao, M.V. Bule, S. Chen, Structural characterization of lignin: A potential source of antioxidants guaiacol and 4-vinylguaiacol, *Int. J. Biol. Macromol.* 75 (2015) 58–66. doi:10.1016/j.ijbiomac.2014.12.049.
- [36] S.R. Chandrasekaran, D. Murali, K.A. Marley, R.A. Larson, K.M. Doll, B.R. Moser, J. Scott, B.K. Sharma, Antioxidants from Slow Pyrolysis Bio-Oil of Birch Wood: Application for Biodiesel and Biobased Lubricants, *ACS Sustain. Chem. Eng.* 4 (2016) 1414–1421. doi:10.1021/acssuschemeng.5b01302.
- [37] E.B. Hassan, E.M. El-Giar, P. Steele, Evaluation of the antioxidant activities of different bio-oils and their phenolic distilled fractions for wood preservation, *Int. Biodeterior. Biodegrad.* 110 (2016) 121–128. doi:10.1016/j.ibiod.2016.03.015.
- [38] N. Gil-Lalaguna, A. Bautista, A. Gonzalo, J.L. Sánchez, J. Arauzo, Obtaining biodiesel antioxidant additives by hydrothermal treatment of lignocellulosic bio-oil, *Fuel Process. Technol.* 166 (2017) 1–7. doi:10.1016/j.fuproc.2017.05.020.
- [39] M.R. Rover, R.C. Brown, Quantification of total phenols in bio-oil using the Folin–Ciocalteu method, *J. Anal. Appl. Pyrolysis*. 104 (2013) 366–371. doi:10.1016/j.jaap.2013.06.011.
- [40] C.A. Luengo, M.O. Cencig, Biomass Pyrolysis in Brazil: Status Report, in: A.V. Bridgwater, G. Grassi (Eds.), *Biomass Pyrolysis Liq. Upgrad. Util.*, Springer Netherlands, Dordrecht, 1991: pp. 299–309. doi:10.1007/978-94-011-3844-4\_13.
- [41] C. Amen-Chen, H. Pakdel, C. Roy, Separation of phenols from Eucalyptus wood tar, *Biomass Bioenergy*. 13 (1997) 25–37. doi:10.1016/S0961-9534(97)00021-4.
- [42] C.A. Mullen, A.A. Boateng, N.M. Goldberg, I.M. Lima, D.A. Laird, K.B. Hicks, Bio-oil and bio-char production from corn cobs and stover by fast pyrolysis, *Biomass Bioenergy*. 34 (2010) 67–74. doi:10.1016/j.biombioe.2009.09.012.
- [43] D. Fu, S. Farag, J. Chaouki, P.G. Jessop, Extraction of phenols from lignin microwave-pyrolysis oil using a switchable hydrophilicity solvent, *Bioresour. Technol.* 154 (2014) 101–108. doi:10.1016/j.biortech.2013.11.091.
- [44] S. Thangalazhy-Gopakumar, S. Adhikari, H. Ravindran, R.B. Gupta, O. Fasina, M. Tu, S.D. Fernando, Physiochemical properties of bio-oil produced at various temperatures from pine wood using an auger reactor, *Bioresour. Technol.* 101 (2010) 8389–8395. doi:10.1016/j.biortech.2010.05.040.
- [45] V.L. Singleton, J.A. Rossi, Colorimetry of Total Phenolics with Phosphomolybdic-Phosphotungstic Acid Reagents, *Am. J. Enol. Vitic.* 16 (1965) 144–158.
- [46] S.I. Mussatto, L.F. Ballesteros, S. Martins, J.A. Teixeira, Extraction of antioxidant phenolic compounds from spent coffee grounds, *Sep. Purif. Technol.* 83 (2011) 173–179. doi:10.1016/j.seppur.2011.09.036.
- [47] T.C.P. Dinis, V.M.C. Madeira, L.M. Almeida, Action of Phenolic Derivatives (Acetaminophen, Salicylate, and 5-Aminosalicylate) as Inhibitors of Membrane Lipid Peroxidation and as Peroxyl Radical Scavengers, *Arch. Biochem. Biophys.* 315 (1994) 161–169. doi:10.1006/abbi.1994.1485.
- [48] L.L.S. Canabady-Rochelle, C. Harscoat-Schiavo, V. Kessler, A. Aymes, F. Fournier, J.-M. Girardet, Determination of reducing power and metal chelating ability of antioxidant peptides: Revisited methods, *Food Chem.* 183 (2015) 129–135. doi:10.1016/j.foodchem.2015.02.147.
- [49] H.-C. Wu, C.-Y. Shiau, Hua-Ming, Chen, T.-K. Chiou, Antioxidant activities of carnosine, anserine, some free amino acids and their combination, *J. Food Ad Drug Anal.* 11 (2003) 148–153.

- [50] L. Sadat, C. Cakir-Kiefer, M.-A. N'Negue, J.-L. Gaillard, J.-M. Girardet, L. Miclo, Isolation and identification of antioxidative peptides from bovine  $\alpha$ -lactalbumin, *Int. Dairy J.* 21 (2011) 214–221. doi:10.1016/j.idairyj.2010.11.011.
- [51] M. Oyaizu, Studies on products of browning reactions: Antioxidative activities of product of browning reaction prepared from glucosamine, *Jpn. J. Nutri.* 44 (1986) 307–315.
- [52] N. Nenadis, L.-F. Wang, M. Tsimidou, H.-Y. Zhang, Estimation of Scavenging Activity of Phenolic Compounds Using the ABTS <sup>•+</sup> Assay, *J. Agric. Food Chem.* 52 (2004) 4669–4674. doi:10.1021/jf0400056.
- [53] *The Chemistry of Phenols*, John Wiley & Sons, 2004.
- [54] R. Bortolomeazzi, N. Sebastianutto, R. Toniolo, A. Pizzariello, Comparative evaluation of the antioxidant capacity of smoke flavouring phenols by crocin bleaching inhibition, DPPH radical scavenging and oxidation potential, *Food Chem.* 100 (2007) 1481–1489. doi:10.1016/j.foodchem.2005.11.039.
- [55] M.C. Foti, Antioxidant properties of phenols, *J. Pharm. Pharmacol.* 59 (2007) 1673–1685. doi:10.1211/jpp.59.12.0010.
- [56] J.C. Danilewicz, Review of Reaction Mechanisms of Oxygen and Proposed Intermediate Reduction Products in Wine: Central Role of Iron and Copper, *Am. J. Enol. Vitic.* 54 (2003) 73–85.
- [57] M. (Musashino N.C. Oyaizu, Antioxidative activities of browning products of glucosamine fractionated by organic solvent and thin-layer chromatography, *J. Jpn. Soc. Food Sci. Technol. Jpn.* (1988). <http://agris.fao.org/agris-search/search.do?recordID=JP8903946> (accessed May 2, 2017).

## Conclusion et perspectives

Les calculs quantiques ont été utilisés en tant qu'outil afin d'étudier les structures des composés phénoliques dans leur état isolé et en présence soit d'une molécule d'eau, soit d'une molécule de liquide ionique. Les conformations les plus stables présentent le groupement hydroxyle dans le plan du noyau benzénique. De plus, la présence de liaisons hydrogène intramoléculaires stabilise les conformations des composés phénoliques dans leur état isolé (guaiacol, syringol, pyrocatechol et vanilline).

En présence d'une molécule d'eau, trois conformations sont favorisées. Dans la conformation dite « translinéaire », la molécule d'eau est à perpendiculaire au noyau benzénique et se comporte comme un accepteur envers le groupement hydroxyle du composé phénolique (phénol, pyrocatechol et crésols). Dans la conformation cyclique, la molécule d'eau interagit à la fois en tant qu'accepteur envers le groupement hydroxyle et donneur envers le groupement methoxy du composé phénolique (guaiacol, syringol). Enfin, une conformation spécifique à la vanilline a été déterminée, pour laquelle où la molécule d'eau interagit en tant que donneur avec le groupement aldéhyde. L'étude du système {phenol – liquide ionique choline bis(trifluoromethylsulfonide)imide} montre que le phénol a une plus grande énergie d'interaction avec le liquide ionique qu'avec l'eau et suggère que ce liquide ionique pourrait être utilisé comme solvant pour l'extraction des composés phénoliques à partir d'une phase aqueuse.

La solubilité des composés phénoliques dans l'eau a été mesurée dans une gamme de température entre 293 et 323K à pression atmosphérique. Des équilibres liquide-liquide ont été observés pour le phénol, le guaiacol, les crésols et le syringol (supérieur à 313K), et des équilibres solide-liquide dans le cas du pyrocatechol, de la vanilline et du le syringol (inférieur à 308K). Parmi les molécules étudiées, le pyrocatechol et phénol sont les deux composés les plus solubles dans l'eau, probablement grâce à la disponibilité de leurs groupements hydroxyles. La solubilité de l'eau dans les phases phénoliques a également été étudiée dans le cas des équilibres liquide-liquide entre 293 et 323K. Ces travaux montrent que les modèles de coefficient d'activité tels que le modèle NRTL permettent de représenter les mesures expérimentales avec une déviation inférieure à 0.2%.

Le liquide ionique choline bis(trifluoromethylsulfonide)imide [Choline][NTf<sub>2</sub>] a été étudié comme solvant possible pour l'extraction de composés phénoliques à partir d'une phase

aqueuse. Ainsi, les systèmes ternaires {eau + composé phénolique (phénol, guaiacol, syringol et pyrocatechol) + [Choline][NTf<sub>2</sub>]} ont été étudiés à 298K à pression atmosphérique. Les systèmes comprenant le phénol, le syringol et le pyrocatechol présentent des diagrammes de phases de type 4 du fait de leur état solide à température ambiante, alors que le système ternaire {eau + guaiacol + [Choline][NTf<sub>2</sub>]} présente un diagramme de type 2. De plus, l'utilisation du [Choline][NTf<sub>2</sub>] permet une extraction rapide, efficace à température ambiante et ne nécessite qu'une faible quantité de solvant. Enfin, la détermination des paramètres des modèles thermodynamiques NRTL et UNIQUAC ont permis le dimensionnement d'une colonne multi-étagées. Cette colonne s'inscrit dans le schéma d'un procédé comprenant également un flash et un séparateur dans le but de récupérer les composés phénoliques à partir d'une phase aqueuse avec une faible demande énergétique ainsi que le recyclage du liquide ionique.

Après avoir étudié l'efficacité du liquide ionique sur l'extraction de molécules modèles contenues dans une phase aqueuse, l'extraction des composés phénoliques a été effectuée sur six bio-huiles réelles produites à partir de la pyrolyse rapide de lignine. Deux extractions liquide-liquide ont été effectuées. Premièrement, les composés phénoliques ont été extraits à partir de la bio-huile en utilisant une solution aqueuse basique. Ils sont ensuite récupérés en utilisant soit de l'acétate d'éthyle soit le liquide ionique [Choline][NTf<sub>2</sub>]. L'extraction avec la [Choline][NTf<sub>2</sub>] permet la récupération des composés avec un fort taux d'extraction (70% dans le cas du phénol) en une seule étape, comparé à l'acétate d'éthyle qui en requiert quatre. A partir du troisième lavage avec la [Choline][NTf<sub>2</sub>], aucun composé phénolique n'a été observé par spectroscopie de masse. La [Choline][NTf<sub>2</sub>] est donc un excellent solvant pour la récupération des composés phénoliques dans une phase aqueuse.

Enfin, les propriétés antioxydantes de huit composés phénoliques ont été étudiées à partir de cinq dosages spectrophotométriques réalisés en microplaques. Les résultats ont été comparés à des molécules de références spécifiques à chaque test afin de classer les composés phénoliques en fonction de chacune des propriétés étudiées. Le guaiacol est le composé répondant le plus au réactif de Folin-Ciocalteu. De plus, les composés phénoliques présentent un pouvoir réducteur et une activité antiradicalaire élevés. Cependant, ces composés ont une activité en tant que chélateurs de métaux très faible, voire inexistante, dans les rangs de concentrations étudiés.

Ce projet de thèse s'inscrit dans un projet plus large et nécessite encore d'approfondir certaines pistes de recherche.

Tout d'abord, les calculs quantiques ont été effectués sur les systèmes {composés phénoliques + eau} ainsi que sur le système {phénol - [Choline][NTf<sub>2</sub>]}. Cependant, il serait nécessaire d'étudier plus de systèmes {composés phénoliques - [Choline][NTf<sub>2</sub>]} afin de mieux comprendre les interactions entre le liquide ionique et les composés phénoliques d'un point de vue moléculaire. De plus, les calculs quantiques constituent, dans le cadre de ce projet, la première étape de la mise en place d'une étude multi-échelle pour l'extraction des composés phénoliques. Les informations structurales acquises dans cette thèse permettront dans un avenir proche de déterminer les propriétés thermodynamiques de ces systèmes à l'aide de la dynamique moléculaire.

D'un point de vue macroscopique, l'optimisation de la première étape d'extraction du procédé, c'est-à-dire la première extraction liquide-liquide des composés phénoliques à l'aide d'une solution aqueuse est nécessaire et requiert une étude sur la cinétique de dissolution et sur l'influence de différents paramètres tels que le pH et la température sur les performances du procédé.

La récupération des composés cibles à partir de la phase liquide ionique peut être effectuée *via* une unité de distillation. Afin de dimensionner une telle colonne, des données expérimentales d'équilibre liquide-vapeur sont nécessaires pour la détermination des paramètres thermodynamiques. La phase vapeur résultante de cette colonne de distillation est supposée contenir de l'eau et le composé phénolique, facilement séparables par refroidissement des vapeurs jusqu'à température ambiante puis par filtration (dans le cas d'un équilibre solide-liquide) ou par décantation (équilibre liquide-liquide).

Enfin, une étude technico-économique serait nécessaire afin d'évaluer la faisabilité du procédé, en prenant notamment en compte l'énergie nécessaire au bon fonctionnement de la colonne de distillation et au refroidissement des vapeurs, ainsi que du coût du liquide ionique et de son recyclage. Ainsi, une étude de la durabilité de liquide ionique après un certain nombre d'extractions serait également nécessaire.



## **APPENDIX**



## Appendix I: Computational study on the molecular conformations of phenolic compounds.

Remark: Distances are in angstroms, angle in degrees, energies in Hartrees.  $\Delta E$  are in  $\text{kJ}\cdot\text{mol}^{-1}$  and are calculated compared to the most stable conformation  $C_1$ . Atoms in grey, white and red represent carbon, hydrogen and oxygen atoms respectively.

**Figure S1:** The potential energy curves for phenol at the B3LYP/cc-pVTZ level of theory as a function of the variation of the C2-C3-O3-H3 dihedral angle

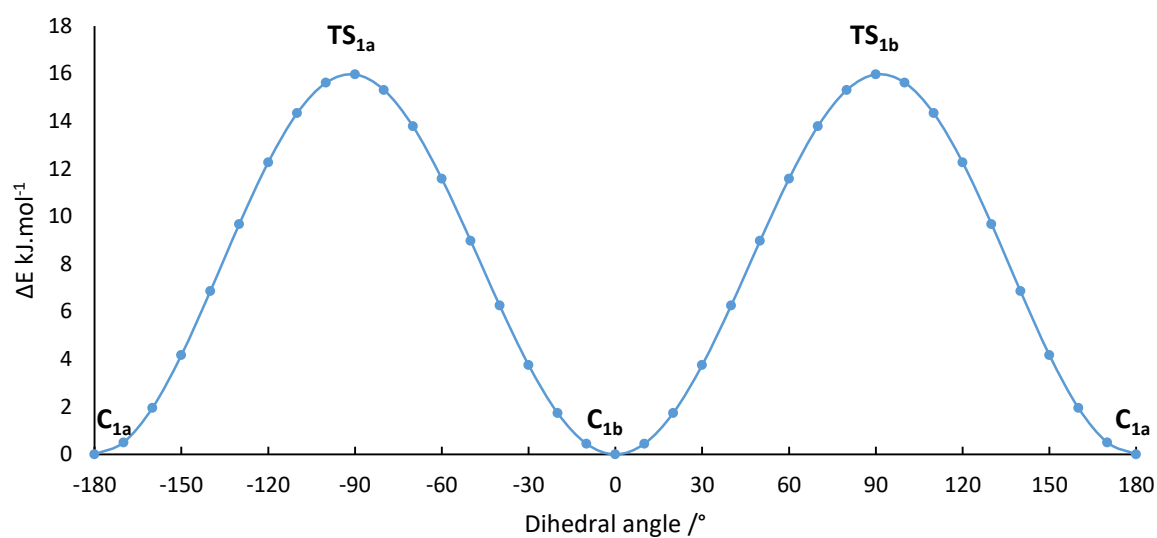


**Figure S2:** Potential Energy Surface of o-cresol as a function of the torsion of the C2-C3-O3-H3 (hydroxy) and C3-C4-C7-H7 (methyl) angles at B3LYP/cc-pVTZ.

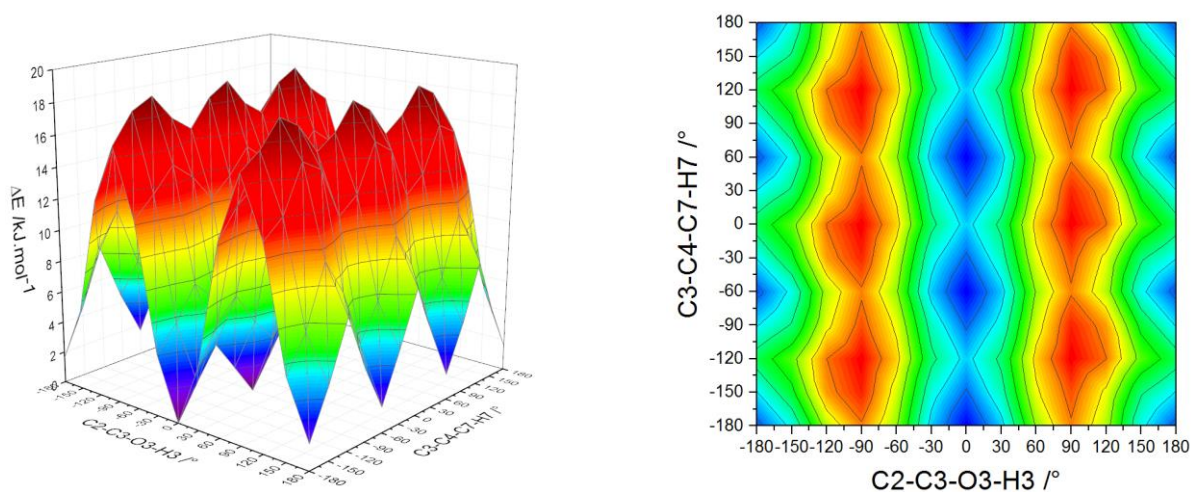


**Figure S3:** The potential energy curves for o-cresol at the B3LYP/cc-pVTZ level of theory as a function of variation of dihedral angle: ■ variation of the C3-C4-C7-H7 dihedral angle with the C2-C3-O3-H3 angle fixed at 0°, ● variation of the C3-C4-C7-H7 dihedral angle with the C2-C3-O3-H3 angle fixed at 180°, ▲ variation of the C2-C3-O3-H3 dihedral angle with the C3-C4-C7-H7 angle fixed at 180°.

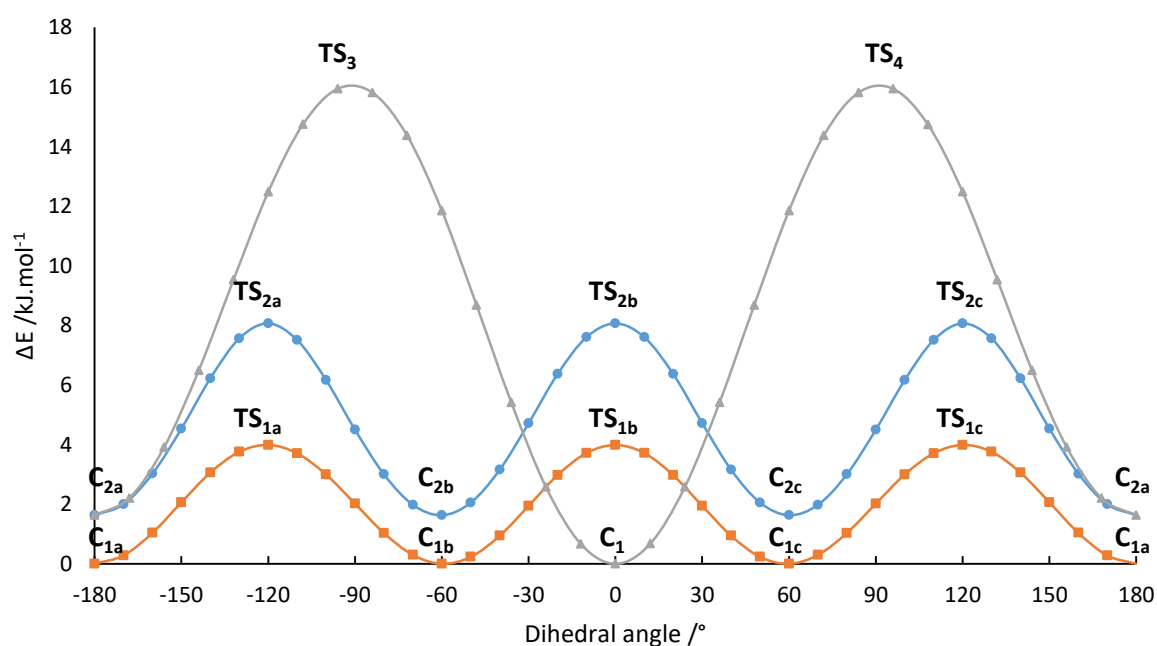


**Figure S4:** Potential Energy Surface of m-cresol as a function of the torsion of C2-C3-O3-H3 (hydroxy) and C4-C5-C7-H7 (methyl) angles at B3LYP/cc-pVTZ.

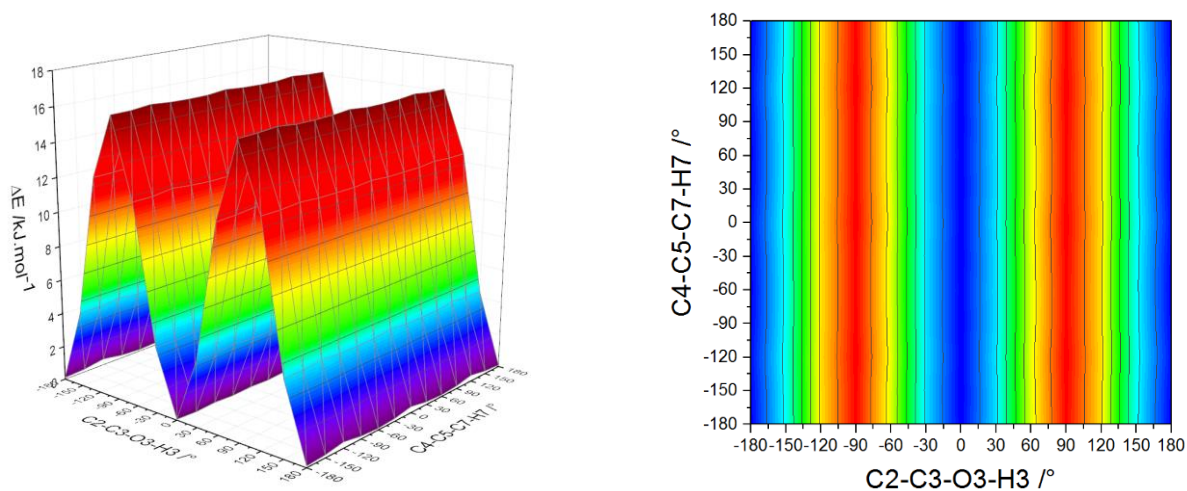
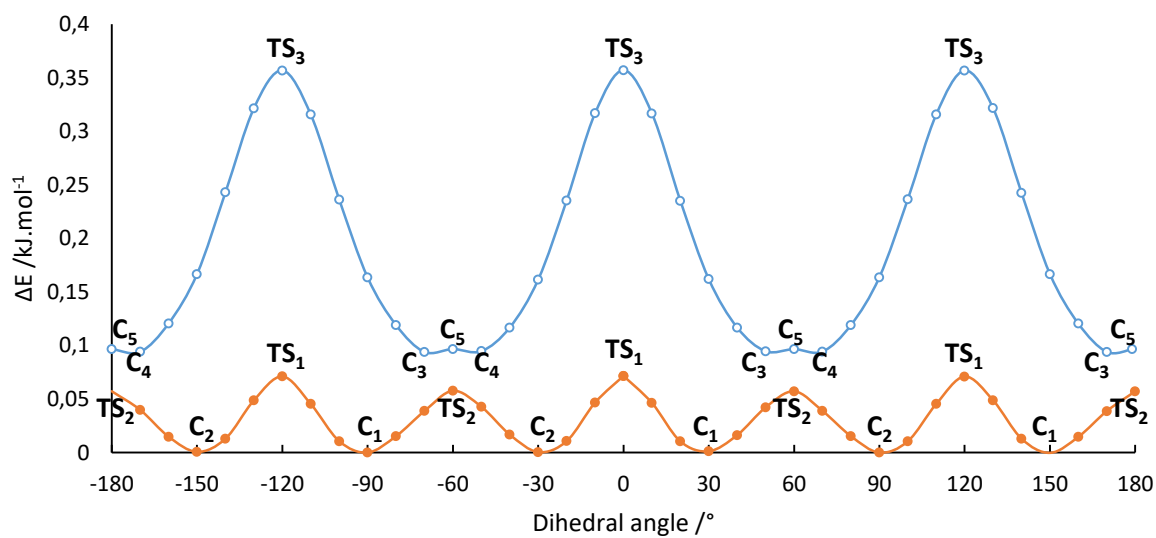


**Figure S5:** The potential energy curves for m-cresol at the B3LYP/cc-pVTZ level of theory as a function of variation of the C4-C5-C7-H7 dihedral angle: ● C2-C3-O3-H3 fixed at 0°, ○ C2-C3-O3-H3 fixed at 180°.

a)



b)

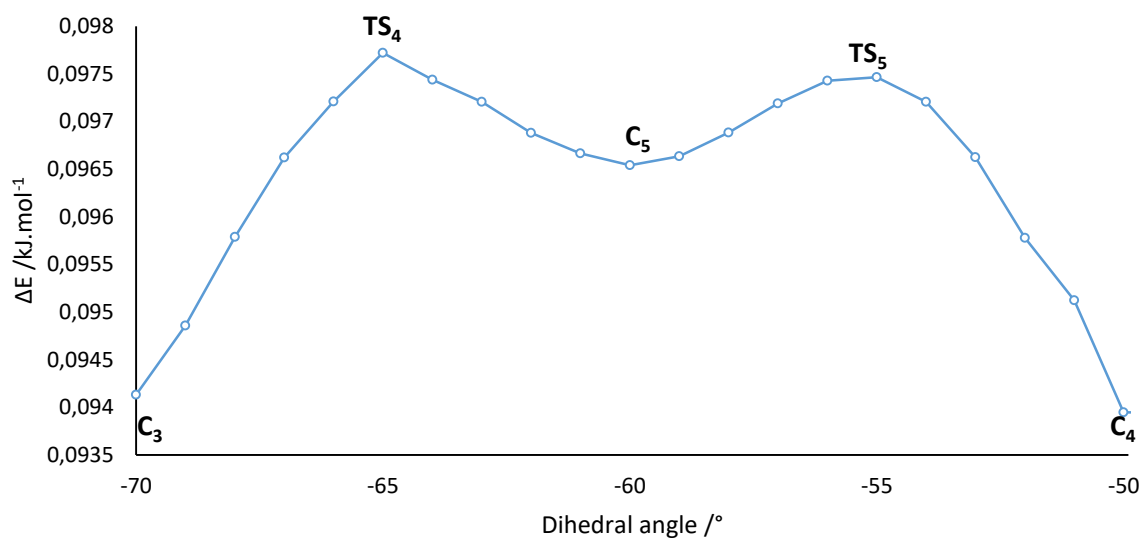


**Figure S6:** The potential energy curves for m-cresol at the B3LYP/cc-pVTZ level of theory as a function of variation of the C2-C3-O3-H3 dihedral angle:  $\blacktriangle$  C4-C5-C7-H7 angle fixed at  $180^\circ$

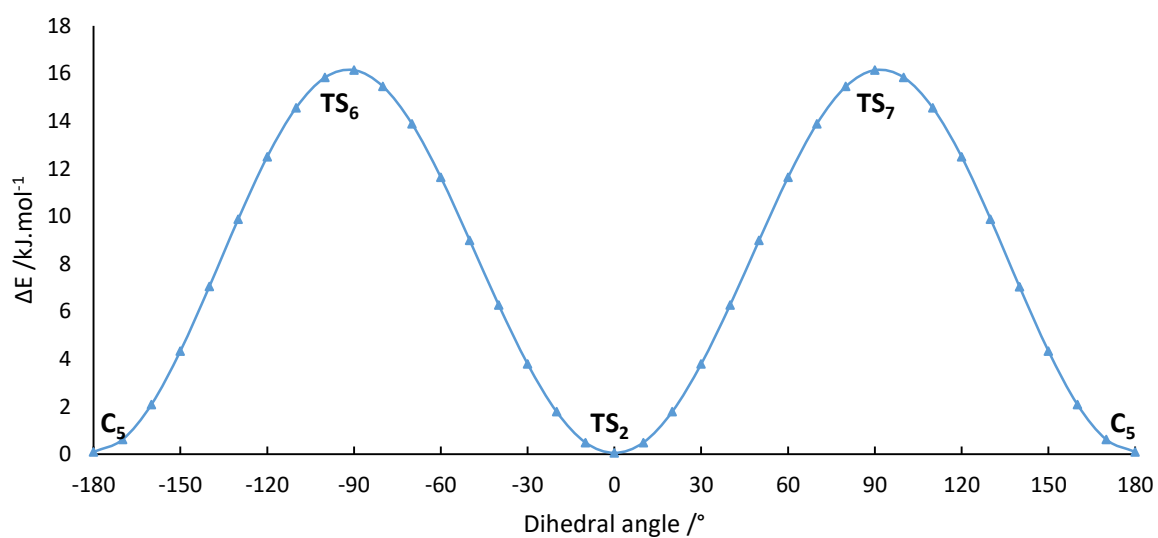


**Figure S7:** Potential Energy Surface of p-cresol as a function of the torsion of C2-C3-O3-H3 (hydroxy) and C5-C6-C7-H7 (methyl) angles at B3LYP/cc-pVTZ.

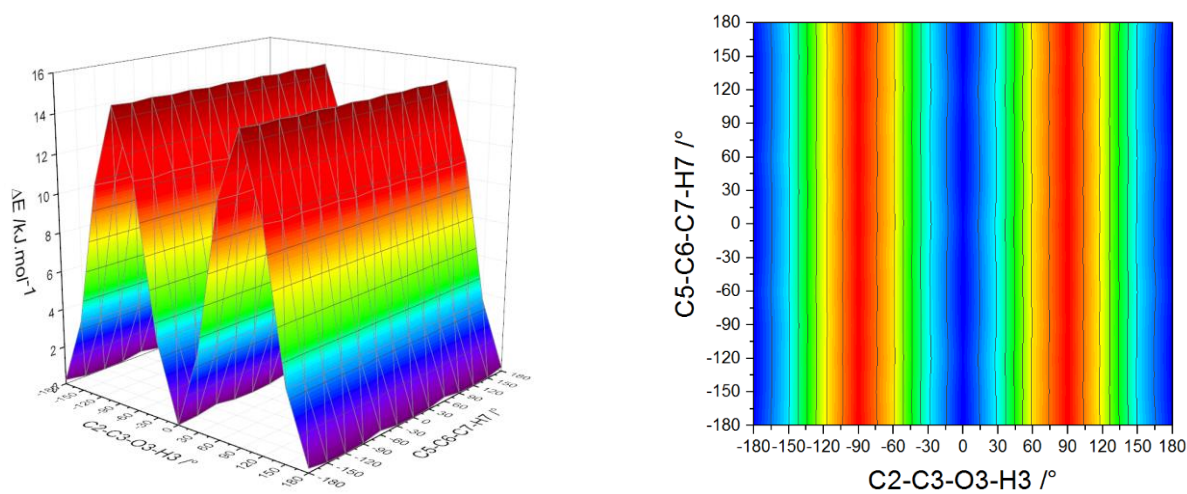
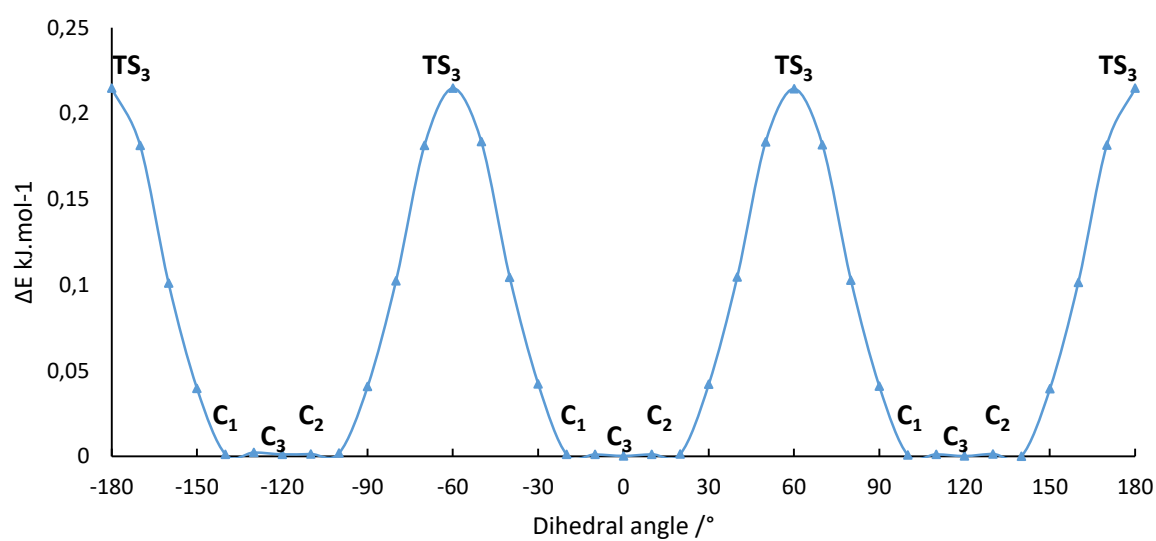
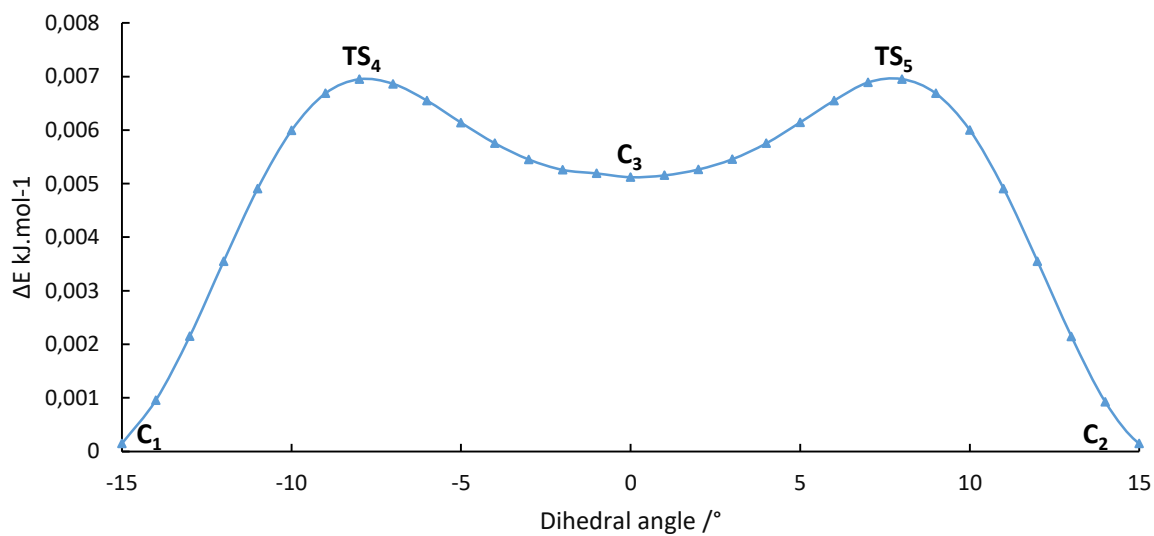


**Figure S8:** The potential energy curves for p-cresol at the B3LYP/cc-pVTZ level of theory as a function of variation of the C5-C6-C7-H7 dihedral angle: ▲ C2-C3-O3-H3 fixed at 180°.

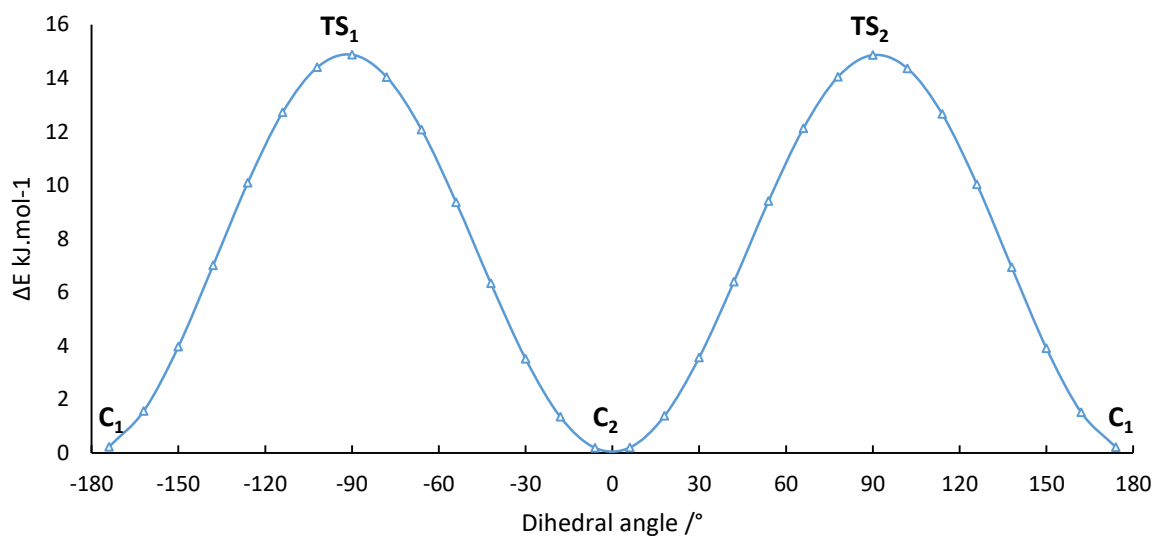
a)



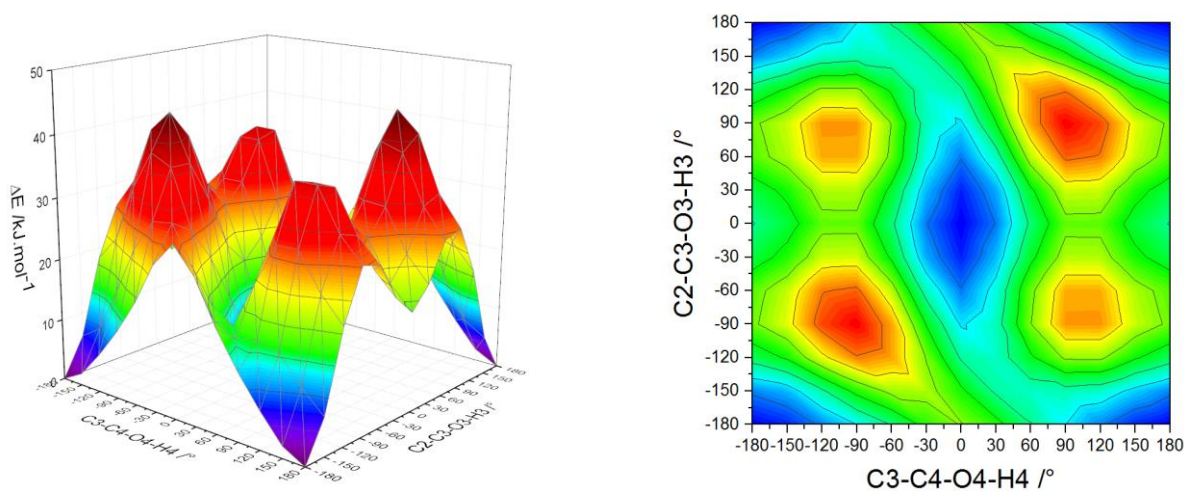
b)



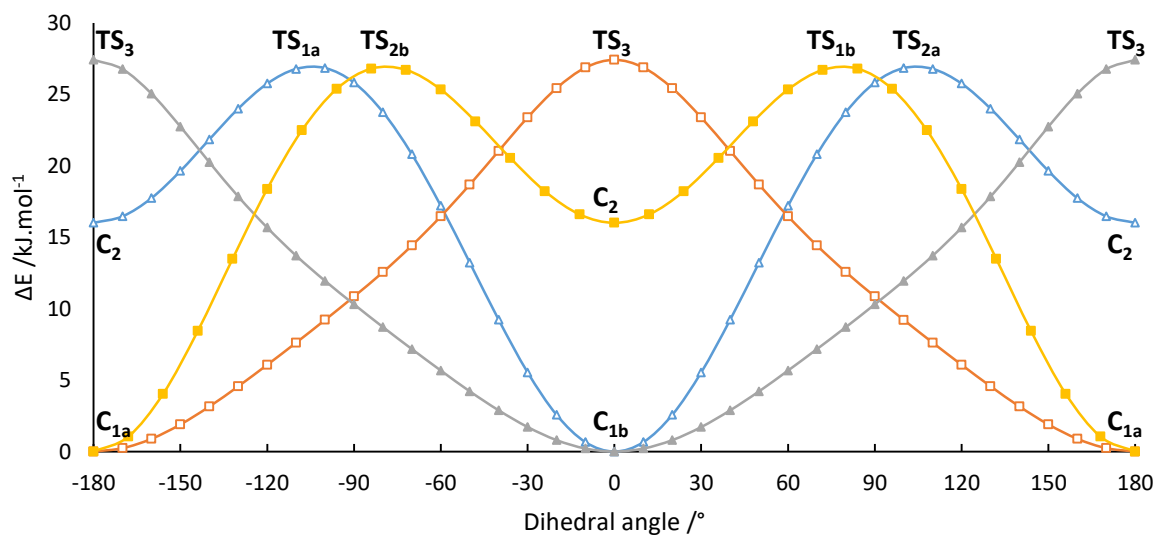
**Figure S9:** The potential energy curves for p-cresol at the B3LYP/cc-pVTZ level of theory as a function of variation of the C2-C3-O3-H3 dihedral angle:  $\Delta$  C5-C6-C7-H7 fixed at 90°



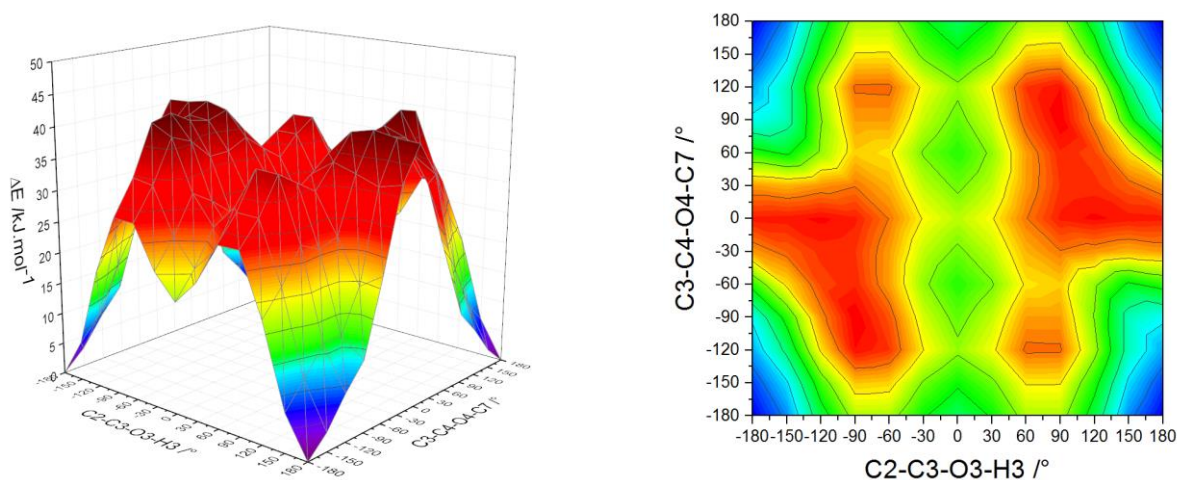
**Figure S10 :** Potential Energy Surface of pyrocatechol as a function of the torsion of C3-C4-O4-H4 (hydroxy) and C2-C3-O3-H3 (hydroxy) angles at B3LYP/cc-pVTZ.



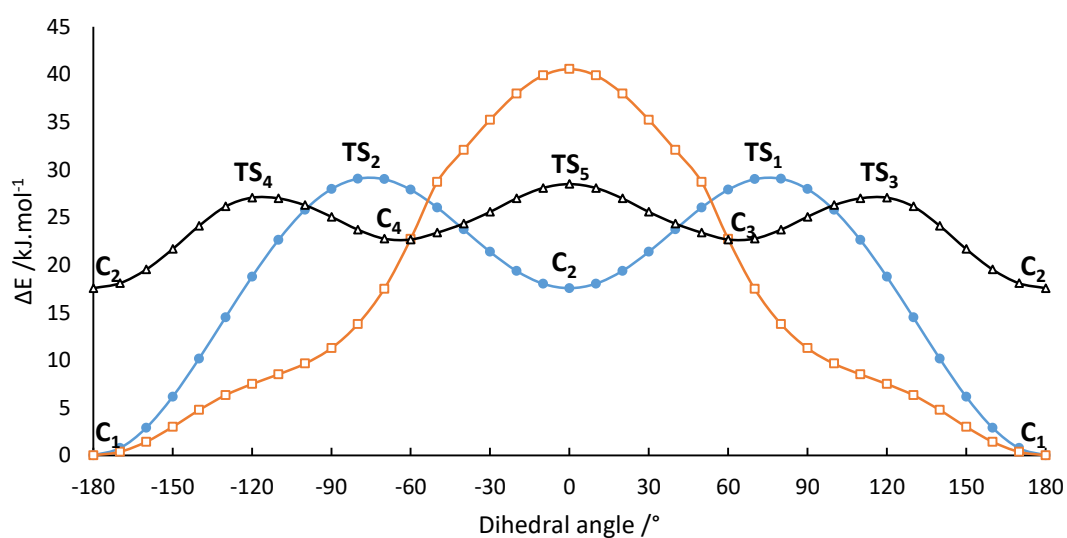
**Figure S11:** The potential energy curves for pyrocatechol at the B3LYP/cc-pVTZ level of theory as a function of variation of dihedral angle:  $\Delta$  variation of the C3-C4-O4-H4 dihedral angle with the C2-C3-O3-H3 angle fixed at  $0^\circ$ ,  $\blacktriangle$  variation of the C2-C3-O3-H3 dihedral angle with the C3-C4-O4-H4 angle fixed at  $0^\circ$ ,  $\square$  variation of the C3-C4-O4-H4 dihedral angle with the C2-C3-O3-H3 angle fixed at  $180^\circ$ ,  $\blacksquare$  variation of the C2-C3-O3-H3 dihedral angle with the C3-C4-O4-H4 angle fixed at  $180^\circ$ .



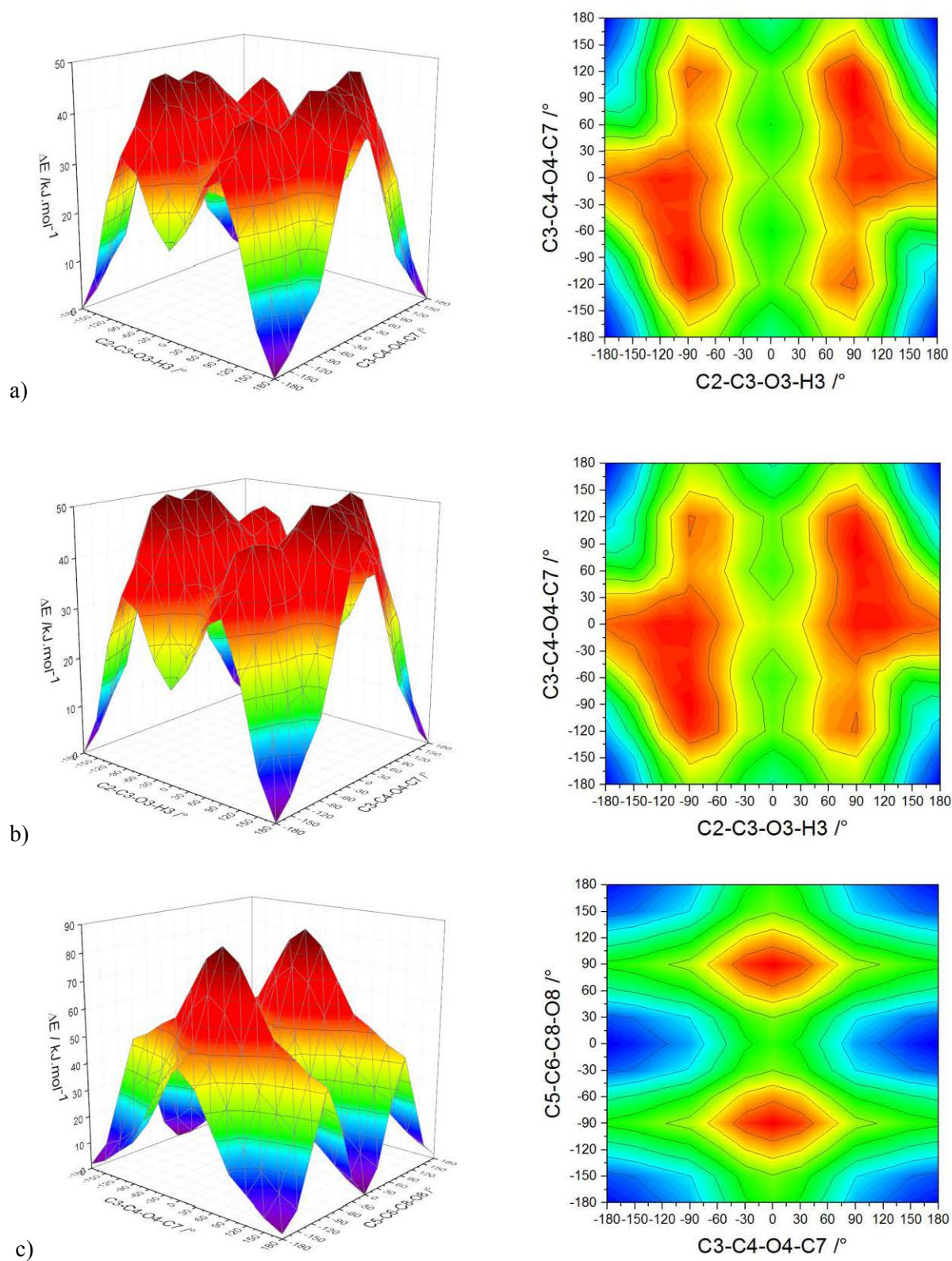
**Figure S12 :** Potential Energy Surface of guaiacol as a function of the torsion of C2-C3-O3-H3 (hydroxy) and C3-C4-O4-C7 (methoxy) angles at B3LYP/cc-pVTZ.



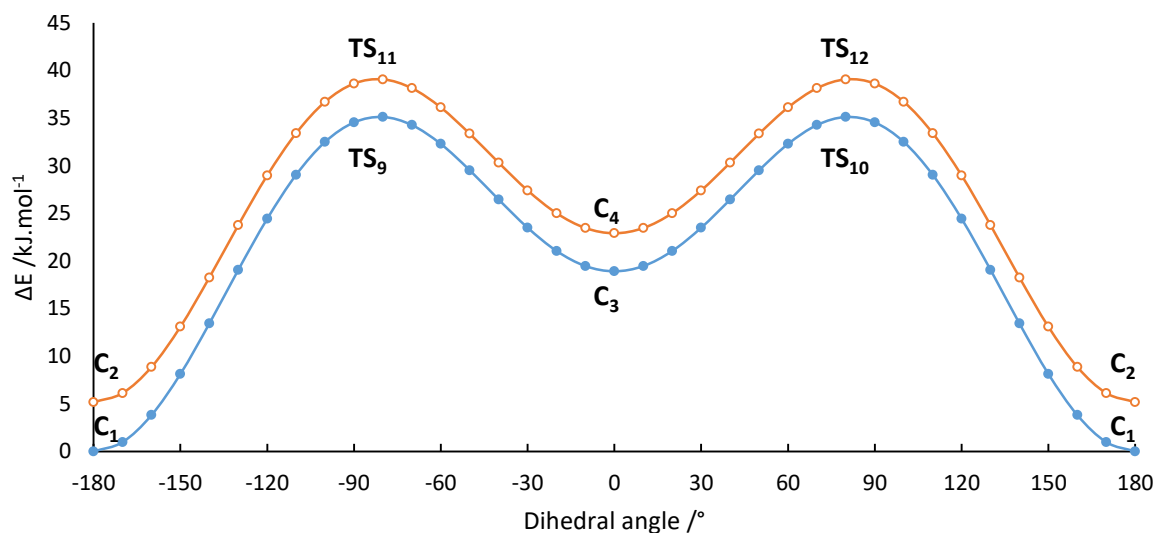
**Figure S13:** The potential energy curves for guaiacol at the B3LYP/cc-pVTZ level of theory as a function of variation of dihedral angle:  $\Delta$  variation of the C3-C4-O4-C7 dihedral angle with the C2-C3-O3-H3 angle fixed at  $0^\circ$ ,  $\square$  variation of the C3-C4-O4-C7 dihedral angle with the C2-C3-O3-H3 angle fixed at  $180^\circ$ ,  $\bullet$  variation of the C2-C3-O3-H3 dihedral angle with the C3-C4-O4-C7 angle fixed at  $180^\circ$ .



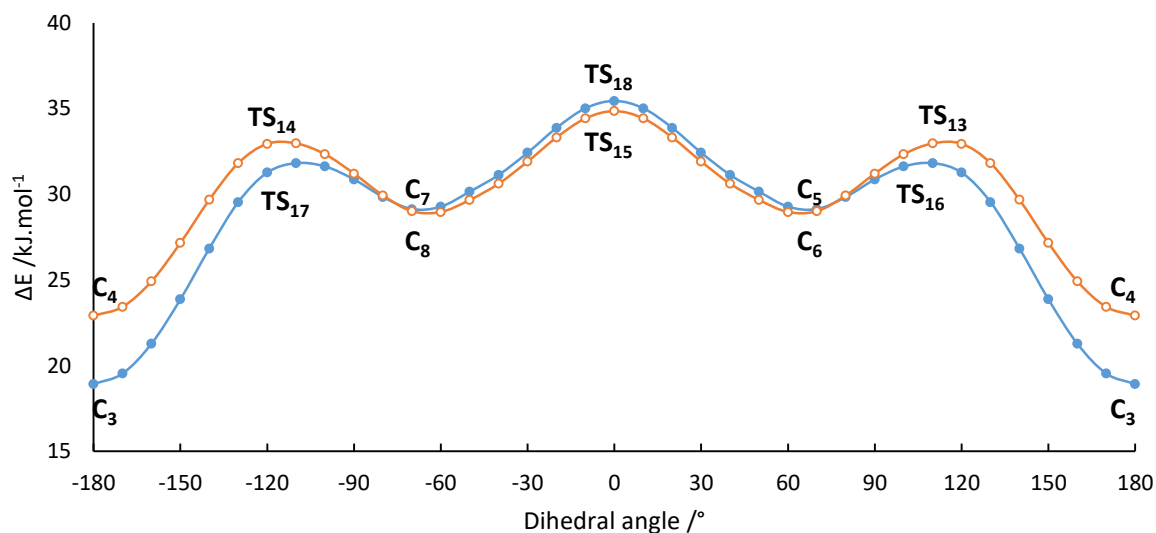
**Figure S14** : Potential Energy Surface of vanillin as a function of the torsion of C2-C3-O3-H3 (hydroxy) and C3-C4-O4-C7 (methoxy) angles with C5-C6-C8-O8 (aldehyde) frozen at a) 180°, b) frozen at 0°, c) Potential Energy Surface of vanillin as a function of the torsion of C3-C4-O4-C7 (methoxy) and C5-C6-C8-O8 (aldehyde) with C2-C3-O10-H11 (hydroxy) frozen at 180°, at B3LYP/cc-pVTZ.



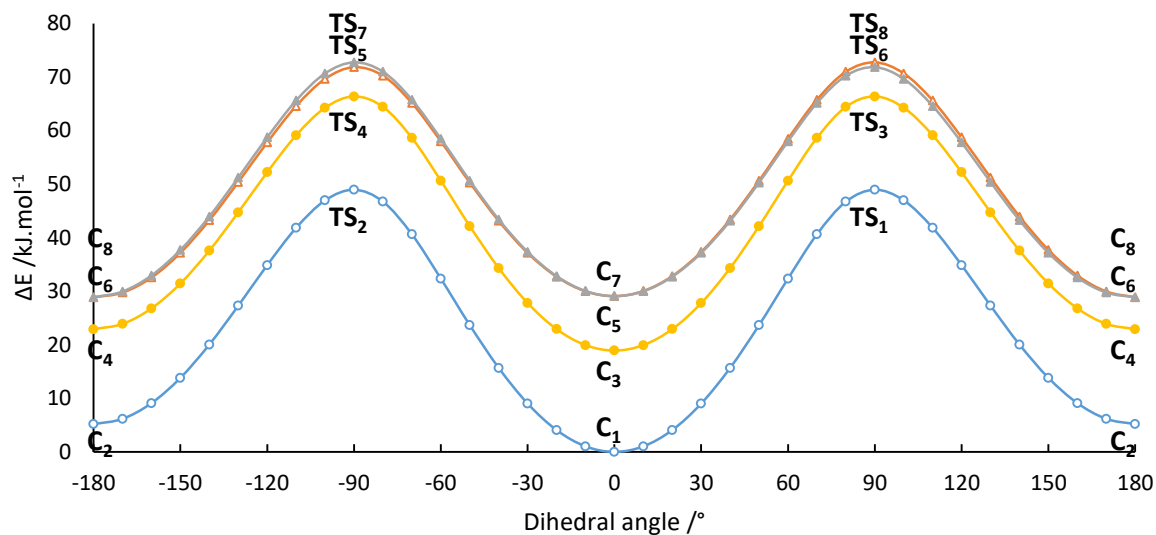
**Figure S15:** The potential energy curves for vanillin at the B3LYP/cc-pVTZ level of theory as a function of variation of C2-C3-O3-H3 dihedral angle:  $\circ$  C5-C6-C8-O8 fixed at  $180^\circ$  and C3-C4-O4-C7 at  $180^\circ$ ,  $\bullet$  C5-C6-C8-O8 fixed at  $0^\circ$  and C3-C4-O4-C7 at  $180^\circ$ .



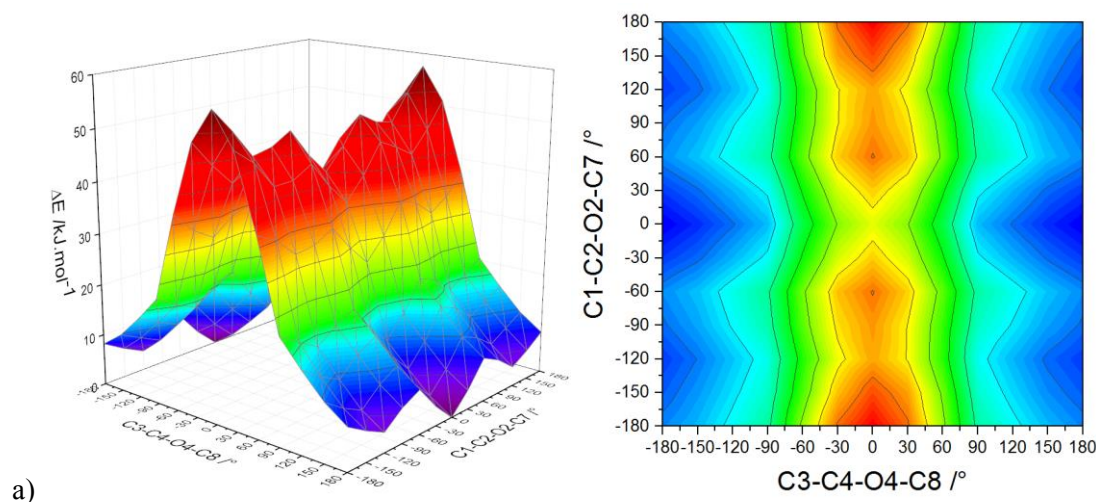
**Figure S16:** The potential energy curves for vanillin at the B3LYP/cc-pVTZ level of theory as a function of variation of the C3-C4-O4-C7 dihedral angle:  $\circ$  C5-C6-C8-O8 fixed at  $180^\circ$  and C2-C3-O3-H3 at  $0^\circ$ ,  $\bullet$  C5-C6-C8-O8 fixed at  $0^\circ$  and C2-C3-O3-H3 at  $0^\circ$ .

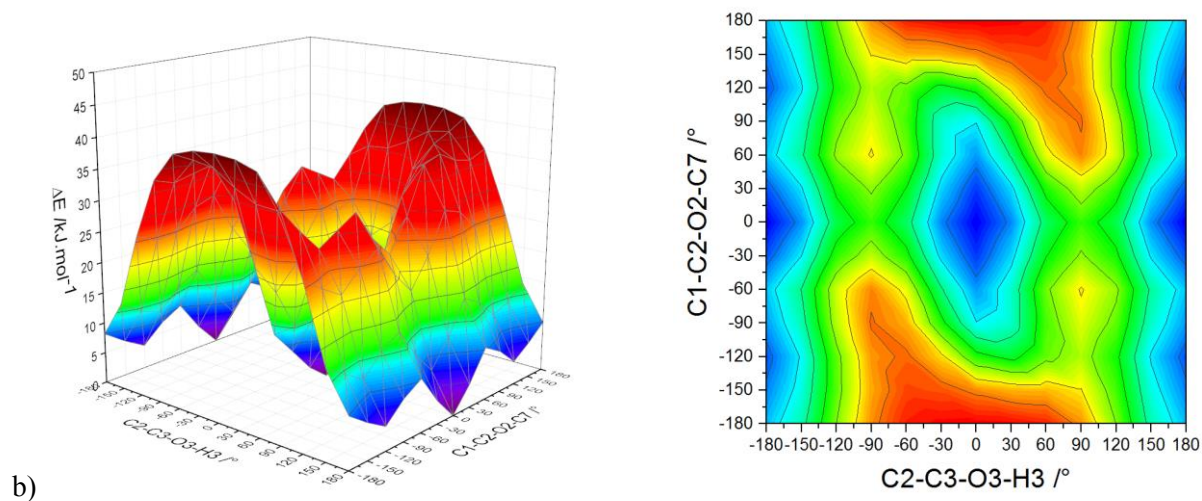


**Figure S17:** The potential energy curves for vanillin at the B3LYP/cc-pVTZ level of theory as a function of variation of the C5-C6-C8-O8 dihedral angle:  $\circ$  C2-C3-O3-H3 fixed at  $180^\circ$  and C3-C4-O4-C7 at  $180^\circ$ ,  $\bullet$  C2-C3-O3-H3 fixed at  $0^\circ$  and C3-C4-O4-C7 at  $180^\circ$ ,  $\blacktriangle$  C2-C3-O3-H3 fixed at  $0^\circ$  and C3-C4-O4-C7 at  $65^\circ$ ,  $\triangle$  C2-C3-O3-H3 fixed at  $0^\circ$  and C3-C4-O4-C7 at  $-65^\circ$ .

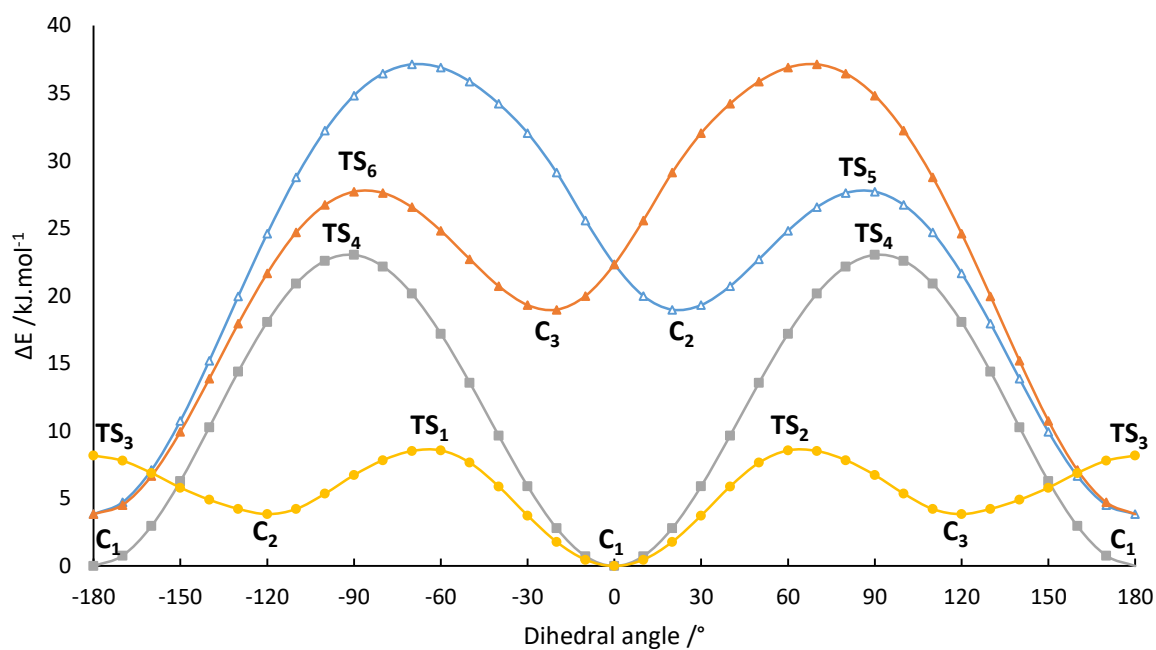


**Figure S18:** a) Potential Energy Surface of syringol as a function of the torsion of C1-C2-O2-C7 (methoxyl) and C3-C4-O4-C8 (methoxyl) angles with C2-C3-O3-H3 (hydroxy) frozen at  $180^\circ$  at B3LYP/cc-pVTZ, b) Potential Energy Surface of syringol as a function of the torsion of C1-C2-O2-C7 (methoxyl) and C2-C3-O3-H3 (hydroxyl) angles with C3-C4-O4-C8 (methoxyl) frozen at  $180^\circ$  at B3LYP/cc-pVTZ.

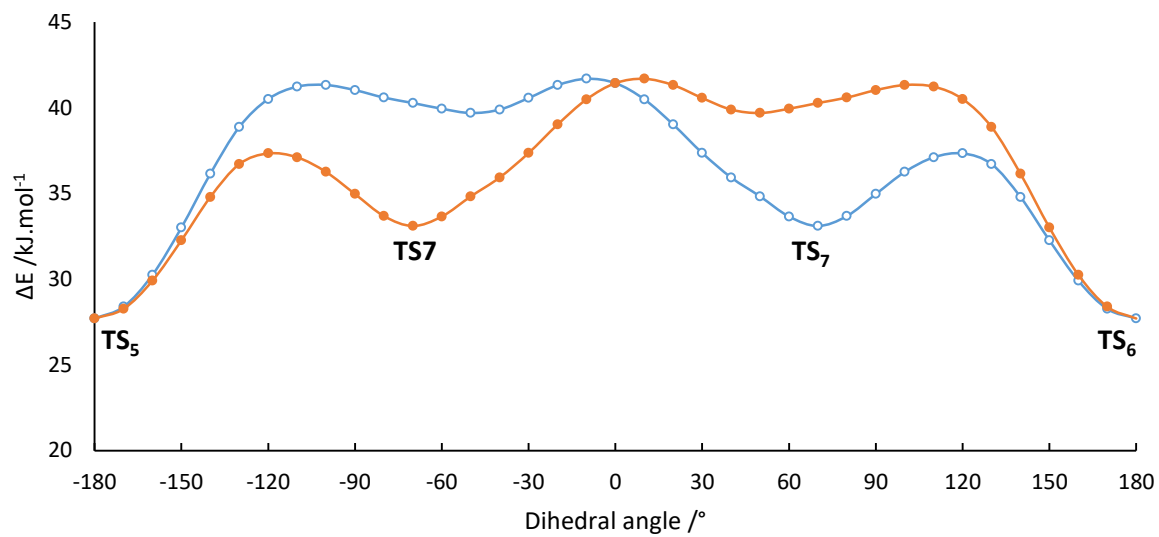




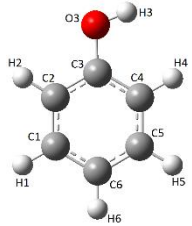
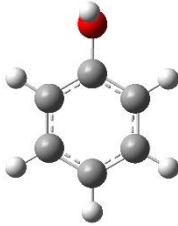
**Figure S19:** The potential energy curves for syringol at the B3LYP/cc-pVTZ level of theory as a function of variation of dihedral angle: ● variation of  $\text{C1-C2-O2-C7}$  while  $\text{C2-C3-O3-H3}$  and  $\text{C3-C4-O4-C8}$  fixed at  $180^\circ$ , ■ variation of  $\text{C2-C3-O3-H3}$  while  $\text{C3-C4-O4-C8}$  fixed at  $180^\circ$  and  $\text{C1-C2-O2-C7}$  at  $0^\circ$ , ▲ variation of  $\text{C2-C3-O3-H3}$  while  $\text{C3-C4-O4-C8}$  fixed at  $180^\circ$  and  $\text{C1-C2-O2-C7}$  at  $120^\circ$ , △ variation of  $\text{C2-C3-O3-H3}$  while  $\text{C3-C4-O4-C8}$  fixed at  $180^\circ$  and  $\text{C1-C2-O2-C7}$  at  $-120^\circ$



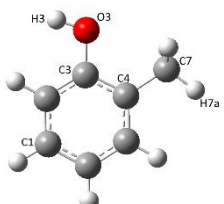
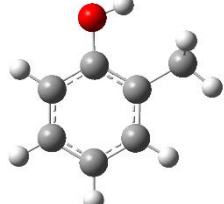
**Figure S20:** The potential energy curves for syringol at the B3LYP/cc-pVTZ level of theory as a function of variation of the C3-C4-O13-C18 dihedral angle: ● C2-C3-O3-H3 fixed at 90° and C1-C2-O2-C7 at -120°, ○ C2-C3-O3-H3 fixed at -90° and C1-C2-O2-C7 at 120°.



**Table S1:** Optimized geometry structures of conformer C<sub>1</sub> and transition state TS<sub>1</sub> of phenol at the B3LYP/cc-pVTZ level of theory.

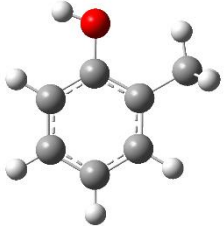
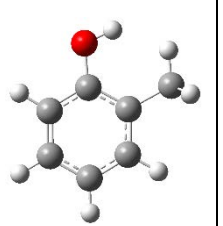
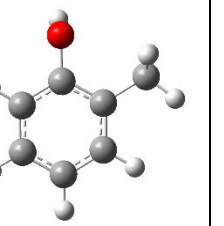
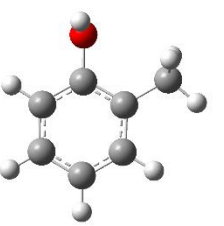
		
	C <sub>1</sub>	TS <sub>1</sub>
Energy (Hartree)	-307.585694	-307.579611
ΔE (kJ.mol <sup>-1</sup> )	0	15.9691837
C1-C2	1.3873	1.3901
C2-C3	1.3931	1.3905
C3-C4	1.3928	1.3905
C4-C5	1.3901	1.3901
C5-C6	1.3891	1.3905
C6-C1	1.3919	1.3905
C1-H1	1.082	1.082
C2-H2	1.081	1.0816
C4-H4	1.084	1.0816
C5-H5	1.082	1.082
C6-H6	1.081	1.0815
C3-O3	1.3668	1.3877
O3-H3	0.9623	0.9621
C1-C2-C3	119.6243	119.7326
C2-C3-C4	120.0201	120.2481
C3-C4-C5	119.805	119.7326
C4-C5-C6	120.5188	120.3048
C5-C6-C1	119.2708	119.6755
C6-C1-C2	120.761	120.3048
C2-C1-H1	119.2733	119.6322
C6-C1-H1	119.9657	120.0628
C1-C2-H2	121.4174	121.2156
C3-C2-H2	118.9582	119.0483
C2-C3-O3	117.4572	119.8392
C4-C3-O3	122.5226	119.8392
C3-O3-H3	109.425	109.6553
C3-C4-H4	119.9383	119.0483
C5-C4-H4	120.2568	121.2156
C4-C5-H5	119.3449	119.6322
C6-C5-H5	120.1363	120.0628
C1-C6-H6	120.3816	120.1617
C5-C6-H6	120.3476	120.1617
C2-C3-O3-H3	-180	91.5558
C4-C3-O3-H3	0	-91.5558

**Table S2a:** Optimized geometry structures of conformers C<sub>1</sub> and C<sub>2</sub> of o-cresol at the B3LYP/cc-pVTZ level of theory.

		
	C <sub>1</sub>	C <sub>2</sub>
Energy (Hartree)	-346.917339	-346.916717
$\Delta E$ (kJ.mol <sup>-1</sup> )	0	1.63061928
C1-C2	1.39	1.3871
C2-C3	1.3907	1.3912
C3-C4	1.4008	1.4009
C4-C5	1.3915	1.3937
C5-C6	1.3918	1.3891
C6-C1	1.3873	1.39
C1-H1	1.0817	1.0818
C2-H2	1.0843	1.0812
C5-H5	1.0831	1.0832
C6-H6	1.0812	1.0812
C3-O3	1.3703	1.3689
O3-H3	0.9621	0.9616
C4-C7	1.5031	1.506
C7-H7a	1.089	1.0948
C11-H7b	1.0917	1.0884
C11-H7c	1.0917	1.0948
C1-C2-C3	120.0779	119.916
C2-C3-C4	121.0818	120.9754
C3-C4-C5	117.581	117.8558
C4-C5-C6	121.9622	121.7142
C5-C6-C1	119.4443	119.3894
C6-C1-C2	119.8529	120.1493
C2-C1-H1	119.655	119.5694
C6-C1-H1	120.4921	120.2814
C1-C2-H2	120.2796	121.4284
C3-C2-H2	119.6425	118.6557
C2-C3-O3	122.0263	116.9756
C4-C3-O3	116.8919	122.049
C3-O3-H3	109.292	109.8098
C3-C4-C7	120.1986	120.5565
C5-C4-C7	122.2204	121.5878
C4-C7-H7a	110.7876	112.0398
C4-C7-H7b	111.3089	110.7963
C4-C7-H7c	111.3089	112.0399

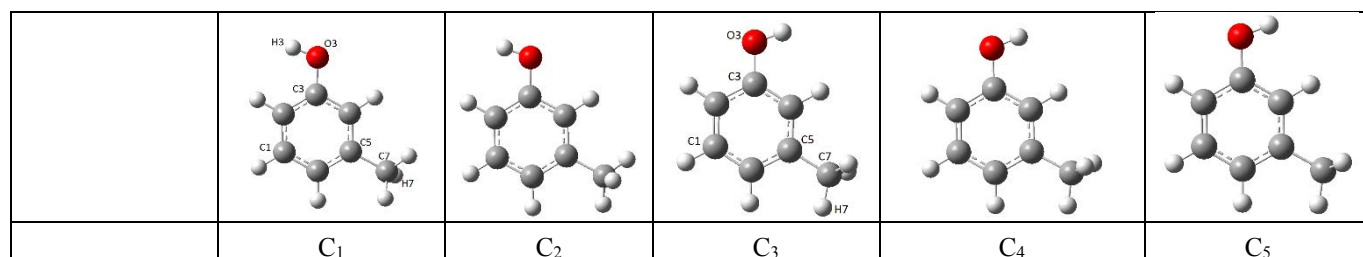
H7a-C7-H7b	108.3938	107.1285
H7a-C7-H7c	108.3938	107.437
H7b-C7-H7c	106.4837	107.1284
C4-C5-H5	118.5007	118.6466
C6-C5-H5	119.5371	119.6392
C1-C6-H6	120.4317	120.4885
C5-C6-H6	120.1241	120.1222
C2-C3-O3-H3	0	-179.9992
C4-C3-O3-H3	-180	0.0009
C3-C4-C7-H7a	180	60.42
C3-C4-C7-H7b	-59.3122	179.9995
C3-C4-C7-H7c	59.3121	-60.4211
C5-C4-C7-H7a	0	-119.58
C5-C4-C7-H7b	120.6878	-0.0005
C5-C4-C7-H7c	-120.6879	119.5789

**Table S2b:** Optimized geometry structures of transition states TS<sub>1</sub>-TS<sub>4</sub> of o-cresol at the B3LYP/cc-pVTZ level of theory.

				
	TS <sub>1</sub>	TS <sub>2</sub>	TS <sub>3</sub>	TS <sub>4</sub>
Energy (Hartree)	-346.91582	-346.914267	-346.911245	-346.911245
$\Delta E$ (kJ.mol <sup>-1</sup> )	3.98721557	8.06393445	15.998458	15.998458
C1-C2	1.3875	1.3841	1.3896	1.3896
C2-C3	1.3936	1.3949	1.3888	1.3888
C3-C4	1.3996	1.4003	1.3987	1.3987
C4-C5	1.394	1.3971	1.3946	1.3946
C5-C6	1.3891	1.386	1.39	1.39
C6-C1	1.389	1.3917	1.3888	1.3888
C1-H1	1.0817	1.0818	1.0817	1.0817
C2-H2	1.0844	1.0812	1.0817	1.0817
C5-H5	1.0836	1.0837	1.083	1.083
C6-H6	1.0813	1.0812	1.0817	1.0817
C3-O3	1.3716	1.369	1.3898	1.3898
O3-H3	0.9619	0.9611	0.9623	0.9623
C4-C7	1.5071	1.51	1.5039	1.5039
C7-H7a	1.0861	1.0911	1.089	1.089
C11-H7b	1.0919	1.0914	1.0928	1.0904
C11-H7c	1.0919	1.0914	1.0904	1.0928

C1-C2-C3	120.3299	120.3439	120.0742	120.0742
C2-C3-C4	120.8958	120.7105	121.2474	121.2474
C3-C4-C5	117.4751	117.6072	117.6614	117.6614
C4-C5-C6	122.19	122.1181	121.5661	121.5661
C5-C6-C1	119.357	119.2658	119.8181	119.8181
C6-C1-C2	119.7522	119.9545	119.6306	119.6306
C2-C1-H1	119.7231	119.6746	119.94	119.94
C6-C1-H1	120.5247	120.3709	120.4288	120.4288
C1-C2-H2	120.2012	121.3903	121.2305	121.2305
C3-C2-H2	119.4689	118.2658	118.6918	118.6918
C2-C3-O3	121.2704	115.9238	119.3221	119.3221
C4-C3-O3	117.8339	123.3657	119.3398	119.3398
C3-O3-H3	109.1157	109.8449	109.9162	109.9162
C3-C4-C7	121.5545	123.101	120.6015	120.6015
C5-C4-C7	120.9704	119.2918	121.7369	121.7369
C4-C7-H7a	111.5846	114.1712	110.8596	110.8596
C4-C7-H7b	110.8847	110.9974	111.5705	111.1894
C4-C7-H7c	110.8847	110.9974	111.1894	111.5705
H7a-C7-H7b	108.0521	106.4369	107.8164	108.6545
H7a-C7-H7c	108.0521	106.4369	108.6545	107.8164
H7b-C7-H7c	107.2139	107.4321	106.575	106.575
C4-C5-H5	118.3773	118.4217	118.8384	118.8384
C6-C5-H5	119.4327	119.4602	119.5955	119.5955
C1-C6-H6	120.4495	120.5499	120.2665	120.2665
C5-C6-H6	120.1934	120.1844	119.9141	119.9141
C2-C3-O3-H3	-0.0001	-180	-90.3889	90.3889
C4-C3-O3-H3	179.9999	0	93.0283	-93.0283
C3-C4-C7-H7a	-0.0004	0	174.8375	-174.8375
C3-C4-C7-H7b	120.5061	120.2962	-64.9817	-53.8509
C3-C4-C7-H7c	-120.5069	-120.2963	53.8509	64.9817
C5-C4-C7-H7a	179.9997	180	-4.9858	4.9858
C5-C4-C7-H7b	-59.4938	-59.7038	115.195	125.9724
C5-C4-C7-H7c	59.4931	59.7037	-125.9724	-115.195

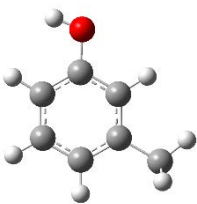
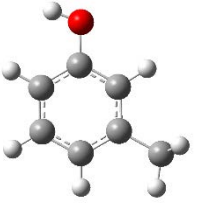
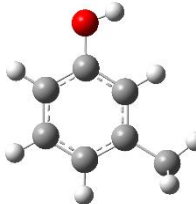
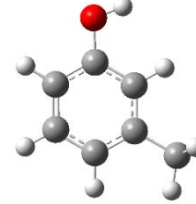
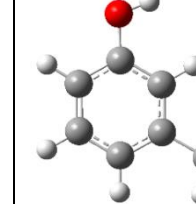
**Table S3a:** Optimized geometry structures of conformers C<sub>1</sub>-C<sub>5</sub> of m-cresol at the B3LYP/cc-pVTZ level of theory.



Energy (Hartree)	-346.917009	-346.917009	-346.9169734	-346.916973	-346.916972
$\Delta E$ (kJ.mol <sup>-1</sup> )	0	0	0.094071665	0.09407167	0.09724852
C1-C2	1.3895	1.3895	1.3854	1.3854	1.3852
C2-C3	1.3919	1.3919	1.3933	1.3933	1.3935
C3-C4	1.3921	1.3921	1.3908	1.3908	1.3905
C4-C5	1.3918	1.3918	1.396	1.396	1.3962
C5-C6	1.3971	1.3971	1.3927	1.3927	1.3924
C1-C6	1.3879	1.3879	1.3921	1.3921	1.3924
C1-H1	1.0821	1.0821	1.0821	1.0821	1.0821
C2-H2	1.0837	1.0837	1.0807	1.0807	1.0807
C4-H4	1.0821	1.0821	1.0854	1.0854	1.0854
C6-H6	1.0822	1.0822	1.082	1.082	1.082
C3-O3	1.3675	1.3675	1.3673	1.3673	1.3673
O3-H3	0.9622	0.9622	0.9623	0.9623	0.9623
C5-C7	1.5068	1.5068	1.5068	1.5068	1.5068
C7-H7a	1.0898	1.09	1.0927	1.0914	1.0921
C7-H7b	1.09	1.0898	1.0914	1.0927	1.0921
C7-H7c	1.0931	1.0931	1.0891	1.0891	1.089
C1-C2-C3	119.1953	119.1953	119.0	119.0224	119.0232
C2-C3-C4	120.212	120.212	120.2	120.2041	120.2071
C3-C4-C5	120.6779	120.6779	120.9	120.8572	120.8547
C4-C5-C6	118.8942	118.8942	118.6	118.6483	118.6473
C5-C6-C1	120.3143	120.3143	120.3	120.3296	120.3347
C6-C1-C2	120.7058	120.7058	120.9	120.9382	120.933
C2-C1-H1	119.3955	119.3955	119.4	119.3559	119.3634
C6-C1-H1	119.8983	119.8983	119.7	119.7059	119.7036
C1-C2-H2	120.5633	120.5633	121.7	121.7189	121.7238
C3-C2-H2	120.2407	120.2408	119.3	119.2584	119.253
C2-C3-O3	122.5079	122.5078	117.4	117.4265	117.4103
C4-C3-O3	117.2799	117.2799	<b>122.4</b>	122.3692	122.3826
C3-O3-H3	109.327	109.327	109.4	109.3909	109.3909
C3-C4-H4	118.5027	118.5027	119.5	119.4725	119.4699
C5-C4-H4	120.8192	120.8192	119.7	119.6702	119.6754
C4-C5-C7	120.3638	120.3639	120.1	120.1307	120.0837
C6-C5-C7	120.7307	120.7307	121.2	121.2174	121.269
C5-C7-H7a	111.4912	111.3304	111.1	111.4134	111.2782
C5-C7-H7b	111.3305	111.4912	111.4	111.1179	111.2772
C5-C7-H7c	110.891	110.891	111.3	111.2805	111.2731
H7a-C7-H7b	108.2222	108.2223	107.2	107.1774	107.1508
H7a-C7-H7c	107.3809	107.3358	107.7	108.0012	107.8357
H7b-C7-H7c	107.336	107.381	108.0	107.6595	107.835
C1-C6-H6	119.9295	119.9295	120.0	119.9549	119.9526
C5-C6-H6	119.7561	119.7561	119.7	119.7155	119.7127
C2-C3-O3-H3	0.0553	-0.0541	179.993	-179.9951	-180.0004
C4-C3-O3-H3	-179.784	179.7834	0.0943	-0.0964	-0.0004

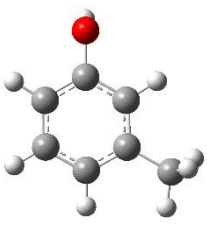
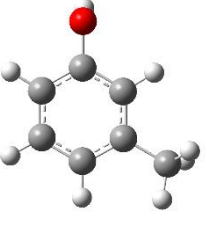
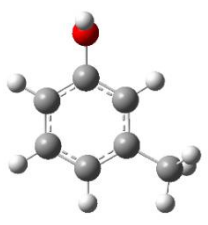
C4-C5-C7-H7a	29.2172	-150.1841	-70.5265	-48.9105	-59.7111
C4-C5-C7-H7b	150.1835	-29.2176	48.9148	70.5309	59.713
C4-C5-C7-H7c	-90.3811	90.3808	169.5112	-169.507	180.0002
C6-C5-C7-H7a	-152.0165	31.05	108.7767	131.7868	120.2897
C6-C5-C7-H7b	-31.0502	152.0164	-131.782	-108.7717	-120.2862
C6-C5-C7-H7c	88.3852	-88.3852	-11.1856	11.1904	0.001

**Table S3b:** Optimized geometry structures of transition states TS<sub>1</sub>-TS<sub>7</sub> of m-cresol at the B3LYP/cc-pVTZ level of theory.

					
	TS <sub>1</sub>	TS <sub>2</sub>	TS <sub>3</sub>	TS <sub>4</sub>	TS <sub>5</sub>
Energy (Hartree)	-346.916982	-346.916987	-346.916873	-346.916972	-346.916972
$\Delta E$ (kJ.mol <sup>-1</sup> )	0.07170241	0.05783976	0.3573568	0.09816744	0.09816744
C1-C2	1.3909	1.3879	1.3881	1.3852	1.3852
C2-C3	1.3905	1.3934	1.3905	1.3934	1.3934
C3-C4	1.3937	1.3904	1.3938	1.3906	1.3906
C4-C5	1.3902	1.3934	1.393	1.3962	1.3962
C5-C6	1.3986	1.3953	1.3957	1.3925	1.3925
C1-C6	1.3865	1.3896	1.3892	1.3923	1.3923
C1-H1	1.0821	1.0821	1.0822	1.0821	1.0821
C2-H2	1.0837	1.0837	1.0807	1.0807	1.0807
C4-H4	1.0819	1.0823	1.085	1.0854	1.0854
C6-H6	1.0824	1.082	1.0824	1.082	1.082
C3-O3	1.3674	1.3676	1.3673	1.3673	1.3673
O3-H3	0.9622	0.9622	0.9623	0.9623	0.9623
C5-C7	1.5068	1.507	1.507	1.5068	1.5068
C7-H7a	1.0919	1.0919	1.0918	1.0924	1.0918
C7-H7b	1.0919	1.0919	1.0918	1.0918	1.0924
C7-H7c	1.089	1.0891	1.0894	1.089	1.089
C1-C2-C3	119.1809	119.2074	119.0044	119.0231	119.0231
C2-C3-C4	120.201	120.2195	120.1709	120.206	120.206
C3-C4-C5	120.7	120.6679	120.9035	120.8557	120.8557
C4-C5-C6	118.8843	118.8936	118.6337	118.6477	118.6477
C5-C6-C1	120.2993	120.3338	120.2937	120.3329	120.3329
C6-C1-C2	120.7346	120.6778	120.9938	120.9346	120.9346
C2-C1-H1	119.3539	119.4401	119.2753	119.3615	119.3615
C6-C1-H1	119.9116	119.8821	119.731	119.704	119.704
C1-C2-H2	120.5451	120.5867	121.6674	121.723	121.723
C3-C2-H2	120.274	120.2059	119.3281	119.254	119.2539

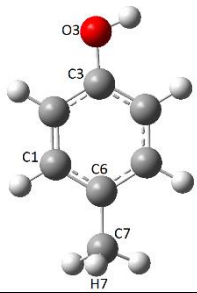
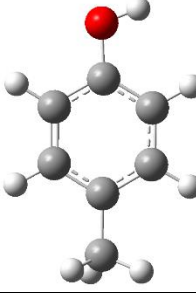
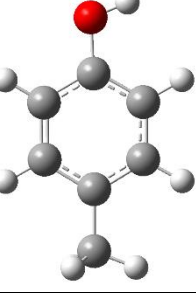
C2-C3-O3	122.605	122.4105	117.62	117.414	117.414
C4-C3-O3	117.194	117.37	122.2091	122.38	122.38
C3-O3-H3	109.3258	109.332	109.3922	109.3907	109.3907
C3-C4-H4	118.4805	118.5119	119.4431	119.4714	119.4714
C5-C4-H4	120.8195	120.8201	119.6534	119.6729	119.6729
C4-C5-C7	120.6581	120.0231	120.7123	120.0886	120.0886
C6-C5-C7	120.4576	121.0833	120.654	121.2629	121.2629
C5-C7-H7a	111.1203	111.1989	111.1393	111.2009	111.34
C5-C7-H7b	111.1206	111.1988	111.1393	111.3402	111.2012
C5-C7-H7c	111.496	111.3541	111.5869	111.2785	111.2785
H7a-C7-H7b	107.0811	107.11	107.0954	107.1502	107.1502
H7a-C7-H7c	107.9169	107.8958	107.8415	107.7612	107.919
H7b-C7-H7c	107.9171	107.8957	107.8415	107.9192	107.7615
C1-C6-H6	119.9279	119.9176	119.9644	119.9531	119.9531
C5-C6-H6	119.7729	119.7487	119.7419	119.7141	119.7141
C2-C3-O3-H3	0	0	180	179.9972	-179.9972
C4-C3-O3-H3	179.9999	180	0	0.0431	-0.043
C4-C5-C7-H7a	120.4283	-59.6302	120.4147	-64.4475	-54.982
C4-C5-C7-H7b	-120.4436	59.6376	-120.4146	54.9663	64.4317
C4-C5-C7-H7c	-0.0074	-179.9964	0	175.4069	-175.4222
C6-C5-C7-H7a	-59.5711	120.3701	-59.5853	115.228	125.3414
C6-C5-C7-H7b	59.5569	-120.3621	59.5854	-125.3582	-115.2448
C6-C5-C7-H7c	179.9931	0.0038	-180	-4.9176	4.9012

Table S3b (continued):

				
	TS <sub>6a</sub>	TS <sub>6b</sub>	TS <sub>7a</sub>	TS <sub>7b</sub>
Energy (Hartree)	-346.910862	-346.910856	-346.910862	-346.910856
$\Delta E$ (kJ.mol <sup>-1</sup> )	16.1384234	16.1545965	16.1384234	16.1545965
C1-C2	1.3883	1.3883	1.3883	1.3883
C2-C3	1.3906	1.3906	1.3906	1.3906
C3-C4	1.3884	1.3884	1.3884	1.3884
C4-C5	1.3959	1.3959	1.3959	1.3959
C5-C6	1.3942	1.3942	1.3942	1.3942
C1-C6	1.3907	1.3907	1.3907	1.3907
C1-H1	1.0821	1.0821	1.0821	1.0821
C2-H2	1.0812	1.0812	1.0812	1.0812
C4-H4	1.0828	1.0828	1.0828	1.0828
C6-H6	1.0825	1.0825	1.0825	1.0825

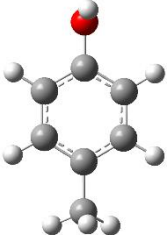
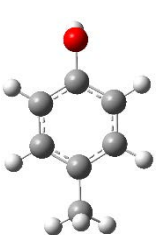
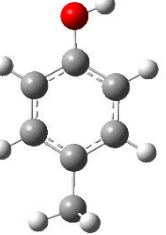
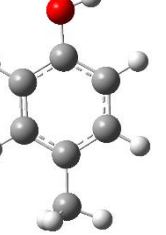
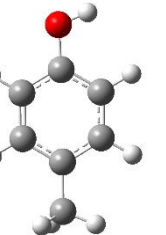
C3-O3	1.3885	1.3885	1.3885	1.3885
O3-H3	0.962	0.962	0.962	0.962
C5-C7	1.5069	1.5069	1.5069	1.5069
C7-H7a	1.091	1.0927	1.0927	1.091
C7-H7b	1.0927	1.091	1.091	1.0927
C7-H7c	1.0893	1.0893	1.0893	1.0893
C1-C2-C3	119.1224	119.1233	119.1224	119.1233
C2-C3-C4	120.436	120.4339	120.436	120.4339
C3-C4-C5	120.7877	120.7907	120.7876	120.7907
C4-C5-C6	118.4398	118.4377	118.4399	118.4377
C5-C6-C1	120.7202	120.7215	120.7202	120.7215
C6-C1-C2	120.492	120.4919	120.492	120.4919
C2-C1-H1	119.7083	119.7085	119.7084	119.7085
C6-C1-H1	119.7996	119.7989	119.7996	119.7989
C1-C2-H2	121.5223	121.5181	121.5222	121.5181
C3-C2-H2	119.3531	119.3527	119.3531	119.3527
C2-C3-O3	119.817	119.8198	119.817	119.8198
C4-C3-O3	119.6798	119.6681	119.6799	119.6681
C3-O3-H3	109.6101	109.6055	109.6101	109.6055
C3-C4-H4	118.6008	118.5946	118.6008	118.5946
C5-C4-H4	120.6085	120.6094	120.6085	120.6094
C4-C5-C7	120.3607	120.3554	120.3605	120.3554
C6-C5-C7	121.193	121.2048	121.1932	121.2048
C5-C7-H7a	111.4042	111.1237	111.0405	111.3311
C5-C7-H7b	111.0404	111.3311	111.404	111.1237
C5-C7-H7c	111.3686	111.362	111.3688	111.362
H7a-C7-H7b	107.1394	107.1496	107.1395	107.1496
H7a-C7-H7c	108.055	107.6264	107.6405	108.0558
H7b-C7-H7c	107.6406	108.0558	108.0549	107.6264
C1-C6-H6	119.7373	119.7337	119.7374	119.7337
C5-C6-H6	119.5419	119.5431	119.5418	119.5431
C2-C3-O3-H3	-92.0186	-91.95	92.0186	91.95
C4-C3-O3-H3	90.9486	91.2515	-90.9486	-91.2515
C4-C5-C7-H7a	-47.2309	-72.22	-72.1046	-47.1356
C4-C5-C7-H7b	72.1047	47.1356	47.2311	72.22
C4-C5-C7-H7c	-167.9501	167.8012	167.9502	-167.8012
C6-C5-C7-H7a	133.7048	107.238	106.9596	133.4064
C6-C5-C7-H7b	-106.9596	-133.4064	-133.7047	-107.238
C6-C5-C7-H7c	12.9856	-12.7409	-12.9856	12.7409

**Table S4a:** Optimized geometry structures conformers C<sub>1</sub>-C<sub>3</sub> of p-cresol at the B3LYP/cc-pVTZ level of theory.

			
	C <sub>1</sub>	C <sub>2</sub>	C <sub>3</sub>
Energy (Hartree)	-346.9160442	-346.9160442	-346.9160423
ΔE (kJ.mol <sup>-1</sup> )	0	0	0.004988
C1-C2	1.3858	1.3858	1.3854
C2-C3	1.3928	1.3928	1.3932
C3-C4	1.3903	1.3903	1.3899
C4-C5	1.391	1.391	1.3914
C5-C6	1.3922	1.3922	1.3918
C6-C1	1.3975	1.3975	1.3979
C1-H1	1.0833	1.0833	1.0834
C2-H2	1.0812	1.0812	1.0812
C3-O3	1.3684	1.3684	1.3684
O3-H16	0.9621	0.9621	0.9622
C4-H4	1.0841	1.0841	1.0841
C5-H10	1.083	1.083	1.083
C6-C7	1.5071	1.5071	1.5072
C7-H7a	1.0931	1.0931	1.0895
C7-H7b	1.0912	1.0897	1.0922
C7-H7c	1.0897	1.0912	1.0922
C1-C2-C3	119.7696	119.7696	119.7768
C2-C3-C4	119.5137	119.5138	119.5149
C3-C4-C5	119.9258	119.9257	119.9164
C4-C5-C6	121.5307	121.5307	121.5419
C5-C6-C1	117.5123	117.5124	117.5098
C6-C1-C2	121.7475	121.7475	121.7402
C2-C1-H1	118.8764	118.8764	118.8717
C6-C1-H1	119.376	119.376	119.3881
C1-C2-H2	121.2038	121.2038	121.2103
C3-C2-H2	119.0263	119.0263	119.0128
C2-C3-O3	117.6481	117.648	117.6248
C4-C3-O3	122.8379	122.8379	122.8603
C3-O3-H3	109.3358	109.3358	109.3322
C3-C4-H4	120.0478	120.0478	120.0629
C5-C4-H4	120.0261	120.0262	120.0208
C4-C5-H5	118.9481	118.9481	118.9444

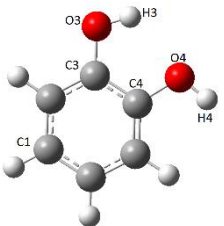
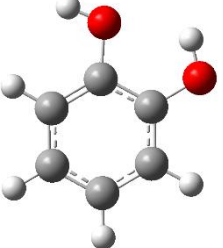
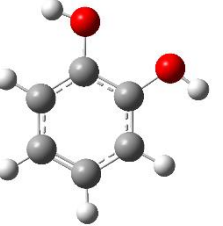
C6-C5-H5	119.5211	119.5211	119.5136
C1-C6-C7	121.0152	121.0152	120.9547
C5-C6-C7	121.4675	121.4675	121.5355
C6-C17-H7a	111.4326	111.4326	111.2455
C6-C17-H7b	111.4731	111.3165	111.472
C6-C17-H7c	111.3165	111.4731	111.4734
H7a-C7-H7b	107.1238	107.4575	107.6742
H7a-C7-H7c	107.4574	107.1238	107.6751
H7b-C7-H7c	107.821	107.821	107.087
C2-C3-O3-H3	-179.899	179.8991	179.9992
C4-C3-O3-H3	-0.0892	0.0891	-0.0006
C1-C6-C7-H7a	-74.1968	74.1947	179.9913
C1-C6-C7-H7b	45.4283	-165.8627	-59.8123
C1-C6-C7-H7c	165.8606	-45.4303	59.7928
C5-C6-C7-H7a	104.9726	-104.9747	-0.0092
C5-C6-C7-H7b	-135.402	14.9679	120.1873
C5-C6-C7-H7c	-14.97	135.4003	-120.208

**Table S4b:** Optimized geometry structures of transition states TS<sub>1</sub>-TS<sub>5</sub> of p-cresol at the B3LYP/cc-pVTZ level of theory.

					
	TS <sub>1</sub>	TS <sub>2</sub>	TS <sub>3</sub>	TS <sub>4</sub>	TS <sub>5</sub>
Energy (Hartree)	-346.9103731	-346.91038	-346.9159607	-346.9160416	-346.9160416
ΔE (kJ.mol <sup>-1</sup> )	14.88942054	14.87146212	0.219255505	0.00672128	0.00672128
C1-C2	1.3894	1.3894	1.3885	1.3856	1.3856
C2-C3	1.3894	1.3893	1.3903	1.393	1.393
C3-C4	1.3894	1.3893	1.3927	1.39	1.39
C4-C5	1.3894	1.3894	1.3884	1.3913	1.3913
C5-C6	1.3952	1.3952	1.3949	1.392	1.392
C6-C1	1.3952	1.3952	1.3948	1.3977	1.3977
C1-H1	1.0832	1.0832	1.083	1.0834	1.0834
C2-H2	1.0817	1.0817	1.0811	1.0812	1.0812
C3-O3	1.3886	1.3885	1.3685	1.3684	1.3684
O3-H16	0.962	0.962	0.9621	0.9622	0.9622
C4-H4	1.0817	1.0817	1.0842	1.0841	1.0841
C5-H10	1.0832	1.0832	1.0834	1.083	1.083
C6-C7	1.507	1.507	1.5074	1.5071	1.5071
C7-H7a	1.0933	1.0932	1.0894	1.0896	1.0896

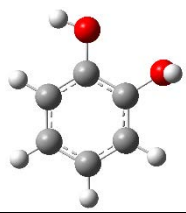
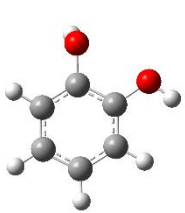
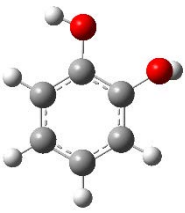
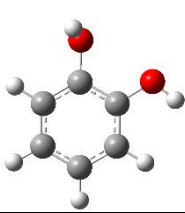
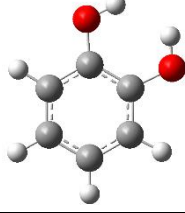
C7-H7b	1.0901	1.0901	1.0922	1.0928	1.0917
C7-H7c	1.0901	1.0901	1.0922	1.0917	1.0928
C1-C2-C3	119.8824	119.8811	119.736	119.7743	119.7743
C2-C3-C4	119.7089	119.7127	119.5024	119.5145	119.5145
C3-C4-C5	119.8824	119.8811	119.9711	119.9195	119.9195
C4-C5-C6	121.3251	121.325	121.497	121.5381	121.5381
C5-C6-C1	117.8723	117.8745	117.4995	117.5107	117.5107
C6-C1-C2	121.3251	121.325	121.794	121.7427	121.7427
C2-C1-H1	119.2264	119.227	118.8737	118.8732	118.8732
C6-C1-H1	119.4477	119.448	119.3323	119.3841	119.3841
C1-C2-H2	120.9772	120.9775	121.1605	121.208	121.208
C3-C2-H2	119.134	119.14	119.1035	119.0175	119.0175
C2-C3-O3	120.1012	120.1117	117.8049	117.6326	117.6326
C4-C3-O3	120.1012	120.1117	122.6926	122.8528	122.8528
C3-O3-H3	109.5757	109.6026	109.3481	109.3335	109.3335
C3-C4-H4	119.134	119.1401	119.9758	120.0576	120.0576
C5-C4-H4	120.9772	120.9774	120.053	120.0229	120.0229
C4-C5-H5	119.2264	119.227	118.9369	118.9468	118.9468
C6-C5-H5	119.4477	119.448	119.5661	119.515	119.515
C1-C6-C7	121.061	121.0545	121.5002	120.9758	120.9758
C5-C6-C7	121.0611	121.0548	121.0003	121.5117	121.5117
C6-C17-H7a	111.1815	111.161	111.5016	111.2689	111.2689
C6-C17-H7b	111.4223	111.4268	111.2055	111.4592	111.4863
C6-C17-H7c	111.4222	111.4267	111.5016	111.4863	111.4592
H7a-C7-H7b	107.2939	107.2939	107.6532	107.5506	107.7598
H7a-C7-H7c	107.294	107.2942	107.1111	107.7598	107.5506
H7b-C7-H7c	108.0213	108.033	107.6532	107.1007	107.1007
C2-C3-O3-H3	91.7166	-91.4573	-180	-179.937	179.9367
C4-C3-O3-H3	-91.7166	91.4572	0	-0.0518	0.0518
C1-C6-C7-H7a	-89.5532	-89.2418	0	172.0074	-172.007
C1-C6-C7-H7b	30.084	30.3847	120.1625	-67.9461	-51.6765
C1-C6-C7-H7c	150.8095	151.1315	-120.163	51.6765	67.9461
C5-C6-C7-H7a	89.5629	89.2624	179.9999	-8.4908	8.4908
C5-C6-C7-H7b	-150.8	-151.111	-59.8376	111.5557	128.8217
C5-C6-C7-H7c	-30.0744	-30.3643	59.8374	-128.822	-111.556

**Table S5a:** Optimized geometry structures of conformers C<sub>1</sub>-C<sub>2</sub> of pyrocatechol at the B3LYP/cc-pVTZ level of theory.

			
	C <sub>1a</sub>	C <sub>1b</sub>	C <sub>2</sub>
Energy (Hartree)	-382.838132	-382.838132	-382.832032
$\Delta E$ (kJ.mol <sup>-1</sup> )	0	0	16.0158388
C1-C2	1.3918	1.393	1.3925
C2-C3	1.3867	1.385	1.3882
C3-C4	1.3996	1.3996	1.4034
C4-C5	1.385	1.3867	1.3882
C5-C6	1.393	1.3918	1.3925
C6-C1	1.388	1.388	1.3857
C1-H1	1.0812	1.0809	1.081
C2-H2	1.0812	1.084	1.0842
C3-O3	1.3625	1.377	1.3651
O3-H3	0.9651	0.9613	0.9622
C4-O4	1.377	1.3625	1.3651
O4-H4	0.9613	0.9651	0.9622
C5-H5	1.084	1.0812	1.0842
C6-H6	1.0809	1.0812	1.081
C1-C2-C3	120.175	119.947	120.9685
C2-C3-C4	119.4107	120.4056	119.3564
C3-C4-C5	120.4056	119.4107	119.3564
C4-C5-C6	119.947	120.175	120.9685
C5-C6-C1	119.775	120.2866	119.6751
C6-C1-C2	120.2866	119.775	119.6751
C2-C1-H1	119.5291	119.701	119.7391
C6-C1-H1	120.1843	120.524	120.5858
C1-C2-H2	121.3565	120.455	120.1072
C3-C2-H2	118.4685	119.598	118.9243
C2-C3-O3	120.0209	124.2765	123.3621
C4-C3-O3	120.5683	115.3179	117.2815
C3-O3-H3	108.107	109.9613	108.9569
C3-C4-O4	115.3179	120.5683	117.2815
C5-C4-O4	124.2765	120.0209	123.3621
C4-O4-H4	109.9613	108.107	108.9569
C4-C5-H5	119.598	118.4685	118.9243
C6-C5-H5	120.455	121.3565	120.1072
C1-C6-H6	120.524	120.1843	120.5858

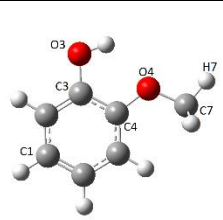
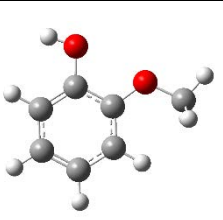
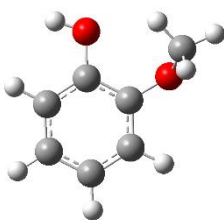
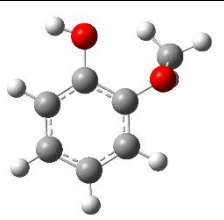
C5-C6-H6	119.701	119.5291	119.7391
C2-C3-O3-H3	-180	0	0
C4-C3-O3-H3	0	-180	-180
C3-C4-O4-H4	-180	0	-180
C5-C4-O4-H4	0	180	0

**Table S5b:** Optimized geometry structures of transition states TS<sub>1</sub>-TS<sub>3</sub> of pyrocatechol at the B3LYP/cc-pVTZ level of theory.

					
	TS <sub>1a</sub>	TS <sub>1b</sub>	TS <sub>2a</sub>	TS <sub>2b</sub>	TS <sub>3</sub>
Energy (Hartree)	-382.827872	-382.827872	-382.827872	-382.827872	-382.827685
$\Delta E$ (kJ.mol <sup>-1</sup> )	26.9387327	26.9387327	26.9387327	26.9387327	27.4292286
C1-C2	1.3898	1.391	1.3898	1.391	1.3868
C2-C3	1.3923	1.3876	1.3923	1.3876	1.3905
C3-C4	1.4011	1.4011	1.4011	1.4011	1.3996
C4-C5	1.3876	1.3923	1.3876	1.3923	1.3905
C5-C6	1.391	1.3898	1.391	1.3898	1.3868
C6-C1	1.3881	1.3881	1.3881	1.3881	1.3902
C1-H1	1.0815	1.081	1.0815	1.081	1.0811
C2-H2	1.0842	1.0821	1.0842	1.0821	1.0814
C3-O3	1.3636	1.3813	1.3636	1.3813	1.3762
O3-H3	0.9623	0.9621	0.9623	0.9621	0.9598
C4-O4	1.3813	1.3636	1.3813	1.3636	1.3762
O4-H4	0.9621	0.9623	0.9621	0.9623	0.9598
C5-H5	1.0821	1.0842	1.0821	1.0842	1.0814
C6-H6	1.081	1.0815	1.081	1.0815	1.0811
C1-C2-C3	120.5978	120.9488	120.5978	120.9488	120.8104
C2-C3-C4	119.3705	119.5568	119.3705	119.5568	119.4401
C3-C4-C5	119.5568	119.3705	119.5568	119.3705	119.4401
C4-C5-C6	120.9488	120.5978	120.9488	120.5978	120.8104
C5-C6-C1	119.4426	120.0813	119.4426	120.0813	119.7495
C6-C1-C2	120.0813	119.4426	120.0813	119.4426	119.7495
C2-C1-H1	119.5409	120.0475	119.5409	120.0475	119.7105
C6-C1-H1	120.3776	120.5083	120.3776	120.5083	120.5399
C1-C2-H2	120.1552	120.9605	120.1552	120.9605	121.3359
C3-C2-H2	119.2457	118.0848	119.2457	118.0848	117.8537
C2-C3-O3	122.8547	121.2058	122.8547	121.2058	116.5121
C4-C3-O3	117.774	119.1594	117.774	119.1594	124.0478

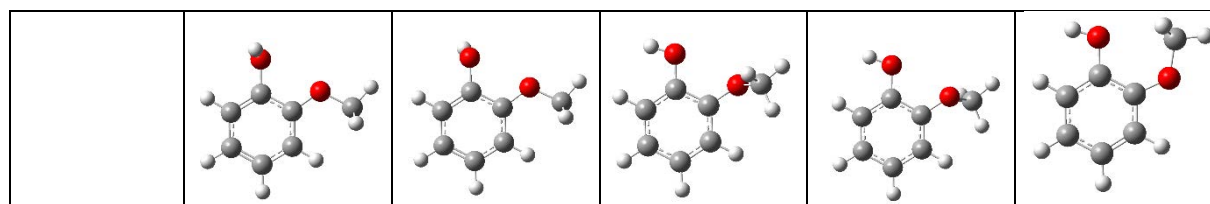
C3-O3-H3	108.9467	109.8856	108.9467	109.8856	112.345
C3-C4-O4	119.1594	117.774	119.1594	117.774	124.0478
C5-C4-O4	121.2058	122.8547	121.2058	122.8547	116.5121
C4-O4-H4	109.8856	108.9467	109.8856	108.9467	112.345
C4-C5-H5	118.0848	119.2457	118.0848	119.2457	117.8537
C6-C5-H5	120.9605	120.1552	120.9605	120.1552	121.3359
C1-C6-H6	120.5083	120.3776	120.5083	120.3776	120.5399
C5-C6-H6	120.0475	119.5409	120.0475	119.5409	119.7105
C2-C3-O3-H3	1.758	78.8651	-1.758	-78.8651	180
C4-C3-O3-H3	-178.5682	-104.3604	178.5682	104.3604	0
C3-C4-O4-H4	-104.3605	-178.5681	104.3605	178.5681	0
C5-C4-O4-H4	78.8651	1.758	-78.8651	-1.758	180

**Table S6a:** Optimized geometry structures of conformers C<sub>1</sub>-C<sub>4</sub> of guaiacol at the B3LYP/cc-pVTZ level of theory.

				
	C <sub>1</sub>	C <sub>2</sub>	C <sub>3</sub>	C <sub>4</sub>
Energy (Hartree)	-422.152656	-422.145969	-422.144057	-422.144057
ΔE (kJ.mol <sup>-1</sup> )	0	17.5579262	22.5764382	22.5764382
C1-C2	1.3931	1.3939	1.3902	1.3902
C2-C3	1.3845	1.3857	1.3907	1.3907
C3-C4	1.4049	1.4086	1.4035	1.4035
C4-C5	1.3865	1.39	1.389	1.389
C5-C6	1.3958	1.3955	1.3906	1.3906
C6-C1	1.3856	1.3832	1.3878	1.3878
C1-H1	1.0813	1.0811	1.0814	1.0814
C2-H2	1.0812	1.0843	1.0845	1.0845
C3-O3	1.3616	1.3652	1.3683	1.3683
O3-H3	0.9657	0.9622	0.9622	0.9622
C4-O4	1.3724	1.36	1.3707	1.3707
O4-C7	1.4183	1.4161	1.4294	1.4294
C7-H7a	1.0867	1.0867	1.0875	1.0875
C7-H7b	1.0927	1.0936	1.0897	1.0936
C7-H7c	1.0927	1.0936	1.0936	1.0897
C5-H5	1.0798	1.0795	1.0815	1.0815

C6-H6	1.0811	1.0812	1.0811	1.0811
C1-C2-C3	120.0639	120.8437	120.6681	120.6681
C2-C3-C4	119.7447	119.6986	119.6119	119.6119
C3-C4-C5	120.1111	119.098	119.1223	119.1223
C4-C5-C6	119.7349	120.678	121.1363	121.1363
C5-C6-C1	120.1474	120.1012	119.5528	119.5528
C6-C1-C2	120.1979	119.5803	119.9006	119.9006
C2-C1-H1	119.5409	119.7585	119.5942	119.5942
C6-C1-H1	120.2611	120.6612	120.5045	120.5045
C1-C2-H2	121.4189	120.1846	120.1953	120.1953
C3-C2-H2	118.5172	118.9716	119.1324	119.1324
C2-C3-O3	120.0524	123.1496	122.476	122.476
C4-C3-O3	120.2029	117.1518	117.9087	117.9087
C3-O3-H3	107.5813	108.811	109.0406	109.0406
C3-C4-O4	114.0008	115.7353	121.8608	121.8608
C5-C4-O4	125.8881	125.1667	118.9086	118.9086
C4-O4-C7	118.4357	118.227	116.4125	116.4125
O4-C7-H7a	106.2267	105.9505	106.0969	106.0969
O4-C7-H7b	111.2643	111.5864	111.5802	110.5954
O4-C7-H7c	111.2644	111.5864	110.5954	111.5802
H7a-C7-H7b	109.3459	109.2449	109.569	109.2743
H7a-C7-H7c	109.3459	109.2449	109.2743	109.569
H7b-C7-H7c	109.3249	109.1454	109.6452	109.6452
C4-C5-H5	120.4987	119.9282	117.6837	117.6837
C6-C5-H5	119.7664	119.3938	121.1767	121.1767
C1-C6-H6	120.4421	120.4686	120.4672	120.4672
C5-C6-H6	119.4104	119.4302	119.9795	119.9795
C2-C3-O3-H3	179.9998	0.0001	-0.6325	0.6325
C4-C3-O3-H3	-0.0001	-179.9999	178.692	-178.692
C3-C4-O4-C7	179.9991	179.9999	67.794	-67.794
C5-C4-O4-C7	-0.0009	-0.0001	-116.0239	116.0239
C4-O4-C7-H7a	-179.9994	-179.9999	177.3193	-177.3193
C4-O4-C7-H7b	-61.0865	-61.2006	-63.404	-58.93
C4-O4-C7-H7c	61.0876	61.2008	58.93	63.404

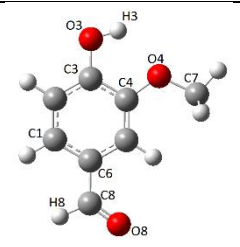
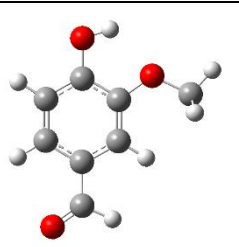
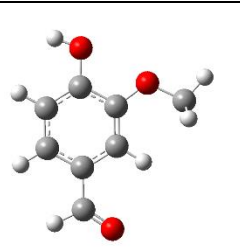
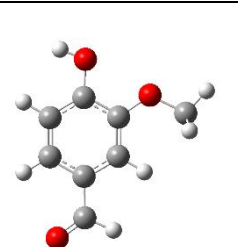
**Table S6b:** Optimized geometry structures of transition states TS<sub>1</sub>-TS<sub>5</sub> of guaiacol at the B3LYP/cc-pVTZ level of theory.



	TS <sub>1</sub>	TS <sub>2</sub>	TS <sub>3</sub>	TS <sub>4</sub>	TS <sub>5</sub>
Energy (Hartree)	-422.141555	-422.141555	-422.142323	-422.142323	-422.141806
$\Delta E$ (kJ.mol <sup>-1</sup> )	29.1468045	29.1468045	27.1303154	27.1303154	28.4875414
C1-C2	1.3926	1.3926	1.3899	1.3899	1.3869
C2-C3	1.3848	1.3848	1.3918	1.3918	1.3927
C3-C4	1.4068	1.4068	1.4026	1.4026	1.4056
C4-C5	1.3938	1.3938	1.3894	1.3894	1.3963
C5-C6	1.393	1.393	1.3909	1.3909	1.3855
C6-C1	1.3854	1.3854	1.388	1.388	1.3886
C1-H1	1.0811	1.0811	1.0814	1.0814	1.0809
C2-H2	1.0821	1.0821	1.0843	1.0843	1.0849
C3-O3	1.3815	1.3815	1.3641	1.3641	1.3763
O3-H3	0.962	0.962	0.9623	0.9623	0.9619
C4-O4	1.3587	1.3587	1.3715	1.3715	1.363
O4-C7	1.4171	1.4171	1.4239	1.4239	1.426
C7-H7a	1.0867	1.0867	1.0875	1.0875	1.0877
C7-H7b	1.0936	1.0933	1.0932	1.0929	1.089
C7-H7c	1.0933	1.0936	1.0929	1.0932	1.089
C5-H5	1.0795	1.0795	1.0817	1.0817	1.0813
C6-H6	1.0817	1.0817	1.0811	1.0811	1.0811
C1-C2-C3	120.8347	120.8347	120.65	120.65	121.731
C2-C3-C4	119.909	119.909	119.4567	119.4567	119.399
C3-C4-C5	119.0791	119.0791	119.4032	119.4032	118.1335
C4-C5-C6	120.3337	120.3337	120.9212	120.9212	122.0258
C5-C6-C1	120.5047	120.5047	119.5905	119.5905	119.6263
C6-C1-C2	119.3362	119.3362	119.9758	119.9758	119.0844
C2-C1-H1	120.0619	120.0619	119.6084	119.6084	119.9621
C6-C1-H1	120.6002	120.6002	120.4154	120.4154	120.9535
C1-C2-H2	121.0202	121.0202	120.1666	120.1666	119.9938
C3-C2-H2	118.1385	118.1385	119.1815	119.1815	118.2752
C2-C3-O3	121.0104	121.0104	122.823	122.823	120.6731
C4-C3-O3	119.0047	119.0047	117.7203	117.7203	119.9279
C3-O3-H3	109.8416	109.8416	108.8835	108.8835	108.4392
C3-C4-O4	116.2107	116.2107	118.181	118.181	127.4663
C5-C4-O4	124.7093	124.7093	122.3562	122.3562	114.4002
C4-O4-C7	118.3435	118.3435	116.1747	116.1747	123.2267
O4-C7-H7a	105.9261	105.9261	106.3683	106.3683	104.851
O4-C7-H7b	111.6449	111.5423	110.9109	111.9834	111.7555
O4-C7-H7c	111.5423	111.6449	111.9834	110.9109	111.7555
H7a-C7-H7b	109.2301	109.2422	109.4087	109.0248	109.5575
H7a-C7-H7c	109.2422	109.2301	109.0248	109.4087	109.5575
H7b-C7-H7c	109.1706	109.1706	109.0762	109.0762	109.2627
C4-C5-H5	120.2669	120.2669	118.721	118.721	116.9472
C6-C5-H5	119.3982	119.3982	120.3507	120.3507	121.027

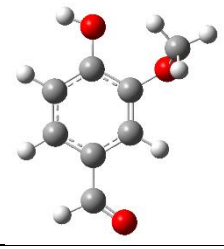
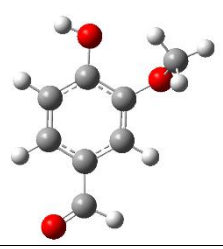
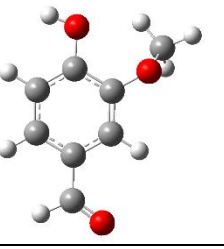
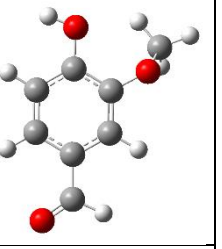
C1-C6-H6	120.2684	120.2684	120.46	120.46	120.6175
C5-C6-H6	119.2267	119.2267	119.9473	119.9473	119.7561
C2-C3-O3-H3	78.4924	-78.4924	-0.8524	0.8524	0
C4-C3-O3-H3	-104.6793	104.6793	179.1249	-179.1249	-180
C3-C4-O4-C7	-178.3007	178.3007	119.0176	-119.0176	-0.0001
C5-C4-O4-C7	2.0387	-2.0387	-63.8079	63.8079	179.9999
C4-O4-C7-H7a	179.0159	-179.0159	-178.1519	178.1519	-180
C4-O4-C7-H7b	-62.1858	-60.2586	-59.2714	-62.8385	-61.3996
C4-O4-C7-H7c	60.2586	62.1858	62.8385	59.2714	61.3996

**Table S7a:** Optimized geometry structures of conformer C<sub>1</sub>-C<sub>8</sub> of vanillin at the B3LYP/cc-pVTZ level of theory.

				
	C <sub>1</sub>	C <sub>2</sub>	C <sub>3</sub>	C <sub>4</sub>
Energy (Hartree)	-535.5228871	-535.5209158	-535.5156801	-535.5141589
$\Delta E$ (kJ.mol <sup>-1</sup> )	0	5.17543811	18.92179472	22.9158891
C1-C2	1.3887	1.3844	1.3892	1.3849
C2-C3	1.386	1.3898	1.3877	1.3913
C3-C4	1.4131	1.4076	1.4164	1.4111
C4-C5	1.3771	1.3816	1.3815	1.3857
C5-C6	1.4041	1.4023	1.4032	1.4017
C6-C1	1.3918	1.3946	1.3892	1.3918
C1-H1	1.0826	1.0807	1.0824	1.0805
C2-H2	1.0807	1.081	1.0838	1.0841
C3-O3	1.352	1.3527	1.356	1.3565
O3-H3	0.967	0.9668	0.9629	0.9629
C4-O4	1.3672	1.3694	1.3548	1.357
O4-C7	1.4227	1.4206	1.4204	1.4183
C7-H7a	1.0919	1.0862	1.0927	1.0863
C7-H7b	1.0919	1.0924	1.0927	1.0933
C7-H7c	1.0862	1.0924	1.0862	1.0933
C5-H5	1.0798	1.0814	1.0794	1.0809
C6-C8	1.4683	1.4701	1.4692	1.4708
C8-H8	1.1091	1.1108	1.1094	1.1104
C8=O8	1.2119	1.2104	1.2114	1.2105
C1-C2-C3	119.6222	119.9744	120.4645	120.8246

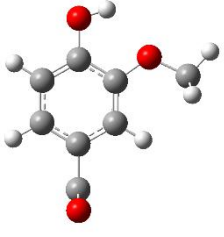
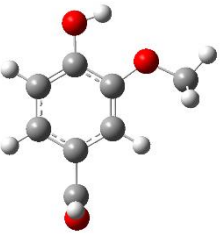
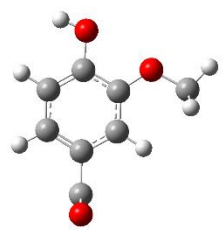
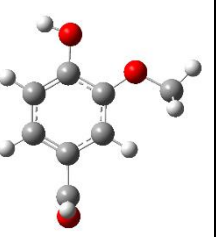
C2-C3-C4	120.1292	120.1066	120.0737	120.0226
C3-C4-C5	120.0579	119.7774	118.9632	118.7248
C4-C5-C6	119.7005	119.9979	120.7192	120.9918
C5-C6-C1	119.9738	119.8694	119.9229	119.8102
C6-C1-C2	120.5164	120.2743	119.8564	119.6259
C2-C1-H1	119.8872	120.9853	120.1328	121.2288
C6-C1-H1	119.5964	118.7405	120.0109	119.1453
C1-C2-H2	121.7108	121.5861	120.4599	120.3044
C3-C2-H2	118.667	118.4394	119.0756	118.871
C2-C3-O3	120.021	119.8315	123.0581	122.95
C4-C3-O3	119.8497	120.0619	116.8681	117.0274
C3-O3-H3	107.8427	107.9205	109.2873	109.2679
C3-C4-O4	113.639	113.8739	115.5094	115.6918
C5-C4-O4	126.3031	126.3487	125.5274	125.5833
C4-O4-C7	118.2047	118.4091	117.995	118.2282
O4-C7-H7a	111.0343	106.1746	111.3776	105.8967
O4-C7-H7b	111.0343	111.1476	111.3776	111.4952
O4-C7-H7c	106.1166	111.1476	105.838	111.4952
H7a-C7-H7b	109.4517	109.4051	109.2591	109.2875
H7a-C7-H7c	109.5715	109.4051	109.4585	109.2875
H7b-C7-H7c	109.5715	109.4901	109.4585	109.2945
C4-C5-H5	122.1809	120.8614	121.5263	120.2468
C6-C5-H5	118.1186	119.1406	117.7545	118.7614
C1-C6-C8	120.0196	120.9837	119.88	120.9117
C5-C6-C8	120.0066	119.1469	120.1971	119.278
C6-C8-H8	114.3225	114.3012	114.2868	114.3453
C6-C8=O8	125.2015	125.4054	125.2462	125.3328
H8-C8=O8	120.476	120.2934	120.467	120.3219
C2-C3-O3-H3	-179.9999	180.0	0.0	0.0
C4-C3-O3-H3	0.0001	0.0	-180.0	180.0
C3-C4-O4-C7	-179.9997	-180.0	-180.0	-180.0
C5-C4-O4-C7	0.0003	0.0	0.0	0.0
C1-C6-C8-H8	0.0	179.9996	-0.0006	-179.9999
C1-C6-C8=O8	180.0	0.0004	180.0005	-0.0002
C5-C6-C8-H8	-180.0	-0.0004	179.9995	0.0002
C5-C6-C8=O8	0.0001	-179.9996	0.0005	-180.0002

Table S7a (continued):

				
	C <sub>5</sub>	C <sub>6</sub>	C <sub>7</sub>	C <sub>8</sub>
Energy (Hartree)	-535.5118158	-535.5118966	-535.5118158	-535.5118965
$\Delta E$ (kJ.mol <sup>-1</sup> )	29.06764564	28.85555775	29.06756687	28.85558401
C1-C2	1.386	1.3816	1.386	1.3816
C2-C3	1.3921	1.3964	1.3921	1.3964
C3-C4	1.4109	1.4055	1.4109	1.4055
C4-C5	1.3807	1.3853	1.3807	1.3853
C5-C6	1.3995	1.3963	1.3995	1.3963
C6-C1	1.393	1.3962	1.393	1.3962
C1-H1	1.0827	1.0808	1.0827	1.0808
C2-H2	1.084	1.0843	1.084	1.0843
C3-O3	1.3592	1.3599	1.3592	1.3599
O3-H3	0.9629	0.9629	0.9629	0.9629
C4-O4	1.3672	1.3679	1.3672	1.3679
O4-C7	1.4311	1.4314	1.4311	1.4314
C7-H7a	1.087	1.0871	1.087	1.0871
C7-H7b	1.0898	1.0895	1.093	1.0931
C7-H7c	1.093	1.0931	1.0898	1.0895
C5-H5	1.0811	1.0829	1.0811	1.0829
C6-C8	1.4713	1.4719	1.4713	1.4719
C8-H8	1.1098	1.1095	1.1098	1.1095
C8=O8	1.21	1.2103	1.21	1.2103
C1-C2-C3	120.2368	120.6643	120.2369	120.6643
C2-C3-C4	120.01	119.9421	120.0099	119.9421
C3-C4-C5	119.0574	118.734	119.0574	118.734
C4-C5-C6	121.0682	121.4408	121.0682	121.4408
C5-C6-C1	119.3927	119.319	119.3928	119.319
C6-C1-C2	120.2294	119.891	120.2294	119.8909
C2-C1-H1	119.9437	121.1111	119.9436	121.1111
C6-C1-H1	119.8265	118.9972	119.8266	118.9972
C1-C2-H2	120.4871	120.326	120.487	120.3261
C3-C2-H2	119.2723	119.0052	119.2724	119.0051
C2-C3-O3	122.4782	122.289	122.4783	122.2891
C4-C3-O3	117.509	117.7658	117.509	117.7658
C3-O3-H3	109.5059	109.4719	109.5058	109.4719
C3-C4-O4	121.2421	121.8633	121.2421	121.8633
C5-C4-O4	119.5831	119.2806	119.583	119.2806

C4-O4-C7	116.4433	116.5393	116.4433	116.5392
O4-C7-H7a	106.0285	106.0161	106.0285	106.0161
O4-C7-H7b	111.5219	111.5221	110.5189	110.5338
O4-C7-H7c	110.5188	110.5338	111.5221	111.5221
H7a-C7-H7b	109.5447	109.5895	109.3423	109.3416
H7a-C7-H7c	109.3423	109.3415	109.5444	109.5896
H7b-C7-H7c	109.7994	109.7547	109.7993	109.7546
C4-C5-H5	119.3645	118.0507	119.3645	118.0506
C6-C5-H5	119.5645	120.5054	119.5645	120.5055
C1-C6-C8	119.8299	120.9345	119.8299	120.9344
C5-C6-C8	120.7768	119.7463	120.7768	119.7463
C6-C8-H8	114.2266	114.3905	114.2266	114.3905
C6-C8=O8	125.2739	125.1105	125.274	125.1105
H8-C8=O8	120.4995	120.4989	120.4994	120.499
C2-C3-O3-H3	-0.5764	-0.8038	0.5765	0.8022
C4-C3-O3-H3	178.8139	178.5612	-178.8138	-178.5624
C3-C4-O4-C7	70.5382	68.5826	-70.5385	-68.5831
C5-C4-O4-C7	-113.44	-115.4867	113.4399	115.4862
C1-C6-C8-H8	0.1474	179.5253	-0.1451	-179.5254
C1-C6-C8=O8	-179.7962	-0.4883	179.7962	0.4883
C5-C6-C8-H8	179.873	-0.6793	-179.8705	0.6791
C5-C6-C8=O8	-0.0706	179.3071	0.0707	-179.3071

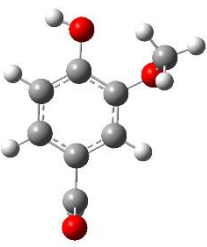
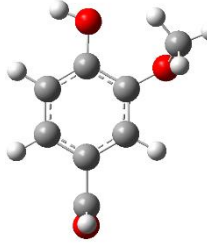
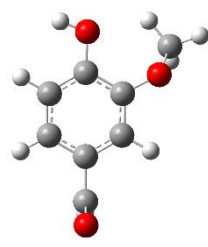
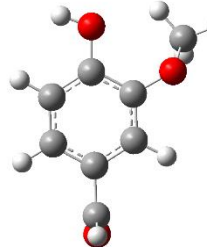
**Table S7b:** Optimized geometry structures of transition states TS<sub>1</sub>-TS<sub>18</sub> of vanillin at the B3LYP/cc-pVTZ level of theory.

				
	TS <sub>1</sub>	TS <sub>2</sub>	TS <sub>3</sub>	TS <sub>4</sub>
Energy (Hartree)	-535.50424601	-535.504246	-535.49760499	-535.49760499
ΔE (kJ.mol <sup>-1</sup> )	48.9421818	48.9421818	66.37817981	66.37817981
C1-C2	1.3923	1.3923	1.3933	1.3933
C2-C3	1.3838	1.3838	1.3849	1.3849
C3-C4	1.4055	1.4055	1.4096	1.4096
C4-C5	1.386	1.386	1.3895	1.3895
C5-C6	1.3982	1.3982	1.398	1.398
C6-C1	1.388	1.388	1.3853	1.3853
C1-H1	1.0815	1.0815	1.0813	1.0813
C2-H2	1.081	1.081	1.0839	1.0839

C3-O3	1.359	1.359	1.3625	1.3625
O3-H3	0.9658	0.9658	0.9624	0.9624
C4-O4	1.3688	1.3688	1.3565	1.3565
O4-C7	1.4203	1.4203	1.418	1.418
C7-H7a	1.0923	1.0923	1.0864	1.0864
C7-H7b	1.0925	1.0863	1.0931	1.0933
C7-H7c	1.0863	1.0925	1.0933	1.0931
C5-H5	1.0802	1.0802	1.0798	1.0798
C6-C8	1.4991	1.4991	1.4991	1.4991
C8-H8	1.1104	1.1104	1.1104	1.1104
C8=O8	1.2039	1.2039	1.2038	1.2038
C1-C2-C3	120.2251	120.2251	121.0147	121.0147
C2-C3-C4	119.6495	119.6495	119.5839	119.5839
C3-C4-C5	120.1713	120.1713	119.1665	119.1665
C4-C5-C6	119.7895	119.7895	120.7282	120.7282
C5-C6-C1	119.9623	119.9623	119.9141	119.9141
C6-C1-C2	120.2006	120.2006	119.5909	119.5909
C2-C1-H1	119.5675	119.5675	119.7734	119.7734
C6-C1-H1	120.2301	120.2301	120.6336	120.6336
C1-C2-H2	121.1393	121.1393	119.8728	119.8728
C3-C2-H2	118.6352	118.6352	119.1123	119.1123
C2-C3-O3	120.0751	120.0751	123.3202	123.3202
C4-C3-O3	120.2754	120.2754	117.0959	117.0959
C3-O3-H3	107.7967	107.7967	109.0384	109.0384
C3-C4-O4	114.0672	114.0672	115.7702	115.7702
C5-C4-O4	125.7613	125.7613	125.0631	125.0631
C4-O4-C7	118.5815	118.5815	118.4068	118.4068
O4-C7-H7a	111.1512	111.1512	105.8817	105.8817
O4-C7-H7b	111.1862	106.1457	111.4831	111.4931
O4-C7-H7c	106.1457	111.1862	111.4931	111.4831
H7a-C7-H7b	109.4836	109.4324	109.3191	109.2756
H7a-C7-H7c	109.4324	109.4836	109.2756	109.3191
H7b-C7-H7c	109.37	109.37	109.3038	109.3038
C4-C5-H5	120.4419	120.4419	119.8925	119.8925
C6-C5-H5	119.7637	119.7637	119.3746	119.3746
C1-C6-C8	120.524	120.524	120.551	120.551
C5-C6-C8	119.5092	119.5092	119.5298	119.5298
C6-C8-H8	115.6811	115.6811	115.6573	115.6573
C6-C8=O8	124.2543	124.2543	124.2552	124.2552
H8-C8=O8	120.0646	120.0646	120.0875	120.0875
C2-C3-O3-H3	179.5993	-179.5993	0.4474	-0.4474
C4-C3-O3-H3	-0.3665	0.3665	-179.5337	179.5337
C3-C4-O4-C7	178.9743	-178.9743	179.4375	-179.4375
C5-C4-O4-C7	-0.879	0.879	-0.4017	0.4017
C1-C6-C8-H8	90.1326	-90.1326	89.6514	-89.6514

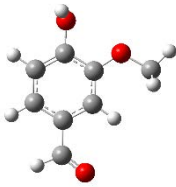
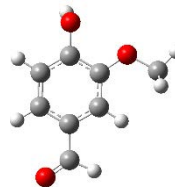
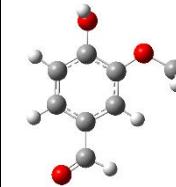
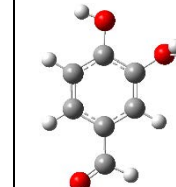
C1-C6-C8=O8	-89.9139	89.9139	-90.4111	90.4111
C5-C6-C8-H8	-89.0952	89.0952	-89.5213	89.5213
C5-C6-C8=O8	90.8583	-90.8583	90.4162	-90.4162

Table S7b (continued):

				
	TS <sub>5</sub>	TS <sub>6</sub>	TS <sub>7</sub>	TS <sub>8</sub>
Energy (Hartree)	-535.49552745	-535.4951961	-535.49519615	-535.4955275
$\Delta E$ (kJ.mol <sup>-1</sup> )	71.83276107	72.70264174	72.70258923	71.83276107
C1-C2	1.3893	1.3891	1.3891	1.3893
C2-C3	1.3901	1.3901	1.3901	1.3901
C3-C4	1.4041	1.4041	1.4041	1.4041
C4-C5	1.3887	1.3887	1.3887	1.3887
C5-C6	1.393	1.393	1.393	1.393
C6-C1	1.3901	1.3902	1.3902	1.3901
C1-H1	1.0817	1.0817	1.0817	1.0817
C2-H2	1.0841	1.0841	1.0841	1.0841
C3-O3	1.3657	1.3658	1.3658	1.3657
O3-H3	0.9624	0.9624	0.9624	0.9624
C4-O4	1.3674	1.3676	1.3676	1.3674
O4-C7	1.4317	1.431	1.431	1.4317
C7-H7a	1.0872	1.0872	1.0872	1.0872
C7-H7b	1.0892	1.0892	1.0933	1.093
C7-H7c	1.093	1.0933	1.0892	1.0892
C5-H5	1.0818	1.0819	1.0819	1.0818
C6-C8	1.4994	1.4998	1.4998	1.4994
C8-H8	1.11	1.1102	1.1102	1.11
C8=O8	1.2037	1.2034	1.2034	1.2037
C1-C2-C3	120.8276	120.8348	120.8348	120.8276
C2-C3-C4	119.5032	119.4994	119.4994	119.5032
C3-C4-C5	119.196	119.1924	119.1923	119.196
C4-C5-C6	121.1844	121.19	121.19	121.1844
C5-C6-C1	119.3596	119.3474	119.3474	119.3596
C6-C1-C2	119.923	119.921	119.921	119.923
C2-C1-H1	119.616	119.6154	119.6153	119.616
C6-C1-H1	120.4603	120.4576	120.4576	120.4603
C1-C2-H2	119.906	119.902	119.902	119.906
C3-C2-H2	119.2637	119.2559	119.2559	119.2637

C2-C3-O3	122.6215	122.5997	122.5997	122.6215
C4-C3-O3	117.8709	117.8975	117.8975	117.8709
C3-O3-H3	109.304	109.2827	109.2827	109.304
C3-C4-O4	122.0905	122.0673	122.0674	122.0905
C5-C4-O4	118.6094	118.618	118.618	118.6094
C4-O4-C7	116.6805	116.7082	116.7083	116.6805
O4-C7-H7a	105.963	105.9762	105.9762	105.963
O4-C7-H7b	111.5348	111.5749	110.5129	110.4987
O4-C7-H7c	110.4987	110.5128	111.575	111.5348
H7a-C7-H7b	109.6561	109.6469	109.2986	109.3325
H7a-C7-H7c	109.3325	109.2986	109.6469	109.6561
H7b-C7-H7c	109.7712	109.7466	109.7465	109.7712
C4-C5-H5	117.6674	117.6563	117.6562	117.6674
C6-C5-H5	121.1482	121.1441	121.1441	121.1482
C1-C6-C8	120.5334	120.4929	120.4929	120.5334
C5-C6-C8	120.1061	120.1549	120.1549	120.1061
C6-C8-H8	115.6773	115.688	115.6881	115.6773
C6-C8=O8	124.1221	124.1398	124.1397	124.1221
H8-C8=O8	120.2005	120.1722	120.1722	120.2005
C2-C3-O3-H3	-0.175	-1.2885	1.2885	0.175
C4-C3-O3-H3	179.0515	178.0319	-178.0318	-179.0515
C3-C4-O4-C7	66.8861	66.7574	-66.7572	-66.8861
C5-C4-O4-C7	-116.8562	-117.2972	117.2975	116.8562
C1-C6-C8-H8	88.9927	-89.2798	89.2795	-88.9927
C1-C6-C8=O8	-91.0083	90.6492	-90.6494	91.0083
C5-C6-C8-H8	-90.6705	89.9189	-89.9193	90.6705
C5-C6-C8=O8	89.3285	-90.1522	90.1517	-89.3285

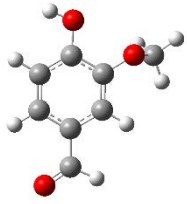
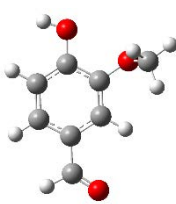
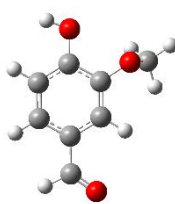
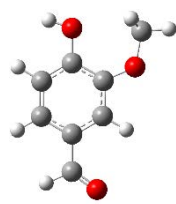
Table S7b (continued):

					
	TS <sub>9</sub>	TS <sub>10</sub>	TS <sub>11</sub>	TS <sub>12</sub>	TS <sub>13</sub>
Energy (Hartree)	-535.509514	-535.509514	-535.5080031	-535.5080031	-535.5102963
$\Delta E$ (kJ.mol <sup>-1</sup> )	35.11110031	35.11110031	39.07799451	39.07799451	33.05719791
C1-C2	1.3898	1.3898	1.3856	1.3856	1.3812
C2-C3	1.3852	1.3852	1.389	1.389	1.3975

C3-C4	1.4138	1.4138	1.4085	1.4085	1.4052
C4-C5	1.3863	1.3863	1.3905	1.3905	1.3852
C5-C6	1.3998	1.3998	1.3985	1.3985	1.3969
C6-C1	1.3903	1.3903	1.3926	1.3926	1.3966
C1-H1	1.0824	1.0824	1.0805	1.0805	1.0808
C2-H2	1.0816	1.0816	1.0818	1.0818	1.0841
C3-O3	1.3751	1.3751	1.3755	1.3755	1.3557
O3-H3	0.9625	0.9625	0.9626	0.9626	0.9629
C4-O4	1.3538	1.3538	1.3557	1.3557	1.3684
O4-C7	1.4211	1.4211	1.4192	1.4192	1.4263
C7-H7a	1.0862	1.0862	1.0863	1.0863	1.0871
C7-H7b	1.0924	1.0927	1.093	1.0933	1.0928
C7-H7c	1.0927	1.0924	1.0933	1.093	1.0927
C5-H5	1.0794	1.0794	1.0809	1.0809	1.0831
C6-C8	1.474	1.474	1.4754	1.4754	1.4711
C8-H8	1.109	1.109	1.1102	1.1102	1.1099
C8=O8	1.2101	1.2101	1.209	1.209	1.2104
C1-C2-C3	120.4889	120.4889	120.8427	120.8427	120.6354
C2-C3-C4	120.2446	120.2446	120.2166	120.2166	119.8154
C3-C4-C5	118.9981	118.998	118.7381	118.738	118.9898
C4-C5-C6	120.3401	120.3401	120.6074	120.6074	121.2342
C5-C6-C1	120.351	120.351	120.2652	120.2652	119.3617
C6-C1-C2	119.576	119.5759	119.3278	119.3278	119.9599
C2-C1-H1	120.4006	120.4006	121.4863	121.4863	121.1361
C6-C1-H1	120.0222	120.0222	119.1843	119.1843	118.9037
C1-C2-H2	121.2574	121.2574	121.1306	121.1306	120.3015
C3-C2-H2	118.2465	118.2465	118.0204	118.0205	119.0616
C2-C3-O3	120.8163	120.8163	120.7208	120.7208	122.6125
C4-C3-O3	118.8544	118.8544	118.9734	118.9733	117.572
C3-O3-H3	110.4463	110.4463	110.4355	110.4355	109.3277
C3-C4-O4	115.9882	115.9882	116.1957	116.1957	118.2227
C5-C4-O4	125.0123	125.0123	125.065	125.065	122.7134
C4-O4-C7	118.1351	118.1351	118.3724	118.3724	116.3307
O4-C7-H7a	105.8205	105.8205	105.8743	105.8743	106.277
O4-C7-H7b	111.3453	111.4435	111.446	111.5606	110.8572
O4-C7-H7c	111.4435	111.3453	111.5606	111.4461	111.88
H7a-C7-H7b	109.4374	109.4426	109.2804	109.2688	109.4586
H7a-C7-H7c	109.4426	109.4374	109.2688	109.2804	109.0858
H7b-C7-H7c	109.2775	109.2775	109.3235	109.3234	109.2126
C4-C5-H5	121.8254	121.8254	120.5731	120.5731	119.0663
C6-C5-H5	117.8334	117.8334	118.8182	118.8182	119.6933
C1-C6-C8	119.6677	119.6677	120.8088	120.8088	120.9382
C5-C6-C8	119.9814	119.9814	118.9259	118.9259	119.6977
C6-C8-H8	114.3456	114.3456	114.4013	114.4013	114.3708
C6-C8=O8	125.1067	125.1067	125.1793	125.1793	125.1948

H8-C8=O8	120.5477	120.5477	120.4194	120.4195	120.4344
C2-C3-O3-H3	-81.0287	81.0287	-81.9706	81.9696	-0.8196
C4-C3-O3-H3	102.3098	-102.3098	101.4561	-101.457	179.0698
C3-C4-O4-C7	178.5833	-178.5832	178.2177	-178.2173	118.303
C5-C4-O4-C7	-1.8489	1.849	-2.1922	2.1926	-64.8616
C1-C6-C8-H8	-0.0805	0.0805	-179.6638	179.6637	179.4709
C1-C6-C8=O8	179.8731	-179.8731	0.3692	-0.3693	-0.5457
C5-C6-C8-H8	179.9316	-179.9316	0.2826	-0.2827	0.0384
C5-C6-C8=O8	-0.1148	0.1149	-179.6844	179.6843	-179.9782

Table S7b (continued):

					
	TS <sub>14</sub>	TS <sub>15</sub>	TS <sub>16</sub>	TS <sub>17</sub>	TS <sub>18</sub>
Energy (Hartree)	-535.5102963	-535.5096123	-535.5107649	-535.5107649	-535.5093859
$\Delta E$ (kJ.mol <sup>-1</sup> )	33.05719791	34.85311868	31.82675733	31.82686236	35.44729558
C1-C2	1.3812	1.3789	1.3856	1.3856	1.383
C2-C3	1.3975	1.3982	1.3935	1.3935	1.3939
C3-C4	1.4052	1.4072	1.41	1.41	1.4127
C4-C5	1.3852	1.3927	1.3803	1.3803	1.3887
C5-C6	1.3969	1.3915	1.3995	1.3995	1.3937
C6-C1	1.3966	1.3961	1.3936	1.3936	1.3934
C1-H1	1.0808	1.0803	1.0828	1.0828	1.0822
C2-H2	1.0841	1.0847	1.0838	1.0838	1.0844
C3-O3	1.3557	1.368	1.3555	1.3555	1.3674
O3-H3	0.9629	0.9625	0.9629	0.9629	0.9625
C4-O4	1.3684	1.3602	1.3684	1.3684	1.3586
O4-C7	1.4263	1.4279	1.4276	1.4276	1.4278
C7-H7a	1.0871	1.0872	1.0929	1.0871	1.0887
C7-H7b	1.0927	1.0887	1.0925	1.0925	1.0887
C7-H7c	1.0928	1.0887	1.0871	1.0929	1.0871
C5-H5	1.0831	1.0827	1.0816	1.0816	1.081
C6-C8	1.4711	1.4725	1.4705	1.4705	1.4724
C8-H8	1.1099	1.1094	1.1096	1.1096	1.1098
C8=O8	1.2104	1.2102	1.2105	1.2105	1.2098
C1-C2-C3	120.6354	121.7534	120.2006	120.2006	121.3484
C2-C3-C4	119.8154	119.7448	119.8486	119.8486	119.842
C3-C4-C5	118.9898	117.7086	119.3341	119.3341	117.9417
C4-C5-C6	121.2342	122.3506	120.9118	120.9118	122.0428
C5-C6-C1	119.3617	119.4073	119.3759	119.3759	119.4896

C6-C1-C2	119.9599	119.0354	120.3244	120.3244	119.3355
C2-C1-H1	121.1361	121.477	119.9319	119.9318	120.3445
C6-C1-H1	118.9037	119.4877	119.7437	119.7436	120.32
C1-C2-H2	120.3015	120.1048	120.4492	120.4492	120.2858
C3-C2-H2	119.0616	118.1418	119.3488	119.3488	118.3658
C2-C3-O3	122.6125	120.4938	122.7928	122.7928	120.6151
C4-C3-O3	117.572	119.7614	117.3586	117.3586	119.543
C3-O3-H3	109.3277	108.8878	109.388	109.388	108.926
C3-C4-O4	118.2227	127.5914	118.4053	118.4054	127.2235
C5-C4-O4	122.7134	114.7001	122.1968	122.1968	114.8348
C4-O4-C7	116.3307	123.4057	115.8119	115.8119	123.7602
O4-C7-H7a	106.277	104.7649	110.8493	106.3368	111.7039
O4-C7-H7b	111.88	111.674	111.5109	111.5109	111.7039
O4-C7-H7c	110.8572	111.674	106.3368	110.8492	104.709
H7a-C7-H7b	109.0858	109.5852	109.3181	109.3202	109.462
H7a-C7-H7c	109.4586	109.5852	109.443	109.4429	109.5738
H7b-C7-H7c	109.2126	109.4472	109.3202	109.3181	109.5738
C4-C5-H5	119.0663	117.2993	120.1343	120.1344	118.5168
C6-C5-H5	119.6933	120.3501	118.9496	118.9495	119.4404
C1-C6-C8	120.9382	121.0489	119.9677	119.9677	119.7822
C5-C6-C8	119.6977	119.5438	120.6548	120.6549	120.7282
C6-C8-H8	114.3708	114.4266	114.2891	114.2891	114.1314
C6-C8=O8	125.1948	125.0587	125.2202	125.2202	125.3865
H8-C8=O8	120.4344	120.5147	120.4907	120.4907	120.4821
C2-C3-O3-H3	0.8196	0.0	-0.4761	0.4757	-0.0001
C4-C3-O3-H3	-179.0698	-180.0	179.4877	-179.488	179.9999
C3-C4-O4-C7	-118.303	-0.0001	110.6251	-110.625	-0.0001
C5-C4-O4-C7	64.8616	179.9999	-72.2989	72.299	179.9999
C1-C6-C8-H8	-179.4709	180.0	0.1167	-0.1159	0.0
C1-C6-C8=O8	0.5457	0.0	-179.8062	179.807	-180.0
C5-C6-C8-H8	-0.0384	0.0	-179.4271	179.4279	-180.0
C5-C6-C8=O8	179.9782	180.0	0.65	-0.6492	0.0

**Table S8a:** Optimized geometry structures of conformer C<sub>1</sub>-C<sub>8</sub> of syringol at the B3LYP/cc-pVTZ level of theory.

	C <sub>1</sub>	C <sub>2</sub>	C <sub>3</sub>
Energy (Hartree)	-536.7126247	-536.7111726	-536.7111726

$\Delta E$ (kJ.mol <sup>-1</sup> )	0	3.812567315	3.812567315
C1-C2	1.3956	1.3946	1.3946
C2-C3	1.3991	1.3947	1.3947
C3-C4	1.3972	1.4027	1.4027
C4-C5	1.3912	1.3874	1.3874
C5-C6	1.3891	1.3938	1.3938
C6-C1	1.3892	1.3846	1.3846
C1-H1	1.0788	1.0807	1.0807
C2-O2	1.3604	1.3702	1.3702
O2-C7	1.4159	1.4297	1.4297
C7-H7a	1.0868	1.0876	1.0876
C7-H7b	1.0935	1.0893	1.0936
C7-H7c	1.0935	1.0936	1.0893
C3-O3	1.3611	1.364	1.364
O3-H3	0.9657	0.966	0.966
C4-O4	1.3734	1.3732	1.3732
O4-C8	1.4179	1.4186	1.4186
C8-H8a	1.0926	1.0926	1.0926
C8-H8b	1.0868	1.0867	1.0925
C8-H8c	1.0926	1.0925	1.0867
C5-H85	1.079	1.0792	1.0792
C6-H6	1.0811	1.081	1.081
C1-C2-C3	119.4694	119.488	119.4879
C2-C3-C4	119.5982	119.487	119.4871
C3-C4-C5	121.0033	120.864	120.864
C4-C5-C6	118.8151	119.0876	119.0875
C5-C6-C1	121.0246	120.5323	120.5323
C6-C1-C2	120.0893	120.5312	120.5313
C2-C1-H1	120.2568	117.9912	117.991
C6-C1-H1	119.6539	121.4748	121.4749
C1-C2-O2	125.097	118.6529	118.653
C3-C2-O2	115.4335	121.7599	121.76
C2-O2-C7	118.2665	116.619	116.6188
O2-C7-7a	105.9295	106.0236	106.0234
O2-C7-7b	111.6138	111.6435	110.5419
O2-C7-7c	111.6138	110.5421	111.643
H7a-C7-H7b	109.22	109.6556	109.2414
H7a-C7-H7c	109.22	109.2412	109.656
H7b-C7-H7c	109.1578	109.6526	109.6528
C2-C3-O3	119.5752	120.4181	120.4179
C4-C3-O3	120.8266	120.0899	120.09
C3-O3-H3	106.9576	107.096	107.0959
C3-C4-O4	113.4649	113.4076	113.4077
C5-C4-O4	125.5318	125.7235	125.7235
C4-O4-C8	118.4378	118.4222	118.422

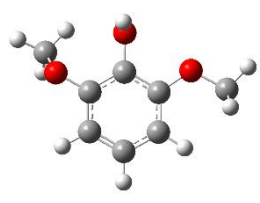
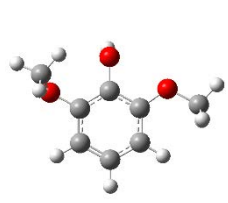
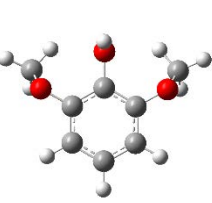
O4-C8-H8a	111.2857	111.2328	111.2327
O4-C8-H8b	106.1968	106.2068	111.2085
O4-C8-H8c	111.2857	111.2085	106.2067
H8a-C8-H8b	109.3344	109.3489	109.3595
H8a-C8-H8c	109.3331	109.3594	109.349
H8b-C8-H8c	109.3344	109.4167	109.4168
C4-C5-H5	120.9212	120.7722	120.7723
C6-C5-H5	120.2637	120.1396	120.1396
C1-C6-H6	119.4576	119.9734	119.9734
C5-C6-H6	119.5178	119.4933	119.4932
C1-C2-O2-C7	0	-119.4051	119.405
C3-C2-O2-C7	180	64.2344	-64.2342
C2-C3-O3-H3	180	179.183	-179.1825
C4-C3-O3-H3	0	-0.0013	0.0021
C3-C4-O4-C8	180	177.8372	-177.8372
C5-C4-O4-C8	0	-1.3661	1.3661

**Table S8b:** Optimized geometry structures of transition states TS<sub>1</sub>-TS<sub>7</sub> of syringol at the B3LYP/cc-pVTZ level of theory.

	TS <sub>1</sub>	TS <sub>2</sub>	TS <sub>3</sub>	TS <sub>4</sub>
Energy (Hartree)	-536.7093355	-536.7093355	-536.7095105	-536.7038725
$\Delta E$ (kJ.mol <sup>-1</sup> )	8.635978385	8.635978385	8.17648963	22.9789011
C1-C2	1.3952	1.3952	1.401	1.3967
C2-C3	1.3933	1.3933	1.3972	1.4004
C3-C4	1.404	1.404	1.4057	1.4004
C4-C5	1.3871	1.3871	1.3849	1.3967
C5-C6	1.3941	1.3941	1.3941	1.3876
C6-C1	1.3847	1.3847	1.38	1.3876
C1-H1	1.0809	1.0809	1.0806	1.0786
C2-O2	1.3718	1.3718	1.3622	1.3598
O2-C7	1.4238	1.4238	1.4266	1.4171
C7-H7a	1.0876	1.0876	1.0876	1.0868
C7-H7b	1.0933	1.093	1.089	1.0934
C7-H7c	1.093	1.0933	1.089	1.0931
C3-O3	1.3594	1.3594	1.3713	1.3764
O3-H3	0.9658	0.9658	0.9662	0.9627
C4-O4	1.3724	1.3724	1.3747	1.3598
O4-C8	1.4185	1.4185	1.4183	1.4171

C8-H8a	1.0927	1.0926	1.0925	1.0934
C8-H8b	1.0867	1.0867	1.0867	1.0868
C8-H8c	1.0926	1.0927	1.0925	1.0931
C5-H85	1.0792	1.0792	1.0788	1.0786
C6-H6	1.081	1.081	1.0811	1.0817
C1-C2-C3	119.8394	119.8394	118.6613	120.0545
C2-C3-C4	119.3175	119.3174	119.2411	119.7965
C3-C4-C5	120.8038	120.8039	121.7745	120.0545
C4-C5-C6	119.2103	119.2103	118.411	119.3061
C5-C6-C1	120.5571	120.5571	120.6089	121.4722
C6-C1-C2	120.2678	120.2678	121.3033	119.3061
C2-C1-H1	119.0474	119.0474	117.3352	120.8129
C6-C1-H1	120.6735	120.6734	121.3615	119.8809
C1-C2-O2	122.2506	122.2506	114.4767	124.5027
C3-C2-O2	117.8509	117.8509	126.8621	115.4421
C2-O2-C7	116.0267	116.0267	122.7718	118.3765
O2-C7-7a	106.3678	106.3678	104.8984	105.9118
O2-C7-7b	110.9385	111.9523	111.7094	111.6585
O2-C7-7c	111.9524	110.9386	111.7094	111.5305
H7a-C7-H7b	109.3843	109.0667	109.6209	109.2225
H7a-C7-H7c	109.0667	109.3843	109.6209	109.2374
H7b-C7-H7c	109.0634	109.0634	109.191	109.1938
C2-C3-O3	120.1705	120.1705	122.2316	120.057
C4-C3-O3	120.5118	120.5118	118.5273	120.057
C3-O3-H3	107.0476	107.0477	106.4581	110.1853
C3-C4-O4	113.4937	113.4937	112.8862	115.4421
C5-C4-O4	125.7008	125.7007	125.3392	124.5027
C4-O4-C8	118.4554	118.4554	118.4483	118.3765
O4-C8-H8a	111.272	111.2315	111.2091	111.6585
O4-C8-H8b	106.1959	106.1959	106.2028	105.9118
O4-C8-H8c	111.2315	111.272	111.2091	111.5305
H8a-C8-H8b	109.3491	109.3718	109.3937	109.2225
H8a-C8-H8c	109.3511	109.3512	109.3653	109.1938
H8b-C8-H8c	109.3718	109.3491	109.3937	109.2374
C4-C5-H5	120.767	120.767	121.1155	120.8129
C6-C5-H5	120.0219	120.0219	120.4736	119.8809
C1-C6-H6	119.9691	119.9691	119.7665	119.2638
C5-C6-H6	119.4709	119.4709	119.6247	119.2638
C1-C2-O2-C7	-64.4148	64.4148	-179.9998	2.5396
C3-C2-O2-C7	118.3885	-118.3885	0.0002	-177.7603
C2-C3-O3-H3	179.2477	-179.2478	180	-91.7232
C4-C3-O3-H3	-0.5712	0.5711	0	91.7232
C3-C4-O4-C8	179.9381	-179.9381	180	177.7603
C5-C4-O4-C8	-0.5333	0.5334	0	-2.5396

Table S8b (continued):

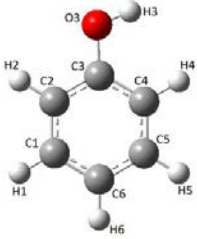
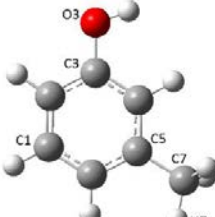
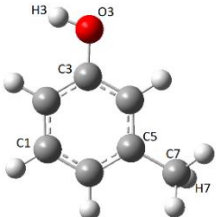
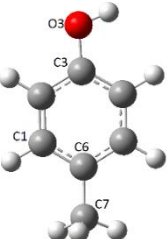
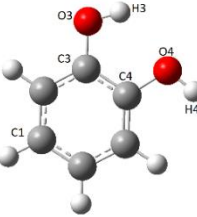
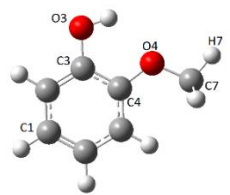
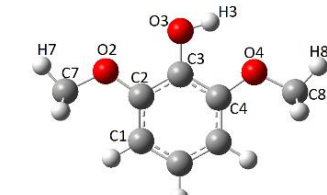
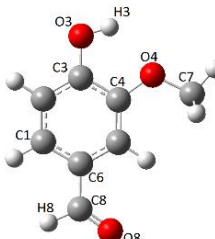
			
	TS <sub>5</sub>	TS <sub>6</sub>	TS <sub>7</sub>
Energy (Hartree)	-536.7021593	-536.7021593	-536.7000751
$\Delta E$ (kJ.mol <sup>-1</sup> )	27.47693396	27.47693396	32.94915858
C1-C2	1.3939	1.3939	1.3914
C2-C3	1.3948	1.3948	1.3999
C3-C4	1.4054	1.4054	1.3999
C4-C5	1.3939	1.3939	1.3914
C5-C6	1.3918	1.3918	1.3882
C6-C1	1.3842	1.3842	1.3882
C1-H1	1.0806	1.0806	1.0809
C2-O2	1.3721	1.372	1.3714
O2-C7	1.4309	1.4309	1.4308
C7-H7a	1.0933	1.0894	1.0876
C7-H7b	1.0877	1.0877	1.0894
C7-H7c	1.0894	1.0933	1.0933
C3-O3	1.3804	1.3804	1.3847
O3-H3	0.963	0.963	0.9633
C4-O4	1.3594	1.3594	1.3714
O4-C8	1.4176	1.4176	1.4308
C8-H8a	1.0867	1.0867	1.0894
C8-H8b	1.0934	1.0931	1.0876
C8-H8c	1.0931	1.0934	1.0933
C5-H85	1.0788	1.0788	1.0809
C6-H6	1.0816	1.0816	1.0815
C1-C2-C3	120.3016	120.3016	119.9334
C2-C3-C4	119.7279	119.7278	119.6576
C3-C4-C5	119.7115	119.7116	119.9334
C4-C5-C6	119.7399	119.7399	120.0296
C5-C6-C1	120.9396	120.9396	120.3987
C6-C1-C2	119.5772	119.5772	120.0296
C2-C1-H1	118.6608	118.6607	118.3939
C6-C1-H1	121.7595	121.7596	121.5686
C1-C2-O2	118.8137	118.8136	118.7788
C3-C2-O2	120.7897	120.7899	121.1394
C2-O2-C7	115.9396	115.9398	116.1759
O2-C7-7a	110.4832	111.3698	106.114
O2-C7-7b	106.1377	106.1376	111.4127
O2-C7-7c	111.3698	110.4832	110.5024

H7a-C7-H7b	109.2469	109.7957	109.7477
H7a-C7-H7c	109.7315	109.7314	109.2472
H7b-C7-H7c	109.7956	109.2469	109.7384
C2-C3-O3	120.5609	120.561	120.166
C4-C3-O3	119.6655	119.6655	120.166
C3-O3-H3	109.7855	109.7855	109.4471
C3-C4-O4	115.5837	115.5836	121.1394
C5-C4-O4	124.6977	124.6977	118.7788
C4-O4-C8	118.3228	118.3228	116.1759
O4-C8-H8a	105.9175	105.9175	111.4127
O4-C8-H8b	111.5968	111.5093	106.114
O4-C8-H8c	111.5093	111.5967	110.5024
H8a-C8-H8b	109.2785	109.2617	109.7477
H8a-C8-H8c	109.2617	109.2785	109.7384
H8b-C8-H8c	109.1945	109.1945	109.2472
C4-C5-H5	120.5686	120.5686	118.3939
C6-C5-H5	119.6894	119.6894	121.5686
C1-C6-H6	119.817	119.817	119.7998
C5-C6-H6	119.2432	119.2433	119.7998
C1-C2-O2-C7	-112.4609	112.4616	-114.8616
C3-C2-O2-C7	71.0722	-71.0715	69.5705
C2-C3-O3-H3	88.1524	-88.1538	90.5903
C4-C3-O3-H3	-94.3132	94.3117	-90.5903
C3-C4-O4-C8	-179.2679	179.268	-69.5705
C5-C4-O4-C8	1.7055	-1.7056	114.8616

## Appendix II: Computational study of phenolic compounds-water clusters

All energies (Energy, ZPE and BSSE) are given in Hartree.

**Table S1:** Ground states from previous chapter

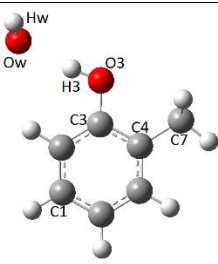
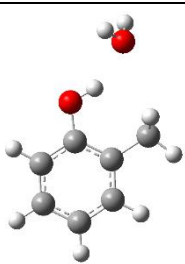
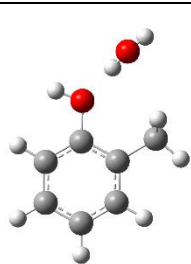
	Phenol	O-cresol	Cis m-cresol	Trans m-cresol	P-cresol
					
Energy	-307.58569373	-346.91733851	-346.91697335	-346.91700918	-346.91604419
ZPE	0.104535	0.132027	0.131776	0.131661	0.131703
	Pyrocatechol	Guaiacol	Syringol	Vanillin	
					
Energy	-382.8381324	-422.1526564	-536.7126247	-535.5228871	
ZPE	0.108759	0.137271	0.169649	0.146730	

**Table S2:** Most stable conformations in the phenol-water complex

C <sub>1</sub>		C <sub>2</sub>		C <sub>3</sub>	
Energy	-384.0580447	Energy	-384.0534532	Energy	-384.0487753
ZPE	0.128519	ZPE	0.128515	ZPE	0.127204
BSSE	0.00300398	BSSE	0.00316664	BSSE	0.0028299
C1-C2	1.387	C1-C2	1.388	C1-C2	1.388
C2-C3	1.396	C2-C3	1.392	C2-C3	1.393
C3-C4	1.396	C3-C4	1.391	C3-C4	1.393
C4-C5	1.390	C4-C5	1.390	C4-C5	1.390
C5-C6	1.390	C5-C6	1.389	C5-C6	1.390
C1-C6	1.392	C1-C6	1.392	C1-C6	1.392
C1-H1	1.082	C1-H1	1.082	C1-H1	1.083
C2-H2	1.081	C2-H2	1.081	C2-H2	1.081
C3-O3	1.359	C3-O3	1.376	C3-O3	1.368
O3-H3	0.973	O3-H3	0.962	O3-H3	0.962
C4-H4	1.083	C4-H4	1.084	C4-H4	1.084
C5-H5	1.083	C5-H5	1.082	C5-H5	1.082
C6-H6	1.081	C6-H6	1.081	C6-H6	1.081
Ow-Hw1	0.962	Ow-Hw1	0.966	Ow-Hw1	0.962
Ow-Hw2	0.962	Ow-Hw2	0.961	Ow-Hw2	0.962
C1-C2-C3	119.9	C1-C2-C3	119.2	C1-C2-C3	119.5
C2-C3-C4	119.6	C2-C3-C4	120.6	C2-C3-C4	120.0
C3-C4-C5	119.8	C3-C4-C5	119.5	C3-C4-C5	119.8
C4-C5-C6	120.7	C4-C5-C6	120.4	C4-C5-C6	120.6
C5-C6-C1	119.1	C5-C6-C1	119.4	C5-C6-C1	119.0
C6-C1-C2	120.7	C6-C1-C2	120.8	C6-C1-C2	121.0
C2-C1-H1	119.3	C2-C1-H1	119.2	C2-C1-H1	119.2
C6-C1-H1	120.0	C6-C1-H1	120.0	C6-C1-H1	119.8
C1-C2-H2	121.3	C1-C2-H2	121.7	C1-C2-H2	121.5
C3-C2-H2	118.8	C3-C2-H2	119.2	C3-C2-H2	119.0
C2-C3-O3	117.8	C2-C3-O3	117.5	C2-C3-O3	117.5
C4-C3-O3	122.6	C4-C3-O3	121.9	C4-C3-O3	122.5
C3-O3-H3	110.5	C3-O3-H3	109.9	C3-O3-H3	109.4
C3-C4-H4	119.5	C3-C4-H4	120.1	C3-C4-H4	119.9
C5-C4-H4	120.6	C5-C4-H4	120.3	C5-C4-H4	120.3

C4-C5-H5	119.2	C4-C5-H5	119.4	C4-C5-H5	119.3
C6-C5-H5	120.0	C6-C5-H5	120.2	C6-C5-H5	120.0
C1-C6-H6	120.4	C1C6-H6	120.3	C1C6-H6	120.1
C5-C6-H6	120.4	C5-C6-H6	120.3	C5-C6-H6	121.0
H3-Ow	1.867	Hw1-O3	2.025	H6-Ow	2.596
O3-Ow	2.837	Ow-O3	2.964	C6-Ow	3.529
O3-H3-Ow	174.5	Ow-Hw1-O3	163.8	C6-H6-Ow	144.2
H3-Ow-Hw1	113.5	Hw1-O3-H3	131.3	H6-Ow-Hw1	94.1
H3-Ow-Hw2	113.5	Hw1-O3-C3	118.6	H6-Ow-Hw2	94.1
Hw1-Ow-Hw2	105.6	Hw1-Ow-Hw2	104.2	Hw1-Ow-Hw2	104.8

**Table S3:** Most stable conformations in the o-cresol-water complex

C <sub>1</sub>		C <sub>2</sub>		C <sub>3</sub>	
					
Energy	-423.38956669	Energy	-423.38686924	Energy	-423.38486912
ZPE	0.15585700	ZPE	0.15574000	ZPE	0.15615900
BSSE	0.00303859	BSSE	0.00301221	BSSE	0.00324132
C1-C2	1.390	C1-C2	1.387	C1-C2	1.390
C2-C3	1.394	C2-C3	1.394	C2-C3	1.389
C3-C4	1.403	C3-C4	1.403	C3-C4	1.399
C4-C5	1.391	C4-C5	1.394	C4-C5	1.393
C5-C6	1.392	C5-C6	1.389	C5-C6	1.391
C1-C6	1.388	C1-C6	1.390	C1-C6	1.387
C1-H1	1.082	C1-H1	1.082	C1-H1	1.082
C2-H2	1.083	C2-H2	1.082	C2-H2	1.084
C3-O3	1.362	C3-O3	1.363	C3-O3	1.381
O3-H3	0.973	O3-H3	0.970	O3-H3	0.963
C4-C7	1.503	C4-C7	1.505	C4-C7	1.504
C7-H7a	1.089	C7-H7a	1.089	C7-H7a	1.089
C7-H7b	1.092	C7-H7b	1.094	C7-H7b	1.092
C7-H7c	1.092	C7-H7c	1.092	C7-H7c	1.091
C5-H5	1.083	C5-H5	1.083	C5-H5	1.083
C6-H6	1.081	C6-H6	1.081	C6-H6	1.081
Ow-Hw1	0.962	Ow-Hw1	0.962	Ow-Hw1	0.961
Ow-Hw2	0.962	Ow-Hw2	0.963	Ow-Hw2	0.967

C1-C2-C3	120.1	C1-C2-C3	120.4	C1-C2-C3	119.9
C2-C3-C4	120.6	C2-C3-C4	120.5	C2-C3-C4	121.5
C3-C4-C5	117.9	C3-C4-C5	117.9	C3-C4-C5	117.2
C4-C5-C6	121.9	C4-C5-C6	122.0	C4-C5-C6	122.0
C5-C6-C1	119.3	C5-C6-C1	119.2	C5-C6-C1	119.5
C6-C1-C2	120.1	C6-C1-C2	120.1	C6-C1-C2	119.7
C2-C1-H1	119.5	C2-C1-H1	119.6	C2-C1-H1	119.7
C6-C1-H1	120.4	C6-C1-H1	120.3	C6-C1-H1	120.6
C1-C2-H2	120.6	C1-C2-H2	121.3	C1-C2-H2	120.3
C3-C2-H2	119.3	C3-C2-H2	118.3	C3-C2-H2	119.8
C2-C3-O3	122.2	C2-C3-O3	116.6	C2-C3-O3	121.3
C4-C3-O3	117.1	C4-C3-O3	122.9	C4-C3-O3	117.2
C3-O3-H3	110.5	C3-O3-H3	113.1	C3-O3-H3	109.2
C3-C4-C7	119.9	C3-C4-C7	121.0	C3-C4-C7	120.8
C5-C4-C7	122.1	C5-C4-C7	121.2	C5-C4-C7	122.0
C4-C7-H7a	110.9	C4-C7-H7a	110.6	C4-C7-H7a	110.6
C4-C7-H7b	111.3	C4-C7-H7b	111.6	C4-C7-H7b	111.2
C4-C7-H7c	111.3	C4-C7-H7c	112.4	C4-C7-H7c	111.5
H7a-C7-H7b	108.4	H7a-C7-H7b	107.5	H7a-C7-H7b	108.2
H7a-C7-H7c	108.4	H7a-C7-H7c	107.7	H7a-C7-H7c	108.3
H7b-C7-H7c	106.4	H7b-C7-H7c	106.7	H7b-C7-H7c	106.9
C4-C5-H5	118.6	C4-C5-H5	118.4	C4-C5-H5	118.4
C6-C5-H5	119.5	C6-C5-H5	119.5	C6-C5-H5	119.5
C1-C6-H6	120.5	C1-C6-H6	120.6	C1-C6-H6	120.4
C5-C6-H6	120.2	C5-C6-H6	120.2	C5-C6-H6	120.1
-	-	-	-	-	-
H3-Ow	1.869	H3-Ow	1.95784	Hw2-O3	2.003
O3-Ow	2.838	O3-Ow	2.84210	Ow-O3	2.969
O3-H3-Ow	174.1	O3-H3-Ow	150.43741	Ow-Hw2-O3	178.0
H3-Ow-Hw1	113.6	H3-Ow-Hw1	112.6	Hw2-O3-C3	123.5
H3-Ow-Hw2	113.6	H3-Ow-Hw2	100.4	Hw2-O3-H3	108.3
Hw1-Ow-Hw2	105.6	Hw1-Ow-Hw2	105.1	Hw1-Ow-Hw2	104.4

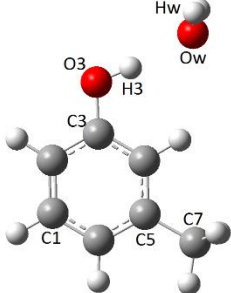
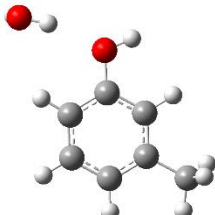
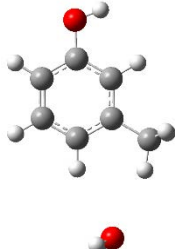
**Table S3:** Most stable conformations in the o-cresol-water complex (continued)

	C <sub>4</sub>	C <sub>5</sub>	C <sub>6</sub>
Energy	-423.38481890	Energy	-423.38093425
ZPE	0.15622300	ZPE	0.15479800
		Energy	-423.38064003
		ZPE	0.15478100

BSSE	0.00342001	BSSE	0.00295046	BSSE	0.00293258
C1-C2	1.390	C1-C2	1.390	C1-C2	1.390
C2-C3	1.389	C2-C3	1.391	C2-C3	1.391
C3-C4	1.399	C3-C4	1.400	C3-C4	1.401
C4-C5	1.393	C4-C5	1.392	C4-C5	1.391
C5-C6	1.391	C5-C6	1.392	C5-C6	1.392
C1-C6	1.387	C1-C6	1.388	C1-C6	1.388
C1-H1	1.082	C1-H1	1.082	C1-H1	1.082
C2-H2	1.084	C2-H2	1.085	C2-H2	1.084
C3-O3	1.380	C3-O3	1.372	C3-O3	1.370
O3-H3	0.963	O3-H3	0.962	O3-H3	0.962
C4-C7	1.504	C4-C7	1.504	C4-C7	1.503
C7-H7a	1.089	C7-H7a	1.089	C7-H7a	1.089
C7-H7b	1.092	C7-H7b	1.092	C7-H7b	1.092
C7-H7c	1.091	C7-H7c	1.092	C7-H7c	1.092
C5-H5	1.083	C5-H5	1.083	C5-H5	1.083
C6-H6	1.081	C6-H6	1.081	C6-H6	1.082
Ow-Hw1	0.961	Ow-Hw1	0.962	Ow-Hw1	0.962
Ow-Hw2	0.967	Ow-Hw2	0.962	Ow-Hw2	0.962
C1-C2-C3	119.9	C1-C2-C3	120.0	C1-C2-C3	120.2
C2-C3-C4	121.6	C2-C3-C4	121.1	C2-C3-C4	121.1
C3-C4-C5	117.2	C3-C4-C5	117.8	C3-C4-C5	117.5
C4-C5-C6	122.0	C4-C5-C6	121.6	C4-C5-C6	121.9
C5-C6-C1	119.6	C5-C6-C1	119.6	C5-C6-C1	119.7
C6-C1-C2	119.7	C6-C1-C2	119.9	C6-C1-C2	119.6
C2-C1-H1	119.7	C2-C1-H1	119.6	C2-C1-H1	120.2
C6-C1-H1	120.6	C6-C1-H1	120.5	C6-C1-H1	120.2
C1-C2-H2	120.3	C1-C2-H2	120.3	C1-C2-H2	120.2
C3-C2-H2	119.8	C3-C2-H2	119.7	C3-C2-H2	119.6
C2-C3-O3	121.4	C2-C3-O3	122.0	C2-C3-O3	122.0
C4-C3-O3	117.0	C4-C3-O3	117.0	C4-C3-O3	116.9
C3-O3-H3	109.4	C3-O3-H3	109.1	C3-O3-H3	109.2
C3-C4-C7	120.7	C3-C4-C7	120.3	C3-C4-C7	120.2
C5-C4-C7	122.1	C5-C4-C7	121.9	C5-C4-C7	122.3
C4-C7-H7a	110.6	C4-C7-H7a	110.3	C4-C7-H7a	110.8
C4-C7-H7b	111.1	C4-C7-H7b	111.3	C4-C7-H7b	111.3
C4-C7-H7c	111.7	C4-C7-H7c	111.3	C4-C7-H7c	111.3
H7a-C7-H7b	108.2	H7a-C7-H7b	108.7	H7a-C7-H7b	108.4
H7a-C7-H7c	108.4	H7a-C7-H7c	108.7	H7a-C7-H7c	108.4
H7b-C7-H7c	106.6	H7b-C7-H7c	106.4	H7b-C7-H7c	106.5
C4-C5-H5	118.4	C4-C5-H5	118.4	C4-C5-H5	118.5
C6-C5-H5	119.5	C6-C5-H5	120.0	C6-C5-H5	119.6
C1-C6-H6	120.4	C1-C6-H6	120.4	C1-C6-H6	120.3

C5-C6-H6	120.1	C5-C6-H6	120.0	C5-C6-H6	120.0
-	-	H5-Ow	2.573	-	-
-	-	C5-Ow	3.618	-	-
-	-	C5-H5-Ow	161.9	-	-
-	-	H5-Ow-Hw1	115.0	-	-
-	-	H5-Ow-Hw2	115.0	-	-
-	-	H5-Ow-H7a	51.3	-	-
Hw2-O3	2.017	H7a-Ow	2.837	H1-Ow	2.585
Ow-O3	2.979	C7-Ow	3.858	C1-Ow	3.520
Ow-Hw2-O3	173.3	C7-H7a-Ow	156.2	C1-H1-Ow	144.3
Hw2-O3-C3	115.3	H7a-Ow-Hw1	85.5	H1-Ow-Hw1	91.0
Hw2-O3-H3	109.5	H7a-Ow-Hw2	85.5	H1-Ow-Hw2	91.0
Hw1-Ow-Hw2	104.5	Hw1-Ow-Hw2	104.9	Hw1-Ow-Hw2	104.7

**Table S4:** Most stable conformations in the m-cresol-water complex

C <sub>1</sub> cis		C <sub>2</sub> cis		C <sub>3</sub> cis	
					
Energy	-423.3891244	Energy	-423.3847969	Energy	-423.3806221
ZPE	0.15567	ZPE	0.155728	ZPE	0.154624
BSSE	0.003039	BSSE	0.003174	BSSE	0.00292329
C1-C2	1.385	C1-C2	1.386	C1-C2	1.386
C2-C3	1.396	C2-C3	1.392	C2-C3	1.393
C3-C4	1.394	C3-C4	1.389	C3-C4	1.391
C4-C5	1.396	C4-C5	1.396	C4-C5	1.396
C5-C6	1.393	C5-C6	1.393	C5-C6	1.394
C1-C6	1.393	C1-C6	1.392	C1-C6	1.392
C1-H1	1.082	C1-H1	1.082	C1-H1	1.083
C2-H2	1.081	C2-H2	1.081	C2-H2	1.081
C3-O3	1.359	C3-O3	1.377	C3-O3	1.368
O3-H3	0.973	O3-H3	0.962	O3-H3	0.962
C4-H4	1.084	C4-H4	1.085	C4-H4	1.086
C5-C7	1.508	C5-C7	1.507	C5-C7	1.507
C7-H7a	1.092	C7-H7a	1.093	C7-H7a	1.093
C7-H7b	1.089	C7-H7b	1.089	C7-H7b	1.088
C7-H7c	1.092	C7-H7c	1.091	C7-H7c	1.093
C6-H6	1.082	C6-H6	1.082	C6-H6	1.082

-	-				
Ow-Hw1	0.962	Ow-Hw1	0.961	Ow-Hw1	0.962
Ow-Hw2	0.962	Ow-Hw2	0.966	Ow-Hw2	0.962
-	-				
C1-C2-C3	119.4	C1-C2-C3	118.6	C1-C2-C3	118.9
C2-C3-C4	119.8	C2-C3-C4	120.8	C2-C3-C4	120.2
C3-C4-C5	120.9	C3-C4-C5	120.6	C3-C4-C5	120.9
C4-C5-C6	118.9	C4-C5-C6	118.5	C4-C5-C6	118.6
C5-C6-C1	120.2	C5-C6-C1	120.5	C5-C6-C1	120.3
C6-C1-C2	120.9	C6-C1-C2	121.0	C6-C1-C2	121.0
C2-C1-H1	119.4	C2-C1-H1	119.3	C2-C1-H1	119.2
C6-C1-H1	119.7	C6-C1-H1	119.7	C6-C1-H1	119.7
C1-C2-H2	121.6	C1-C2-H2	122.0	C1-C2-H2	121.8
C3-C2-H2	119.0	C3-C2-H2	119.4	C3-C2-H2	119.3
C2-C3-O3	117.7	C2-C3-O3	117.4	C2-C3-O3	117.4
C4-C3-O3	122.5	C4-C3-O3	121.8	C4-C3-O3	122.3
C3-O3-H3	110.5	C3-O3-H3	109.9	C3-O3-H3	109.2
C3-C4-H4	119.1	C3-C4-H4	119.6	C3-C4-H4	119.4
C5-C4-H4	120.0	C5-C4-H4	119.8	C5-C4-H4	119.7
C4-C5-C7	120.0	C4-C5-C7	120.2	C4-C5-C7	120.4
C6-C5-C7	121.1	C6-C5-C7	121.3	C6-C5-C7	121.0
C5-C7-H7a	111.3	C5-C7-H7a	111.1	C5-C7-H7a	111.1
C5-C7-H7b	111.3	C5-C7-H7b	111.3	C5-C7-H7b	111.2
C5-C7-H7c	111.2	C5-C7-H7c	111.4	C5-C7-H7c	111.1
H7a-C7-H7b	107.9	H7a-C7-H7b	107.6	H7a-C7-H7b	108.2
H7a-C7-H7c	107.1	H7a-C7-H7c	107.2	H7a-C7-H7c	107.0
H7b-C7-H7c	107.8	H7b-C7-H7c	108.0	H7b-C7-H7c	108.2
C1-C6-H6	120.0	C1-C6-H6	119.9	C1-C6-H6	120.5
C5-C6-H6	119.8	C5-C6-H6	119.6	C5-C6-H6	119.2
H3-Ow	1.873	Hw2-Ow	2.021	H6-O7	2.726
O3-Ow	2.842	Ow-O3	2.963	C6-Ow	3.726
O3-Hw-Ow	173.5	Ow-Hw2-O3	164.4	C6-H6-Ow	153.6
H3-Ow-Hw1	112.5	Hw2-O3-C3	118.8	H6-Ow-Hw1	90.1
H3-Ow-Hw2	112.5	Hw2-O3-H3	131.2	H6-Ow-Hw2	90.1
Hw1-Ow-Hw2	105.6	Hw1-Ow-Hw2	104.2	H6-Ow-H7b	52.2
-	-	-	-	H7b-Ow	2.642
-	-	-	-	C7-Ow	3.696
-	-	-	-	C7-H7b-Ow	162.8
-	-	-	-	H7b-Ow-Hw1	118.9
-	-	-	-	H7b-Ow-Hw2	118.9
-	-	-	-	Hw1-Ow-Hw2	104.9

**Table S4:** Most stable conformations in the m-cresol-water complex (continued)

C <sub>1</sub> trans		C <sub>2</sub> trans	
Energy	-423.3891357	Energy	-423.3850142
ZPE	0.155522	ZPE	0.155728
BSSE	0.003017	BSSE	0.00322
C1-C2	1.389	C1-C2	1.390
C2-C3	1.396	C2-C3	1.389
C3-C4	1.394	C3-C4	1.391
C4-C5	1.392	C4-C5	1.392
C5-C6	1.397	C5-C6	1.398
C1-C6	1.389	C1-C6	1.387
C1-H1	1.083	C1-H1	1.082
C2-H2	1.082	C2-H2	1.084
C3-O3	1.359	C3-O3	1.377
O3-H3	0.973	O3-H3	0.962
C4-H4	1.083	C4-H4	1.082
C5-C7	1.507	C5-C7	1.507
C7-H7a	1.090	C7-H7a	1.089
C7-H7b	1.093	C7-H7b	1.093
C7-H7c	1.090	C7-H7c	1.090
C6-H6	1.082	C6-H6	1.082
-	-	-	-
Ow-Hw1	0.962	Ow-Hw1	0.961
Ow-Hw2	0.962	Ow-Hw2	0.966
-	-	-	-
C1-C2-C3	119.3	C1-C2-C3	118.9
C2-C3-C4	119.8	C2-C3-C4	120.8
C3-C4-C5	121.0	C3-C4-C5	120.3
C4-C5-C6	118.9	C4-C5-C6	118.9
C5-C6-C1	120.1	C5-C6-C1	120.5
C6-C1-C2	120.9	C6-C1-C2	120.6
C2-C1-H1	119.3	C2-C1-H1	119.4
C6-C1-H1	119.8	C6-C1-H1	120.0
C1-C2-H2	120.9	C1-C2-H2	120.6
C3-C2-H2	119.8	C3-C2-H2	120.4
C2-C3-O3	122.6	C2-C3-O3	121.9
C4-C3-O3	117.6	C4-C3-O3	117.3
C3-O3-H3	110.4	C3-O3-H3	109.8
C3-C4-H4	118.3	C3-C4-H4	118.7

C5-C4-H4	120.7	C5-C4-H4	121.0
C4-C5-C7	120.3	C4-C5-C7	120.3
C6-C5-C7	120.7	C6-C5-C7	120.7
C5-C7-H7a	111.4	C5-C7-H7a	111.4
C5-C7-H7b	111.0	C5-C7-H7b	110.9
C5-C7-H7c	111.5	C5-C7-H7c	111.3
H7a-C7-H7b	107.3	H7a-C7-H7b	107.5
H7a-C7-H7c	108.2	H7a-C7-H7c	108.3
H7b-C7-H7c	107.3	H7b-C7-H7c	107.3
C1-C6-H6	120.0	C1-C6-H6	119.8
C5-C6-H6	119.8	C5-C6-H6	119.7
H3-Ow	1.870	Hw2-Ow	2.016
O3-Ow	2.839	Ow-O3	2.959
O3-Hw-Ow	174.0	Ow-Hw2-O3	164.5
H3-Ow-Hw1	113.2	Hw2-O3-C3	119.1
H3-Ow-Hw2	112.9	Hw2-O3-H3	130.8
Hw1-Ow-Hw2	105.6	Hw1-Ow-Hw2	104.2

**Table S5:** Most stable conformations in the p-cresol-water complex

C <sub>1</sub>		C <sub>2</sub>		C <sub>3</sub>		C <sub>4</sub>	
Energy	-423.388168	Energy	-423.383993	Energy	-423.379773	Energy	-423.379557
ZPE	0.155757	ZPE	0.155675	ZPE	0.154602	ZPE	0.154395
BSSE	0.00301463	BSSE	0.00318947	BSSE	0.00292021	BSSE	0.0027472
C1-C2	1.385	C1-C2	1.386	C1-C2	1.386	C1-C2	1.389
C2-C3	1.395	C2-C3	1.392	C2-C3	1.393	C2-C3	1.390
C3-C4	1.393	C3-C4	1.388	C3-C4	1.390	C3-C4	1.392
C4-C5	1.391	C4-C5	1.392	C4-C5	1.392	C4-C5	1.389
C5-C6	1.392	C5-C6	1.392	C5-C6	1.393	C5-C6	1.395
C1-C6	1.398	C1-C6	1.398	C1-C6	1.397	C1-C6	1.396
C1-H1	1.084	C1-H1	1.083	C1-H1	1.084	C1-H1	1.083
C2-H2	1.082	C2-H2	1.082	C2-H2	1.081	C2-H2	1.082
C3-O3	1.360	C3-O3	1.378	C3-O3	1.370	C3-O3	1.370
O3-H3	0.972	O3-H3	0.962	O3-H3	0.962	O3-H3	0.962
C4-H4	1.083	C4-H4	1.084	C4-H4	1.084	C4-H4	1.084
C5-H5	1.083	C5-H5	1.083	C5-H5	1.083	C5-H5	1.084

C6-C7	1.507	C6-C7	1.507	C6-C7	1.508	C6-C7	1.508
C7-H7a	1.090	C7-H7a	1.089	C7-H7a	1.089	C7-H7a	1.093
C7-H7b	1.093	C7-H7b	1.092	C7-H7b	1.093	C7-H7b	1.093
C7-H7c	1.093	C7-H7c	1.092	C7-H7c	1.093	C7-H7c	1.089
-	-	-	-	-	-	-	-
Ow-Hw1	0.962	Ow-Hw1	0.966	Ow-Hw1	0.962	Ow-Hw1	0.962
Ow-Hw2	0.962	Ow-Hw2	0.961	Ow-Hw2	0.962	Ow-Hw2	0.962
-	-	-	-	-	-	-	-
C1-C2-C3	120.086	C1-C2-C3	119.3	C1-C2-C3	119.7	C1-C2-C3	119.8
C2-C3-C4	119.117	C2-C3-C4	120.1	C2-C3-C4	119.6	C2-C3-C4	119.5
C3-C4-C5	119.957	C3-C4-C5	119.7	C3-C4-C5	120.1	C3-C4-C5	119.9
C4-C5-C6	121.739	C4-C5-C6	121.5	C4-C5-C6	121.2	C4-C5-C6	121.5
C5-C6-C1	117.401	C5-C6-C1	117.6	C5-C6-C1	117.8	C5-C6-C1	117.6
C6-C1-C2	121.701	C6-C1-C2	121.8	C6-C1-C2	121.7	C6-C1-C2	121.6
C2-C1-H1	118.919	C2-C1-H1	118.8	C2-C1-H1	118.9	C2-C1-H1	119.5
C6-C1-H1	119.380	C6-C1-H1	119.4	C6-C1-H1	119.5	C6-C1-H1	118.9
C1-C2-H2	121.092	C1-C2-H2	121.4	C1-C2-H2	121.2	C1-C2-H2	121.2
C3-C2-H2	118.822	C3-C2-H2	119.2	C3-C2-H2	119.1	C3-C2-H2	119.0
C2-C3-O3	117.903	C2-C3-O3	117.6	C2-C3-O3	117.6	C2-C3-O3	117.8
C4-C3-O3	122.980	C4-C3-O3	122.3	C4-C3-O3	122.8	C4-C3-O3	122.6
C3-O3-H3	110.424	C3-O3-H3	109.9	C3-O3-H3	109.2	C3-O3-H3	109.2
C3-C4-H4	119.674	C3-C4-H4	120.3	C3-C4-H4	120.0	C3-C4-H4	120.0
C5-C4-H4	120.368	C5-C4-H4	120.1	C5-C4-H4	119.9	C5-C4-H4	120.1
C4-C5-H5	118.853	C4-C5-H5	118.9	C4-C5-H5	119.4	C4-C5-H5	118.9
C6-C5-H5	119.408	C6-C5-H5	119.6	C6-C5-H5	119.4	C6-C5-H5	119.6
C1-C6-C7	120.985	C1-C6-C7	120.9	C1-C6-C7	121.1	C1-C6-C7	121.2
C5-C6-C7	121.614	C5-C6-C7	121.5	C5-C6-C7	121.2	C5-C6-C7	121.2
C6-C7-H7a	111.248	C6-C7-H7a	111.3	C6-C7-H7a	110.7	C6-C7-H7a	111.3
C6-C7-H7b	111.559	C6-C7-H7b	111.4	C6-C7-H7b	111.5	C6-C7-H7b	111.3
C6-C7-H7c	111.559	C6-C7-H7c	111.4	C6-C7-H7c	111.5	C6-C7-H7c	111.1
H7a-C7-H7b	107.608	H7a-C7-H7b	107.7	H7a-C7-H7b	108.0	H7a-C7-H7b	107.0
H7a-C7-H7c	107.609	H7a-C7-H7c	107.7	H7a-C7-H7c	108.0	H7a-C7-H7c	108.0
H7b-C7-H7c	107.033	H7b-C7-H7c	107.1	H7b-C7-H7c	107.0	H7b-C7-H7c	108.0
-	-	-	-	-	-	-	-
H3-Ow	1.871	Hw1-O3	2.016	H5-Ow	2.556	H1-Ow	2.612
O3-Ow	2.840	Ow-O3	2.957	C5-Ow	3.602	C1-Ow	3.635
O3-H3-Ow	173.896	Ow-Hw1-O3	164.1	C5-H5-Ow	162.0	C1-H1-Ow	157.3
H3-Ow-Hw1	112.647	Hw1-O3-C3	118.6	H5-Ow-Hw1	115.6	H1-Ow-Hw1	98.1
H3-Ow-Hw2	112.646	Hw1-O3-H3	131.4	H5-Ow-Hw2	115.6	H1-Ow-Hw2	98.1
-	-	-	-	H5-Ow-H7a	51.5	H1-Ow-H7c	52.8
-	-	-	-	H7a-Ow	2.853	H7c-Ow	2.702
-	-	-	-	C7-Ow	3.869	C7-Ow	3.737

-	-	-	-	C7-H7a-Ow	155.2	C7-H7c-Ow	158.8
-	-	-	-	H7a-Ow-Hw1	86.1	H7c-Ow-Hw1	123.9
-	-	-	-	H7a-Ow-Hw2	86.1	H7c-Ow-Hw2	123.9
Hw1-Ow-Hw2	105.6	Hw1-Ow-Hw2	104.2	Hw1-Ow-Hw2	104.9	Hw1-Ow-Hw2	104.9

**Table S6:** Most stable conformations in the pyrocatechol-water complex

C <sub>1</sub>		C <sub>2</sub>		C <sub>3</sub>	
Energy	-459.3116508	Energy	-459.3096333	Energy	-459.3062329
ZPE	0.132908	ZPE	0.133208	ZPE	0.132765
BSSE	0.00301704	BSSE	0.00379451	BSSE	0.00315835
C1-C2	1.393	C1-C2	1.388	C1-C2	1.392
C2-C3	1.386	C2-C3	1.394	C2-C3	1.386
C3-C4	1.402	C3-C4	1.403	C3-C4	1.397
C4-C5	1.387	C4-C5	1.388	C4-C5	1.385
C5-C6	1.394	C5-C6	1.390	C5-C6	1.393
C1-C6	1.388	C1-C6	1.389	C1-C6	1.388
C1-H1	1.081	C1-H1	1.081	C1-H1	1.081
C2-H2	1.081	C2-H2	1.081	C2-H2	1.082
C3-O3	1.364	C3-O3	1.352	C3-O3	1.371
O3-H3	0.966	O3-H3	0.977	O3-H3	0.965
C4-O4	1.369	C4-O4	1.388	C4-O4	1.376
O4-H4	0.974	O4-H4	0.962	O4-H4	0.961
C5-H5	1.083	C5-H5	1.085	C5-H5	1.084
C6-H6	1.081	C6-H6	1.081	C6-H6	1.081
-	-	-	-	-	-
Ow-Hw1	0.962	Ow-Hw1	0.962	Ow-Hw1	0.966
Ow-Hw2	0.962	Ow-Hw2	0.968	Ow-Hw2	0.961
-	-	-	-	-	-
C1-C2-C3	120.0	C1-C2-C3	121.4	C1-C2-C3	119.7
C2-C3-C4	119.8	C2-C3-C4	118.0	C2-C3-C4	120.0
C3-C4-C5	120.0	C3-C4-C5	120.6	C3-C4-C5	120.1
C4-C5-C6	119.9	C4-C5-C6	120.8	C4-C5-C6	119.8
C5-C6-C1	120.0	C5-C6-C1	119.2	C5-C6-C1	119.9
C6-C1-C2	120.1	C6-C1-C2	120.1	C6-C1-C2	120.4
C2-C1-H1	119.6	C2-C1-H1	119.6	C2-C1-H1	119.5
C6-C1-H1	120.3	C6-C1-H1	120.3	C6-C1-H1	120.2

C1-C2-H2	121.4	C1-C2-H2	121.2	C1-C2-H2	121.7
C3-C2-H2	118.6	C3-C2-H2	117.4	C3-C2-H2	118.6
C2-C3-O3	120.3	C2-C3-O3	117.7	C2-C3-O3	120.1
C4-C3-O3	119.9	C4-C3-O3	124.3	C4-C3-O3	119.9
C3-O3-H3	107.2	C3-O3-H3	114.0	C3-O3-H3	108.4
C3-C4-O4	115.4	C3-C4-O4	118.2	C3-C4-O4	115.4
C5-C4-O4	124.7	C5-C4-O4	121.2	C5-C4-O4	124.5
C4-O4-H4	111.1	C4-O4-H4	108.6	C4-O4-H4	110.1
C4-C5-H5	119.3	C4-C5-H5	119.0	C4-C5-H5	119.7
C6-C5-H5	120.8	C6-C5-H5	120.2	C6-C5-H5	120.5
C1-C6-H6	120.4	C1-C6-H6	120.9	C1-C6-H6	120.4
C5-C6-H6	119.6	C5-C6-H6	119.9	C5-C6-H6	119.6
-	-	-	-	-	-
H3-O4	2.114	H3-Ow	1.828	H3-O4	2.136
O3-O4	2.669	O3-Ow	2.797	O3-O4	2.671
O3-H3-O4	114.9	O3-H3-Ow	171.2	O3-H3-O4	113.4
-	-	H3-Ow-Hw1	108.8	-	-
-	-	H3-Ow-Hw2	84.3	-	-
-	-	-	-	-	-
H4-Ow	1.830	Hw2-O4	1.970	Hw1-O3	2.020
O4-Ow	2.803	Ow-O4	2.796	Ow-O3	2.955
O4-H4-Ow	176.8	Ow-Hw2-O4	142.0	Ow-Hw1-O3	162.3
H4-Ow-Hw1	116.4	Hw2-O4-C4	129.6	Hw1-O3-C3	117.2
H4-Ow-Hw2	116.4	Hw2-O4-H4	121.2	Hw1-O3-H3	134.3
Hw1-Ow-Hw2	105.8	Hw1-Ow-Hw2	105.8	Hw1-Ow-Hw2	104.2

**Table S6:** Most stable conformations in the pyrocatechol-water complex (continued)

C <sub>4</sub>		C <sub>5</sub>	
Energy	-459.3043594	Energy	-459.3014494
ZPE	0.132453	ZPE	0.131489
BSSE	0.00304883	BSSE	0.00291252
C1-C2	1.393	C1-C2	1.392
C2-C3	1.391	C2-C3	1.387
C3-C4	1.405	C3-C4	1.400
C4-C5	1.388	C4-C5	1.385
C5-C6	1.393	C5-C6	1.393
C1-C6	1.386	C1-C6	1.388
C1-H1	1.082	C1-H1	1.082

C2-H2	1.083	C2-H2	1.081
C3-O3	1.357	C3-O3	1.363
O3-H3	0.973	O3-H3	0.965
C4-O4	1.368	C4-O4	1.377
O4-H4	0.962	O4-H4	0.961
C5-H5	1.085	C5-H5	1.084
C6-H6	1.081	C6-H6	1.081
-	-	-	-
Ow-Hw1	0.962	Ow-Hw1	0.962
Ow-Hw2	0.962	Ow-Hw2	0.962
-	-	-	-
C1-C2-C3	121.0	C1-C2-C3	120.1
C2-C3-C4	118.9	C2-C3-C4	119.4
C3-C4-C5	119.7	C3-C4-C5	120.5
C4-C5-C6	121.0	C4-C5-C6	120.1
C5-C6-C1	119.5	C5-C6-C1	119.5
C6-C1-C2	119.9	C6-C1-C2	120.6
C2-C1-H1	119.6	C2-C1-H1	119.4
C6-C1-H1	120.5	C6-C1-H1	120.1
C1-C2-H2	120.4	C1-C2-H2	121.5
C3-C2-H2	118.5	C3-C2-H2	118.5
C2-C3-O3	123.5	C2-C3-O3	120.0
C4-C3-O3	117.6	C4-C3-O3	120.6
C3-O3-H3	110.0	C3-O3-H3	108.1
C3-C4-O4	117.3	C3-C4-O4	115.3
C5-C4-O4	123.0	C5-C4-O4	124.3
C4-O4-H4	108.6	C4-O4-H4	109.9
C4-C5-H5	118.9	C4-C5-H5	119.6
C6-C5-H5	120.1	C6-C5-H5	120.3
C1-C6-H6	120.7	C1-C6-H6	120.3
C5-C6-H6	119.8	C5-C6-H6	120.3
H3-Ow	1.867	H6-Ow	2.581
O3-Ow	2.835	C6-Ow	3.519
O3-H3-Ow	173.4	C6-H6-Ow	144.7
H3-Ow-Hw1	111.7	H6-Ow-Hw1	91.4
H3-Ow-Hw2	111.7	H6-Ow-Hw2	91.4
Hw1-Ow-Hw2	105.5	Hw1-Ow-Hw2	104.7

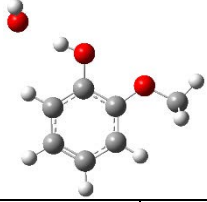
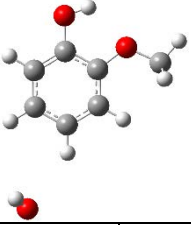
**Table S7:** Most stable conformations in the guaiacol-water complex

C <sub>1</sub>		C <sub>2</sub>		C <sub>3</sub>		C <sub>4</sub>	
Energy	-498.622534	Energy	-498.622508	Energy	-498.62088	Energy	-498.618481
ZPE	0.161824	ZPE	0.161558	ZPE	0.16131	ZPE	0.160537
BSSE	0.00388331	BSSE		BSSE	0.00316542	BSSE	0.00273665
C1-C2	1.387	C1-C2	1.3888	C1-C2	1.393	C1-C2	1.393
C2-C3	1.396	C2-C3	1.3916	C2-C3	1.383	C2-C3	1.385
C3-C4	1.403	C3-C4	1.408	C3-C4	1.402	C3-C4	1.406
C4-C5	1.388	C4-C5	1.3893	C4-C5	1.387	C4-C5	1.389
C5-C6	1.389	C5-C6	1.3924	C5-C6	1.395	C5-C6	1.397
C1-C6	1.391	C1-C6	1.3864	C1-C6	1.386	C1-C6	1.386
C1-H1	1.082	C1-H1	1.0814	C1-H1	1.081	C1-H1	1.081
C2-H2	1.081	C2-H2	1.0813	C2-H2	1.082	C2-H2	1.081
C3-O3	1.355	C3-O3	1.3533	C3-O3	1.371	C3-O3	1.361
O3-H3	0.979	O3-H3	0.9752	O3-H3	0.966	O3-H3	0.966
C4-O4	1.393	C4-O4	1.3825	C4-O4	1.372	C4-O4	1.368
O4-C7	1.437	O4-C7	1.4224	O4-C7	1.419	O4-C7	1.426
C7-H7a	1.088	C7-H7a	1.0873	C7-H7a	1.087	C7-H7a	1.087
C7-H7b	1.091	C7-H7b	1.0915	C7-H7b	1.093	C7-H7b	1.091
C7-H7c	1.091	C7-H7c	1.0924	C7-H7c	1.093	C7-H7c	1.092
C5-H5	1.082	C5-H5	1.0796	C5-H5	1.080	C5-H5	1.080
C6-H6	1.081	C6-H6	1.081	C6-H6	1.081	C6-H6	1.081
-	-	-	-	-	-	-	-
Ow-Hw1	0.962	Ow-Hw1	0.9681	Ow-Hw1	0.966	Ow-Hw1	0.964
Ow-Hw2	0.972	Ow-Hw2	0.9619	Ow-Hw2	0.961	Ow-Hw2	0.962
-	-	-	-	-	-	-	-
C1-C2-C3	120.8	C1-C2-C3	121.2	C1-C2-C3	119.6	C1-C2-C3	120.1
C2-C3-C4	118.3	C2-C3-C4	118.5	C2-C3-C4	120.4	C2-C3-C4	119.8
C3-C4-C5	120.7	C3-C4-C5	120.1	C3-C4-C5	119.9	C3-C4-C5	119.9
C4-C5-C6	120.5	C4-C5-C6	120.5	C4-C5-C6	119.6	C4-C5-C6	119.8
C5-C6-C1	119.2	C5-C6-C1	119.7	C5-C6-C1	120.3	C5-C6-C1	120.2
C6-C1-C2	120.5	C6-C1-C2	120.0	C6-C1-C2	120.3	C6-C1-C2	120.2
C2-C1-H1	119.4	C2-C1-H1	119.6	C2-C1-H1	119.5	C2-C1-H1	119.6
C6-C1-H1	120.1	C6-C1-H1	120.4	C6-C1-H1	120.3	C6-C1-H1	120.3
C1-C2-H2	121.3	C1-C2-H2	121.3	C1-C2-H2	121.8	C1-C2-H2	121.4
C3-C2-H2	117.9	C3-C2-H2	117.5	C3-C2-H2	118.7	C3-C2-H2	118.5
C2-C3-O3	118.3	C2-C3-O3	117.6	C2-C3-O3	120.1	C2-C3-O3	120.1
C4-C3-O3	123.4	C4-C3-O3	123.9	C4-C3-O3	119.5	C4-C3-O3	120.1

C3-O3-H3	112.0	C3-O3-H3	113.6	C3-O3-H3	107.9	C3-O3-H3	107.5
C3-C4-O4	120.1	C3-C4-O4	116.4	C3-C4-O4	114.1	C3-C4-O4	114.1
C5-C4-O4	119.3	C5-C4-O4	123.5	C5-C4-O4	126.1	C5-C4-O4	126.0
C4-O4-C7	113.9	C4-O4-C7	118.1	C4-O4-C7	118.4	C4-O4-C7	118.5
O4-C7-H7a	106.7	O4-C7-H7a	106.2	O4-C7-H7a	106.2	O4-C7-H7a	105.9
O4-C7-H7b	110.2	O4-C7-H7b	110.9	O4-C7-H7b	111.2	O4-C7-H7b	110.7
O4-C7-H7c	110.9	O4-C7-H7c	111.6	O4-C7-H7c	111.2	O4-C7-H7c	110.9
H7a-C7-H7b	109.7	H7a-C7-H7b	109.4	H7a-C7-H7b	109.4	H7a-C7-H7b	109.8
H7a-C7-H7c	109.7	H7a-C7-H7c	109.2	H7a-C7-H7c	109.4	H7a-C7-H7c	109.2
H7b-C7-H7c	109.6	H7b-C7-H7c	109.4	H7b-C7-H7c	109.4	H7b-C7-H7c	110.2
C4-C5-H5	118.3	C4-C5-H5	120.1	C4-C5-H5	120.5	C4-C5-H5	120.3
C6-C5-H5	121.2	C6-C5-H5	119.4	C6-C5-H5	119.9	C6-C5-H5	119.9
C1-C6-H6	120.6	C1-C6-H6	120.7	C1-C6-H6	120.4	C1-C6-H6	120.5
C5-C6-H6	120.1	C5-C6-H6	119.6	C5-C6-H6	119.3	C5-C6-H6	119.4
-	-	-	-	-	-	-	-
-	-	H3-Ow	1.867	H3-O4	2.088	H3-O4	2.094
-	-	O3-Ow	2.821	O3-O4	2.638	O3-O4	2.646
-	-	O3-H3-Ow	165.3	O3-H3-O4	114.4	O3-H3-O4	114.6
-	-	H3-Ow-Hw1	80.5	-	-	-	-
-	-	H3-Ow-Hw2	107.0	-	-	-	-
-	-	-	-	-	-	-	-
H3-Ow	1.823	Hw1-O4	1.962	Hw1-O3	2.013	Hw1-C4	2.903
O3-Ow	2.795	Ow-O4	2.794	Ow-O3	2.950	Hw1-C5	2.548
O3-H3-Ow	171.9	Ow-Hw-O4	142.6	Ow-Hw1-O3	163.0	Hw1-C6	3.1
H3-Ow-Hw1	113.8	Hw1-O4-C4	126.1	Hw1-O3-C3	117.4	Ow-Hw1-C4	125.9
H3-Ow-Hw2	84.8	Hw1-O4-C7	113.5	Hw1-O3-H3	134.6	Ow-Hw1-C5	141.0
-	-	Hw1-Ow-Hw2	105.9	Hw1-Ow-Hw2	104.1	Ow-Hw1-C6	165.8
-	-	-	-	-	-	-	-
Hw2-O4	1.904	-	-	-	-	H5-Ow	3.219
Ow-O4	2.748	-	-	-	-	H5-Ow-H7b	47.651
Ow-Hw2-O4	143.7	-	-	-	-	H5-Ow-Hw1	42.7
Hw2-O4-C4	116.6	-	-	-	-	H5-Ow-Hw2	128.6
Hw2-O4-C7	109.3	-	-	-	-	-	-
Hw1-Ow-Hw2	106.4	-	-	-	-	Hw1-C6-H6	102.7
-	-	-	-	-	-	Hw1-C6-C1	111.83
-	-	-	-	-	-	Hw1-C5-H5	80.22
-	-	-	-	-	-	C5-H5-Ow	87.66
-	-	-	-	-	-	Hw1-C4-O4	97.73
-	-	-	-	-	-	Hw1-C4-C3	113.50
-	-	-	-	-	-	C4-Hw1-C6	47.05
-	-	-	-	-	-	-	-
-	-	-	-	-	-	H7b-Ow	2.580
-	-	-	-	-	-	C7-Ow	3.525
-	-	-	-	-	-	C7-H7b-ow	144.4
-	-	-	-	-	-	H7b-Ow-Hw1	84.3

-	-	-	-	-	-	H7b-Ow-Hw2	106.1
-	-	-	-	-	-	Hw1-Ow-Hw2	104.4

**Table S7:** Most stable conformations in the guaiacol-water complex (continued)

C <sub>5</sub>		C <sub>6</sub>		C <sub>7</sub>	
					
Energy	-498.618224	Energy	-498.618061	Energy	-498.6159584
ZPE	0.161067	ZPE	0.160835	ZPE	0.160019
BSSE	0.00372955	BSSE	0.00306242	BSSE	0.00300959
C1-C2	1.391	C1-C2	1.394	C1-C2	1.393
C2-C3	1.387	C2-C3	1.389	C2-C3	1.384
C3-C4	1.398	C3-C4	1.411	C3-C4	1.405
C4-C5	1.387	C4-C5	1.390	C4-C5	1.387
C5-C6	1.392	C5-C6	1.396	C5-C6	1.396
C1-C6	1.390	C1-C6	1.383	C1-C6	1.386
C1-H1	1.081	C1-H1	1.082	C1-H1	1.082
C2-H2	1.081	C2-H2	1.083	C2-H2	1.081
C3-O3	1.369	C3-O3	1.357	C3-O3	1.362
O3-H3	0.970	O3-H3	0.973	O3-H3	0.966
C4-O4	1.380	C4-O4	1.363	C4-O4	1.372
O4-C7	1.438	O4-C7	1.414	O4-C7	1.419
C7-H7a	1.087	C7-H7a	1.087	C7-H7a	1.087
C7-H7b	1.091	C7-H7b	1.094	C7-H7b	1.093
C7-H7c	1.091	C7-H7c	1.094	C7-H7c	1.093
C5-H5	1.082	C5-H5	1.080	C5-H5	1.080
C6-H6	1.081	C6-H6	1.081	C6-H6	1.081
-	-	-	-	-	-
Ow-Hw1	0.961	Ow-Hw1	0.962	Ow-Hw1	0.962
Ow-Hw2	0.967	Ow-Hw2	0.962	Ow-Hw2	0.962
-	-	-	-	-	-
C1-C2-C3	119.4	C1-C2-C3	120.9	C1-C2-C3	120.0
C2-C3-C4	120.2	C2-C3-C4	119.3	C2-C3-C4	119.7
C3-C4-C5	120.0	C3-C4-C5	119.4	C3-C4-C5	120.2
C4-C5-C6	119.8	C4-C5-C6	120.7	C4-C5-C6	119.9
C5-C6-C1	120.0	C5-C6-C1	119.9	C5-C6-C1	119.9
C6-C1-C2	120.5	C6-C1-C2	119.8	C6-C1-C2	120.5
C2-C1-H1	119.5	C2-C1-H1	119.7	C2-C1-H1	119.3
C6-C1-H1	120.0	C6-C1-H1	120.5	C6-C1-H1	120.2
C1-C2-H2	121.5	C1-C2-H2	120.5	C1-C2-H2	121.5

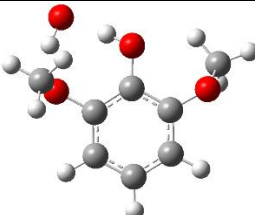
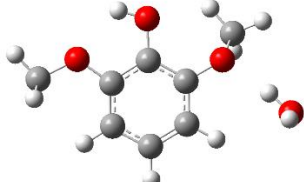
C3-C2-H2	119.1	C3-C2-H2	118.6	C3-C2-H2	118.5
C2-C3-O3	120.2	C2-C3-O3	123.2	C2-C3-O3	120.1
C4-C3-O3	119.5	C4-C3-O3	117.5	C4-C3-O3	120.2
C3-O3-H3	106.1	C3-O3-H3	109.9	C3-O3-H3	107.5
C3-C4-O4	116.4	C3-C4-O4	115.6	C3-C4-O4	114.0
C5-C4-O4	123.5	C5-C4-O4	124.9	C5-C4-O4	125.9
C4-O4-C7	115.6	C4-O4-C7	118.2	C4-O4-C7	118.4
O4-C7-H7a	106.2	O4-C7-H7a	106.0	O4-C7-H7a	106.2
O4-C7-H7b	110.8	O4-C7-H7b	111.7	O4-C7-H7b	111.2
O4-C7-H7c	110.4	O4-C7-H7c	111.7	O4-C7-H7c	111.2
H7a-C7-H7b	109.2	H7a-C7-H7b	109.2	H7a-C7-H7b	109.4
H7a-C7-H7c	110.0	H7a-C7-H7c	109.2	H7a-C7-H7c	109.4
H7b-C7-H7c	110.2	H7b-C7-H7c	109.0	H7b-C7-H7c	109.3
C4-C5-H5	119.4	C4-C5-H5	120.0	C4-C5-H5	120.5
C6-C5-H5	120.8	C6-C5-H5	119.3	C6-C5-H5	119.7
C1-C6-H6	120.2	C1-C6-H6	120.6	C1-C6-H6	120.3
C5-C6-H6	119.8	C5-C6-H6	119.5	C5-C6-H6	119.9
-	-	-	-	-	-
H3-O4	2.119			H3-O4	2.098
O3-O4	2.686			O3-O4	2.649
O3-H3-O4	115.8			O3-H3-O4	114.5
-	-	-	-	-	-
-	-	-	-	-	-
-	-	-	-	-	-
Hw2-O3	2.082	H3-Ow	1.870	H1-Ow	3.383
Ow-O3	2.986	O3-Ow	2.839	C1-Ow	3.887
Ow-Hw2-O3	155.0	O3-H3-Ow	173.4	C1-H1-Ow	109.9
Hw2-O3-C3	102.3	H3-Ow-Hw1	112.0	H1-Ow-Hw1	61.7
Hw2-O3-H3	90.6	H3-Ow-Hw2	112.0	H1-Ow-Hw2	61.7
O3-Hw2-Ow	155.0	Hw1-Ow-Hw2	105.5	H1-Ow-H6	46.6
-	-	-	-	-	-
H7c-Ow	2.621	-	-	H6-Ow	2.614
C7-Ow	3.598	-	-	C6-Ow	3.538
C7-H7c-Ow	148.6	-	-	C6-H6-Ow	143.1
H7c-Ow-Hw1	103.3	-	-	H6-Ow-Hw1	87.4
H7c-Ow-Hw2	92.1	-	-	H6-Ow-Hw2	87.4
Hw1-Ow-Hw2	104.5	-	-	Hw1-Ow-Hw2	104.7

**Table S8:** Most stable conformations in the syringol-water complex

C <sub>1</sub>		C <sub>2</sub>		C <sub>3</sub>	
Energy	-613.1824950	Energy	-613.1822066	Energy	-613.1812441
ZPE	0.194031	ZPE	0.193791	ZPE	0.19375
BSSE	0.00390755	BSSE	0.00392028	BSSE	0.00390508
C1-C2	1.392	C1-C2	1.394	C1-C2	1.388
C2-C3	1.396	C2-C3	1.400	C2-C3	1.402
C3-C4	1.412	C3-C4	1.408	C3-C4	1.407
C4-C5	1.391	C4-C5	1.392	C4-C5	1.390
C5-C6	1.394	C5-C6	1.390	C5-C6	1.389
C1-C6	1.383	C1-C6	1.386	C1-C6	1.387
C1-H1	1.081	C1-H1	1.079	C1-H1	1.081
C2-O2	1.393	C2-O2	1.383	C2-O2	1.393
O2-C7	1.436	O2-C7	1.422	O2-C7	1.436
C7-H7a	1.091	C7-H7a	1.092	C7-H7a	1.091
C7-H7b	1.088	C7-H7b	1.087	C7-H7b	1.091
C7-H7c	1.091	C7-H7c	1.091	C7-H7c	1.088
C3-O3	1.354	C3-O3	1.352	C3-O3	1.357
O3-H3	0.979	O3-H3	0.974	O3-H3	0.981
C4-O4	1.359	C4-O4	1.360	C4-O4	1.370
O4-C8	1.416	O4-C8	1.415	O4-C8	1.430
C8-H8a	1.087	C8-H8a	1.087	C8-H8a	1.088
C8-H8b	1.094	C8-H8b	1.094	C8-H8b	1.094
C8-H8c	1.094	C8-H8c	1.094	C8-H8c	1.089
C5-H5	1.079	C5-H5	1.079	C5-H5	1.081
C6-H6	1.081	C6-H6	1.081	C6-H6	1.081
-	-	-	-	-	-
Ow-Hw1	0.972	Ow-Hw1	0.968	Ow-Hw1	0.972
Ow-Hw2	0.962	Ow-Hw2	0.962	Ow-Hw2	0.962
-	-	-	-	-	-
C1-C2-C3	121.7	C1-C2-C3	121.1	C1-C2-C3	121.4
C2-C3-C4	118.2	C2-C3-C4	118.4	C2-C3-C4	118.1
C3-C4-C5	120.0	C3-C4-C5	120.4	C3-C4-C5	120.1
C4-C5-C6	120.4	C4-C5-C6	120.0	C4-C5-C6	120.9
C5-C6-C1	120.2	C5-C6-C1	120.6	C5-C6-C1	119.7
C6-C1-C2	119.4	C6-C1-C2	119.5	C6-C1-C2	119.8
C2-C1-H1	118.8	C2-C1-H1	120.5	C2-C1-H1	118.6
C6-C1-H1	121.7	C6-C1-H1	120.0	C6-C1-H1	121.6

C1-C2-O2	119.1	C1-C2-O2	123.2	C1-C2-O2	119.1
C3-C2-O2	119.3	C3-C2-O2	115.7	C3-C2-O2	119.4
C2-O2-C7	113.8	C2-O2-C7	118.1	C2-O2-C7	113.9
O2-C7-H7a	110.2	O2-C7-H7a	111.6	O2-C7-H7a	110.9
O2-C7-H7b	106.7	O2-C7-H7b	106.2	O2-C7-H7b	110.2
O2-C7-H7c	110.9	O2-C7-H7c	110.9	O2-C7-H7c	106.7
H7a-C7-H7b	109.7	H7a-C7-H7b	109.2	H7a-C7-H7b	109.7
H7a-C7-H7c	109.6	H7a-C7-H7c	109.4	H7a-C7-H7c	109.7
H7b-C7-H7c	109.7	H7b-C7-H7c	109.4	H7b-C7-H7c	109.7
C2-C3-O3	123.8	C2-C3-O3	124.2	C2-C3-O3	123.1
C4-C3-O3	118.0	C4-C3-O3	117.3	C4-C3-O3	118.8
C3-O3-H3	111.4	C3-O3-H3	112.8	C3-O3-H3	111.5
C3-C4-O4	115.1	C3-C4-O4	114.9	C3-C4-O4	121.5
C5-C4-O4	124.8	C5-C4-O4	124.6	C5-C4-O4	118.3
C4-O4-C8	118.3	C4-O4-C8	118.3	C4-O4-C8	116.9
O4-C8-H8a	105.9	O4-C8-H8a	105.9	O4-C8-H8a	106.0
O4-C8-H8b	111.7	O4-C8-H8b	111.7	O4-C8-H8b	110.5
O4-C8-H8c	111.6	O4-C8-H8c	111.6	O4-C8-H8c	111.6
H8a-C8-H8b	109.2	H8a-C8-H8b	109.2	H8a-C8-H8b	109.2
H8a-C8-H8c	109.2	H8a-C8-H8c	109.2	H8a-C8-H8c	109.7
H8b-C8-H8c	109.1	H8b-C8-H8c	109.1	H8b-C8-H8c	109.8
C4-C5-H5	120.1	C4-C5-H5	120.3	C4-C5-H5	117.8
C6-C5-H5	119.4	C6-C5-H5	119.7	C6-C5-H5	121.3
C1-C6-H6	120.2	C1-C6-H6	119.7	C1-C6-H6	120.2
C5-C6-H6	119.6	C5-C6-H6	119.7	C5-C6-H6	120.1
H3-Ow	1.827	Hw1-O2	1.963	H3-Ow	1.800
O3-Ow	2.800	Ow-O2	2.794	O3-Ow	2.776
O3-H3-Ow	172.4	Ow-Hw1-O2	142.4	O3-H3-Ow	173.3
H3-Ow-Hw1	84.2	Hw1-O2-C2	125.7	H3-Ow-Hw1	85.5
H3-Ow-Hw2	113.0	Hw1-O2-C7	114.0	H3-Ow-Hw2	114.1
-	-	-	-	-	-
Hw1-O2	1.899	H3-Ow	1.887	Hw1-O2	1.905
Ow-O2	2.749	O3-Ow	2.835	Ow-O2	2.748
Ow-Hw1-O2	144.5	O3-H3-Ow	163.5	Ow-Hw1-O2	143.5
Hw1-O2-C2	116.4	H3-Ow-Hw1	79.5	Hw1-O2-C2	115.7
Hw1-O2-C7	110.2	H3-Ow-Hw2	105.4	Hw1-O2-C7	110.6
Hw1-Ow-Hw2	106.3	Hw1-Ow-Hw2	105.8	Hw1-Ow-Hw2	106.4

**Table S8:** Most stable conformations in the syringol-water complex (continued)

C <sub>4</sub>		C <sub>5</sub>	
			
Energy	-613.1809618	Energy	-613.1803805
ZPE	0.193682	ZPE	0.193428
BSSE	0.00384962	BSSE	0.00307344
C1-C2	1.388	C1-C2	1.387
C2-C3	1.401	C2-C3	1.403
C3-C4	1.407	C3-C4	1.393
C4-C5	1.390	C4-C5	1.394
C5-C6	1.389	C5-C6	1.385
C1-C6	1.387	C1-C6	1.394
C1-H1	1.081	C1-H1	1.079
C2-O2	1.393	C2-O2	1.372
O2-C7	1.437	O2-C7	1.419
C7-H7a	1.091	C7-H7a	1.092
C7-H7b	1.091	C7-H7b	1.092
C7-H7c	1.088	C7-H7c	1.087
C3-O3	1.357	C3-O3	1.363
O3-H3	0.980	O3-H3	0.966
C4-O4	1.370	C4-O4	1.379
O4-C8	1.429	O4-C8	1.436
C8-H8a	1.088	C8-H8a	1.087
C8-H8b	1.094	C8-H8b	1.092
C8-H8c	1.089	C8-H8c	1.088
C5-H5	1.081	C5-H5	1.081
C6-H6	1.081	C6-H6	1.081
-	-	-	-
Ow-Hw1	0.973	Ow-Hw1	0.961
Ow-Hw2	0.961	Ow-Hw2	0.969
-	-	-	-
C1-C2-C3	121.5	C1-C2-C3	120.7
C2-C3-C4	118.1	C2-C3-C4	119.3
C3-C4-C5	120.1	C3-C4-C5	120.1
C4-C5-C6	120.9	C4-C5-C6	120.0
C5-C6-C1	119.7	C5-C6-C1	120.7
C6-C1-C2	119.8	C6-C1-C2	119.2
C2-C1-H1	118.7	C2-C1-H1	120.7
C6-C1-H1	121.6	C6-C1-H1	120.1
C1-C2-O2	119.2	C1-C2-O2	125.9

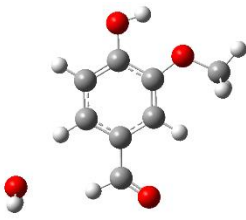
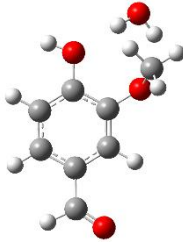
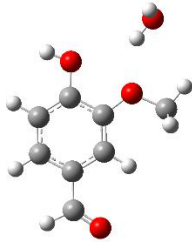
C3-C2-O2	119.3	C3-C2-O2	113.4
C2-O2-C7	113.9	C2-O2-C7	118.4
O2-C7-H7a	110.2	O2-C7-H7a	111.2
O2-C7-H7b	110.8	O2-C7-H7b	111.2
O2-C7-H7c	106.7	O2-C7-H7c	106.2
H7a-C7-H7b	109.6	H7a-C7-H7b	109.4
H7a-C7-H7c	109.7	H7a-C7-H7c	109.4
H7b-C7-H7c	109.7	H7b-C7-H7c	109.4
C2-C3-O3	123.1	C2-C3-O3	120.2
C4-C3-O3	118.7	C4-C3-O3	120.5
C3-O3-H3	111.6	C3-O3-H3	107.1
C3-C4-O4	121.5	C3-C4-O4	120.9
C5-C4-O4	118.2	C5-C4-O4	118.9
C4-O4-C8	116.9	C4-O4-C8	116.3
O4-C8-H8a	106.0	O4-C8-H8a	106.0
O4-C8-H8b	110.5	O4-C8-H8b	110.3
O4-C8-H8c	111.5	O4-C8-H8c	110.9
H8a-C8-H8b	109.2	H8a-C8-H8b	109.5
H8a-C8-H8c	109.7	H8a-C8-H8c	109.9
H8b-C8-H8c	109.8	H8b-C8-H8c	110.1
C4-C5-H5	117.8	C4-C5-H5	118.4
C6-C5-H5	121.3	C6-C5-H5	121.6
C1-C6-H6	120.2	C1-C6-H6	119.5
C5-C6-H6	120.1	C5-C6-H6	119.8
H3-Ow	1.815	H3-O2	2.078
O3-Ow	2.790	O3-O2	2.636
O3-H3-Ow	172.9	O3-H3-O2	115.0
H3-Ow-Hw1	84.7	-	-
H3-Ow-Hw2	115.7	-	-
-	-	-	-
Hw1-O2	1.897	Hw2-O4	1.941
Ow-O2	2.743	Ow-O4	2.902
Ow-Hw1-O2	143.9	Ow-Hw2-O4	171.1
Hw1-O2-C2	117.2	Hw2-O4-C4	114.5
Hw1-O2-C7	110.4	Hw2-O4-C8	111.4
Hw1-Ow-Hw2	106.4	Hw1-Ow-Hw2	104.5

**Table S9:** Most stable conformations in the vanillin-water complex

C <sub>1</sub>		C <sub>2</sub>		C <sub>3</sub>		C <sub>4</sub>	
Energy	-611.996059	Energy	-611.993001	Energy	-611.991426	Energy	-611.990232
ZPE	0.171318	ZPE	0.171203	ZPE	0.170737	ZPE	0.170605
BSSE	0.00316235	BSSE	0.00275848	BSSE	0.00374504	BSSE	0.00310668
C1-C2	1.387	C1-C2	1.388	C1-C2	1.382	C1-C2	1.390
C2-C3	1.387	C2-C3	1.387	C2-C3	1.399	C2-C3	1.384
C3-C4	1.414	C3-C4	1.414	C3-C4	1.412	C3-C4	1.411
C4-C5	1.377	C4-C5	1.376	C4-C5	1.379	C4-C5	1.378
C5-C6	1.407	C5-C6	1.405	C5-C6	1.398	C5-C6	1.403
C1-C6	1.395	C1-C6	1.393	C1-C6	1.397	C1-C6	1.392
C1-H1	1.083	C1-H1	1.082	C1-H1	1.083	C1-H1	1.083
C1-H2	1.081	C1-H2	1.081	C1-H2	1.081	C1-H2	1.081
C3-O3	1.350	C3-O3	1.350	C3-O3	1.342	C3-O3	1.361
O3-H3	0.968	O3-H3	0.967	O3-H3	0.982	O3-H3	0.967
C4-O4	1.364	C4-O4	1.366	C4-O4	1.388	C4-O4	1.367
O4-C7	1.428	O4-C7	1.423	O4-C7	1.437	O4-C7	1.424
C7-H7a	1.091	C7-H7a	1.092	C7-H7a	1.091	C7-H7a	1.092
C7-H7b	1.091	C7-H7b	1.092	C7-H7b	1.092	C7-H7b	1.092
C7-H7c	1.086	C7-H7c	1.086	C7-H7c	1.087	C7-H7c	1.086
C5-H5	1.080	C5-H5	1.080	C5-H5	1.082	C5-H5	1.080
C6-C8	1.460	C6-C8	1.461	C6-C8	1.469	C6-C8	1.470
C8-H8	1.107	C8-H8	1.105	C8-H8	1.110	C8-H8	1.109
C8=O8	1.219	C8=O8	1.220	C8=O8	1.212	C8=O8	1.211
-	-	-	-	-	-	-	-
Ow-Hw1	0.961	Ow-Hw1	0.971	Ow-Hw1	0.962	Ow-Hw1	0.961
Ow-Hw2	0.973	Ow-Hw2	0.961	Ow-Hw2	0.970	Ow-Hw2	0.965
-	-	-	-	-	-	-	-
C1-C2-C3	119.5	C1-C2-C3	119.6	C1-C2-C3	120.6	C1-C2-C3	119.1
C2-C3-C4	120.2	C2-C3-C4	120.2	C2-C3-C4	118.6	C2-C3-C4	120.7
C3-C4-C5	120.3	C3-C4-C5	120.0	C3-C4-C5	120.5	C3-C4-C5	119.9
C4-C5-C6	119.5	C4-C5-C6	119.7	C4-C5-C6	120.6	C4-C5-C6	119.6
C5-C6-C1	120.0	C5-C6-C1	120.0	C5-C6-C1	119.0	C5-C6-C1	120.1
C6-C1-C2	120.6	C6-C1-C2	120.5	C6-C1-C2	120.7	C6-C1-C2	120.6
C2-C1-H1	119.8	C2-C1-H1	119.9	C2-C1-H1	119.8	C2-C1-H1	119.8
C6-C1-H1	119.6	C6-C1-H1	119.6	C6-C1-H1	119.5	C6-C1-H1	119.6
C1-C2-H2	121.7	C1-C2-H2	121.7	C1-C2-H2	121.5	C1-C2-H2	122.1

C3-C2-H2	118.7	C3-C2-H2	118.7	C3-C2-H2	117.9	C3-C2-H2	118.8
C2-C3-O3	120.1	C2-C3-O3	120.0	C2-C3-O3	117.9	C2-C3-O3	120.1
C4-C3-O3	119.8	C4-C3-O3	119.8	C4-C3-O3	123.5	C4-C3-O3	119.2
C3-O3-H3	107.7	C3-O3-H3	107.9	C3-O3-H3	113.2	C3-O3-H3	108.0
C3-C4-O4	113.7	C3-C4-O4	113.6	C3-C4-O4	119.0	C3-C4-O4	113.7
C5-C4-O4	126.0	C5-C4-O4	126.3	C5-C4-O4	120.5	C5-C4-O4	126.4
C4-O4-C7	118.0	C4-O4-C7	118.2	C4-O4-C7	114.6	C4-O4-C7	118.2
O4-C7-H7a	111.2	O4-C7-H7a	111.0	O4-C7-H7a	110.6	O4-C7-H7a	111.0
O4-C7-H7b	110.9	O4-C7-H7b	111.0	O4-C7-H7b	110.7	O4-C7-H7b	111.0
O4-C7-H7c	105.9	O4-C7-H7c	106.1	O4-C7-H7c	106.6	O4-C7-H7c	106.1
H7a-C7-H7b	108.9	H7a-C7-H7b	109.5	H7a-C7-H7b	109.6	H7a-C7-H7b	109.5
H7a-C7-H7c	110.0	H7a-C7-H7c	109.6	H7a-C7-H7c	109.5	H7a-C7-H7c	109.6
H7b-C7-H7c	109.9	H7b-C7-H7c	109.6	H7b-C7-H7c	109.7	H7b-C7-H7c	109.6
C4-C5-H5	121.2	C4-C5-H5	122.1	C4-C5-H5	120.3	C4-C5-H5	122.2
C6-C5-H5	119.4	C6-C5-H5	118.3	C6-C5-H5	119.1	C6-C5-H5	118.2
C1-C6-C8	118.9	C1-C6-C8	119.7	C1-C6-C8	120.3	C1-C6-C8	120.0
C5-C6-C8	121.1	C5-C6-C8	120.3	C5-C6-C8	120.6	C5-C6-C8	119.9
C6-C8-H8	114.3	C6-C8-H8	115.5	C6-C8-H8	114.3	C6-C8-H8	114.4
C6-C8=O8	126.5	C6-C8=O8	124.8	C6-C8=O8	125.3	C6-C8=O8	125.1
H8-C8=O8	119.3	H8-C8=O8	119.7	H8-C8=O8	120.4	H8-C8=O8	120.6
-	-	-	-	-	-	-	-
H3-O4	2.079	H3-O4	2.081			H3-O4	2.071
O3-O4	2.634	O3-O4	2.634			O3-O4	2.626
O3-H3-O4	114.7	O3-H3-O4	114.5			O3-H3-O4	114.6
-	-	-	-	-	-	-	-
Hw2-O8	1.912	-	-	Hw2-O4	1.951	Hw2-O3	2.058
Ow-O8	2.869	-	-	Ow-O4	2.751	Ow-O3	2.980
Ow-Hw2-O8	167.3	-	-	Ow-Hw2-O4	138.1	Ow-Hw2-O3	159.1
Hw2-O8-C8	132.1	-	-	Hw2-O4-C4	122.2	Hw2-O3-C3	116.3
-	-	-	-	Hw2-O4-C7	111.2	Hw2-O3-H3	135.6
-	-	-	-	-	-	-	-
H5-Ow	2.294	Hw1-O8	1.930	H3-Ow	1.796	H2-Ow	2.611
C5-Ow	3.342	Ow-O8	2.9	O3-Ow	2.770	C2-Ow	3.471
C5-H5-Ow	163.0	Ow-Hw1-O8	159.1	O3-H3-Ow	170.7	C2-H2-Ow	136.1
H5-Ow-Hw1	123.1	Hw1-O8=C8	103.7	H3-Ow-Hw1	115.2	H2-Ow-Hw1	101.3
H5-Ow-Hw2	68.2	-	-	H3-Ow-Hw2	86.0	H2-Ow-Hw2	68.3
-	-	-	-	-	-	-	-
Hw1-Ow-Hw2	104.5	Hw1-Ow-Hw2	104.3	Hw1-Ow-Hw2	106.6	Hw1-Ow-Hw2	104.4

**Table S9:** Most stable conformations in the vanillin-water complex (continued)

C <sub>5</sub>		C <sub>6</sub>		C <sub>7</sub>		C <sub>8</sub>	
							
Energy	-611.989647	Energy	-611.987722	Energy	-611.979607	Energy	-611.984074
ZPE	0.170479	ZPE	0.169728	ZPE	0.169492	ZPE	0.169894
BSSE	0.00308246	BSSE	0.00298724	BSSE	0.00350349	BSSE	0.00299216
C1-C2	1.389	C1-C2	1.389	C1-C2	1.387	C1-C2	1.390
C2-C3	1.392	C2-C3	1.386	C2-C3	1.390	C2-C3	1.387
C3-C4	1.419	C3-C4	1.413	C3-C4	1.409	C3-C4	1.414
C4-C5	1.380	C4-C5	1.377	C4-C5	1.380	C4-C5	1.380
C5-C6	1.404	C5-C6	1.404	C5-C6	1.399	C5-C6	1.403
C1-C6	1.390	C1-C6	1.393	C1-C6	1.393	C1-C6	1.389
C1-H1	1.083	C1-H1	1.083	C1-H1	1.083	C1-H1	1.082
C1-H2	1.082	C1-H2	1.081	C1-H2	1.084	C1-H2	1.084
C3-O3	1.346	C3-O3	1.353	C3-O3	1.363	C3-O3	1.358
O3-H3	0.975	O3-H3	0.967	O3-H3	0.963	O3-H3	0.963
C4-O4	1.358	C4-O4	1.369	C4-O4	1.370	C4-O4	1.357
O4-C7	1.418	O4-C7	1.422	O4-C7	1.435	O4-C7	1.425
C7-H7a	1.093	C7-H7a	1.092	C7-H7a	1.090	C7-H7a	1.092
C7-H7b	1.093	C7-H7b	1.092	C7-H7b	1.092	C7-H7b	1.092
C7-H7c	1.087	C7-H7c	1.086	C7-H7c	1.086	C7-H7c	1.086
C5-H5	1.079	C5-H5	1.080	C5-H5	1.081	C5-H5	1.080
C6-C8	1.466	C6-C8	1.468	C6-C8	1.473	C6-C8	1.471
C8-H8	1.110	C8-H8	1.107	C8-H8	1.109	C8-H8	1.109
C8=O8	1.213	C8=O8	1.214	C8=O8	1.209	C8=O8	1.211
-	-	-	-	-	-	-	-
Ow-Hw1	0.963	Ow-Hw1	0.962	Ow-Hw1	0.962	Ow-Hw1	0.961
Ow-Hw2	0.963	Ow-Hw2	0.962	Ow-Hw2	0.964	Ow-Hw2	0.966
-	-	-	-	-	-	-	-
C1-C2-C3	120.5	C1-C2-C3	119.8	C1-C2-C3	119.9	C1-C2-C3	120.2
C2-C3-C4	119.6	C2-C3-C4	120.1	C2-C3-C4	120.2	C2-C3-C4	120.2
C3-C4-C5	119.3	C3-C4-C5	120.1	C3-C4-C5	119.2	C3-C4-C5	119.2
C4-C5-C6	120.7	C4-C5-C6	119.6	C4-C5-C6	120.8	C4-C5-C6	120.4
C5-C6-C1	119.7	C5-C6-C1	120.2	C5-C6-C1	119.5	C5-C6-C1	120.0
C6-C1-C2	120.1	C6-C1-C2	120.2	C6-C1-C2	120.4	C6-C1-C2	120.0
C2-C1-H1	120.0	C2-C1-H1	120.3	C2-C1-H1	119.9	C2-C1-H1	120.1
C6-C1-H1	119.8	C6-C1-H1	119.5	C6-C1-H1	119.8	C6-C1-H1	120.0
C1-C2-H2	120.8	C1-C2-H2	121.6	C1-C2-H2	120.5	C1-C2-H2	120.5
C3-C2-H2	118.7	C3-C2-H2	118.6	C3-C2-H2	119.6	C3-C2-H2	119.3

C2-C3-O3	123.2	C2-C3-O3	120.1	C2-C3-O3	122.6	C2-C3-O3	123.4
C4-C3-O3	117.2	C4-C3-O3	119.8	C4-C3-O3	117.1	C4-C3-O3	116.4
C3-O3-H3	110.5	C3-O3-H3	107.8	C3-O3-H3	110.1	C3-O3-H3	109.8
C3-C4-O4	115.4	C3-C4-O4	113.7	C3-C4-O4	120.1	C3-C4-O4	115.2
C5-C4-O4	125.3	C5-C4-O4	126.3	C5-C4-O4	120.5	C5-C4-O4	125.6
C4-O4-C7	117.9	C4-O4-C7	118.1	C4-O4-C7	115.6	C4-O4-C7	118.9
O4-C7-H7a	111.5	O4-C7-H7a	111.1	O4-C7-H7a	111.2	O4-C7-H7a	111.0
O4-C7-H7b	111.5	O4-C7-H7b	111.1	O4-C7-H7b	110.3	O4-C7-H7b	111.1
O4-C7-H7c	105.9	O4-C7-H7c	106.2	O4-C7-H7c	106.3	O4-C7-H7c	105.2
H7a-C7-H7b	109.1	H7a-C7-H7b	109.4	H7a-C7-H7b	109.9	H7a-C7-H7b	109.5
H7a-C7-H7c	109.4	H7a-C7-H7c	109.6	H7a-C7-H7c	109.2	H7a-C7-H7c	110.1
H7b-C7-H7c	109.4	H7b-C7-H7c	109.6	H7b-C7-H7c	109.9	H7b-C7-H7c	109.9
C4-C5-H5	121.6	C4-C5-H5	122.2	C4-C5-H5	119.6	C4-C5-H5	121.6
C6-C5-H5	117.7	C6-C5-H5	118.2	C6-C5-H5	119.6	C6-C5-H5	118.0
C1-C6-C8	120.0	C1-C6-C8	119.7	C1-C6-C8	119.9	C1-C6-C8	119.9
C5-C6-C8	120.3	C5-C6-C8	120.1	C5-C6-C8	120.7	C5-C6-C8	120.1
C6-C8-H8	114.2	C6-C8-H8	114.0	C6-C8-H8	114.3	C6-C8-H8	114.3
C6-C8=O8	125.5	C6-C8=O8	125.2	C6-C8=O8	125.1	C6-C8=O8	125.1
H8-C8=O8	120.3	H8-C8=O8	120.7	H8-C8=O8	120.6	H8-C8=O8	120.6
-	-	-	-	-	-	-	-
-	-	H3-O4	2.081	Hw2-O3	2.126	-	-
-	-	O3-O4	2.636	Ow-O3	3.090	-	-
-	-	O3-H3-O4	114.7	Ow-Hw2-O3	178.9	-	-
-	-	-	-	Hw2-O3-C3	121.8	-	-
-	-	-	-	Hw2-O3-H3	119.4	-	-
-	-	-	-	-	-	-	-
-	-	H8-Ow	2.786	Hw1-O4	2.765	Hw2-O4	2.102
-	-	C8-Ow	3.799	Ow-O4	3.157	Ow-O4	2.940
-	-	C8-H8-Ow	152.1	Ow-Hw1-O4	105.3	Ow-Hw2-O4	144.2
-	-	H8-Ow-Hw1	90.4	Hw1-O4-C4	125.5	Hw2-O4-C4	131.6
-	-	H8-Ow-Hw2	90.4	Hw1-O4-C7	98.2	Hw2-O4-C7	108.9
-	-	H8-Ow-H1	52.4	Hw1-O4-Hw2	32.1	O4-Hw2-O3	65.1
-	-	-	-	-	-	-	-
H3-Ow	1.834	H1-Ow	2.492	Hw2-O4	2.679	Hw2-O3	2.645
O3-Ow	2.806	C1-Ow	3.539	Ow-O4	3.157	Ow-O3	3.496
O3-H3-Ow	175.0	C1-H1-Ow	162.3	Ow-Hw2-O4	111.1	Ow-Hw2-O3	147.1
H3-Ow-Hw1	114.2	H1-Ow-Hw1	119.1	Hw2-O4-C7	90.5	Hw2-O3-C3	110.8
H3-Ow-Hw2	114.2	H1-Ow-Hw2	119.1	Hw2-O4-C4	103.1	Hw2-O3-H3	138.7
-	-	-	-	O4-Hw2-O3	67.8	-	-
Hw1-Ow-Hw2	105.7	Hw1-Ow-Hw2	104.8	Hw1-Ow-Hw2	103.1	Hw1-Ow-Hw2	104.0



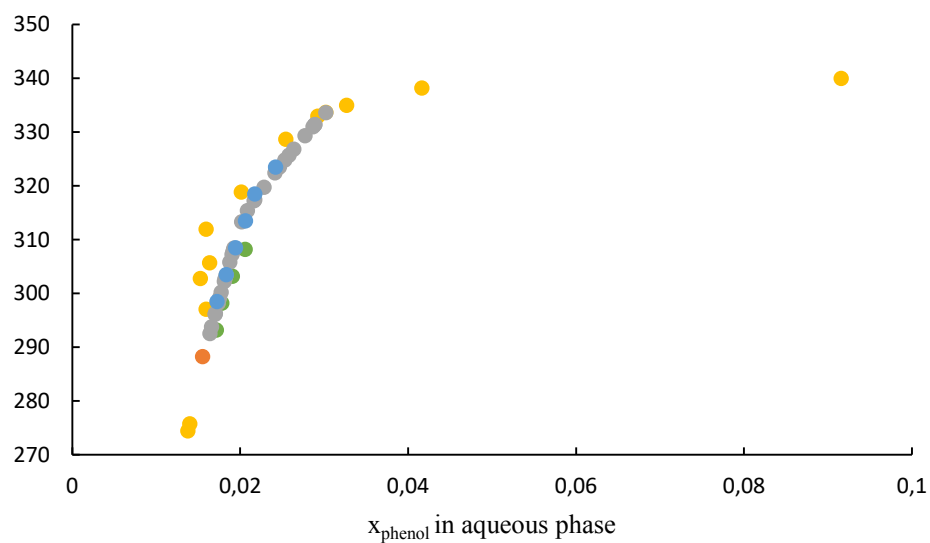
**Appendix III: Phase equilibria of phenolic compounds in water or ethanol****Table S1:** Maximum wavenlength of the phenolic compounds

Compounds	Wavenlength $\lambda$ (nm)
Phenol	269
Guaiacol	274
Syringol	266
Pyrocatechol	275
o-Cresol	270
m-Cresol	271
p-Cresol	276
Vanillin	229

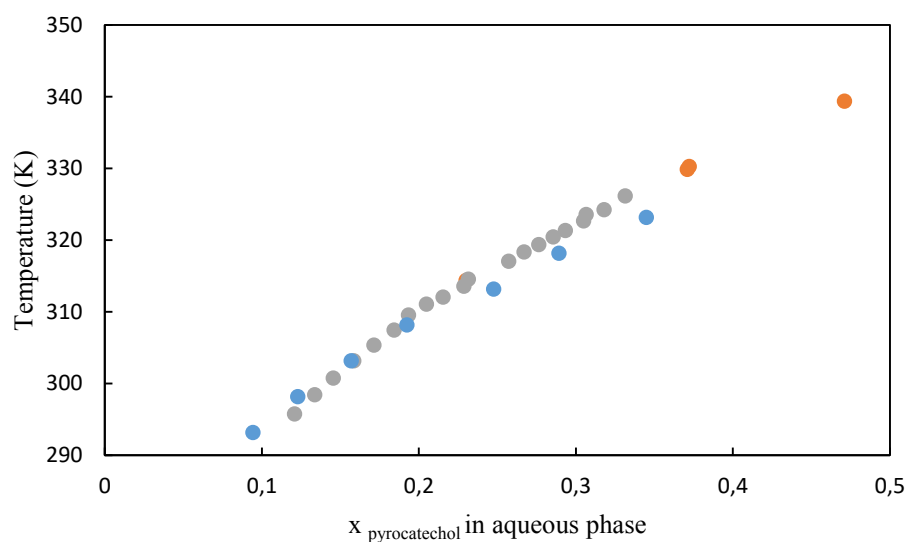
**Table S2:** Antoine parameters

	o-Cresol <sup>a</sup>		Phenol <sup>a</sup>		Guaiacol <sup>a</sup>		Ethanol <sup>b</sup>	
A	6.9117	mmHg	7.1345	mmHg	4.36309	bar	16.8969	kPa
B	1435.5	mmHg.°C <sup>-1</sup>	1516.07	mmHg.°C <sup>-1</sup>	1753.447	bar.K <sup>-1</sup>	3803.98	kPa.°C <sup>-1</sup>
C	165.16	°C	174.57	°C	-74.81	K	-41.68	°C

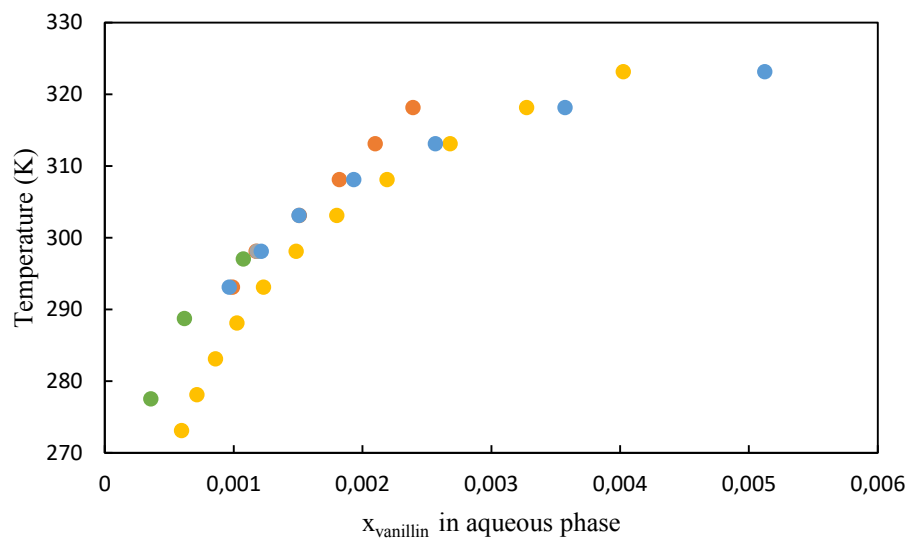
a: equation  $\log(P) = A - \frac{B}{C+T}$ , b: equation  $\ln(P) = A - \frac{B}{C+T}$

**Figure S1: Phenol-water system**

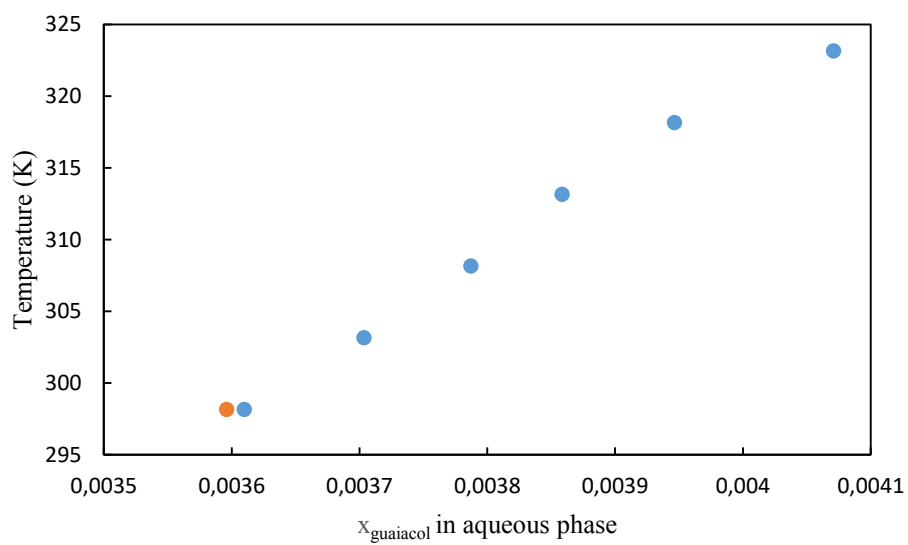
● experimental measurements, ● Achard et al[31], ● Campbell et al[32], ● Hill et al[33], ● Jaoui et al[34]

**Figure S2: Pyrocatechol–water system**

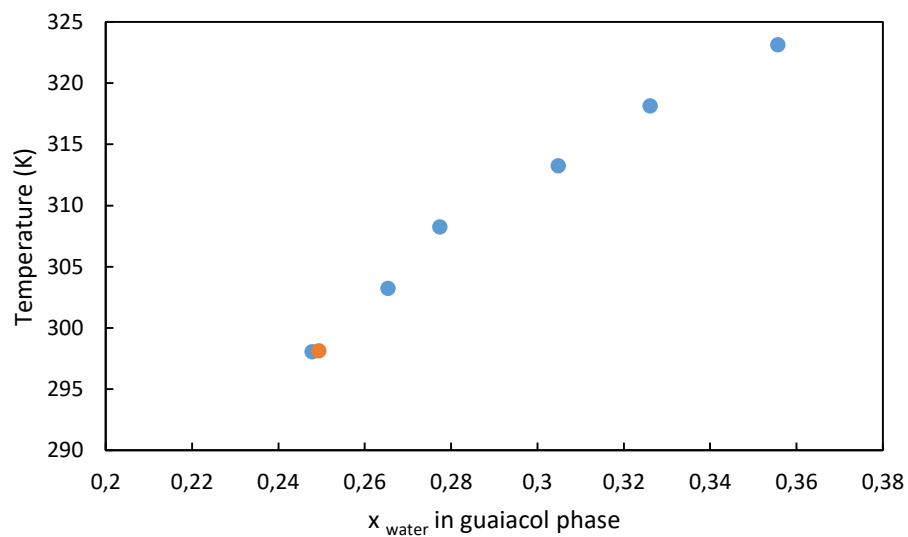
● experimental measurements, ● walker et al[29], ● xia et al[30]

**Figure S3:** Vanillin-water system

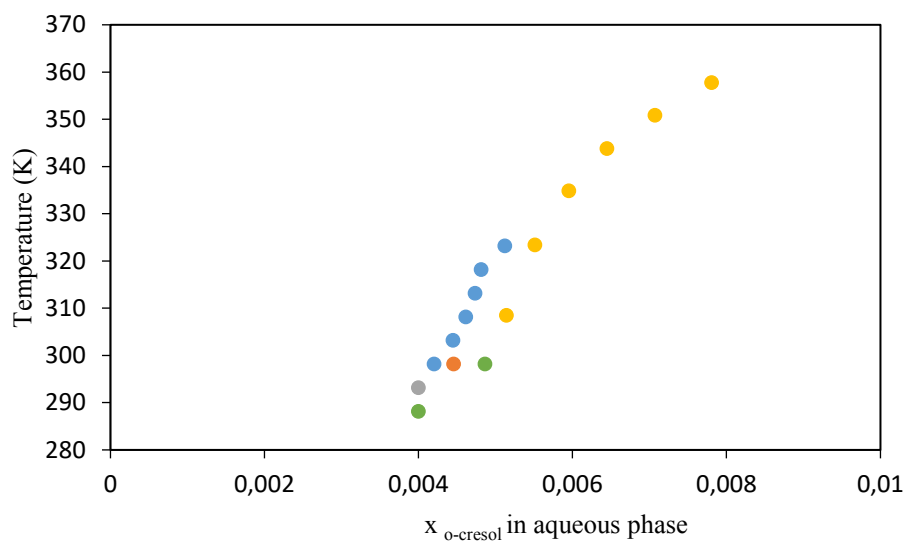
● experimental measurements, ● Cartwright [26], ● Mange et al [27], ● Noubigh et al [28]

**Figure S4:** Guaiacol-water system

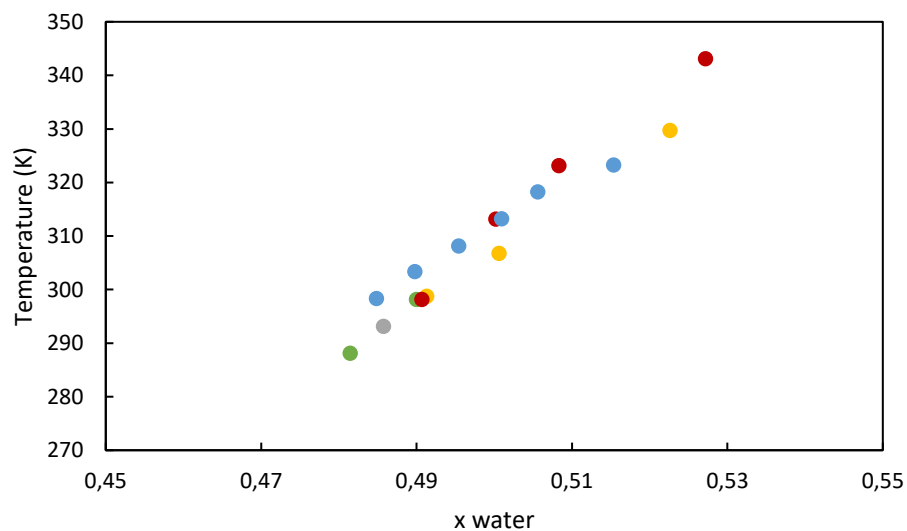
● experimental measurements, ● Tam et al[20]



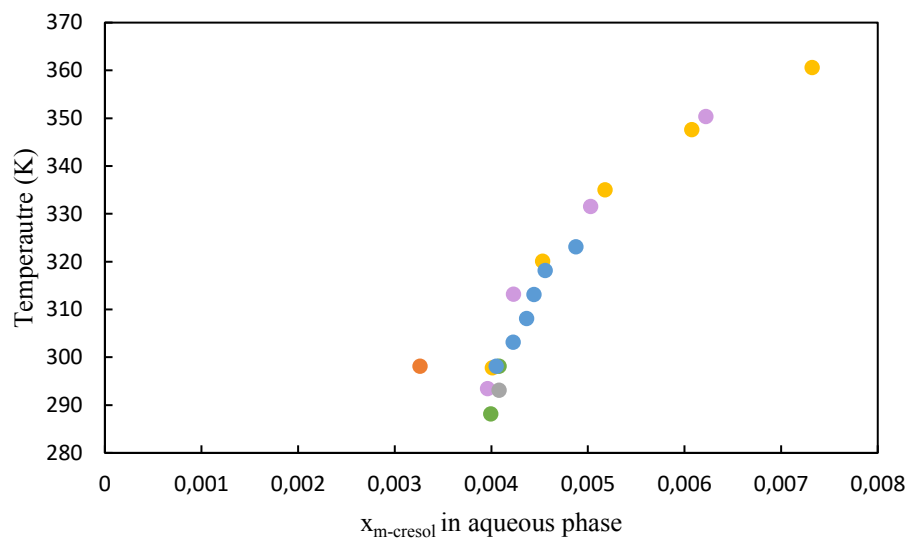
● experimental measurements, ● Shedlovsky [35]

**Figure S5:** o-Cresol-water system

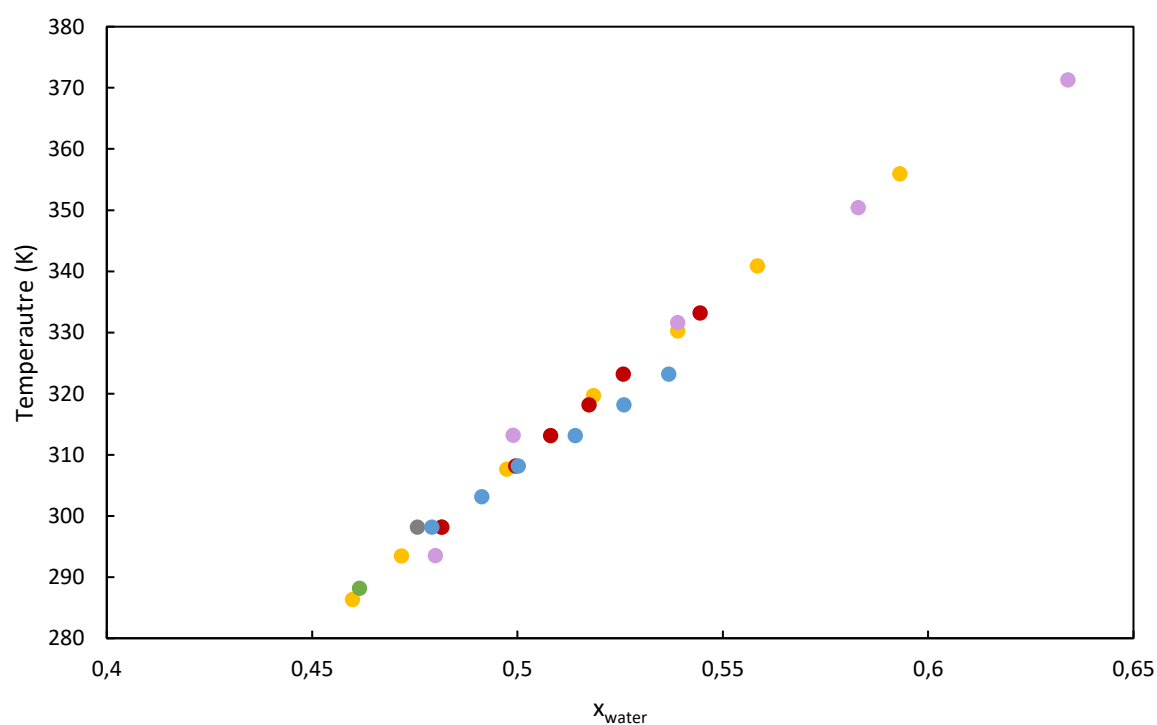
● experimental measurements, ● Sidgwick et al[21], ● Varhanickova et al[22], ● Bailey et al[23], ● Brusset et al[24]



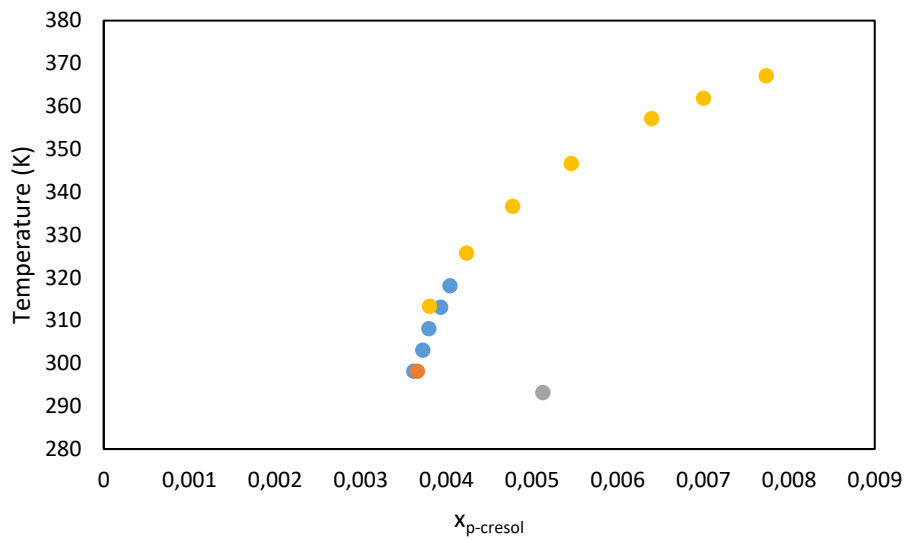
● experimental measurements, ● Sidgwick et al[21], ● Bailey et al[23], ● Brusset et al[24], ● Klauck et al[36]

**Figure S6:** m-Cresol-water system

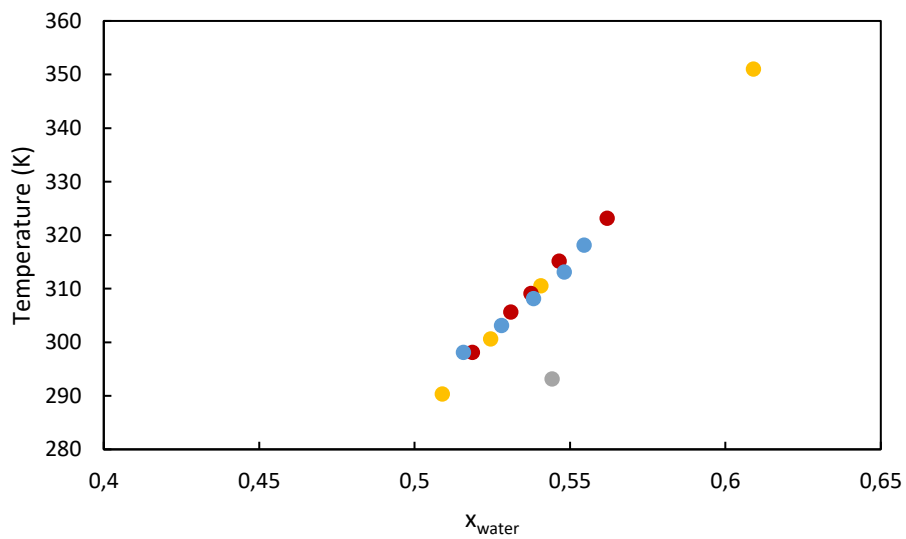
● experimental measurements, ● Sidgwick et al[21], ● Varhanickova et al[22], ● Bailey et al[23], ● Brusset et al[24], ● Leet et al[25]



● experimental measurements, ● Sidgwick et al[21], ● Bailey et al[23], ● Brusset et al[24], ● Leet et al[25], ● Klauck et al[36]

**Figure S7:** p-Cresol-water system

● experimental measurements, ● Sidgwick et al[21], ● Varhanickova et al[22], ● Bailey et al[23]



● experimental measurements, ● Sidgwick et al[21], ● Klauck et al[36], ● Bailey et al[23]

**Figure S8:** Vapor-Liquid equilibria of the phenol-ethanol system in function of the molar fraction of phenol at different pressures. Pressures: ● 0.09 bar, ● 0.165 bar, ● 0.335 bar, ● 0.5 bar, ● 0.7 bar, ● 0.83 bar, ● 0.99 bar, ● experimental measurements.

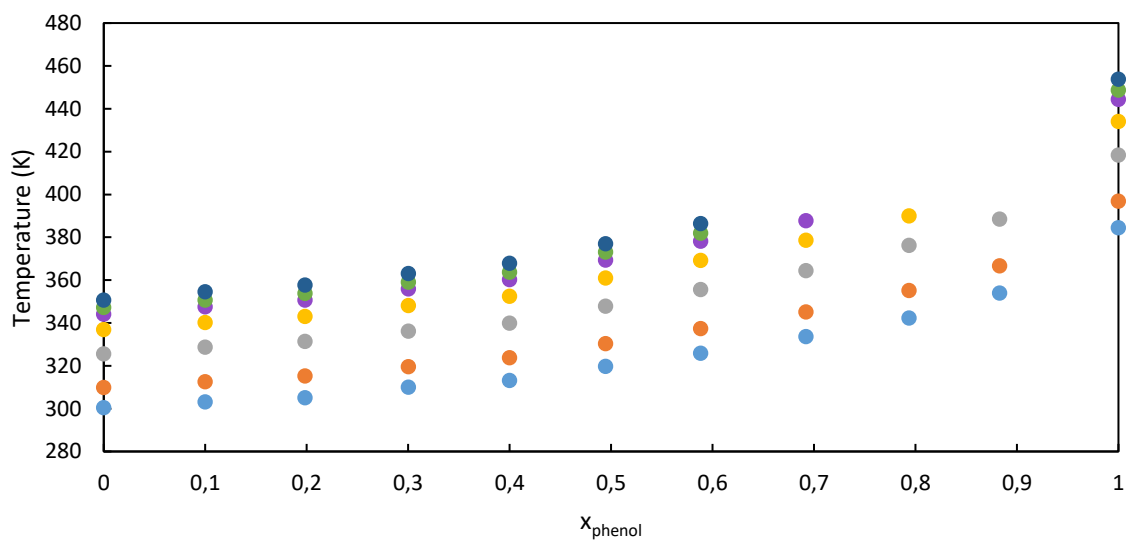
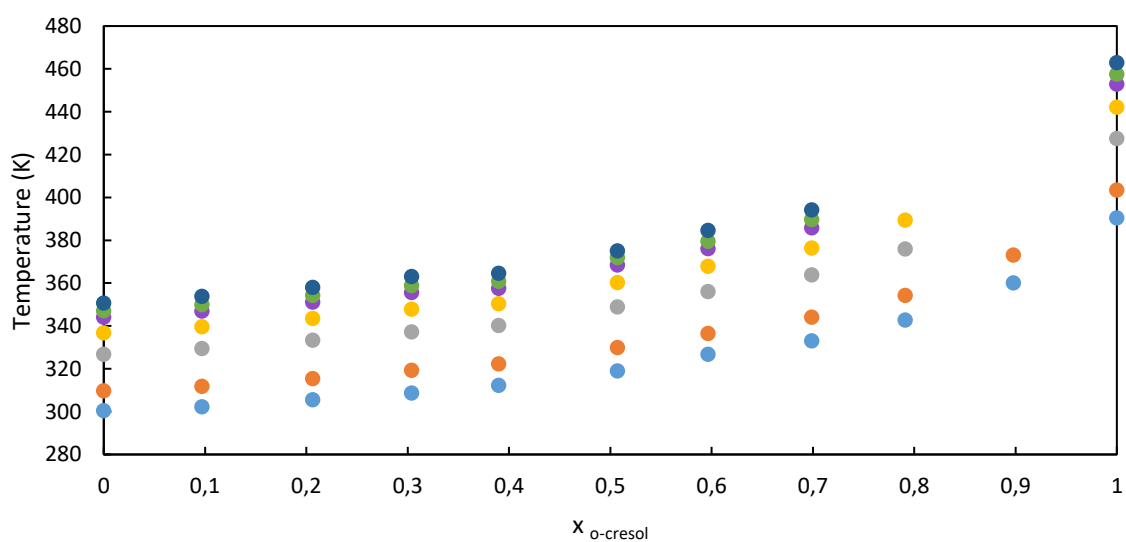


**Figure S9:** Vapor-Liquid equilibria of the o-cresol-ethanol system in function of the molar fraction of o-cresol at different pressures. Pressures: ● 0.09 bar, ● 0.165 bar, ● 0.335 bar, ● 0.5 bar, ● 0.7 bar, ● 0.83 bar, ● 0.99 bar, ● experimental measurements.



### Appendix IV: Extraction of phenolic compounds from aqueous solution using choline bis(trifluoromethylsulfonyl)imide

**Table S1:** Operating conditions of the GC-FID for the quantification of phenolic compounds.

Element	Characteristic	Description
Columns	Type	Supelco SPB <sup>TM</sup> -5 poly(5% diphenyl/95% dimethyl siloxane) FUSED SILICA Capillary Column 30m x 0.25mm x 0.25µm film thickness
	Flow	1.90 mL/min
	Carrier gas	Helium
Oven	Temperature	383.15 K
Injector	Injection volume	0.1µL
	Split ratio	100
	Temperature	523.15 K
Detector	Type	Flame Ionization Detector FID
	Temperature	523.15 K

**Table S2:** Operating conditions of the GC-TCD for the quantification of water.

Element	Characteristic	Description
Columns	Type	Alltech GS-Q Porous divinylbenzene homopolymer, length 30 m, ID 0.53 mm
	Flow	4.5 mL/min
	Carrier gas	Helium
Oven	Temperature	353.15 K for 2 min then increase of 10K/min until 523.15K for 120 min
Injector	Injection volume	1.0 µL
	Split ratio	1
	Temperature	503.15 K
Detector	Type	Thermal Conductivity Detector TCD
	Temperature	573.15 K

**Table S3:** parameters of the Othmer-Tobias consistency test for each system

	$a_1$	$b_1$	$r^2$
phenol	-4.5020	0.1071	0.9968
guaiacol	-5.2595	0.2163	0.9853
syringol	-4.8311	-0.1304	0.9984
pyrocatechol	-6.3953	1.6892	0.9956

**Table S4:** Values of the binary parameters for the NRTL Equation.

System	ij	$\Delta g_{ij}$ (J.mol <sup>-1</sup> )	$\Delta g_{ji}$ (J.mol <sup>-1</sup> )	$\alpha$	rmsd
[choline][NTf <sub>2</sub> ] (1) +	12	-3355	9145	0.3	0.0051
Phenol (2) + water (3)	13	-1944	19616		
	23	-2094	11665		
[choline][NTf <sub>2</sub> ] (1) +	12	-2289	6670	0.3	0.0045
Guaiacol (2) + water (3)	13	-2560	12900		
	23	1928	13070		
[choline][NTf <sub>2</sub> ] (1) +	12	6152	17616	0.3	0.0044
Syringol (2) + water (3)	13	-494	25806		
	23	-1264	18995		
[choline][NTf <sub>2</sub> ] (1) +	12	-500	11000	0.3	0.0135
Pyrocatechol (2) + water (3)	13	-2500	13500		
	23	-4000	13500		

**Table S5** : Values of binary parameters for the UNIQUAC Equation for the ternary mixtures

System	ij	$\Delta u_{ij}$ (J.mol <sup>-1</sup> )	$\Delta u_{ji}$ (J.mol <sup>-1</sup> )	rmsd
[choline][NTf <sub>2</sub> ] (1) + Phenol (2) + water (3)	12	-920	-910	0.0041
	13	950	344	
	23	-2030	4052	
[choline][NTf <sub>2</sub> ] (1) + Guaiacol (2) + water (3)	12	3750	-850	0.0033
	13	600	700	
	23	300	2150	
[choline][NTf <sub>2</sub> ] (1) + Syringol (2) + water (3)	12	-520	-1520	0.0044
	13	1790	-498	
	23	-868	2702	
[choline][NTf <sub>2</sub> ] (1) + Pyrocatechol (2) + water (3)	12	-983	4015	0.0046
	13	775	392	
	23	-1210	3075	

**Table S6** : UNIQUAC parameters [39]

component	r	q
water <sup>a</sup>	0.920	1.40
[Choline][NTf <sub>2</sub> ]	7.190	5.952
phenol <sup>a</sup>	3.5517	2.68
guaiacol	4.5307	3.512
syringol	3.939	3.351
pyrocatechol	2.406	2.125

**Table S7:** Thermodynamics properties of water, [choline][NTf<sub>2</sub>] and phenolic compounds.

Compounds	C <sub>p</sub> kJ.kg <sup>-1</sup> .K <sup>-1</sup>	ΔH <sub>vap</sub> kJ.kg <sup>-1</sup>	T <sub>b</sub> °C
Water	Liquid : 4.184 Vapor : 1.914	2260.75	100
[Choline][NTf <sub>2</sub> ]	1.15	/	>350
Phenol	2.355	487.80	182
Guaiacol	2.043	400.22	205
Syringol	2.082	364.94	261
Pyrocatechol	1.708	503.07	245

$$Q = m^{vapor} h^{vapor} + m^{liquid} h^{liquid} - m^{extract} h^{extract}$$

Q, m and h correspond respectively to the energy, mass and enthalpy. Superscript refers to the phase.

Because we supposed that only the ionic liquid remains to the liquid phase in the flash, we got:

$$m^{liquid} = m^{extract} * w_{IL}^{extract} \text{ and } m^{vapor} = m^{extract} * (1 - w_{IL}^{extract})$$

We assume that the excess enthalpy is equal to 0 and the state reference is taken at 25°C and 1 atmosphere in the liquid phase. The heat capacity is supposed to be only varying with temperature and calculated at the average between the boiling temperature of the phenolic compound and reference temperature. For instance, the heat capacity of phenol is calculated at the temperature of 103.5 °C. Water is considered liquid between 25 and 100°C, and gas above 100°C. The enthalpy of vaporization are calculated at the boiling point of each compound.

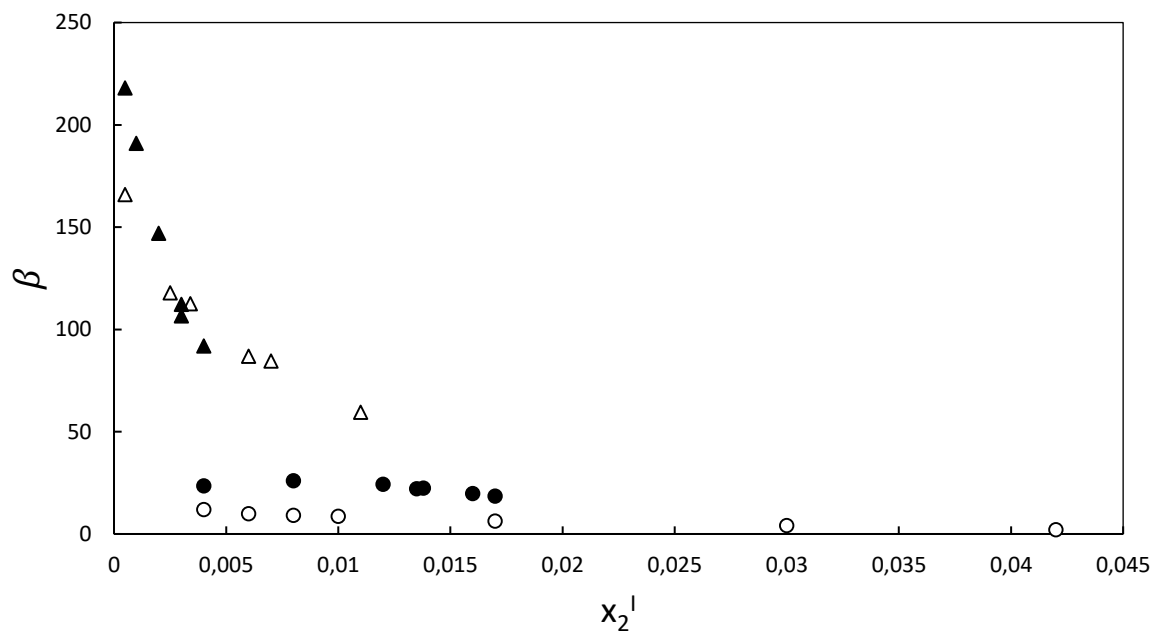
Therefore, we obtain:

$$Q = m^{vapor} \{ [w_{PC}^{vapor} * (\Delta_{vap} H_{PC} + C_{p_{PC}}^{liquid} * (T_{b_{PC}} - 25))] \\ + w_{water}^{vapor} [(C_{p_{water}}^{vapor} * (T_{b_{PC}} - 100) + \Delta_{vap} H_{water} + C_{p_{water}}^{liquid} * (100 - 25))] \} \\ + m^{liquid} * C_{p_{IL}}^{liquid} * (T_{b_{PC}} - 25)$$

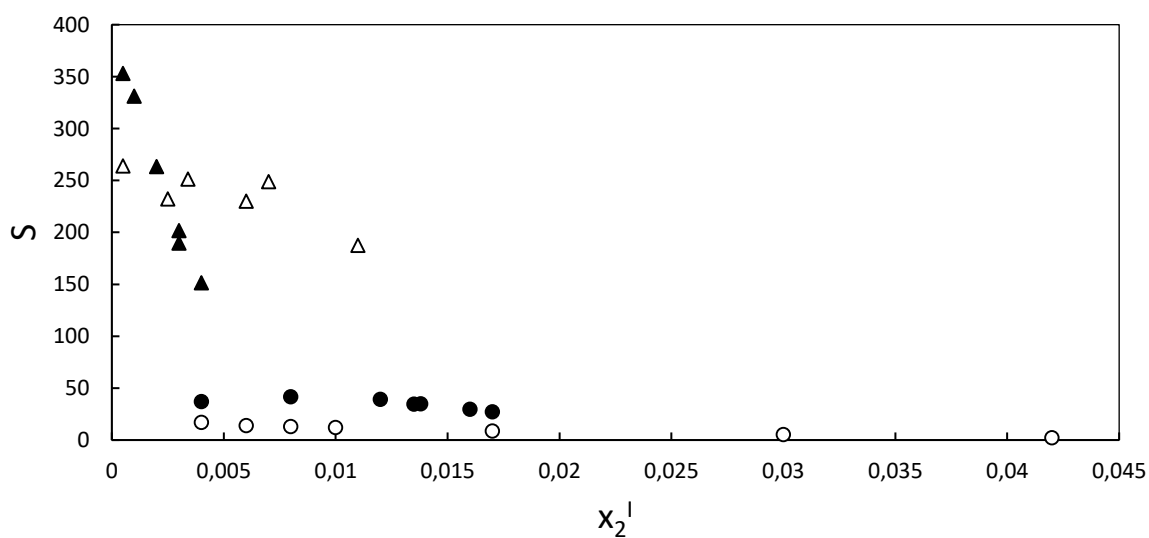
With Q the energy in kJ, w and Cp are the massic fraction and the heat capacity. Superscripts refers to the phase, and subscripts to the compound.

To convert the results in kJ/kg of phenolic compounds:  $Q \left( \frac{kJ}{kg} \right) = \frac{Q (kJ)}{m^{extract} * w_{PC}^{extract}}$

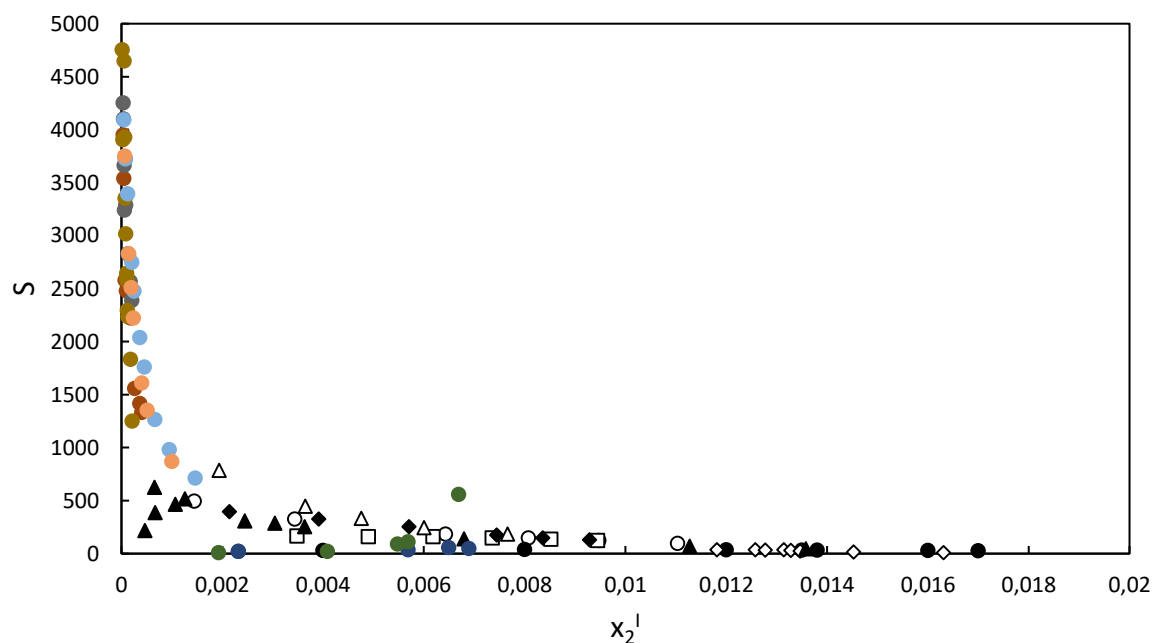
**Figure S1 :** Plot of the solute distribution ration  $\beta$  as a function of the mole fraction of phenolic compound in the aqueous phase for the investigated systems: ● phenol,  $\Delta$  guaiacol,  $\blacktriangle$  syringol,  $\circ$  pyrocatechol.



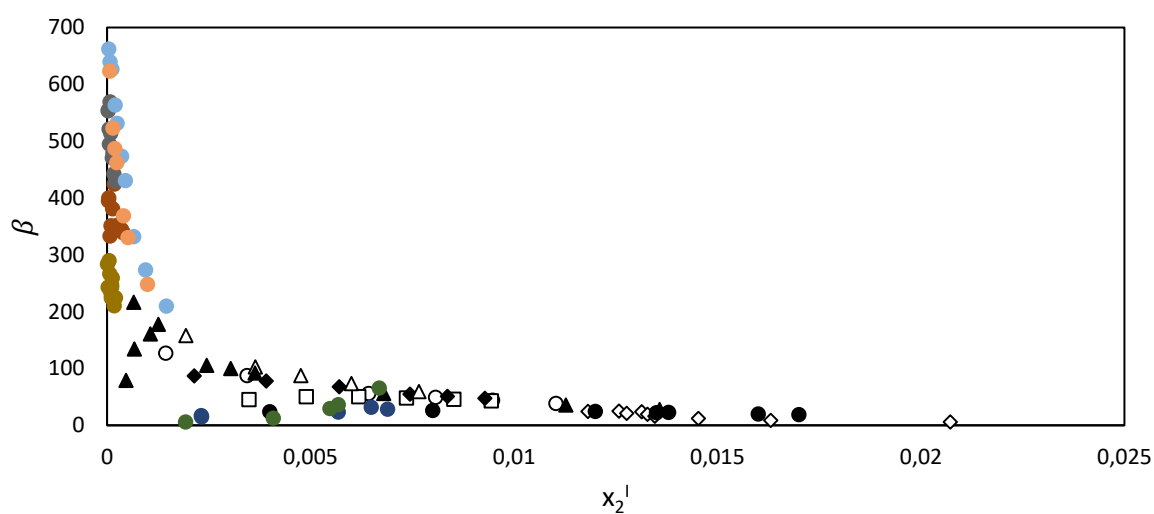
**Figure S2 :** Plot of the selectivity  $S$  as a function of the mole fraction of phenolic compound in the aqueous phase for the investigated systems: ● phenol,  $\Delta$  guaiacol,  $\blacktriangle$  syringol,  $\circ$  pyrocatechol.



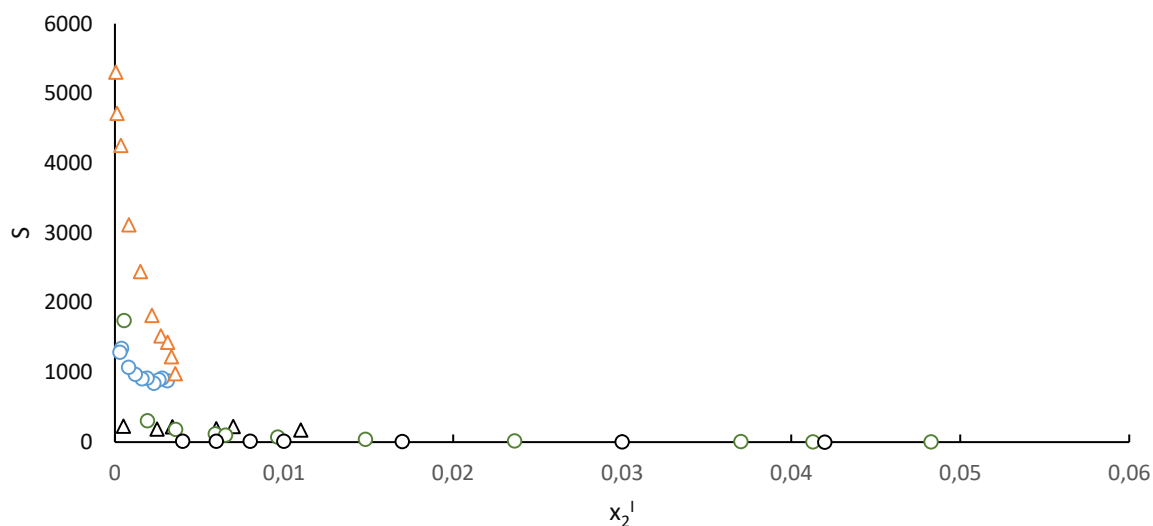
**Figure S3** : plot of the selectivity  $S$  vs the molar fraction of phenol in the aqueous phase:  $\circ$  1-octanol,  $\square$  cyclohexanone,  $\Delta$  isobutylacetate,  $\blacklozenge$  2-ethyl-1-hexanol [28],  $\blacktriangle$  2-butanone,  $\diamond$  2-propanol [16],  $\bullet$  MTBK [19],  $\bullet$  MBK [17],  $\bullet$  2-methoxy-2-methylpropane [12],  $\bullet$  toluene [24],  $\bullet$  m-xylene [24],  $\bullet$  2-pentanone [20],  $\bullet$  MIPK [21],  $\bullet$  experimental data



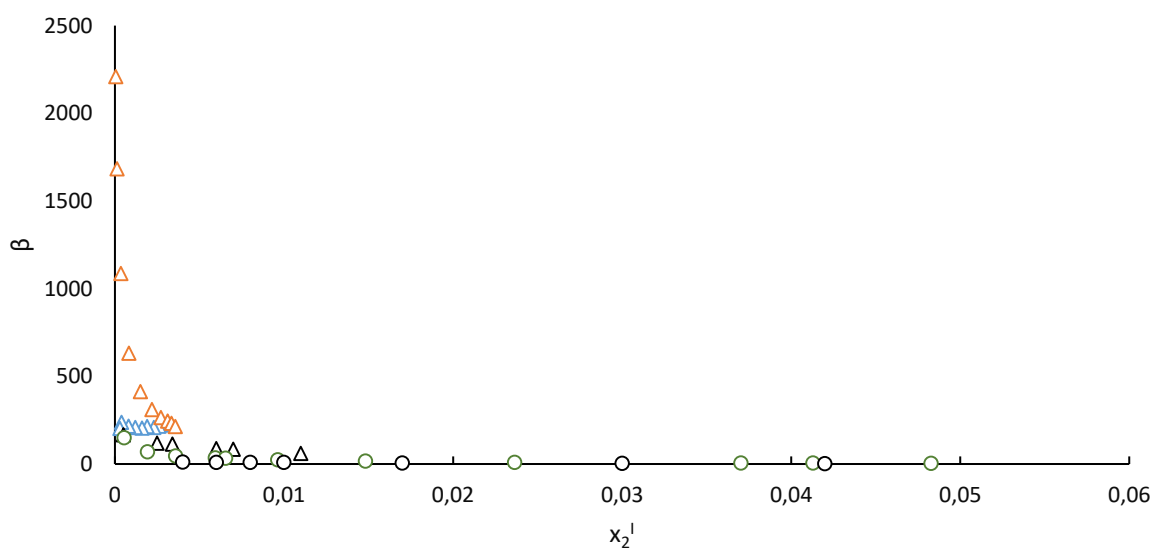
**Figure S4** : Plot of the solute distribution ratio  $\beta$  vs the molar fraction of phenol in the aqueous phase:  $\circ$  1-octanol,  $\square$  cyclohexanone,  $\Delta$  isobutylacetate,  $\blacklozenge$  2-ethyl-1-hexanol [28],  $\blacktriangle$  2-butanone,  $\diamond$  2-propanol [16],  $\bullet$  MTBK [19],  $\bullet$  MBK [17],  $\bullet$  2-methoxy-2-methylpropane [12],  $\bullet$  toluene [24],  $\bullet$  m-xylene [24],  $\bullet$  2-pentanone [20],  $\bullet$  MIPK [21],  $\bullet$  experimental data



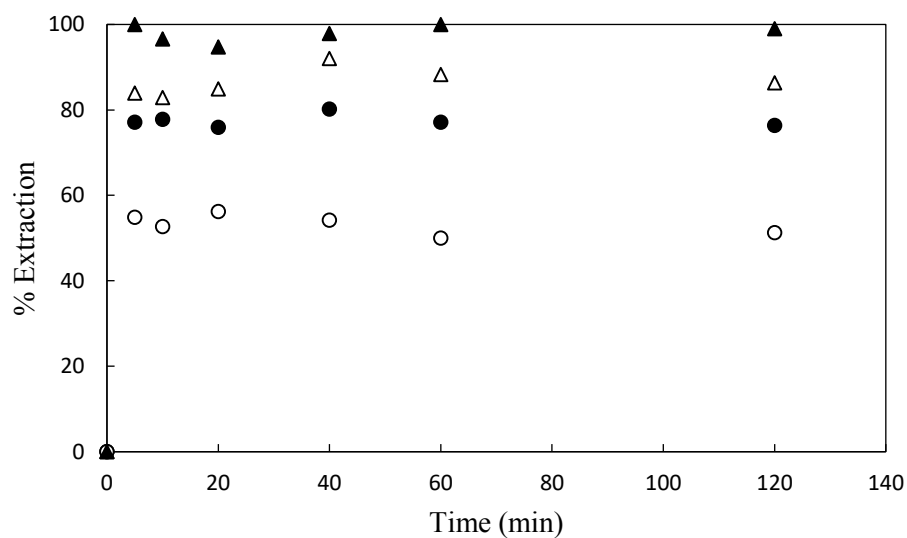
**Figure S5 :** plot of the selectivity  $S$  vs the molar fraction of phenolic compound in the aqueous phase:  $\triangle$  {water – guaiacol - P666,14[N(CN)<sub>2</sub>]} [26]  $\triangle$  {water – guaiacol - ethyl acetate} [26]  $\triangle$  {water – guaiacol – [choline][NTf<sub>2</sub>]} experimental measurements;  $\circ$  {water – pyrocatechol - n-butyl acetate} [27],  $\circ$  {water – pyrocatechol – [choline][NTf<sub>2</sub>]} experimental measurements.



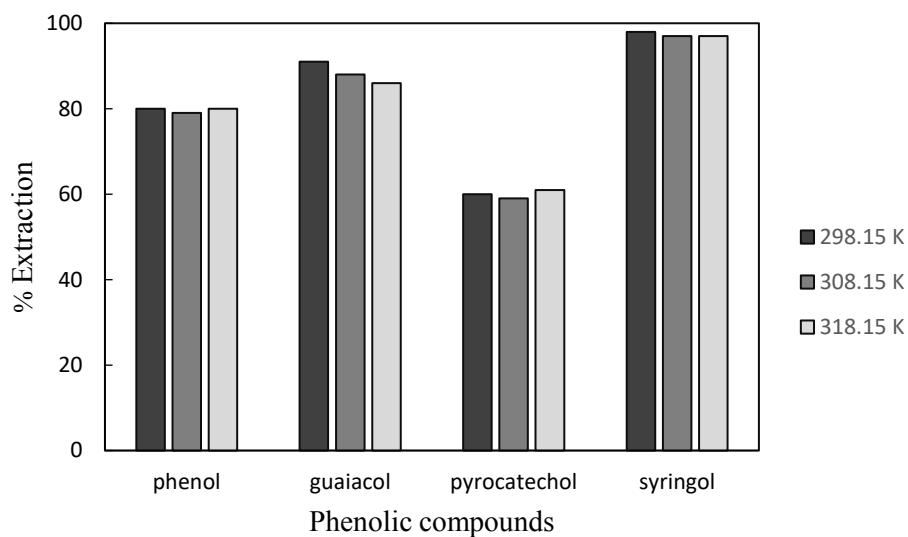
**Figure S6 :** plot of solute distribution ratio  $\beta$  vs the molar fraction of phenolic compound in the aqueous phase:  $\triangle$  {water – guaiacol - P666,14[N(CN)<sub>2</sub>]} [26]  $\triangle$  {water – guaiacol - ethyl acetate} [26]  $\triangle$  {water – guaiacol – [choline][NTf<sub>2</sub>]} experimental measurements;  $\circ$  {water – pyrocatechol - n-butyl acetate} [27],  $\circ$  {water – pyrocatechol – [choline][NTf<sub>2</sub>]} experimental measurements.



**Figure S7:** Plot of the percentage of extraction for each compound as a function of time: ● phenol, △ guaiacol, ▲ syringol, ○ pyrocatechol. Temperature 298.15 K and ratio of ionic liquid/water equal to 1.

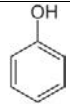
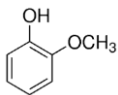
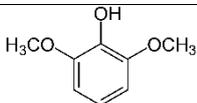
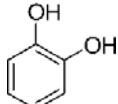
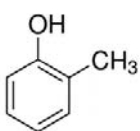
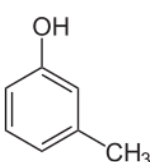
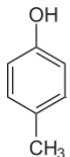
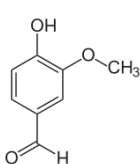


**Figure S8:** Influence of the temperature on the efficiency of the extraction process.

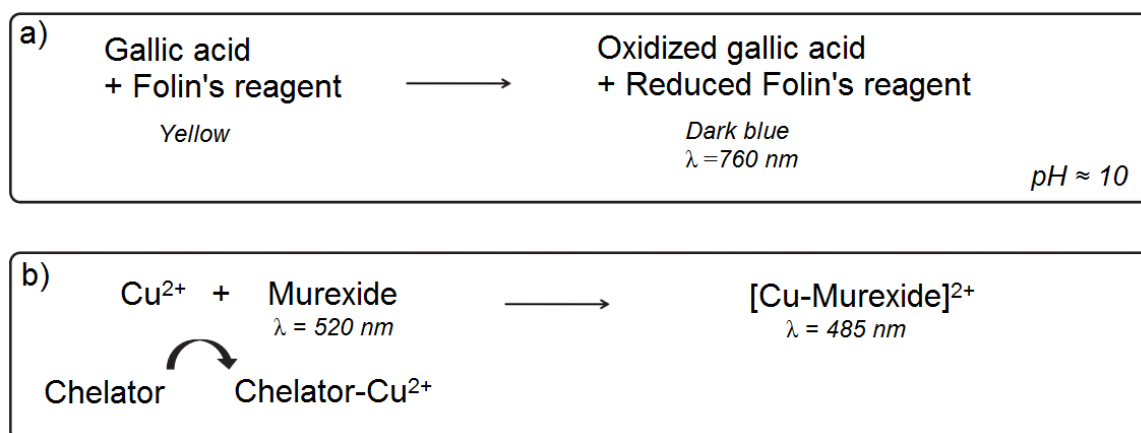


## Appendix V: Antioxidant Properties of Phenolic Compounds

Table S1: Structure and properties of the eight phenolic compounds (Sigma Aldrich; purity > 99 %).

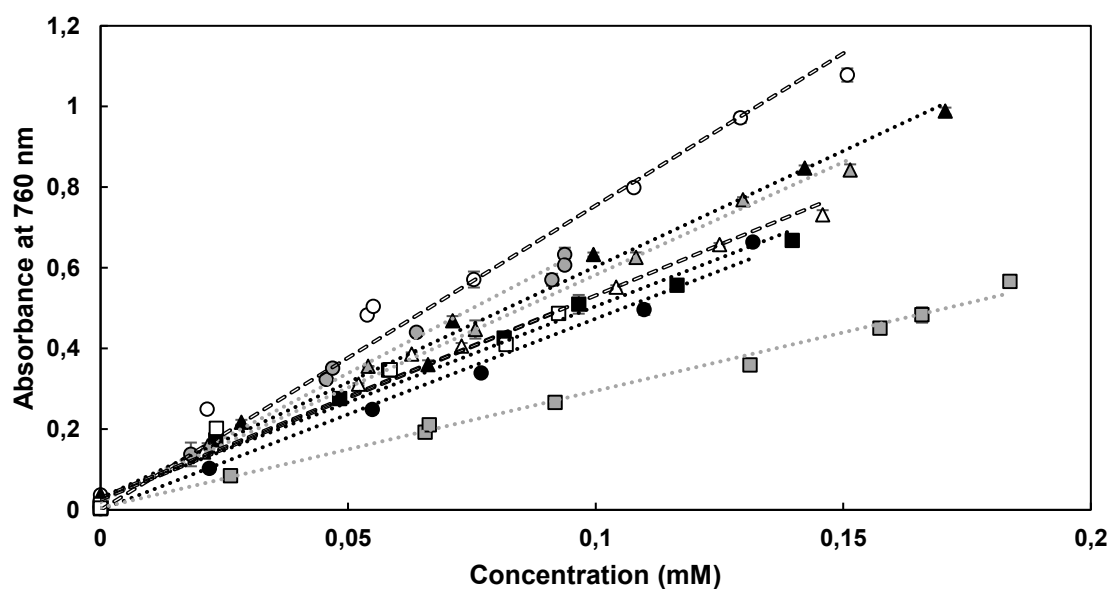
Name	Abbreviation	Formula	pKa	Molar mass (g.mol <sup>-1</sup> )
Phenol	Phenol		9.95	94.11
2-methoxyphenol	Guaiacol		9.98	124.14
2,6-dimethoxyphenol	Syringol		9.98	154.16
1,2-benzenediol	Pyrocatechol		9.5	110.11
2-Methylphenol	O-cresol		10.3	108.14
3-Methylphenol	M-cresol		10.2	108.14
4-Methylphenol	P-cresol		10.2	108.14
4-Hydroxy-3-methoxybenzaldehyde	Vanillin		7.5	152.15

**Figure S1.** Chemical reactions involved in the assays. a) Quantification of total phenols by Folin-Ciocalteu. b) Copper chelation capacity. The principle of the other tests used in this study are described elsewhere (Canabady-Rochelle et al, 2015).

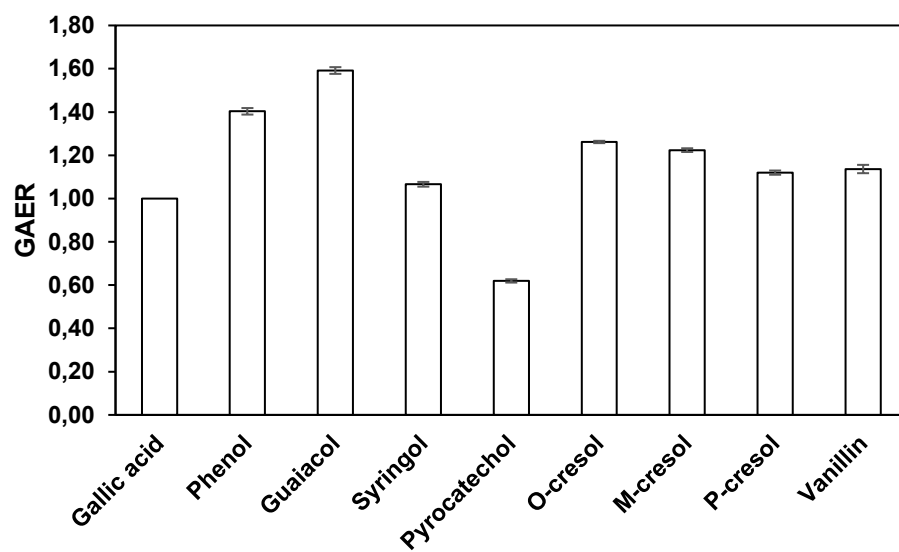
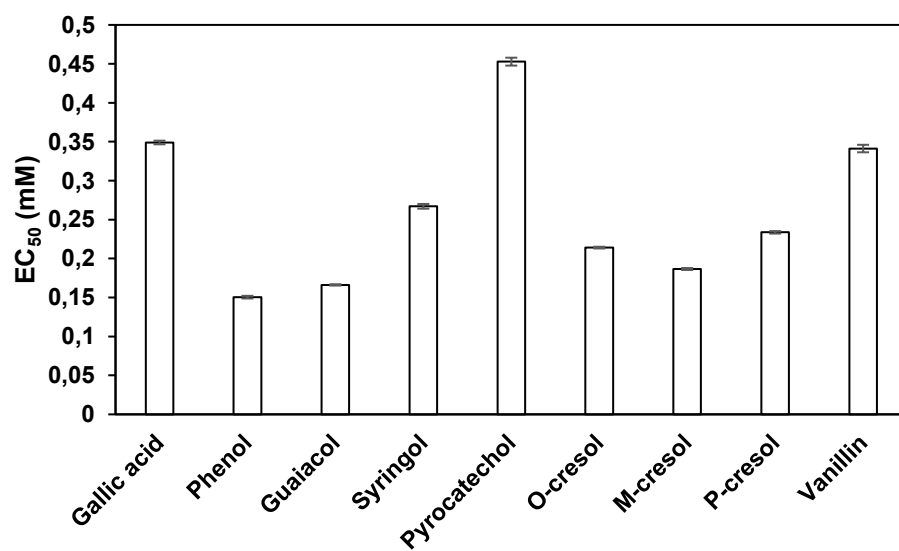


### I. Dosage of phenols by the Folin-Ciocalteu method

**Figure S2:** Linearization of the absorbance as a function of the concentration of the compounds:  
 ● Reference (Gallic acid), ○ Phenol, ◊ Guaiacol, ■ Syringol, □ Pyrocatechol, ◻ Vanillin, ▲ O-cresol, ▲ M-cresol, ▲ P-cresol



The standard deviation are so low that it cannot be observed at this scale.

**Figure S3:** Gallic Acid Equivalent Response (GAER)**Figure S4:** EC<sub>50</sub> of the response of the compounds to Folin's reagent

## II. Iron(II) chelating activity

Figure S5: EDTA Equivalent Chelation Capacity (EECC) indice

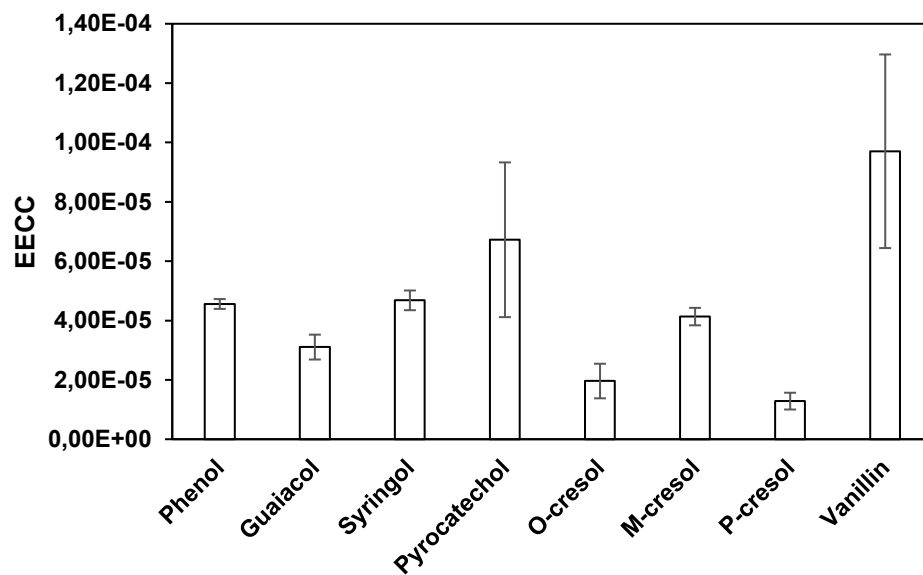
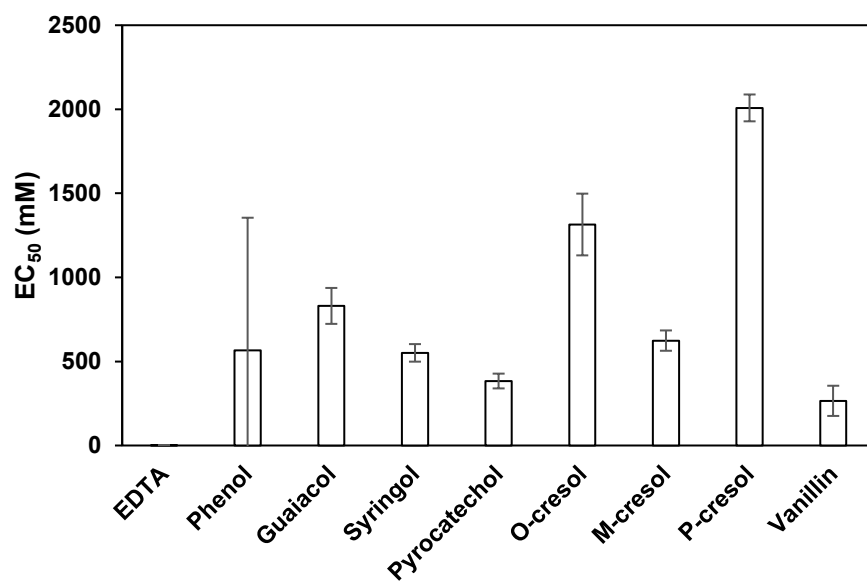
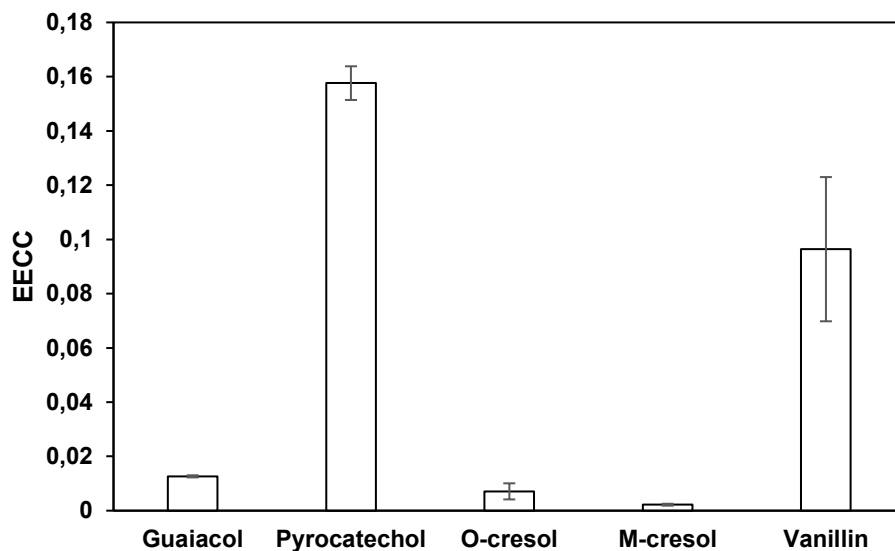


Figure S6: EC<sub>50</sub> of the iron chelation capacity



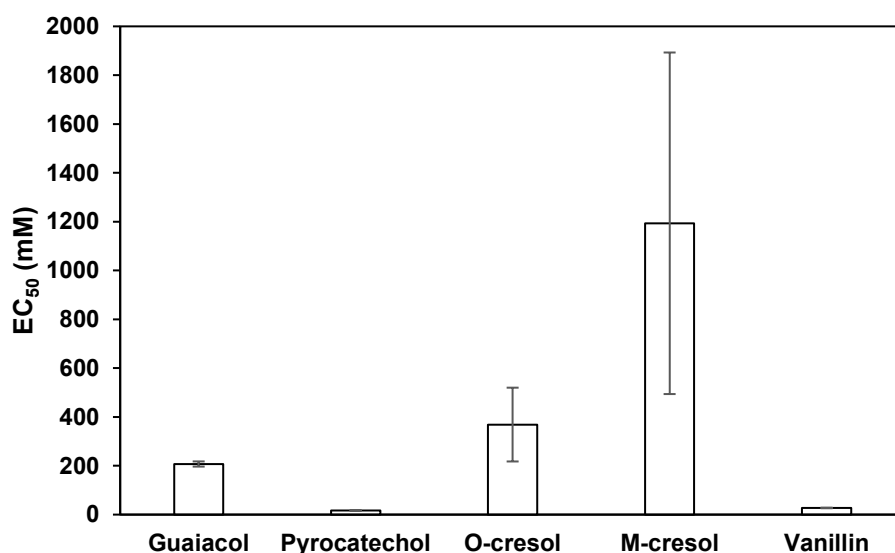
### III. Copper(II) chelating activity

**Figure S7:** EDTA Equivalent Chelation Capacity (EECC) indice



It was not possible to calculate the EECC for phenol, syringol and p-cresol because of the non-linearity of the results for these compounds

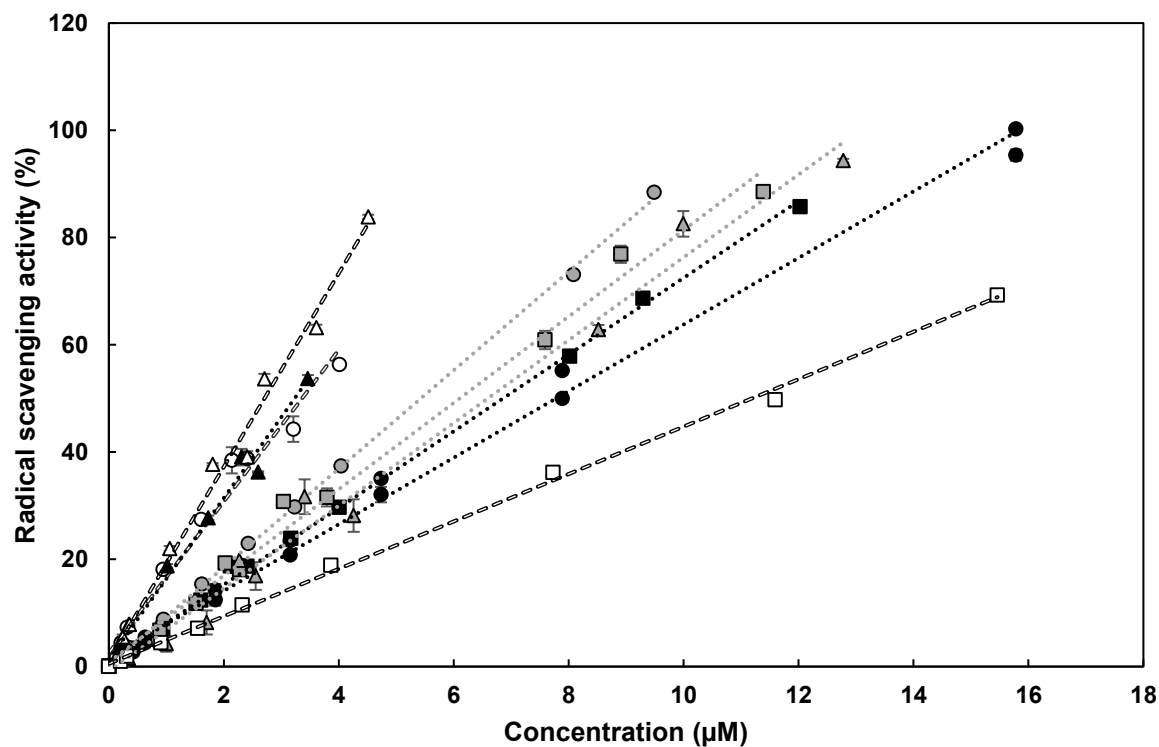
**Figure S8:** EC<sub>50</sub> of the copper chelation capacity



It was not possible to calculate the EC<sub>50</sub> for phenol, syringol and p-cresol because of the non-linearity of the results for these compounds.

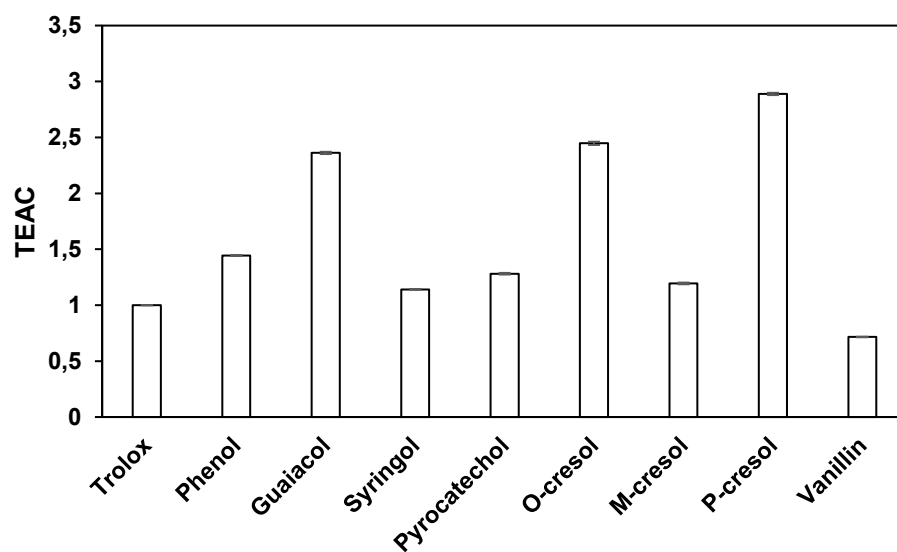
#### IV. Radical Scavenging activity

**Figure S9:** linearization of the radical scavenging activity (%) as a function of the concentration of the compounds ( $\mu\text{M}$ ): ● Reference (Trolox), ○ Phenol, ○ Guaiacol, ■ Syringol, ■ Pyrocatechol, □ Vanillin, ▲ O-cresol, ▲ M-cresol, ▲ P-cresol

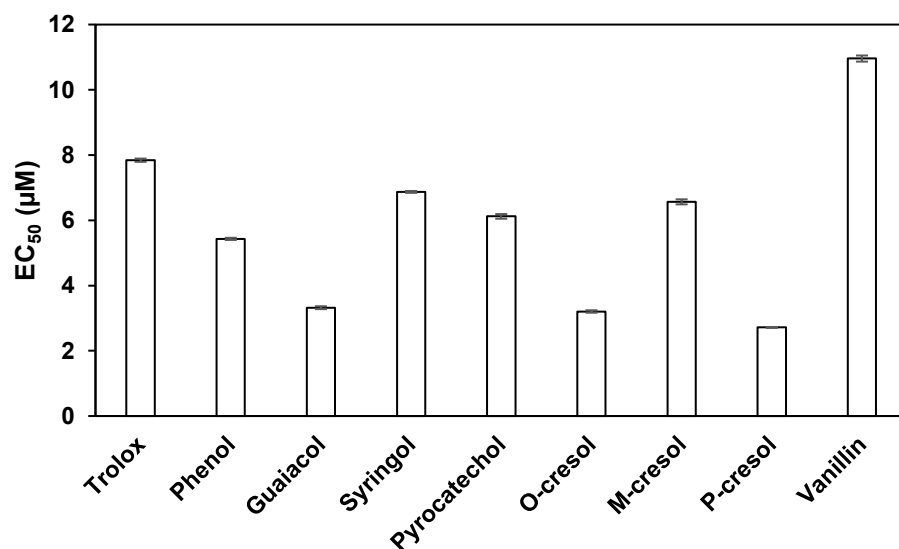


The standard deviation are so low that it cannot be observed at this scale.

**Figure S10:** Trolox Equivalent Antioxidant Capacity (TEAC) indice



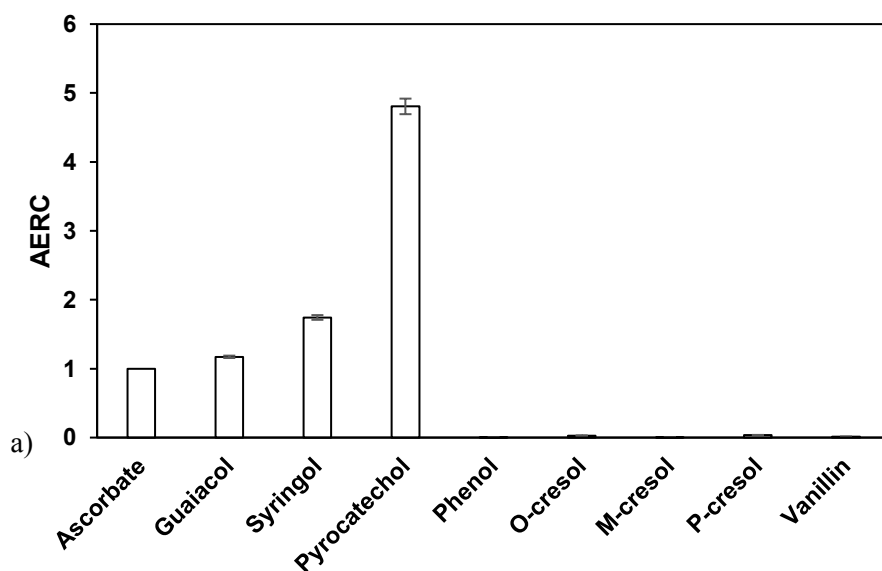
The standard deviation are so low that it cannot be observed at this scale.

**Figure S11:** EC<sub>50</sub> of radical scavenging activity

The standard deviation are so low that it cannot be observed at this scale.

## V. Reducing capacity

**Figure S12:** Ascorbate Equivalent Reducing Capacity (AERC) indice a) All the studied phenolic compounds. b) Focus on the phenolic compounds with the lowest AERC.



The standard deviation are so low that it cannot be observed at this scale.

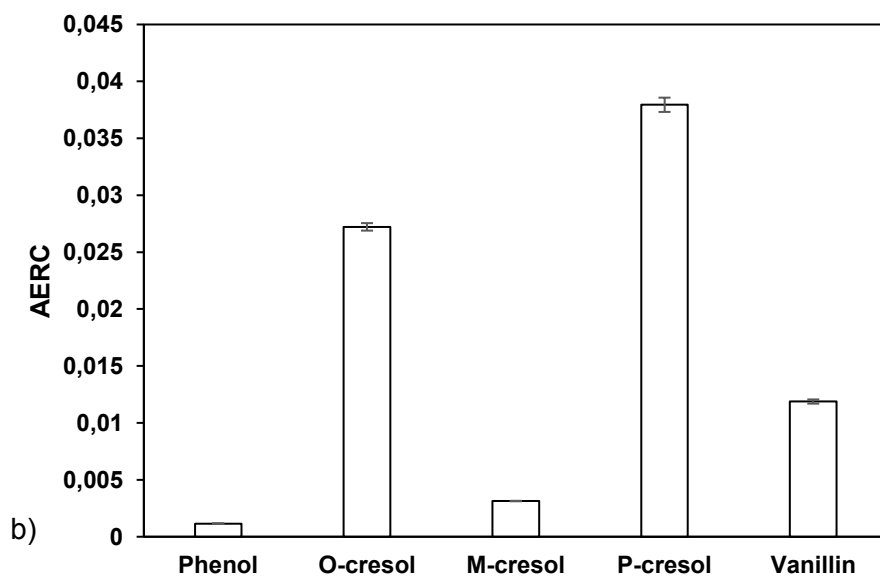
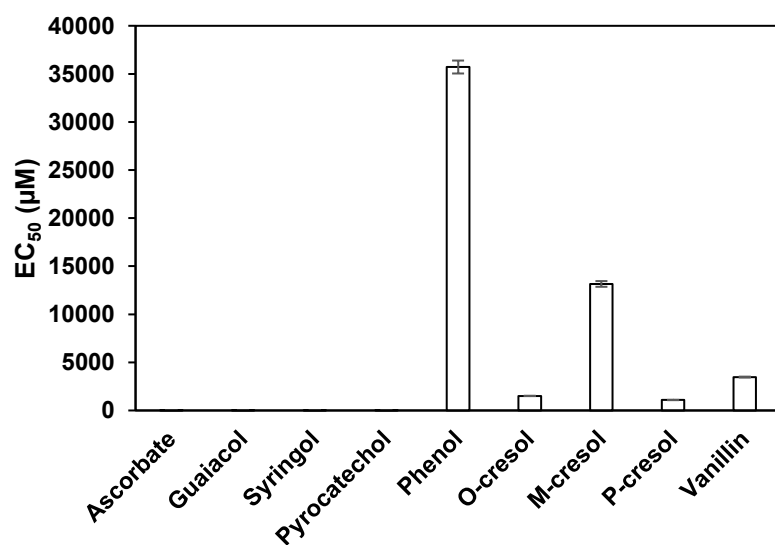


Figure S13: EC<sub>50</sub> of the reducing capacity



The standard deviation are so low that it cannot be observed at this scale.



## Extraction of phenolic compounds from lignin bio-oil.

### Abstract

The lignocellulosic biomass is mostly composed of cellulose, hemicellulose and lignin. Upon thermal conversion of lignin, a bio-oil rich in phenolic compounds is obtained. These latter are then generally recovered through several liquid-liquid extraction involving aqueous and organic solvents. In this work we investigated, by a multi-scale study, the feasibility and the efficiency of the ionic liquid [Choline][NTf<sub>2</sub>] for the extraction of these phenolic compounds by liquid-liquid extraction. Indeed, such a solvent could improve the extraction efficiency and at the same time, reduce the toxicity and the cost of the classic organic solvents. Quantum calculations were performed in order to better understand the interaction governing the key systems of these extractions. The structures of the phenolic compounds in their isolated forms and in contact with solvents show that the conformations are stabilized by the presence of hydrogen bonds. More, the determination of the interaction energies indicates that the [Choline][NTf<sub>2</sub>] ionic liquid is efficient for the extraction of phenolic compounds present in aqueous solution. Furthermore, the study of phase diagrams of binary systems {water-phenolic compound} and ternary systems {water-phenolic compound-[Choline][NTf<sub>2</sub>]} show that the extraction of these compounds is also possible at a macroscopic scale. Then, the NRTL parameters coming from these experiments allowed the simulation of the extraction of three compounds mostly present in the bio-oils, namely phenol, guaiacol and syringol, as so at low cost. Finally, the extraction of these compounds from bio-oil obtained from lignin fast pyrolysis was also particularly efficient with the [Choline][NTf<sub>2</sub>] ionic liquid. Therefore, this multi-scale study demonstrated that [Choline][NTf<sub>2</sub>] is an excellent solvent for the recovery of phenolic compounds. Lastly, the study of the antioxidant properties testify the added-value of these compounds, especially through their reducing power and their radical scavenging capacity.

**Keywords:** phenolic compounds, bio-oils, extraction, gas chromatography, process design, *ab initio* calculations, antioxidant properties.

## Extraction de composés phénoliques à partir d'une bio-huile de lignine.

### Résumé

La biomasse ligno-cellulosique est principalement constituée de cellulose, d'hémicellulose et de lignine. Par conversion thermo-chimique, la lignine se transforme en bio-huile riche en composés phénoliques. Ces composés phénoliques sont généralement récupérés à l'aide de plusieurs étapes d'extractions liquide-liquide consécutives impliquant des solvants aqueux et organiques. A l'aide d'une approche multi-échelle, nous avons étudié, la faisabilité et l'efficacité d'un liquide ionique, la [Choline][NTf<sub>2</sub>], pour l'extraction liquide-liquide de ces composés. En effet, l'utilisation de ce solvant permettrait d'améliorer l'efficacité d'extraction, tout en diminuant la toxicité et les coûts liés à l'utilisation de solvants organiques classiques. Des calculs quantiques ont été effectués afin de mieux comprendre les interactions régissant les systèmes clés de ces extractions. Les structures des composés phénoliques dans leur état isolé ou en présence de solvant montrent que les conformations sont stabilisées par la présence de liaisons hydrogène. De plus, la détermination des énergies d'interaction indique que la [Choline][NTf<sub>2</sub>] est efficace pour l'extraction de composés phénoliques présents en solution aqueuse. Par ailleurs, la détermination des diagrammes de phases des systèmes binaires {eau-composé + phénolique} et des systèmes ternaires {eau + composé phénolique + [Choline][NTf<sub>2</sub>]} montre que l'extraction des composés est également possible à une échelle macroscopique. Les paramètres NRTL issus de ces expériences ont permis de simuler l'extraction de trois composés phénoliques majoritairement présents dans les bio-huiles, *i.e.* le phénol, le guaiacol et le syringol, et ce, à moindre coût. Enfin, l'extraction de ces composés à partir d'une bio-huile obtenue par pyrolyse rapide de lignine a également été particulièrement efficace avec le liquide ionique [Choline][NTf<sub>2</sub>]. De ce fait, cette étude multi-échelle a permis de montrer que la [Choline][NTf<sub>2</sub>] est un excellent solvant pour la récupération des composés phénoliques. Enfin, l'étude des propriétés anti-oxydantes témoigne de la valeur ajoutée de ces composés, notamment à travers leur pouvoir réducteur et leur propriété anti-radicalaire.

**Mots-clés :** composés phénoliques, bio-huiles, extraction, chromatographie gazeuse, dimensionnement de procédés, calculs *ab initio*, propriétés antioxydantes.